Government of **Western Australia**
Department of **Mines and Petroleum**

RECORD 2014/6

ALBANY–FRASER OROGEN SEISMIC AND MAGNETOTELLURIC (MT) WORKSHOP 2014: EXTENDED ABSTRACTS

compiled by
CV Spaggiari and IM Tyler



Geological Survey of Western Australia

ROYALTIES FOR REGIONS
EXPLORATION INCENTIVE SCHEME

Australian Government
Geoscience Australia

Centre for EXPLORATION TARGETING

ANSIR NATIONAL RESEARCH FACILITY FOR EARTH SOUNDING

INDEPENDENCE GROUP NL

ANGLOGOLD ASHANTI

Government of Western Australia
Department of Mines and Petroleum

Record 2014/6

ALBANY–FRASER OROGEN SEISMIC AND MAGNETOTELLURIC (MT) WORKSHOP 2014: EXTENDED ABSTRACTS

compiled by
CV Spaggiari and IM Tyler

Perth 2014

Geological Survey of
Western Australia

MINISTER FOR MINES AND PETROLEUM
Hon. Bill Marmion MLA

DIRECTOR GENERAL, DEPARTMENT OF MINES AND PETROLEUM
Richard Sellers

EXECUTIVE DIRECTOR, GEOLOGICAL SURVEY OF WESTERN AUSTRALIA
Rick Rogerson

REFERENCE
The recommended reference for this publication is:

(a) For reference to an individual contribution:

Occhipinti, SA, Doyle, MG, Spaggiari, CV, Korsch, RJ, Cant, G, Martin, K, Kirkland, CL, Savage, J, Less, T, Bergin, L and Fox, L 2014, Interpretation of the deep seismic reflection line 12GA-T1: northeast Albany–Fraser Orogen, *in* Albany–Fraser Orogen seismic and magnetotelluric (MT) workshop 2014: extended abstracts *compiled by* CV Spaggiari and IM Tyler: Geological Survey of Western Australia, Record 2014/6, p. 52–68.

(b) For reference to the publication:

Spaggiari, CV and Tyler IM (compilers) 2014, Albany–Fraser Orogen seismic and magnetotelluric (MT) workshop 2014: extended abstracts: Geological Survey of Western Australia, Record 2014/6, 182p.

National Library of Australia Card Number and ISBN 978-1-74168-634-0

Grid references in this publication refer to the Geocentric Datum of Australia 1994 (GDA94). Locations mentioned in the text are referenced using Map Grid Australia (MGA) coordinates, Zones 51 and 52. All locations are quoted to at least the nearest 100 m.

Published 2014 by Geological Survey of Western Australia
This Record is published in digital format (PDF) and is available online at <www.dmp.wa.gov.au/GSWApublications>.

Further details of geological products and maps produced by the Geological Survey of Western Australia are available from:
Information Centre
Department of Mines and Petroleum
100 Plain Street
EAST PERTH WESTERN AUSTRALIA 6004
Telephone: +61 8 9222 3459 Facsimile: +61 8 9222 3444
www.dmp.wa.gov.au/GSWApublications

Contents

Plates

1. Interpreted pre-Mesozoic bedrock geology of the northeast region of the Albany–Fraser Orogen including seismic line 12GA-T1 (1:250 000)
2. Interpreted pre-Mesozoic bedrock geology of the east Albany–Fraser Orogen and southeast Yilgarn Craton including seismic line 12GA-AF3 (1:500 000)
3. Interpreted pre-Mesozoic bedrock geology of the Albany–Fraser Orogen and southeast Yilgarn Craton including seismic lines 12GA-AF1 and 12GA-AF2 (1:500 000)
4. Geological interpretation of the Albany–Fraser Orogen and southeast Yilgarn Craton seismic lines 12GA-AF1, 12GA-AF2, 12GA-AF3, 12GA-T1

Acquisition and processing of the 2012 Albany–Fraser Orogen deep reflection seismic survey

by

RD Costelloe[1], J Holzschuh[1], and T Fomin[1]

Introduction

Geoscience Australia (GA), in collaboration with the Geological Survey of Western Australia (GSWA) and the Tropicana Joint Venture, comprising AngloGold Ashanti Australia Ltd and the Independence Group NL, contracted Terrex Seismic to collect the Albany–Fraser Orogen seismic survey from 23 April to 5 June 2012. The survey consisted of four lines, 12GA-AF1, 12GA-AF2, 12GA-AF3 and 12GA-T1. The lines were located on local roads and along the Trans-Australian Railway access road. Figure 1 shows the location of the lines. The survey was designed as a transect across the Albany–Fraser zone in Western Australia and to image the relationship between the Yilgarn Craton to the west, the Albany–Fraser Orogen in the centre, and the Madura Province beneath the Eucla Basin to the east. A total of 671.9 km of deep crustal seismic data was collected.

Acquisition of the reflection seismic data

Logistics of the seismic survey

Acquisition of the reflection seismic data commenced on 23 April 2012 at the western end of line 12GA-AF2 (AF2). AF2 was completed on 2 May 2012 about 25 km northeast of Esperance covering 158.4 km. Line 12GA-AF1 (AF1) then commenced from the west on Fisheries Road, about 15 km northeast of Esperance. AF1 was collected up to the boundary with the Cape Arid National Park and was completed on 10 May 2012, covering 114.06 km. The crew then mobilized on 11 May 2012 to the western end of line 12GA-AF3 (AF3) about 130 km to the east of Kalgoorlie on the Trans-Australian Railway access road. Recording continued until 27 May 2012 when the line was finished near Haig. AF3 covered 319.12 km in total. Two days of testing commenced and the camp was moved to the Tropicana site to the north. Acquisition of line 12GA-T1 (T1) commenced on 1 June 2012 from the north and was completed on 5 June 2012, covering a total of 80.32 km. The average production for the whole survey was about 17 km per day.

The data acquisition crew was accommodated in a mobile trailer camp which contained all accommodation, kitchen, dining, laundry, workshop and office facilities. The data acquisition proceeded with the crew operating along the verges of the shire roads for lines AF1 and AF2. The railway access road provided good access for the vibrators and crew vehicles and for the camp trailers for line AF3. T1 was located along a narrow track leading to the Plumridge Lakes Nature Reserve and some minor vegetation clearing had to be done to allow access to crew heavy vehicles. As the crew was operating along public roads, a traffic management firm was contracted to provide signage of traffic hazards and to manage seismic crew and public traffic around the back and front crews and the vibrators.

Recording parameters

Table 1 shows the recording parameters that were used for the acquisition of the Albany–Fraser Orogen seismic survey. The parameters were chosen based on previous deep seismic data collection experience and on sweep frequency parameter testing, which was completed before the start of the survey. A set of tests was designed for the Eucla Basin section of line AF3, and is described in a later section.

The seismic data were recorded using an active spread of 300 channels, spread over 12 km. SM24 10 Hz geophones were used in the receiver array, with 12 geophones per station. The 12 geophones were evenly spread over the 40 m station, with approximately 3.3 m between geophones, with arrays centred on the surveyed peg locations. The geophone array was designed to have some effect in attenuating surface wave noise (Pritchett, 1990), and to be easily deployed in the field. Each geophone string of 12 consisted of two sets of six series-connected geophones, the two strings connected in parallel.

1 Minerals and Natural Hazards Division, Geoscience Australia, GPO Box 378, Canberra ACT 2601

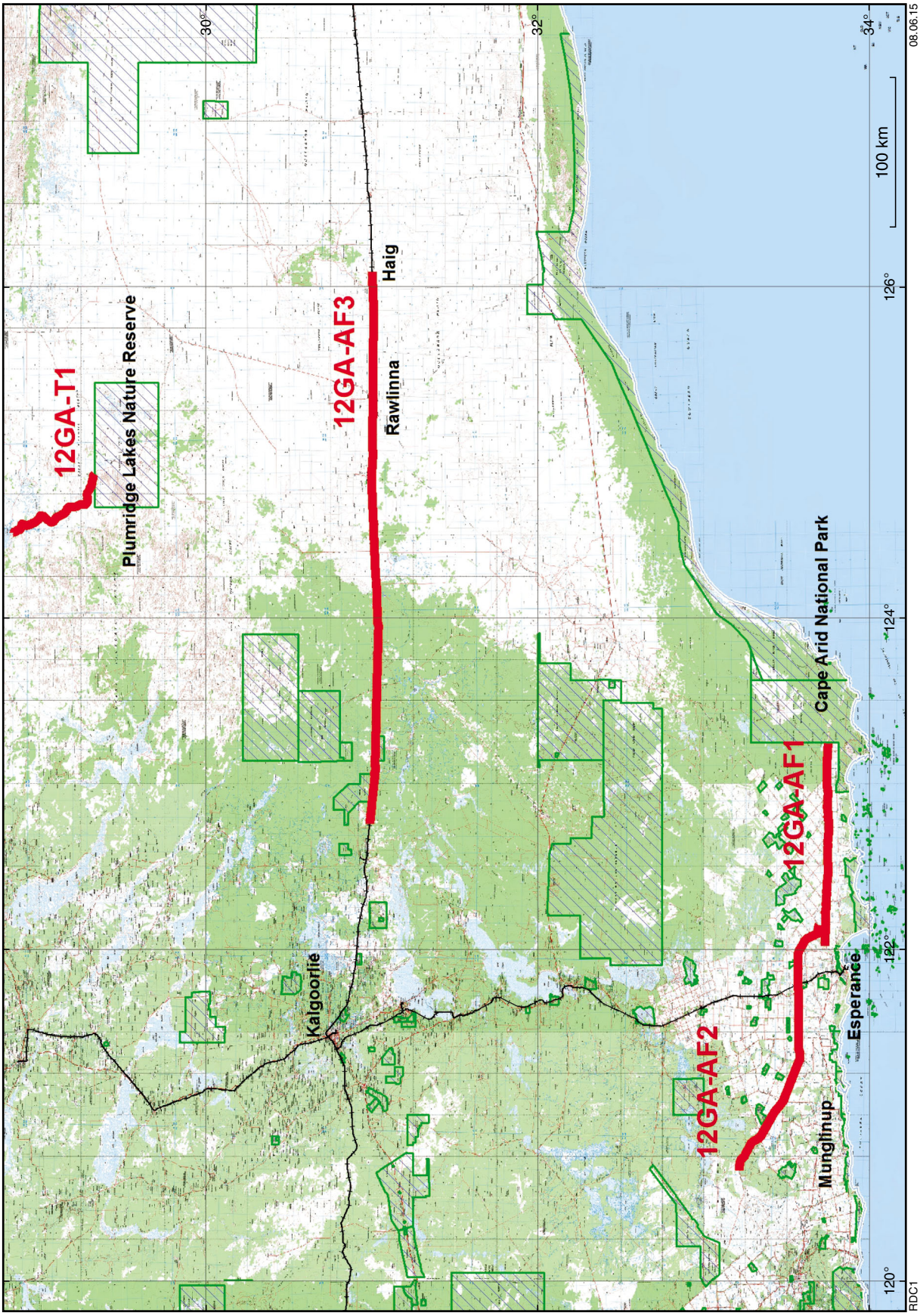

Figure 1. Location of the Albany–Fraser seismic lines

The source array, consisting of three AHV-IV Hemi-50 vibrators, was located at the centre of the 12 km spread, giving a maximum source-to-receiver offset of 6 km. The vibrators were spaced with the pads 15 m apart. The vibrators moved up 15 m between sweeps so that the trailing vibrators moved to the locations previously occupied by the vibrator in front of it. Three sweeps were recorded for each vibration point (VP), with each sweep individually cross-correlated with its reference sweep and all three cross-correlated records stacked together to produce the SEG-D shot record for each VP. Each sweep ranged over a different frequency range as shown in Table 1. The three sweeps together gave a weighted array covering 60 m per VP. The array helped to reduce source-generated surface wave noise in the in-line direction. VPs were spaced every second station, 80 m apart, and the centre of the vibrator array was located midway between survey stations.

Table 1. Data acquisition parameters

Source	3 IVI Hemi-50 vibrators
Source array	15 m pad to pad, 15 m moveup
Sweep length	3 x 12 s
Sweep frequency	6–64 Hz, 10–96 Hz, 8–80 Hz
Vibration point (VP) interval	80 m
Receiver group	12 geophones @ 3.3 m spacing
Group interval	40 m
Number of recorded channels	300
Nominal fold	75
Recording instrument	Sercel 428XL
Record length	20 s
Sampling interval	2 ms

Field QC and data management

The seismic data were recorded to disk in SEG-D demultiplexed format using a Sercel 428XL recording system, and then transferred each day to the on-site geophysicist via a USB memory stick. The data were recorded at 2 ms sampling rate with no low-cut filter and a 0.8 Nyquist frequency (200 Hz) high-cut filter. The sweeps were 12 s duration, with 20 s listening time, resulting in 20 s stacked correlated records. At the end of each day's recording, a laptop running Paradigm DISCO/ Focus software on Red Hat Enterprise was used to run a processing sequence to view the shot data and create brute stacks for quality control of the data. At the end of each line, two identical LTO data tapes (A and B) were created containing all the SEG-D data for that line. Each SEG-D stacked correlated record was 11.5 MB in size, and total data volume of 93.8 GB was recorded for the survey.

Processing of the reflection seismic data

Hardware and software

The reflection seismic data were processed by the Onshore Seismic and Magnetotelluric Section of GA in Canberra. The data were initially processed using Paradigm DISCO/ Focus software on a Red Hat Enterprise Linux Sun Fire X4600 M2 server, with the final processing steps and archiving of the data done on the replacement server for the X4600, an HP DL585 server running Paradigm Echos software on Red Hat Enterprise Linux.

Table 2. Final processing sequence

Crooked line geometry
SEG-D to DISCO format conversion
Inner trace edits
Notch filter
Common midpoint sort
Gain recovery
Spectral equalization
Floating datum residual refraction statics
Velocity analysis
Residual statics
NMO and stretch mute
Bandpass filter
Velocity analysis
Offset regularization and DMO
Common midpoint stack
Post-stack time migration
Coherency enhancement
Mean datum statics
Trace amplitude scaling

Processing overview

Standard deep crustal seismic processing procedures were used as summarized in Table 2 and briefly explained in the following sections.

Crooked-line geometry

This initial process defined the acquisition geometry of each line. The roads along which the survey was conducted were not straight, so crooked-line geometry was defined for each line. For this 2D survey, the bends in the lines can affect the resulting image. At sharp bends in the lines there is likely to be smearing and poor resolution of shallow data.

Also, deeper dipping structures may not image correctly, depending on the relative directions of the line and the dip of the structures. Line T1 had the most significant bends and so was most affected by these imaging issues.

SEG-D to DISCO format conversion

The field data were recorded in SEG-D Revision 1 format. The data were loaded into the processing system from the LTO tapes and converted into the internal DISCO format for processing.

Trace edits

The inner two traces nearest to the vibrators (trace 150 and 151) were omitted from the processing as the source array actually extended across them creating significant early time noise.

Notch filter

A 50 Hz notch filter was applied to selected traces of some shots on lines AF1 and AF2 where the data were significantly affected by powerline interference.

Common depth point sort

The shot data were sorted into common depth point (CDP) bins, which had been defined in the crooked-line geometry process. The CDP bins were defined at 20 m intervals based on the source-receiver midpoint locations. A line of best fit through those midpoints, called the CDP line, was generated and which differs from the surveyed station line. All traces from any shots which had source-receiver midpoints that fell within the predefined CDP location bins, were gathered into the same CDP bin along the previously defined crooked-line geometry.

Gain recovery

A time-variant gain was applied to the data to account for the spherical divergence of the seismic energy as it propagated from the source.

Spectral equalization

Spectral equalization was used to attenuate source generated and random noise, especially ground-roll, relative to the higher frequencies of the sweep signal.

Floating datum refraction statics

Refraction static corrections (time shifts) were applied to the traces to compensate for the time variations caused by varying topography and near-surface regolith thickness and velocity. These near-surface low velocity layers can cause differing delays to the reflection signal which, if not corrected, can degrade the stack (Cox, 1999). Refraction statics were also applied to set the reference datum level of the seismic data to a specified elevation. For the lines in this survey, a datum of 400 m AHD was used, so zero time on the final data corresponds to 400 m AHD. Refraction statics were calculated based on picking first breaks on shot records, and the long wavelength average statics subtracted, to leave residual refraction statics on a floating datum, which at this stage of the processing left the data essentially surface referenced. The method of calculating the statics is based on the works of Taner et al. (1988).

Velocity analysis

First-pass velocity analyses were done at regular intervals along the lines, using coherency plots and/or constant velocity stacks.

Residual statics

Residual statics were calculated and applied. Residual statics make small adjustments to the refraction statics based on cross-correlating traces within CDP gathered in a selected time gate, to maximize the correlation to further improve the stack response.

Normal moveout and stretch mute

Normal moveout (NMO) corrections were applied based on the first-pass velocity analyses. NMO is required because each CDP gather contains traces with differing source to receiver offsets. Delays resulting from the differing offsets, and therefore differing raypaths of the seismic signal, are compensated for by the NMO correction. Muting of the early time (less than 1 s) data is required as the NMO process significantly stretches the far offset data.

Bandpass filter

A bandpass filter was applied to the data to remove noise outside the seismic sweep signal frequency band.

Offset regularization and dip moveout

Offset regularization and dip moveout (DMO) (Deregowski and Rocca, 1981) were applied to enable dipping and flat reflections to stack with the same NMO correction. DMO shifts reflections both within and between CDP gathers based on apparent dip of coherent events.

Velocity analysis

A second pass of velocity analysis was to pick appropriate velocity field to stack the DMO data.

NMO and stretch mute

NMO corrections were applied to the DMO corrected gathers based on the DMO velocity analyses.

Common midpoint stack

The stack process sums the NMO/DMO corrected data for each CDP gather at each time sample. The signal to random noise ratio is improved by the square root of the number of traces stacked (fold). The Albany–Fraser Orogen data were stacked to a nominal fold of 75 traces per CDP, giving a theoretical signal-to-noise ratio improvement of 8.7.

Post-stack time migration

Migration is the final imaging process and moves data to its correct spatial location based on dip. Dipping reflections visible on the stack move up dip and become steeper and shorter. Diffractions visible on the stack should collapse to a small region on the migration. Figure 2 displays a small section of line AF2, which shows high reflectivity in the upper crust. The upper panel is the stacked section and the lower panel is the migrated section. The display shows how migration has collapsed a large diffraction and has moved linear dipping reflections from their pre-migration locations on the stack section to their true locations on the migrated section.

Time migration methods were applied to the stacked data using a smoothed velocity model derived from the stacking velocities. Two different algorithms were used: omega-x finite difference migration; and Kirchhoff migration. Both algorithms are described in Yilmaz (2001).

Coherency enhancement

Coherency enhancement was applied to enhance data satisfying continuity over several traces and within specified dip limits.

Mean datum statics

The average refraction statics were applied to the data, shifting it from surface reference to the datum of 400 m AHD.

Trace amplitude scaling

A final automatic gain control scaling was applied to the data for display to equalize the displayed amplitudes of the data.

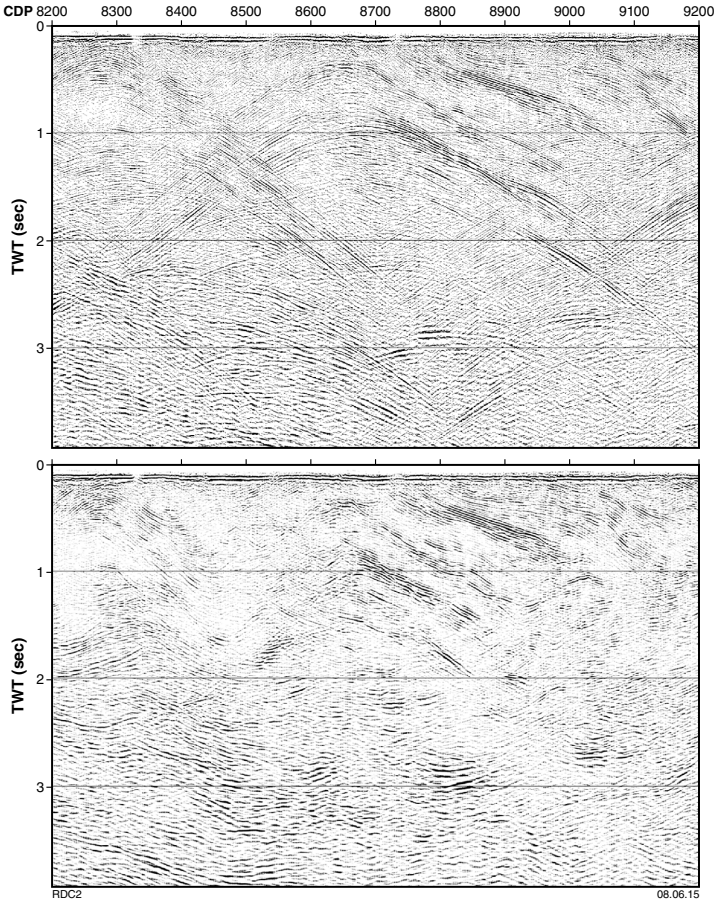

Figure 2. Stack (upper) and migration (lower) of a small section of line 12GA-AF2

Testing program

A review of previous surveys over the Eucla Basin was made during design of the survey, as the effectiveness of the standard source and recording parameters were unknown in the carbonate terrain of the Eucla Basin which would be encountered when recording line AF3. A testing program was designed, to be implemented on line AF3, once there was a noticeable degradation of data quality being collected using the standard parameters. Previous surveys over other areas of the Eucla Basin had resulted in poor imaging using the seismic method (Leven and Barton, 1991). As part of the testing program, 4.5 Hz geophone strings (enough for 150 channels of 12 per channel) were used to compare the data quality obtained with that obtained using the standard 10 Hz geophones. Increased bandwidth, especially in the low frequencies, was expected to improve the data interpretability where there was significant scattering of energy, as was expected in the karst limestone areas of the Eucla Basin. Previous seismic acquisition programs have been unable to record interpretable seismic data in areas of surface limestones (Wei and Hall, 2011). Data for line AF3 were recorded to the end of the planned line using the standard parameters, as the data quality remained acceptable. After production was completed on the line, some testing was done using the 4.5 Hz geophones in a parallel spread to the production spread, using various sweep parameters, as shown in Table 3.

The testing program included two basic changes to the normal acquisition parameters; a comparison of 4.5 Hz geophones to the 10 Hz geophones, and a comparison of low frequency, non-linear sweeps against higher frequency linear sweeps. Both changes were aimed at acquiring more low frequency signal in the data.

A parallel spread of 150 channels of 4.5 Hz geophones was laid on the southern side of the track being used as the seismic line, with the 10 Hz spread on the northern side, so that 150 channels of data with 10 Hz geophones and 150 channels of data with 4.5 Hz geophones were simultaneously recorded. Table 3 shows the acquisition parameters of the testing program that was conducted.

Table 3. Test sweep parameters

Test	*VP range*	*Sweep type*	*Frequency range*
1	10675.5	Linear	3–48 Hz
	10910.5		3–24 Hz
			3–16 Hz
2	10824.5	Linear	3–64 Hz
	10848.5		10–96 Hz
			8–80 Hz
3	10824.5	Non-linear 9 dB/Oct	3–48 Hz
	10844.5		3–24 Hz
			3–16 Hz
4	10824.5	Non-linear 9 dB/Oct	3–64 Hz
	10833.5		10–96 Hz
			8–80 Hz

The section of line common to all tests lies from station 10674 to station 10984, with a maximum of 10 fold. Each sweep was correlated and stored as a separate record. For the experimental VPs, the vibrators did not move up between sweeps but vibrated all three sweeps from the centre position of the array.

Results of the testing program

Generally, the linear sweeps show better data quality than the non-linear sweeps, and the 10 Hz geophones show a similar response to the 4.5 Hz geophones. The wider bandwidth sweeps (Table 3, tests 2 and 4) also show improved data quality compared to the lower frequency sweeps (Table 3, tests 1 and 3). The tests confirm what was observed during production on AF3, i.e. that the original acquisition parameters are effective in imaging through the limestones of the Eucla Basin in this area, and are as good as or better than the other tested parameters.

Data archiving

The final processed data were converted to SEG-Y format, with the SEG-Y trace headers loaded with correct metadata. The SEG-Y EBCDIC headers contain a summary of the acquisition and processing parameters used. Images of the final stack and migrated data were created from the final SEG-Y data at 1:100 000 scale for the full 20 s, and 1:50 000 scale for the top 8 s of data. The final processed data, metadata and images for this survey are available for download from the GA website at <www.ga.gov.au/minerals/projects/current-projects/seismic-acquisition-processing.html>.

References

Cox, M 1999, Static Corrections for Seismic Reflection Surveys. Tulsa, Oklahoma: Society of Exploration Geophysicists.

Deregowski, SM and Rocca, F 1981, Geometrical Optics and Wave Theory of Constant Offset Sections in Layered Media: Geophysical Prospecting, v. 29, p. 374–406.

Leven, J and Barton, T 1991, Seismic Field Trials on the Nullarbor Plain, South Australia: BMR Record 1991/87.

Pritchett, WC 1990, Acquiring Better Seismic Data, New York: Chapman and Hall.

Taner, MT, Lu, L, and Baysal, E 1988, Unified method for 2-D and 3-D refraction statics with first break picking by supervised learning: 58th Annual International Meeting, Society of Exploration Geophysicists, Expanded Abstracts, p. 772–774. Tulsa, Oklahoma: Society of Exploration Geophysicists.

Wei, Z, and Hall, MA 2011, Analyses of vibrator and geophone behaviour on hard and soft ground: The Leading Edge, v. 30, p. 132–137.

Yilmaz, O 2001, Seismic Data Analysis, Tulsa, Oklahoma: Society of Exploration Geophysicists.

A magnetotelluric survey across the Albany–Fraser Orogen and adjacent Yilgarn Craton, southwestern Australia

by

J Spratt[1], M Dentith[2], S Evans[3], CV Spaggiari, K Gessner, and IM Tyler

Introduction

Magnetotelluric soundings at 163 locations across the Albany–Fraser Orogen, southwestern Australia, have provided 2D conductivity models of the crust and uppermost lithospheric mantle beneath four regional transects. Figure 1 shows the locations of stations on regional potential field datasets, and the major tectonic zones.

Magnetotellurics (MT) is an electromagnetic geophysical method that involves measuring and relating natural time-varying electric and magnetic fields, induced by the interaction between the Earth's geomagnetic field and solar winds and by worldwide thunderstorms, in order to resolve the electrical conductivity structure of the subsurface of the Earth. The relationship between these horizontal and mutually perpendicular fields recorded at each station provides amplitude (apparent resistivity) and phase lags as a function of frequency (or period, the inverse of frequency), commonly referred to as MT response curves. With increasing depth there is an exponential decrease in the amplitudes of the electromagnetic fields, the so-called skin-depth phenomenon. As the depth of penetration — or skin depth — of these fields is directly related to frequency (the lower the frequency, the greater the depth) and the resistivity of the material (the greater the resistivity, the greater the depth), estimates of resistivity versus depth can be made beneath each site.

Data acquisition and processing

The MT data were collected by Moombarriga Geoscience over four deployments during the period 24 April 2012 to 12 April 2013. Data were acquired at 5–10 km station spacing along roads with station tracks providing information along four main MT profiles: AF3 (same location as seismic line 12GA-AF3); CUN; FR; YFB (Fig.1). Time series data were recorded for an average of 40 hours at each site in an effort to resolve apparent resistivity and phase to a period of 1000 s. In addition, time-domain electromagnetic soundings were made at each MT station comprising the traverses to quantify static shift.

Two horizontal components of the electric field (Ex and Ey) and three components of the magnetic field variation (Hx, Hy, and Hz) were measured at each site except at sites where the vertical (Hz) component was omitted because of difficult site conditions. Electric dipoles and horizontal coils were installed in magnetic north–south and east–west azimuths and the electric dipoles at all sites were approximately 100 m in length. The electric field was measured using non-polarizing (Pb/PbCl2 solution) electrodes. Electromagnetic soundings of the near surface at each station were made using a Zonge ZT20 transmitter and SmarTEM24 receiver with a three-component RVR. A 100 m-sided square transmitter loop (Tx area = 10 000 m^2) was used with sides oriented north–south and east–west. The receiver coil had an effective area of 10 000 m^2.

The MT data were processed using modern, robust, remote-referencing techniques. Prior to 2D modelling, MT data are typically analysed to determine the regional geoelectric strike direction as well as the degree of dimensionality in order to generate an accurate representation of a 2D Earth. For a 1D Earth the conductivity structure is layered and independent of the geoelectric strike direction. Within a 2D Earth model conductivity structure varies laterally so that the apparent resistivity is different along and across geological, or more correctly geoelectrical strike, therefore apparent resistivities and phases need to be calculated in both directions (or modes). The transverse-electric (TE) mode describes current flowing parallel to geoelectric strike and is predominantly sensitive to current concentration and flow patterns. The transverse-magnetic (TM) mode describes current flow perpendicular to strike and is more sensitive to charges induced on lateral boundaries. Dimensionality and geoelectric strike analysis on these data reveal variable strike directions both laterally and with depth, highlighting the need for regional 3D inversions.

1 Independent consultant, Wakefield, Quebec, Canada

2 Centre for Exploration Targeting, The University of Western Australia

3 Moombarriga Geoscience, Perth, Western Australia

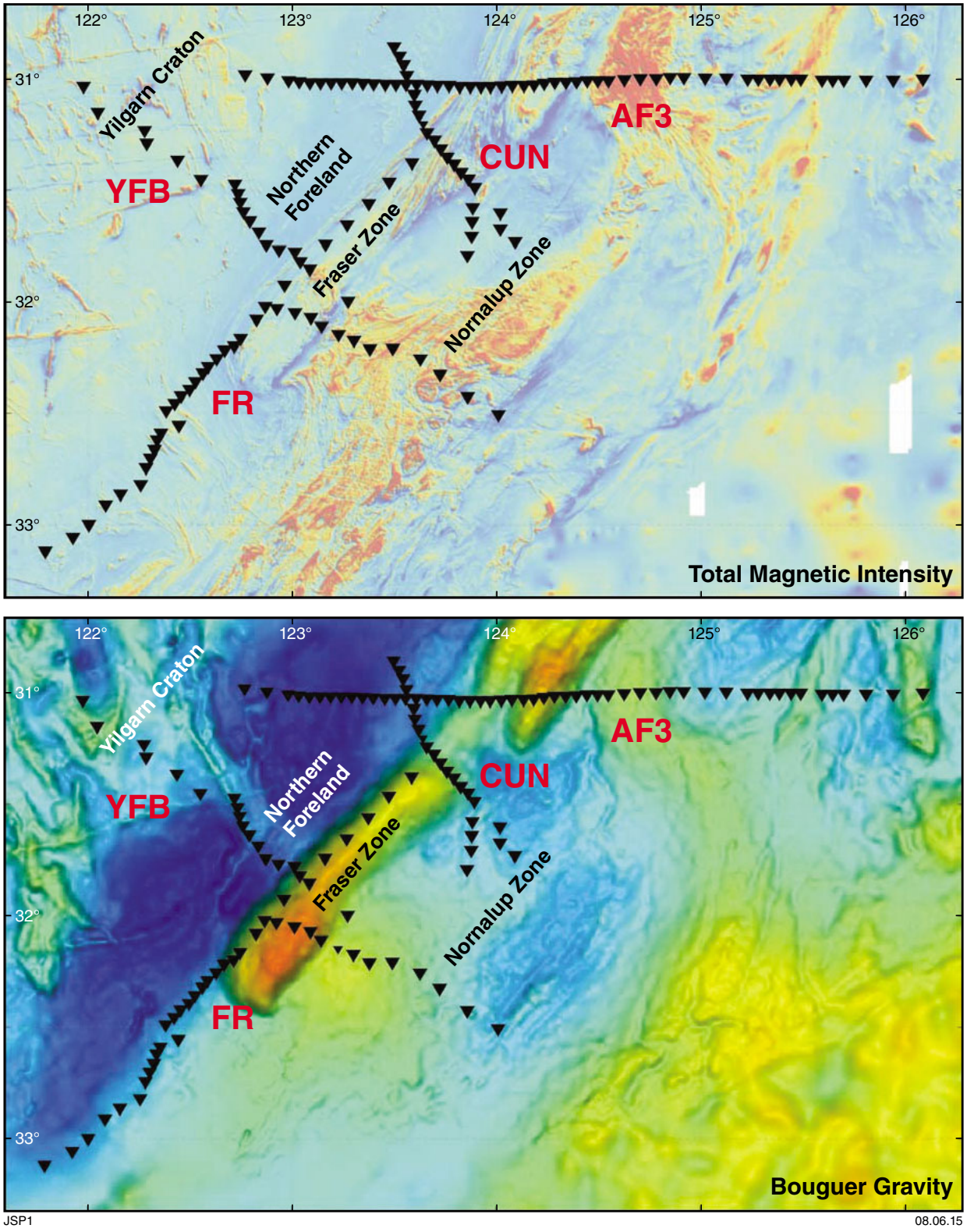

Figure 1. **Regional potential field maps showing the locations of the MT stations and modelled profiles**

The WinGlink™ interpretation software package, which implements the inversion algorithm of Rodi and Mackie (2001), was used to generate 2D models along the profiles. Inversions were executed from the MT responses recalculated at the appropriate geoelectric strike direction(s). The inversion program searches for the smoothest, best-fit model with the least deviation from the starting model (Mackie and Madden, 1993). The models derived, therefore, represent the minimum structure required to fit the data with an acceptable misfit.

Models were generated along each profile using different components of the data, with and without the inclusion of data deemed 3D, and at differing strike angles in order to assess the change in the observed conductivity structure and resolve features that are robust in the data. A uniform grid Laplacian operator and tau value of 3 were applied. The preferred models for each profile were generated with data presumed to be affected by 3D distortion removed, have structure that appears to be robust between inversions using different data components and modelling parameters, and have the lowest overall RMS value. The reliability of conductivity variations in the models was tested with feature testing. This involves ascertaining whether the variation has a significant effect on the fit of the modelled data and hence whether it is a required component of the model.

Interpretations and discussion

The results from 2D modelling are shown in Figure 2. Preliminary interpretation suggests:

- The Yilgarn Craton beneath the northwestern extent of the YFB profile shows anomalously low resistivities within the upper crust, compared to the high resistivities typically imaged beneath stable Archean cratons. These low resistivities may be the result of graphite or sulfide mineralization along fault planes or within metasedimentary units in greenstone belts (e.g. black shales in the Black Flag Group).

- In general, the Albany–Fraser Orogen has high crustal resistivities, with values >10 000 ohm.m, that are cut by steeply dipping or near-vertical, less resistive zones. The high resistivities are consistent with felsic granites and granulite-grade metamorphic assemblages.

- Several of the less resistive, steeply dipping or near-vertical structures show an excellent correlation with the location of known faults. These structures are not highly conductive as they are still within the range typical of crystalline rocks, with values greater than 2000 ohm.m, and are visible by MT methods due to the extremely resistive nature of the host rock. This suggests that the fault zones are dry with minimal mineralization along the fault plane. Most of the faults are shown to extend to lower crustal depths, and some may extend deeper; however, the presence of a lower crustal conductor masks their response.

- The Cundeelee Fault is imaged in profiles AF3 and YFB, and is shown to extend to at least 25 km depth. This contrasts with the interpreted flattening of the Cundeelee Fault at 4.3 s two-way time (TWT) in the seismic data, which equates to approximately 13 km (Spaggiari et al., 2014). However, the electrical structure suggests that the Cundeelee Fault does not correspond with the northwestern edge of the Northern Foreland. Although the Cundeelee Fault is currently defined to mark the boundary between the Northern Foreland and the Yilgarn Craton in this region, the boundary is in fact transitional, as the Northern Foreland represents reworked Yilgarn Craton, and is defined by a difference in strain, and locally, metamorphic grade (Spaggiari et al., 2011). Therefore, the MT data (and also the seismic data along 12GA-AF3, Plate 4), indicate that the effect of reworking on the Yilgarn Craton extends much further northwest than previously recognized. This is consistent with a northeast trending series of long wavelength, low anomalies in regional gravity data (Fig. 1) that correlate well with the MT data. Therefore, in this region, the boundary of the Northern Foreland should perhaps be considered to be further to the northwest.

- Along the FR and AF3 profiles, the Fraser Shear Zone appears to mark the northeastern (FR) and southwestern (AF3) edge of an ~25 km wide, low resistivity zone, which is likely due to the juxtaposition of lower resistivity rocks with high resistivity rocks of the Fraser Zone.

- Although the cause remains uncertain, MT studies worldwide have revealed much of the lower continental crust to exhibit relatively uniform reduced resistivities, typically 10–100 times less resistive than middle to upper crustal values. The enhanced conductivity within the crust of the Yilgarn Craton inhibits the MT data from imaging the base of the crust and model resolution is poor at 40–60 km beneath the northwestern-most extent of the YFB profile. Moderately low resistivities are observed at lower crustal depths beneath each of the four profiles impeding accurate estimates for the electric Moho depth at these locations. However, along parts of the AF3 and CUN profiles an increase in resistivity is observed between 35–40 km, which is consistent with seismic crustal thickness estimates (Kennett, 2014; Korsch et al., 2014).

- In general, where the models are found to be reliable, high mantle resistivities are imaged beneath the Yilgarn Craton. This is consistent with old colder stable lithoshere beneath the Archean Yilgarn Craton that is juxtaposed against juvenile, more fertile Paleoproterozoic upper mantle beneath the orogenic belt.

- The complex tectonic history of the Albany–Fraser Orogen has resulted in a deep electrical structure that is largely 3D. 2D models of the deep structure are, therefore, unreliable with large differences in models derived at differing geoelectric strike angles.

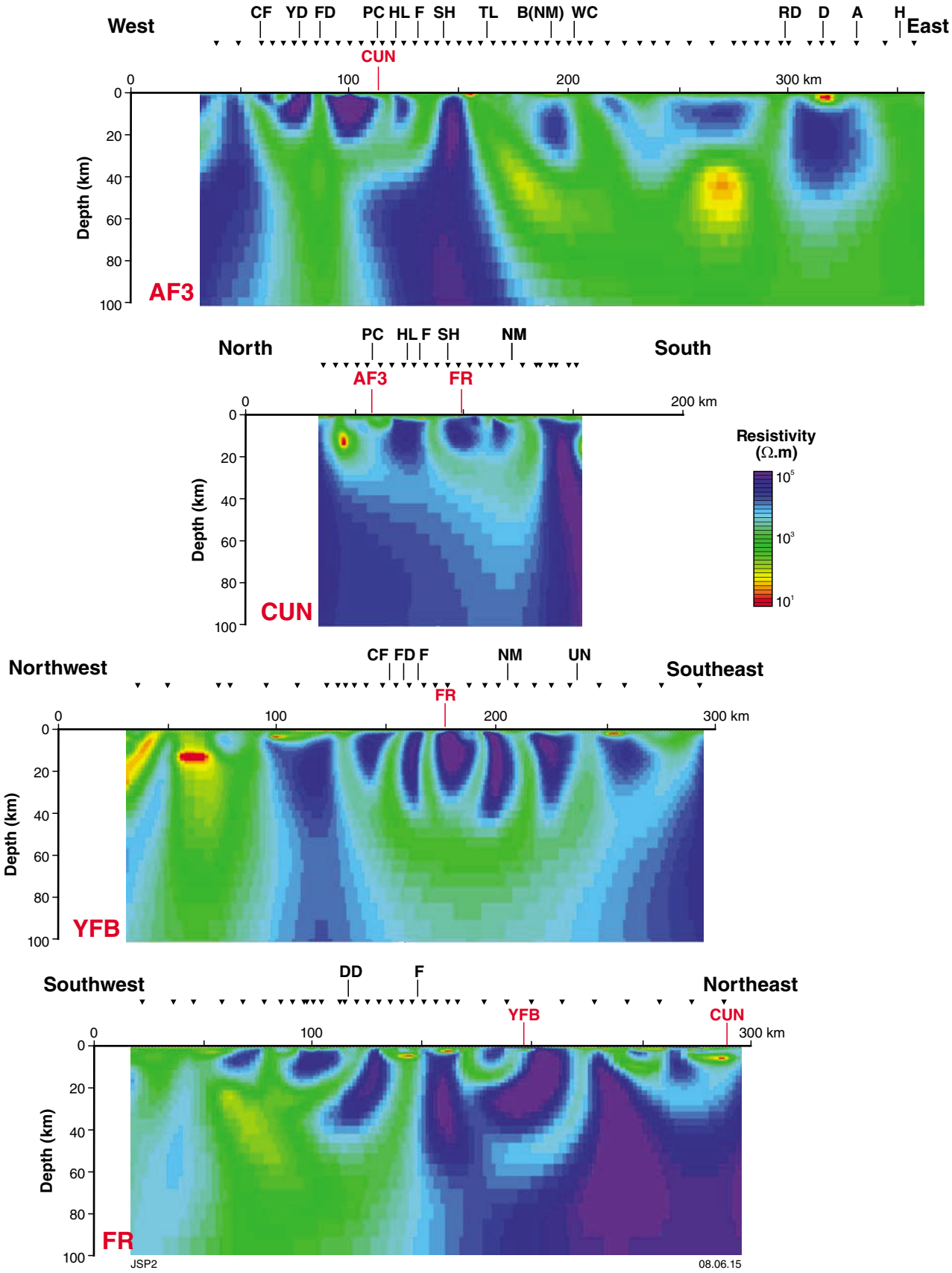

Figure 2. **Resistivity cross-sections. See Figure 1 for locations. Various major faults and shear zones are labelled: A – Anniversary; B – Boonderoo; CF – Cundeelee; D – Diesel; DD – Dundas; F – Fraser; FD – Frog Dam; H – Honeymoon; HL – Harris Lake; NM – Newman; PC – Ponton Creek; RD – Rodona; SH – Spy Hill; TL – Transline; UN – unnamed; WC – Woodcutters; YD – Yellow Dam.**

References

Kennett, BLN 2014, The nature of the lithosphere in the vicinity of the Albany–Fraser seismic lines, *in* Albany–Fraser Orogen seismic and magnetotelluric (MT) workshop 2014: extended abstracts *compiled by* CV Spaggiari and IM Tyler: Geological Survey of Western Australia, Record 2014/6, p. 135–141.

Korsch, RJ, Spaggiari, CV, Occhipinti, SA, Doublier, MP, Clark, DJ, Dentith, MC, Doyle, MG, Kennett, BLN, Gessner, K, Neumann, NL, Belousova, EA, Tyler, IM, Costelloe, RD, Fomin, T and Holzschuh, J 2014, Geodynamic implications of the 2012 Albany–Fraser deep seismic reflection survey: a transect from the Yilgarn Craton across the Albany–Fraser Orogen to the Madura Province, *in* Albany–Fraser Orogen seismic and magnetotelluric (MT) workshop 2014: extended abstracts *compiled by* CV Spaggiari and IM Tyler: Geological Survey of Western Australia, Record 2014/6, p. 142–173.

Mackie, RL and Madden, TR 1993, Three dimensional magnetotelluric inversion using conjugate gradients: Geophysical Journal international, v. 115, p. 215–229.

Rodi, W and Mackie, RL 2001, Nonlinear conjugate gradients algorithm for 2D magnetotelluric inversion: Geophysics, v. 66, p. 174–187.

Spaggiari, CV, Kirkland, CL, Pawley, MJ, Smithies, RH, Wingate, MTD, Doyle, MG, Blenkinsop, TG, Clark, C, Oorschot, CW, Fox, LJ and Savage, J 2011, The geology of the east Albany–Fraser Orogen — a field guide: Geological Survey of Western Australia, Record 2011/23, 97p.

Spaggiari, CV, Occhipinti, SA, Korsch, RJ, Doublier, MP, Clark, DJ, Dentith, MC, Gessner, K, Doyle, MG, Tyler, IM, Kennett, BLN, Costelloe, RD, Fomin, T and Holzschuh, J 2014b, Interpretation of Albany–Fraser seismic lines 12GA-AF1, 12GA-AF2 and 12GA-AF3: implications for crustal architecture, *in* Albany–Fraser Orogen seismic and magnetotelluric (MT) workshop 2014: extended abstracts *compiled by* CV Spaggiari and IM Tyler: Geological Survey of Western Australia, Record 2014/6, p. 28–51.

Geological framework of the Albany–Fraser Orogen

by

CV Spaggiari, CL Kirkland, RH Smithies, SA Occhipinti*, and MTD Wingate

Introduction

The margins of the Archean Yilgarn Craton record a long and variable geodynamic history, from at least the latest Neoarchean. These margins are either truncated or reworked, or were formed by a combination of these processes. For example, the western margin of the Yilgarn Craton is truncated by the late Mesoproterozoic to Neoproterozoic Darling Fault Zone, whereas the northern margin of the Yilgarn Craton is truncated by the c. 2000 Ma collision of the Glenburgh Terrane, and also reworked during several episodes of tectonism following that collision (Johnson et al., 2011). While the history of the eastern margin of the Yilgarn Craton is obscure due to thick cover of the Officer Basin, the southern and southeastern margins of the Yilgarn Craton record a long history of reworking, which has become increasingly evident in the Albany–Fraser Orogen. Hence, the Albany–Fraser Orogen not only provides insight into Paleoproterozoic and Mesoproterozoic tectonic events and supercontinent configurations (e.g. Johnson, 2013), but through the analysis of that reworking, provides insight into the history of more distal or previously unrecognized components of the Yilgarn Craton (e.g. Kirkland et al., 2014).

This review summarizes the tectonic framework and history of the Albany–Fraser Orogen to provide context for the various contributions in this volume, including: interpretations of the four deep reflection seismic lines (Spaggiari et al., 2014a; Occhipinti et al., 2014; Korsch et al., 2014); the potential field modelling (Brisbout et al., 2014; Murdie et al., 2014); the geochronology, isotope geology, and geochemistry (Kirkland et al., 2014a; Smithies et al., 2014a); and the mineral systems (Tyler et al., 2014). The interpreted bedrock geology of the eastern part of the central Albany–Fraser Orogen, and the east Albany–Fraser Orogen, is presented in the three plates that accompany this volume. Plate 4 contains cross-sections of the geology in these maps constrained by the interpretations of the seismic data. This review does not attempt to summarize historical work — such material can be found elsewhere (e.g. Spaggiari et al., 2009, 2011).

* AngloGold Ashanti Ltd, Level 13, St Martins Tower, PO Box Z5046, Perth WA 6831

The Albany–Fraser Orogen comprises two main tectonic units that reflect its relationship to the Yilgarn Craton — the Northern Foreland and the Kepa Kurl Booya Province (Figs 1 and 2). The Northern Foreland originated as part of the Archean Yilgarn Craton, and in general overlies the non-reworked part of the craton in various thrust sheets (Plate 4). The Kepa Kurl Booya Province (Spaggiari et al., 2009; 2011) is defined as the crystalline basement of the Albany–Fraser Orogen. It includes four fault-bound geographical and structural zones (Tropicana, Biranup, Fraser, and Nornalup) that contain rocks with variable protolith ages and geological histories (Spaggiari et al., 2009, 2011; Occhipinti et al., 2014; Kirkland et al., 2014). Three sedimentary basins are present: the 1815–1600 Ma Barren Basin; the 1600–1305 Ma Arid Basin; and the 1280–1215 Ma Ragged Basin (Spaggiari et al., 2014b; Waddell, 2014). Within the Biranup Zone and throughout the Nornalup Zone Mesoproterozoic granitic intrusions belong to either the 1330–1280 Ma Recherche Supersuite or to the 1200–1125 Ma Esperance Supersuite, coinciding with Stages I and II of the Albany–Fraser Orogeny, respectively (Fig. 2). A single occurrence of Recherche Supersuite granite occurs in the Northern Foreland near Bald Rock dated at 1299 ± 14 Ma (GSWA 83690, Nelson, 1995). The eastern extent of the Albany–Fraser Orogen coincides with the Rodona Shear Zone, which separates the orogen from the Madura Province (Fig. 1; Plates 2 and 3). These units, and the tectonic events that formed them, are described briefly below, followed by a summary of recently proposed tectonic models (Spaggiari et al., 2014b). Further details and references can be found in Spaggiari et al. (2009, 2011, 2012, 2014b), Kirkland et al. (2011a,b), and Smithies et al. (2013).

Northern Foreland

The Northern Foreland is defined as the portion of the Archean Yilgarn Craton that was intruded by Paleoproterozoic magmatic rocks, and reworked during the Mesoproterozoic Albany–Fraser Orogeny (Fig. 2; Plates 1, 2 and 3). Its position reflects its proximity to the Yilgarn Craton during orogenesis; hence, the term ‘foreland’. It consists of greenschist and amphibolite to granulite facies, Archean gneisses and granites, remnant greenstones, and younger dolerite dykes. The Munglinup

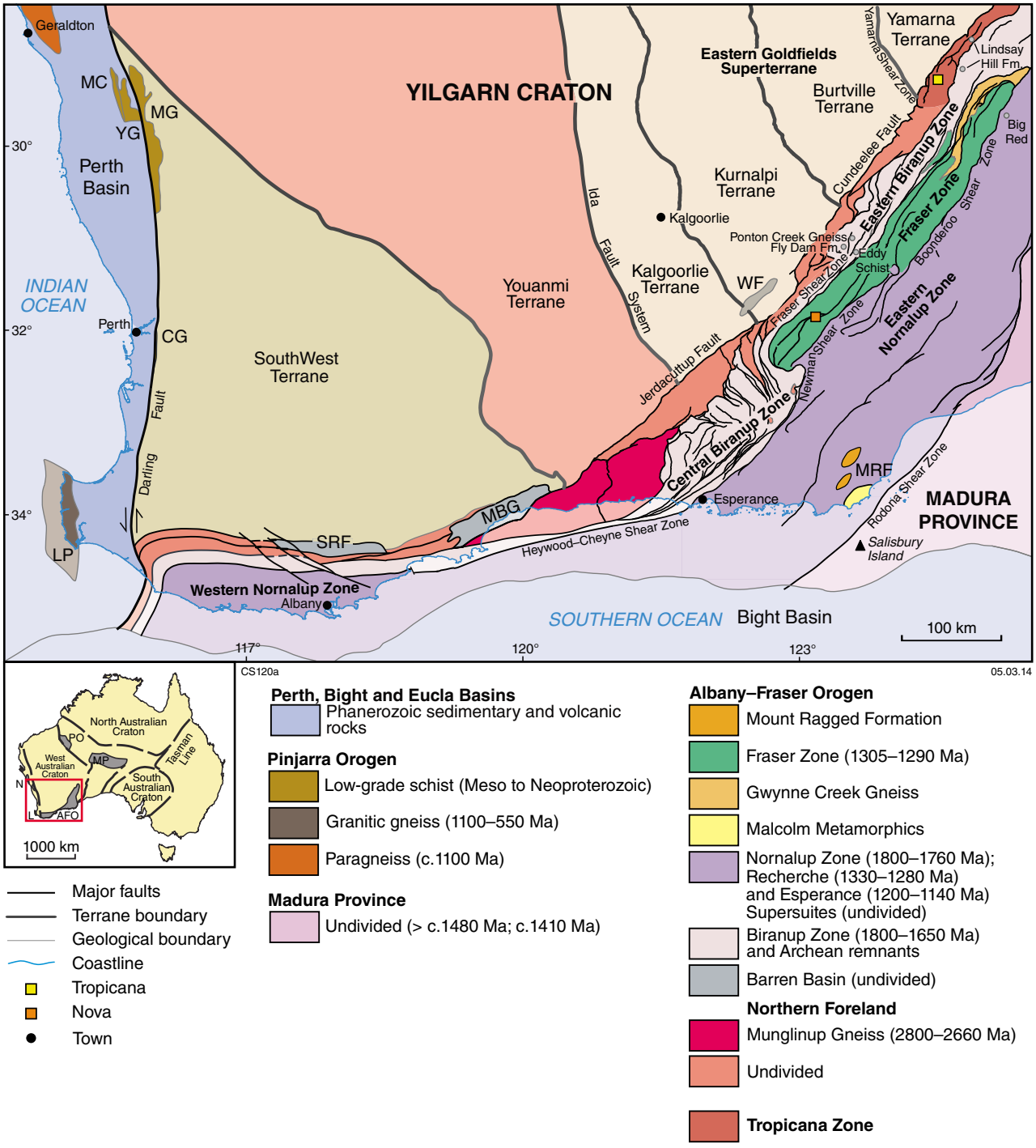

Figure 1. Simplified, pre-Mesozoic interpreted bedrock geology of the Albany–Fraser Orogen and tectonic subdivisions of the Yilgarn Craton (from Spaggiari et al., 2014b). Abbreviations used: SRF – Stirling Range Formation; MBG – Mount Barren Group; WF – Woodline Formation; MRF – Mount Ragged Formation; CG – Cardup Group; LP – Leeuwin Province; MC – Mullingarra Complex; MG – Moora Group. Inset: AFO – Albany–Fraser Orogen; MP – Musgrave Province; PO – Paterson Orogen; L – Leeuwin Province; N – Northhampton Province.

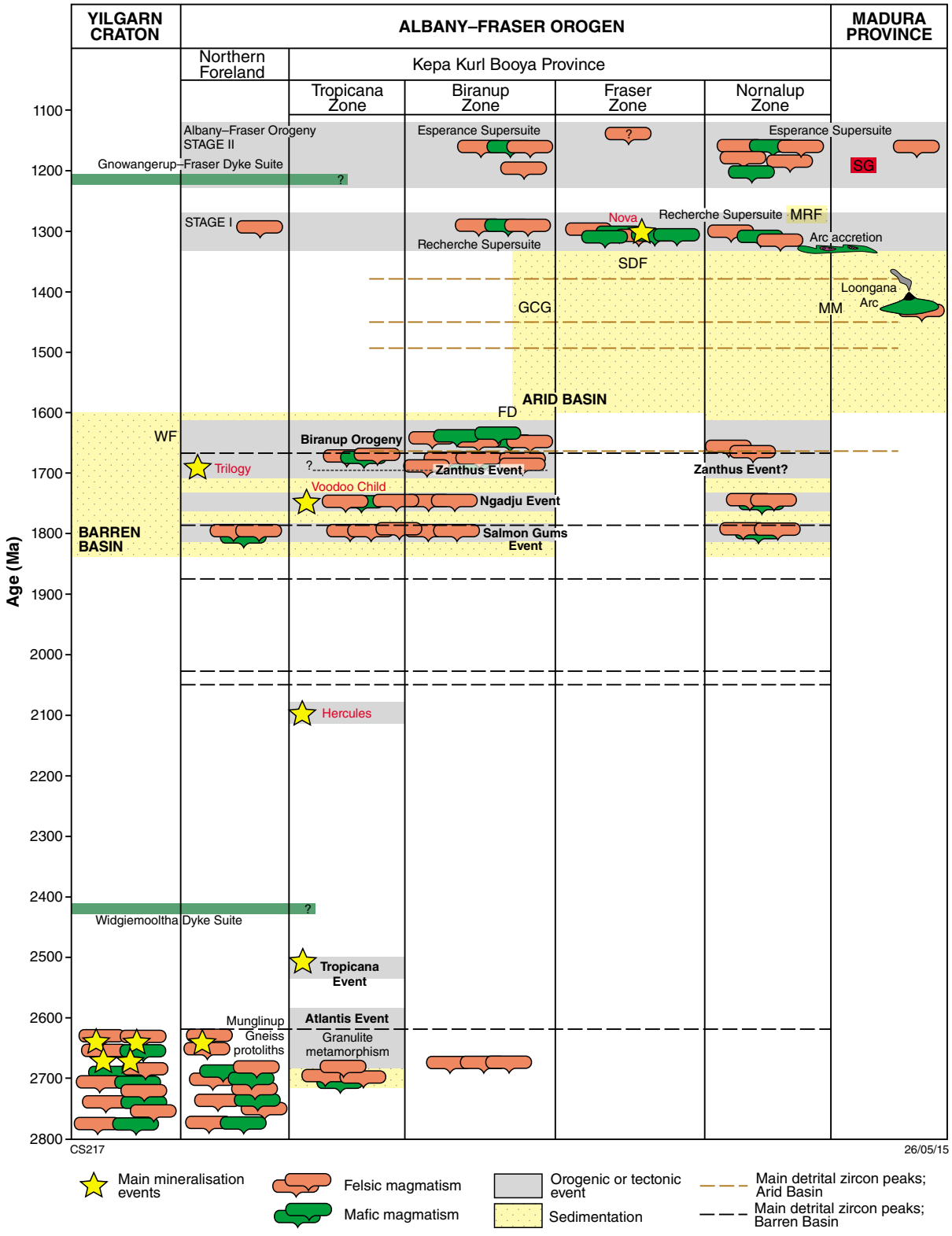

Figure 2. Time–space plot of the Albany–Fraser Orogen and Madura Province. Abbreviations used: FD – Fly Dam Formation; GCG – Gwynne Creek Gneiss; MM – Malcolm Metamorphics; MRF – Mount Ragged Formation; SDF – Snowys Dam Formation; SG – Salisbury Gneiss; WF – Woodline Formation.

Gneiss, with protolith ages of 2717–2640 Ma, is a major component of the Northern Foreland and is preserved in thrust sheets in the central part of the orogen (Plates 3 and 4). It is bounded to the east by the Red Island Shear Zone, which is interpreted as the major boundary between the Munglinup Gneiss (Northern Foreland) and Biranup Zone rocks of the Kepa Kurl Booya Province (Fig. 1; see line 12GA-AF2 on Plate 4). The Munglinup Gneiss comprises amphibolite- to granulite-facies orthogneiss interlayered with lenses of metamorphosed mafic rocks, some of which are interpreted as metamorphosed mafic dykes or sills. Minor banded metachert (jaspilite), amphibolitic schist, serpentinite, and metamorphosed ultramafic rocks are interpreted as remnants of Archean greenstone sequences.

Deformation in the Northern Foreland varied from moderate- to high-strain ductile conditions under amphibolite- to granulite-facies conditions in the Munglinup Gneiss (and the southern part of the Mount Barren Group of the Barren Basin), to low to moderate strain, brittle to semibrittle, under greenschist to amphibolite facies conditions. This variation generally reflects lower strain conditions and lower metamorphic grade with increasing distance towards the craton, as well as the exhumation of different crustal levels. Geochronological data indicate metamorphism and deformation occurred between 1210 and 1180 Ma, during Stage II (1225–1140 Ma) of the Albany–Fraser Orogeny, although early deformation may be as old as Archean. At least three phases of folding are recognized in the Munglinup Gneiss, which is also locally sheared and boudinaged. Megascale fold interference patterns are well defined in aeromagnetic imagery, due to the presence of magnetite in the metamorphic fabrics. The northern limit of the Northern Foreland is defined by the presence of discontinuous and widely spaced shear zones. Mafic dykes in the central Albany–Fraser Orogen also show the effects of increased deformation intensity, from north to south, within the Northern Foreland. In the north, magmatic textures and clear intrusive relationships are preserved, whereas towards the south, the mafic dykes are metamorphosed and rotated parallel to the regional trend of the orogen.

Kepa Kurl Booya Province

Archean to Paleoproterozoic units

Tropicana Zone

The newly named Tropicana Zone (Fig. 2; Plate 1; Occhipinti et al., 2014) contains Archean rocks that have an affinity to the Yilgarn Craton, but their geological evolution is distinct, and cannot be readily correlated with adjacent terranes, such as the adjacent Yamarna Terrane (Occhipinti et al., 2014; Kirkland et al., 2014a). Differences include the presence of c. 2700 Ma sanukitoid granites (Kirkland et al., 2014; Smithies et al., 2014a), and Archean gneisses that underwent upper amphibolite to granulite facies metamorphism over a prolonged period from c. 2718 to 2554 Ma (Kirkland et al., 2014; Doyle et al., 2014). Furthermore, the Tropicana Zone has been emplaced an unknown distance into its current position overlying the Yamarna Terrane of the Yilgarn Craton via the c. 2500 Ma Plumridge Detachment (Plate 4; Occhipinti et al., 2014). It is for this reason that it is not included in the Northern Foreland of the Albany–Fraser Orogen, i.e. because it formed in a different structural position. Hence, the Tropicana Zone is defined as part of the Kepa Kurl Booya Province.

Two units have been defined in the Tropicana Zone: the Tropicana Gneiss and the Hercules Gneiss (Plate 1). The Tropicana Gneiss includes interlayered granitic gneiss that incorporates tonalitic and dioritic compositions, mafic gneiss (including metagabbro and metamorphosed ultramafic rocks), garnet gneiss, and minor metachert and meta-iron formation (see also Spaggiari et al., 2011 and Doyle et al., 2014). Locally, the Tropicana Gneiss is intruded by Paleoproterozoic granite of Biranup Zone affinity (Fig. 2). The Hercules Gneiss is only known from diamond drillcores from the Neale Project area (Atlantis and Hercules prospects), and is dominated by Neoarchean metadiorite and quartz metamonzodiorite gneiss (Kirkland et al., 2014). This gneissic fabric is locally crosscut by microgranite veins dated at 1783 ± 3 Ma (GSWA 192550, Kirkland et al., 2014), and fine- to medium-grained mafic rocks.

The Tropicana Zone shares a similar geological history to the Northern Foreland and Biranup Zone from at least 1800 Ma, with deposition of Barren Basin sediments (Lindsay Hill Formation), and intrusion of Paleoproterozoic granitic rocks such as the c. 1800 Ma Black Dragon Gneiss, the c. 1763 Ma McKay Creek Metasyenogranite (associated with the Voodoo Child Formation), the c. 1710 Ma Bobbie Point Metasyenogranite, and most likely 1690–1670 Ma metagranitic and metagabbroic rocks similar to those dated in the adjacent Pleiades Lakes area of the Biranup Zone (Fig. 2; Plate 1; Spaggiari et al., 2011; Occhipinti et al., 2014).

Biranup and Nornalup zones

The Biranup Zone is dominated by strongly deformed orthogneiss, with lesser amounts of metagabbroic and hybrid rocks that range in age from 1810 to 1625 Ma, and which flank the entire southern and southeastern margin of the Yilgarn Craton (Figs 1 and 2). Isolated remnants of Archean granite with Yilgarn Craton affinity occur within the Biranup Zone and this, combined with the isotopic and geochemical affinities of the Paleoproterozoic intrusive rocks, indicates a direct association with the Yilgarn Craton during their emplacement. The Paleoproterozoic magmatic rocks intrude metasedimentary rocks of the Barren Basin (see below). The Nornalup Zone is the southern- and easternmost unit of the Albany–Fraser Orogen and also spans its entire length (Fig. 1), although much of the original basement appears to be masked by intrusions of the Recherche and Esperance Supersuites.

In the east Albany–Fraser Orogen, the Nornalup Zone is separated from the Biranup and Fraser Zones by the Newman and Boonderoo Shear Zones and from the Madura Province by the Rodona Shear Zone.

Salmon Gums Event

The oldest dated Paleoproterozoic intrusive rocks are 1810–1800 Ma granitic gneisses that occur in both the Biranup and Nornalup Zones, marking the earliest phase of Paleoproterozoic magmatic activity recognized so far. This event, here named the Salmon Gums Event (after the locality Salmon Gums; Fig. 2), coincided with deposition of the Stirling Range Formation (Rasmussen et al., 2004), which corresponds to the earliest recognized period of formation of the Barren Basin. Metagranodiorite and metadiorite of the Black Dragon Gneiss is dated at c. 1800 Ma and occurs adjacent to the Tropicana Zone (Plate 1; Doyle et al., 2014). In the central Biranup Zone two diamond drillcores from south of Salmon Gums (Hopkinson, 2010) intersected layered, mafic and felsic granitic gneiss that yielded 1806 ± 6 Ma and 1804 ± 6 Ma zircon U–Pb dates, interpreted to reflect magmatic crystallization (hole SGD001, GSWA 192502, Kirkland et al., 2014b; hole SGD002, GSWA 192504, preliminary data, respectively). In the eastern Nornalup Zone migmatitic, monzogranitic gneiss containing angular mafic inclusions is exposed about 12 km east of Boingaring Rocks, and has yielded a zircon U–Pb date of 1809 ± 8 Ma, interpreted as the age of magmatic crystallization (GSWA 194785, Kirkland et al., 2014). All of these granites contain mafic enclaves.

Ngadju Event

The 1810–1800 Ma magmatic event was followed by a second phase of magmatic activity between 1780 and 1760 Ma, here named the Ngadju Event after the Ngadju people (Fig. 2). This event is recorded in the Biranup and Nornalup Zones, as well as the Tropicana Zone, and coincided with widespread sediment deposition and the formation of various sub-basins of the Barren Basin (Spaggiari et al., 2014b). In the central Biranup Zone, the diamond drillcores from south of Salmon Gums (Hopkinson, 2010) also intersected granitic gneiss that yielded a date of 1779 ± 7 Ma, interpreted as the magmatic crystallization age (hole SGD003, GSWA 192505, Kirkland et al., 2014c). In the eastern Nornalup Zone, strongly deformed metamonzogranite in the Newman Shear Zone yielded a date of 1763 ± 11 Ma, interpreted as the magmatic crystallization age (Kirkland et al., 2012a). The similarity in magmatic ages in both the Biranup and Nornalup zones implies that these zones shared the Paleoproterozoic (and likely Archean) substrate, prior to intrusion of the Fraser Zone and Recherche Supersuite during Stage I of the Albany–Fraser Orogeny (Fig. 2). Thus, the large shear zone system that separates the Biranup and Nornalup Zones (Coramup and Heywood–Cheyne Shear Zones, Fig. 1; Plate 3) is interpreted as a long-lived, reactivated structure that reflects an earlier history of rift-related extension (see also Spaggiari et al., 2014a,b).

Biranup Orogeny

Several phases of mildly alkaline granite magmatism produced widespread syenogranitic rocks throughout the eastern Biranup Zone from c. 1710 Ma through to at least 1650 Ma, during the Biranup Orogeny (Spaggiari et al., 2011). During this period sedimentation and formation of the Barren Basin was ongoing, with deposition of units such as the Woodline Formation and the Fly Dam Formation (Spaggiari et al., 2014b). The c. 1680 Ma Zanthus Event (Fig. 2) is a compressional phase of the Biranup Orogeny that produced folding under upper amphibolite to granulite facies conditions in Biranup Zone granitic gneiss that intruded Barren Basin psammitic gneiss (Ponton Creek Gneiss, Fig. 1; Kirkland et al., 2011a). Younger igneous rocks produced during the Biranup Orogeny include the c. 1660 Ma Eddy Suite, which is dominated by rapakivi-textured metagranodiorite mingled with metagabbro. These rocks have intruded Barren Basin semipelitic schist.

Other metagranitic rocks of both the central and eastern Biranup Zone include metamonzogranite, metagranodiorite, and rare tonalitic gneiss, with most ages falling in the range 1690–1660 Ma (Nelson et al., 1995; Kirkland et al., 2011a; Spaggiari et al., 2009). The central and eastern Biranup Zone are dominated by Paleoproterozoic gneisses that contain evidence of partial melting and migmatization, and have therefore undergone upper amphibolite to granulite facies metamorphism. Most homogeneous zircon overgrowths in these rocks indicate that high-grade metamorphism occurred during Stage II from c. 1225 to 1150 Ma, although some Stage I metamorphic dates of c. 1300 Ma occur in the Nornalup Zone (Kirkland et al., 2011a, 2014a; Spaggiari et al., 2014b).

Mesoproterozoic units

Fraser Zone

The Fraser Zone is bounded by the Fraser Shear Zone (previously named the Fraser Fault; Myers, 1985) along its northwestern edge and southern tip, and by the Newman and Boonderoo Shear Zones along its southeastern edge (Fig. 1; Plates 1, 2 and 3). It is dominated by high-grade metamorphic rocks that have a strong, distinct geophysical signature in both aeromagnetic and gravity data — the latter reflecting high density attributed to the dominance of metagabbroic rocks. All of the northern part of the Fraser Zone is obscured by Cretaceous to Cenozoic cover rocks of the Bight and Eucla Basins, but the gravity data indicate that it is an approximately 425 km long, northeasterly trending, fault-bound unit that is up to 50 km wide. The Fraser Zone contains the 1305–1290 Ma Fraser Range Metamorphics (Spaggiari et al., 2009), which comprise thin to voluminous sheets of metagabbroic rocks that range in thickness from several centimetres up to several hundred metres, interlayered with sheets of metamonzogranitic to metasyenogranitic gneisses, pyroxene-bearing granitic gneisses, and hybrid

magmatic rocks. All are interlayered at various scales with amphibolite to granulite facies pelitic, semipelitic, and psammitic gneiss, and locally calc-silicate and iron-rich metasedimentary rocks of the Snowys Dam Formation, which forms part of the Mesoproterozoic Arid Basin (Fig. 2; Spaggiari et al., 2014b). Metagranitic rocks range in composition from metamonzogranite to metasyenogranite. Whole-rock geochemical data for felsic rocks within the Fraser Zone permits these rocks to be subdivided into two broad groups; one compositionally similar to granites representing the majority of the 1330–1280 Ma Recherche Supersuite, the other likely reflecting melts derived locally through melting of the metasedimentary components of the Fraser Zone (Smithies et al., 2013).

Much of the northwestern side of the Fraser Zone is dominated by tightly to isoclinally folded, strongly foliated to mylonitic rocks, whereas the least deformed and thickest examples of metagabbroic sheets occur in the southeast, reflecting a significant difference in strain until the Newman Shear Zone is reached along the southeastern boundary (Fig.1; see also Brisbout et al., 2014). Aeromagnetic and gravity data indicate a repetition of this architecture along strike to the northeast beneath the Eucla Basin, where the Fraser Zone is crossed by seismic line 12GA-AF3.

Peak metamorphic temperatures and pressures recorded in the metapelitic rocks of the Snowys Dam Formation reached approximately 850°C at pressures of 7–9 kbars at c. 1290 Ma, followed by a period of isobaric cooling at pressures of about 9 kbars (Clark et al., 2014). All isotopic results from the Fraser Zone indicate a short time interval for both mafic and felsic igneous crystallization, predominantly between 1305 and 1290 Ma, and essentially coeval granulite-facies metamorphism (Fig. 2). The close temporal correspondence between mafic to felsic magmatism and the age of granulite-facies metamorphism implies that magmatism provided the thermal impetus for metamorphism (Clark et al., 2014). All U–Pb zircon geochronology in the Fraser Zone indicates tectonothermal activity during Stage I of the Albany–Fraser Orogeny, with no evidence of Stage II. This suggests that the Fraser Zone had cooled and strengthened sufficiently to inhibit zircon growth during Stage II, and that the Fraser Zone behaved as a resistant lozenge at that time (Clark et al., 2014). This is consistent with the interpretation that during Stage II the Fraser Zone was translated to the southwest, as indicated by the differential kinematics on its bounding shear zones (Spaggiari et al., 2011, 2013, 2014a).

The Fraser Zone is interpreted to represent a structurally modified, middle- to deep-crustal 'hot zone', formed by the repeated intrusion of gabbroic magma from a mantle upwelling into quartzofeldspathic country rock, either beneath an intercontinental rift, or in a distal back-arc setting (Spaggiari et al., 2011; Smithies et al., 2013; Clark et al., 2014). Whole-rock geochemical data indicate that an oceanic-arc setting, as interpreted by Condie and Myers (1999), is unlikely because the enriched crustal component of the gabbroic rocks of the Fraser Zone is better explained by assimilation from an older, felsic basement that included a Sr-depleted component of Archean — or reworked Archean — crust (Smithies et al., 2013). This interpretation is supported by previous and recent Nd- and Hf-isotopic data (Fletcher et al., 1991; Kirkland et al., 2011b), and the presence of Paleoproterozoic basement rocks in the eastern Nornalup Zone.

Sedimentary Basins

Barren Basin

The Barren Basin evolved over a period of more than 200 million years (1815–1600 Ma) and is interpreted to have extended at least 1000 km along the southern and southeastern Yilgarn Craton margin. It comprises Paleoproterozoic metasedimentary rocks belonging to the Stirling Range Formation, Mount Barren Group, Lindsay Hill Formation, Woodline Formation (Woodline Sub-basin), Fly Dam Formation, and unnamed occurrences of psammitic to semipelitic schist and gneiss (Fig. 1; Plates 1, 2 and 3; Spaggiari et al., 2011, 2014b). These units overlie the Yilgarn Craton, the Northern Foreland, the Biranup Zone, and the Nornalup Zone, and are interpreted to be the structural and erosional remnants of a much larger basin system that evolved along, and in the distal reaches of, the southern and southeastern Yilgarn Craton margin.

At least three main depositional phases are recognized, each closely following magmatic events (Fig. 2). The first commenced prior to c. 1800 Ma with deposition of the Stirling Range Formation, followed by deposition of the Mount Barren Group by 1693 ± 4 Ma (Vallini et al., 2005), and deposition of the Coramup Gneiss, the Ponton Creek psammitic gneiss, Big Red paragneiss, and the Lindsay Hill Formation between 1710 and 1650 Ma, coincident with the Biranup Orogeny. This was followed shortly afterwards by deposition of the Woodline and Fly Dam Formations, possibly in the late stages of, or shortly after, the Biranup Orogeny (Spaggiari et al., 2014b).

Depositional environment

The majority of sedimentary units of the Barren Basin comprise quartz-rich lithologies including cross-bedded sandstones, pure sandstones (now quartzites), pebbly sandstones, and siltstones. For the most part, the preserved units indicate moderate to high energy, fluvial to shallow marine (tidal or deltaic) conditions, indicative of broad, relatively shallow basins. However, a potential bias may exist due to the dominance of units sampled on or adjacent to the Yilgarn Craton. The Big Red paragneiss, which occurs in the Nornalup Zone and is the farthest outboard Barren Basin unit (Fig. 1), is interlayered with metamorphosed iron-rich layers, perhaps indicative of a deeper marine setting. The interbedded sandstone and mudstone protoliths of the Fly Dam Formation may also be indicative of deeper water. The relationships suggest on- or near-craton fluvial to shallow marine deposition, with the basin system gradually deepening away from the craton as time progressed — from c. 1727 Ma, based on the conservative estimate of the maximum depositional age of the Big Red paragneiss (Spaggiari et al., 2014b, and references therein).

Detrital zircon ages and provenance

The most dominant age component of Barren Basin detritus is Neoarchean, mostly spanning the range 2750–2600 Ma (Fig. 2). The Neoarchean ages are consistent with the ages of granites and greenstones of the Yilgarn Craton (Cassidy et al., 2006, and references therein), and given its close proximity and uncomformable contact relationships with some units, the Yilgarn Craton is regarded as the most likely source (Spaggiari et al., 2014b). The Barren Basin also contains several significant age components of zircon detritus spanning 2550–1900 Ma that imply sources distal to the Albany–Fraser Orogen, or alternatively, unrecognized or destroyed basement components. The largest detrital zircon age maxima in the 2550–1900 Ma range occur at c. 2250 and 2035 Ma. Barren Basin metasedimentary rocks from drillcore from the Big Red prospect in the Nornalup Zone (Fig. 1) yielded significant detrital age components between 2575 and 2450 Ma, with a probability peak at c. 2457 Ma. The 2575–2450 Ma age range also appears as minor age components in the Woodline Formation and the Coramup Gneiss (Spaggiari et al., 2014b, and references therein; Kirkland et al., 2014).

After the Neoarchean component, the second largest detrital zircon age component in much of the Barren Basin spans the range 1900–1600 Ma, with the largest probability peak defined between 1700 and 1650 Ma (Fig. 2). Subsidiary probability peaks are defined between 1800 and 1750 Ma, and a smaller peak at c. 1875 Ma. The 1700–1650 Ma age range matches that observed from magmatic rocks emplaced during the Biranup Orogeny, and the 1800–1750 age range matches granitic magmatism in the Biranup and Nornalup Zones during the Salmon Gums and Ngadju Events (Fig. 2). The c. 1875 Ma peak is unknown, and may indicate an as yet unrecognized magmatic event in the Albany–Fraser Orogen, or alternatively, detritus from a distal source (Spaggiari et al., 2014b).

The magmatic episodes appear to have provided substantial amounts of detritus to the basin system, much of which was mixed with detritus sourced from the Yilgarn Craton (Spaggiari et al., 2014b). These interpretations are supported by Lu–Hf data (Kirkland et al., 2011b, 2014a). There appears to have been a close link in the timing between depositional phases and pulses of magmatism, potentially indicative of relatively rapid, cyclical uplift and erosion releasing detritus into the evolving basin system. Although not constrained, potential coeval volcanism may also have supplied detritus to the basin.

Arid Basin

Several successions of metasedimentary rocks have maximum depositional ages younger than the youngest Biranup Zone magmatism (c. 1625 Ma), but have been affected by Stage I tectonism. These sedimentary successions belong to the Arid Basin and include the Malcolm Metamorphics of the eastern Nornalup Zone (formerly the Malcolm Gneiss; Myers, 1995), the Gwynne Creek Gneiss in the northeastern part of the orogen, and the Snowys Dam Formation of the Fraser Zone (Figs 1 and 2; Spaggiari et al., 2011, 2014b). Also included are paragneissic rocks from the western Nornalup Zone such as those found at Whalehead Rock near Albany (Fig. 1; Love, 1999).

The Malcolm Metamorphics are dominated by siliciclastic metasedimentary rocks, but also include layers of mafic amphibolitic schist and less abundant calc-silicate rocks. Two samples of upper amphibolite, migmatitic semipelitic schist yielded maximum depositional ages of 1455 ± 16 Ma (upper intercept age in sample PM-11-011) and 1456 ± 21 Ma (upper intercept age in GSWA 194867, preliminary data), constraining the maximum depositional age to c. 1450 Ma (Adams, 2012). Although part of the Arid Basin, the Malcolm Metamorphics may have originated in the Madura Province, potentially as a fore-arc deposit to the Loongana Arc (see below), they occur in a fault slice close to the Rodona Shear Zone, and may represent an interleaved unit on the Nornalup Zone – Madura Province boundary.

The Gwynne Creek Gneiss occurs in the northeastern part of the Albany–Fraser Orogen, between the Fraser and Biranup Zones, east of the Tropicana gold deposit (Fig. 1; Plate 1). The unit is dominated by psammitic and semipelitic gneiss, and also includes layered, finely laminated, quartzofeldspathic gneiss with layer-parallel leucosome rocks. Minor metagranitic, metamafic, and meta-ultramafic rocks intrude the metasedimentary rocks, and are possibly related to the Fraser Zone intrusions (Spaggiari et al., 2011). Alternatively, they may represent earlier magmatic activity during deposition of the Arid Basin. The metasedimentary rocks are also intruded by late, coarse to very coarse, K-feldspar-rich pegmatites. The Gwynne Creek Gneiss has a maximum depositional age of 1483 ± 12 Ma (based on one analysis), with a more conservative estimate of 1533 ± 11 Ma based on six analyses (Kirkland et al., 2011a).

The Snowys Dam Formation is part of the Fraser Range Metamorphics of the Fraser Zone and is typically intercalated with layers of mafic granulite or amphibolite that are interpreted as sills or sheets of the Fraser Zone gabbroic intrusions, although it is possible that some may represent earlier magmatic activity. The southwestern exposures of the Snowys Dam Formation are predominantly garnet-rich pelitic and semipelitic gneisses, with locally iron-rich metasedimentary rocks, and quartz-rich psammitic gneiss (e.g. the Gnamma Hill and Mount Malcolm areas). Locally, these rocks are interlayered with metasedimentary rocks that have calc-silicate affinities, and may represent metamorphosed marls, or volcaniclastic protoliths.

Maximum depositional ages of the Snowys Dam Formation indicate that deposition occurred not long before mafic magmatism. Garnet–biotite semipelitic gneiss from near Mount Malcolm yielded the youngest maximum depositional age of 1332 ± 21 Ma (single zircon analysis), or the more conservative estimate of 1363 ± 9 Ma (24 youngest analyses; GSWA 194778, Kirkland et al., 2012b). Zircon rims from the same sample yielded a metamorphic date of 1298 ± 12 Ma, identical to

metamorphic zircons from mafic granulite at the American Quarry (1292 ± 6 Ma; GSWA 194718, Kirkland et al., 2011c).

Depositional environment

The depositional environment of the Arid Basin is difficult to interpret based on the limited data available and highly variable basin fill. This includes interbedded sandstone and mudstone, calcareous rocks or marls, iron-rich horizons, and probable volcaniclastic or volcanic successions. In contrast to the Barren Basin, there is no evidence of fluvial deposits, and the sequences appear to be generally finer grained, less quartz-rich and less mature (Spaggiari et al., 2014b).

Detrital zircon ages and provenance

The most dominant age component of Arid Basin zircon detritus is Mesoproterozoic, spanning the range 1425–1375 Ma, with slightly lesser volumes in the ranges 1475–1425 Ma and 1375–1325 Ma (Fig. 2; Spaggiari et al., 2014b). The dominant age component of 1425–1375 Ma is found in the Snowys Dam Formation of the Fraser Zone, although this unit is also where the majority of the data comes from. The second most dominant detrital age component in the Arid Basin spans the range 1700–1650 Ma, with minor components in the ranges 1825–1725 Ma and 1625–1600 Ma. The 1700–1650 Ma age range occurs in the Snowys Dam Formation, but is most dominant in the Gwynne Creek Gneiss. All three Arid Basin units contain minor age components in the range 1600–1475 Ma. The smallest age components in all units occur between 2750 and 2600 Ma, 2550 and 2450 Ma, and from 2075 to 2025 Ma (Spaggiari et al., 2014b).

Detrital zircon analysis shows that the Snowys Dam Formation and the Malcolm Metamorphics have an unusual provenance, and that the dominant age range of detritus from c. 1455 Ma through to 1375 Ma does not correspond with any known sources from the Albany–Fraser Orogen (Spaggiari et al., 2014b). Furthermore, zircons of this age have the most juvenile Lu–Hf isotopic signature recorded in the Albany–Fraser Orogen, pointing to an exotic source with newly formed crust of different character. That source is interpreted as the c. 1410 Ma Loongana oceanic-arc, with which this detritus shares a similar isotopic and age signature (Spaggiari et al., 2014b; Kirkland et al., 2014a).

The second largest age component in the Arid Basin spans the range 1700–1650 Ma and can be readily correlated with known sources produced by the Biranup Orogeny. The flanking age range of 1825–1725 Ma also correlates well with known ages of magmatic rocks of the Biranup and Nornalup Zones. This detritus is likely to have shed from uplifted portions of these zones, and/or from the earlier deposition or recycling of these sediments into the Arid Basin, before being mixed with the c. 1455 to 1375 Ma sediments (Spaggiari et al., 2014b). The small number of both Neoarchean detrital zircons and Paleoproterozoic zircon detritus in the age range 2550–1900 Ma in the Arid Basin indicates that recycling from the Barren Basin was minimal, based on the prevalence of detrital zircons of these age groups in the Barren Basin. The small volume of Neoarchean detrital zircons also implies that input from the adjacent Yilgarn Craton was minimal at this time (Spaggiari et al., 2014b).

Ragged Basin

The Ragged Basin represents a restricted sequence of which the only known unit is the Mount Ragged Formation, which is exposed in the eastern Nornalup Zone (Figs 1 and 2). The Mount Ragged Formation is interpreted to have been deposited sometime between Stages I and II of the Albany–Fraser Orogeny (Clark et al., 2000). The metasedimentary component of the Salisbury Gneiss, which is exposed on Salisbury Island (Fig. 1), is interpreted as having been deposited at a similar time to the Mount Ragged Formation; however, there is little constraint on its depositional age. It lies within the Madura Province, and is not considered part of the Ragged Basin.

The Mount Ragged Formation comprises upper-greenschist to lower-amphibolite facies metasedimentary rocks dominated by pale grey, medium-grained, well-sorted, planar cross-bedded quartzite, locally interbedded with pelite or metasiltstone. Poorly sorted, quartz-pebble conglomerates interbedded with thick layers of well-sorted granular, quartz-dominated gritstones also occur locally (Waddell, 2014). The succession has been interpreted as deposited in a shallow intracratonic basin (Clark et al., 2000), although more recent work has refined this interpretation as a shallow basin fed by a large fluvial system dominated by a shifting complex of sandy braided channels (Waddell, 2014). The sequence is interpreted to gradually coarsen upwards, which implies a distal fluvial environment characterized by channel migration and abandonment evolving to a proximal fluvial environment characterized by rapid periods of sedimentation, producing coarser deposits (Waddell, 2014).

Previously published SHRIMP U–Pb data from the Mount Ragged Formation indicate a maximum depositional age of 1321 ± 24 Ma, but include a single grain dated at 1261 ± 31 Ma (Clark et al., 2000). From this it was difficult to establish whether the Mount Ragged Formation was distinct from other sedimentary rocks of the Arid Basin. The age of 1321 ± 24 Ma was interpreted as consistent with local derivation from the underlying Recherche Supersuite, and the contact was interpreted as an angular unconformity (Clark et al., 2000). Recently acquired geochronology from detrital zircons from the Ragged Range and nearby Diamonds Hill supports the interpretation that the Mount Ragged Formation is younger than the Arid Basin, and indicates that the maximum depositional age could be as young as 1234 ± 32 Ma (based on a single analysis, preliminary data, GSWA 194875). The same sample yielded the youngest conservative estimate for the maximum age of deposition at 1314 ± 19 Ma (based on 14 analyses). Other samples have also yielded younger, single zircon analyses at

1300 ± 28 and 1290 ± 84 Ma (GSWA 194866, Kirkland et al., 2014f; GSWA194874, Kirkland et al., 2014g, respectively). Although sparse, these young single grains appear to occur in all samples, including that of Clark et al. (2000), suggesting deposition took place during the latest part of Stage I of the Albany–Fraser Orogeny, or after it. The significant age component of 1350–1325 Ma is coincident with the early part of Stage I.

Amphibolite-facies metamorphism (4–5 kbars, 550°C) and growth of the 1154 ± 15 Ma rutile, indicate that these rocks were buried and metamorphosed during Stage II (Clark et al., 2000). This is further constrained by the recently dated, undeformed granite intrusion that crops out at Scott Rock, dated at 1175 ± 12 Ma (GSWA 192586, Kirkland et al., 2014e). Aeromagnetic imagery indicates that this granite crosscuts the fold and thrust architecture of the Mount Ragged Formation (Plate 3; Waddell, 2014).

Madura Province

The basement geology of the Madura Province lies completely under cover of the Bight and Eucla Basins, and is interpreted from geophysical interpretations and a small number of exploration and GSWA stratigraphic drillholes (Fig. 3). The province is defined as the area of basement bounded by the Rodona Shear Zone to the west, and the Mundrabilla Shear Zone to the east (Fig. 1; Plates 2 and 3). The Rodona Shear Zone is a wide, northeast-trending, east-dipping, high-strain zone that coincides with the eastern edge of the Albany–Fraser Orogen (Spaggiari et al., 2012, 2014a). Kinematic interpretations from aeromagnetic data indicate a period of west-directed thrusting overprinted by sinistral shearing. The Mundrabilla Shear Zone is a prominent, north–south structure that abruptly loses its magnetic signature to the north under the Officer Basin. It is a wide, straight, shear zone, which suggests it is subvertical, with drag fabrics indicative of a sinistral shear sense, at least during its more recent history. The shear zone is coincident with a surface fault and present-day scarp through the Miocene limestones of the Eucla Basin. Aeromagnetic data indicate a complex structural architecture for the Madura Province, with a dominant northeasterly regional trend (Spaggiari et al., 2012).

The only rock record from within the Rodona Shear Zone is from drillcore from the Hannah 1 prospect (Fig. 3; northeast of Caiguna). This drillhole intersected a coincident magnetic and gravity high, that has a boudin-like geometry. The drillcore contains metadiorite dated at 1170 ± 4 Ma (GSWA 182203, Kirkland et al., 2012c; Spaggiari et al., 2014a). Similar geophysical anomalies occur to the north of this, mainly within the shear zone. The deformed c. 1170 Ma metadiorite from the Hannah 1 drillcore indicates that at least the latest phase of deformation was after c. 1170 Ma.

In the Forrest Zone of the Coompana Province, the Eucla 1 petroleum well intersected a distinct ovoid feature of high magnetic intensity, interpreted as one of a series of northeast-trending granitic intrusions that are dragged into, and cut by, sinistral movement on the Mundrabilla Shear Zone (Fig. 3; Spaggiari et al., 2012). These magnetic intrusions have a similar signature to magnetic intrusions of the Esperance Supersuite in the eastern Nornalup Zone (Spaggiari et al., 2014a). Small rock chips from the base of the well, which are interpreted as derived from a granitic rock, provided a date of 1140 ± 8 Ma, interpreted as the magmatic crystallization age of the granite (GSWA 194773; Kirkland et al., 2011d). A single analysis of an unzoned zircon yielded a date of 1598 ± 14 Ma, interpreted as either the age of an inherited component within the granite, or the age of zircon incorporated from another rock unit (e.g. sedimentary rock) within the drillhole.

Diamond drillcore from the Moodini prospect within the Mundrabilla Shear Zone (about 15 km east of Moodini, Fig. 3), drilled by Venus Metals in March 2011, comprises texturally variable metagranite that is mostly porphyritic, locally with a fine-grained quench texture suggesting rapid cooling (Fig. 4a,b). It is locally cut by coarse pegmatite with large K-feldspars and white mica. The metagranite contains a subhorizontal foliation or linear fabric with a rodded morphology. The fabric is crosscut by localized alteration zones containing quartz, epidote, and possible prehnite in veins. The metagranite has a high magnetic susceptibility, and overlies a discrete north-trending magnetic high in the centre of the Mundrabilla Shear Zone. Zircons from this metagranite have been dated at 1132 ± 9 Ma (hole DDH MORCD 002, 592.83 – 593.39 m depth interval, GSWA 192566, preliminary data), interpreted as the age of magmatic crystallization of the granite. This indicates that sinistral movement on the Mundrabilla Shear Zone either occurred during emplacement of this granite, or after it. The date of the Moodini granite is also within uncertainty of the date from the Eucla 1 granite, and is likely to be part of the same magmatic event.

Madura Province basement rocks

Drilling at the Burkin prospect — which lies east of the Rodona Shear Zone and within the hinge of an interpreted antiformal structure approximately 65 km north of seismic line 12GA-AF3 (Plate 2, Fig. 3) — intersected a complex succession of heterogeneous gneissic rocks, iron-rich layered quartz–chlorite–garnet schist, metamorphosed banded iron-formation, and amphibolite (Benson, 2009; Spaggiari et al., 2012). Core with patches of potentially migmatitic, leucocratic material which crosscut a folded fabric, was sampled for U–Pb zircon geochronology (GSWA 182485, Kirkland et al., 2012d). Three zircon cores (either inherited or detrital) were dated at c. 2408 to 2293 Ma, while four grains provided a possible maximum depositional age of c. 1538 Ma (if the gneiss is interpreted to have a sedimentary protolith). Fourteen analyses of a mix of zircon rims and discrete homogeneous crystals provided a date of 1478 ± 4 Ma, interpreted as high-temperature metamorphism associated with migmatization and production of the leucocratic material (Kirkland et al., 2012b). Alternatively, the 1478 ± 4 Ma date could be a detrital zircon age component of the host rock.

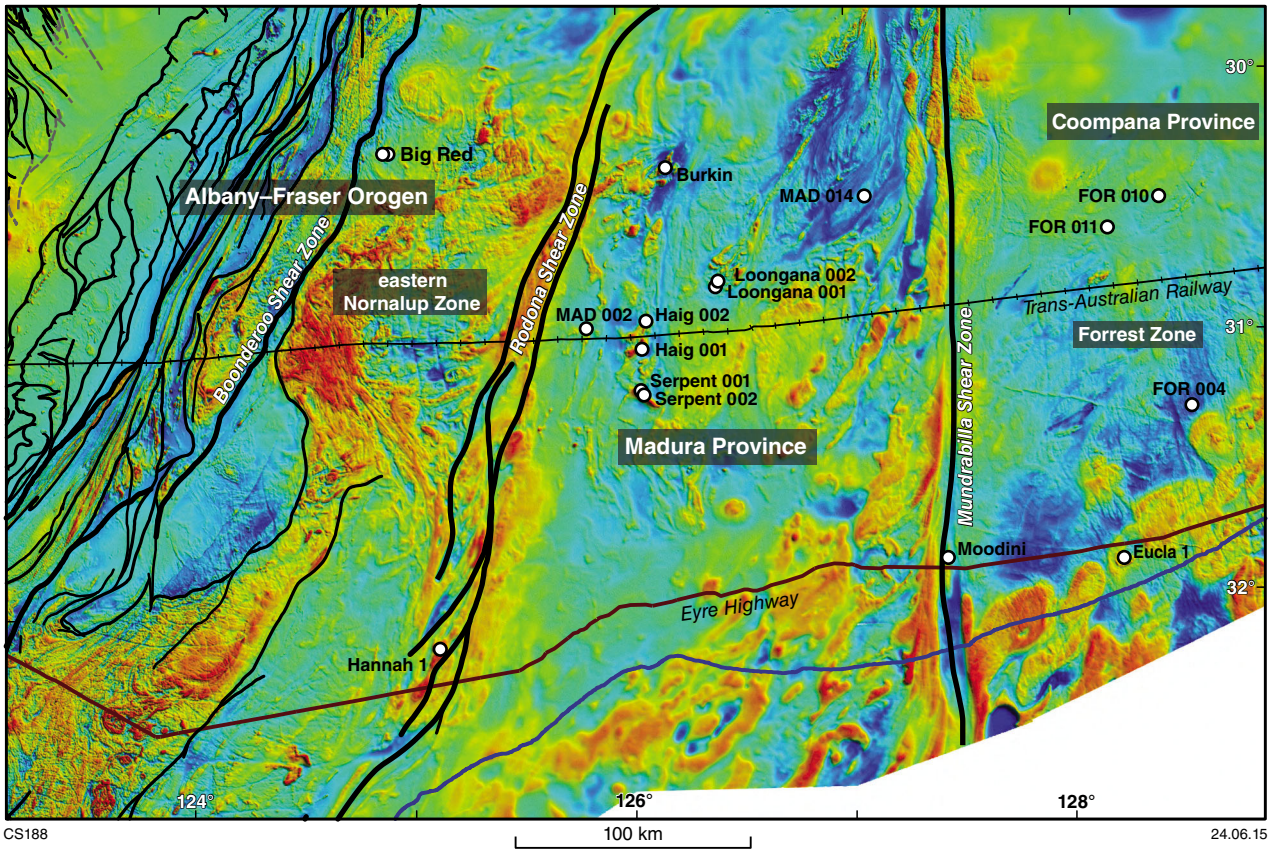

Figure 3. Reduced-to-pole aeromagnetic image over the east Albany–Fraser Orogen and Eucla Basin, showing major tectonic basement units and simplified structures, and the locations of drillcore sites, including the sites of the 2013 GSWA stratigraphic drilling program.

In 2013, GSWA drilled two stratigraphic holes in the Madura Province; MAD002 and MAD014 (Fig. 3). MAD002 is located about 4 km north of common depth point (CDP) 20 660 in seismic line 12GA-AF3 (Plate 2), and intersected basement at 389 m. Here, the basement consists of amphibolite schist interlayered with leucogranite veins and pods that are either parallel to the schistosity, or more locally, transgress it (Fig. 4c,d). The drillhole is coincident with a north-northeasterly trending, magnetic fabric of moderate susceptibility. In map view, this magnetic fabric occurs between the westerly dipping Pinto Shear Zone and the westerly dipping Honeymoon Shear Zone, which is interpreted to overlie the gabbroic rocks of the Haig Cave Supersuite (new name, after Haig Cave; seismic line 12GA-AF3; Plates 2 and 4; Spaggiari et al., 2014a).

Haig Cave Supersuite

The Haig Cave Supersuite comprises c. 1410 Ma gabbroic and metagranitic rocks from six diamond drillcores from the Loongana, Haig, and Serpent prospects, which are all from an area of roughly 3500 km^2 located in the central part of the Madura Province (Plate 2; Fig 3). These prospects overlie distinct gravity highs but have variable aeromagnetic signatures.

Weakly layered, medium-grained, mafic cumulate rocks form the basement lithology at the Serpent prospect, and also greatly dominate the Haig prospect, but here are intruded by medium- to coarse-grained trondhjemitic plagiogranite. At both Haig and Serpent geochemically distinct mafic cumulate rocks occur, indicating that distinct intrusive chambers were sampled (Spaggiari et al., 2014b). In Loongana core LNGD001, the upper portion of the basement component is dominated by weakly layered, medium-grained, mafic cumulate rocks, but it also includes an approximately 13 m thick interval of medium-grained, peridotitic cumulate rocks. The lower part of the basement component is dominated by medium- to coarse-grained trondhjemitic plagiogranite, which is also the dominant lithology in LNGD002 (Spaggiari et al., 2014b).

The c. 1410 Ma age of the Haig Cave Supersuite is constrained by dating of the granitic and gabbroic rocks from the Loongana core (see Spaggiari et al., 2012, 2014b, for details and references). Although undated, the Haig and Serpent drillcores are included in the Loongana Supersuite because of lithological and geochemical similarities. Dated zircons from plagiogranite from the Loongana core have juvenile Hf-isotopic compositions (εHf -2.5 to +11.5), with a median εHf of +7.8, and approach mantle-like values, which at 1410 Ma was εHf +12.1 (Spaggiari et al., 2014b). The isotopic and

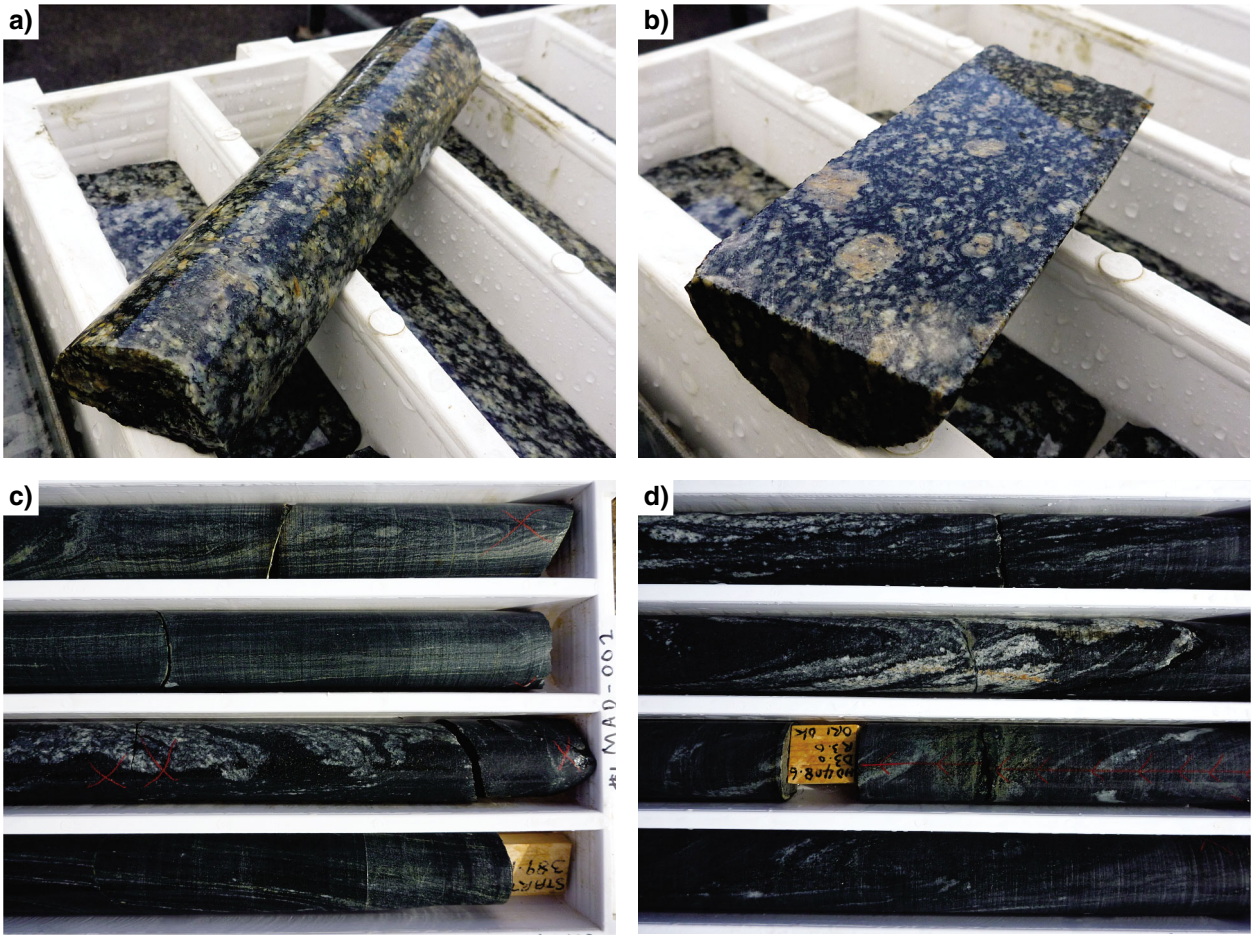

Figure 4. **Photographs of drillcore from the Madura Province: a) quench texture in metagranite from Moodini core; b) foliated porphyritic metagranite from Moodini core; c) laminated amphibolite schist interlayered with leucogranite veins, upper section of basement core at approximately 389 m depth; d) laminated amphibolite schist interlayered with leucogranite veins parallel to the schistosity, approximately 408 m depth**

geochemical interpretations suggest that the Haig Cave Supersuite formed in an oceanic-arc setting, with little contribution from continental material (Spaggiari et al., 2014b).

The isotopic values also overlap those found in detrital zircons in the age range 1425–1375 Ma from the Arid Basin, consistent with derivation from the Haig Cave Supersuite. If these zircons were sourced from the Madura Province, they must have been deposited in the Arid Basin by at least c. 1300 Ma, before being intruded by Recherche Supersuite granitic rocks, and the Fraser Zone gabbros.

Salisbury Gneiss

On Salisbury Island (Fig. 1), the Salisbury Gneiss comprises pelitic gneisses and mafic granulite, porphyritic granitic gneiss, and a two-pyroxene metagabbro that is undeformed in its core but deformed and amphibolitic at its margins (Clark, 1999). Outcrops of migmatitic pelitic gneiss record granulite-facies metamorphic conditions of approximately 800°C and >5 MPa (Clark, 1999; Clark et al., 2000). Migmatitic leucosome derived from partial melting of the pelitic gneiss yielded dates of 1214 ± 8 Ma (18 core analyses) and 1182 ± 13 Ma (six rim analyses; Clark et al., 2000). The c. 1214 Ma date provides a minimum age of deposition of the pelitic rocks. This date was interpreted as the age of crystallization of the leucosome, whereas the younger date of 1182 ± 13 Ma was interpreted to reflect zircon growth during decompression from peak metamorphic conditions (Clark et al., 2000). A lack of evidence for Stage I metamorphism led Clark (1999) to interpret deposition of the sediments to have occurred after that event.

Tectonic significance of the Madura Province

Although poorly constrained, all data from the Madura Province collected so far indicate that its geological evolution was different from that of the Albany–Fraser Orogen, until at least 1330 Ma. The presence of the

Loongana oceanic-arc suggests a largely oceanic environment, although it may contain limited older basement components locally (e.g. Burkin prospect). The Rodona Shear Zone is interpreted as a suture between the Albany–Fraser Orogen and Madura Province, which probably formed in the early part of Stage I of the Albany–Fraser Orogeny with accretion of the Loongana oceanic-arc (see below), but has since been modified.

The eastern extent of the Madura Province is ambiguous because it is not clear whether the Mundrabilla Shear Zone also represents a suture, separating the largely oceanic realm of the Madura Province from the Forrest Zone of the Coompana Province. The presence of deformed granites dated at c. 1140 and 1132 Ma indicate that sinistral movement on the Mundrabilla Shear Zone was much later than the accretion of the Loongana oceanic-arc, and was coincident with the later part of Stage II of the Albany–Fraser Orogeny. This movement may have been up to 200 km displacement, and probably pre-dated the Giles Event at c. 1070 Ma in the Musgrave Province (Smithies et al., 2014b). Note that for consistency, we have adopted the naming convention of Korsch et al. (2014), where the Forrest Zone (previously Forrest Province, e.g. Spaggiari et al., 2012), is part of the Coompana Province. These tectonic elements are poorly constrained, but are the subject of ongoing work including GSWA stratigraphic drilling, and interpretation of the recently acquired deep reflection seismic survey, the Eucla–Gawler line.

Tectonic evolution

Proposed models

A summary of tectonic models for the Paleoproterozoic and early part of Stage I of the Albany–Fraser Orogeny are presented below. The models are based on interpretations of the major basin-forming events, and their potential link to magmatism. Full models and details are provided in Spaggiari et al. (2014b).

Barren Basin

The Barren Basin evolved over a period of more than 200 million years (1815–1600 Ma) and is interpreted to have extended at least 1000 km along the southern Yilgarn Craton margin. It is dominated by mature, quartz-rich metasedimentary rocks interpreted to have formed in either a continental rift or a back-arc setting, during which the most dominant source of detritus was shed from the Yilgarn Craton as it underwent extension. This was mixed with locally derived detritus from synmagmatic rocks. If the Barren Basin was formed in a back-arc setting, the subduction zone and magmatic arc must have been a substantial distance outboard of the Yilgarn Craton margin.

Extension of the southern Yilgarn Craton was underway by c. 1805 Ma, resulting in a horst and graben architecture exposing basement highs. Detritus was sourced from the Yilgarn Craton hinterland, the basement highs, and potentially mixed with external sources. These sediments were fed into dominantly fluvial to deltaic, or shallow marine systems, producing the c. 1800 Ma Stirling Range Formation, and potentially even the lowermost unit of the Mount Barren Group, the Steere Formation. Mantle melting produced lower crustal melts and granitic intrusions along middle crustal shear zones, weakening the crust. Extension and magmatism was again prevalent between 1780 and 1760 Ma producing an asymmetric, melt lubricated detachment leading to doming and a core-complex mode of extension (Fig. 5a). This potentially increased the rate of extension and crustal thinning, widening the basin. Although volumetrically minor, gabbroic rocks are typically mingled with the granitic rocks, and indicate an ongoing link to the mantle as the crust thinned. It is likely that volcanism was also prevalent at this time, although the only known example are the dacitic rocks from the Voodoo Child Formation in the Tropicana Zone, which are also associated with mafic–ultramafic rocks (Less, 2013).

During the Biranup Orogeny (1710–1650 Ma), magmatism had increased volumetrically and by 1660 Ma included a greater input of more isotopically juvenile mantle material, forming mingled granitic and gabbroic intrusions such as those defined by the Eddy Suite (Kirkland et al., 2011a,b). The increased magmatism led to thermal subsidence and deepening of the basin, increased sediment load, and formation of deeper depositional centres flanked by topographic highs. Volcanism is again inferred. The compressional c. 1680 Ma Zanthus Event may reflect a brief period of basin inversion, perhaps releasing the first detritus of Biranup Orogeny age into the Barren Basin, feeding units such as the Fly Dam Formation, and to a lesser extent, the Woodline Formation. The Fly Dam Formation, which has a maximum depositional age of c. 1617 Ma, may represent the last stage of basin formation, which may have been due to thermal subsidence following the Biranup Orogeny.

An explanation for the distinct period of quiescence between 1600 and 1455 Ma, shown by the provenance from both the Barren and Arid Basins — and the magmatic history of the Albany–Fraser Orogen — is that the continental rift (or back-arc) described above evolved into a marginal ocean basin, forming an ocean–continent transition and passive margin. If a convergent margin setting is invoked, the quiescent period would indicate substantial retreat of the accompanying subduction zone. This marginal basin marks the initial setting of the Arid Basin.

Arid Basin

By c. 1500 Ma the Arid Basin was a marginal basin that lay outboard of the Yilgarn Craton and Biranup Zone, with the Nornalup Zone as an ocean–continent transition (OCT). These zones define a passive margin that provided the bulk of the detritus to the basin at that time. By c. 1455 Ma the tectonic setting changed to one of convergence, and the marginal basin included an east-dipping ocean–ocean subduction zone and the Loongana oceanic-arc (Fig. 5b). This configuration is based on the interpretation of the c. 1410 Ma Haig Cave Supersuite as an oceanic-arc, which must have been isolated from

a) c. 1770 Ma

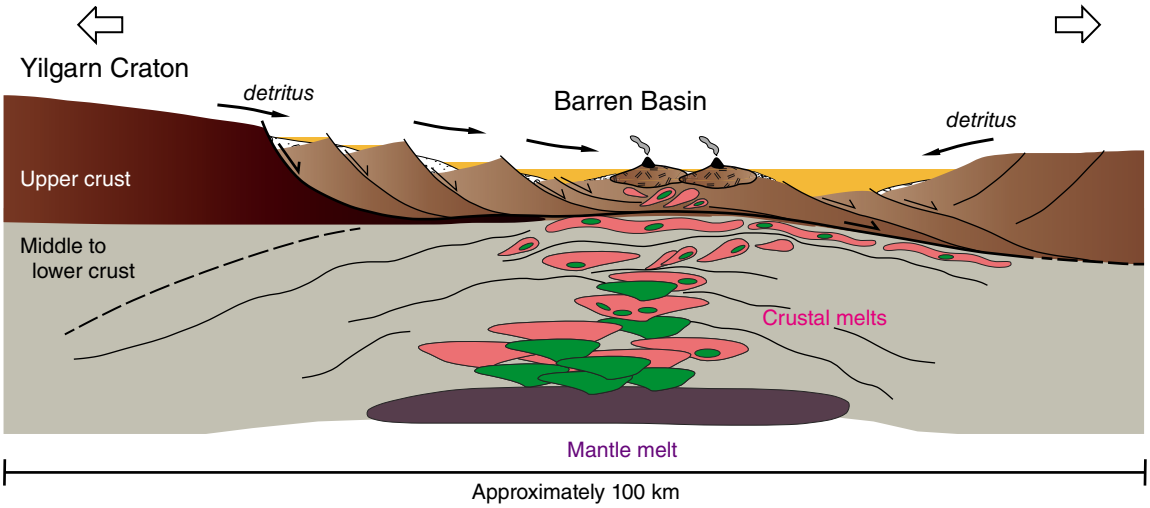

b) c. 1410 Ma

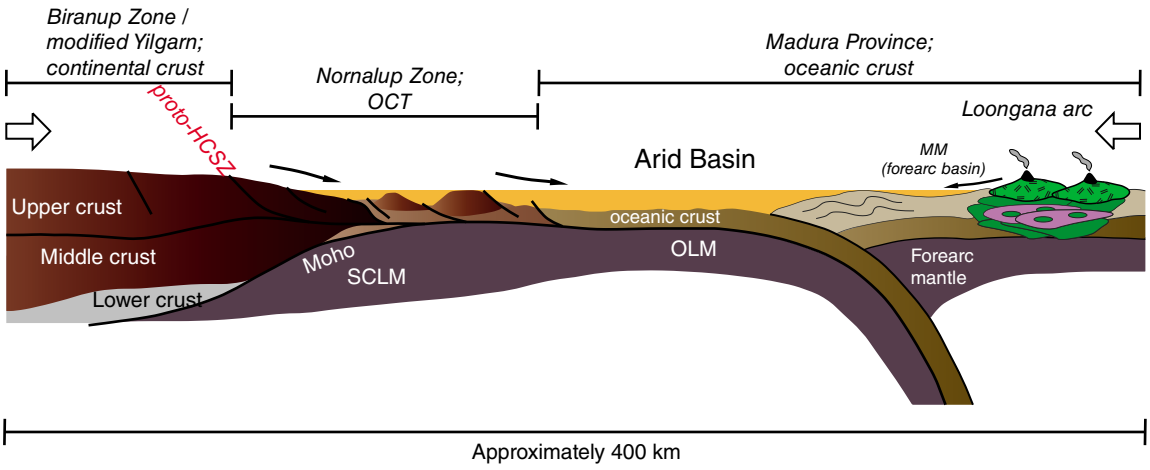

c) c. 1330 Ma

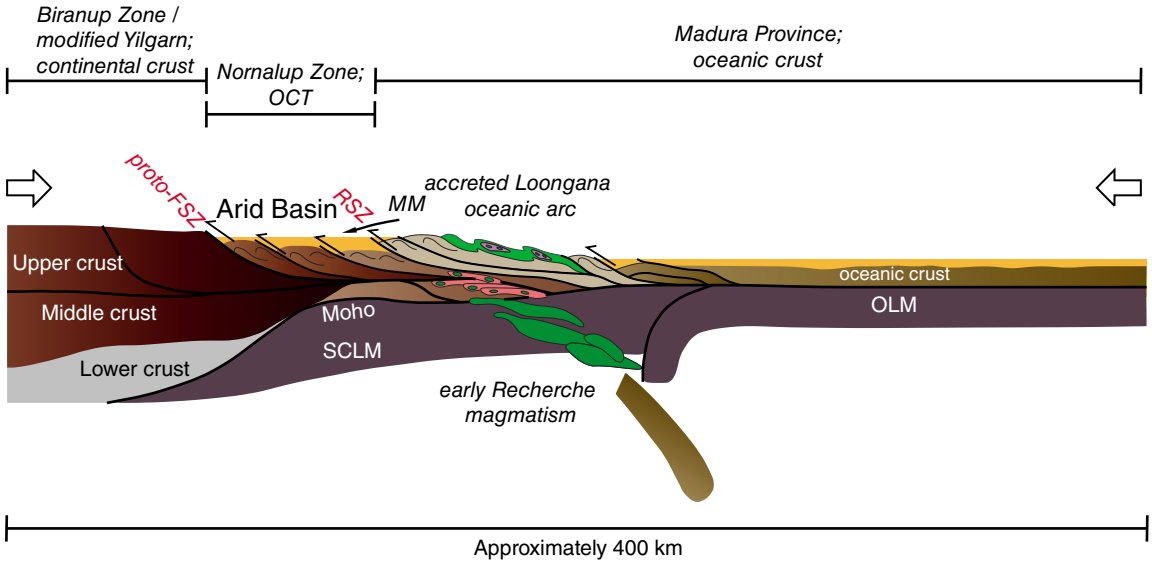

CS220 27.05.15

Figure 5. (facing) Tectonic evolution of the Barren and Arid Basins: a) extension and magmatism between 1780–1760 Ma produced an asymmetric, melt-lubricated detachment leading to doming and a core-complex mode of extension, and widening of the Barren Basin; b) formation of the Arid Basin as dominantly a marginal basin. Convergent setting and development of the Loongana oceanic-arc at c. 1400 Ma, with the Malcolm Metamorphics interpreted as fore-arc basin sediments; c) closure of the marginal basin, oceanic-arc accretion and slab detachment triggered the onset of Stage I, and early Recherche Supersuite magmatism. Sediments were transferred from the Loongana oceanic-arc and its environs to the Arid Basin via a foreland fold and thrust system. Abbreviations used: SCLM – sub-continental lithospheric mantle; OLM – oceanic lithospheric mantle; OCT– ocean–continent transition; MM – Malcolm Metamorphics; HCSZ – Heywood–Cheyne Shear Zone; FSZ – Fraser Shear Zone; RSZ – Rodona Shear Zone. Green indicates mafic/mantle component; pink indicates crustal melt/granitic component. From Spaggiari et al. (2014b).

any significant mass of continental crust to produce the mafic–ultramafic rocks and low-K plagiogranites present. It is also consistent with the lack of evidence of tectonic activity in the Biranup and Nornalup Zones (the passive margin hinterland) at this time. It is feasible that after c. 1455 Ma the Malcolm Metamorphics were deposited in either a fore-arc or accretionary prism setting onto an oceanic substrate (cf. Adams, 2012), west of the newly formed oceanic-arc.

Sedimentation was continuing well after formation of the Loongana oceanic-arc, until at least c. 1332 Ma (maximum depositional age of the Snowys Dam Formation). Therefore, it is likely that any sediment derived from the oceanic-arc must have either been recycled, or deposited after the oceanic-arc (and subduction) had changed position. The simplest way to explain deposition of the younger Arid Basin sediments onto the Biranup and Nornalup Zone substrate would be to invoke west-directed, oceanic-arc soft collision and accretion onto the passive margin, feeding detritus westwards in a foreland basin system, towards the craton and hinterland (Fig. 5c). The exact timing of this is speculative, but the closure of the marginal ocean basin and termination of east-dipping ocean–ocean subduction in the Madura Province could be viewed as marking the onset of Stage I of the Albany–Fraser Orogeny. If this is correct, the earliest intrusions of the Recherche Supersuite at c. 1330 Ma may have been caused by this event, through initial crustal thickening producing partial melting of the upper crust, with the addition of a mantle component. Oceanic-arc accretion would have produced large-scale compressional structures, forming a suture zone between the Albany–Fraser Orogen (eastern Nornalup Zone) and the Madura Province, marked by the Rodona Shear Zone.

As Stage I of the Albany–Fraser Orogeny progressed, convergence continued and west-dipping subduction was initiated accommodating the continued consumption of the remaining Madura Province oceanic crust, east of the Loongana oceanic-arc. Roll-back of the renewed subduction zone produced an extensional regime, placing the Albany–Fraser Orogen into a back-arc setting that accommodated the main pulse of magmatism which produced the remainder of the Recherche Supersuite and the Fraser Zone gabbros by c. 1300 Ma. By this time, deposition of the Arid Basin had also ceased. West-dipping subduction and roll-back led to the collision or accretion of the South Australian – Mawson Craton, leaving a remnant portion of the oceanic realm that now defines the Madura Province. Therefore, the Madura Province can be broadly interpreted as a suture zone between the Albany–Fraser Orogen and the Coompana Province, with an as yet unidentified major structure marking the western extent of the Coompana Province. That structure most likely lies in the Forrest Zone, beneath the Eucla Basin, and has been intruded by c. 1140 Ma granites, and cut by the Mundrabilla Shear Zone.

References

Adams, M 2012, Structural and geochronological evolution of the Malcolm Gneiss, Nornalup Zone, Albany–Fraser Orogen, Western Australia: Geological Survey of Western Australia, Record 2012/4, 122p.

Benton, J 2009, Diamond Drilling at E69/1972, 19 August 2009 – 16 September 2009, Holes BKD1 – BKD2, Gunson Resources Limited, Burkin Nickel Project: Digirock Pty Ltd, Perth, Western Australia, Statutory mineral exploration report, A085906, (unpublished).

Brisbout, LI, Spaggiari, CV and Aitken, ARA 2014, Integrating outcrop, aeromagnetic and gravity data: models of the east Albany–Fraser Orogen, *in* Albany–Fraser Orogen seismic and magnetotelluric (MT) workshop 2014: extended abstracts *compiled by* CV Spaggiari and IM Tyler: Geological Survey of Western Australia, Record 2014/6, p. 102–117.

Cassidy, KF, Champion, DC, Krapez, B, Barley, ME, Brown, SJA, Blewett, RS, Groenewald, PB and Tyler, IM 2006, A revised geological framework for the Yilgarn Craton, Western Australia: Geological Survey of Western Australia, Record 2006/8, 8p.

Clark, DJ 1999, Thermo-tectonic evolution of the Albany–Fraser Orogen, Western Australia: University of New South Wales, Sydney, New South Wales, PhD thesis (unpublished).

Clark, DJ, Hensen, BJ and Kinny, PD 2000, Geochronological constraints for a two-stage history of the Albany–Fraser Orogen, Western Australia: Precambrian Research, v. 102, no. 3, p. 155–183.

Clark, C, Kirkland, CL, Spaggiari, CV, Oorschot, C, Wingate, MTD and Taylor, RJ 2014, Proterozoic granulite formation driven by mafic magmatism: An example from the Fraser Range Metamorphics, Western Australia v. 240, p. 1–21.

Condie, KC and Myers, JS 1999, Mesoproterozoic Fraser Complex: geochemical evidence for multiple subduction-related sources of lower crustal rocks in the Albany–Fraser Orogen, Western Australia: Australian Journal of Earth Sciences, v. 46, p. 875–882.

Doyle, MG, Blenkinsop, TG, Crawford, AJ, Fletcher, IR, Foster, J, Fox-Wallace, L, Large, RR, Mathur, R, McNaughton, NJ, Meffre, S, Muhling, JR, Occhipinti, SA, Rasmussen, B and Savage, J 2014, Tropicana deposit, Western Australia: an integrated approach to understanding granulite-hosted gold and the Tropicana Gneiss, *in* Albany–Fraser Orogen seismic and magnetotelluric (MT) workshop 2014: extended abstracts *compiled by* CV Spaggiari and IM Tyler: Geological Survey of Western Australia, Record 2014/6, p. 69–76.

Fletcher, IR, Myers, JS and Ahmat, AL 1991, Isotopic evidence on the age and origin of the Fraser Complex, Western Australia: a sample of Mid-Proterozoic lower crust: Chemical Geology: Isotope Geoscience, v. 87, p. 197–216.

Hopkinson, A 2010, Salmon Gums Project EIS Report DA2009/076; Triton Gold Limited: Geological Survey of Western Australia, Statutory mineral exploration report, A088000 (unpublished).

Johnson, SP 2013, The birth of supercontinents and the Proterozoic assembly of Western Australia: Geological Survey of Western Australia, 78p.

Johnson, SP, Sheppard, S, Rasmussen, B, Wingate, MTD, Kirkland, CL, Muhling, JR, Fletcher, IR and Belousova, E 2011, Two collisions, two sutures: Punctuated pre-1950 Ma assembly of the West Australian Craton during the Ophthalmian and Glenburgh Orogenies: Precambrian Research, v. 189, p. 239–262.

Kirkland, CL, Spaggiari, CV, Pawley, MJ, Wingate, MTD, Smithies, RH, Howard, HM, Tyler, IM, Belousova, EA and Poujol, M 2011a, On the edge: U–Pb, Lu–Hf, and Sm–Nd data suggests reworking of the Yilgarn Craton margin during formation of the Albany–Fraser Orogen: Precambrian Research, v. 187, p. 223–247, doi:10.1016/j.precamres.2011.03.002.

Kirkland, CL, Spaggiari, CV, Wingate, MTD, Smithies, RH, Belousova, EA, Murphy, R and Pawley, MJ 2011b, Inferences on crust–mantle interaction from Lu–Hf isotopes: a case study from the Albany–Fraser Orogen: Geological Survey of Western Australia, Record 2011/12, 25p.

Kirkland, CL, Wingate, MTD and Spaggiari, CV 2011c, 194718: mafic granulite, American Granulite Quarry; Geochronology Record 993: Geological Survey of Western Australia, 4p.

Kirkland, CL, Wingate, MTD, Spaggiari, CV and Tyler, IM 2011d, 194773: granitic rock, Eucla No. 1 drillhole; Geochronology Record 1001: Geological Survey of Western Australia, 4p.

Kirkland, CL, Wingate, MTD and Spaggiari, CV 2012a, 194784: metamonzogranite, Newman Rock; Geochronology Record 1026: Geological Survey of Western Australia, 4p.

Kirkland, CL, Wingate, MTD and Spaggiari, CV 2012b, 194778: migmatitic garnet–biotite gneiss, Mount Malcolm; Geochronology Record 1067: Geological Survey of Western Australia, 6p.

Kirkland, CL, Wingate, MTD, Hall, CE and Spaggiari, CV 2012c, 182203, metagabbro, Hannah prospect; Geochronology Record 1049: Geological Survey of Western Australia, 5p.

Kirkland, CL, Wingate, MTD and Spaggiari, CV 2012d, 182485: migmatitic gneiss, Burkin prospect; Geochronology Record 1054: Geological Survey of Western Australia, 4p.

Kirkland, CL, Spaggiari, CV, Smithies, RH and Wingate, MTD 2014a, Cryptic progeny of craton margins: Geochronology and Isotope Geology of the Albany–Fraser Orogen with implications for evolution of the Tropicana Zone, *in* Albany–Fraser Orogen seismic and magnetotelluric (MT) workshop 2014: extended abstracts *compiled by* CV Spaggiari and IM Tyler: Geological Survey of Western Australia, Record 2014/6, p. 89–101.

Kirkland, CL, Wingate, MTD and Spaggiari, CV 2014b, 192502: granitic gneiss, Aloa Downs; Geochronology Record 1157: Geological Survey of Western Australia, 4p.

Kirkland, CL, Wingate, MTD, and Spaggiari, CV 2014c, 192505: granitic gneiss, Bishops Road; Geochronology Record 1158: Geological Survey of Western Australia, 4p.

Kirkland, CL, Wingate, MTD and Spaggiari, CV 2014d, 194785: metatonalite, east of Boingaring Rocks; Geochronology Record 1161: Geological Survey of Western Australia, 4p.

Kirkland, CL, Wingate, MTD and Spaggiari, CV 2014e, 192586: monzogranite, Scott Rocks; Geochronology Record 1216: Geological Survey of Western Australia, 4p.

Kirkland, CL, Wingate, MTD and Spaggiari, CV 2014f, 194874: psammitic schist, Tower Peak; Geochronology Record 1219: Geological Survey of Western Australia, 6p

Kirkland, CL, Wingate, MTD and Spaggiari, CV 2014g, 194866: psammitic schist, The Diamonds Hill; Geochronology Record 1218: Geological Survey of Western Australia, 7p.

Korsch, RJ, Spaggiari, CV, Occhipinti, SA, Doublier, MP, Clark, DJ, Dentith, MC, Doyle, MG, Kennett, BLN, Gessner, K, Neumann, NL, Belousova, EA, Tyler, IM, Costelloe, RD, Fomin, T and Holzschuh, J 2014, Geodynamic implications of the 2012 Albany–Fraser deep seismic reflection survey: a transect from the Yilgarn Craton across the Albany–Fraser Orogen to the Madura Province, *in* Albany–Fraser Orogen seismic and magnetotelluric (MT) workshop 2014: extended abstracts *compiled by* CV Spaggiari and IM Tyler: Geological Survey of Western Australia, Record 2014/6, p. 142–173.

Less, T 2013 Newly recognised Paleoproterzoic gold-silver mineralization in the Albany-Fraser orogeny, *in* Future understanding of tectonics, ores, resources, environment and sustainability *edited by* Z Chang, R Goldfarb, T Blenkinsop, C Palczek, D Cooke, K Camuti and J Carranza: FUTORES Conference, Economic Geology Research Unit Contribution 68, James Cook University, Townsville, Australia, 2–5 June 2013, p. 31.

Love, GJ 1999, A study of wall-rock contamination in a tonalitic gneiss from King Point, near Albany, Western Australia: Curtin University, Perth, Western Australia, Honours thesis (unpublished).

Murdie, RE, Gessner, K, Occhipinti, SA, Spaggiari, CV and Brett, J 2014, Interpretation of gravity and magnetic data across the Albany–Fraser Orogen, *in* Albany–Fraser Orogen seismic and magnetotelluric (MT) workshop 2014: extended abstracts *compiled by* CV Spaggiari and IM Tyler: Geological Survey of Western Australia, Record 2014/6, p. 118–134.

Myers, JS 1985, The Fraser Complex: a major layered intrusion in Western Australia, *in* Professional papers for 1983: Geological Survey of Western Australia, Report 14, p. 57–66.

Myers, JS 1995, Geology of the Esperance 1:1 000 000 sheet (2nd edition): Geological Survey of Western Australia, 1:1 000 000 Geological Series Explanatory Notes, 10p.

Nelson, DR 1995, 83690: biotite granodiorite gneiss, Bald Rock; Geochronology Record 78: Geological Survey of Western Australia, 4p.

Nelson, DR, Myers, JS and Nutman, AP 1995, Chronology and evolution of the Middle Proterozoic Albany–Fraser Orogen, Western Australia: Australian Journal of Earth Sciences, v. 42, p. 481–495.

Occhipinti, SA, Doyle, M, Spaggiari, CV, Korsch, R, Cant, G, Martin, K, Kirkland, CL, Savage, J, Less, T, Bergin, L and Foz, L 2014, Interpretation of the deep seismic reflection line 12GA-T1: northeastern Albany–Fraser Orogen, *in* Albany–Fraser Orogen seismic and magnetotelluric (MT) workshop 2014: extended abstracts *compiled by* CV Spaggiari and IM Tyler: Geological Survey of Western Australia, Record 2014/6, p. 52–68.

Rasmussen, B, Fletcher, IR, Bengtson, S and McNaughton, N 2004, SHRIMP U–Pb dating of diagenetic xenotime in the Stirling Range Formation, Western Australia: 1.8 billion year minimum age for the Stirling biota: Precambrian Research, v. 133, p. 329–337.

Smithies, RH, Spaggiari, CV, Kirkland, CL, Howard, HM and Maier, WD 2013, Petrogenesis of gabbros of the Mesoproterozoic Fraser Zone: constraints on the tectonic evolution of the Albany–Fraser Orogen: Geological Survey of Western Australia, Record 2013/5, 29p.

Smithies, RH, Spaggiari, CV, Kirkland, CL and Maier, WD 2014a, Geochemistry and petrogenesis of igneous rocks in the Albany–Fraser Orogen, *in* Albany–Fraser Orogen seismic and magnetotelluric (MT) workshop 2014: extended abstracts *compiled by* CV Spaggiari and IM Tyler: Geological Survey of Western Australia, Record 2014/6, p. 77–88.

Smithies, RH, Kirkland, CL, Korhonen, FJ, Aitken, ARA, Howard, HM, Maier, WD, Wingate, MTD, Quentin de Gromard, R and Gessner, K 2014b, The Mesoproterozoic thermal evolution of the Musgrave Province in central Australia – Plume vs the geological record: Gondwana Research, in press. http://dx.doi.org/10.1016/j.gr.2013.12.014.

Spaggiari, CV, Bodorkos, S, Barquero-Molina, M, Tyler, IM and Wingate, MTD 2009, Interpreted bedrock geology of the south Yilgarn and central Albany–Fraser Orogen, Western Australia: Geological Survey of Western Australia, Record 2009/10, 84p.

Spaggiari, CV, Kirkland, CL, Pawley, MJ, Smithies, RH, Wingate, MTD, Doyle, MG, Blenkinsop, TG, Clark, C, Oorschot, CW, Fox, LJ and Savage, J 2011, The geology of the east Albany–Fraser Orogen — a field guide: Geological Survey of Western Australia, Record 2011/23, 97p.

Spaggiari, CV, Kirkland, CL, Smithies, RH, Wingate, MTD 2012, What lies beneath — interpreting the Eucla basement, in GSWA 2012 extended abstracts: promoting the prospectivity of Western Australia: Geological Survey of Western Australia, Record 2012/2, p. 25–27.

Spaggiari, CV, Occhipinti, SA, Korsch, RJ, Doublier, MP, Clark, DJ, Dentith, MC, Gessner, K, Doyle, MG, Tyler, IM, Kennett, BLN, Costelloe, RD, Fomin, T and Holzschuh, J 2014a, Interpretation of Albany–Fraser seismic lines 12GA-AF1, 12GA-AF2 and 12GA-AF3: implications for crustal architecture, *in* Albany–Fraser Orogen seismic and magnetotelluric (MT) workshop 2014: extended abstracts *compiled by* CV Spaggiari and IM Tyler: Geological Survey of Western Australia, Record 2014/6 p. 28–51.

Spaggiari, CV, Kirkland, CL, Smithies, RH and Wingate, MTD 2014b, Tectonic links between sedimentary cycles, basin formation and magmatism in the Albany–Fraser Orogen, Western Australia: Geological Survey of Western Australia Report, Report 133, 63p.

Spaggiari, CV, Smithies, RH, Kirkland, CL, Howard, HM, Maier, WD and Clark, C 2013, melting, mixing, and emplacement: evolution of the Fraser Zone, Albany–Fraser Orogen, *in* GSWA 2013 extended abstracts: promoting the prospectivity of Western Australia: Geological Survey of Western Australia, Record 2013/2, p. 1–5.

Vallini, DA, Rasmussen, B, Krapež, B, Fletcher, IR and McNaughton, N 2005, Microtextures, geochemistry and geochronology of authigenic xenotime constraining the cementation history of a Paleoproterozoic metasedimentary sequence: Sedimentology, v. 52, p. 101–122.

Waddell, P-J 2014, Sedimentological and structural evolution of the Mount Ragged Formation, Nornalup Zone, Albany–Fraser Orogen, Western Australia: Geological Survey of Western Australia, Report 129, 116p.

Interpretation of Albany–Fraser seismic lines 12GA-AF1, 12GA-AF2 and 12GA-AF3: implications for crustal architecture

by

CV Spaggiari, SA Occhipinti[2], RJ Korsch[1], MP Doublier[1], DJ Clark[1], MC Dentith[3], K Gessner, MG Doyle[2], IM Tyler, BLN Kennett[4], RD Costelloe[1], T Fomin[1], and J Holzschuh[1]

Introduction

The aim of this study is to examine the crustal architecture of the Albany–Fraser Orogen, and to examine its relationship to the adjoining Yilgarn Craton by tracking the craton's subsurface extent beneath the orogen. The deep crustal structure of the Albany–Fraser Orogen provides insight into the processes that drove Paleoproterozoic rifting and magmatism along the craton margin, and Mesoproterozoic tectonic assembly. The upper crustal portion of the seismic images show the Mesoproterozoic fold and thrust belt architecture present in the Albany–Fraser Orogen that, although complex, in general terms relates to the tectonic assembly of the West Australian Craton and the South Australian Craton. Commencing in the Yilgarn Craton in the west, and finishing in the Madura Province in the east, the seismic lines provide a complete image and interpreted cross-section of the orogen.

In April to June 2012, 672 line km of vibroseis-source, deep seismic reflection data were acquired along four traverses (12GA-AF1, 158.4 km; 12GA-AF2, 114.04 km; 12GA-AF3, 319.12 km; and 12GA-T1, 80.32 km), collectively referred to as the Albany–Fraser seismic survey. The lines were designed to cross the various tectonic units and major shear zones of the east Albany–Fraser Orogen, and the eastern part of the central Albany–Fraser Orogen (Fig. 1; Plates 1, 2 and 3). The project is, in part, a collaborative project between Geoscience Australia (GA) and the Geological Survey of Western Australia (GSWA), and is part of the ongoing cooperation under the National Geoscience Agreement (NGA). This contribution covers the results and interpretation of seismic lines 12GA-AF1, 12GA-AF2 and 12GA-AF3; 12GA-T1 is presented in Occhipinti et al. (2014), and will not be discussed here.

Details of the acquisition and processing techniques followed for the deep seismic survey are provided in Costelloe et al. (2014). We undertake conversion from two-way travel time (TWT) to depth using an effective P-wave velocity for the crust of 6000 ms^{-1}, so that 1 s TWT is approximately equal to 3 km depth, with the exception of sedimentary rocks in the Eucla Basin and for the Cenozoic regolith, where we assume much slower P-wave velocities of 2500–3800 ms^{-1}.

Acquisition and processing techniques of deep crustal reflection seismic lines are designed to provide images of the crust and uppermost mantle that can be interpreted and shown as two-dimensional (2D) cross-sections of the present-day geological architecture. Although the processed seismic reflection data provide images of reflections to work with, the process of interpretation is analogous to drawing basic structural and lithological cross-sections from mapped surface data, where features that are away from the plane of section are taken into account. This includes analysing their geometrical extent, estimating apparent dip where features are not perpendicular to the line of section, and taking crosscutting relationships into account (i.e. the law of superposition). Because of the 2D nature of the seismic lines, the orientations of structures are apparent dips, and apparent dip directions. While the interpretations presented here have been derived from the seismic reflection images, they have also been guided by interpreted bedrock geology maps (Plates 1, 2, and 3), which in turn are based on field and drillcore relationships, and magnetic and gravity data interpretation compiled between 2008 and 2013. Modelling of the potential field data are presented in Murdie et al. (2014).

1 Minerals and Natural Hazards Division, Geoscience Australia, GPO Box 378, Canberra ACT 2601

2 AngloGold Ashanti Ltd, Level 13, St Martins Tower, PO Box Z5046, Perth WA 6831

3 Centre for Exploration Targeting, School of Earth and Environment, The University of Western Australia, 35 Stirling Highway, Crawley WA 6009

4 Research School of Earth Sciences, The Australian National University, Canberra ACT 0200

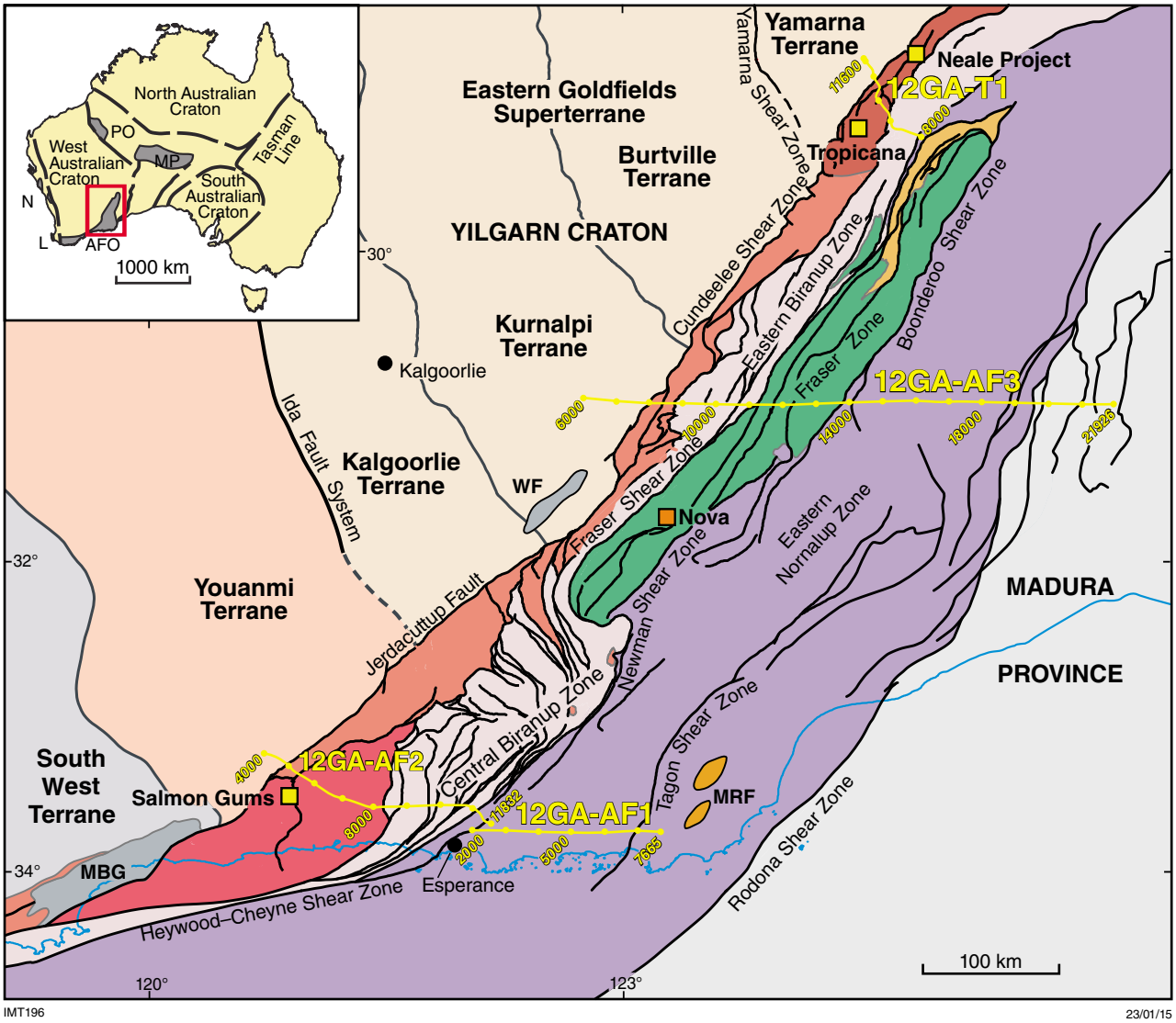

ALBANY–FRASER OROGEN

- Mount Ragged Formation
- Fraser Zone (1305–1290 Ma)
- Gwynne Creek Gneiss
- Nornalup Zone (1800–1650 Ma); Recherche (1330–1280 Ma) and Esperance (1200–1140 Ma) Supersuites (undivided)
- Biranup Zone (1800–1650 Ma) and Archean remnants
- Barren Basin (undivided)
- Tropicana Zone (2720–1650 Ma)
- Munglinup Gneiss (2800–2660 Ma)
- Northern Foreland, undivided

- Major faults
- Terrane boundary
- Geological boundary
- Coastline
- Gold
- Nickel–copper
- Town

Figure 1. Simplified, pre-Mesozoic interpreted bedrock geology of the Albany–Fraser Orogen and tectonic subdivisions of the Yilgarn Craton (modified from Spaggiari et al., 2014b) showing the location of the Albany–Fraser deep crustal seismic reflection lines; Abbreviations used: MBG – Mount Barren Group; WF – Woodline Formation; MRF – Mount Ragged Formation. Inset: AFO – Albany–Fraser Orogen; MP – Musgrave Province; PO – Paterson Orogen; L – Leeuwin Province; N – Northampton Province

Large areas of the seismic lines cross regions with very sparse outcrop, or regions that are buried by younger cover rocks, such as the Eucla Basin (figure 1, Spaggiari et al., 2012). This has made interpretation difficult, so that there is a high degree of uncertainty in many areas, even near the surface. Other issues include deciding whether reflections are out of plane, and whether they link to other reflections, how far to migrate reflections, and deciding the geological significance of large areas of non-reflectivity. The interpretation methodology includes delineating reflective versus non-reflective zones, which generally corresponds to particular units, marking out the truncations of reflections (usually interpreted as faults or shear zones, or intrusions), and tracking the geometries of reflections, e.g. folded layers. It is important to note that like any other geophysical dataset, not all geological features can be imaged. Only surfaces or packages with different acoustic impedance are detected, so the integration of other datasets is vital. Despite the above, the seismic images have allowed us to track the orientation and extent of major shear zones and the accompanying geology to great depths, permitting interpretations of the underlying geology. In the future, these interpretations will be tested in 3D models that will include passive seismic data (acquisition in progress), and inversions and modelling of potential field data.

The three seismic lines covered by this abstract are described in detail below, from west to east, and also south to north. The images and interpreted sections are shown in Figures 2, 3 and 4, and in greater detail in Plate 4, which also gives the common depth point (CDP) numbers. The lines of section, including the Tropicana line 12GA-T1, are shown in Figure 1, and on three interpreted bedrock geology maps in Plates 1 (line 12GA-T1), Plate 2 (12GA-AF3), and Plate 3 (12GA-AF1 and 12GA-AF2). All four plates accompany this volume. The legend for the lithological units for each section in Figures 2, 3 and 4 is shown in Figure 5. A geological overview of the Albany–Fraser Orogen is given in Spaggiari et al. (2014a) and Kirkland et al. (2014a).

Interpretation of seismic line 12GA-AF2

Seismic line 12GA-AF2 is 114.04 km long and, from west to east, commences in the Youanmi Terrane of the Yilgarn Craton and crosses the central and east Albany–Fraser Orogen to the boundary between the Biranup and Nornalup Zones, just northwest of Esperance (Figs 1 and 2; Plates 3 and 4). From west to east, the line tracks in a southeasterly direction, then turns easterly, before a major bend to the southeast. This line geometry was deliberately chosen to facilitate overlap with the western end of 12GA-AF1. Due to changes in the geometry of geological features related to the bend, the reflections at this eastern end of the line do not match exactly those in the westernmost part of line 12GA-AF1, and should only be interpreted as far east as about CDP 11 600. No magnetotelluric (MT) data was collected along this line because it is located too close to the Southern Ocean.

Yilgarn Craton and Northern Foreland

The westernmost part of 12GA-AF2 has imaged the poorly exposed southern part of the Southern Cross Domain of the Youanmi Terrane. In this region the boundary between the Yilgarn Craton and its reworked counterpart, the Northern Foreland of the Albany–Fraser Orogen, is defined as the southeasterly dipping Jerdacuttup Fault (CDP 4870; Myers, 1990; Witt, 1998), although the seismic image shows a similar fault reaching the surface west of the Jerdacuttup Fault, at CDP 4500. The Northern Foreland is distinguished from the Yilgarn Craton by the degree of Proterozoic deformation in the former. Based on fold geometries in outcrop, and aeromagnetic data interpretation, the Jerdacuttup Fault was previously inferred to mark a major change from Archean northwesterly trending structures to Proterozoic northeasterly trending structures (Myers, 1990; Witt, 1998; Spaggiari et al., 2009). The Jerdacuttup Fault is not exposed, and has been mapped using magnetic imagery. The unnamed fault imaged in the seismic line northwest of the Jerdacuttup Fault is not visible in the magnetic data because this area is heavily overprinted by more than one suite of Proterozoic mafic dykes (see Spaggiari et al., 2009), and is also extensively fractured. Because of the abundance of intrusions and structures the unnamed fault cannot be mapped laterally, so we continue to use the Jerdacuttup Fault as marking the boundary between the Yilgarn Craton and Northern Foreland (Albany–Fraser Orogen) in this region.

From the western end of line 12GA-AF2, east to the Jerdacuttup Fault, the upper crust of the Youanmi Terrane is dominated by granitic rocks and is generally only weakly to moderately reflective. The thickness varies from about 2.0 s TWT (~6 km) at about CDP 4100 to about 3.7 s TWT (~11 km) at about CDP 4500. The Northern Foreland has a similar seismic character as far east as the Cascade Shear Zone, and is of a similar thickness. Two mafic sills of unknown age are interpreted from two sets of very strong subhorizontal reflections in the upper crust at 0.3 – 0.7 s TWT (~1–2 km depth), similar to those imaged on previous seismic lines farther to the north in the Youanmi Terrane (Ivanic et al., 2013). The westernmost sill appears to crosscut the fault west of the Jerdacuttup Fault. 12GA-AF2 crossed a small greenstone belt interpreted from a linear magnetic anomaly at about CDP 5300, but this was not imaged.

Below the Youanmi Terrane, and continuing for the entire length of 12GA-AF2, is a strongly reflective middle to lower crust where the reflections dip gently to the southeast over the western two-thirds of the section, and are subhorizontal in the eastern part. We interpret this as the Yarraquin Seismic Province, which has previously been defined as the moderately to strongly reflective middle to lower crust underlying the Youanmi Terrane farther north (Korsch et al., 2013; Korsch et al., 2014). Hence, the Youanmi Terrane (sensu stricto) is confined to only the upper crust, and its base is defined as the contact with the Yarraquin Seismic Province (Korsch et al., 2013a).

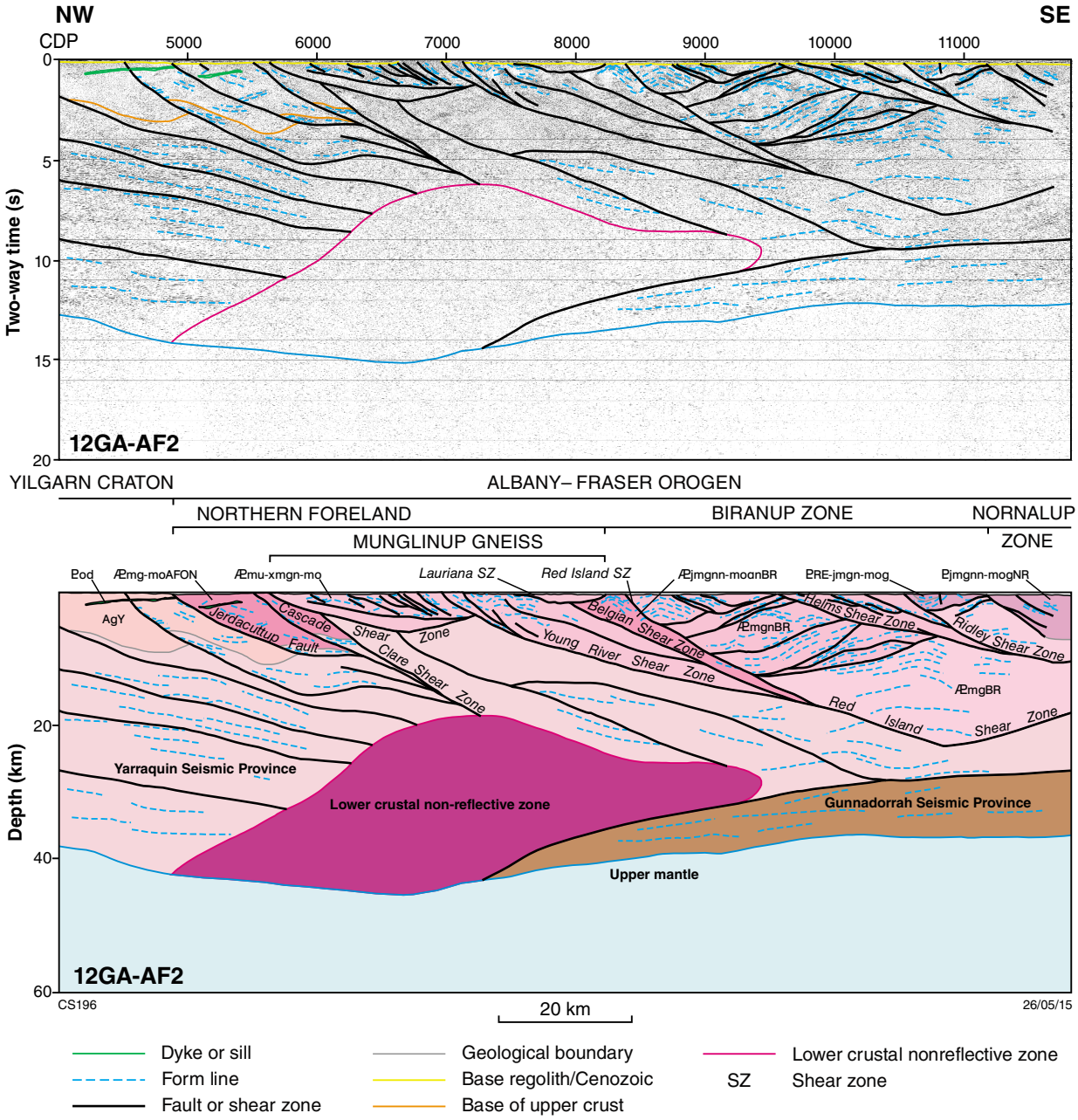

Figure 2. Migrated section for seismic line 12GA-AF2, showing the seismic image with interpreted linework (upper) and solid geology interpreted section (lower). Display is to 20 s TWT (~60 km) depth, and shows vertical scale equal to the horizontal scale, assuming a crustal velocity of 6000 ms^{-1} for the entire section. See Figure 5 for the units legend.

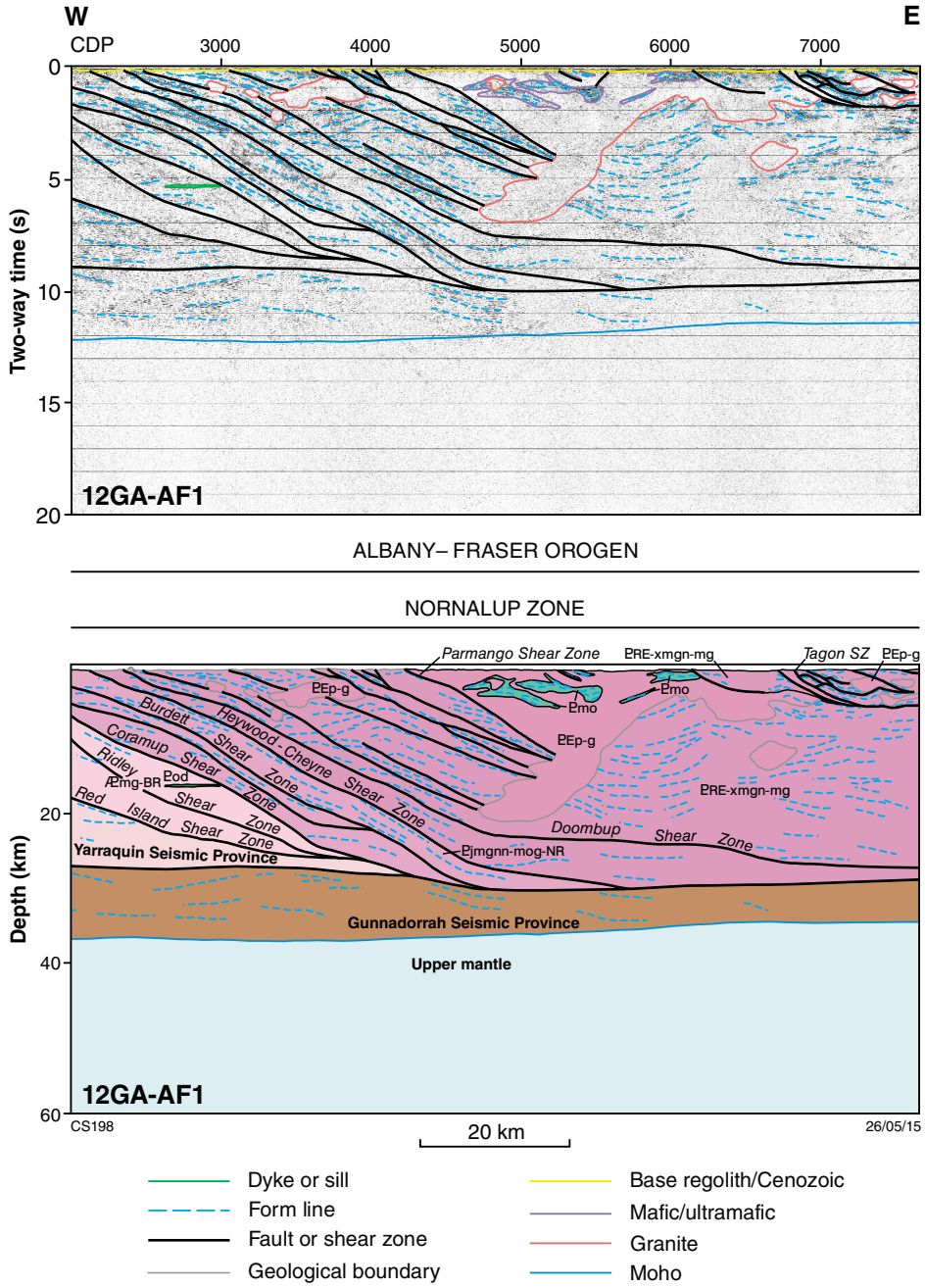

Figure 3. Migrated section for seismic line 12GA-AF1, showing the seismic image with interpreted linework (upper) and solid geology interpreted section (lower). Display is to 20 s TWT (~60 km) depth, and shows vertical scale equal to the horizontal scale, assuming a crustal velocity of 6000 ms^{-1} for the entire section. See Figure 5 for the units legend.

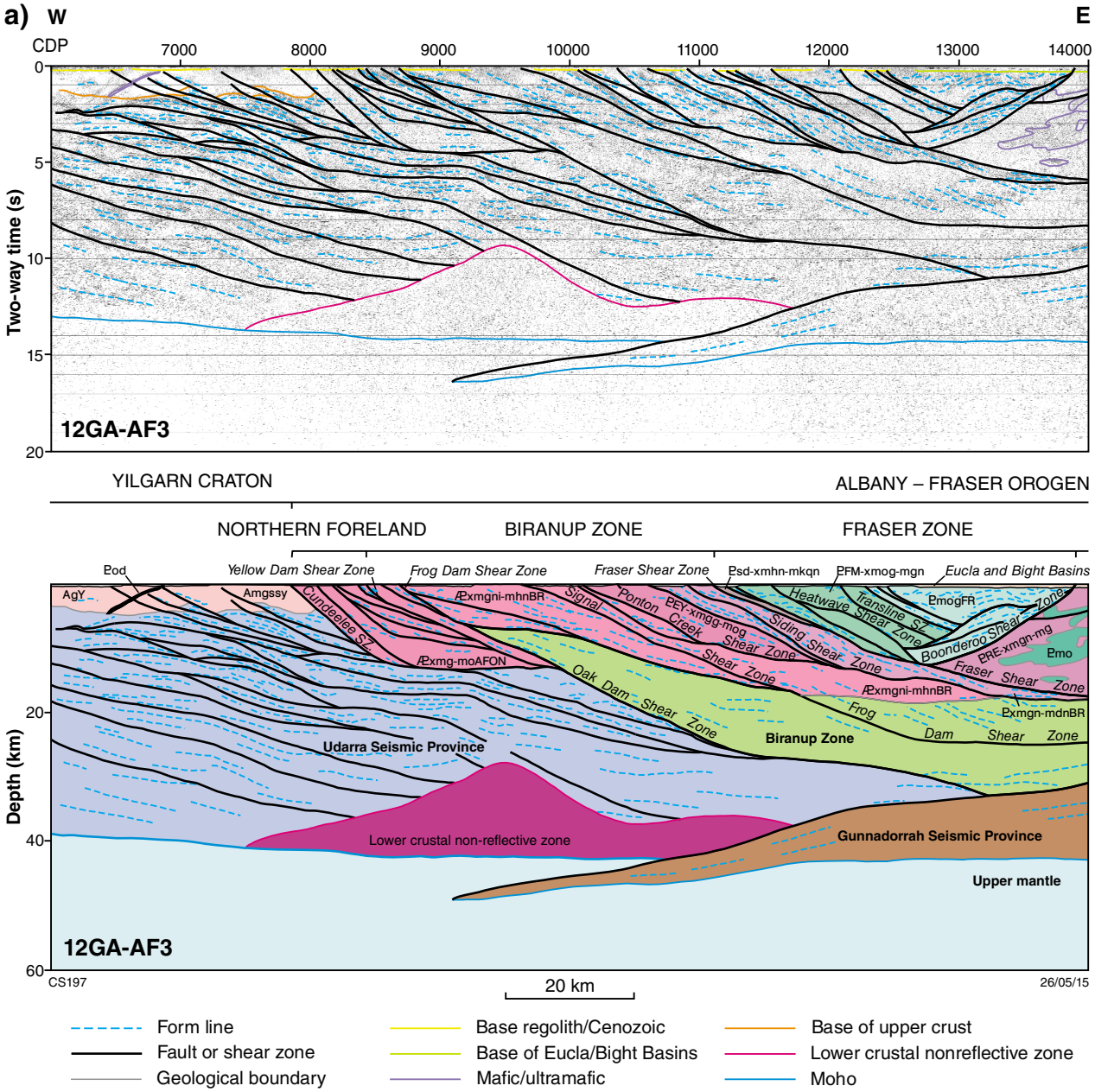

Figure 4. Migrated sections for seismic line 12GA-AF3, showing the seismic image with interpreted linework (upper) and solid geology interpreted section (lower). Display is to 20 s TWT (~60 km) depth, and shows vertical scale equal to the horizontal scale, assuming a crustal velocity of 6000 ms^{-1} for the entire section. The western part of the section is shown in a), and the eastern part in b). See Figure 5 for the units legend.

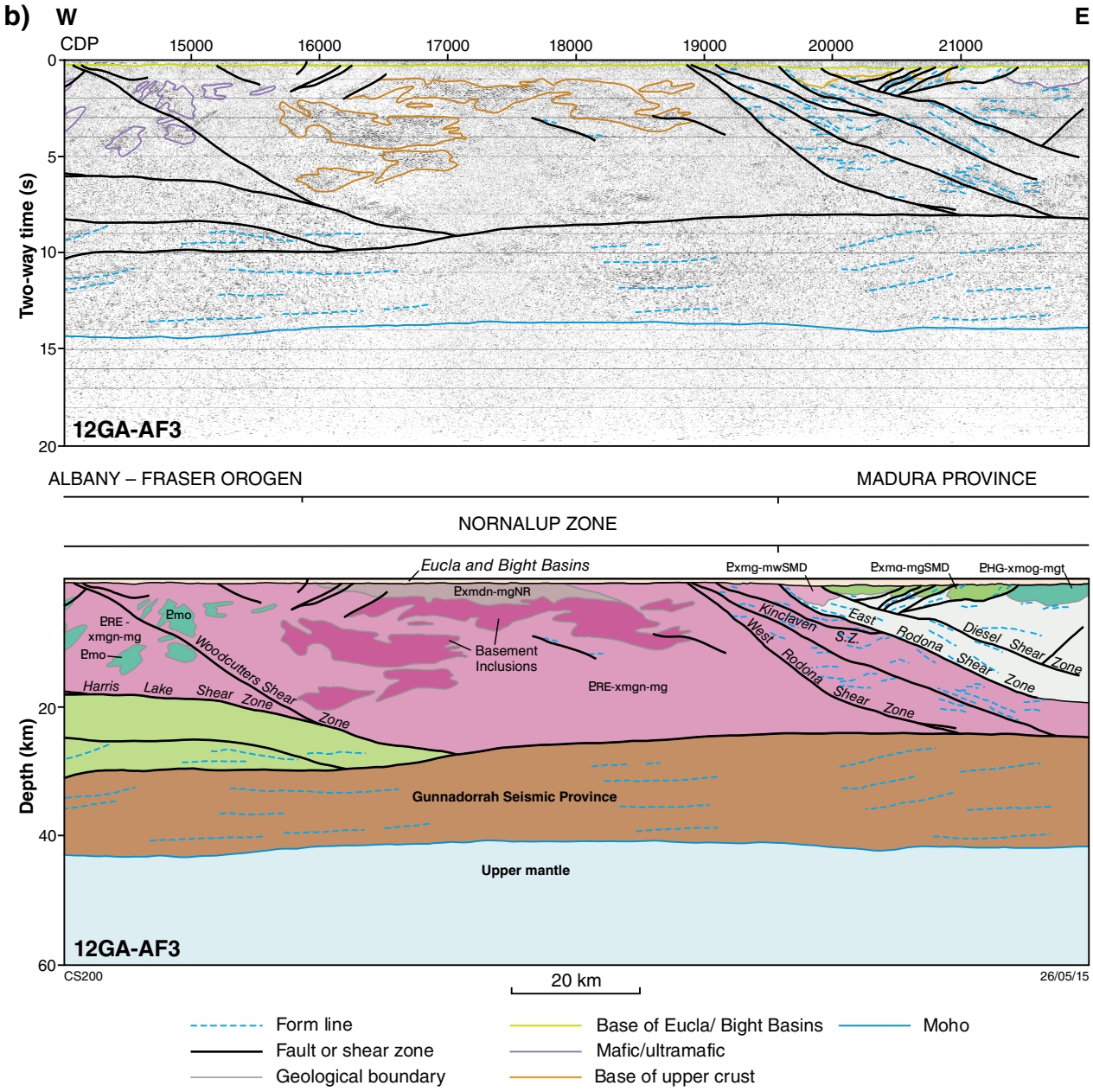

Figure 4. continued

Figure 5. Reference for the units shown in the migrated sections in Figures 2, 3 and 4

Overall there is a predominant southeast dip and listric form to the structures in this part of the Youanmi Terrane and Northern Foreland, and a thrust movement sense is interpreted from the top to the west offsets of the Yarraquin Seismic Province below. This confirms that the Northern Foreland has been thrust over the Youanmi Terrane, as has previously been interpreted (Myers, 1990; Witt, 1998; Spaggiari et al., 2009).

Munglinup Gneiss

Southeast of the Cascade Shear Zone, but still within the Northern Foreland, are fault-bound slices of reworked Yilgarn lithologies at higher metamorphic grade, named the Munglinup Gneiss (in Myers, 1995). The Cascade Shear Zone is interpreted as a thrust with a gentle southeast dip, placing upper amphibolite, Munglinup Gneiss over greenschist facies rocks of the Northern Foreland. The Cascade Shear Zone has a scooped shape and links to the southeasterly dipping Young River Shear Zone to the east at about 1.2 s TWT (~4 km depth) below CDP 7230 (Fig. 6). Above the Cascade Shear Zone is another rather flat-lying shear zone that separates relatively non-reflective Munglinup Gneiss from a more strongly reflective package that contains reflections indicative of an anastomosing and folded fabric, with a predominant southeast dip. The Cascade Shear Zone also truncates major shear zones within the Yarraquin Seismic Province below. East-northeasterly trending, dextral strike-slip faults cut major shear zones in this region, including both the Cascade and Young River Shear Zones (Plate 3).

Farther east, the Munglinup Gneiss occurs within another fault slice between the Young River Shear Zone and the folded Lauriana Shear Zone to CDP 8230 (Fig. 6). In this section are large-scale refolded folds visible in aeromagnetic data (Spaggiari et al., 2009, 2011), which are also visible in the seismic section, particularly just east of the Lort River Shear Zone at CDP 7120 (Fig. 6). The Lauriana Shear Zone is also folded into a broad, northwesterly trending synform between CDPs 7500 and 8230, and overlies the older Belgian Shear Zone, which to the east bounds a slice of Archean Munglinup Gneiss and Paleoproterozoic interlayered granitic and mafic gneiss which includes c. 1800 and 1670 Ma rocks that are part of the Biranup Zone (Hopkinson, 2010; GSWA 192502, Kirkland et al., 2014b; GSWA 192504, preliminary data). The Belgian Shear Zone links to the southeasterly dipping Red Island Shear Zone (named after Red Island off the South Coast, which the shear runs through) at depth, which defines the main boundary between the Northern Foreland (Munglinup Gneiss) and the Biranup Zone (Figs 2 and 7). The Red Island Shear Zone also cuts the folded Lauriana Shear Zone near the surface (Plate 3). Although complex, the crosscutting relationships help constrain the relative timing of movement along these shear zones, with the Belgian Shear Zone preserving the oldest movement, and the Young River and Red Island Shear Zones showing the youngest movement (Plate 3). The fault slice of combined Munglinup Gneiss and Biranup Zone rocks bounded by the Belgian and Red Island Shear Zones is contained within the thrust slice bounded by the Cascade and Red Island Shear Zones (see Plate 3). These relationships, and the presence of both Archean Munglinup Gneiss and Paleoproterozoic Biranup Zone granitic gneiss in the same drillcores at Salmon Gums (Hopkinson, 2010; GSWA 192502, Kirkland et al., 2014b; GSWA 192505, Kirkland et al., 2014c; GSWA 192507, Kirkland et al., 2013a; GSWA 192508, Kirkland et al., 2014d; GSWA 192504, preliminary data), are consistent with the Paleoproterozoic history of magmatic intrusion directly into Yilgarn Craton crust (Spaggiari et al., 2014a; Smithies et al., 2014; Kirkland et al., 2011a,b, 2014a). The relationships show that the Northern Foreland (Munglinup Gneiss) and Biranup Zone are not simply fault-bound entities juxtaposed by major shear zones, but are also autochthonous.

The Munglinup Gneiss is underlain by the Yarraquin Seismic Province, which between CDPs 6330 and 7220 only reaches a maximum thickness of about 6 km (2 s TWT). There is similarity in seismic character between these two units, and given that the Munglinup Gneiss most likely represents deeper slices of reworked Yilgarn Craton (Spaggiari et al., 2009, 2011), it is feasible that in this region it may also have been derived from the Yarraquin Seismic Province. Although dominantly granitic, the Munglinup Gneiss contains distinct layering of felsic and mafic lithologies, which may help define its reflective character. This may also correlate with the upper portion of the Yarraquin Seismic Province.

Biranup Zone

The Red Island Shear Zone marks the main boundary between the Northern Foreland and the dominantly Paleoproterozoic gneissic rocks of the Biranup Zone. In this region the Biranup Zone gneisses are mostly granitic, often garnet rich, and typically interlayered with mafic gneiss. The Biranup Zone not only contains remnants of Yilgarn Craton granite (Kirkland et al., 2011a; Spaggiari et al., 2011), but is also dominated by granitic rocks that were formed by recycling of Archean felsic material that is interpreted as Yilgarn Craton basement (Kirkland et al., 2011b; Smithies et al., 2014). Although in this region the Red Island Shear Zone marks the main boundary of the Biranup Zone, it does not mark the eastern extent of the Yarraquin Seismic Province, which continues below the Biranup Zone, and is consistent with the derivation of Biranup Zone magmatic rocks from Yilgarn Craton basement (Kirkland et al., 2011a,b; Smithies et al., 2014). This suggests that the Biranup Zone was not thrust a substantial distance over the Yarraquin Seismic Province, (i.e. it could not have been displaced a distance greater than extended Yilgarn Craton crust), and/or that the Yarraquin Seismic Province (and inferred Yilgarn heritage) continued a considerable distance to the east and southeast.

The Red Island Shear Zone also marks a distinct change in magnetic character, from a refolded-fold pattern to the northwest, to a linear, shear-related fabric to the southeast. This shear-related fabric extends about 50 km or so across strike as far as the Heywood–Cheyne Shear Zone, and encompasses the boundary between the Biranup and Nornalup Zones, which is described below.

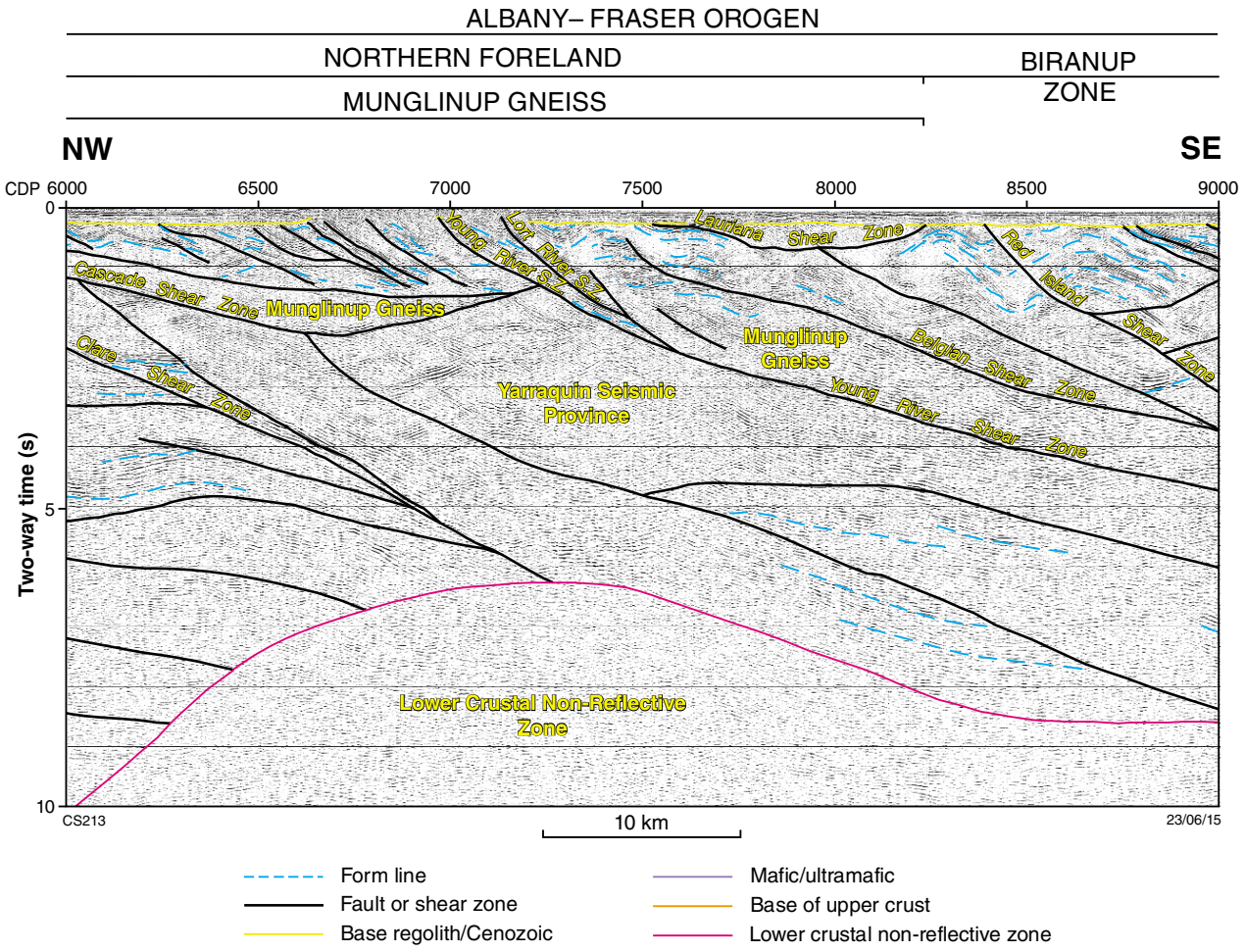

Figure 6. Detail of part of seismic line 12GA-AF2 showing the Munglinup Gneiss in the upper crust

On seismic line 12GA-AF2, the Biranup Zone is dominantly highly reflective, with packages of reflections and shear zones dipping both to the east and west. The westerly dipping shear zones appear to be earlier, and for the most part truncated by the easterly dipping shear zones, such as the Red Island, Helms, Speddingup, Ridley, and Coramup Shear Zones, which all have a moderate easterly to southeasterly dip (Figs 2 and 7). None of the earlier westerly dipping shear zones are exposed at the surface in the vicinity of the seismic line, although one cuts close to the Helms Shear Zone at about CDP 9540. The magnetic data show that the area between the Red Island and Speddingup Shear Zones is dominated by northerly trending folds, and is structurally complex, making 2D interpretation of the seismic image difficult. For example, a doubly plunging antiform is present between the Red Island and Bishops Hat Shear Zones, which is itself folded into a broad synform to the east (Plates 3 and 4). These folds sit above one of the westerly dipping shear zones, and may relate to an earlier deformation event of both folding and shearing, that predates later movement on the large, east to southeasterly dipping shear zones. The Helms Shear Zone also appears to be folded away from the line of section to the south. It is possible that this folding and shearing event was linked to northerly trending folding observed in the adjacent Munglinup Gneiss, although these may also be Archean in age and therefore earlier (Spaggiari et al., 2009). Another possibility is the westerly dipping shear zones may be related to an earlier extensional architecture, representing the tops of tilted blocks. If this were the case, the folded horizons may have formed during inversion processes along the major east to southeasterly dipping shear zones. This would fit with the Paleoproterozoic rift model proposed by Spaggiari et al. (2014b).

East of the Ridley Shear Zone, between CDPs 10 600 and 10 810, is the southern tip of an interpreted sheet of Recherche Supersuite metagranite, truncated by the steeply east-dipping, sinistral strike-slip Jenabillup Shear Zone. The metagranite has been dated to the northeast at Mount Burdett at 1299 ± 18 Ma, which is interpreted as the igneous crystallization age (GSWA 83697, Nelson, 1995). The extent of this metagranite sheet is interpreted from magnetic and gravity data.

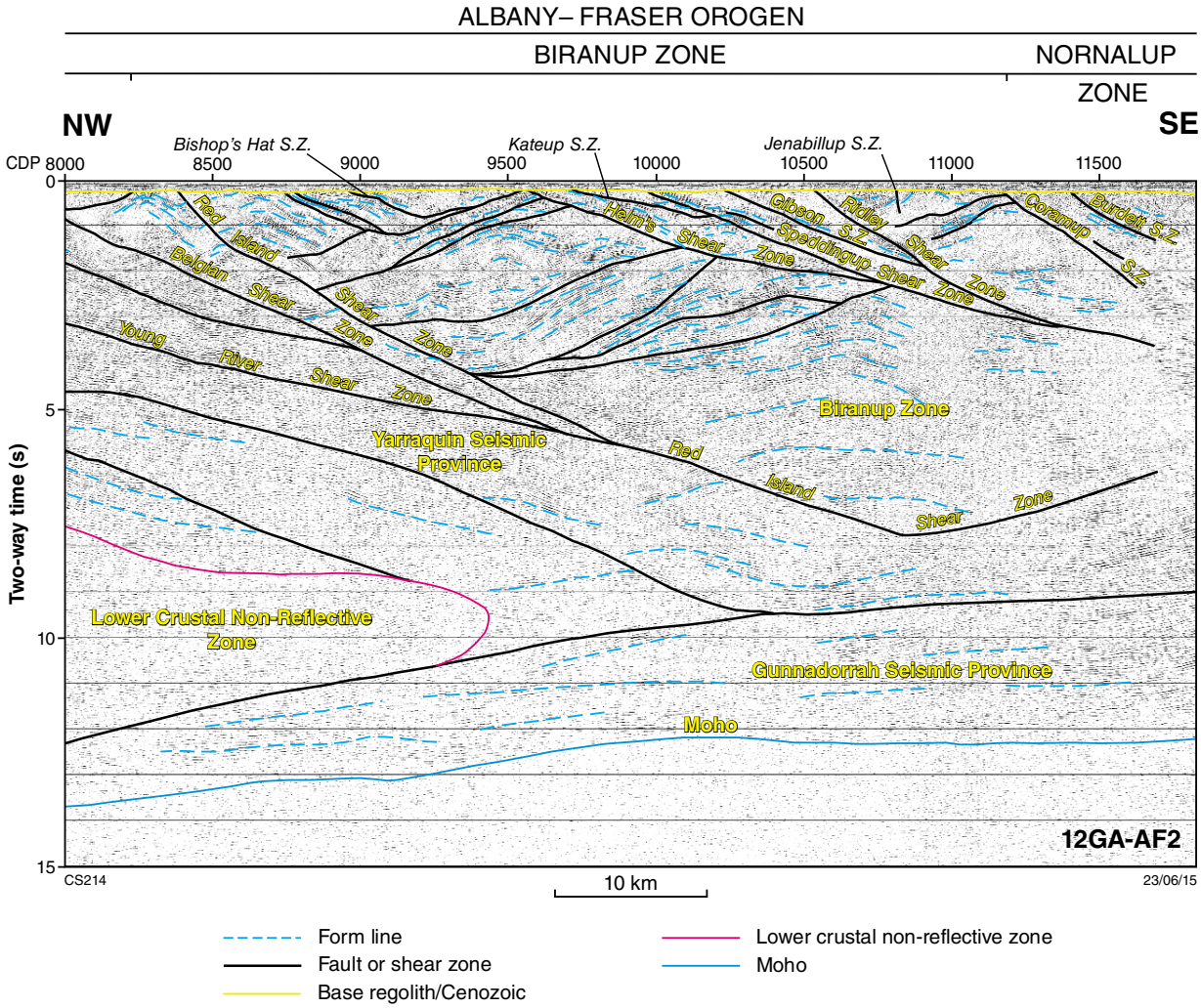

Figure 7. Detail of part of seismic line 12GA-AF2 showing the Biranup Zone

Where Biranup Zone rocks cannot be tracked to the surface, and correlated with surface outcrops, we have shown them on the cross-section as Biranup Zone undivided. These terminate against the southeasterly dipping Coramup Shear Zone at the eastern end of line 12GA-AF2.

Coramup Shear Zone

The Coramup Shear Zone is here defined as the main boundary between the Biranup and Nornalup zones, based on interpreted relationships in the seismic images from both 12GA-AF2 and 12GA-AF1, and to some extent, the magnetic data. Previously, the boundary was interpreted as the Heywood–Cheyne Shear Zone (Spaggiari and Pawley, 2012), which marks the easternmost extent of the linear, shear-related fabric in the magnetic data. In any case, the distinction between the Biranup and Nornalup Zones is to some degree blurred, as both contain Paleoproterozoic granitic rocks that are indistinguishable both geochemically and isotopically (Spaggiari et al., 2011), although the data are very sparse in the Nornalup Zone. The Nornalup Zone is also much more thoroughly overprinted by both the Recherche and Esperance Supersuites.

The Coramup Shear Zone contains both metagranitic rocks and metasedimentary rocks of the Barren Basin (Coramup Gneiss) and has been mapped on the coast at Butty Head as a high strain zone. P-T conditions indicate granulite facies metamorphism and range from 850 to 700°C over time, and vary from about 7–10 kbars, and back down to 5–6 kbars (Bodorkos and Clark, 2004a). Early metamorphism and D1 deformation are interpreted to have occurred during Stage I (c. 1290 Ma), and subsequent events during Stage II, of the Albany–Fraser Orogeny (Bodorkos and Clark, 2004a). Detailed structural analysis was interpreted to show reverse movement sense on the southeasterly dipping gneissic foliation (D_1), locally overprinted by intense, northeasterly trending dextral shearing and transpression (D_2), followed by narrow,

north-northeasterly trending mylonitic or pseudotachylitic sinistral shear zones (D_3) (Bodorkos and Clark, 2004b). These interpretations are consistent with the seismic and magnetic data. The Burdett Shear Zone crosses line 12GA-AF2 at about CDP 11400, and is another major, southeasterly dipping shear zone subparallel to the Coramup Shear Zone.

Lower crust on 12GA-AF2

A major feature of the lower crust in 12GA-AF2 is a large subhorizontal elongate body, with roughly 90 km maximum width and 25 km maximum thickness defined by its non-reflective seismic character of reduced impedance contrast (Fig. 2; Plate 4). This body truncates southeasterly dipping shear zones and reflections in the Yarraquin Seismic Province, and extends to the Moho, coincident with where the Moho appears to be deepest in this section (15.1 s TWT [~45 km depth]). This body is also coincident with a large, long wavelength positive gravity anomaly which indicates it is made of relatively dense material, such as mafic–ultramafic cumulate (Murdie et al., 2014). Because of the large size, our preferred interpretation of this feature is a former source region for magmatism that contains a combination of crustal melts (or mush), and melt residuals from a magmatic event. These have obliterated the fabrics in the Yarraquin Seismic Province. There are several possibilities for the timing of this magmatism, but the truncations of the shear zones, some of which appear to extend into the Albany–Fraser Orogen above, suggest it was relatively late, and probably during either Stage I or Stage II of the Albany–Fraser Orogeny. One possibility is that it was synchronous with the intrusions of the c. 1210 Ma Gnowangerup – Fraser Dyke Suite that are abundant in this region.

Alternative interpretations of this lower crustal non-reflective zone is that it is a large alteration zone associated with crustal thickening, or a large zone of extensive deformation which has obliterated the earlier seismic fabric. Similar zones of reduced impedance contrast have been observed in mineralized regions; for example, in the lower crust beneath the Olympic Dam deposit in South Australia (Drummond et al., 2006). This was interpreted to be the source-region for the magma of the Hiltaba Suite granite hosting the deposit. All of these interpretations have merit, and the large non-reflective zone may be the result of a combination of these processes, where syndeformation magmatism has released and mobilized fluids.

Interpretation of seismic line 12GA-AF1

Seismic line 12GA-AF1 is 158.4 km long and has minor overlap with the eastern end of line 12GA-AF2. 12GA-AF1 is entirely within the Nornalup Zone and runs parallel to the coast, which is about 20–30 km to the south. At its western end the seismic line crosses the continuation of the approximately 50 km-wide shear zone system (Red Island Shear Zone to Heywood–Cheyne Shear Zone) that contains the Coramup Shear Zone, defined as the boundary between the Biranup and Nornalup Zones (see 'Coramup Shear Zone' section above). No MT data were collected along this line because it is located too close to the Southern Ocean.

Nornalup Zone

The western end of line 12GA-AF1 lies within granitic and mafic gneiss of the eastern Nornalup Zone (Fig. 1). In the field and geophysically, Paleoproterozoic granitic gneiss is indistinguishable from Mesoproterozoic granitic gneiss of the Recherche Supersuite, so their spatial distributions are difficult to map. Because of this, the geological subdivisions on line 12GA-AF1, and also in this region on the geological map (Plate 3), remain very general. Where possible, we have mapped out intrusions of the Esperance Supersuite based on magnetic character and shape (Plate 3), and as non-reflective or weakly reflective zones in the seismic image (Fig. 3; Plate 4). The interpretation of Esperance Supersuite granites as strongly magnetic, ovoid to elongate masses is supported by recent geochronology where homogeneous monzogranite with a locally developed, weak foliation trending 040° was dated at 1172 ± 5 Ma (GSWA 194849, preliminary data). The monzogranite gave high magnetic susceptibility readings in the field, and is located within a large, positive magnetic anomaly (Fig. 8). Small mafic pods and wisps within the monzogranite have even higher magnetic susceptibility readings that range 5000–8000 x 10^{-5} SI. This monzogranite occurs to the east of the southeasterly dipping Parmango Shear Zone (see below).

The western part of line 12GA-AF1 shows the eastern continuation of major shear zones described on line 12GA-AF2 (Red Island, Ridley, Coramup, Burdett, and Heywood–Cheyne Shear Zones) to great depths (Fig. 3). The Red Island Shear Zone continues to dip moderately to the southeast at depth, but flattens slightly before reaching the Coramup Shear Zone, which truncates it. It separates both the Biranup and Nornalup Zones from the underlying Yarraquin Seismic Province, which extends as far east as about CDP 4250. This is about 150 km across strike from the Jerdacuttup Fault, which marks the boundary between the Yilgarn Craton and the Northern Foreland. The Coramup, Burdett, and Heywood–Cheyne Shear Zones also flatten with depth and sole onto the Gunnadorrah Seismic Province (new name, after Gunnadorrah Homestead; Korsch et al., 2014) (Fig. 3). Beyond the Heywood–Cheyne Shear Zone to the east, no distinction between upper and middle crust is possible because there are no obvious differences in reflectivity. It is highly likely, however, that the lower crust, which comprises the Gunnadorrah Seismic Province, is more dense (mafic) and distinct from the middle to upper crust in this region (Murdie et al., 2014).

Between the Heywood–Cheyne and Parmango Shear Zones at CDP 4230, the crust in the seismic image is dominated by easterly dipping, highly reflective packages separated by a series of easterly dipping shear zones. The kinematic history of these shear zones is unknown, but curved reflections in the hanging walls could indicate

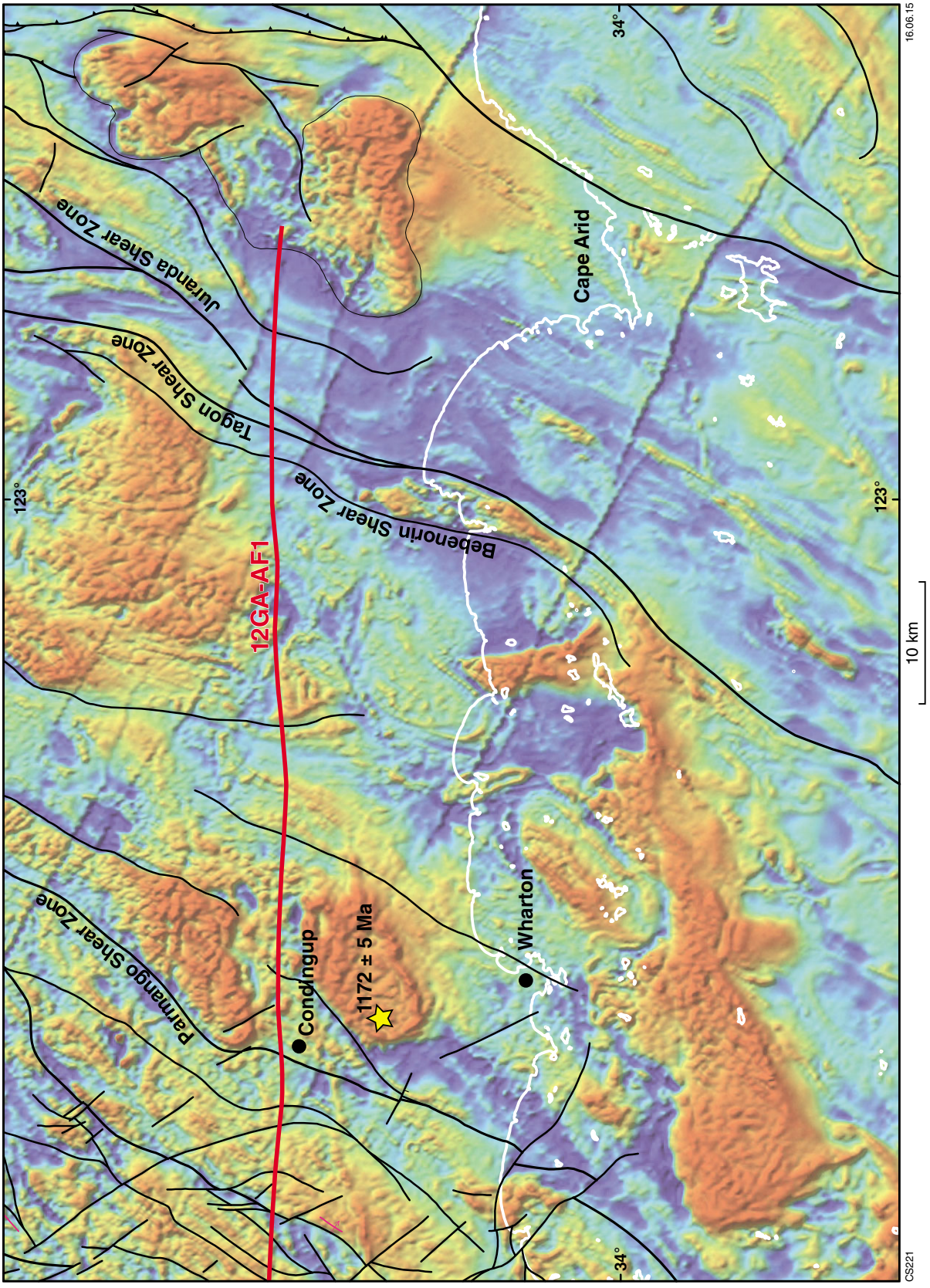

Figure 8. **Reduced-to-pole aeromagnetic image of part of the eastern Nornalup Zone, showing the eastern end of line 12GA-AF1, major shear zones, and strongly magnetic (in red) Esperance Supersuite intrusions. The location of dated sample GSWA 194849 (preliminary data), which is coincident with one of these intrusions, is shown.**

rollover anticlines and a dominant thrust sense of displacement. Alternatively, the curved reflections could have formed during inversion of extensional shear zones, or they could indicate S–C relationships and a normal movement sense. While shear zones are visible in the magnetic data, it is difficult to determine any shear sense. We have interpreted that this region is dominated by the Recherche Supersuite, which would include remnants of Nornalup Zone basement. The seismic packages, and the shear zones, are interpreted to have been intruded locally by irregularly shaped bodies of Esperance Supersuite granite.

East of the Parmango Shear Zone, stretching approximately 40 km east, is a large, variably reflective to non-reflective zone that appears to crosscut the southeasterly dipping shears, including the Parmango Shear Zone. The variably reflective to non-reflective zone thins at depth, and extends down to the middle crust to 7 s TWT (~21 km). We interpret that this zone is dominated by Esperance Supersuite granitic intrusions, where the deeper portion is inferred to be a residual source region from which magma was injected along several shear zones. An alternative interpretation is that this could be a large alteration zone related to shearing, and/or a conduit, which has obliterated any earlier structures.

The interpretation of the dominantly Esperance Supersuite granitic rocks in this area is consistent with the recently dated monzogranite described above (GSWA 194849, preliminary data) that occurs as a large ovoid, strongly magnetic body in the hangingwall of the Parmango Shear Zone. Rafts of highly reflective material, surrounded by the weakly reflective granitic material, are interpreted to be dominantly mafic in composition. These relationships, as imaged in the seismic line, may be considered large-scale analogues of the outcrops of magmatic rocks along the coast to the south, where phases of mingled granitic and mafic material have been successively intruded and deformed multiple times (Fig. 9). This coastal section runs parallel to the length of Fisheries Road, along which line 12GA-AF1 was acquired (Costelloe et al., 2014), and provides an important constraint on the interpretation. The coastal exposures are interpreted as a magma chamber, where crosscutting relationships of magma mingling textures, fabric formation, and net-veining are indicative of successive pulses of magma injection. The geochemistry of these rocks is consistent with occurrences of Recherche Supersuite intruded by Esperance Supersuite granites (Smithies et al., 2014).

This variably reflective to non-reflective zone ends at about CDP 6710, coincident with the moderately southeasterly dipping Bebenorin Shear Zone, which is just west of and parallel to the Tagon Shear Zone. The Tagon Shear Zone is a major structure that separates a northeasterly trending region of moderately to strongly magnetic granitic rocks to the west, from similar but less magnetic rocks to the east (Plates 2 and 3). In the hangingwall of the Tagon Shear Zone the upper crust is dominated by a series of easterly dipping listric shear zones. Curved reflections and internal shears are interpreted as rollover anticlines, indicating a dominant thrust sense of displacement for both the Tagon Shear Zone and the Juranda Shear Zone, which occurs just to the east. The listric Tagon Shear Zone links onto a flat-lying shear, interpreted as a sole thrust, which has a maximum depth of about 1.8 s TWT (~5 km).

Interpretation of seismic line 12GA-AF3

Seismic line 12GA-AF3 is 319.12 km long and commences in the Kurnalpi Terrane of the Yilgarn Craton from west to east, then crosses the entire east Albany–Fraser Orogen, and ends in the Madura Province to the east (Figs 1 and 4; Plates 2 and 4). The seismic line runs due east, from just east of Karonie through to Haig, following the Trans-Australian Railway. MT data were collected along this line and is currently being processed. The recently acquired Eucla–Gawler seismic line commenced at the eastern end of line 12GA-AF3 and followed the railway line across the border of Western Australia to as far east as the Gawler Craton in South Australia, where it tied to the north–south Gawler–Officer–Musgrave–Arunta (GOMA) seismic line. These data are currently being processed.

Yilgarn Craton and Northern Foreland

The westernmost part of seismic line 12GA-AF3 is broadly similar to the north-westernmost part of line 12GA-AF2, except that here the portion of the Yilgarn Craton that is crossed is the southeastern portion of the Kurnalpi Terrane of the Eastern Goldfields Superterrane. In contrast to line 12GA-AF2, the Northern Foreland on line 12GA-AF3 is only about 16 km wide, and lacks the Munglinup Gneiss (Fig. 4a; Plates 2 and 4). The Kurnalpi Terrane was imaged at the surface between CDP 6002 and the Cundeelee Shear Zone at CDP 7850. In this region, the seismic image shows that the Kurnalpi Terrane consists of a thin upper crust, which in general, is only weakly to moderately reflective, and variable in thickness, ranging from about 0.5 s TWT (~1.5 km) at about CDP 7070 to about 1.5 s TWT (~4.5 km) at about CDP 7900. This region of generally weakly reflective crust is interpreted to be dominated by granitic rocks, cut by northerly trending, east-dipping shear zones (Fig. 4a; Plates 2 and 4). A thin package of strong, moderately west-dipping reflections between CDP 6450 and CDP 6840 at 0.3 – 0.7 s TWT (~1–2 km depth) is interpreted as a mafic sill. This sill crosscuts a major, unnamed shear zone.

Below this upper crustal layer the middle to lower crust is highly reflective, and extends to the Moho. It is dominated by easterly dipping reflections and interpreted shear zones, some of which link to shear zones in the upper crust (Kurnalpi Terrane), showing a thrust sense of displacement of the upper crustal boundary. Because of the distinct change in the seismic character at the boundary between the upper and middle crust, and because we are unable to track the strong reflections in the middle to lower crust to the surface, at this stage we confine the Kurnalpi Terrane (sensu stricto) to only the upper crust, and define its base

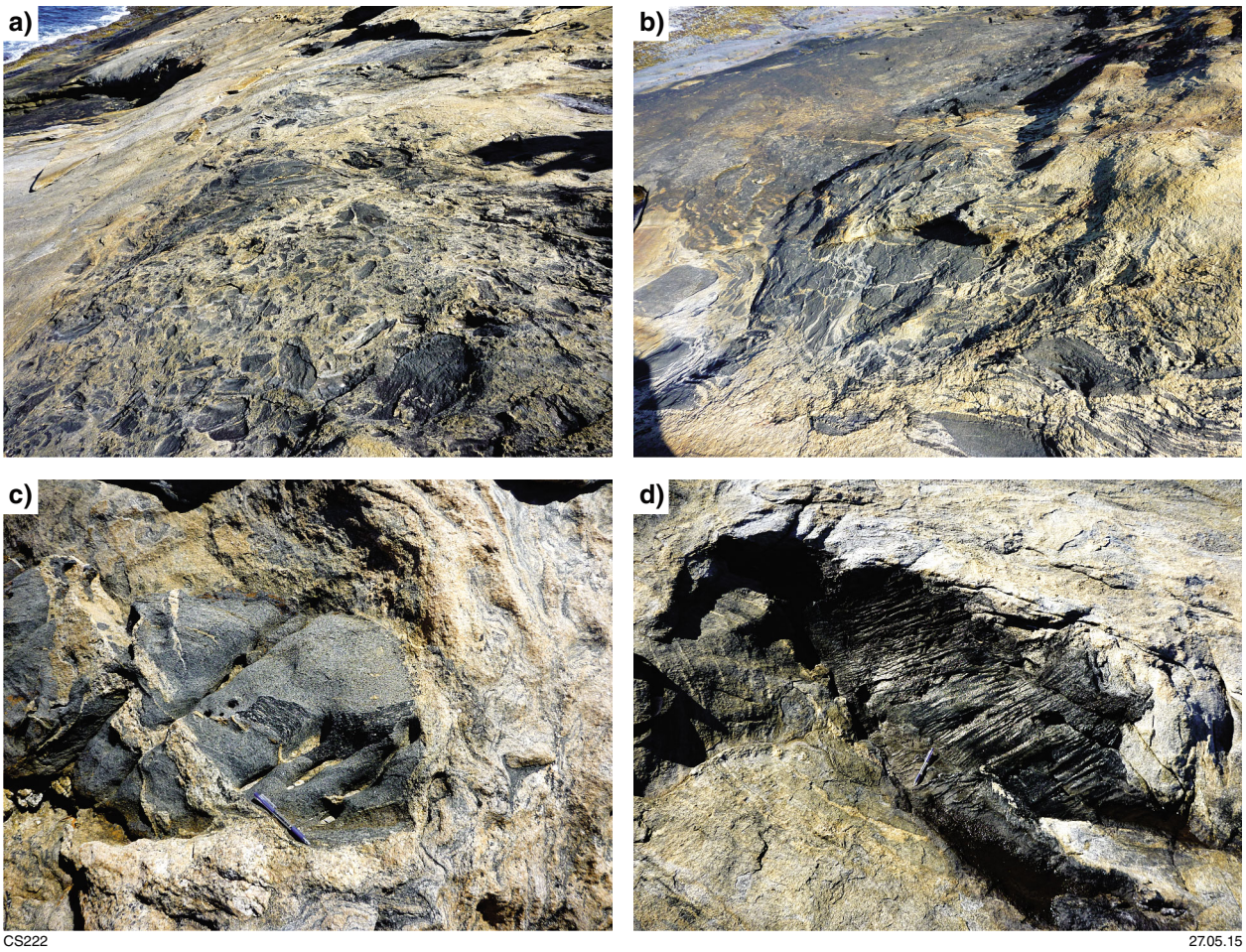

Figure 9. Photographs of magmatic rocks along the south coast east of Esperance, interpreted to be part of a Mesoproterozoic magma chamber imaged in 12GA-AF1: a) pods of mafic material with variable fabric development entrained in granite; b) net-veined mafic enclaves of variable size in deformed granite and gabbro; c) complex intrusive and fabric relationships in mafic enclaves within felsic magmatic rocks showing early fabric in inner mafic enclave (centre), entrained within a mafic enclave, overprinted by net-veining from the felsic host; d) detail of early crenulated mafic enclave enclosed in younger deformed granite gneiss. Note the difference in fabric orientation.

as the contact with the Udarra Seismic Province below (new name, after Udarra Soak; Korsch et al., 2014). The Udarra Seismic Province is defined as a discrete package of rocks which forms the current basement to the granite–greenstone rocks of the Kurnalpi Terrane. It extends from the western edge of the seismic section to the boundary with the Gunnadorrah Seismic Province at a depth of about 11 s TWT (~33 km) at about CDP 13 000, a distance of about 140 km. The Gunnadorrah Seismic Province is distinguished by its subhorizontal, moderately reflective and coherent seismic texture.

The moderately southeasterly dipping Cundeelee Shear Zone (CDP 7850) marks the boundary between the Yilgarn Craton and the Northern Foreland (Fig. 4a; Plates 2 and 4), but as described for line 12GA-AF2, this boundary is gradational and attributed to where a major change in deformation intensity can be mapped. The listric Cundeelee Shear Zone is interpreted as a thrust, placing the Northern Foreland over the Kurnalpi Terrane, and at depth it separates the Northern Foreland from the Udarra Seismic Province down to about 4.4 s TWT (~13 km depth). The Northern Foreland is internally deformed, has an east-dipping wedge-shaped geometry, and occurs in the footwall of the moderately to shallowly, east-dipping Frog Dam Shear Zone near the surface. The wedge-shaped geometry could be interpreted as the lower half of a duplex structure. The western half of the Northern Foreland has a similar seismic character to the Kurnalpi Terrane immediately to the west, being a weakly reflective zone. However, east of the Yellow Dam Shear Zone at CDP 8370, the seismic character changes to highly reflective, with a series of strong reflections dipping to the east and subparallel to the bounding Yellow Dam and Frog Dam shear zones. This zone corresponds with patchy, but distinctly linear, northeasterly trending magnetic anomalies that, in part, have defined the Yellow Dam Shear Zone (Plate 2). The Yellow Dam Shear Zone links to the Oak Dam Shear Zone at depth.

The Frog Dam Shear Zone separates the Northern Foreland from the Biranup Zone. It is a major thrust of extensive length, and has placed upper amphibolite to granulite facies Biranup Zone gneissic rocks over greenschist facies rocks of the Northern Foreland. The shear zone is distinct on magnetic imagery as a curvilinear feature, bounding rocks of lower magnetic intensity and fabric to the west from rocks with much more clearly defined magnetic fabric in the east, corresponding to the gneissic fabric in the latter. This interpretation is well supported by age constraints of granitic rocks from this area, which help delineate the boundary between the Northern Foreland and the Biranup Zone (e.g. metamonzogranite from the Northern Foreland dated at 2619 ± 6 Ma, GSWA 194792, preliminary data; metasyenogranite from the Biranup Zone dated at 1670 ± 7 Ma, GSWA 194727, Kirkland et al., 2012a). The Frog Dam Shear Zone appears to flatten at about 2.4 s TWT (~7 km depth), where an interpreted splay, the Signal Shear Zone, commences. At depth, the Frog Dam Shear Zone overrides and truncates the Oak Dam Shear Zone, and the latter becomes the boundary between the Biranup Zone and the underlying Udarra Seismic Province.

Biranup Zone

The Biranup Zone is dominated by highly reflective, easterly dipping reflective packages interpreted to be bound by subparallel shears. In the upper crust, rollover anticlines in the hanging walls of some shear zones indicate a predominant thrust sense of displacement. Major shear zones, such as the Frog Dam and Oak Dam Shear Zones, cut deep into the middle crust to the seismic provinces below. The highly reflective packages in the upper crust correlate with the upper amphibolite to granulite facies, dominantly granitic gneisses that occur in this region. These rocks extend about 50 km to the east, as far as the Fraser Shear Zone (previously named the Fraser Fault; Myers, 1985), which marks the western boundary of the Fraser Zone.

The granitic protoliths in this part of the Biranup Zone have been dated between 1690 and 1660 Ma (Kirkland et al., 2011a). To the west, and north of the Trans-Australian Railway, they include a succession that occurs along Ponton Creek, where granite has intruded psammitic rocks of the Barren Basin, and has been deformed at c. 1680 Ma during the Zanthus Event (Kirkland et al., 2011a). Similar rocks occur to the south of the Trans-Australian Railway. These rocks are in the footwall position to the fault-bound, c. 1665 Ma Eddy Suite (Plate 4; Kirkland et al., 2011a; Spaggiari et al., 2011), which lies between the easterly dipping Ponton Creek and Harris Lake Shear Zones, and forms a wedge that extends to 4.2 s TWT (~12.5 km depth). The Eddy Suite is dominated by mingled gabbroic and granodioritic rocks that have intruded sedimentary rocks of the Barren Basin. These intrusions represent some of the youngest igneous rocks in the Biranup Zone and indicate addition of a more isotopically juvenile, mantle component, mixed with older recycled crust (Kirkland et al., 2011b; Smithies et al., 2014). Where exposed to the south, the Eddy Suite is bound to the east by the Fraser Shear Zone, where it is interpreted to sole onto the Harris Lake Shear Zone at depth (Fig. 4; Plates 2 and 4).

Overall, on line 12GA-AF3, the Biranup Zone is imaged as a long, easterly dipping crustal slice that flattens at depth at about 6 s TWT (~18 km), where it becomes a subhorizontal slice up to about 15 km thick, which passes below the Fraser Zone, and overlies the eastern end of the Udarra Seismic Province and western parts of the Gunnadorrah Seismic Province. Where we cannot make a correlation with the surface geology we have termed the lower portion of the Biranup Zone 'middle to lower crust Biranup Zone'. We interpret this crust as an extension of the Biranup Zone at depth, although we cannot be certain of this. Another possibility is that it could be reworked Udarra Seismic Province, and include Biranup Zone intrusions. Some major shear zones, such as the Frog Dam Shear Zone, can be traced through to the lower crust as deep as the Gunnadorrah Seismic Province below. To the east, the Harris Lake Shear Zone links to the Fraser Shear Zone at depth, and both pass below the entire width of the Fraser Zone (Fig. 10).

Fraser Zone

The Fraser Zone is a large, Mesoproterozoic, sheeted complex of gabbroic and granitic rocks that have intruded sedimentary rocks of the Arid Basin (Spaggiari et al., 2011; Smithies et al., 2013). In the Fraser Zone, the exposed portion of these rocks that occur to the southwest are defined as the Fraser Range Metamorphics (Spaggiari et al., 2009), but where the metasedimentary component is dominant, such as along the northwestern margin of the Fraser Zone adjacent to the Fraser Shear Zone, they are mapped as the Snowys Dam Formation (Plates 2 and 3; Spaggiari et al., 2014b). No outcrop exists where seismic line 12GA-AF3 crosses the Fraser Zone, due to thick regolith cover over its western side, and the western part of the Eucla Basin to the east, so the interpretation of the units is based on outcrop along strike to the southwest, and gravity and magnetic data.

In seismic line 12GA-AF3, the Fraser Zone is imaged as a distinct V-shaped entity, bound to the west by the Fraser Shear Zone at CDP 11 100, and to the east by the westerly dipping Boonderoo Shear Zone at CDP 13 880, which marks the boundary with the eastern Nornalup Zone (Fig. 10). The maximum depth of the Fraser Zone is imaged at about 4.2 s TWT (~13 km), along the moderately, easterly dipping Fraser Shear Zone. When viewed together with its bounding shear zones, the V-shape becomes a Y-shape, where the tail of the Y is defined by the Fraser Shear Zone. This geometry is consistent with that modelled to the southwest using gravity and magnetic data, where sensitivity testing has shown it to be the most robust geometry (Brisbout et al., 2014). Internally, the V-shaped geometry is subdivided by easterly dipping shear zones in the west (Spy Hill, Heatwave, Transline, and Ballast Shear Zones), and westerly dipping shear zones in the east. Crosscutting relationships of these shear zones are complex, and probably reflect interleaving along strike, rather than simple back-thrusting along the westerly dipping shear zones. A large, broad antiform has been imaged on the eastern side of the Fraser Zone, between CDP 13 000 and CDP 13 400.

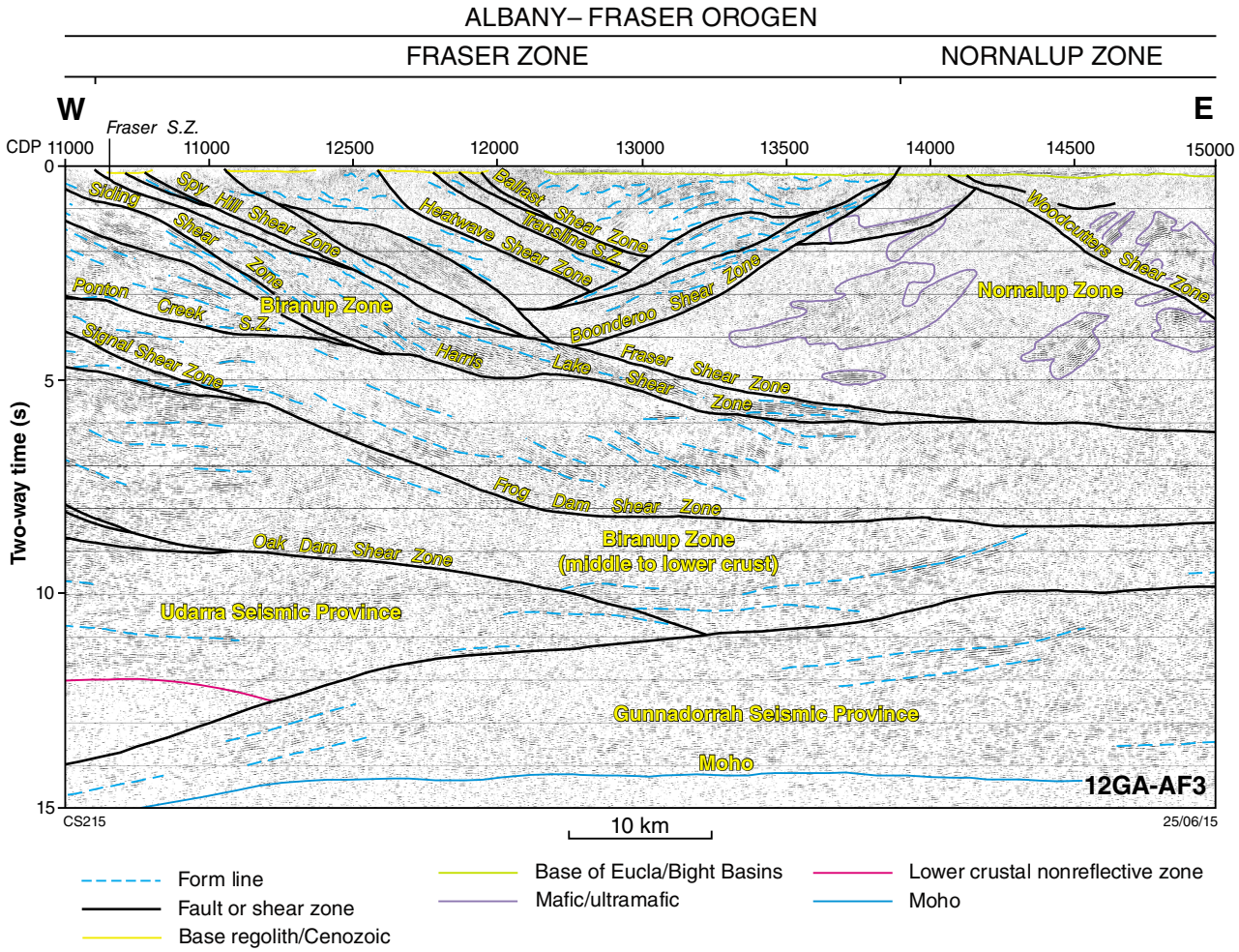

Figure 10. Detail of part of seismic line 12GA-AF3 showing the Fraser Zone

The subdivision in the V-shape is also evident in gravity and magnetic data, and is interpreted to reflect a more voluminous gabbroic package east of the Transline Shear Zone, similar to that on the eastern side of the Fraser Zone where it is exposed in the southwest, but as a separate fault-bounded slice. The western side is interpreted to reflect a greater proportion of metasedimentary material interlayered with metamorphosed gabbro and granite sheets. The strongly linear magnetic texture is interpreted to reflect this layering, but is overprinted by a strong to locally mylonitic fabric, particularly adjacent to the Fraser Shear Zone. These features are observed in outcrop to the southwest, where they show a similar magnetic texture (Spaggiari et al., 2011).

Nornalup Zone

On seismic line 12GA-AF3, the eastern Nornalup Zone lies between the Boonderoo Shear Zone at about CDP 13 880, and the East Rodona Shear Zone at about CDP 19 540 (Fig. 4b; Plates 2 and 3). In this region, the eastern Nornalup Zone is covered by rocks of the Eucla Basin and underlying Bight Basin. The seismic character is similar to the central part of the eastern Nornalup Zone on line 12GA-AF1; it is weakly reflective, and again interpreted to be dominated by granitic material. Because of the weak reflectivity, it has been difficult to map out specific units above the middle to lower crustal Biranup Zone, and Gunnadorrah Seismic Province. Much of the eastern Nornalup Zone in this region has been termed ‘Recherche Supersuite dominant’, although we recognize that the lower crust is possibly more dense and of different composition (Murdie et al., 2014), being a likely source region for much of the magmatic products observed at the surface. Intrusions of the Recherche and Esperance Supersuites appear to have masked much of the original Paleoproterozoic basement features, not only in the seismic data, but also in the magnetic and gravity data. Some of the more recognizable features in the geophysical data are described below.

Within the weakly reflective areas are subhorizontal, irregularly shaped, highly reflective zones interpreted as rafts or lenses within the dominantly granitic material. In the west, these are interpreted to be mafic in composition,

based on a stronger gravity signature indicative of denser material. In the east, the reflective material is interpreted as a combination of basement remnants and metasedimentary material. This is based in part on a lower gravity signature compared to the west, and also on the presence of Paleoproterozoic metasedimentary rocks in drillcore from about 80 km to the north of the seismic line that are intruded by both Recherche and Esperance Supersuite granites (Big Red prospect; Spaggiari et al., 2014b).

East of the Fraser Zone, the area of westerly dipping shear zones and reflections are truncated by the easterly dipping Woodcutters Shear Zone at CDP 14 070. This coincides with the western extent of a large, distinct, northwesterly trending gravity ridge and coincident magnetic high that extends as far east as the West Rodona Shear Zone, south of seismic line 12GA-AF3. The magnetic high is strongest in the northwest, and defines a set of tight, northwesterly trending folds that occur in the hangingwall of the Woodcutters Shear Zone.

To the east, between CDP 15 900 and CDP 17 850 on seismic line 12GA-AF3, both the magnetic susceptibility and gravity signature are much lower. This area is interpreted as dominantly Nornalup Zone basement, consisting of metasedimentary gneiss intruded by granitic rocks. The area is also coincident with a distinct change in strike orientation of the magnetic fabric, swinging from the zone of northwesterly trending, tight folding in the west, to an east–west fabric that is visible in the area of lower magnetic susceptibility to the east (Plate 2). This fabric is parallel to the seismic line, so although largely non-reflective and poorly imaged, would show as subhorizontal.

Rodona Shear Zone

The Rodona Shear Zone is an unexposed, major structure that can be traced in magnetic and gravity data along strike for over 500 km (Plates 2 and 3). The southern portion runs offshore around Point Culver, east of Israelite Bay, and the northern extent is deeply buried under the Officer Basin. Although the remainder is entirely under cover of the Eucla Basin, the Rodona Shear Zone is interpreted as the boundary between the eastern Nornalup Zone (and the Albany–Fraser Orogen) and the Madura Province, based on differences in what is known about the geological history from either side (see also Clark et al., 2000; Spaggiari et al., 2012, 2014b; Plates 2 and 3).

In seismic line 12GA-AF3, at CDP 18 810, the weakly reflective, subhorizontal reflections described in the eastern Nornalup Zone are truncated by a series of variable, but dominantly easterly dipping reflections of moderate strength, which define a zone about 14 km wide at the surface, and which extends to the eastern end of the seismic line at depth. This area corresponds with a complex zone of shear-related deformation interpreted in magnetic data, and mapped as the Rodona Shear Zone (Plates 2 and 3). Because of the width of the zone, we have named the western and eastern limits as the West Rodona and East Rodona Shear Zones, respectively (CDP 18 810 to 19 540; Plate 4). The Kinclaven Shear Zone lies within this zone, and links to the East Rodona Shear Zone at depth. The West Rodona Shear Zone extends to the Gunnadorrah Seismic Province at 8 s TWT (~24 km depth), but does not appear to cut through it.

Although unexposed, the unit within the Rodona Shear Zone is interpreted to be dominantly Recherche Supersuite, or at least of Albany–Fraser Orogen affinity, based on similarities in magnetic and gravity data with the adjacent Nornalup Zone. It is highly likely, however, that slices of Madura Province rocks also occur within the Rodona Shear Zone, and recent work suggests the Malcolm Metamorphics, which are exposed on the coast to the south, may be one such example (Plate 3; Spaggiari et al., 2014b).

The only rock record from within the Rodona Shear Zone is from drillcore from the Hannah 1 prospect, located to the south (northeast of Caiguna). This drillhole intersected a coincident magnetic and gravity high that has a boudin-like geometry. The drillcore contains metadiorite dated at 1170 ± 4 Ma (GSWA 182203, Kirkland et al., 2012b), and is part of the Esperance Supersuite. Similar geophysical anomalies occur to the north of this, mainly within the shear zone.

Kinematic history

In the magnetic data, the east–west fabric described between CDP 15 900 and CDP 17 850 on seismic line 12GA-AF3 in the eastern Nornalup Zone (see 'Nornalup Zone' section above) swings to a northeasterly trend adjacent to the northeasterly trending West Rodona Shear Zone. This foliation deflection is interpreted to be indicative of sinistral shear sense. Similar sinistral foliation deflections occur to the south, between the West Rodona and East Rodona Shear Zones. These locally cut interpreted thrusts suggest an earlier phase of thrusting which was responsible for the current easterly dip, overprinted by sinistral, possibly transpressional, shearing. The deformed c. 1170 Ma metadiorite from the Hannah Prospect drillcore indicates that at least the latest phase of deformation was after c. 1170 Ma.

Madura Province

Seismic line 12GA-AF3 crossed the westernmost part of the Madura Province, from the East Rodona Shear Zone at CDP 19 540, to the eastern end of the section. Very little is known about the Madura Province as it lies entirely under cover of the Eucla and Bight Basins, and only eight exploration drillholes have intersected the basement to reasonable depths (summarized in Spaggiari et al., 2012). The best known of these drillcores are those from the Loongana prospect, which lies to the east of the end of the seismic line (Plate 2). The Loongana drillholes are located over a distinct gravity anomaly, and intersected metagabbro, locally with peridotitic cumulate, interlayered with trondhjemitic plagiogranite (Spaggiari et al., 2014b). Both the metagabbro and metagranite have been dated between 1410 and 1400 Ma (see summary in Spaggiari et al., 2014b). The geochemistry and isotopic character

of these rocks, and also the metagabbroic rocks from both the Haig and Serpent drillcores nearby (Tillick, 2011; Tillick and Hunt, 2010), are consistent with the formation of an oceanic-arc, with little contribution from continental material, and indicates a largely oceanic setting for this part of the Madura Province at c. 1400 Ma (Spaggiari et al., 2014b). Collectively, these rocks are named the Haig Cave Supersuite (after Haig Cave).

In 2013, GSWA drilled two stratigraphic holes in the Madura Province; MAD002 and MAD014. MAD002 is located about 4 km north of CDP 20 660 (Fig. 11), and intersected basement at 389 m. Here, the basement consists of amphibolite schist interlayered with leucogranite veins and pods that are either parallel to the schistosity, or more locally, transgress it. The drillhole is coincident with a north-northeasterly trending, magnetic fabric of moderate susceptibility. In map view, this magnetic fabric occurs between the westerly dipping Pinto Shear Zone (CDP 20 500) and the westerly dipping Honeymoon Shear Zone (CDP 21 390), which, on the seismic section, overlies the gabbroic rocks of the Haig Cave Supersuite (Figs 4c and 11; Plates 2 and 4). In line 12GA-AF3, drillhole MAD002 occurs in weakly to non-reflective crust, which we have separated from the lower-upper to middle, more reflective crust. Interestingly, the Haig Cave Supersuite does not appear to have strong reflectivity, although, because it occurs at the far eastern edge of the section, it may not have been fully imaged.

The westerly dipping shear zones (Pinto, Anniversary, and Honeymoon Shear Zones (Fig. 11) either sole onto, or are cut by, the easterly dipping Diesel Shear Zone, which lies parallel to the East Rodona Shear Zone, and is probably related to that structure. In the magnetic data, the Honeymoon Shear Zone appears to be folded into two, along-strike antiforms cored by the Haig Cave Supersuite, but now cut by the unconformity of the overlying Bight Basin (Plate 2). One possibility is that the westerly dip of the reflectors and shear zones in this area may represent the western limb of a large, antiformal structure that has been truncated by the Rodona Shear Zone.

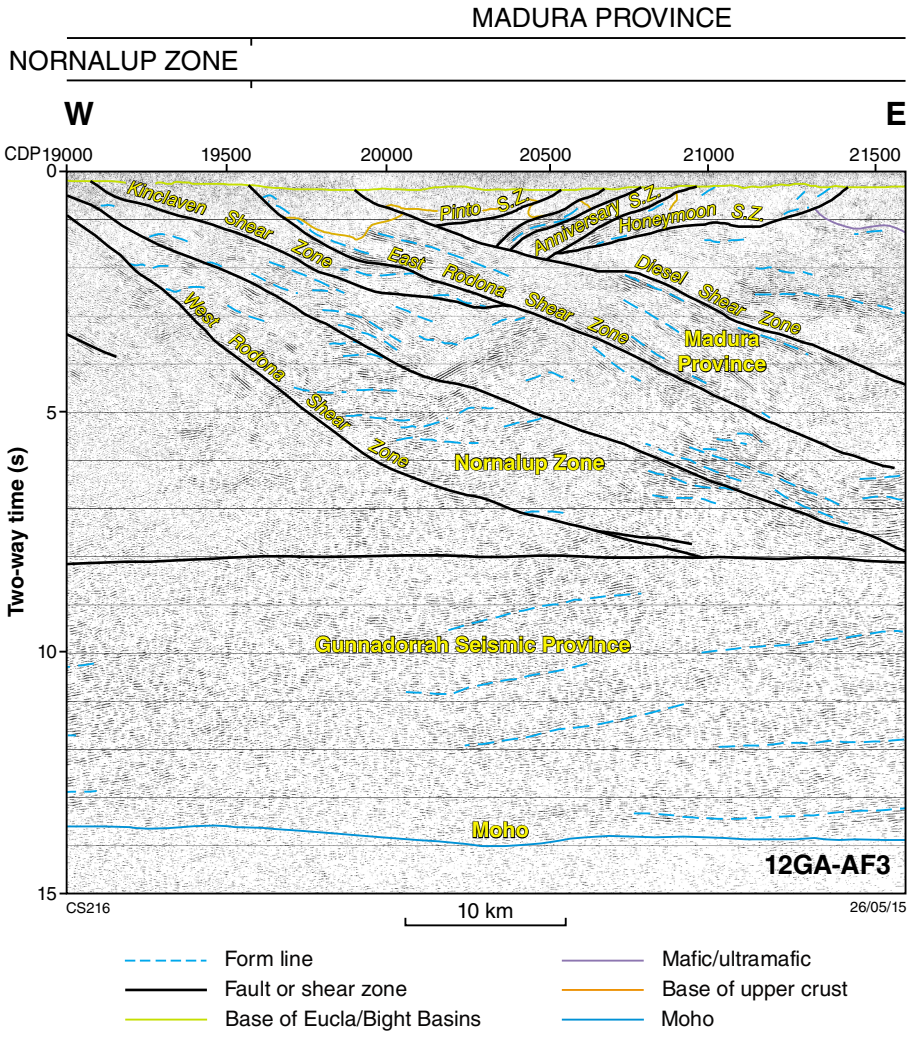

Figure 11. Detail of part of seismic line 12GA-AF3 showing the Madura Province

Lower crust on 12GA-AF3

The long length of 12GA-AF3 (319.12 km) has provided an image of the lower crust across the entire Albany–Fraser Orogen. Much of the lower crust, from beneath the Biranup Zone through to the eastern end of the section, is characterized by subhorizontal reflections with moderate to strong reflectivity, which is substantially different from the middle crust above it. Because of the difference in seismic character, this lower crustal zone is defined as the Gunnadorrah Seismic Province (Korsch et al., 2014). This seismic province is up to 5.5 s TWT (~16 km) thick at the eastern end, and gradually tapers to a thin wedge in the west.

The tapered western end of the Gunnadorrah Seismic Province lies beneath an interpreted low-angle, westerly dipping thrust at about CDP 10 650, which is also interpreted to cut through the Moho (Fig. 4a; Plate 4). The vertical displacement is estimated to be 2.3 s TWT (~7 km). An alternative interpretation is that the Moho is not faulted, but that the crust thickens considerably from about 13 s TWT (~39 km) at the western end of the line to about 16.3 s TWT (~49 km) centred below CDP 10 650, and then shallows eastwards to a depth of about 14 s TWT (~42 km) (Kennett, 2014).

Interestingly, this complication in the Moho coincides with another large zone of reduced impedance contrast (relatively non-reflective zone) of similar size to that interpreted on line 12GA-AF2. As in 12GA-AF2, the non-reflective zone occurs where the crust is thickest. However, there is no large, long wavelength gravity anomaly associated with the non-reflective zone on 12GA-AF3, and the modelling suggests a much less dense composition (Murdie et al., 2014). Nevertheless, as in 12GA-AF2, we have interpreted this non-reflective zone as a zone of crustal melt and melt residuals, which here can be interpreted as having a more felsic composition. Alternatively, as described above for 12GA-AF2, the non-reflectivity may be due to alteration, perhaps associated with magmatism and/or deformation.

Discussion

Crustal architecture and kinematics

The three seismic lines described above (12GA-AF2, 12GA-AF1 and 12GA-AF3) all show a series of structures with a predominant, moderate, easterly or southeasterly dip, particularly in the middle to upper crust. Most of these structures are interpreted as shear zones that show a thrust sense of displacement. This interpretation is consistent with mapped structures, both in magnetic data and in outcrop. As discussed below, however, it is highly likely that many of the thrusts are inverted, extensional structures. The truncated, westerly dipping shear zones in the Biranup Zone in seismic line 12GA-AF2 (Figs 2 and 7) could be interpreted as earlier extensional features representing the tops of tilted blocks. This would fit with a model of Paleoproterozoic extension and rifting (Spaggiari et al., 2014b). Seismic line 12GA-AF3 does not appear to preserve the same, early west-dipping structures in the Biranup Zone, perhaps because of the effects of the c. 1680 Ma Zanthus Event that has been recognized in this area (Kirkland et al., 2011a).

The prevalence of Albany–Fraser Orogeny, Stage II metamorphic dates throughout the east Albany–Fraser Orogen (e.g. Kirkland et al., 2011a, 2014a) is likely to reflect the formation of the present day crustal architecture imaged by the seismic data. These metamorphic dates are likely to constrain the timing of crustal thickening during folding and thrusting under relatively high temperature conditions (upper amphibolite to granulite facies), although more work is required to establish this. Thrusting during Stage II is supported by a recent study of the Mount Ragged Formation (Plate 3), which was deposited either during the late stages of, or after, Stage I of the Albany–Fraser Orogeny, and is interpreted to have a fold and thrust architecture (Waddell, 2014).

Thrusts have also been mapped in the central and west Albany–Fraser Orogen, particularly in relation to northwest-vergent folding in coastal exposures. At Bremer Bay, Paleoproterozoic Biranup Zone gneisses show large-scale, northwest-vergent, c. 1180 Ma F_3 folding, which is bracketed by two phases of boudinage (Spaggiari et al., 2009; Barquero-Molina, 2009). Northwest-vergent, asymmetric folding has also been mapped in the Mount Barren Group (see also Witt, 1998), and dates of xenotime and monazite of 1206 ± 6 and 1194 ± 8 Ma, respectively, were interpreted to record static overprinting of peak D_2 assemblages that were assumed to have formed during Stage I of the Albany–Fraser Orogeny (Dawson et al., 2003). However, given that no Stage I dates have been recorded in the Mount Barren Group, it is likely that these Stage II dates record both deformation and metamorphism during Stage II. Similar, northwest-vergent, asymmetric folds within the Biranup Zone were also mapped along the Pallinup River (Central Domain, Beeson et al., 1988), but these structures have not been dated. All of these areas have a similarity in the dominant northwest-vergent fold style, and the available geochronology suggests that this folding may have occurred more or less synchronously during Stage II of the Albany–Fraser Orogeny. Although largely unconstrained in timing, northwest-vergent folding is also commonly observed in the east Albany–Fraser Orogen, particularly in the Northern Foreland and Biranup Zone (Spaggiari et al., 2011).

Even though the Stage II timing is prevalent, at least one phase of thrusting may also have occurred during Stage I. For example, the folding and pop-up architecture of the Fraser Zone suggests a period of compression (see below), and the lack of Stage II dates within the Fraser Zone, coupled with the metamorphic Stage I dates (Clark et al., 2014), indicate that some exhumation and folding occurred during this time. Stage I metamorphism has also been recorded in the far northeast in the Gwynne Creek Gneiss (Plate 1), which contains refolded folds (Spaggiari et al., 2011).

Strike-slip shearing is also a feature of at least the late stages of the structural evolution of the Albany–Fraser Orogen, and is largely interpreted from magnetic data. It appears to be more prevalent towards the east, from between the Red Island and Heywood–Cheyne Shear Zones to the Rodona Shear Zone. In the latter, some thrusts appear to be cut by sinistral strike-slip shear zones (Plate 3). It is not clear whether these strike-slip shear zones are simply not imaged in the seismic data, or whether they have moderate dips, and may be transpressional structures. The seismic reflection technique can only image dips of structures up to about 60°. Overall, it is clear that much more work, particularly detailed fieldwork, is required to unravel the details of the timing and kinematics of the major shear zones throughout the Albany–Fraser Orogen, and their relationships with magmatism.

Structural emplacement of the Fraser Zone

In seismic line 12GA-AF3, the Fraser Zone is interpreted as a distinct V-shaped entity (Figs 4 and 10; Plate 4). The maximum depth of the Fraser Zone is imaged at about 4.2 s TWT (~13 km), along the moderately, easterly dipping Fraser Shear Zone. When combined with the V-shape of the Fraser Zone, the Fraser Shear Zone can be interpreted to form the tail of a Y-shape.

There are several ways the Y-shaped geometry could be interpreted to have formed, so it is relevant to provide a brief overview of the structures observed in the Fraser Range Metamorphics to the southwest. These rocks are dominated by a well-developed, northeasterly trending, predominantly steeply southeast-dipping, gneissic foliation. In general, this foliation is axial planar to tight to isoclinal, northeasterly trending folds of the layering, which are, in turn, cut by thrusts and shear zones. Deformation under high temperature conditions up to 850º C took place shortly after intrusion of the gabbroic and granitic sheets between about 1305 and 1290 Ma (Spaggiari et al., 2013; Clark et al., 2014). Evidence for this is provided by the dating of late, metagranitic veins containing large euhedral garnets that crosscut the foliation, dated at 1283 ± 8 Ma (Stage I; GSWA 194780, Kirkland et al., 2013b).

Major shear zones such as the Coramup and Heywood–Cheyne Shear Zones that occur to the southwest of the Fraser Zone (see sections 12GA-AF2 and 12GA-AF1) are interpreted to have an early history related to Paleoproterozoic extension. These large, crustal-scale shears are interpreted to have been utilized by the intrusion of the Fraser Zone sheeted complex during Stage I of the Albany–Fraser Orogeny (Spaggiari et al., 2014b), prior to the formation of the current bounding shear zones (Fraser, Newman, and Boonderoo Shear Zones). The relatively short time between intrusion and deformation and metamorphism suggests the stress field may have rapidly switched from extensional or transtensional (accommodating Mesoproterozoic magma emplacement) to contractional or transpressional (Spaggiari et al., 2013). This switch probably drove the first period of exhumation of the Fraser Zone along the bounding shear zones, possibly resulting in the formation of a pop-up architecture between the Biranup and Nornalup Zones (Spaggiari et al., 2013). This could account for the Y-shaped geometry, with initial formation of the Fraser and Harris Lake Shear Zones acting as the main floor thrusts during emplacement of the Fraser Zone over the Biranup Zone. At the same time, the formation of the Boonderoo and Newman Shear Zones as westerly dipping shear zones was probably accommodated by synmagmatic intrusions of the Recherche Supersuite into the eastern Nornalup Zone, softening and weakening the crust on the eastern side of the Fraser Zone.

Subsequent translational deformation, probably during Stage II of the Albany–Fraser Orogeny, is interpreted to have brought the Fraser Zone to its current location. This is indicated by lower temperature shear zone fabrics and the kinematics in the bounding shear zones to the southwest. These include discrete L-tectonites and L–S tectonites along the Newman Shear Zone, indicative of both vertical movement (southeast side up), and sinistral strike-slip movement. In contrast, mylonitic fabrics along the Fraser Shear Zone are all indicative of dextral shear (Spaggiari et al., 2011, 2013). The differential kinematics have been interpreted as wholesale southwestward translation of the Fraser Zone, contributing to the formation of the 'S-bend' termination (see Spaggiari et al., 2011). If correct, this implies that the initial intrusion and emplacement of the Fraser Zone during Stage I took place an unknown distance to the northeast.

Influence of magmatic processes on crustal architecture

Both seismic lines 12GA-AF1 and 12GA-AF3 show large areas of weak to non-reflective crust, within the eastern Nornalup Zone. We have interpreted the crust in these areas to have been heavily intruded by dominantly granitic rocks of the Recherche and Esperance Supersuites, as is evident from outcrop along the South Coast, east of Esperance (Plate 3). These areas, particularly those on 12GA-AF1, truncate dipping reflections and easterly dipping shear zones. Although more work is needed to constrain the interaction between deformation and magmatic emplacement processes, based on the relationships of fabrics within meta-igneous rocks that show repeated intrusion and deformation (Fig. 9), it is highly likely that the emplacement of these magmatic rocks was facilitated by shear zone development during deformation. The high temperature conditions and variable orientations of these sheeted intrusions have probably not produced coherent, linear, layered areas that would equate to well-defined, coherent reflections in the seismic data, perhaps with the exception of some of the rafts or large enclaves interpreted in 12GA-AF3. Hence, it is possible that these non-reflective zones may not always equate to the youngest intrusions, but may simply be areas dominated by variably oriented magmatic fabrics that do not produce coherent reflections in the seismic image.

Magmatic processes have played a significant role throughout the entire history of the Albany–Fraser Orogen, and all major tectonic events have been accompanied by voluminous magmatism (Spaggiari et al., 2014b; Smithies et al., 2014). This has no doubt left its mark on the structural fabric of the orogen.

Middle to lower crust

The middle to lower crust is dominated by easterly dipping reflections and interpreted shear zones that are generally shallow at depth and are truncated by, or sole onto the top of, the Gunnadorrah Seismic Province. These are punctuated by weakly reflective to non-reflective zones, some of which may relate to magmatic and/or alteration processes, as discussed above. Two of these features are distinct in the western part of the lower crust, one in line 12GA-AF2 and one in line 12GA-AF3. One interpretation of these non-reflective zones is that they are areas of crustal melt and melt residuals that do not contain coherent fabrics that can be imaged. They may also be large zones of alteration, possibly driven by magmatic processes linked to upper mantle heat. As discussed above, it is not clear whether these non-reflective zones are relatively early or late features, because, although in the 2D images they appear to be crosscut various shear zones, this may simply be because they do not contain fabrics or layers that image as coherent reflections.

Interpreting the middle to lower crust is problematic for many reasons, such as whether it is viable to extrapolate large, individual shear zones evident near the surface or in the upper crust downwards to the middle or lower crust. The question arises, how might the crust be partitioned vertically? In many localities the seismic images certainly do show consistent packages of reflections that can be traced long distances, but it is important to recognize that the interpretation of individual structures is simplistic and limited to 2D, and more likely reflects zones of particular rock packages in particular orientations. This means that caution should be exercized in extrapolating known structural relationships from the surface to the middle or lower crust.

Following on from this, the middle to lower crust contains regions of seismic character that cannot be correlated with the upper crust — the Yarraquin, Udarra, and Gunnadorrah Seismic Provinces. The age and origin of these seismic provinces are unknown, although both the Yarraquin and Udarra Seismic Provinces have also been interpreted below the Youanmi and Kurnalpi Terranes, respectively, which suggests they are likely to have an affinity with the Yilgarn Craton. Although the amount of craton-vergent, thrust-related displacement cannot be measured, this suggests that previous interpretations of isotopic and geochemical data, and models of extension and rifting (Kirkland et al., 2011a,b, 2014a; Smithies et al., 2013; Spaggiari et al., 2014b; Smithies et al., 2014), are consistent with the seismic interpretations presented here.

The Albany–Fraser Orogen has often been regarded as a Mesoproterozoic Grenvillian collisional orogen, but when the basin history and magmatic evolution are taken into account, it is clear that the orogen has been dominated by extensional processes throughout much of its history, particularly during the Paleoproterozoic (Clark et al., 2014; Spaggiari et al., 2014b; Smithies et al., 2014). The geometry of the listric or shallowly dipping to subhorizontal structures in the middle to lower crust are consistent with an extensional architecture, and are interpreted as inverted structures. Although speculative, the flat-lying geometry of the Gunnadorrah Seismic Province could indicate that this seismic province represents highly attenuated and modified Yilgarn Craton crust. However, the interpreted low-angle westerly dipping thrust that offsets the Moho in seismic line 12GA-AF3, is at odds with this. If the thrust was originally extensional, it would be expected to dip the other way, as most of the thrusts dip to the east or southeast. An extensional regime or detachment could, however, produce tilting of the Gunnadorrah Seismic Province to the west, although it is unclear how this might manifest itself in the lower crust or along the Moho. Alternatively, the inferred thrust could reflect subhorizontal wedging of the lower crust during compression, or, as indicated by Kennett (2014), the thrust may not exist, and there is simply a bulge in the Moho in this region. In addition, it is not clear whether the Rodona Shear Zone, which marks the eastern edge of the Albany–Fraser Orogen, truncates the Gunnadorrah Seismic Province, or soles onto it. Future work on the continuation of seismic line 12GA-AF3, the Eucla–Gawler line, should help clarify this.

Conclusions

The interpretation of the three seismic lines, 12GA-AF2, 12GA-AF1 and 12GA-AF3, described here has provided a 2D cross-section of the entire crust of the east Albany–Fraser Orogen. The interpretations show that the orogen has a dominantly east- to southeast-dip, that generally shallows or flattens at depth. Major shear zones are either truncated by, or sole onto, the Yarraquin, Udarra, or Gunnadorrah Seismic Provinces at depth.

The Coramup Shear Zone separates the Biranup Zone from the eastern Nornalup Zone, and although this shear zone and several subparallel major shear zones form one of the most significant shear zone systems in the orogen, it is not interpreted as a suture zone. This is because of the similarities in the geological evolution of the Biranup and Nornalup Zones, which together, form part of the Kepa Kurl Booya Province. Furthermore, in seismic line 12GA-AF3, the along-strike continuation of that boundary, here represented by the bounding shear zones of the Fraser Zone in the upper crust, shows the Biranup–Nornalup boundary as flat-lying beneath the Fraser Zone, and extending to the top of the Gunnadorrah Seismic Province to the east (Fraser and Harris Lake Shear Zones).

The middle to lower crust contains regions of seismic character that cannot be correlated with the upper crust — the Yarraquin, Udarra, and Gunnadorrah Seismic Provinces. The age and origin of these seismic provinces are unknown, although both the Yarraquin and Udarra Seismic Provinces have also been interpreted below the

Youanmi and Kurnalpi Terranes, respectively, which suggests they are likely to have an affinity with the Yilgarn Craton. This suggests that the Yilgarn Craton can be tracked under the Albany–Fraser Orogen at least as far as under the Fraser Zone in line 12GA-AF3, and at least halfway under the eastern Nornalup Zone in line 12GA-AF1, but beneath interpreted Biranup Zone. Although the amount of craton-vergent, thrust-related displacement cannot be measured, it is highly likely that this portion of the Yilgarn Craton was significantly extended and thinned during the Proterozoic, and, therefore, the generally listric to flat-lying structures represent an inverted, extensional architecture. This is consistent with the history of basin formation and magmatism in the orogen.

The seismic images also show large areas of weakly to non-reflective crust, where structures are interpreted to be masked by magmatic processes of deformation-related intrusion. This is consistent with the repeated history of voluminous magmatism in the orogen, leading to partial melting of the crust. An excellent example of this is the preservation of an interpreted magma chamber that is exposed on the South Coast east of Esperance, which may correlate with the variably reflective to non-reflective broad zone imaged in line 12GA-AF1.

References

Barquero-Molina, M 2010, Kinematics of bidirectional extension and coeval NW-directed contraction in orthogneisses of the Biranup Complex, Albany–Fraser Orogen, southwestern Australia: Geological Survey of Western Australia, Report 109, 205p.

Beeson, J, Delour, CP and Harris, LB 1988, A structural and metamorphic traverse across the Albany Mobile Belt, Western Australia: Precambrian Research, v. 40–41, p. 117–136, doi:10.1016/0301-9268(88)90064-2.

Bodorkos, S and Clark, DJ 2004a, Evolution of a crustal-scale transpressive shear zone in the Albany Fraser Orogen, SW Australia: 1. P–T conditions of Mesoproterozoic metamorphism in the Coramup Gneiss: Journal of Metamorphic Geology, v. 22, no. 8, p. 691–711, doi: 10.1111/j.1525-1314.2004.00543.x.

Bodorkos, S and Clark, DJ 2004b, Evolution of a crustal-scale transpressive shear zone in the Albany Fraser Orogen, SW Australia: 2. Tectonic history of the Coramup Gneiss and a kinematic framework for Mesoproterozoic collision of the West Australian and Mawson cratons: Journal of Metamorphic Geology, v. 22, no. 8, p. 713–731, doi: 10.1111/j.1525-1314.2004.00544.x.

Brisbout, LI, Spaggiari, CV and Aitken, ARA 2014, Integrating outcrop, aeromagnetic and gravity data: models of the east Albany–Fraser Orogen, *in* Albany–Fraser Orogen seismic and magnetotelluric (MT) workshop 2014: extended abstracts *compiled by* CV Spaggiari and IM Tyler: Geological Survey of Western Australia, Record 2014/6, p. 102–117.

Clark, DJ, Hensen, BJ and Kinny, PD 2000, Geochronological constraints for a two-stage history of the Albany–Fraser Orogen, Western Australia: Precambrian Research, v. 102, no. 3, p. 155–183.

Clark, C, Kirkland, CL, Spaggiari, CV, Oorschot, C, Wingate, MTD and Taylor, RJ 2014, Proterozoic granulite formation driven by mafic magmatism: An example from the Fraser Range Metamorphics, Western Australia v. 240, p. 1–21.

Costelloe, RD, Holzschuh, J and Fomin, T 2014, Acquisition and processing of the 2012 Albany–Fraser deep reflection seismic survey, *in* Albany–Fraser Orogen seismic and magnetotelluric (MT) workshop 2014: extended abstracts *compiled by* CV Spaggiari and IM Tyler: Geological Survey of Western Australia, Record 2014/6, p. 1–6.

Dawson, GC, Krapež, B, Fletcher, IR, McNaughton, N and Rasmussen, B 2003, 1.2 Ga thermal metamorphism in the Albany–Fraser Orogen of Western Australia: consequence of collision or regional heating by dyke swarms?: Journal of the Geological Society, London, v. 160, p. 29–37.

Drummond, B, Lyons, P, Goleby, B and Jones, L 2006, Constraining models of the tectonic setting of the giant Olympic Dam iron oxide–copper–gold deposit, South Australia, using deep seismic reflection data: Tectonophysics, v. 420, p. 91–103.

Hopkinson, A 2010, Salmon Gums Project EIS Report DA2009/076; Triton Gold Limited: Geological Survey of Western Australia, Statutory mineral exploration report, A088000 (unpublished).

Ivanic, TJ, Wingate, MTD, Korsch, RJ, Blewett, RS, Jones, LEA, Wyche, S, Zibra, I, Doublier, MP, Romano, SS, Pawley, MJ, Van Kranendonk, MJ, Gessner, K, Hall, CE, Chen, SF Patison, N and Costelloe, RD 2013, Preliminary interpretation of the Youanmi deep seismic reflection lines for Proterozoic intrusive rocks, *in* Youanmi and Southern Carnarvon seismic and magnetotelluric (MT) workshop *compiled by* S Wyche, TJ Ivanic and I Zibra: Geological Survey of Western Australia, Record 2013/6, p. 77–81.

Kennett, BLN 2014, The nature of the lithosphere in the vicinity of the Albany–Fraser seismic lines, *in* Albany–Fraser Orogen seismic and magnetotelluric (MT) workshop 2014: extended abstracts *compiled by* CV Spaggiari and IM Tyler: Geological Survey of Western Australia, Record 2014/6, p. 135–141.

Kirkland, CL, Spaggiari, CV, Pawley, MJ, Wingate, MTD, Smithies, RH, Howard, HM, Tyler, IM, Belousova, EA and Poujol, M 2011a, On the edge: U–Pb, Lu–Hf, and Sm–Nd data suggests reworking of the Yilgarn Craton margin during formation of the Albany–Fraser Orogen: Precambrian Research, v. 187, p. 223–247, doi:10.1016/j.precamres.2011.03.002.

Kirkland, CL, Spaggiari, CV, Wingate, MTD, Smithies, RH, Belousova, EA, Murphy, R and Pawley, MJ 2011b, Inferences on crust–mantle interaction from Lu–Hf isotopes: a case study from the Albany–Fraser Orogen: Geological Survey of Western Australia, Record 2011/12, 25p.

Kirkland, CL, Spaggiari, CV, Smithies, RH and Wingate, MTD 2014a, Cryptic progeny of craton margins: Geochronology and Isotope Geology of the Albany–Fraser Orogen with implications for evolution of the Tropicana Zone, *in* Albany–Fraser Orogen seismic and magnetotelluric (MT) workshop 2014: extended abstracts *compiled by* CV Spaggiari and IM Tyler: Geological Survey of Western Australia, Record 2014/6, p. 89–101.

Kirkland, CL, Wingate, MTD, Spaggiari, CV and Pawley, MJ 2012a, 194727: metasyenogranite, Uraryie Rock; Geochronology Record 1021: Geological Survey of Western Australia, 4p.

Kirkland, CL, Wingate, MTD, Hall, CE and Spaggiari, CV 2012b, 182203, metagabbro, Hannah prospect; Geochronology Record 1049: Geological Survey of Western Australia, 5p.

Kirkland, CL, Wingate, MTD, and Spaggiari, CV 2013a, 192507: granitic gneiss, Bishops Road; Geochronology Record 1088: Geological Survey of Western Australia, 4p.

Kirkland, CL, Wingate, MTD and Spaggiari, CV 2013b, 194780: granite pegmatite, Wyralinu Hill; Geochronology Record 1093: Geological Survey of Western Australia, 4p.

Kirkland, CL, Wingate, MTD and Spaggiari, CV 2014b, 192502: granitic gneiss, Aloa Downs; Geochronology Record 1157: Geological Survey of Western Australia, 4p.

Kirkland, CL, Wingate, MTD, and Spaggiari, CV 2014c, 192505: granitic gneiss, Bishops Road; Geochronology Record 1158: Geological Survey of Western Australia, 4p.

Kirkland, CL, Wingate, MTD, and Spaggiari, CV 2014d, 192508: granitic gneiss, Bishops Road; Geochronology Record 1159: Geological Survey of Western Australia, 4p.

Korsch, RJ, Blewett, RS, Wyche, S, Zibra, I, Ivanic, TJ, Doublier, MP, Romano, SS, Pawley, MP, Johnson, SP, Van Kranendonk, MJ, Jones, LEA, Kositcin, N, Gessner, K, Hall, CE, Chen, SF, Patison, N, Kennett, BLN, Jones, T, Goodwin, JA, Milligan, PM and Costelloe, RD 2013, Geodynamic implications of the Youanmi and Southern Carnarvon deep seismic reflection surveys: a ~1300 km traverse from the Pinjarra Orogen to the eastern Yilgarn Craton, *in* Youanmi and Southern Carnarvon seismic and magnetotelluric (MT) workshop *compiled by* S Wyche, TJ Ivanic I and Zibra: Geological Survey of Western Australia, Record 2013/6, p. 141–158.

Korsch, RJ, Spaggiari, CV, Occhipinti, SA, Doublier, MP, Clark, DJ, Dentith, MC, Doyle, MG, Kennett, BLN, Gessner, K, Neumann, NL, Belousova, EA, Tyler, IM, Costelloe, RD, Fomin, T and Holzschuh, J 2014, Geodynamic implications of the 2012 Albany–Fraser deep seismic reflection survey: a transect from the Yilgarn Craton across the Albany–Fraser Orogen to the Madura Province, *in* Albany–Fraser Orogen seismic and magnetotelluric (MT) workshop 2014: extended abstracts *compiled by* CV Spaggiari and IM Tyler: Geological Survey of Western Australia, Record 2014/6, p. 142–173.

Murdie, RE, Gessner, K, Occhipinti, SA, Spaggiari, CV and Brett, J 2014, Interpretation of gravity and magnetic data across the Albany–Fraser Orogen, *in* Albany–Fraser Orogen seismic and magnetotelluric (MT) workshop 2014: extended abstracts *compiled by* CV Spaggiari and IM Tyler: Geological Survey of Western Australia, Record 2014/6, p. 118–134.

Myers, JS 1985, The Fraser Complex: a major layered intrusion in Western Australia, in Professional papers for 1983: Geological Survey of Western Australia, Report 14, p. 57–66.

Myers, JS 1990, Albany–Fraser Orogen: Geological Survey of Western Australia, Memoir 3, p. 255–263.

Myers, JS 1995, Geology of the Esperance 1:1 000 000 sheet (2nd edition): Geological Survey of Western Australia, 1:1 000 000 Geological Series Explanatory Notes, 10p.

Nelson, DR 1995, 83697: biotite monzogranite gneiss, Mount Burdett; in Compilation of SHRIMP U–Pb zircon geochronology data, 1994: Western Australia Geological Survey, Record 1995/3, p. 56–58.

Occhipinti, SA, Doyle, M, Spaggiari CV, Korsch, R, Cant, G, Martin, K, Kirkland, CL, Savage, J, Less, T, Bergin, L and Foz, L 2014, Interpretation of the deep seismic reflection line 12GA-T1: northeastern Albany–Fraser Orogen, *in* Albany–Fraser Orogen seismic and magnetotelluric (MT) workshop 2014: extended abstracts *compiled by* CV Spaggiari and IM Tyler: Geological Survey of Western Australia, Record 2014/6, p. 52–68.

Smithies, RH, Spaggiari, CV, Kirkland, CL, Howard, HM and Maier, WD 2013, Petrogenesis of gabbros of the Mesoproterozoic Fraser Zone: constraints on the tectonic evolution of the Albany–Fraser Orogen: Geological Survey of Western Australia, Record 2013/5, 29p.

Smithies, RH, Spaggiari, CV, Kirkland, CL and Maier, WD 2014, Geochemistry and petrogenesis of igneous rocks in the Albany–Fraser Orogen, *in* Albany–Fraser Orogen seismic and magnetotelluric (MT) workshop 2014: extended abstracts *compiled by* CV Spaggiari and IM Tyler: Geological Survey of Western Australia, Record 2014/6, p. 77–88.

Spaggiari, CV, Bodorkos, S, Barquero-Molina, M, Tyler, IM and Wingate, MTD 2009, Interpreted bedrock geology of the south Yilgarn and central Albany–Fraser Orogen, Western Australia: Geological Survey of Western Australia, Record 2009/10, 84p.

Spaggiari, CV, Kirkland, CL, Pawley, MJ, Smithies, RH, Wingate, MTD, Doyle, MG, Blenkinsop, TG, Clark, C, Oorschot, CW, Fox, LJ and Savage, J 2011, The geology of the east Albany–Fraser Orogen — a field guide: Geological Survey of Western Australia, Record 2011/23, 97p.

Spaggiari, CV, Kirkland, CL, Smithies, RH, Wingate, MTD 2012, What lies beneath — interpreting the Eucla basement, in GSWA 2012 extended abstracts: promoting the prospectivity of Western Australia: Geological Survey of Western Australia, Record 2012/2, p. 25–27.

Spaggiari, CV, Kirkland, CL, Smithies, RH, Occhipinti, SA and Wingate, MTD 2014a, Geological framework of the Albany–Fraser Orogen, *in* Albany–Fraser Orogen seismic and magnetotelluric (MT) workshop 2014: extended abstracts *compiled by* CV Spaggiari and IM Tyler: Geological Survey of Western Australia, Record 2014/6, p. 12–27.

Spaggiari, CV, Kirkland, CL, Smithies, RH and Wingate, MTD 2014b, Tectonic links between sedimentary cycles, basin formation and magmatism in the Albany–Fraser Orogen, Western Australia: Geological Survey of Western Australia Report, Report 133, 63p.

Spaggiari, CV and Pawley, MJ 2012, Interpreted pre-Mesozoic bedrock geology of the east Albany–Fraser Orogen and southeast Yilgarn Craton (1:500 000), *in* The geology of the east Albany–Fraser Orogen — a field guide *compiled by* CV Spaggiari, CL Kirkland, MJ Pawley, RH Smithies, MTD Wingate, MG Doyle, TG Blenkinsop, C Clark, CW Oorschot, LJ Fox and J Savage: Geological Survey of Western Australia, Record 2011/23, Plates 1 and 1A.

Spaggiari, CV, Smithies, RH, Kirkland, CL, Howard, HM, Maier, WD and Clark, C 2013, melting, mixing, and emplacement: evolution of the Fraser Zone, Albany–Fraser Orogen, *in* GSWA 2013 extended abstracts: promoting the prospectivity of Western Australia: Geological Survey of Western Australia, Record 2013/2, p. 1–5.

Tillick, D 2011, Final Report of Co-funded Government – Industry Drilling Program at the Haig Prospect, Eucla Project, August 2011, Teck Australia Pty Ltd, 24p.

Tillick, D and Hunt, D 2010, Eucla Project, C283/2008, Combined Annual Report for the Period 1 April 2009 to 31 March 2010, Teck Australia Pty Ltd, 13p.

Waddell, P-J 2014, Sedimentological and structural evolution of the Mount Ragged Formation, Nornalup Zone, Albany–Fraser Orogen, Western Australia: Geological Survey of Western Australia, Report 129, 116p.

Witt, WK 1998, Geology and mineral resources of the Ravensthorpe and Cocanarup 1:100 000 sheets: Geological Survey of Western Australia, Report 54, 152p.

Interpretation of the deep seismic reflection line 12GA-T1: northeastern Albany–Fraser Orogen

by

SA Occhipinti[1], M Doyle[1], CV Spaggiari, R Korsch[2], G Cant[1], K Martin[1], CL Kirkland, J Savage[1], T Less[1], L Bergin[1], and L Fox[1]

Introduction and aims of the seismic survey

The Albany–Fraser Orogen in Western Australia consists of the southern and southeastern margins of the West Australian Craton (Fig. 1). The orogen contains components of the Yilgarn Craton preserved as fragments and basement to younger Paleoproterozoic and Mesoproterozoic rocks (Nelson et al., 1995; Kirkland et al., 2011; Spaggiari et al., 2011, 2014a). The east Albany–Fraser Orogen has been interpreted to extend northeast under younger sedimentary rocks of the Gunbarrel and Officer Basins towards the Musgrave Province, with a total potential strike length exceeding 1000 km (Kirkland et al., 2011). Along its northwestern margin the orogen is in both faulted contact with the Yilgarn Craton, and uncomformably overlain by the Carboniferous to Permian sedimentary sequences (Paterson Formation) that fill the Gunbarrel Basin.

Outcrop through the northeastern Albany–Fraser Orogen is very sparse due to widespread sand cover, and geological interpretation is largely reliant on public domain magnetic and gravity data (e.g. Spaggiari et al., 2011; Blenkinsop and Doyle, 2014). Integration of magnetic interpretations with geochronological and geochemical analysis of areas where outcrop or diamond drillcore is available, has guided regional-scale interpretations of the Precambrian basement (Plate 1; Kirkland et al., 2011; Spaggiari et al., 2011; Doyle et al., 2015).

Three deep seismic reflection surveys were acquired by Geoscience Australia (GA), the Geological Survey of Western Australia (GSWA), and the Australian National Seismic Imaging Resource (ANSIR during 2012; Plate 4). A fourth line was acquired in collaboration with Tropicana Joint Venture partners, AngloGold Ashanti Limited (70% and manager) and Independence Group NL (30%) through ANSIR. All four lines were processed by Geoscience Australia. Details of the data acquisition and processing are provided by Costello et al. (2014).

The northernmost seismic line (12GA-T1) traverses, from west to east, the Gunbarrel Basin, the Tropicana Zone (Tropicana Domain, Doyle et al., 2013) and the dominantly Paleoproterozoic Biranup Zone. The transect provides an insight into the deep crustal structure (Fig. 2; Plates 1 and 4) and crosses major faults and boundaries between geological domains of different ages. The line follows the sinuous route of the Rason Lake Road and thus is not perfectly perpendicular to the trend of the major structures and overall magnetic grain of the Precambrian basement. Major structures such as the Gunbarrel Fault, Blue Robin, Rusty Nail, and Sydney Simpson Shear Zones are crossed by the line. In addition to the acquisition of seismic reflection data, magnetotellurics (MT) data were also acquired along line 12GA-T1. The principal aims of acquiring the seismic reflection and MT data along line 12GA-T1 were to:

- establish the broad geological context of this gold endowed region within the broader Albany–Fraser Orogen
- ascertain the location and nature of the major crustal-scale faults, including those bounding the dominantly Archean (Tropicana Zone), Proterozoic (Biranup Zone) and Paleozoic (Paterson Formation) elements
- determine the deep crustal architecture of the Tropicana Zone
- clarify the relationship between the Tropicana Zone and the Northern Foreland (reworked Yilgarn Craton).

The northeastern, poorly exposed part of the Albany–Fraser Orogen contains the Tropicana gold deposit. The deposit was discovered in 2005 by the AngloGold Ashanti Greenfields exploration team, and is the largest greenfields gold discovery in Australia for the last decade (Kendall et al., 2007; Doyle et al., 2007, 2013). The Tropicana Deposit has a known strike length of approximately 5 km and comprises four known mineralized zones, which from north to south are: the Boston Shaker, Tropicana, Havana and Havana South Zones.

1 2601AngloGold Ashanti Ltd, Level 13, St Martins Tower, PO Box Z5046, Perth WA 6831

2 Minerals and Natural Hazards Division, Geoscience Australia, GPO Box 378, Canberra ACT 2601

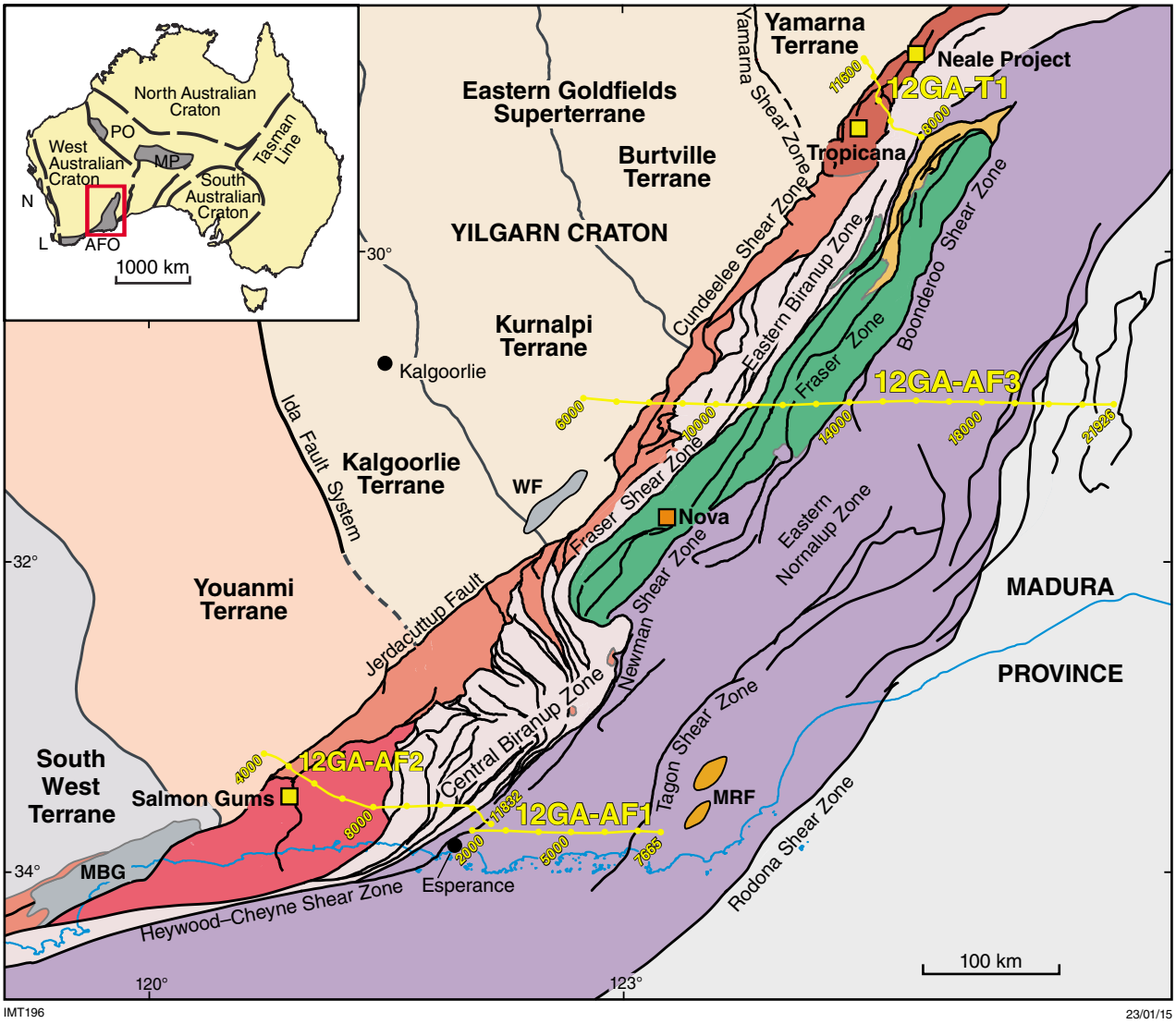

Figure 1. Simplified, pre-Mesozoic interpreted bedrock geology of the Albany–Fraser Orogen and tectonic subdivisions of the Yilgarn Craton (modified from Spaggiari et al., 2014c) showing the location of the Albany–Fraser deep crustal seismic reflection lines. Abbreviations used: MBG – Mount Barren Group; WF – Woodline Formation; MRF – Mount Ragged Formation. Inset: AFO – Albany–Fraser Orogen; MP – Musgrave Province; PO – Paterson Orogen; L – Leeuwin Province; N – Northampton Province

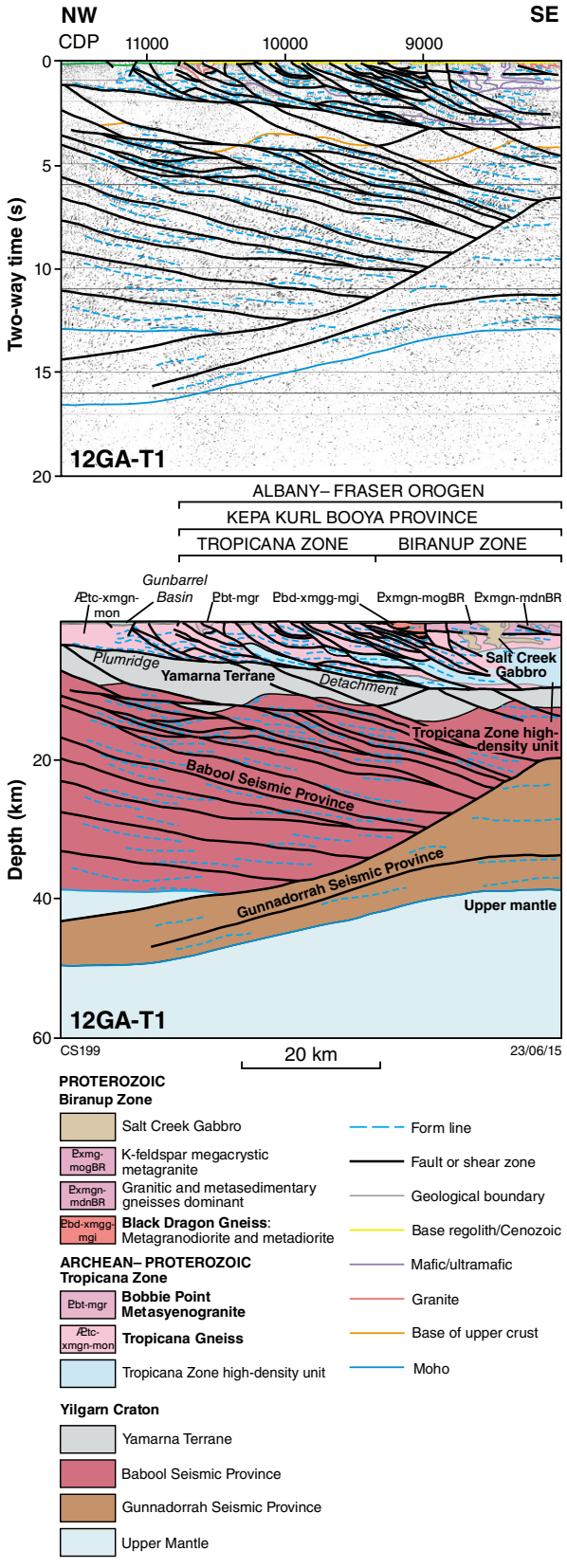

Figure 2. Interpreted linear (top) and solid (bottom) geology of deep crustal seismic line 12GA-T1 (extracted from Plate 4)

Resources as at December 2012 total 7.89 Moz of contained gold, including measured resources of 29.8 Mt at 2.12 g/t Au for 2.03 Moz, indicated resources of 76.4 Mt at 1.95 g/t Au for 4.78 Moz and inferred resources of 11.9 Mt at 2.83 g/t Au for 1.08 Moz (Doyle et al., 2013). Processing of ore and recovery of gold commenced in 2013.

In this contribution we report the results of an interpretation of the 12GA-T1 seismic line, in the context of the geological interpretation undertaken in the region by AngloGold Ashanti geoscientists and GSWA. Our interpretation attempts to establish a geodynamic synthesis of the northeastern part of the Albany–Fraser Orogen which can explain the deep crustal architecture that has been interpreted from the 12GA-T1 seismic line.

Interpretation of seismic line 12GA-T1

The 12GA-T1 seismic line provides an image from the surface to the upper mantle down to 20 seconds two-way travel time (s TWT; ~60 km; Korsch et al., 2014). The crust can be mapped as either being reflective, reflective to moderately reflective, or relatively non-reflective.

From the surface to depths corresponding to approximately 3 s TWT (approximately 9 km), features such as a sedimentary basin sequences, granitic intrusions, and possible mafic intrusions are interpreted (Fig. 2; Plate 4). The upper crustal reflective to moderately reflective data shows features interpreted as major faults or shear zones. Structures identifiable in the seismic section correlate closely with the position of faults interpreted from regional magnetic data (Plates 1 and 4). In seismic line 12GA-T1, the apparent dips of structures are mostly shallow to moderate to the east or southeast. This interpretation is largely consistent with 3D models derived from the inversion of magnetic data that illustrates faults and shear zones with mostly moderate to shallow, east or southeasterly dips, or locally steep easterly dips. However, due to the 2D nature of the seismic line, and the variable orientations of structures relative to the orientation of the seismic line, the dips of the structures are apparent dips, as are the dip directions. Beneath the lower crust in line 12GA-T1 the Moho is defined by a contrast between lower crust (moderately reflective to reflective) and mostly non-reflective upper mantle (Fig. 2; Plate 4). The location and apparent dip of the Moho varies considerably along seismic line 12GA-T1. The discontinuity is present at depths as shallow as 13 s TWT (39 km) and as deep as approximately 16.5 s TWT (49.5 km). This variation in the depth of the Moho is interpreted to represent the base of two different seismic provinces that have been juxtaposed along a low-angle fault located near common depth point (CDP) 10 550, with a vertical displacement of the Moho across the fault of about 3.5 s TWT (10 km), indicating a thrust movement sense (Korsch et al., 2014). The fault has an apparent moderate northwest dip, and can be traced upwards into the middle crust to a depth of about 6.6 s TWT (19 km) at the southeastern end of the seismic line.

To the northwest, the Moho discontinuity is interpreted to lie at about 13 s TWT (about 39 km) beneath the Babool Seismic Province, which Korsch et al. (2013) considered to be a section of middle to lower crust underlying the reworked Yamarna Terrane. To the southeast, the Moho underlies the newly defined Gunnadorrah Seismic Province to a depth of 16.5 s TWT (49.5 km; Korsch et al., 2014).

The upper crustal part of line 12GA-T1 is dominated by an interpreted parautochthonous unit, here named the Tropicana Zone of the Kepa Kurl Booya Province (see below). The Tropicana Zone is in fault contact with the Yilgarn Craton to the northwest, and with the Northern Foreland to the southwest (Fig. 1; Plates 1 and 4). In the northwest, the Tropicana Zone is overlain by the Carboniferous to Permian Gunbarrel Basin, and to the east is in fault contact with the Biranup Zone. The Tropicana Zone is considered to have a distinctly different geological history to the adjacent Northern Foreland, that occurs to the southwest (see also Blenkinsop and Doyle, 2014; Kirkland et al., 2014). Within the Tropicana Zone, major structures include the Pipeline, Phoenix, Rusty Nail, Angel Eyes, Tumbleweed, Thorny Devil, Black Dragon, Blue Robin, Chimera, and Sydney Simpson Shear Zones (Figs 3 and 4; Plates 1 and 4). These all lie above a distinctive set of strong reflections with an apparent shallow southeast dip, here named the Plumridge Detachment. This forms the boundary between the Tropicana Zone and the underlying reworked Yamarna Terrane. Most of the named shear zones mentioned above, including the Plumridge Detachment, have shallow to moderate, east or southeast apparent dips. Exceptions include the Phoenix, Chimera and Sydney Simpson Shear Zones that appear to dip steeply towards the east to southeast.

Upper crustal units and seismic provinces

In the Albany–Fraser Orogen and adjacent Yilgarn Craton, the upper crust can be divided into several distinct tectonic units, based on geological mapping, interpretation of geophysical datasets, drillhole data, and geochemical and geochronological studies (Spaggiari et al., 2009, 2011, 2014a; Kirkland et al., 2014; Smithies et al., 2014). In seismic line 12GA-T1, these include the Yamarna Terrane of the Yilgarn Craton and the Northern Foreland and Kepa Kurl Booya Province of the Albany–Fraser Orogen. The Kepa Kurl Booya Province comprises the Tropicana, Biranup, Fraser, and Nornalup Zones, which together define the crystalline basement of the Albany–Fraser Orogen (Spaggiari et al., 2009, 2011). The Northern Foreland is defined as the clearly recognizable, reworked component of the Yilgarn Craton that lies between the craton and Kepa Kurl Booya Province, that is, in the foreland position (Myers, 1990; Spaggiari et al., 2009). In general, the tectonic units are separated by major faults or shear zones, which in seismic line 12GA-T1 do not always directly correspond with previously interpreted upper crustal geology.

The Tropicana Zone occurs in the upper crustal part of the section and contains gneissic units that are either exposed, or are close to the present-day surface (described as the Plumridge Terrane by Blenkinsop and Doyle, 2014; Doyle et al., 2014, 2015). The Yamarna Terrane is identifiable in the upper crustal part of the section, but does not extend to the surface, with its shallowest point at about 1.2 s TWT (3.6 km). The Babool and Gunnadorrah Seismic Provinces occupy the middle to lower crustal region imaged in line 12GA-T1. The seismic character of these tectonic units and the seismic provinces are described in detail by Korsch et al. (2014).

Tropicana Zone

The Tropicana Zone is a newly defined tectonic unit that includes the Tropicana gold deposit, and extends an unknown distance under cover to the northeast. It is approximately 27 km wide in the Tropicana mine region, and is bound to the east by the Biranup Zone and to the west by the Gunbarrel Fault, and Gunbarrel Basin (Figs 1 and 3; Plate 1). Its eastern boundary is defined by Blenkinsop and Doyle (2014) as the northeast-trending Black Dragon Thrust (herein called the Black Dragon Shear Zone). However, in interpreting seismic line 12GA-T1, it was found that the boundary between the Tropicana Zone (defined by the extent of the Tropicana Gneiss) and Biranup Zone is the Sydney Simpson and Blue Robin Shear Zones, which are also interpreted to have thrust displacements, and overlie the Black Dragon Shear Zone (Plates 1 and 4). The southern boundary of the Tropicana Zone, and contact with the Northern Foreland, is interpreted as a thrust, located approximately 45 km south-southwest of the Tropicana Gold Mine (Fig. 1; Plate 1).

The principal units of the Tropicana Zone are the Archean Tropicana Gneiss (defined around the Tropicana gold deposit and from sparse outcrops) and the Hercules Gneiss defined around Beadell Resources' Neale Project area, including the Hercules and Atlantis prospects, northeast of Tropicana (Fig. 3; Kirkland et al., 2014). The Tropicana Zone also includes younger Paleoproterozoic rocks that either overlie, or intrude, the Archean basement. The Hercules Gneiss, which lies completely under regolith and Permian Paterson Formation cover and is only known from drillcores, is dominated by granulite facies, Archean felsic to intermediate (dioritic) granitic gneiss (Kirkland et al., 2014). Outcrop of the Tropicana Gneiss is sparse, thus observations are largely restricted to analysis of drillcore sampled by the AngloGold Ashanti – Independence Group NL's Tropicana Joint Venture mineral exploration project. The Tropicana Gneiss is dominated by amphibolite to granulite facies felsic and mafic gneiss, foliated metagranite, chert, quartzite and banded meta-iron formation (Doyle et al., 2009; Fox-Wallace, 2010; Blenkinsop and Doyle, 2014). Although the Tropicana Gneiss is mostly in fault contact with the younger (Paleoproterozoic) Biranup Zone rocks, intrusions of Biranup Zone-related Paleoproterozoic igneous rocks into both the Tropicana Gneiss and Hercules Gneiss suggest that, like the Biranup Zone, the Tropicana Zone had the

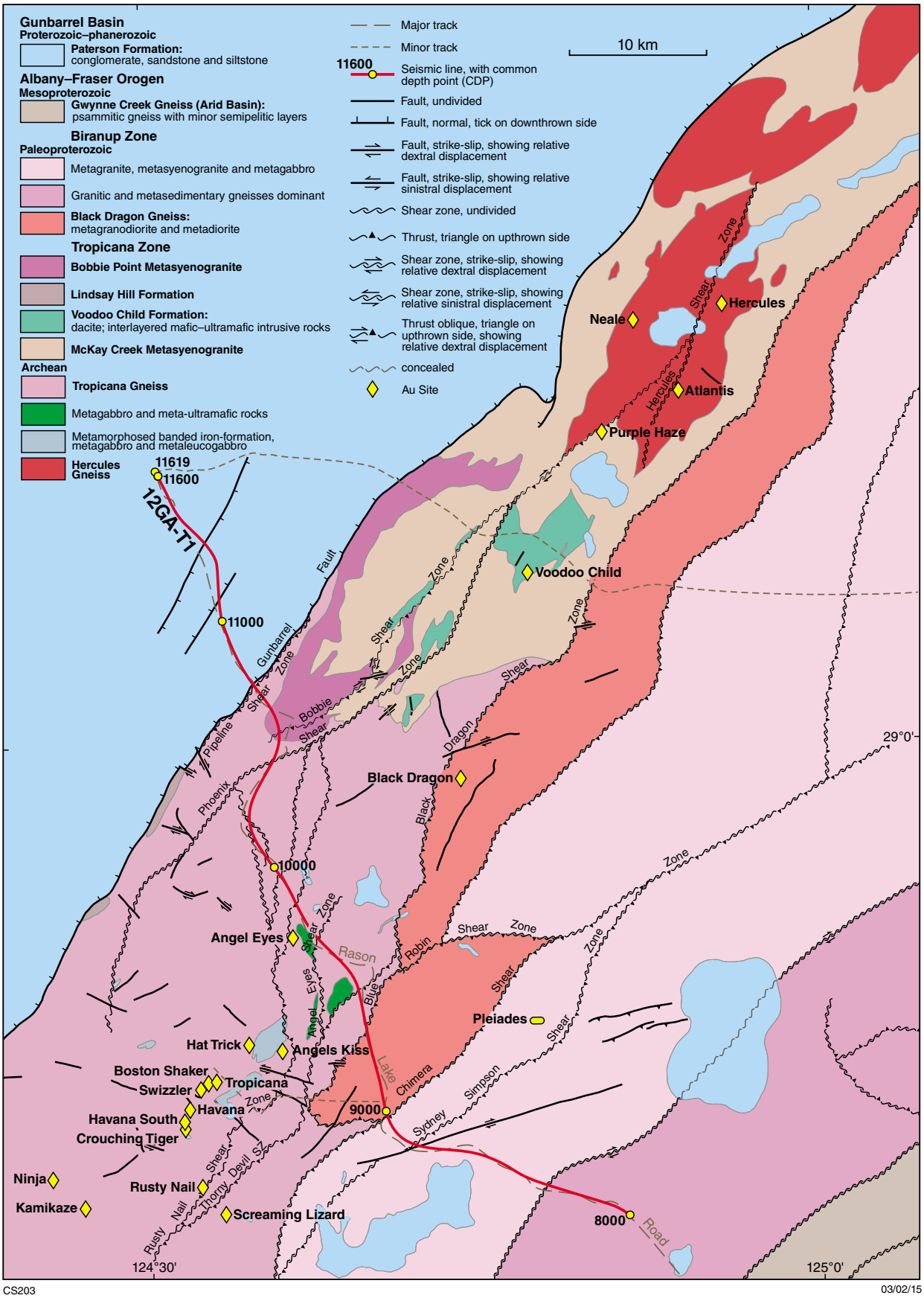

Figure 3. Pre-Mesozoic interpreted bedrock geology of the northeastern Albany–Fraser Orogen showing the Tropicana Zone (simplified from Plate 1)

same, autochthonous relationship to the Yilgarn Craton during the Paleoproterozoic (Kirkland et al., 2011, 2014).

In seismic line 12GA-T1, the Tropicana Zone is reflective to moderately reflective and occupies only the upper crust. It thins from southeast to northwest, from about 3.2 s TWT (about 10 km depth) below CDP 8002 to about 1.2 s TWT (about 3.6 km) below CDP 11 617. The Tropicana Zone has been broadly subdivided into two components in the seismic interpretation. The main component is taken to represent the high-grade gneissic rocks (Tropicana Gneiss) observed in drillcore and in outcrop from the region. This package of rocks exhibits moderate to locally weak reflectivity in seismic line 12GA-T1. Another, more reflective package is also present both within and beneath the Tropicana Gneiss and has been interpreted as a separate unit named herein the 'Tropicana Zone high-density unit'.

The Tropicana Zone high-density unit thickens to the east. The location of this more reflective unit is broadly coincident with a regional gravity high. The top of the region of high-gravity response has been calculated through inversion of the regional and detailed gravity data by AngloGold Ashanti geophysicists and is located at about 3.4 km below the present landform surface. This corresponds with the top of the highly reflective unit at the southeastern end of seismic line 12GA-T1. Alternatively, the higher gravity response may be in part due to the Gunnadorrah Seismic Province being thicker in the southeast than in the northwest, as illustrated by Murdie et al. (2014).

Geochronology and mineralization

A detailed account of the deformation and metamorphism of the Tropicana gneissic rock package and formation of the Tropicana gold deposit is given in Blenkinsop and Doyle (2014) and the geochronology of the zone is described in Doyle et al. (2015) and in Kirkland et al. (2014).

In recent years efforts have been made by GSWA, AngloGold Ashanti and Independence Group's Tropicana Joint Venture, and Beadell Resources to understand the age, origin and tectonothermal history of the Tropicana and Hercules Gneisses. The following is a summary of what is known with regards to the ages of protolith rocks, their metamorphism, and the timing of mineralization hosted in the Tropicana and Hercules Gneisses in the Tropicana Zone.

Moderately foliated granite exposed northwest of the Tropicana Gold Mine is one of several occurrences that have yielded Archean dates within the Tropicana Zone (MGA Zone 51, 650037E, 6770830N; GSWA 182435, Kirkland et al., 2013a). The metagranite is equigranular, heavily retrogressed, and contains K-feldspar rich veins that are subparallel to a foliation (Kirkland et al., 2013a). Zircons from this metagranite contain oscillatory zoning, consistent with igneous crystallization. However, these oscillatory zoned zircons commonly contain unzoned rims and are highly rounded in nature, which is consistent with them having crystallized under high-grade metamorphic conditions (Kirkland et al., 2013a; Rubbato et al., 2001; Möller and Kennedy, 2006; Korhonen et al., 2013). Moreover, the low U content and high Th/U ratio (1.4 – 2.72) of these unzoned rims are consistent with crystallization under very high-grade metamorphic conditions (Möller and Kennedy, 2006; Korhonen et al., 2013), rather than with igneous crystallization. A date of 2722 ± 15 Ma was obtained from analyses of the oscillatory zoned cores from four zircons extracted from the foliated granite and interpreted to represent the magmatic crystallization age of the granite (Kirkland et al., 2013a). A much younger date of 2640 ± 1 Ma on 10 analyses from the unzoned highly rounded rims is likely to represent a high-grade metamorphic overprint of the granite. Kirkland et al. (2013a) noted the alternative that the c. 2640 Ma age could be the igneous crystallization age of the granite, with the older c. 2722 Ma being an inheritance age. However, our preferred interpretation is that the 2640 ± 10 Ma date records the age of high-grade metamorphism, whereas the older c. 2722 Ma date is the age of igneous crystallization of the metamorphosed granitic rock.

In the Tropicana Zone, orogenic gold mineralization occurred after high-grade metamorphism at c. 2520 Ma (Doyle et al., 2013, 2015; Blenkinsop and Doyle, 2014). The gold mineralization event was associated with the formation of biotite and pyrite in the deposit and its timing is constrained by the 2515 ± 8 Ma $^{40}Ar/^{39}Ar$ age of biotite, and a late Archean Re–Os date from pyrite (Doyle et al., 2013, 2015). The gold mineralization at Tropicana is unlike many typical Archean lode gold deposits in that it is not directly associated with quartz and carbonate veining. Blenkinsop and Doyle (2014) suggest that a U–Pb date from rutile of 2524 ± 8 Ma recording cooling through 500–550°C, and the $^{40}Ar/^{39}Ar$ date of 2515 ± 8 Ma from biotite, are both consistent with exhumation along a retrograde path from peak granulite facies metamorphism to greenschist facies. Recent work by Kirkland et al. (2014) suggests that granulite facies zircon growth occurred continuously in the Hercules Gneiss between 2718 and 2554 Ma, implying that the Tropicana Zone represents a deep crustal level of neo-Archean crust. The deeply rooted Tropicana Zone likely remained in the granulite facies field between about 2700 and 2550 Ma. This was prior to initial exhumation through amphibolite facies at c. 2520 Ma, into greenschist facies crustal levels at about 2515 Ma. This period of exhumation is coeval with gold mineralization and with a deformation and metamorphic event called the Tropicana Event that impacted and refertilized the dehydrated gneissic crust (Doyle et al., 2015). Thus, the Tropicana Event reflects exhumation on a retrograde path from peak granulite-facies metamorphic conditions (Doyle et al., 2014, 2015).

Much of the gold at Tropicana was precipitated in K-feldspar-rich host rocks — either quartzofeldspathic orthogneiss or K-feldspar-rich pegmatitic rocks that originated from the local partial melting of the rock package (Doyle et al., 2009). The K-feldspar-rich pegmatitic rock and the enclosing quartzofeldspathic orthogneiss commonly contain gradational boundaries supporting the suggestion that the pegmatitic rock may have formed as a diatexitic migmatite (Mehnert, 1968;

Sawyer, 2008) due to partial melting and alteration of the host rocks that enclose it, and the introduction of a metasomatic, hydrothermal fluid. The timing of migmatization is not well constrained.

The temperature and pressure of gold mineralization at Tropicana has not been precisely determined; however, it is likely to have formed above 350°C (Doyle et al., 2013) in the greenschist facies, supported by the observation that gold mineralization is associated with greenschist facies assemblages. For example, biotite with pyrite and gold replaces metamorphic biotite and amphibole, in shear zones defined by elongate biotite and pyrite in some parts of the deposit (Blenkinsop and Doyle, 2014). In other zones at Tropicana, biotite–sericite and minor chlorite assemblages (stable in the greenschist facies) crystallized in both shears and exsolution fabrics in brecciated K-feldspar pegmatitic rocks, and are associated with gold mineralization (Blenkinsop and Doyle, 2014).

Kirkland et al. (2011) interpreted granitic gneisses and foliated metagranites to have been tectonically reworked during multiple Paleo- to Mesoproterozoic events, as evident in other parts of the Albany–Fraser Orogen. Dating of late Paleoproterozoic granitic veins within the Tropicana Zone support this suggestion, although many of the gneisses in the Tropicana Zone appear to have escaped significant Paleo- to Mesoproterozoic deformation and metamorphism, as evident from the preservation of their Archean gneissic fabrics (see Blenkinsop and Doyle, 2014; Kirkland et al., 2014).

Yilgarn Craton – Yamarna Terrane

The Archean granite–greenstones of the Yilgarn Craton are part of the West Australian Craton. The Yilgarn Craton consists of several granite–greenstone terranes that formed between 3730 and 2620 Ma (Cassidy et al., 2006). In the northern part of the Albany–Fraser Orogen, the reworked Yamarna Terrane is interpreted to be present only in the upper crust, beneath the low-angle Plumridge Detachment, which separates it from the Tropicana Zone (Figs 2 and 4; Plate 4). This detachment is approximately 300 m wide and has an apparent shallow dip to the east or southeast, similar to its true dip on the basis of structures interpreted from the magnetic data and measured in drillcore (Blenkinsop and Doyle, 2014). The base of the reworked Yamarna Terrane is in contact with the Babool Seismic Province (see below).

The reworked Yamarna Terrane is a relatively non-reflective seismic unit without clearly defined structures, although it is probable that the reworked Yamarna Terrane has been faulted because parts of the terrane appear to be offset from each other. These faults mostly dip moderately to the southeast (apparent dips). However, one fault beneath about CDP 9000 has an apparent dip to the northwest. The non-reflective reworked Yamarna Terrane may have been segmented by extensional faults, stepping down from northwest to southeast. For example, the base of the reworked Yamarna Terrane in the northwestern part of the section at about CDP 11 400 is at about 3.2 s TWT (9.6 km), whereas in the southeastern part of line 12GA-T1 it is deeper at about 4.2 s TWT (12.6 km). The thickness of the reworked Yamarna Terrane also varies considerably along the line. In the northwest and central parts, it is up to about 6 km thick, whereas in the southeast it is approximately 3 km thick. This change in thickness could be due to tectonic reworking consisting of:

- extension of the unit from northwest to southeast (i.e. thinning of the unit to the southeast)
- both extension of the unit from northwest to southeast and displacement of parts of the terrane due to overthrusting of the Tropicana Zone.

The extensional structures are likely to have formed sometime between 2635 and 2520 Ma. This age is bracketed by the age of the youngest Archean rocks in the Yamarna Terrane (c. 2635 Ma; Korsch et al., 2013) and the probable age of formation of the Plumridge Detachment that cuts them, separating them from the overlying Tropicana Zone. The main movement along the Plumridge Detachment can be bracketed by the 2700–2640 Ma protolith and metamorphic ages of orthogneisses in the Tropicana Zone, and the overprinting greenschist facies event that has been dated at c. 2520 Ma (Blenkinsop and Doyle, 2014).

The Babool and Gunnadorrah Seismic Provinces

The Babool Seismic Province was first defined by Korsch et al. (2013) as the highly reflective middle to lower crust that occurs below the Yamarna Terrane in the Yilgarn–Officer–Musgrave (YOM) seismic survey. Herein, the Babool Seismic Province is used to describe the moderately to strongly reflective middle and lower crust that extends beneath the reworked Yamarna Terrane across the whole of seismic line 12GA-T1 (Fig. 2). The base of the Babool Seismic Province is bound to the east by a west-dipping fault that separates it from the Gunnadorrah Seismic Province, and also offsets the Moho. Korsch et al. (2014) suggest that the Babool Seismic Province corresponds to older basement below the Yamarna Terrane, based on the presence of xenocrystic zircons as old as c. 2940 Ma in rocks within the Yamarna Terrane, and older isotopic model ages (Wyche et al., 2012; Pawley et al., 2012).

The Gunnadorrah Seismic Province has only recently been defined, and is interpreted to be present in the middle to lower crust in all four Albany–Fraser Orogen seismic lines (Korsch et al., 2014). It is suggested that the Gunnadorrah Seismic Province forms a continuous unit to the south, as it is interpreted to be present in the lower crust beneath the Nornalup Zone in seismic line 12GA-AF3, and even farther south on lines 12GA-AF1 and 12GA-AF2 (Spaggiari et al., 2014b; Korsch et al., 2014). In line 12GA-T1, the Gunnadorrah Seismic Province contains moderately reflective middle to lower crust that can be imaged to depths of about 16.5 s TWT (49.5 km) below CDP 10 800. The offset of seismic reflections in the lower crust suggest that the Gunnadorrah Seismic Province has been underthrust beneath the Babool Seismic Province. The Gunnadorrah Seismic Province appears to truncate shear zones in the Babool Seismic Province, which

suggests that it was juxtaposed after these shear zones formed. These shear zones could be as old as Neoarchean, given that they occur in both the Babool Seismic Province and the upper crustal reworked Yamarna Terrane. However, like the upper crustal Yamarna Terrane itself, some of these shear zones are demonstrably cut by the Plumridge Detachment, and therefore are likely to have formed between c. 2635 and 2520 Ma (Blenkinsop and Doyle, 2014).

Biranup Zone and related rocks in the Tropicana Zone

On seismic line 12GA-T1, the Biranup Zone is bound to the west by the Blue Robin Shear Zone, and extends to the southeastern end of the line. Although rocks of the Biranup Zone are mostly in fault contact with the older Tropicana Gneiss, both map and field relationships show that Biranup Zone-related rocks have intruded the Archean rocks of the Tropicana Zone, as well as Yilgarn Craton rocks of the Northern Foreland (Spaggiari et al., 2011, 2014a; Plates 1, 2 and 3). These relationships are supported by geochronological and Lu–Hf data (Kirkland et al., 2011, 2014). In addition, metasedimentary rocks of the Paleoproterozoic Barren Basin were deposited on both the Yilgarn Craton and the Tropicana Zone (Spaggiari et al., 2011, 2014c). Paleoproterozoic rocks, which include the volcano-sedimentary rocks of the Voodoo Child Formation (Fig. 3; Plate 1), have all been metamorphosed in the greenschist facies in the Tropicana Zone (Less, 2013). However, south of the Tropicana Zone rocks of the Biranup Zone, and some Barren Basin rocks, are of upper amphibolite or granulite facies (Spaggiari et al., 2011, 2014c).

In the area around seismic line 12GA-T1, igneous intrusives are dominantly metagranites, although locally metaleucogabbro, metamelanogabbro and metaperidotite are also present. Geochronology by GSWA and AngloGold Ashanti geologists of Paleoproterozoic rocks in the Tropicana Zone has been mainly restricted to areas of outcrop, generally north and east of the Tropicana deposit. The results indicate that there may be several groups of Paleoproterozoic Biranup Zone-related components in the Tropicana Zone, including:

- metamorphosed granodiorite, quartz diorite, and diorite of the Black Dragon Gneiss (in seismic section 12GA-T1, above and below the Blue Robin Shear Zone) dated at about 1815–1800 Ma (Blenkinsop and Doyle, 2014)
- metamorphosed syenogranite, dacite, and leucogabbro of the Voodoo Child Formation and McKay Creek Metasyenogranite, dated at c. 1760 Ma (Kirkland et al., 2012a; Less, 2013; Doyle et al., 2013; Blenkinsop and Doyle, 2014). Sedimentary rocks from nearby include quartzite of the Lindsay Hill Formation (Barren Basin) that has a maximum depositional age of c. 1990 Ma (Kirkland et al., 2013b)
- various metagranitic rocks in the vicinity of seismic line 12GA-T1 have been dated at c. 1708 Ma (Bobbie Point Metasyenogranite), c. 1690 to 1670 Ma (Pleiades Lakes area, Biranup Zone), and c. 1627 Ma (Kirkland et al., 2010a,b, 2012b,c).

Rocks in the Voodoo Child gold prospect occur in a distinctive zone that can be delineated in the magnetic data. This zone is distinguished by sharp, northeast-trending bounding faults to the east and west that separate it from a zone of generally lower magnetic intensity on either side. Along its southern margin, east-northeast trending faults are interpreted and may form geological boundaries to this domain. The presence of a restricted sequence of sedimentary rocks and an ultramafic–mafic to felsic intrusive succession suggests that the Voodoo Child Formation may have been deposited in a Paleoproterozoic pull-apart basin overlying the Tropicana Zone. This may have been within a distal back-arc basin setting, in response to Paleoproterozoic subduction to the east of the region (cf. Spaggiari et al., 2011, 2014c).

Less (2013) suggested that gold mineralization at the Voodoo Child prospect occurs as two main styles:

- Within intrusions of biotite- and sericite-altered microgranodiorite, commonly hosting amoeboid patches of coarse-grained or micrographic granitoid, where electrum grains are associated with chalcopyrite, pyrite, and sphalerite, concentrated in the coarser granitoids
- Associated with biotite–sericite ± silica alteration principally affecting locally metamorphosed quartz diorite, with Au–Ag mineralization accompanying disseminated pyrite.

According to Less (2013), these styles are indicative of intrusion-related mineralization. At Voodoo Child this may be manifested by apophyses of a larger mineralized or fertile granitoid intrusion at depth, from which fluids have preferentially mineralized a reactive quartz diorite (Less, 2013). Deep-seated, long-lived structures are suggested to have provided the plumbing for magmatism and mineralization at Voodoo Child (Less, 2013). Biranup Zone rocks in the northeastern part of the orogen, and in the vicinity of seismic line 12GA-T1, have a greenschist-facies metamorphic overprint, as do the Paleoproterozoic rocks that intrude the Tropicana Zone. This metamorphic overprint is associated with sericite and epidote alteration of plagioclase, actinolite–tremolite alteration of igneous hornblende in gabbroic rocks, and sericite overprinting highly strained igneous feldspars in granitic rocks (AngloGold Ashanti petrology report, unpublished). Locally, Paleoproterozoic granitic rocks in the Tropicana Zone are moderately to strongly foliated, or are mylonitic. In these cases, the foliation or mylonitic fabric is generally northeast trending, and shear sense indicators around feldspar porphyroclasts indicate dominantly dextral kinematics (e.g. Bobbie Shear Zone, northeast of Tropicana). However, mapping to the east in the Biranup Zone in the Pleiades Lakes region, about 20 km northeast of the eastern part of seismic line 12GA- T1, shows more complex relationships and at least three phases of deformation, including mylonite formation and folding (Stokes, 2014).

Gnowangerup–Fraser Dyke Suite

The east-northeasterly trending Gnowangerup–Fraser Dyke Suite consists of dolerites and gabbros that have intruded the southern Yilgarn Craton and Northern Foreland during Stage II of the Albany–Fraser Orogeny. The suite is part of the Marnda Moorn large igneous province, which extends from the western Yilgarn Craton through to the Albany–Fraser Orogen, and has an average age of c. 1210 Ma (Wingate et al., 2005). Northeasterly trending dykes that intrude the Tropicana Zone cross seismic line 12GA-T1, but are not imaged. In aeromagnetic data these dykes clearly crosscut major structures and have been interpreted as part of the Gnowangerup–Fraser Dyke Suite, but attempts to date them have been unsuccessful (Doyle et al., 2014).

Salt Creek Gabbro

A north-northeast trending zone of mottled magnetic response crosses seismic line 12GA-T1 between CDP 8830 (coincident with the Sydney Simpson Shear Zone) and about CDP 8450 (Fig. 5; Plates 1 and 4). During an early 2000s Ni–Cu–PGE exploration drilling project, Mithril Resources Limited intersected a sequence of metasedimentary rocks, including pelite, amphibolite and quartz–plagioclase–biotite–garnet gneiss intruded by mafic rocks, to the south of seismic line 12GA-T1 (Mithril Resources Limited, 2003, 2005).

The mafic intrusive bodies have variable compositions and mineral assemblages, and have been described as quartz diorite gabbro, gabbro, oligoclase–labradorite–orthopyroxene–clinopyroxene–biotite–magnetite–quartz gabbro, and plagioclase–clinopyroxene–biotite–ilmenite–magnetite–apatite gabbro. Locally, these rocks are weakly mineralized, for example, late actinolite–pyrrhotite–pyrite–chalcopyrite was reported in one sample (Mithril Resources Limited, 2003, 2005).

Based on aeromagnetic data, Mithril Resources Limited (2003, 2005) asserted that the mafic intrusions formed a series of post-tectonic igneous bodies with diameters ranging 2–12 km. They suggested that the intrusions occur along a belt 150 km long and up to about 10 km wide, inferred to have formed along an Archean–Proterozoic suture, and emplaced within varied lithologies and units with differing tectonic histories. For example, in areas closest to the east, and therefore closer to the high-metamorphic grade Fraser Zone, Mithril Resources Limited noted that the rocks intruded are of a higher metamorphic grade than observed elsewhere — described as mafic granulite facies rocks — whereas elsewhere they have intruded into amphibolite facies metasedimentary, felsic or mafic igneous rocks, including graphitic phyllite in the west (Mithril Resources Limited, 2003, 2005).

The gabbroic intrusions were informally named the Salt Creek Complex by Mithril Resources Limited (2003, 2005). The term 'complex' is usually reserved for units comprising a series of related intrusions, so herein it is renamed with the simpler term Salt Creek Gabbro. The unit is only known through limited drillcore (described above), and does not crop out. However, the ovoid to rounded apparent magnetic lows in the magnetic images that largely characterize this zone are coincident with the drilled gabbroic rocks, which return high magnetic susceptibility measurements (Mithril Resources Limited, 2003). This indicates that these rocks have been remanently magnetized and have not been metamorphosed to temperatures higher than the Curie temperature for magnetic minerals (mostly magnetite, about 577°C Curie temperature). The Salt Creek Gabbro appears to intrude the Northern Foreland, and Tropicana and Biranup Zones, and cut-thrust faults with apparent moderate to low-angle east, or southeast dips (Fig. 5). The magnetic texture of the unit along with the absence of evidence for post-emplacement metamorphism suggests that the gabbro was emplaced during or after Stage II (1225–1140 Ma) of the Albany–Fraser Orogeny. The Salt Creek Gabbro may be part of the Gnowangerup–Fraser Dyke Suite, emplaced at c. 1210 Ma, or represent a younger event.

The zone of mottled magnetic response extends northeast of line 12GA-T1, to the Pleiades Lakes area, where it has been interpreted as due to remanence effects in strongly magnetic metagranite and metagabbro of the Biranup Zone (Spaggiari et al., 2011). Whereas this interpretation was based on the only outcrop within the area of mottled magnetic texture, it is feasible that younger intrusions of the Salt Creek Gabbro may underlie Biranup Zone rocks in this area.

Gunbarrel Basin

The late Carboniferous to early Permian Paterson Formation occurs in the region imaged in seismic line 12GA-T1, between the Gunbarrel Fault at CDP 10 760 and the northwestern end of the line at CDP 11 671. The sedimentary sequence unconformably overlies rocks of the Tropicana Zone (Fig. 4). Inversion of magnetic data over the Gunbarrel Basin adjacent to the Tropicana Zone indicates that the depth of the basin could be up to about 1 km.

Drillhole information in the area shows that glaciogenic sedimentary rocks are present to depths of at least 300 m (Anglogold Ashanti, unpublished data); however, along the seismic line 12GA-T1, below CDP 11 200, the Gunbarrel Basin extends to about 600 m depth. It is not known whether glaciogenic rocks are present down to 600 m in this part of the basin. However, 215 km to the south at around MGA Zone 51, 525517E, 6622646N, drillhole data reported by Tulloch Resources in the southernmost part of the Gunbarrel Basin indicates that 557 m of Permian glacial siliciclastic rocks unconformably overlie the Cundeelee Intrusion, a carbonatite complex, suggesting that the lower parts of the Gunbarrel Basin imaged in seismic line 12GA-T1 are glaciogenic rock. Regional interpretation of the Gunbarrel Basin suggests that it has a narrow, northeast striking half-graben geometry, typically with steep westerly to northwesterly dipping normal faults separating it from the Northern Foreland and Tropicana Zone to the southeast (Fig. 4; Plates 1 and 4). These faults are interpreted to have facilitated rapid deepening of the basin in this region, perhaps forming a wedge-shaped geometry shallowing to the northwest.

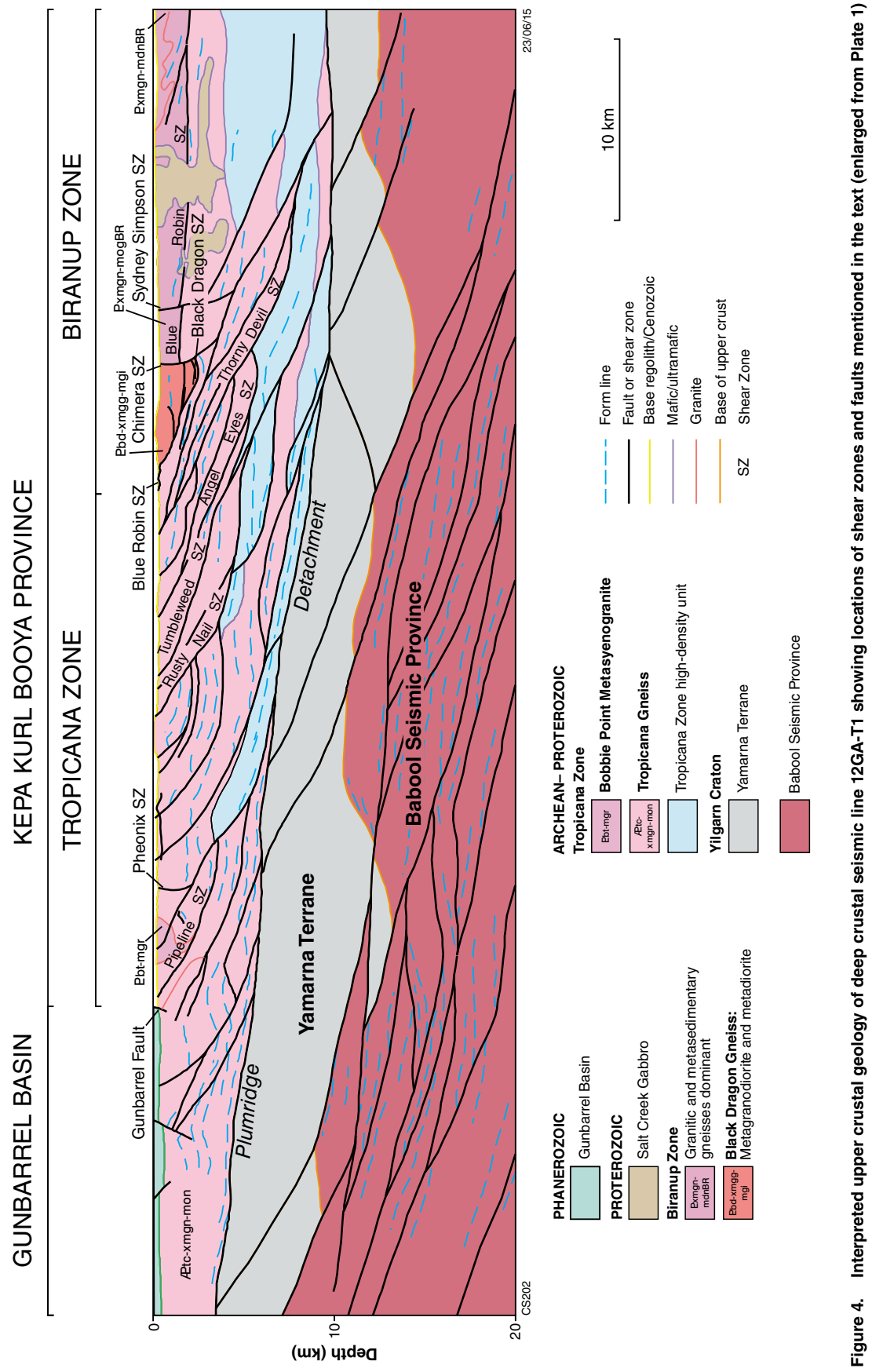

Figure 4. Interpreted upper crustal geology of deep crustal seismic line 12GA-T1 showing locations of shear zones and faults mentioned in the text (enlarged from Plate 1)

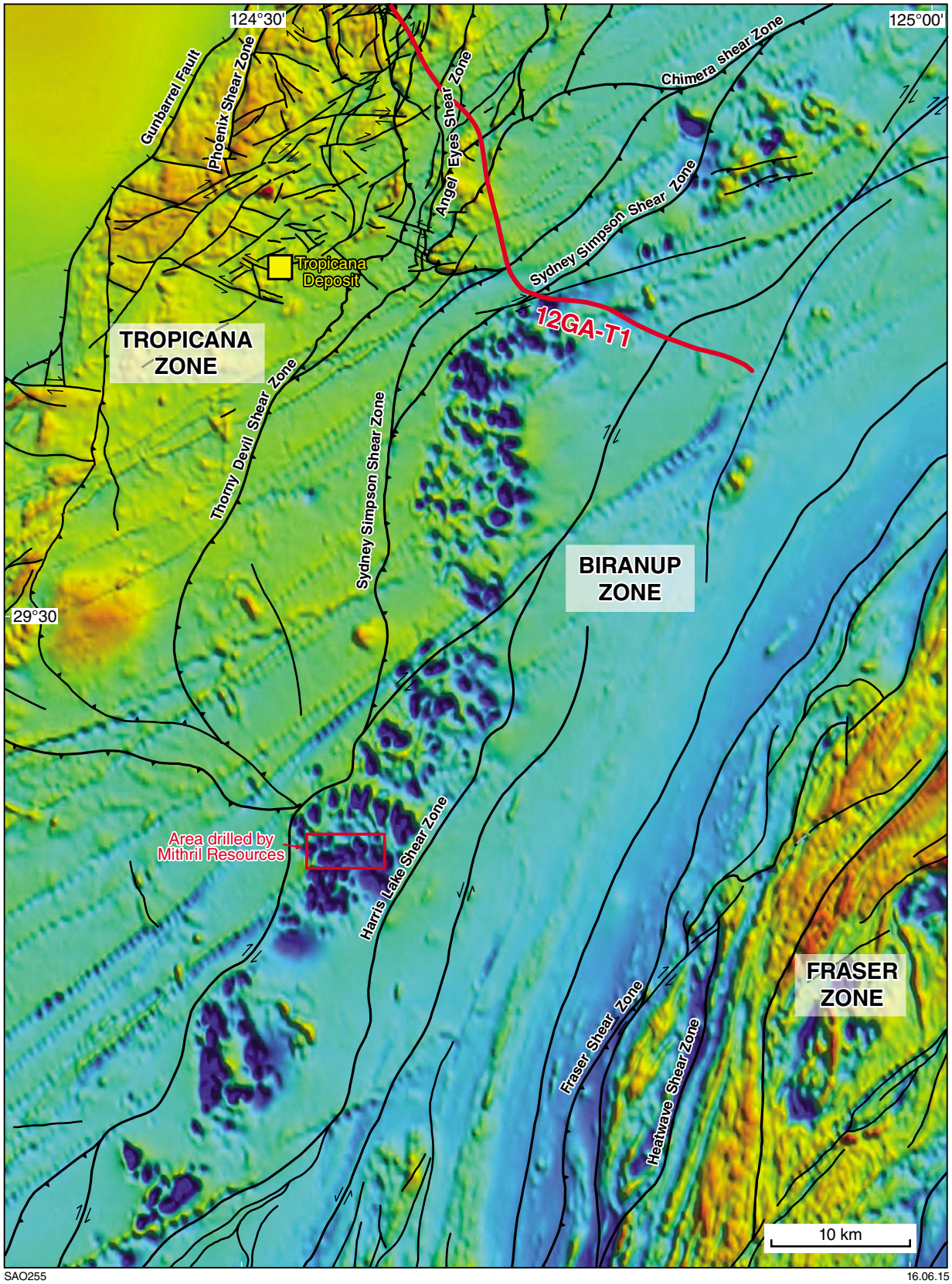

Figure 5. **Reduced-to-pole aeromagnetic image showing the mottled, remanently magnetized features described in the text, and the area drilled by Mithril Resources Limited.**

This is consistent with the gradual change from long to short wavelength features, from southeast to northwest, in magnetic data.

Major shear zones and faults

Many major shear zones and faults have been imaged from the upper through to the lower crust in seismic line 12GA-T1. Overprinting relationships between these and the units that they cut, and structures that they are cut by, provide a relative chronological history of deformation and metamorphism spanning Archean to Phanerozoic tectonism. A brief description of the major structures that have been imaged in the seismic line 12GA-T1, and their relative timing relationships, is provided below.

Shear zones in the reworked Yamarna Terrane and Babool Seismic Province

A large number of shears with shallow to moderately southeast apparent dips variably displace the boundary between the reworked Yamarna Terrane and the Babool Seismic Province, as well as seismic reflections within the Babool Seismic Province. The sense of displacement on these faults is largely extensional in the seismic section, although locally thrust movements may be inferred by offsets of the seismic reflections.

These shallow to moderately southeast dipping shears are cut by the Gunnadorrah Seismic Province in the east and central part of the section, and by the Tropicana Zone overlying the reworked Yamarna Terrane. This suggests that extensional shearing of reworked Yamarna Terrane and the Babool Seismic Province took place between cratonization of the Yilgarn Craton (c. 2630 Ma), and the structural emplacement of the Tropicana Zone, over the reworked Yamarna Terrane (implied to be c. 2520 Ma, see below), and may be indicative of extension along the Yilgarn Craton margin at this time. It is unknown when the Babool Seismic Province was juxtaposed against the Gunnadorrah Seismic Province. However, this must have occurred after the formation of the extensional shear zones present in the combined reworked Yamarna Terrane and Babool Seismic Province, therefore after c. 2630 Ma.

Babool–Gunnadorrah boundary

An apparently moderately northwest-dipping shear zone forms the boundary between the Babool and Gunnadorrah Seismic Provinces in seismic line 12GA-T1. The nature of this boundary is unknown. One interpretation is that the Gunnadorrah Seismic Province was underthrust beneath the Babool Seismic Province at the same time that the Tropicana Zone was thrust over the reworked Yamarna Terrane. However, there is currently little evidence to support this interpretation.

Plumridge Detachment

The boundary between the Tropicana Gneiss of the Tropicana Zone and the underlying reworked Yamarna Terrane, is marked by a distinct shallow, southeasterly dipping detachment fault, here named the Plumridge Detachment. The dip and dip direction of the Plumridge Detachment has been determined using Leapfrog 3D software as being approximately 7° towards 139°, shallowing slightly in the east. Taking into account the variable orientation of seismic line 12GA-T1 with the strike of the geology, this slight change of dip suggests that either the structure does not maintain constant dip along its entire length, or that the detachment may be gently folded in the east. It is suggested that this detachment may have been active during greenschist facies metamorphism and Au mineralization, observed in the upper parts of the Tropicana Gneiss. The detachment must have either initiated in the granulite facies, or been connected to a ramp that initiated in the granulite facies in order to have exhumed these high-grade rocks. The timing of the Plumridge Detachment is constrained by the following three points:

1. The Plumridge Detachment cuts extensional shears observed in the reworked Yamarna Terrane below that are likely to be younger than c. 2630 Ma.

2. Seismic reflections within the Tropicana Gneiss are linked into, or cut by, the Plumridge Detachment, suggesting that the gneissic fabric within the Tropicana Gneiss that had developed by c. 2640 Ma is cut by the detachment.

3. The Plumridge Detachment provides a plausible mechanism of uplift and associated retrogression of the Tropicana Gneiss, resulting in the greenschist facies overprint observed within the mineralized rocks. This greenschist facies metamorphic event, which is concomitant with the age of gold mineralization and associated biotite-alteration at Tropicana is dated at c. 2520 Ma.

Rusty Nail, Pipeline, Angel Eyes, Tumbleweed, and Thorny Devil Shear Zones

The Rusty Nail, Pipeline, Angel Eyes, Tumbleweed, and Thorny Devil Shear Zones all cut the Tropicana Gneiss. These shear zones all dip moderately southeast in seismic section 12GA-T1 (Figs 2 and 4; Plates 1 and 4), and commonly display southeast-over-northwest displacement consistent with thrusting. However, the age of these shear zones is poorly constrained. Although some sole onto the Plumridge Detachment, nowhere along the seismic line 12GA-T1 does the Plumridge Detachment appear to be cut by any structures that extend to the near surface, making it difficult to determine crosscutting relationships. The shear zones listed above cut linear and sublinear magnetic fabrics, interpreted from regional-scale aeromagnetic data which are largely purported to be subparallel to the gneissosity in the Tropicana Gneiss. Where field observations have been possible, the shear zones generally dip moderately to steeply to the south–southeast, and their mineralogy is dominated by quartz–sericite, and locally chlorite, suggesting that they formed in the greenschist facies. This could have been coincident with the late stages

of c. 2520 Ma Au mineralization in the area, and/or later. Evidence for shear development younger than c. 2520 Ma is demonstrated by mylonitic shear zones that crosscut the c. 1708 Ma Bobbie Point Metasyenogranite northeast of Tropicana (Fig. 3; Plate 1), and shear zones that cut or contain Paleoproterozoic rocks (see below).

The Thorny Devil Shear Zone cuts the Tropicana Gneiss, and to the north of seismic line 12GA-T1 is cut by the Black Dragon Shear Zone, which here forms the boundary between the Tropicana Gneiss and the Biranup Zone (Figs 3 and 4). These relationships indicate that these shear zones formed after the intrusion of Paleoproterozoic granitic rocks in the region, and therefore could have been active during the Biranup Orogeny, and/or during Stages I or II of the Mesoproterozoic Albany–Fraser Orogeny.

The Rusty Nail Shear Zone cuts the Tropicana Gneiss, and the highly reflective unit mapped in the Tropicana Gneiss, so may have formed after 2640 Ma (the inferred age of high-grade metamorphism) and possibly prior to, or during Proterozoic orogenic events that occurred in the region.

Blue Robin Shear Zone

In the region of seismic line 12GA-T1, the Blue Robin Shear Zone has a gentle east–southeast dip with thrust displacement separating Paleoproterozoic Biranup Zone metagranites in the hangingwall, from both Tropicana Gneiss and Paleoproterozoic metagranites of the Biranup Zone in the footwall (Fig. 4). The age of formation of this shear zone is difficult to ascertain. It is clearly younger than the Tropicana Gneiss and the Paleoproterozoic Biranup Zone metagranites, which includes the youngest known Biranup Zone granite dated at c. 1627 Ma (Kirkland et al., 2010b). This suggests that emplacement of the Biranup Zone over the Tropicana Zone may have occurred during Stages I or II of the Mesoproterozoic Albany–Fraser Orogeny.

Chimera and Sydney Simpson Shear Zones

The Chimera and Sydney Simpson Shear Zones appear to contain reverse-fault geometries that dip steeply to the southeast (Fig. 4). These shear zones cut the Blue Robin Shear Zone in seismic line 12GA-T1. Work by AngloGold Ashanti geologists in this area indicate that the shear zones formed in the greenschist facies. As the Chimera and Sydney Simpson Shear Zones cut the Blue Robin Shear Zone they must be relatively young, and are therefore interpreted to have formed during Stage II of the Mesoproterozoic Albany–Fraser Orogeny.

Gunbarrel Fault

The Gunbarrel Fault is considered to be a steeply west to northwest dipping normal fault that bounds the Gunbarrel Basin to its east (Figs 3 and 4; Plates 1 and 4; Blenkinsop and Doyle, 2014). In seismic line 12GA-T1 this fault is situated at CDP 11 060. In this region it cuts the Archean Tropicana Gneiss and the Paleoproterozoic Bobbie Point Metasyenogranite, as well as southeasterly dipping shear zones with thrust, reverse, and/or dextral strike slip displacement. To the north of seismic line 12GA-T1 the Gunbarrel Fault cuts the southeast dipping Pipeline Shear Zone, which has thrust-displacement. To the south-southwest the Gunbarrel Fault is interpreted to cut the Cundeelee Shear Zone, which also has thrust displacement (Spaggiari et al., 2014b; Plates 1 and 2).

The Gunbarrel Fault is thought to have initially developed in the late Carboniferous. Between CDPs 11 100 and 11 300 the deepest part of the Gunbarrel Basin has been imaged (at about 600 m), within a graben bounded by north-northwest and south-southeast dipping normal faults.

Discussion and concluding remarks

The Tropicana Zone and northeastern part of the Biranup Zone in the Albany–Fraser Orogen record a prolonged and complicated geological history that prior to c. 1800 Ma is significantly different from that of the Northern Foreland. Geological interpretation of geophysical data, key outcrop studies, geochemical and geochronological analysis has increased the understanding of this region immensely. However, the paucity of outcrop has impeded development of a holistic 4D perspective.

Seismic line 12GA-T1 provides a rare insight into this region by providing a cross-section view through the Tropicana Zone, and northeastern Biranup Zone. This view, when interpreted in the light of other data obtained from surface, or near surface (drillcore samples), has provided key pieces to the puzzle of the geological development of the region. In addition, comparison of the interpretation of this line with interpretations of seismic lines 12GA-A1, 12GA-A2 and 12GA-A3 have provided insights into the development of the Albany–Fraser Orogen as a whole (Spaggiari et al., 2014b; Korsch et al., 2014).

Within seismic line 12GA-T1, the reworked portion of the Yilgarn Craton, purported to be the Yamarna Terrane and the Babool Seismic Province, are deformed by moderate east-southeast dipping faults with normal displacement, suggesting that the eastern edge of the Yilgarn Craton underwent extension (Figs 2, 4 and 6). As discussed above, the precise timing of this extensional deformation is unknown; however, it must have been sometime between cratonization of the Yilgarn Craton (of which the Yamarna Terrane and Babool Seismic Province are a part) and the formation of the overlying Plumridge Detachment and underlying Gunnadorrah–Babool faulted boundary that cut these extensional structures. This extensional event is therefore constrained between c. 2630 and 2520 Ma.

The origin and age of the Gunnadorrah Seismic Province is largely unknown (Spaggiari et al., 2014b; Korsch et al., 2014). It could potentially be another reworked part of the Yilgarn Craton, or another ‘unknown’ crustal element that was thrust under the Yamarna Terrane sometime after extension of that region. It is possible that the Gunnadorrah Seismic Province was juxtaposed at the same

time as the Tropicana Zone was thrust over the reworked Yamarna Terrane – Babool Seismic Province along the gently southeast-dipping Plumridge Detachment (Figs 2, 4 and 6).

The thinning of the Tropicana Zone from the southeast to the northwest and geometry of the linked internal structures are consistent with thrusting along the Plumridge Detachment. High-grade granulite and amphibolite facies gneisses that characterize the Tropicana Gneiss are likely to have formed in the middle to lower crust and were probably exhumed to greenschist facies conditions during top-to-the-northwest directed movement along the detachment. Movement along the Plumridge Detachment must have taken place after the formation of the pervasive high-metamorphic grade gneissosity observed within units of the overlying Tropicana Gneiss, as it deformed the seismic reflection packages observed in line 12GA-T1 that are likely to represent bulk variations in the mineralogy defining the gneissic layering. The gold mineralization within the Tropicana Zone that formed in the greenschist facies (Doyle et al., 2009, 2013; Blenkinsop and Doyle, 2014) may have been concomitant with thrusting along the Plumridge Detachment and exhumation of the Tropicana Gneiss to crustal levels within greenschist facies conditions (Figs 6 and 7).

There appears to have been a hiatus of more than 700 million years in the Tropicana Zone between c. 2520 and 1800 Ma, after which dominantly intrusive rocks formed within the Tropicana Zone until c. 1620 Ma. In the Tropicana Zone granitic rocks as old as c. 1800 Ma are included in the Salmon Gums Event (Spaggiari et al., 2014a). Between 1780 and 1760 Ma, pull-apart basins may have formed over the Tropicana Zone forming depositional centres and/or the foci for intrusions into the basement. The Voodoo Child Formation may have been deposited in one of these areas. The mechanism by which this occurred is not constrained, although it could be explained as related to formation of the Barren Basin (Spaggiari et al., 2014c). Apart from shears that may have formed the boundaries of the pull-apart basins, no obvious structures observed in the Tropicana Zone can be easily attributed to have formed during this time. It may be that during this period extensional processes were prevalent over compression. This could have led to localized formation of sedimentary basins, the local emplacement of felsic-mafic intrusives (Voodoo Child area) and the widespread intrusion of granitic rocks. This could also explain the lack of formation of a widespread foliation that can be ascribed to this period in the Tropicana Zone. However, further work is required to clarify this.

The layered ultramafic–mafic to felsic rock succession of the Voodoo Child Formation is deformed into a regional-scale, northeasterly trending fold (Plate 1). Geological interpretation of the geophysical data suggests that this fold plunges to the southeast. Locally, the fold is cut by dominantly northeasterly trending shears that indicate southeast over northwest thrust movement.

The Tropicana Gneiss, Paleoproterozoic metagranites, metasedimentary rocks, and meta-mafic rocks are all cut by northeast trending shear zones that developed in the greenschist facies. Many of these shear zones have been imaged in seismic line 12GA-T1. Locally, in outcrop and in drillcores, the shear zones appear to be steeply dipping to the southeast and exhibit dextral shear sense indicators such as S–C fabrics and rotated feldspar porphyroclasts in metagranite. In some areas, brittle-ductile shears with dextral kinematics can be mapped at the surface, extended in map view using aeromagnetic data, and have also been interpreted as thrusts, suggesting possible oblique slip in the region.

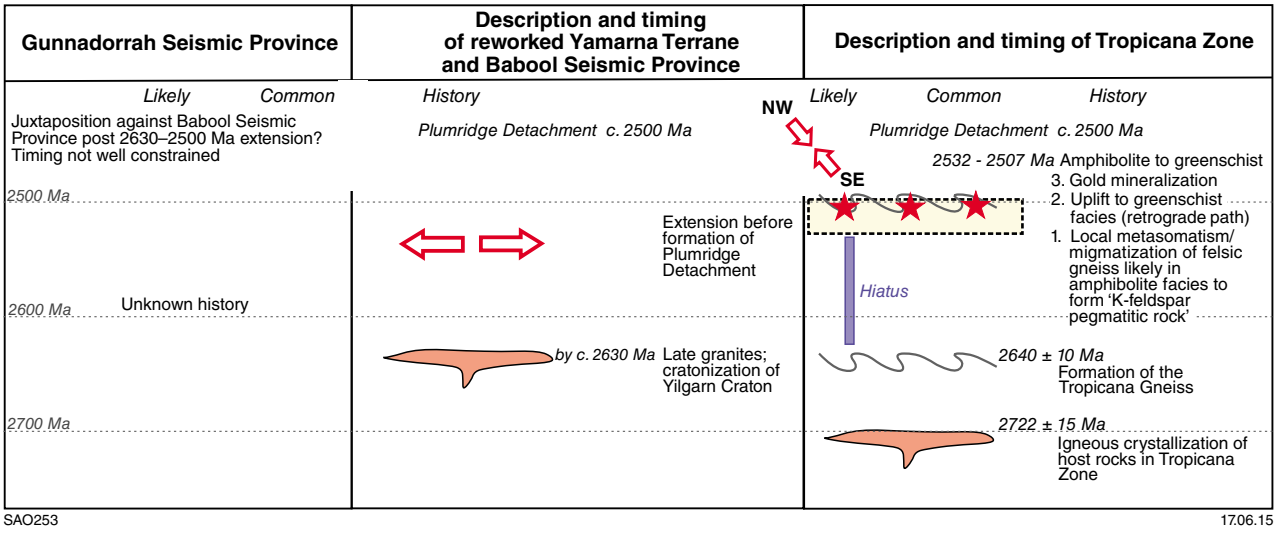

Figure 6. Simplified paragenesis of the Tropicana Zone, reworked Yamarna Terrane, Babool Seismic Province, and Gunnadorrah Seismic Province

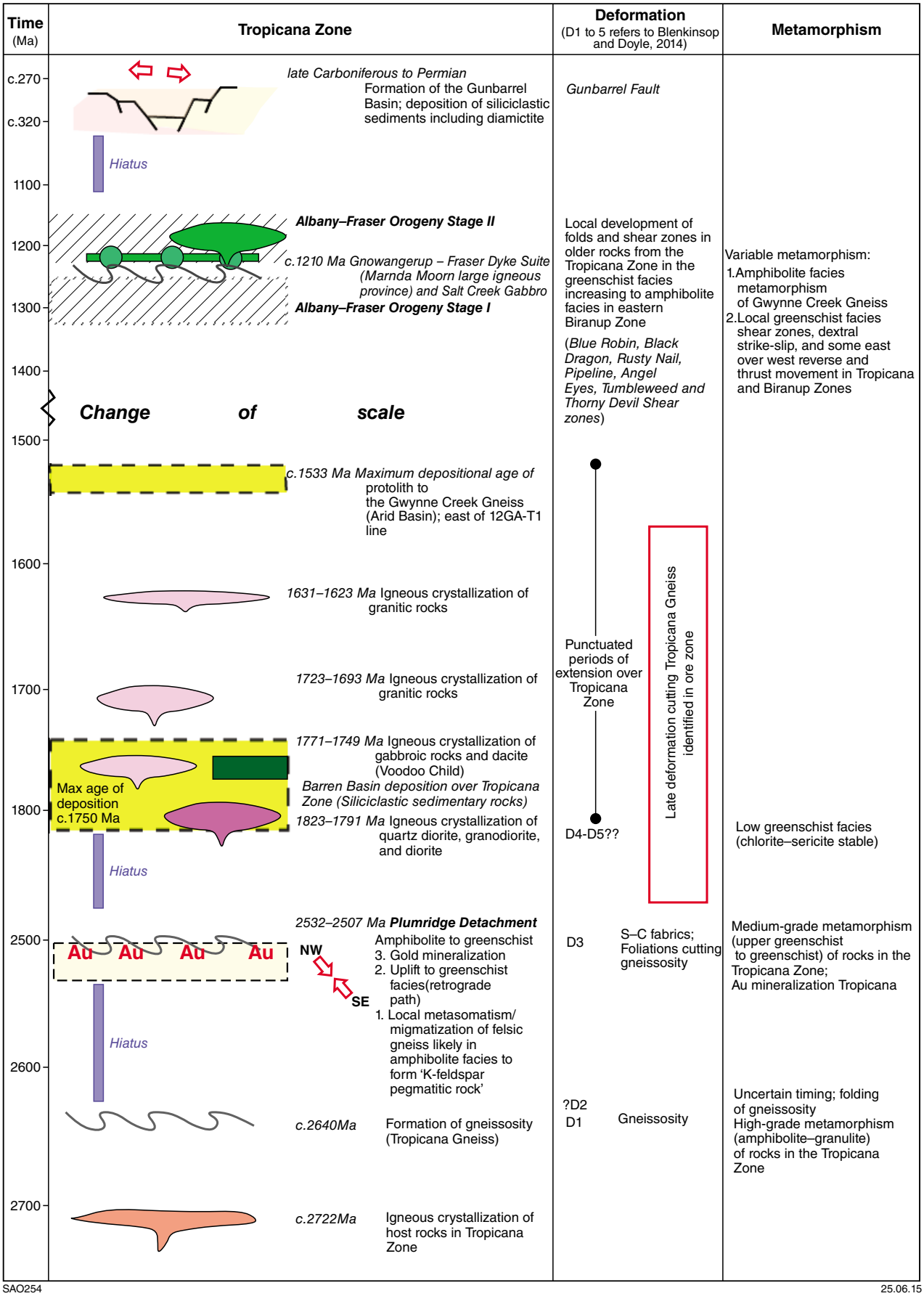

Figure 7. Paragenesis of the upper crustal part of seismic line 12GA-T1

To the east of the Tropicana and Biranup Zones, metasedimentary and metamafic rocks of the Mesoproterozoic Gwynne Creek Gneiss have been metamorphosed at high grade and deformed into northeasterly trending, F_2 folds (Spaggiari et al., 2011; Plate 1). This deformation and metamorphism, although occurring at higher grades, may have been coeval with deformation and metamorphism at greenschist facies conditions observed in northeast trending shear zones within the Tropicana and Biranup Zones in the vicinity of seismic line 12GA-T1.

The precise timing of development of these northeast-trending structures that formed in the greenschist facies is unknown. In the Biranup Zone U–Pb dating of metamorphic zircons suggests that the deformation and metamorphism responsible for the late northeast-trending structures may have occurred during Stage II of the Albany–Fraser Orogeny, although these dates are from higher grade, amphibolite–granulite facies rocks further south (Spaggiari et al., 2011). Zircons obtained from the Gwynne Creek Gneiss to the east indicate metamorphism during both Stages I and II of the Albany–Fraser Orogeny, with a period of uplift between (Kirkland et al., 2011). Therefore, it is feasible that some of the northeast-trending structures in the Tropicana Zone formed during either Stage I or II of the Albany–Fraser Orogeny, or both.

In the Tropicana Zone, northeast-trending structures appear to pre-date the intrusion of east-northeast trending mafic dykes, which, although undated, are inferred to be part of the c. 1210 Ma Gnowangerup – Fraser Dyke Suite. This interpretation is based on aeromagnetic data which show the east-northeast dykes cutting the northeast-trending structures, and on the unmetamorphosed and largely undeformed nature of dykes observed in the field and in drillcore. However, deformed and metamorphosed equivalents are interpreted to occur in the Northern Foreland to the southwest (Spaggiari et al., 2009, 2011).

The Salt Creek Gabbro is an unexposed largely north-northeasterly trending unit of reportedly undeformed mafic gabbroic rocks (Mithril Resources Limited, 2003, 2005). The Salt Creek Gabbro intrudes the Tropicana and Biranup Zones and may extend to the south into the Northern Foreland. Its relationship with the Gnowangerup–Fraser Dyke Suite is not established due to the lack of outcrop and small number of drillholes in the region. However, its emplacement must have post-dated high-grade metamorphism that occurred during the Albany–Fraser Orogeny to the south of the Tropicana Zone.

The Gunbarrel Basin formed on the West Australian Craton during the late Carboniferous to Permian. It mostly overlies the Yilgarn Craton, but also straddles the Tropicana Zone and Northern Foreland. The extent of the Tropicana Zone beneath the basin has not been clearly delineated.

References

Blenkinsop, TG and Doyle, MG 2014, Structural controls on gold mineralization on the margin of the Yilgarn craton, Albany–Fraser orogen: The Tropicana deposit, Western Australia: Journal of Structural Geology, v. 67 p. 189–204.

Cassidy, KF, Champion, DC, Krapez, B, Barley, ME, Brown, SJA, Blewett, RS, Groenewald, PB and Tyler, IM 2006, A revised geological framework for the Yilgarn Craton, Western Australia: Geological Survey of Western Australia, Record 2006/8, 8p.

Costelloe, RD, Holzschuh, J and Fomin, T 2014, Acquisition and processing of the 2012 Albany–Fraser deep reflection seismic survey, *in* Albany–Fraser Orogen seismic and magnetotelluric (MT) workshop 2014: extended abstracts *compiled by* CV Spaggiari and IM Tyler: Geological Survey of Western Australia, Record 2014/6, p. 1–6.

Doyle, MG, Kendall, BM and Gibbs, D 2007, Discovery and characteristics of the Tropicana Gold District, *in* Proceedings of Geoconferences, Kalgoorlie 07 Conference *edited by* FP Bierlein and CM Knox-Robinson: Geoscience Australia Record 2007/14, p. 186–190.

Doyle, MG, Gibbs, D, Savage, J and Blenkinsop, TG 2009, Geology of the Tropicana Gold Project, Western Australia, *in* Smart science for exploration and mining: Economic Geology Research Unit, James Cook University; 10th Biennial SGA Meeting of the Society for Geology Applied to Mineral Deposits, Townsville, Queensland, 17 August 2009: Proceedings volume 1, p. 50–52.

Doyle, M, Savage, J, Blenkinsop, T, Crawford, A and McNaughton, N 2013, Tropicana – Unravelling the complexity of a +6 Million Ounce Gold Deposit Hosted in Granulite Facies Metamorphic Rocks: The Australian Institute of Mining and Metallurgy Publication Series no. 9/2013, p. 87–93.

Doyle, MG, Fletcher, IR, Foster, J, Large, R, Mathur, R, McNaughton, NJ, Meffre, S, Muhling, JR, Phillips, D and Rasmussen, B 2015, Geochronological constraints on the Tropicana Gold Deposit and Albany–Fraser Orogen, Western Australia: Economic Geology, v. 110, p. 1–32.

Fox-Wallace, LJ 2010, Geology of the Hat Trick Prospect in the Tropicana Project area, Western Australia, unpublished BSc (Honours) thesis, James Cook University, Sydney, 104p.

Kendall, B, Doyle, M, and Gibbs, D 2007, Tropicana: The discovery of a new gold province in Western Australia, *in* Proceedings 2007 NewGenGold Conference: Paydirt Media Pty Ltd, Perth, p. 85–95.

Kirkland, CL, Spaggiari, CV, Pawley, MJ, Wingate, MTD, Smithies, RH, Howard, HM, Tyler, IM, Belousova, EA and Poujol, M 2011, On the edge: U–Pb, Lu–Hf, and Sm–Nd data suggests reworking of the Yilgarn Craton margin during formation of the Albany–Fraser Orogen: Precambrian Research, v. 187, p. 223–247.

Kirkland, CL, Spaggiari, CV, Smithies, RH and Wingate, MTD 2014, Cryptic progeny of craton margins: Geochronology and Isotope Geology of the Albany–Fraser Orogen with implications for evolution of the Tropicana Zone, *in* Albany–Fraser Orogen seismic and magnetotelluric (MT) workshop 2014: extended abstracts *compiled by* CV Spaggiari and IM Tyler: Geological Survey of Western Australia, Record 2014/6 p. 89–101.

Kirkland, CL, Wingate, MTD, Spaggiari, CV and Pawley, MJ 2010a, 182435: metagranodiorite, Bobbie Point; Geochronology Record 866: Geological Survey of Western Australia, 4p.

Kirkland, CL, Wingate, MTD, Spaggiari, CV and Pawley, MJ 2010b, 182435: metasyenogranite, Barlett Bluff; Geochronology Record 849: Geological Survey of Western Australia, 4p.

Kirkland, CL, Wingate, MTD and Spaggiari, CV 2013a, 182435: metagranite, Lindsay Hill; Geochronology Record 1137: Geological Survey of Western Australia, 4p.

Kirkland, CL, Wingate, MTD and Spaggiari, CV 2013b, 182405: quartzite, McKay Creek; Geochronology Record 1136: Geological Survey of Western Australia, 5p.

Kirkland, CL, Wingate, MTD, Spaggiari, CV and Pawley, MJ 2012, 182424: metasyenogranite, McKay Creek; Geochronology Record 1017: Geological Survey of Western Australia, 4p.

Kirkland, CL, Wingate, MTD, Spaggiari, CV and Pawley, MJ 2012b, 182426: metasyenogranite, Pleiades Lakes; Geochronology Record 1018: Geological Survey of Western Australia, 4p.

Kirkland, CL, Wingate, MTD, Spaggiari, CV and Pawley, MJ 2012c, 182428: metasyenogranodiorite, Pleiades Lakes; Geochronology Record 1019: Geological Survey of Western Australia, 4p.

Korhonen, FJ, Clark, C, Brown, M, Bhattacharya, S and Taylor, R 2013, How long-lived is ultrahigh temperature (UHT) metamorphism? Constraints from zircon and monazite geochronology in the Eastern Ghats orogenic belt, India: Precambrian Research, v. 234, p. 322–350.

Korsch, RJ, Blewett, RS, Pawley, MJ, Carr, LK, Hocking, RM, Neumann, NL, Smithies, RH, Quentin de Gromard, R, Howard, HM, Kennett, BLN, Aitken, ARA, Holzschuh, J, Duan, J, Goodwin, JA, Jones, T, Gessner, K and Gorczyk, W 2013, Geological setting and interpretation of the southwest half of deep seismic reflection line 11GA-YO1: Yamarna Terrane of the Yilgarn Craton and the western Officer Basin, *in* Yilgarn Craton-Officer Basin-Musgrave Province seismic and MT workshop *edited by* NL Neumann: Geoscience Australia, Record 2013/28, p. 24–50.

Korsch, RJ, Spaggiari, CV, Occhipinti, SA, Doublier, MP, Clark, DJ, Dentith, MC, Doyle, MG, Kennett, BLN, Gessner, K, Neumann, NL, Belousova, EA, Tyler, IM, Costelloe, RD, Fomin, T and Holzschuh, J 2014, Geodynamic implications of the 2012 Albany–Fraser deep seismic reflection survey: a transect from the Yilgarn Craton across the Albany–Fraser Orogen to the Madura Province, *in* Albany–Fraser Orogen seismic and magnetotelluric (MT) workshop 2014: extended abstracts *compiled by* CV Spaggiari and IM Tyler: Geological Survey of Western Australia, Record 2014/6, p. 142–173.

Less, T 2013, Newly recognized Paleoproterzoic gold-silver mineralization in the Albany-Fraser orogeny, *in* Future understanding of tectonics, ores, resources, environment and sustainability *edited by* Z Chang, R Goldfarb, T Blenkinsop, C Palczek, D Cooke, K Camuti and J Carranza: FUTORES Conference, Economic Geology Research Unit Contribution 68, James Cook University, Townsville, Australia 2–5 June 2013, p. 31.

Mehnert, KR 1968, Migmatites and the origin of granitic rocks: Elsevier Publishing Company, Amersterdam, London, New York, 393p.

Mithril Resources Limited 2003, Annual Report, 2003, Plumridge Project EL39/871,872,873,874,931,934 and E69/1573 2002/2003: Geological Survey of Western Australia, Statutory mineral exploration report, Combined Annual Technical Report A66752 (unpublished).

Mithril Resources Limited 2005, Final Report, 2005, Plumridge Project ET 39/871: Geological Survey of Western Australia, Statutory mineral exploration report A070970 (unpublished).

Möller, A and Kennedy, A 2006, Extremely high Th/U in metamorphic zircon: In situ dating of the Labwor Hills granulites: 16th Annual VM Goldschmidt Conference 2006, Abstracts, p. 425.

Murdie, RE, Gessner, K, Occhipinti, SA, Spaggiari, CV and Brett, J 2014, Interpretation of gravity and magnetic data across the Albany–Fraser Orogen, *in* Albany–Fraser Orogen seismic and magnetotelluric (MT) workshop 2014: extended abstracts *compiled by* CV Spaggiari and IM Tyler: Geological Survey of Western Australia, Record 2014/6, p. 118–134.

Myers, JS 1990, Albany–Fraser Orogen: Geological Survey of Western Australia, Memoir 3, p. 255–263.

Nelson, DR, Myers, JS and Nutman, AP 1995, Chronology and evolution of the Middle Proterozoic Albany–Fraser Orogen, Western Australia: Australian Journal of Earth Sciences, v. 42, p. 481–495.

Pawley, MJ, Wingate, MTD, Kirkland, CL, Wyche, S, Hall, CE, Romano, SS and Doublier, MP 2012, Adding pieces to the puzzle: episodic crustal growth and a new terrane in the northeast Yilgarn Craton, Western Australia: Australian Journal of Earth Sciences, v. 59, p. 603–623.

Rubbato, D, Williams, IS and Buick, IS 2001, Zircon and monazite response to prograde metamorphism in the Reynolds Range, central Australia: Contributions to Mineralogy and Petrology, v. 140, p. 158–168.

Sawyer, EW 2008, Atlas of Migmatites: The Canadian Mineralogist, Special Publication 9, NRC Research Press, Ottawa, Ontario, Canada, 371p.

Smithies, RH, Spaggiari, CV, Kirkland, CL and Maier, WD 2014, Geochemistry and petrogenesis of the Albany–Fraser igneous rocks, *in* Albany–Fraser Orogen seismic and magnetotelluric (MT) workshop 2014: extended abstracts *compiled by* CV Spaggiari and IM Tyler: Geological Survey of Western Australia, Record 2014/6 p. 77–88.

Spaggiari, CV, Bodorkos, S, Barquero-Molina, M, Tyler, IM and Wingate, MTD 2009, Interpreted bedrock geology of the south Yilgarn and central Albany–Fraser Orogen, Western Australia: Geological Survey of Western Australia, Record 2009/10, 84p.

Spaggiari, CV, Kirkland, CL, Pawley, MJ, Smithies, RH, Wingate, MTD, Doyle, MG, Blenkinsop, TG, Clark, C, Oorschot, CW, Fox, LJ and Savage, J 2011, The geology of the east Albany–Fraser Orogen — a field guide: Geological Survey of Western Australia, Record 2011/23, 97p.

Spaggiari, CV, Kirkland, CL, Smithies, RH, Occhipinti, SA and Wingate, MTD 2014a, Geological framework of the Albany–Fraser Orogen, *in* Albany–Fraser Orogen seismic and magnetotelluric (MT) workshop 2014: extended abstracts *compiled by* CV Spaggiari and IM Tyler: Geological Survey of Western Australia, Record 2014/6, p. 12–27.

Spaggiari CV, Kirkland CL, Smithies RH and Wingate MTD 2014c, Tectonic links between Proterozoic sedimentary cycles, basin formation and magmatism in the Albany–Fraser Orogen, Western Australia: Geological Survey of Western Australia, Report 133, 63p.

Spaggiari, CV, Occhipinti, SA, Korsch, RJ, Doublier, MP, Clark, DJ, Dentith, MC, Gessner, K, Doyle, MG, Tyler, IM, Kennett, BLN, Costelloe, RD, Fomin, T and Holzschuh, J 2014b, Interpretation of Albany–Fraser seismic lines 12GA-AF1, 12GA-AF2 and 12GA-AF3: implications for crustal architecture, *in* Albany–Fraser Orogen seismic and magnetotelluric (MT) workshop 2014: extended abstracts *compiled by* CV Spaggiari and IM Tyler: Geological Survey of Western Australia, Record 2014/6 p. 28–51.

Stokes, MA 2014, Structural evolution of the Pleiades Lakes Region; northeastern Albany–Fraser Orogen, Western Australia: Geological Survey of Western Australia, Record 2014/15,145p.

Wingate, MTD, Morris, PA, Pirajno, F and Pidgeon, RT 2005, Two large igneous provinces in late Mesoproterozoic Australia, *in* Supercontinents and Earth Evolution Symposium 2005 *edited by* MTD Wingate and SA Pisarevsky: Geological Society of Australia, Abstracts 81, p. 151.

Wyche, S, Kirkland, CL, Riganti, A, Pawley, MJ, Belousova, EA and Wingate, MTD 2012, Isotopic constraints on stratigraphy in the central and eastern Yilgarn Craton, Western Australia: Australian Journal of Earth Sciences, v. 59, p. 657–670.

Tropicana deposit, Western Australia: an integrated approach to understanding granulite-hosted gold and the Tropicana Gneiss

by

MG Doyle[1], TG Blenkinsop[2*], AJ Crawford[3], IR Fletcher[4], J Foster[3#], L Fox-Wallace[1], RR Large[3], R Mathur[5], NJ McNaughton[6], S Meffre[3], JR Muhling[4], SA Occhipinti[1], B Rasmussen[4], and J Savage[1]

Introduction

Exploration models for lode gold deposits have emphasized the relatively low prospectivity of regions dominated by high-metamorphic grade gneisses relative to greenschist facies granite–greenstone terranes. The Tropicana Gold Mine, Western Australia, is the first major greenfields gold discovery in upper amphibolite to granulite facies gneissic rocks at the eastern margin of the highly endowed Yilgarn Craton.

Tropicana is a rare example of a world-class (cf. Schodde and Hronsky, 2006) gold deposit hosted in mid-amphibolite to granulite-facies gneisses. Other well-studied gold deposits hosted in high-grade metamorphic rocks include Hemlo in Canada, Renco in Zimbabwe, Challenger in South Australia, and Big Bell and Griffins Find in Western Australia. A protracted history of reactivation, re-equilibration, and remobilization of gold and associated metals in these deposits makes discerning the precise timing of the principal mineralization event(s) challenging. Research has focused on clarifying the timing of alteration, mineralization and deformation and relative to peak metamorphism.

1 AngloGold Ashanti Ltd, Level 13, St Martins Tower, PO Box Z5046, Perth WA 6831, Australia

2 Economic Geology Research Unit, School of Earth and Environmental Science, James Cook University, Townsville QLD 4811, Australia

3 CODES, University of Tasmania, Hobart TAS 7001, Australia

4 The Institute for Geoscience Research, Curtin University, Perth WA 6845, Australia

5 Department of Geology, Juniata College, 1700 Moore Street, Huntingdon, PA 16652, USA

6 John de Laeter Centre for Isotope Research, Curtin University, Perth WA 6845, Australia

* Current address: School of Earth and Ocean Sciences, Main Building, Park Place, Cardiff CF10 3AT, United Kingdom

\# Current address: Sirius Resources, 5/5 Muford Place, Balcatta WA 6021, Australia

The range of deposit styles are divisible into two categories: a) those deposits formed prior to peak metamorphism (metamorphosed gold deposits); and b) those related to events post-dating peak metamorphism (post-metamorphic gold deposits; Tomkins, 2013). Combined, detailed paragenetic studies, geochronology and theoretical studies suggest that the many gold deposits in high-grade metamorphic rocks can be explained by mineralization at greenschist facies conditions and subsequent metamorphism to mid-amphibolite or granulite facies (e.g. Challenger, Tomkins and Mavrogenes, 2002; Tomkins et al., 2004b; Griffins Find, Tomkins and Grundy, 2009; Hemlo, Tomkins et al., 2004a; Big Bell, Phillips and Powell, 2009). In contrast, multidisciplinary studies support a retrograde timing for shear-controlled gold mineralization at Renco (Blenkinsop and Frei, 1996).

Here we present a summary of studies completed in collaboration with multiple research partners that have placed important constraint on the mineralization, alteration, metamorphic and igneous crystallization events that are represented at the Tropicana gold deposit. Results of the Tropicana studies are placed in the context of the regional seismic line 12GA-T1 in a companion abstract by Occhipinti et al. (2014). The abstract summarizes research outcomes on Tropicana presented in key papers (Doyle et al., 2013; Blenkinsop and Doyle, 2014; Doyle et al., 2015) and readers are referred to those documents as a primary resource.

Project location and resource

The project, located within the remote Great Victoria Desert, is part of the Tropicana Joint Venture, which is 70% owned by AngloGold Ashanti Australia (the manager) and 30% by Independence Group NL (Fig. 1). Economic intercepts returned from diamond and reverse circulation (RC) drilling in mid-2005 at Tropicana prospect and in mid-2006 at Havana prospect formed the foundations for discovery and subsequent resource delineation/definition programs and feasibility studies (Doyle et al., 2007; Kendall et al., 2007). Approval for construction of the project was granted in November

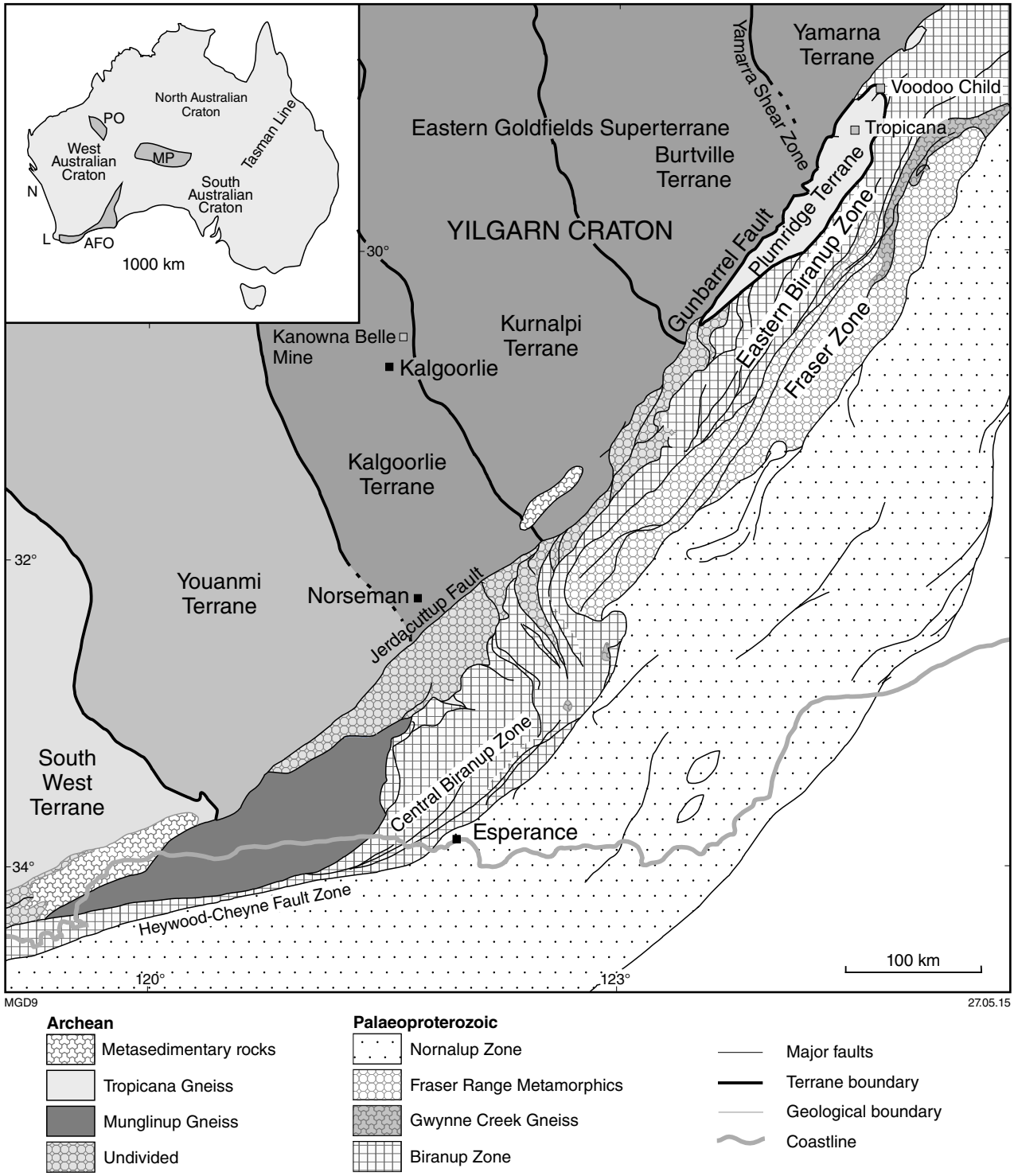

Figure 1. Geological map showing the location of the Tropicana gold deposit in the far northeast of the Albany–Fraser Orogen, and major greenstone-hosted gold deposits in the Yilgarn Craton (modified after Spaggiari et al., 2011)

2010, and construction of the mine commenced in the June quarter of 2011. The first gold pour from openpit mining was completed on schedule in the December quarter of 2013 (Doyle et al., 2013). The approved project will have a 10-year mine life and in the first three years of operation, gold production will be between 470 000 – 490 000 oz/pa at a cash cost of A$580–600/oz.

Reserves as at December 2011 total 56.4 Mt grading 2.16 g/t Au for 3.91 Moz of gold (AngloGold Ashanti Ltd, 2011). In December 2012, the joint venture partners announced an increase in the mineral resource estimate by 1.48 Moz to 7.89 Moz of contained gold, including measured resources of 29.8 Mt at 2.12 g/t Au for 2.03 Moz, indicated resources of 76.4 Mt at 1.95 g/t Au for 4.78 Moz, and inferred resources of 11.9 Mt at 2.83 g/t Au for 1.08 Moz. Mineral resource is inclusive of that mineralization included in ore reserves (AngloGold Ashanti Ltd, 2012; Doyle et al., 2013).

Regional geological setting

Exposures of Precambrian basement rocks are scarce within the northern and central parts of the Albany–Fraser Orogen due to widespread sand cover and locally extensive Tertiary and Permian sedimentary sequences. Acquisition of detailed proprietary magnetic, gravity and airborne EM datasets to supplement lower resolution pre-competitive geophysical data has underpinned interpretations of the regional geology in this region. When combined with geochronological and geochemical studies of rocks sampled from geographically disparate outcrops and exploration drillholes, an incomplete but robust geological and tectonic history can be resolved.

The Tropicana Gneiss (Tropicana domain, of Doyle et al., 2013) includes lithologically diverse associations of orthogneiss and subordinate paragneiss that form part of the eastern margin of the Yilgarn Craton (Doyle et al., 2009; Blenkinsop and Doyle, 2014). The domain is characterized by a gravity high and dominantly north-northwest to northeast-trending magnetic pattern that marks the position of Neoarchean reverse (thrusts) faults that define multiple duplexes, including the Tropicana, Iceberg, and Madras duplexes of Blenkinsop and Doyle (2014).

The Tropicana Gneiss hosts the Tropicana gold deposit and at this latitude is approximately 27 km wide, but has a near surface expression that is greater (~35 km) to the south, and is narrow (a few kilometres) and discontinuous to the north around the Hercules prospect (Blenkinsop and Doyle, 2014). The Tropicana Gneiss is interpreted to extend over a strike length of at least 80 km, although it is obscured by Paleoproterozoic rocks of the Voodoo Child Domain in the Voodoo Child and Hercules prospect areas, 50–70 km north of the Tropicana mine (Blenkinsop and Doyle, 2014).

The Tropicana Gneiss comprises a fault-bound assemblage of rocks with a distinct geological history and is ascribed to the Plumridge Terrane of the Yilgarn Craton by Blenkinsop and Doyle (2014). Structural and lithostratigraphic elements in the Yamarna and Burtville Terranes of the Yilgarn Craton cannot be traced eastward into the Tropicana Gneiss on the basis of magnetic and gravity datasets, although relationships are obscured by thick (>300 m) sedimentary sequences (Paterson Formation) which fill the Gunbarrel Basin. In seismic line 12GA-T1, crustal elements of the Yamarna Terrane are interpreted to extend below Tropicana Gneiss — the contact between the two being marked by an approximately 300 m-thick east-dipping detachment fault, the Plumridge Detachment (Occhipinti et al., 2014).

The Gunbarrel Basin is bound along its eastern margin by the steeply west-dipping, Phanerozoic, Gunbarrel Fault which cuts and displaces Neoarchean and Proterozoic faults and shears dissecting the Tropicana Gneiss. Shears within the Tropicana Gneiss are characterized by sericite–chlorite-dominant assemblages indicative of greenschist facies conditions, in contrast to the upper amphibolite to lower granulite-facies mineral assemblages which characterize peak metamorphism in the gneissic rocks (Doyle et al., 2013; Blenkinsop and Doyle, 2014).

To the east and northeast of the gold mine, the Tropicana Gneiss is in faulted contact with the Black Dragon domain (c. 1800 Ma rocks; Blenkinsop and Doyle, 2014) and Voodoo Child domain (c. 1760 Ma; Bunting et al., 1976; Kirkland et al., 2011; Less, 2013) of the Biranup Zone (Blenkinsop and Doyle, 2014; Occhipinti et al., 2014). Diverse associations of metasedimentary and igneous rocks ranging from c. 1800 to 1620 Ma were ascribed to the Biranup Zone (e.g. Spaggiari et al., 2009; Kirkland et al., 2011; Spaggiari et al., 2011). Hf-isotopic signatures and enclaves of Archean basement are interpreted to record a source incorporating both Archean crust and juvenile mantle-derived components for the Biranup Zone (Kirkland et al., 2011). The Biranup Zone is interpreted to record either an arc to back-arc setting on the active craton margin, or to have been emplaced in post-orogenic extensional basins (e.g. Bunting et al., 1976; Kirkland et al., 2011).

Tropicana geology

Mineral resources at the Tropicana Gold Mine encompass four mineralized zones distributed along an approximately 5 km strike length. They are, from north to south, the Boston Shaker, Tropicana, Havana and Havana South Zones (e.g. Doyle et al., 2007, 2009, 2013; Fig. 2). Mineralization has been intersected along strike to the northwest and southwest of the current mining operation, and intersected down dip of the Havana Zone to a maximum vertical depth of about 1 km.

The dominant lithological associations in the hangingwall to mineralization are garnet-bearing gneiss, amphibolite and granulite, with subordinate chert, banded iron-formation (grunerite–quartz±garnet), quartzofeldspathic gneiss and anatexite facies (Fig. 3). Ore zones are hosted by a range of gneissic rocks, but predominantly within quartzofeldspathic gneiss and compositionally similar anatexite facies; particularly K-feldspar-dominant (syenitic) facies. The footwall package comprises

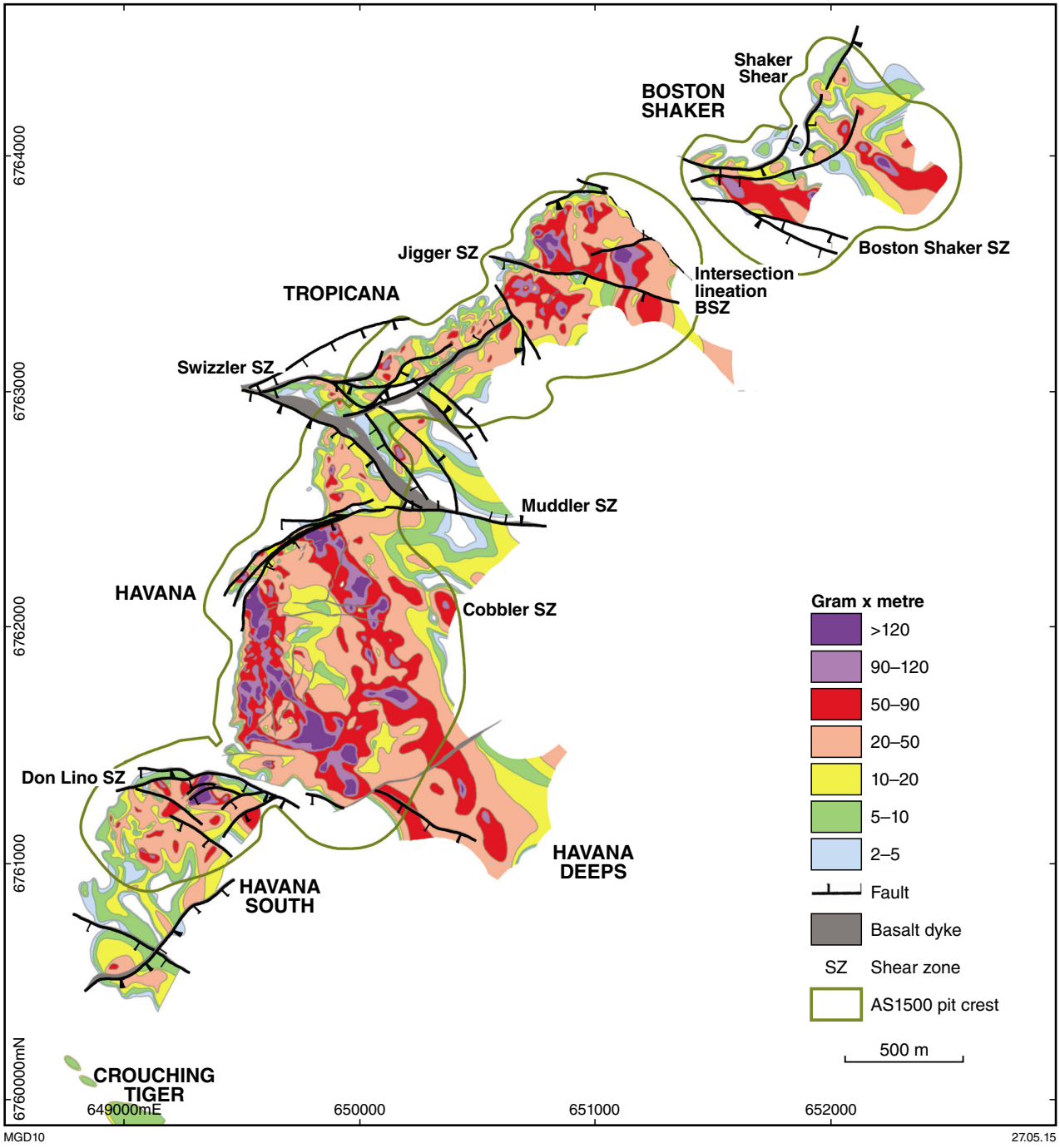

Figure 2. **Structural domains and mesoscopic shear zones of the Tropicana gold deposit, superimposed on a grade (g/t Au) X thickness (m) plot. GDA/UTM grid (after Blenkinsop and Doyle, 2014)**

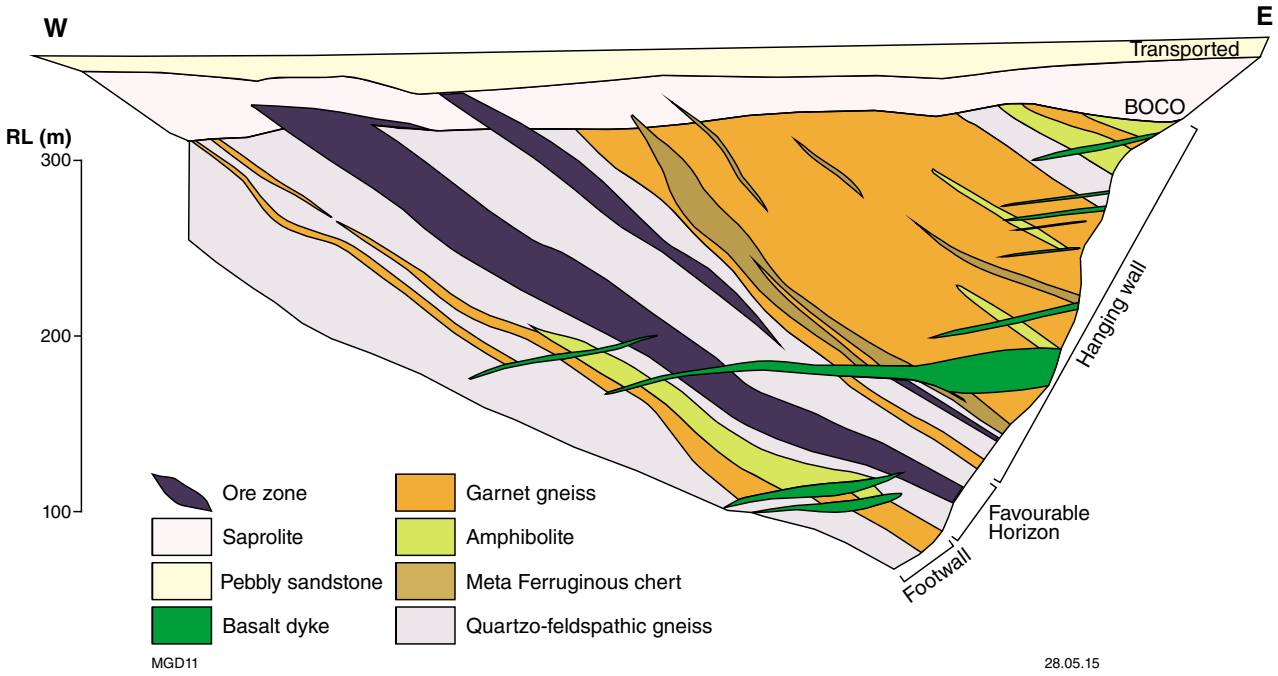

Figure 3. Schematic east–west cross-section of the Tropicana deposit (based on Doyle et al., 2007)

amphibolite, granulite, and both garnet-bearing and felsic gneiss associations. On the basis of lithogeochemistry, the host sequence is interpreted to be dominated by rhyolitic to basaltic metavolcanic rocks (Doyle et al., 2013).

Partial melting of the host sequence has produced anatexite patches, bands and veins (1–20 cm wide). Anatexite and leucosomes are texturally continuous with the gneissosity or intruded parallel to the axial plane of intrafolial folds indicating syndeformational emplacement during peak metamorphism at granulite facies (Doyle et al., 2007; Blenkinsop and Doyle, 2014). Both the host rocks and ore zones are cut by basalt to dolerite intrusions with chilled or weakly sheared margins. Several attempts to date the dykes have been unsuccessful and, on the basis of regional magnetic interpretations, they are ascribed to the c. 1210 Ma (Qiu et al., 1999; Wingate et al., 2000) Gnowangerup–Fraser Dyke Suite providing a minimum age for mineralization (Doyle et al., 2007).

The ore envelope modelled at a ≥0.3 g/t Au is subparallel to dominantly east- to southeast-dipping (~40°) gneissosity and enveloping surfaces of garnet-bearing gneiss divisions in the footwall and hangingwall. Mineralization is localized in shear-controlled lenses that are characterized by biotite–sericite–pyrite–chlorite±calcite±siderite mineral assemblages that are consistent with upper greenschist facies conditions at the time of economic gold mineralization. In lithons between shears, biotite–sericite–pyrite alteration has moved out from fractures and altered metamorphic mineral assemblages. Greenschist facies retrogression is widespread but variable in rocks distal to mineralization.

Gold typically occurs as fine-grained (10–30 µm) inclusions in pyrite and less commonly in fractures cutting K-feldspar, quartz, and monazite. Stylolitic dissolution fabrics, crackle-breccia facies, and shears, fractures and veins with biotite–pyrite±sericite fills are widespread, particularly in higher grade zones, and cut and/or displace peak-metamorphic fabrics (Blenkinsop and Doyle, 2014). Accessory minerals include pyrrhotite, chalcopyrite, electrum and telluride minerals (calaverite, petzite, sylvanite, altaite), and trace minerals include molybdenum, bismuthinite, sphalerite, galena, and bornite.

There is evidence for more than one phase of mineralization, probably at different gold grades, and reactivation of mineralized structures is common. Occurrences of visible gold associated with high-grade intercepts are localized on late sericite fractures which cut across anatectic segregations, gneissic bands and rare deformed quartz veins, and overprint earlier biotite–sericite–pyrite-dominant assemblages.

Tropicana structure

The structural architecture and history of the Tropicana Deposit has been described in detail by Blenkinsop and Doyle (2014) and is summarized below.

Gneissic banding (mm-to-cm scale) is readily measurable in drillcores and available outcrops. The banding is tight to isoclinally folded with east- to southeast-dipping hinge surfaces and gently south-plunging hinges. Many of these folds are rootless, consistent with the development of

gneissic banding during early deformation accompanying metamorphism at amphibolite to granulite facies, as supported by leucosomes that are observed both parallel to the banding and localized along D_1 fold closures (Doyle et al., 2007).

Mapping of outcrop 4 km northeast of the deposit (Fox-Wallace, 2010; Fox-Wallace et al., 2013) defined D_2 folds that are represented in the Tropicana Gold Mine model at the scale of hundreds of metres in the footwall to ore. The D_2 folds are interpreted to record a west to northwest-verging thrust system that is developed regionally during D_2.

The mineralized shear zones developed during D_3 at c. 2520 Ma (see below) during the Tropicana Event (Doyle et al., 2013; Blenkinsop and Doyle, 2014). D_3 shear zones (mm-to-cm wide) are defined by assemblages of biotite, pyrite, sericite, and chlorite and cut across the gneissic banding, although they are generally subparallel to the gneissosity. The shear zones envelop lithons ranging in scale from centimetres to tens of metres in length that are brecciated and fractured. Shear sense indicators include S–C and S–C fabrics, sigma porphyroclasts and oblique foliations, and when linked with mineralogy define a coherent kinematic history. Biotite–pyrite-dominant fabrics as ascribed to D_3 are overprinted by later sericite and/or chlorite fabrics. Gentle folding of the gneissic host postdates D_1 and D_2, and is ascribed to D_3. The typical southeast plunge of the high-grade shoots at Havana is parallel to common intersections of the biotite–pyrite shear zones and hinges of F_3 folds.

In the Tropicana Zone, high-grade ore shells dip more easterly, giving an easterly trend to their intersection. The change in plunge could be a consequence of: a) an initial variation in geometry inherited from D_1 and D_2; or b) reorientation by D_4 or D_5 in the Tropicana Zone, which is distinguished from the other zones by a higher density of late shear zones.

Sericite–chlorite dominant fabrics overprint the biotite–pyrite shears and are characterized by distinct fabrics and kinematics (D_4, D_5). Asymmetric folds with fold hinge surfaces which dip south, and the south-dipping shears are consistent with late deformation events comprising dextral shear on south- and southwest-dipping zones, and are ascribed to D_5.

Tropicana geochronology

The structural and mineralization history of the Tropicana deposit has been established through integration of structural, paragenetic, and geochronological studies. The event history and significance for interpretation of the region are summarized from Doyle et al. (2013), Blenkinsop and Doyle (2014), and Doyle et al. (2015).

SHRIMP U–Pb analysis of zircon and monazite from gneiss hosting the Tropicana gold lodes yield a weighted mean $^{207}Pb/^{206}Pb$ age of 2638 ± 4 Ma. In samples for which both zircon and monazite have been analysed, the ages returned are within error. The centre of some zircon grains yield ages in the range 2.6 – 2.7 Ga, in contrast to monazite which lacks evidence for Pb inheritance. The absence of an inherited Pb component in monazite analyses from the sample pairs implies that the U–Pb system in monazite was completely reset during metamorphism at c. 2638 Ma, or that both zircon and monazite record the magmatic age, and the older zircon ages are from xenocrysts.

Metamorphic zircon is typically characterized by Th/U ratios less than 0.1 (e.g. Rubatto et al., 2001, and references therein). Th/U ratios for zircons in the Tropicana samples are in the range of 1.3 – 0.2, favouring interpretation as an igneous crystallization age.

The timing of peak granulite-facies metamorphism is poorly constrained between c. 2638 and 2520 Ma. Cooling trajectories based on the maximum and minimum uplift rates published in the literature allow the peak of granulite metamorphism recorded at Tropicana to be from close to the host rock emplacement age, to only a few million years prior to mineralization (Doyle et al. 2015).

The oldest statistically significant population of rutile ages (2521 ± 5 Ma) is interpreted to record the formation of tungsten-rich rutile during mineralization at a temperature below the 500–550°C blocking temperature (Doyle et al., 2015). Re–Os of pyrite from Tropicana returned an age of 2505 ± 50 Ma and overlap with those from less precise Pb/Pb pyrite analyses (2.4 – 2.5 Ga). The pyrite dates are within error of the biotite analyses from biotite–pyrite assemblages hosting gold (Blenkinsop and Doyle, 2014).

The dehydrated nature of granulite-facies gneisses under retrograde conditions suggests mineralizing fluids were introduced from an external source at c. 2.5 Ga. The fluid-induced event (Tropicana Event, Doyle et al., 2013) produced a mineral assemblage indicative of greenschist-facies conditions and impacted on the retrograde path from peak metamorphism. Economic gold mineralization is interpreted to have formed during the event during northeast–southwest directed shortening.

The Tropicana Gneiss was exhumed into the greenschist facies window during the Neoarchean and remained relatively unaffected during the Albany–Fraser Orogeny. Evidence for Stage I (1345–1260 Ma) or Stage II (1215–1140 Ma; Clark et al., 2000) of the Albany–Fraser Orogeny is limited. At Tropicana, the Albany–Fraser Orogeny cannot have reached temperatures of about 350°C for an extended period of time, as biotite and rutile ages are robust. The Tropicana Gneiss is interpreted to have represented a 'relatively' stable structural region during the Proterozoic Eon. Deformation was localized along its margins, between constituent structurally bound blocks, and within discrete high-strain mylonitic shear zones that cut both the Archean and Proterozoic domains.

Discussion

The history of the Tropicana Gneiss of the Plumridge terrane falls into two principal periods (Doyle et al., 2013; Blenkinsop and Doyle, 2014; Fig. 4). During the first period, emplacement and metasomatism of the precursor mafic to felsic rocks at c. 2636 Ma was followed by amphibolite to lower granulite facies metamorphism in the period c. 2636 to 2520 Ma. This was followed by

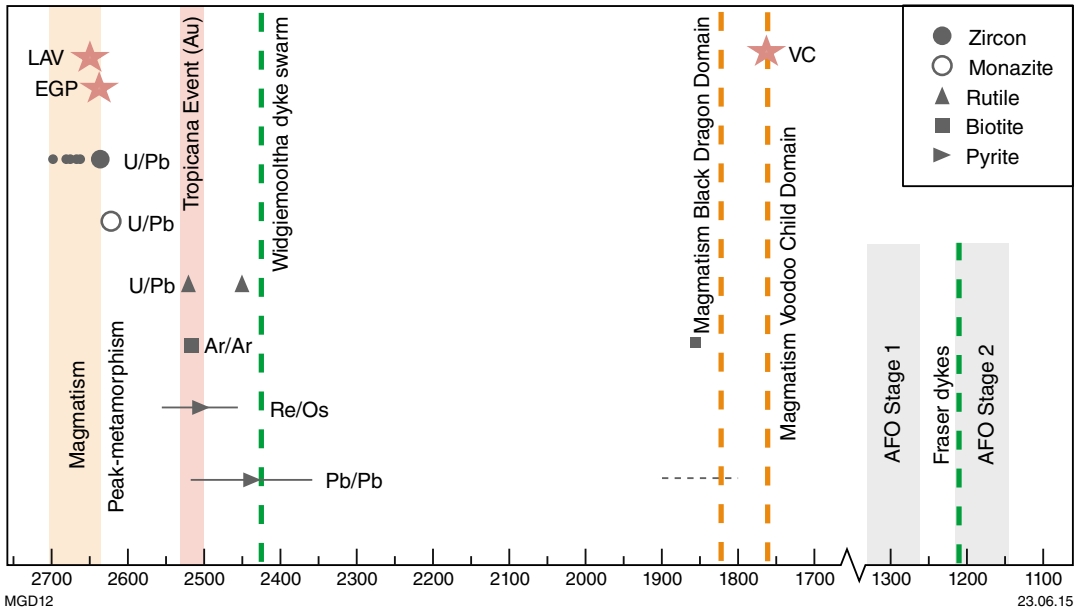

Figure 4. Summary of principal events at the Tropicana gold deposit, Biranup Zone and Albany–Fraser Orogen (AFO). The principal gold events in the Eastern Goldfields Province (EGP), Laverton District (LAV) of the Yilgarn Craton, and Voodoo Child (VC) are also illustrated (after Doyle et al., 2015).

exhumation and juxtaposition of the Archean lower crust against and over upper crust of the Yilgarn Craton. The Plumridge Detachment marks the contact between the Tropicana Gneiss and underlying elements of the Yamarna Terrane (Occhipinti et al., 2014). The second period was associated with northeast–southwest shortening and produced mineral assemblages diagnostic of greenschist facies conditions (Blenkinsop and Doyle, 2014). The age of this deformation and mineralization event, the Tropicana Event, is latest Archean (c. 2520 Ma) and generated economic concentrations of gold at the Tropicana mine. Thrusts mapped in the Tropicana Gold Mine area have listric geometries and merge into the Plumridge Detachment at depth (Occhipinti et al., 2014).

The age of mineralization in the Tropicana Gneiss contrasts with that of peak gold mineralization in the Yilgarn Craton. Mineralization was diachronous across the craton and in the Laverton greenstone belt occurred at c. 2.65 Ga, whereas in the Eastern Goldfields Superterrane, the Southern Cross and Murchison Domains mineralization occurred at 2.64 Ga (e.g. Salier et al., 2005). The Tropicana mineralization occurred at c. 2.5 Ga, a period that coincides with a subordinate peak in juvenile continental crustal production and gold deposit formation (e.g. Goldfarb et al., 2001, 2005).

The timing of the Tropicana mineralization is similar to that recognized in the Eastern Dharwar Craton, India (e.g. Sarma et al., 2008). In the Dharwar Craton, gold ores at Hutti and Kolar were broadly coincident with widespread syntectonic plutonism preceding final stabilization of the craton by c. 2420 Ma (Krogstad et al., 1989). The current study suggests that the final stages in cratonization of the Yilgarn Craton in Australia may have extended into the early Paleoproterozoic and, if so, was preceded by thermal reworking of the lower–middle crust.

The similarity in the position of Tropicana gold deposit and the granulite-hosted Renco gold deposit in Zimbabwe relative to their adjacent cratons is striking. Both comprise shear-hosted ore zones that dip moderately away from the craton and post-dates peak metamorphism (Blenkinsop and Doyle, 2014). They are type examples of Tomkin's (2013) post-metamorphic gold deposit category found in highly metamorphosed terranes.

References

AngloGold Ashanti Ltd 2011, Tropicana Gold Project ore reserve increase: Report to Australian Securities Exchange, 26 July 2011, 2p.

AngloGold Ashanti Ltd 2012, Tropicana Gold Project mineral resource continues to grow: Report to Australian Securities Exchange, 4 December 2012, 3p.

Bierlein, FP, Groves, DI, Goldfarb, RJ and Dube, B 2006, Lithospheric controls on the formation of provinces hosting giant orogenic gold deposits: Mineralium Deposita, v. 40, p. 874–886.

Blenkinsop, TG and Frei, R 1996, Archean and Proterozoic mineralization and tectonics at the Renco mine (Northern Marginal Zone, Limpopo Belt, Zimbabwe): Economic Geology, v. 91, p. 1225–1238.

Blenkinsop, TG and Doyle, MG 2013, Structural controls on gold mineralization on the margin of the Yilgarn Craton, Albany–Fraser Orogeny: the Tropicana deposit, Western Australia, *in* Future understanding of tectonics, ores, resources, environment and sustainability *edited by* Z Chang, R Goldfarb, T Blenkinsop, C Palczek, D Cooke, K Camuti and J Carranza: FUTORES Conference, Economic Geology Research Unit Contribution 68, James Cook University, Townsville, Australia 2–5 June 2013, p. 37.

Blenkinsop, TG and Doyle, MG 2014, Structural controls on gold mineralization on the margin of the Yilgarn Craton, Albany–Fraser Orogen: The Tropicana Deposit, Western Australia: Journal of Structural Geology, v. 67 p. 189–204.

Bunting, JA, de Laeter, JR and Libby, WG 1976, Tectonic subdivisions and geochronology of the northeastern part of the Albany–Fraser Province, Western Australia, *in* Annual Report for 1975: Geological Survey of Western Australia, p. 117–125.

Clark, DJ, Henson, BJ and Kinny, PD 2000, Geochronological constraints for a two-stage history of the Albany–Fraser Orogen: Western Australia: Precambrian Research, v. 102, p. 155–183.

Doyle, MG, Kendall, BM and Gibbs, D 2007, Discovery and characteristics of the Tropicana Gold District, *in* Proceedings of Geoconferences, Kalgoorlie 07 Conference *edited by* FP Bierlein and CM Knox-Robinson: Geoscience Australia Record 2007/14, p. 186–190.

Doyle, MG, Gibbs, D, Savage, J and Blenkinsop, TG 2009, Geology of the Tropicana Gold Project, Western Australia, *in* Smart science for exploration and mining: Economic Geology Research Unit, James Cook University; 10th Biennial SGA Meeting of the Society for Geology Applied to Mineral Deposits, Townsville, Queensland, 17 August 2009: Proceedings volume 1, p. 50–52.

Doyle, M, Savage, J, Blenkinsop, T, Crawford, A and McNaughton, N 2013, Tropicana – Unravelling the complexity of a +6 Million Ounce Gold Deposit Hosted in Granulite Facies Metamorphic Rocks: The Australian Institute of Mining and Metallurgy Publication Series no. 9/2013, p. 87–93.

Doyle, MG, Fletcher, IR, Foster, J, Large, R, Mathur, R, McNaughton, NJ, Meffre, S, Muhling, JR, Phillips, D and Rasmussen, B, 2015 Geochronological constraints on the Tropicana Gold Deposit and Albany–Fraser Orogen, Western Australia: Economic Geology, v. 110, p. 1–32.

Fox-Wallace, LJ 2010, Geology of the Hat Trick Prospect in the Tropicana Project area, Western Australia: James Cook University, Townsville, BSc (Honours) thesis (unpublished), 104p.

Fox, LJ, Blenkinsop, TG and Doyle, MG 2012, Geology of the Hat Trick Prospect, Tropicana Region, Northern Foreland of the Albany Fraser orogeny, WA: Geological Society of Australia, Abstracts 102, p. 39–40.

Goldfarb, RJ, Groves, DI and Gardoll, S 2001, Orogenic gold and geological time: a global synthesis: Ore Geology Reviews, v. 18, p. 1–75.

Goldfarb, RJ, Baker, T, Dubé, B, Groves, D, Hart, CJ and Gosselin, P 2005, Distribution, character, and genesis of gold deposits in metamorphic terranes: Economic Geology 100th Anniversary Volume, p. 407–450.

Kendall, B, Doyle, M and Gibbs, D 2007, Tropicana: The discovery of a new gold province in Western Australia: 2007 NewGenGold Conference, p. 85–95.

Kirkland, CL, Spaggiari, CV, Pawley, MJ, Wingate, MTD, Smithies, RH, Howard, HM, Tyler, IM, Belousova, EA and Poujol, M 2011, On the edge: U–Pb, Lu–Hf, and Sm–Nd data suggests reworking of the Yilgarn craton margin during formation of the Albany–Fraser Orogen: Precambrian Research, v. 187, p. 223–247

Krogstad, EJ, Balakrishnan, S, Mukhopadhyay, DK, Rajamani, V and Hanson, GN 1989, Plate tectonics 2.5 billion years ago: Evidence at Kolar, South India: Science, v. 243, p. 1337–1340.

Less, T 2013, Newly recognized Paleoproterozoic gold-silver mineralization in the Albany–Fraser Orogeny, *in* Future understanding of tectonics, ores, resources, environment and sustainability *edited by* Z Chang, R Goldfarb, T Blenkinsop, C Palczek, D Cooke, K Camuti and J Carranza: FUTORES Conference, Economic Geology Research Unit Contribution 68, James Cook University, Townsville, Australia 2–5 June 2013, p. 31.

Occhipinti, SA, Doyle, M, Spaggiari CV, Korsch, R, Cant, G, Martin, K, Kirkland, CL, Savage, J, Less, T, Bergin, L and Fox, L 2014, Interpretation of the deep seismic reflection line 12GA-T1: northeastern Albany–Fraser Orogen, *in* Albany–Fraser Orogen seismic and magnetotelluric (MT) workshop 2014: extended abstracts *compiled by* CV Spaggiari and IM Tyler: Geological Survey of Western Australia, Record 2014/6, p. 52–68.

Qiu, Y, McNaughton, NJ, Groves, DI and Dunphy, JM 1999, First record of 1.2 Ga mafic granitic magmatism within the Archaean Yilgarn Craton, Western Australia, and its significance: Australian Journal of Earth Sciences, v. 46, p. 421–428.

Rubatto, D, Williams, IS and Buick, I 2001, Zircon and monazite response to prograde metamorphism in the Reynolds Range, Australia: Contributions to Mineralogy and Petrology, v. 140, p. 458–468.

Sarma, DS, McNaughton, NJ, Fletcher, IR, Groves, DI, Mohan, MR and Balaram, V 2008, Timing of gold mineralization in the Hutti gold deposit, Dharwar Craton, South India: Economic Geology, v. 103, p. 1715–1727.

Schodde, RC and Hronsky, JMA 2006, The role of world-class mines in wealth creation: Society of Economic Geologists Special Publication 12, p. 71–90.

Spaggiari, CV, Bodorkos S, Barquero-Molina, M, Tyler, IM and Wingate, MTD 2009, Interpreted bedrock geology of the south Yilgarn and central Albany–Fraser Orogen, Western Australia: Geological Survey of Western Australia, Record 2009/10, 84p.

Spaggiari, CV, Kirkland, CL, Pawley, MJ, Smithies, RH, Wingate, MTD, Doyle, MG, Blenkinsop, TG, Clarke, C, Oorschot, CW, Fox, LJ and Savage, J 2011, The geology of the East Albany–Fraser Orogen – a field guide: Geological Survey of Western Australia, Record 2011/23, 98p.

Tomkins, AG 2013, Gold deposits in highly metamorphosed terranes: The Australian Institute of Mining and Metallurgy Publication Series no. 9/2013, p. 23–25.

Tomkins, AG and Grundy, C 2009, Timing of granulite-hosted gold at Griffin's Find: Constraining the crustal continuum model, *in* Smart science for exploration and mining: Economic Geology Research Unit, James Cook University; 10th Biennial SGA Meeting of the Society for Geology Applied to Mineral Deposits, Townsville, Queensland, 17 August 2009: Proceedings volume 1, p. 381–383.

Tomkins, AG, Pattison, DR and Zaleski, E 2004a, The Hemlo gold deposit, Ontario: An example of melting and mobilization of a precious metal-sulfosalt assemblage during amphibolite facies metamorphism and deformation: Economic Geology, v. 99, p. 1063–1084.

Tomkins, AG, Dunlap, WJ and Mavrogenes, JA 2004b, Geochronological constraints on the polymetamorphic evolution of the granulite-hosted Challenger gold deposit: implications for assembly of the northwest Gawler Craton: Australian Journal of Earth Sciences, v. 51, p. 1–14.

Tomkins, AG and Mavrogenes, JA 2002, Mobilization of gold as a polymetallic melt during pelite anatexis at the Challenger gold deposit, South Australia: A metamorphosed Archean deposit: Economic Geology, v. 97, p. 1249–1271.

Wingate, MTD, Campbell, I and Harris, LB 2000, SHRIMP baddelyite age for the Fraser Dyke Swarm, southeast Yilgarn Craton, Western Australia: Australian Journal of Earth Sciences, v. 47, p. 309–313.

Geochemistry and petrogenesis of igneous rocks in the Albany–Fraser Orogen

by

RH Smithies, CV Spaggiari, CL Kirkland, and WD Maier[1]

Introduction

Like other orogenic belts that surround the Yilgarn Craton, the Albany–Fraser Orogen is dominated by Paleoproterozoic to Mesoproterozoic igneous rocks formed through a complex series of events variably involving recycling of a range of crustal components and periods of crustal refertilization through juvenile mantle magmatic input. The record of crustal evolution of these 'circum-Yilgarn' orogens is typically already cryptic, but their study is further complicated by vast regions of extremely poor outcrop. One of the most fruitful ways of deciphering the crustal evolution of geologically complex regions of continental crust is by tracing the compositional evolution of igneous rocks through time and space. This approach is directly limited by the availability of suitable outcrop. A database of whole-rock analyses obtained so far on mafic to felsic rocks from the central and eastern Albany–Fraser Orogen, is used here to place critical constraints on models used to assess the geological evolution and mineral prospectivity of the region. The dataset used here includes ~250 whole-rock analyses from the WACHEM database (http://geochemistry.dmp.wa.gov.au/geochem/), and approximately half of the felsic samples have also been dated by U–Pb geochronology (www.dmp.wa.gov.au/geochron/). Interpretations and constraints from studies of both geochemical and isotopic datasets have been presented in Smithies et al., (2013, 2014) and Kirkland et al., (2011a,b). The purpose of this article is to summarize some of the key conclusions arising from these studies. The regional geological setting of various units described below is summarized in Spaggiari et al. (2014a, this volume) and Spaggiari et al. (2011, 2014b), and is not repeated here. Constraints on the geochronology of the orogen and its Hf isotopic signature are described in Kirkland et al. (2014, this volume).

1 Department of Geosciences, University of Oulu, Linnanmaa, Oulu 90014, Finland

Mafic and ultramafic rocks

Most analyses of mafic rocks of the Albany–Fraser Orogen have been obtained from the southwestern part of the c. 1300 Ma Fraser Zone (Fig. 1). Recently added to this is a subset of analyses of diamond core samples from the Nova deposit (The Eye prospect; Sirius Resources NL, 2012) drilled just prior to the main discovery as an Exploration Incentive Scheme (EIS) co-funded project. In addition, several other gabbroic samples have been obtained throughout the course of regional mapping. These include: a) samples that, based on field relationships with dated granites, are suspected to relate to Stage I of the Albany–Fraser Orogeny (i.e. are synchronous with the gabbros of the Fraser Zone); b) gabbros which, based on mingling relationships with dated granites or on direct dating of the gabbro itself, were emplaced synchronously with major felsic magmatic events that pre-dated the Mesoproterozoic Albany–Fraser Orogeny (most likely Paleoproterozoic events including the 1710–1650 Ma Biranup Orogeny).

Fraser Zone gabbro

Gabbros of the Fraser Zone intruded metasedimentary country rock and granites of the Recherche Supersuite (Spaggiari et al., 2011). The metasedimentary rocks were deposited in a deep basin (the Arid Basin) shortly prior to gabbroic intrusion. The granites of the Recherche Supersuite include suites that were co-magmatic (and possibly co-genetic) with respect to the gabbros, and suites that formed as a result of gabbroic intrusion and the ensuing high-grade metamorphism.

The gabbros are typically Fe-rich tholeiites with parental magmas derived from a source that was similar to, or possibly slightly more depleted than, a MORB source. Two broad groups of gabbros occur: 'main gabbros' which show no field, petrographic, or geochemical evidence of having interacted with metasedimentary and granitic country-rocks; and various 'hybrid gabbros' which show variable evidence for interaction with crustal components. The main gabbro is parental to the hybrid gabbros but escaped hybridization during ascent or emplacement.

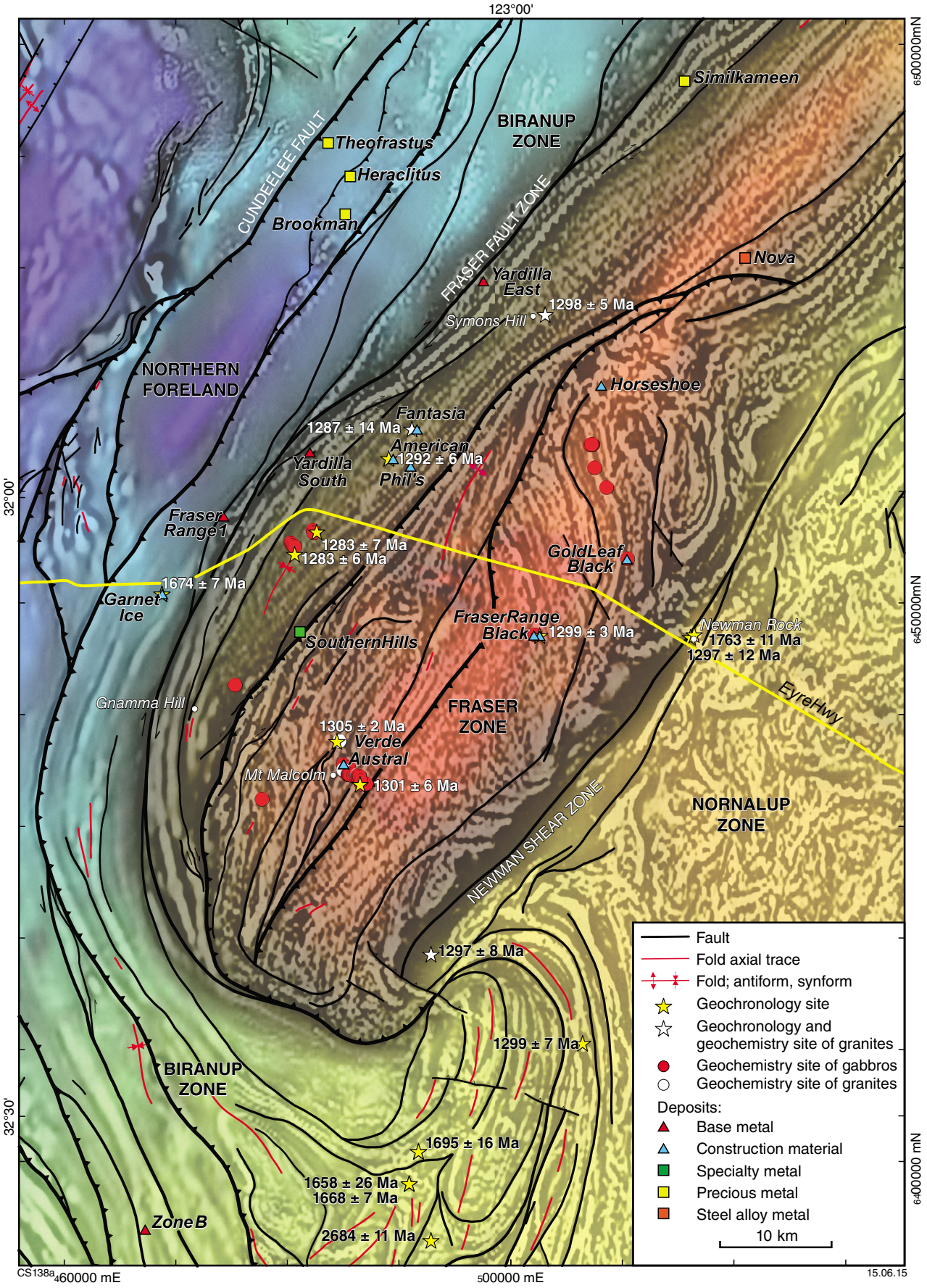

Figure 1. **Gravity image with first vertical derivative aeromagnetic drape of the southwestern part of the Fraser Zone, showing major structures, sample locations and U–Pb (SIMS) ages (from Smithies et al., 2013)**

However, these rocks still contain an enriched crustal component acquired at a deeper level. Previous accounts have suggested this enrichment reflects a subduction addition to the mantle sources that formed a series of discrete, subsequently accreted, ocean island arcs. However, all previous and recent Nd- and Hf-isotopic data are incompatible with that interpretation. For example, the relatively non-radiogenic Nd-isotopic data presented by Fletcher et al. (1991) alone suggests the gabbros cannot have formed in isolation of evolved old 'continental'crust. The observed trace element enrichments are better explained in terms of assimilation of basement that included a Sr-depleted component of Archean, or reworked Archean, crust. This is consistent with Hf-isotopic datasets and inherited zircon components within these rocks, which raise the possibility that a Biranup Zone component interacted with the primitive magmas of the Fraser Zone.

Our preferred model for the petrogenesis of the Fraser Zone gabbros involves mantle upwelling beneath an intracontinental rift, back-arc or possibly continental arc, forming a regional sheeted sill complex or 'hot-zone' that was subsequently structurally modified (Spaggiari et al., 2011). A continental arc seems least likely in view of the absence of calc-alkaline magmas in the Fraser Zone itself. If the enriched trace element signatures in the high-Fe tholeiites that form the main gabbros are better explained by crustal contamination, then a distal back-arc or a truly intracontinental setting appears more likely than an arc-proximal setting. A back-arc setting has also been proposed to explain the high-temperature metamorphism, its temporal link to mafic magmatism, and the determined P–T path (Clark et al., 2014).

Nova (The Eye)

Mafic and ultramafic rocks within the Fraser Zone host significant Ni–Cu sulfide mineralization at Nova (The Eye prospect; Gollam, 2012; Sirius Resources NL, 2012). No published data indicate the timing of emplacement of the intrusion forming The Eye prospect. However, given the volume of mafic magmatism elsewhere in this zone that is temporally constrained, it was likely synchronous with the main c. 1300 Ma mafic magmatism within the Fraser Zone. Apart from the spatial association, and similar contact relationships with metasedimentary country-rocks, the 'main gabbros' (see above) and The Eye share several cursory compositional features including rather high Ni/Cu ratios and depleted PGE concentrations (Fig. 2) (despite the high Ni- and Cu-sulfide abundances at The Eye). Nevertheless, such geochemical similarities might be viewed cautiously given that c. 1665 Ma gabbro from the Eddy Suite, located in the eastern Biranup Zone marginal to the Fraser Zone (see below; Plate 2), have similar chemical compositions.

Certainly, if the main gabbros of the Fraser Zone and The Eye are indeed related to the same general magmatic event, then The Eye is distinguished within that magmatic group in being dominated by mafic and ultramafic cumulates (whereas higher Zr concentrations in the main gabbros likely reflect liquid compositions) that crystallized from a significantly more primitive magma (whole-rock $Mg^{\#}$ up to 83, Cr/V up to 45; Fig. 3). Despite (or, perhaps,

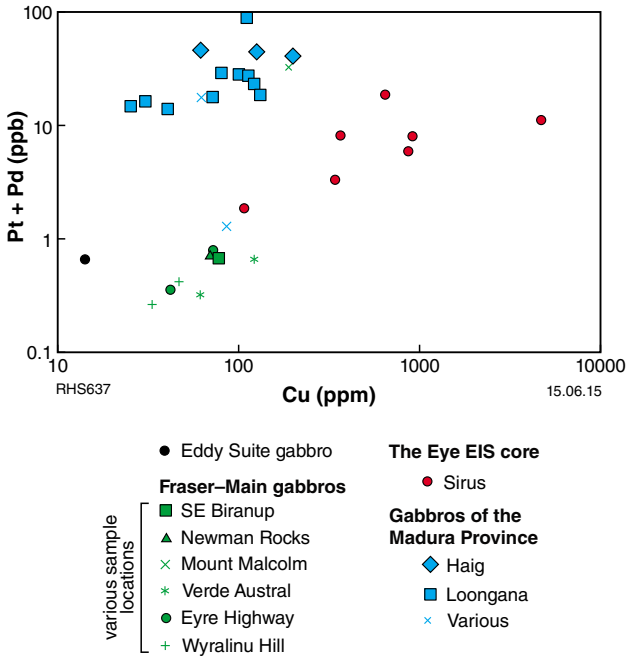

Figure 2. Variations in Pt + Pd vs Cu concentrations for mafic and ultramafic rocks of the Albany–Fraser Orogen and Madura Province

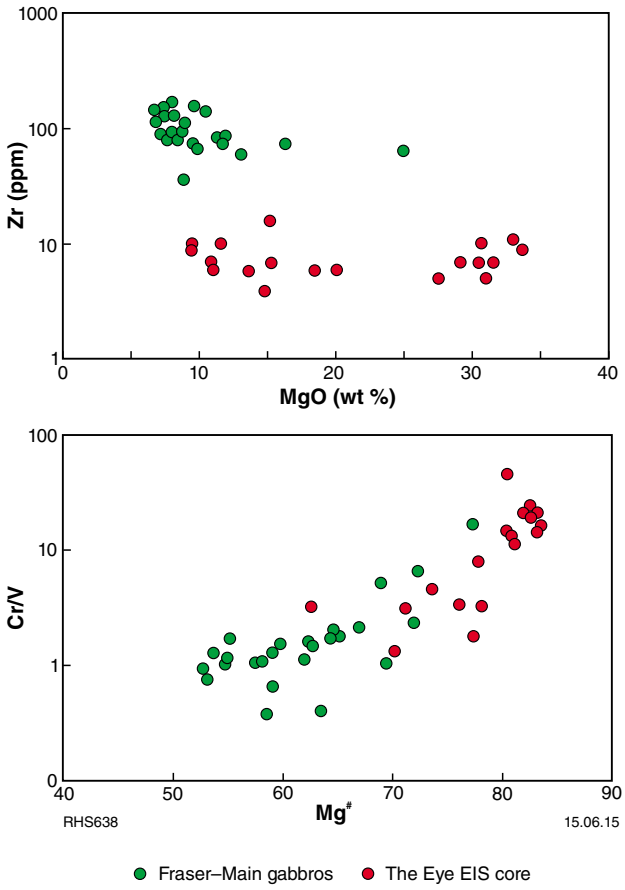

Figure 3. Variations in Zr concentrations and Cr/V ratios for mafic and ultramafic rocks of the Fraser Zone ($Mg^{\#}$ = molecular ratio of Mg/(Mg+total Fe)

because of) their primitive geochemistry, samples from The Eye are also significantly more crustally contaminated than the main gabbros. This is not only evident in their generally higher La/Nb ratios (3–6 c.f. 1–4) but also in the more radiogenic Sr-isotopic compositions of feldspars (initial $^{87}Sr/^{86}Sr$ ~ 0.7057 to 0.7066) and in the more crustal (i.e. higher) $\delta^{34}S$ (up to 4.5) values of their sulfides. Interestingly, Re–Os isotopic data on pyrite from the EIS core at The Eye yields model ages of around 1.82 – 1.71 Ga (GSWA preliminary data), possibly also indicating a sulfur source from a crustal basement to the Fraser Zone. The Re–Os system in these rocks also records isotopic disturbance at c. 1100 Ma, likely during Stage II of the Albany–Fraser Orogeny.

Other gabbros

Several gabbro samples, typically enclaves within Recherche or Esperance Supersuite granite, were collected throughout the eastern Nornalup Zone. The geochemistry of these gabbros shows extensive scatter (Fig. 4), probably reflecting minor contamination from the host granite, but is compatible with a source similar to the MORB-like source that yielded the Fraser gabbro (Fig. 5).

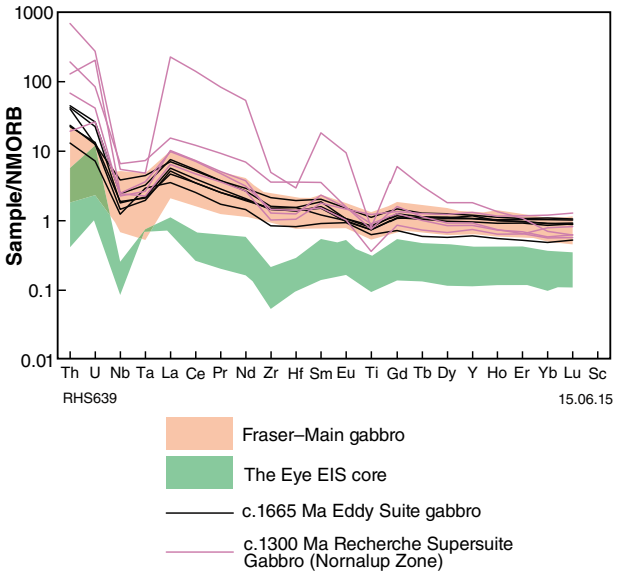

Figure 5. MORB-normalized multi-element spidergram for mafic and ultramafic rocks of the Albany–Fraser Orogen (normalizations after Sun and McDonough, 1989)

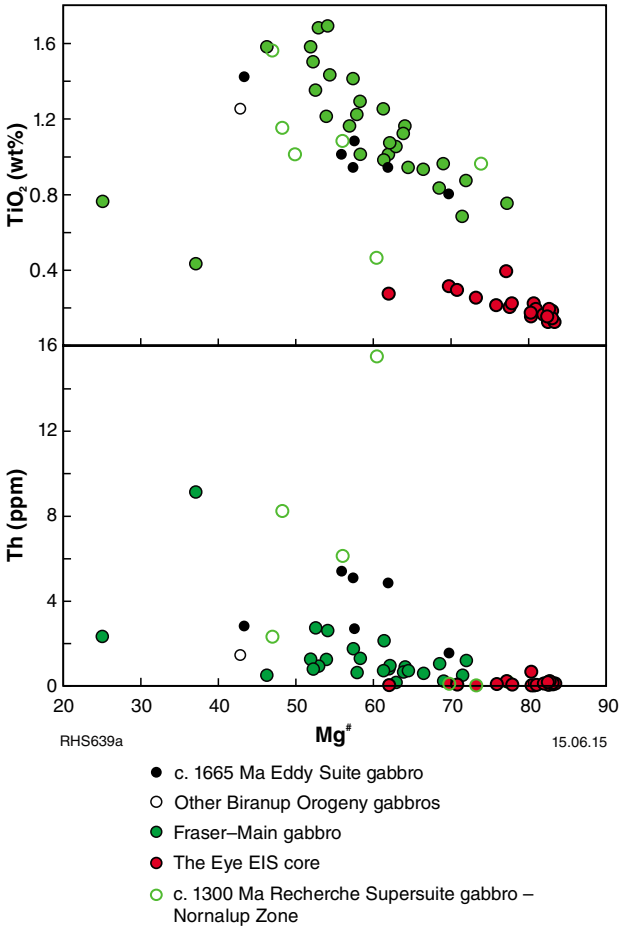

Figure 4. Variations in TiO_2 and Th concentrations for mafic and ultramafic rocks of the Albany–Fraser Orogen

Several other gabbro samples were taken from the eastern Biranup Zone — close to the Fraser Shear Zone marking the western extent of the Fraser Zone. The main sample site was a well exposed transect of the Eddy Suite just southwest of Harris Lake (Plate 2). Fractionated samples of this gabbro and of the co-mingled granite host have been dated at c. 1665 Ma (Kirkland et al., 2011a; Spaggiari et al, 2011). The geochemistry of these gabbros is very difficult to distinguish from samples of the Fraser gabbro, although lower concentrations of TiO_2 and of total Fe and higher Th and U at a given $Mg^{\#}$ do appear to discriminate the older gabbros (Fig. 4). The similarities in compositions of all gabbros discussed here suggest a mantle source that remained compositionally homogeneous over a long period (at least from c. 1665 to 1300 Ma), but also cautions against assigning an age to gabbroic rocks based on chemical composition alone.

Felsic rocks

Here, we use the term ‘granite’ (sensu lato) to refer to all originally intrusive felsic rocks irrespective of subsequent metamorphic or structural history. Of the >150 whole-rock granite analyses, 82 dated samples were assigned to groups based on U–Pb zircon crystallization age. Most (70%) of the dated samples crystallized during or before the 1710–1650 Ma Biranup Orogeny, allowing more tightly defined age groups for that subset of the data. The remaining c. 30% of the dated samples crystallized during the 1345–1140 Ma Albany–Fraser Orogeny and have been subdivided between the existing Stage I (1345–1260 Ma) and Stage II (1215–1140 Ma) orogenic age groups. The geographical distribution of the granites is shown in Figure 6.

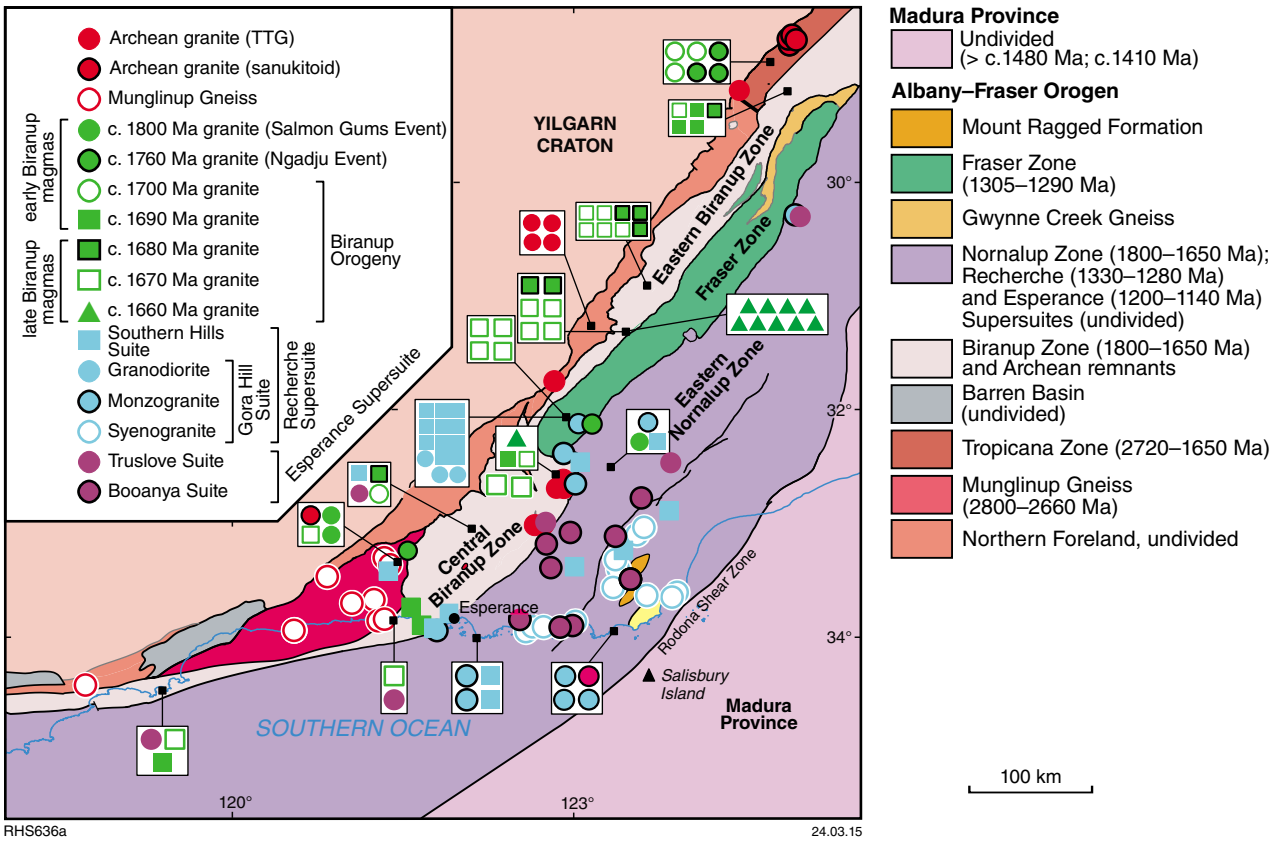

Figure 6. Location of granite samples. Relative position line reflects a northwest–southeast sample traverse through the Albany–Fraser Orogen (see Figure 11).

All undated samples have been assigned to the specific age group to which they show the closest affinity based firstly on field characteristics and relationships (e.g. contact relationships, structural and metamorphic history, geophysical characteristics) and petrology, and then on their geochemical characteristics (i.e. where field relationships were ambiguous). In no case did apparent geochemical affinity take precedence over a clear field classification. However, in several cases, samples with ambiguous field classification showed a clear geochemical affinity to a particular granite age group and were assigned accordingly.

At least 12 granite age-groups covering the period from c. 2722 to 1135 Ma can be identified, each with a generally distinctive compositional range. Granites with ages in the range 1710–1650 Ma fall within the Biranup Orogeny, whereas granites with ages of c. 1800 Ma are part of the Salmon Gums Event, and granites with ages between 1780 and 1760 Ma are part of the Ngadju Event (Spaggiari et al., 2014, this volume).

1. Archean granites
2. The Munglinup Gneiss (also Archean)
3. Granite with crystallization ages c. 1800 Ma (c.1800 Ma granites; Salmon Gums Event)
4. Granite with crystallization ages c. 1760 Ma (c.1760 Ma granites; Ngadju Event)
5. Granite with crystallization ages <1750 and >1695 Ma (c.1700 Ma granites)
6. Granite with crystallization ages between 1695 and >1685 Ma (c. 1690 Ma granites)
7. Granite with crystallization ages between 1685 and >1675 Ma (c. 1680 Ma granites)
8. Granite with crystallization ages between 1675 and >1665 Ma (c. 1670 Ma granites)
9. Granite with crystallization ages between 1665 and >1655 Ma (c. 1660 Ma granites)
10. Granites crystallized during Stage I of the Albany–Fraser Orogeny (Recherche Supersuite)
11. Granites crystallized during Stage II of the Albany–Fraser Orogeny (sodic Esperance Supersuite)
12. Granites mainly crystallized during Stage II of the Albany–Fraser Orogeny (enriched Esperance Supersuite).

Archean granites

Isolated fragments of Archean crust that remain in the Biranup Zone (Kirkland et al., 2011a; Spaggiari et al., 2011) are clearly recognized as such based on their geochemistry, which includes the generally elevated Na_2O and LILE (e.g. Sr) concentrations and depleted K_2O and HREE (e.g. Yb) concentrations typical of most Archean granites (Fig. 7).

Archean felsic rocks in the Northern Foreland and Biranup Zone can be divided between granites representative of the TTG series and Archean sanukitoids. Sanukitoids range to lower silica concentrations (down to ~61 wt%) (Fig. 7). They are thought to form as subduction derived TTG interacts with mantle wedge peridotite (e.g. Shirey and Hanson, 1981; Smithies and Champion, 2000; Martin et al., 2005) to produce a pyroxenitic source capable of yielding felsic melts. These melts are characterized, at c. 60 wt% SiO_2, by $Mg^{\#}$>60 and Cr and Ni concentrations >200 and 100 ppm, respectively, coupled with high concentrations of Sr, Ba and LREE. The occurrence of sanukitoids thus might be used to indicate close proximity to an old tectonic-plate margin and their presence in the Tropicana Zone (Hercules Gneiss, Plate 1; Kirkland et al., 2014 this volume), and elsewhere in the Biranup Zone, might suggest that this zone includes at least two older plate boundaries relating to assembly of the Yilgarn Craton. The observation that the Archean granite group contains samples from at least two compositionally distinctive series (TTG and sanukitoid) likely explains much of the compositional scatter observed for the group. In addition, while there is no clear evidence for compositional modification during metamorphism, several of the sanukitoid samples from the Hercules Gneiss in the Tropicana Zone have anomalously low CaO and correspondingly high K_2O, reflecting significant hydrothermal alteration.

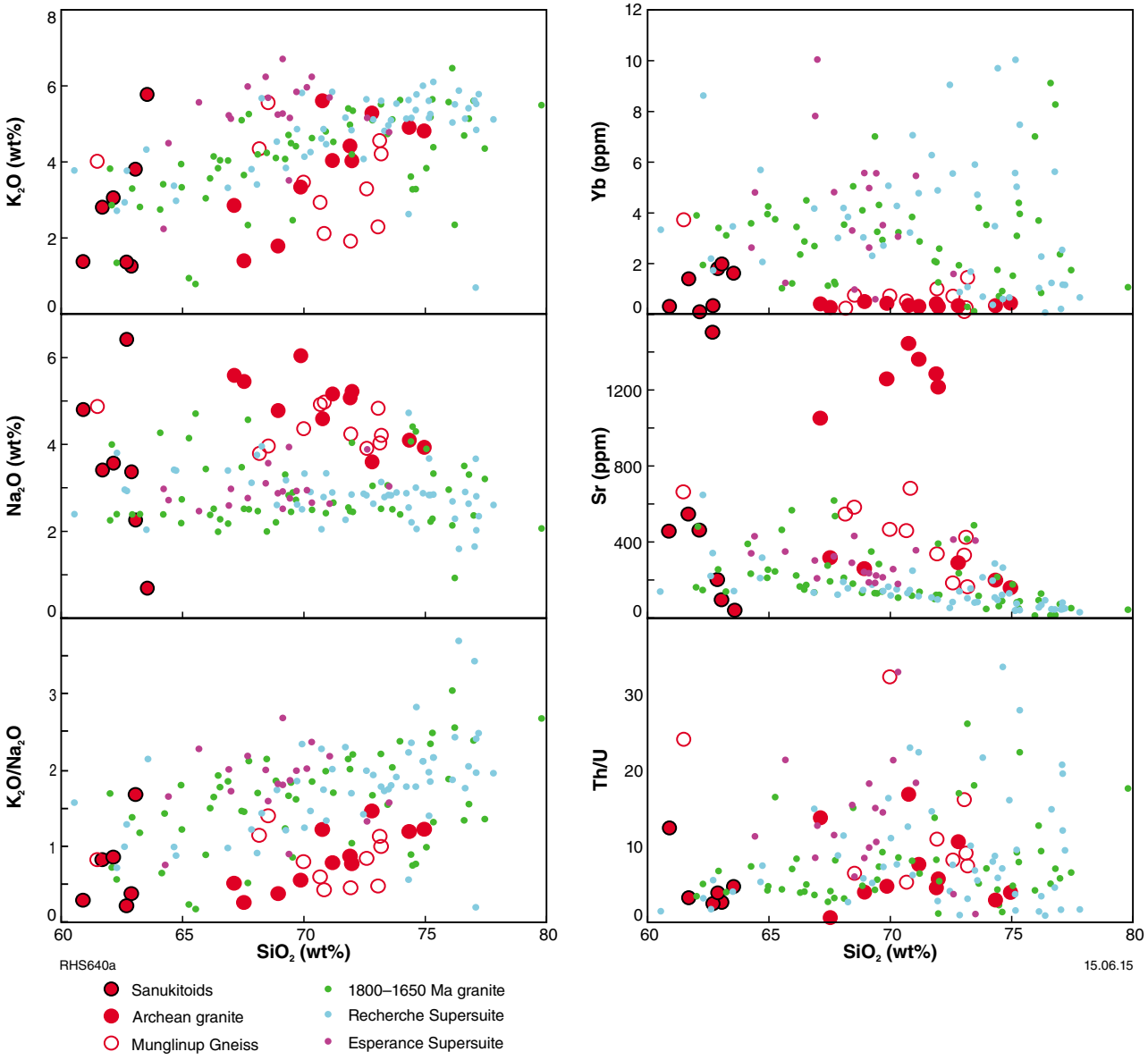

Figure 7. Compositional variation diagrams emphasizing geochemical characteristics of Archean granites from the Albany–Fraser Orogen

The Munglinup Gneiss (Plate 3) comprises an Archean granite protolith that has undergone Mesoproterozoic high-grade metamorphism involving metamorphic segregation, but only minimal anatectic melt loss beyond the sample scale. Compositional differences between the Munglinup Gneiss and other Archean granite with respect to La/Yb and La/Sm ratios possibly identify metamorphic conditions that permitted minor dehydration melting of biotite, but not of hornblende. This is consistent with field relationships that show only limited development of partial melt (leucosomes), generally synchronous with deformation.

Granites of the Biranup and Nornalup Zones

Geochemical data strengthen earlier conclusions based on geochronological and Hf-isotopic data (Kirkland et al., 2011b; Spaggiari et al., 2011) that the post-Archean crustal evolution of the Biranup Zone and Nornalup Zone of the Albany–Fraser Orogen involves recycling of dominantly Archean felsic material in several episodes, each also involving variable inputs of juvenile mantle material. These events progressively mask, but do not destroy, the Archean compositional heritage of the crust.

In terms of granite petrogenesis and crustal evolution, the period from c. 1800 Ma to the end of the Biranup Orogeny at c. 1650 Ma (i.e. including the Salmon Gums Event, the Ngadju Event and the Biranup Orogeny) can be divided in two ('early' and 'late' Biranup magmas). The felsic products of these two events can be broadly distinguished on plots of SiO_2 vs Na_2O, K_2O/Na_2O or Rb/Sr (Fig. 8). Early Biranup magmas include the c. 1800, 1760, 1700 and 1690 Ma granite groups, although the 1690 Ma group shows very transitional characteristics between the early and late Biranup magmas. The early period, as outlined above, essentially involved large-scale remelting of Archean crust, and the range to Nd-isotopic compositions more radiogenic than those of typical Archean granites indicate that crustal evolution throughout this period also involved mantle additions. The compositional characteristics of Archean TTG (e.g. high Al_2O_3, Na_2O, Sr, Ba, La/Yb, low K_2O, HREE – Fig. 7), relating mainly to their high pressure derivation from mafic sources, remains well developed in most of the older granite age groups (e.g. >1680 Ma), but progressive recycling leads to (among other things) increasing K_2O/Na_2O ratios in the younger granites (Fig. 8). The fact that the concentrations of the HREE (e.g. Yb) also remains very low within most of the early Biranup magmas perhaps suggests that recycling of Archean crust at this stage remained within the stability field of garnet. Some exceptions occur with local development of highly sodic granites, but these are often accompanied by rather high HREE concentrations (e.g. Yb >2ppm) suggesting local anatexis of gabbros at low pressure.

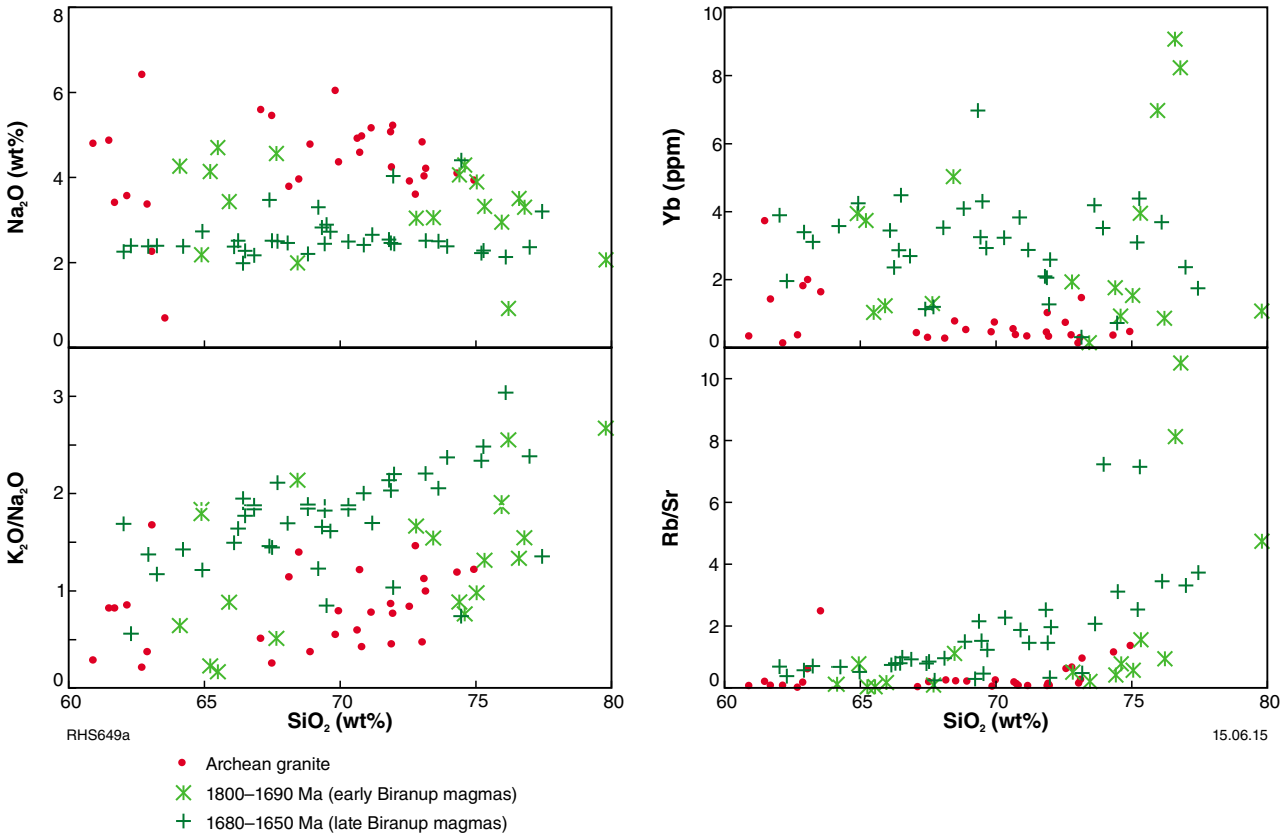

Figure 8. Compositional variation diagrams emphasizing contrasting geochemical characteristics of early and late Biranup magmas

In contrast with the sodic early Biranup magmas, the majority of the high-K late Biranup (c. 1680 to 1650 Ma) magmas show none of the enduring major or trace element (Fig. 8) compositional features that mark the source as recycled Yilgarn Craton crust, although the Nd-isotopic data indicates that Archean material remained a major source component (Fig. 9). The compositional ranges and trends shown by the late Biranup granites are reasonably typical of medium- to high-K calc-alkaline rocks (although the late Biranup magmas tend to have more ferroan compositions) and there are very few, and only subtle, compositional features that can distinguish any of the three age groups that fall within the c. 1680 to 1650 Ma period. The Nd-isotopic compositions of the late Biranup magmas is typically more radiogenic ($\varepsilon_{Nd\ (1670Ma)}$ of -2.73 to -11.86) than Yilgarn Craton felsic crust. It overlaps extensively with the range for the early Biranup magmas, but extends to slightly more radiogenic compositions (Fig. 9). Within the range for the late Biranup magmas, there is also a crude trend to increasingly radiogenic compositions with decreasing age of magmatic group (average $\varepsilon_{Nd\ (1670Ma)}$ of c. 1680 Ma granites = -6.44; c. 1670 Ma granites = -5.72; c. 1660 Ma granites = -3.86). Rather than direct incorporation of Archean crust, geochemical arguments suggest that the source for the high-K late Biranup magmas actually incorporated a high proportion of early Biranup granite, again with addition of a younger and more isotopically juvenile mantle component. Thus, the later magmatic period (c. 1680 to c. 1650 Ma) of the Biranup Orogeny heralds a change in the style of crustal evolution to one that involved recycling of previously recycled Archean felsic crust, and trends to higher concentrations of HREE suggest that this recycling occurred at higher crustal levels (or in thinner crust) than was the case during the period when the early Biranup magmas were produced. Another significant difference, identified through negative correlations between the measure of Nd- and Hf-isotopic decoupling ($\Delta\varepsilon_{Hf}$) and La/Sm, La/Yb and La/Nb ratios, is the indication that deep refractory crust, left behind after extraction of Archean TTG, formed a source component of the late Biranup magmas. In detail, the source for late Biranup granites includes a chemically primitive component formed through variable interaction between mafic mantle melts and the ^{176}Hf-enriched deep crustal residuals of Archean TTG production, and mixing between these and crustal melts dominated by relatively evolved and radiogenic early Biranup source material.

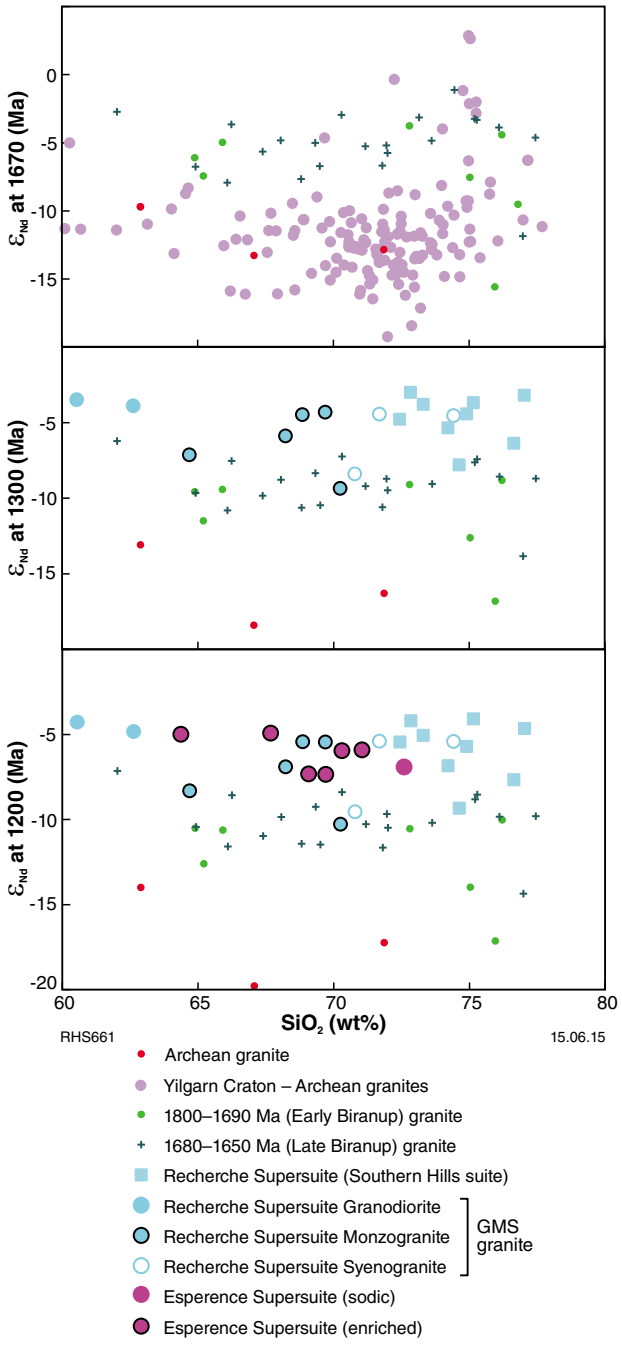

Figure 9. Nd-isotopic compositional variations of granites from the Albany–Fraser Orogen (data for granites of the Yilgarn Craton are from D Champion, written comm, 2014)

Forming close to the transition from early to late Biranup magmatism, and commencement of the Biranup Orogeny, the c. 1700 Ma granites from Bobbie Point (Bobbie Point Metasyenogranite, Tropicana Zone) are unusual. They have A-type compositions reflecting very high-temperature (and likely anhydrous) crustal melting. They also have high HREE (Fig. 7) concentrations and $\Delta\varepsilon_{Hf}$ values suggesting low pressure melting of a crustal source that previously resided at a deeper level within the garnet stability field (Kirkland et al., 2011a). This is consistent with the c. 1700 Ma melting of the Archean rocks of the Tropicana Zone after their emplacement to shallow crustal levels via thrusting along the Plumridge Detachment at c. 2500 Ma (Occhipinti et al., 2014, this volume). This thrust event is not recognized elsewhere in the Albany–Fraser Orogen, but the c. 1700 Ma magmatism likely reflects a period of significant crustal thinning throughout. Although crustal evolution throughout the period from c. 1800 Ma to the end of the Biranup Orogeny was likely controlled by crustal thinning events, the c. 1700 Ma event, perhaps, heralds the beginning of a period of enhanced thinning and uplift of deep crustal source components which continued for the rest of the Biranup Orogeny.

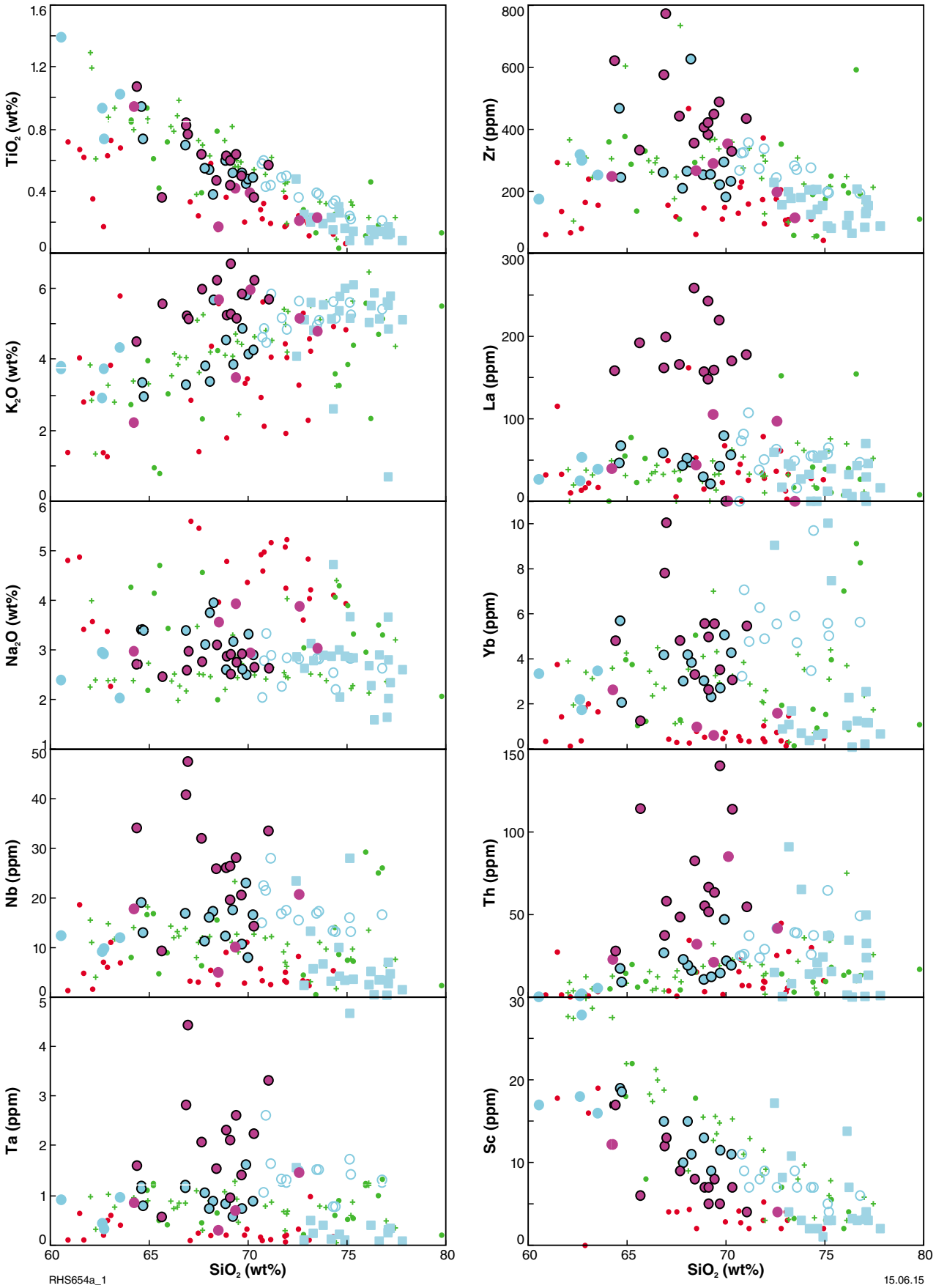

Figure 10. Compositional variation diagrams emphasizing geochemical characteristics of granites formed during the Albany–Fraser Orogeny

Granites of the Albany–Fraser Orogeny

Stage I — Recherche Supersuite

Granites crystallized during Stage I of the Albany–Fraser Orogeny (Recherche Supersuite) were subdivided based solely on composition. A highly silicic (SiO_2 > 72 wt%) group of rocks typically with notable depletions in high field strength elements (HFSE – Nb, Ta, Zr, Hf, Ti – Fig. 10), rare earth elements (REE), Th and U compared to other granites of the Recherche Supersuite with similar silica values is concentrated in and around (but not restricted to) the Fraser Zone and is referred to here as the Southern Hills Suite. Remaining samples of the Recherche Supersuite tend to form a geochemically coherent group that has been subdivided according to silica content into 'Recherche granodiorite' (SiO_2 <64 wt%), 'Recherche monzogranite' (SiO_2 64 to 70.5 wt%), and 'Recherche syenogranite' (SiO_2 >70.5 wt%). These are grouped into the granodiorite–monzogranite–syenogranite (GMS) granites and are found throughout the Fraser and Nornalup Zones, including on the easternmost edge of the Nornalup Zone adjacent to the Rodona Shear Zone and adjoining Madura Province.

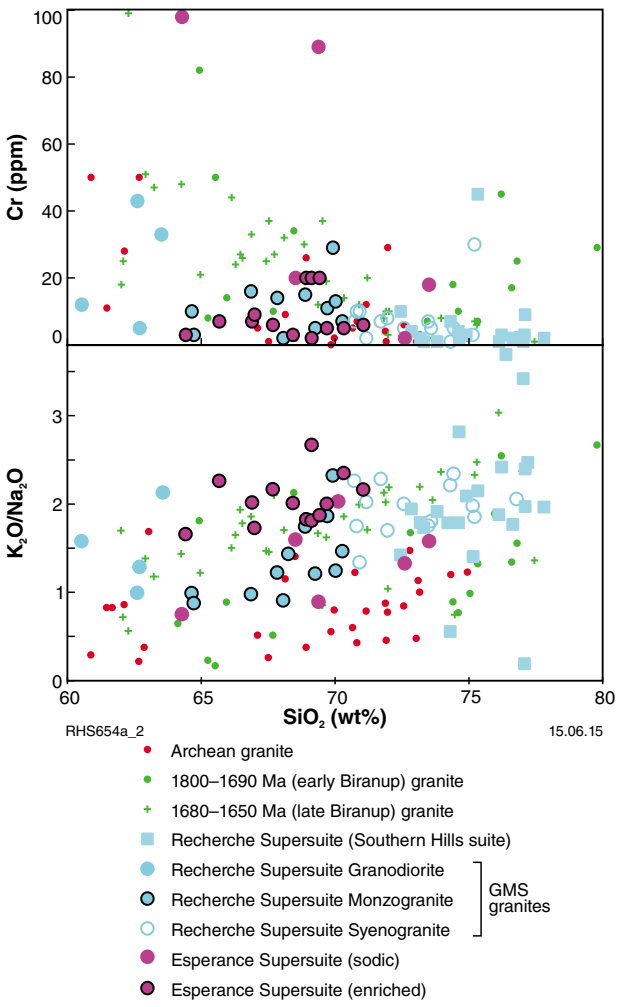

Figure 10. continued

The Southern Hills Suite reflects melting of supercrustal sequences dominated by sedimentary rocks whose source was isotopically primitive (note elevated ε_{Nd} compared with older granites – Fig. 9) with respect to known older crustal components of the Albany–Fraser Orogen. The most likely source of this material is the Madura Province to the east (e.g. Spaggiari et al., 2014).

Except for a few critical trace elements (e.g. Sc, Cr, Ba – Fig. 10), it is extremely difficult to separate the GMS granites from the late Biranup granite groups. All of these rocks or groups are generally calc-alkalic and weakly ferroan and show extensive compositional overlap for most elements. However, in terms of overall trends, the GMS granite series is distinct in that concentrations of Nb, Ta, and Yb increase with increasing SiO_2, whereas those trace elements decrease with increasing SiO_2 in the late Biranup granite groups. Like the late Biranup granites, the GMS granites generally have lower Na_2O and higher K_2O concentrations and higher K_2O/ Na_2O ratios than early Biranup granite groups, Archean granites and the Munglinup Gneiss.

In a broad sense there is a clear and systematic spatial variation in the composition of GMS granites more or less at a right angle to the structural trend of the Albany–Fraser Orogen, such that granodiorite occurs only in the northwest and syenogranite dominates in the southeast. Magmatism also appears to become systematically younger to the northwest.

Based on geochemical and isotopic variations, the GMS granites most likely represent mixing between a crustal source (likely early and late Biranup granites — themselves containing a significant component of recycled Archean crust) and mantle material similar to that which formed the Fraser gabbro (Fraser Zone). This peterogenesis is similar to that of the late Biranup granites although there is no evidence that the deep crustal refractory source component identified within the late Biranup magmas was involved in production of the GMS granites. In addition, the slightly more radiogenic time-integrated Nd-isotopic compositions in the GMS granites reflect a further increment in the proportion of mantle material entering granite source regions. Formation of these granites was within an orogen-wide, lower crustal hot zone. The magmatically active portion of this hot zone migrated from southeast to northwest from c. 1330 to 1283 Ma.

A sharp change in the isotopic composition of the GMS magmas just west of the boundary between the Nornalup Zone and the Madura Province (the Rodona Shear Zone) (Figs 6 and 11) reflects a significant change in basement composition that also marks the southeastern edge of non-radiogenic reworked Archean crust. The c. 1330 to 1315 Ma GMS granites that mark this change have an isotopic signature that suggests significant incorporation of juvenile crust from the Madura Province itself and indicate that the Madura Province and Nornalup Zone were linked either before (in a passive margin setting), or at least by, this time. The current position of these granites adjacent to the Rodona Shear Zone is consistent with its interpretation as suture zone,

defined by a wide zone of tectonically interleaved rocks from both the Nornalup Zone (Albany–Fraser Orogen) and the Madura Province, which had a long-lived, complex structural history (Spaggiari et al., 2014b,c). To the east, the Madura Province has among the most radiogenic Nd-isotopic compositions of Proterozoic Australia. With a virtually identical Nd isotopic evolution trend, it is conceivable that the Musgrave Province (Fig. 12) developed on Madura Province basement (Spaggiari et al., 2014b; Smithies et al., 2014).

Since the boundary between the Nornalup Zone and the Madura Province is where GMS magmatism began, this magmatisim, and the lower crustal hot zone where melting occurred, may have initiated through orogenic collapse, following accretion and obduction of the western edge of the Madura Province (including the Loongana oceanic arc)

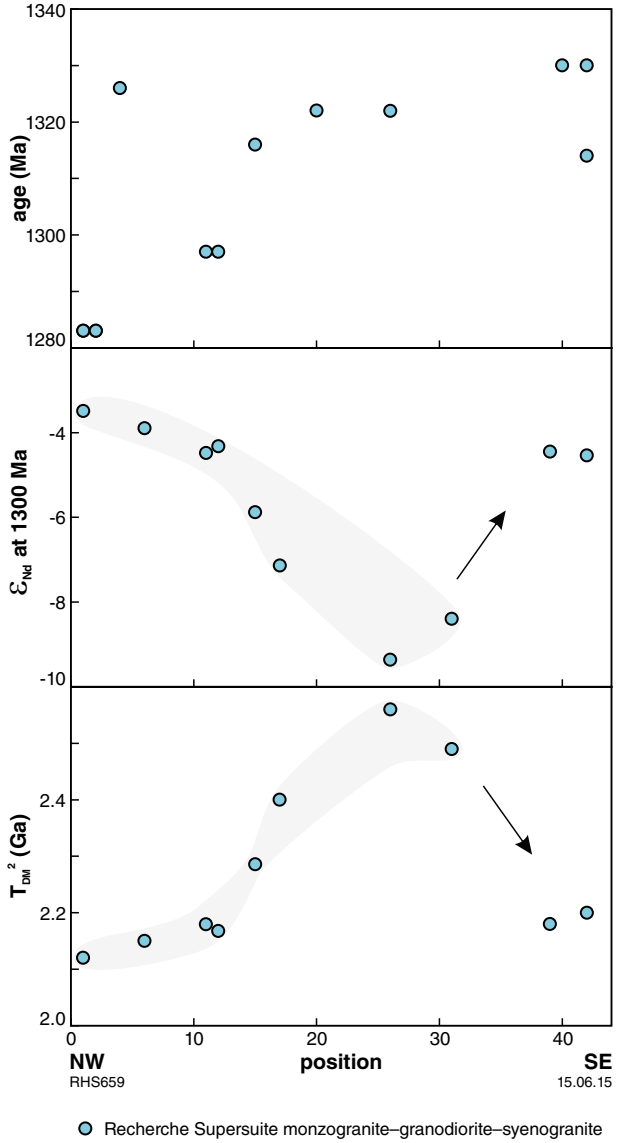

Figure 11. Variations in age and Nd-isotopic compositions of Recherche Supersuite granites along a northwest to southeast traverse through the Albany–Fraser Orogen (see Figure 6).

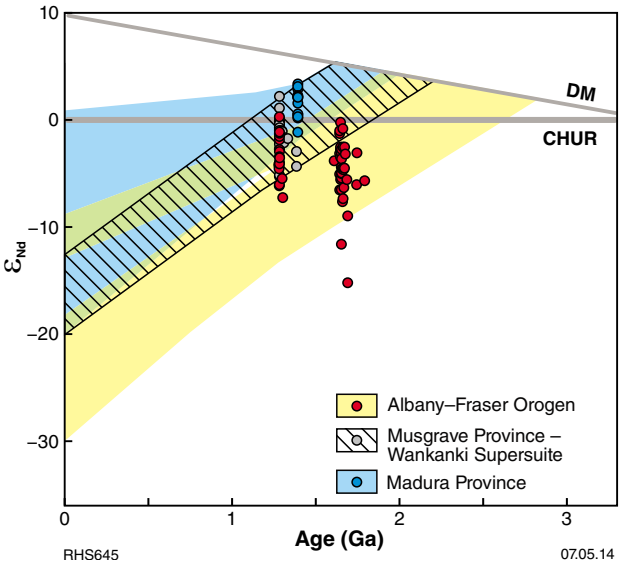

Figure 12. Nd-isotopic evolution diagram comparing the isotopic evolution of magmatic components of the Albany–Fraser Orogen with those of equivalent aged igneous rocks from the Musgrave Province and Madura Province.

over the Nornalup Zone, which would have led to crustal thickening. This is consistent with the tectonic scenario proposed by Spaggiari et al. (2014) to explain the interplay between magmatism and basin development in this region.

Stage II — Esperance Supersuite

Granites formed during Stage II of the Albany–Fraser Orogeny are divided between the 'sodic' Esperance Supersuite granites and the 'enriched' Esperance Supersuite granites (Fig. 10). The sodic Esperance Supersuite granites form a linear belt along the northwestern margin of the known outcrop extent of the Esperance Supersuite (e.g. Mt Ridley, GSWA sample 184374). These rocks in general represent low degree partial melts of locally available lithologies — mainly felsic rocks formed during the Biranup Orogeny — with melting broadly constrained along major shear zones, including the sheared boundary between the Nornalup and Biranup zones (Red Island to Heywood–Cheyne shear zones, Plate 3).

The enriched Esperance Supersuite granites are ferroan, alkali–calcic to alkali rocks with strong enrichments in incompatible trace elements (Fig. 10) characteristic of a specific type of A-type magmatism that results through very high temperature melting of anhydrous lower crust, likely in association with a significant juvenile mantle input. They herald a significant change in magmatism compared with both the sodic Esperance Supersuite granites and the Recherche Supersuite, probably related to higher crustal temperatures associated, again, with significant crustal extension. Time integrated Nd-isotopic compositions are similar to that of both the sodic Esperance Supersuite and the GMS granites suggesting that the composition of the source regions might not have changed.

Conclusions

Geochemical and isotopic analyses of temporally constrained series of rocks provide one of the most powerful means of deciphering the crustal history of geologically complex regions. Despite the typically poor outcrop of the Albany–Fraser Orogen, such studies are already providing a wealth of detailed information that is constraining our models for the crustal evolution of this region. These models will continue to be refined as our dataset increases.

References

Fletcher, IR, Myers, JS and Ahmat, AL 1991, Isotopic evidence on the age and origin of the Fraser Complex, Western Australia: a sample of Mid-Proterozoic lower crust: Chemical Geology: Isotope Geoscience, v. 87, p. 197–216.

Gollam, M 2012, Final drilling report 'The Eye'; Sirius Gold Pty Ltd: Geological Survey of Western Australia, Statutory mineral exploration report, A092733 (unpublished).

Kirkland, CL, Spaggiari, CV, Pawley, MJ, Wingate, MTD, Smithies, RH, Howard, HM, Tyler, IM, Belousova, EA and Poujol, M 2011a, On the edge: U–Pb, Lu–Hf, and Sm–Nd data suggests reworking of the Yilgarn Craton margin during formation of the Albany–Fraser Orogen: Precambrian Research, v. 187, p. 223–247, doi:10.1016/j.precamres.2011.03.002.

Kirkland, CL, Spaggiari, CV, Wingate, MTD, Smithies, RH, Belousova, EA, Murphy, R and Pawley, MJ 2011b, Inferences on crust–mantle interaction from Lu–Hf isotopes: a case study from the Albany–Fraser Orogen: Geological Survey of Western Australia, Record 2011/12, 25p.

Martin, H, Smithies, RH, Rapp, R, Moyen, J-F and Champion, D 2005, An overview of adakite, TTG and sanukitoid: relationships and some implications for crustal evolution: Lithos, v. 79, p.1–24.

Occhipinti, SA, Doyle, M, Spaggiari, CV, Korsch, R, Cant, G, Martin, K, Kirkland, CL,Savage, J, Less, T, Bergin, L and Foz, L 2014, Interpretation of the deep seismic reflection line 12GA-T1: northern Albany–Fraser Orogen, *in* Albany–Fraser Orogen seismic and magnetotelluric (MT) workshop 2014: extended abstracts *compiled by* CV Spaggiari and IM Tyler: Geological Survey of Western Australia, Record 2014/6, p. 52–68.

Shirey, SB and Hanson, GN 1984, Mantle-derived Archaean monzodiorites and trachyandesites: Nature, v. 310, p. 222–224.

Smithies, RH and Champion, DC 2000, The Archaean High-Mg Diorite Suite: Links to Tonalite-Trondhjemite-Granodiorite Magmatism and Implications for Early Archaean Crustal Growth: Journal of Petrology, v. 41, p.1653–1671.

Smithies, RH, Spaggiari, CV, Kirkland, CL, Howard, HM and Maier, WD 2011, Petrogenesis of gabbros of the Mesoproterozoic Fraser Zone: constraints on the tectonic evolution of the Albany–Fraser Orogen: Geological Survey of Western Australia, Record 2013/5, 29p.

Smithies, RH, Spaggiari, CV and Kirkland, CL 2014, Building the crust of the Albany–Fraser Orogen; constraints from granite geochemistry, Western Australia: Geological Survey of Western Australia, Report 150, 49p.

Sirius Resources NL 2012a, Best hit yet at Nova: Report to Australian Securities Exchange, 26 September 2012, 5p.

Spaggiari, CV, Kirkland, CL, Pawley, MJ, Smithies, RH, Wingate, MTD, Doyle, MG, Blenkinsop, TG, Clark, C, Oorschot, CW, Fox, LJ and Savage, J 2011, The Geology of the east Albany–Fraser Orogen — a field guide: Geological Survey of Western Australia, Record 2011/23, 97p.

Spaggiari, CV, Kirkland, CL, Smithies, RH, Wingate, MTD and Occhipinti, SA 2014a, Geological framework of the Albany–Fraser Orogen, *in* East Albany–Fraser Orogen seismic and magnetotelluric (MT) workshop 2014: extended abstracts *compiled by* CV Spaggiari and IM Tyler: Geological Survey of Western Australia, Record 2014/6, p. 12–27.

Spaggiari CV, Kirkland CL, Smithies RH, and Wingate MTD, 2014b, Tectonic links between sedimentary cycles, basin formation and magmatism in the Albany–Fraser Orogen, Western Australia Geological Survey of Western Australia, Report 133, 63p.

Spaggiari, CV, Occhipinti, SA, Korsch, RJ, Doublier, MP, Clark, DJ, Dentith, MC, Gessner, K, Doyle, MG, Tyler, IM, Kennett, BLN, Costelloe, RD, Fomin, T and Holzschuh, J 2014c, Interpretation of seismic lines 12GA-AF1, 12GA-AF2 and 12GA-AF3: implications for crustal architecture, *in* Albany–Fraser Orogen seismic and magnetotelluric (MT) workshop 2014: extended abstracts *compiled by* CV Spaggiari and IM Tyler: Geological Survey of Western Australia, Record 2014/6, p. 28–51.

Sun, S and McDonough, WF 1989, Chemical and isotopic systematics of oceanic basalts: implications for mantle compositions and processes, *in* Magmatism in the Ocean Basins *edited by* AD Saunders and MJ Norry: Geological Society, London, Special Publication 42, p. 313–345.

Cryptic progeny of craton margins: geochronology and isotope geology of the Albany–Fraser Orogen, with implications for evolution of the Tropicana Zone

by

CL Kirkland, CV Spaggiari, RH Smithies, and MTD Wingate

Introduction

Craton margins are dynamic, they are locations of exotic terrane transferral, may be the sites of lithospheric attenuation, rifting, and subsequent reattachment, may be active with redistribution of material by subduction, or may simply be passive. Additionally, craton margins are the sites of first-order lithospheric discontinuities that facilitate the transfer of heat and materials (fluids and magmas), and under favorable circumstances can become mineralization corridors. Craton margins have changed over geological time as a result of the transition from high mantle temperatures and low mantle viscosity in the Archean, to relatively low mantle temperatures in the Proterozoic. Such changes may be expected to result in distinctly different craton margin architectures and processes through earth history and to manifest themselves in different mineralization styles. Nonetheless, on a global scale, the most important hydrothermal gold mineralization is associated with late Archean or Paleozoic to Quaternary convergent (subduction) margin settings (Barley et al., 1989).

The Proterozoic margins of Archean cratons are increasingly recognized as key regions where upgrading of ancient mineral endowments to economically viable levels can occur (Lawley et al., 2014). Additionally, other processes along craton margins, such as terrane transfer, may also play important roles in delivering mineral endowment. Distinguishing the nature of craton margin processes (e.g. terrane accretion, reattachment, rifting, stable) has pertinent implications for regional mineral prospectivity.

One such area where a variety of craton margin processes has been in operation is the Albany–Fraser Orogen, a component of the West Australian Craton, located along the southern and southeastern margins of the Archean Yilgarn Craton (Spaggiari et al., 2011). Towards the west, the orogen is truncated by the late Mesoproterozoic to Neoproterozoic Darling Fault Zone and Pinjarra Orogen, whereas the eastern extent of the orogen is overlain by the Bight and Eucla basins. To the northeast, the orogen is overlain by the Officer and Gunbarrel basins. Further northeast, the Proterozoic Musgrave Province has a similar Mesoproterozoic magmatic history, although the basement units have distinctly different Nd- and Hf-isotopic characteristics (Kirkland et al., 2011a,b). The Albany–Fraser Orogen and Musgrave Province may once have been contiguous, but only after 1400 Ma. The crustal evolution of these two regions prior to 1400 Ma is distinctly different. Between c. 1900 and 1400 Ma Hf-isotopic evolution trends contrast apparent crustal reworking for the Musgrave Province, with progressive juvenile input into unradiogenic Archean crust in the Albany–Fraser Orogen (Kirkland et al., 2012a). The eastern margin of the Albany–Fraser Orogen is covered by the Eucla Basin, but is inferred to extend to the Rodona Shear Zone (Spaggiari et al., 2012). On the eastern side of this structure, the orogen is in contact with the Madura Province, which comprises juvenile c. 1410 Ma tonalites and gabbros (e.g. GSWA 192558, Kirkland et al., 2013a) derived from low- to medium-K tholeiitic parental magmas likely produced in an oceanic-arc setting (Loongana Arc; Spaggiari et al., 2014a). Migmatitic gneiss in drillcores of the Madura Province yield a zircon U–Pb date of c. 1480 Ma, interpreted to reflect migmatization, and a range of protolith ages, indicating a component older than the Loongana Arc in the Madura Province, alternatively all these crystallization ages could reflect detritus (Kirkland et al., 2012b). The Albany–Fraser Orogen is interpreted as a component of the Australo–Antarctic, Albany–Fraser–Wilkes Orogen, which was a coherent entity prior to Gondwana breakup (Fitzsimons, 2003).

Prior to the commencement of the Albany–Fraser Orogen project at the Geological Society of Western Australia (GSWA) in 2006, there were comparatively few isotopic datasets for this region (Nelson et al., 1995a; Clark et al., 1999, 2000). Nonetheless, geological understanding of this region's evolution has advanced rapidly with the recent collection and interpretation of large, high-quality geochronology and isotopic datasets. These datasets have enabled the deciphering of the geological history and crustal evolution of this region. Because of the sparse outcrop, coupled with the dominance of granitic gneisses whose ages cannot be distinguished in outcrop,

GSWA's geochronology program has been fundamental to understanding the tectonic events that have built this orogen. These data, now coupled with geochemistry (Smithies et al., 2014) have facilitated the interpretation of magnetic and gravity datasets, which in unison, provide important constraints for the interpretation of the deep crustal seismic lines (Spaggiari et al., 2014b).

In the following text we present a brief overview of the U–Pb geochronology collected in various lithotectonic zones of the Albany–Fraser Orogen, before evaluating the isotopic signatures of some of these zones. Within this framework we present the results of recent work in the newly defined Tropicana Zone, that includes the Tropicana gold mine and several prospects to the northeast (Occhipinti et al., 2014). Outcrop is sparse in the Tropicana Zone, but drillcores have provided valuable information on the distinct evolution of this zone. In the northeast, buried under deep regolith, are the Hercules and Atlantis prospects (Plate 1). These contain Archean granites with broadly dioritic compositions, and a very narrow range of low silica values from 58.1 to 63.6 w%, classified as sanukitoids. These Archean granites have been named the Hercules Gneiss. The Tropicana Zone is located along the eastern margin of the Yilgarn Craton, in the Great Victoria Desert. The western boundary of the Tropicana Zone is sharply truncated by the Gunbarrel Fault, and a thick sequence of sedimentary rocks of the Gunbarrel Basin (Plates 1 and 4; Occhipinti et al., 2014).

U–Pb geochronology of the major units of the Albany–Fraser Orogen

Figure 1 presents an overview geological map of the various craton margin lithotectonic elements of the Albany–Fraser Orogen. A summary of the SIMS (SHRIMP) zircon geochronology in these zones is presented in this section.

Northern Foreland (Munglinup Gneiss)

The Northern Foreland reflects the margin of the Yilgarn Craton reworked during the Albany–Fraser Orogeny. Geochronological data have shown that the orthogneisses were derived from late Archean precursors, with at least five phases of granitic magmatism: at c. 2720, 2680, 2670, 2660, and 2620 Ma (e.g. Spaggiari et al., 2011; Fig. 2). These crystallization ages are comparable to those of magmatic events elsewhere in the Yilgarn Craton (Cassidy et al., 2006 and references therein). Such similarity is consistent with the interpretation that the granitic precursors to the Munglinup Gneiss were part of the Yilgarn Craton. Hf-isotopic signatures of the Northern Foreland are similar to many terranes and domains of the Yilgarn Craton, although a unique attribution of the Northern Foreland to a specific component of the Yilgarn Craton is not possible (Kirkland et al., 2011b).

Kepa Kurl Booya Province

The Kepa Kurl Booya Province is the crystalline basement of the Albany–Fraser Orogen (Spaggiari et al., 2009), and lies immediately to both the south and east of the Yilgarn Craton. This zone was affected by Stage I intrusion and metamorphism of the Albany–Fraser Orogeny. The Kepa Kurl Booya Province can be considered as comprising four fault-bounded lithotectonic zones named the Biranup, Fraser, and Nornalup zones, and the newly defined Tropicana Zone. Each of these zones contains rocks with variable protolith ages, but similar timing of overprinting metamorphism or intrusion by younger mafic and felsic magmas.

Biranup Zone

The Biranup Zone comprises largely mid-crustal rocks, including orthogneiss and metagabbro with ages of c. 1810 to 1625 Ma (Spaggiari et al., 2011; Fig. 3). The earliest magmatic pulse in this zone occurred at 1810–1800 Ma and was followed by a second event at 1780–1760 Ma. Deposition of a component of the Barren Basin (see below) was followed rapidly by intrusion of a suite of Biranup Zone granitic magmas at 1686 ± 8 Ma (e.g. GSWA 194701, Kirkland et al., 2011c). Deformation during the Zanthus Event, a compressional component of the 1710–1650 Ma Biranup Orogeny, is constrained by 1676 ± 6 Ma folded migmatitic leucosomes and 1679 ± 6 Ma crosscutting axially planar leucosomes (Kirkland et al., 2011a). A younger suite of granitic and gabbroic rocks, which exhibit distinct mingling and local hybridization textures, is dated at 1665 ± 4 Ma (Eddy Suite; Plate 2). The youngest Biranup Zone magma (excluding Stage I and II granite injections) is a metasyenogranite with a zircon U–Pb crystallization age of 1627 ± 4 Ma (GSWA 194736, Kirkland et al., 2010). Initially, the lack of evidence for a Paleoproterozoic magmatic or tectonothermal event in the southern Yilgarn Craton led to the suggestion that the Biranup Zone was an exotic terrane accreted onto the Yilgarn Craton margin during Stage I of the Albany–Fraser Orogeny (e.g. Nelson et al., 1995a). However, more recent isotopic work has shown that the Biranup Zone was likely to have formed autochthonously along the Yilgarn Craton margin (Kirkland et al., 2011a, 2011b), which is consistent with the presence of fragments of Archean granite isolated within it (Spaggiari et al., 2011). Zircon overgrowths were developed widely during Stage II metamorphism in the Biranup Zone.

Fraser Zone

The Fraser Zone is dominated by the Fraser Range Metamorphics, a sequence of high-grade metasedimentary rocks intruded by sheets of metagabbro and metagranite (Smithies et al., 2013; Clark et al., 2014). Mafic and felsic magmatism in the Fraser Zone were contemporaneous and occurred between c. 1310 and 1283 Ma, soon after deposition of the Arid Basin (see below) (Kirkland et al., 2011a; Spaggiari et al., 2011). Magmatic crystallization of mafic intrusive rocks in the Fraser Zone has been

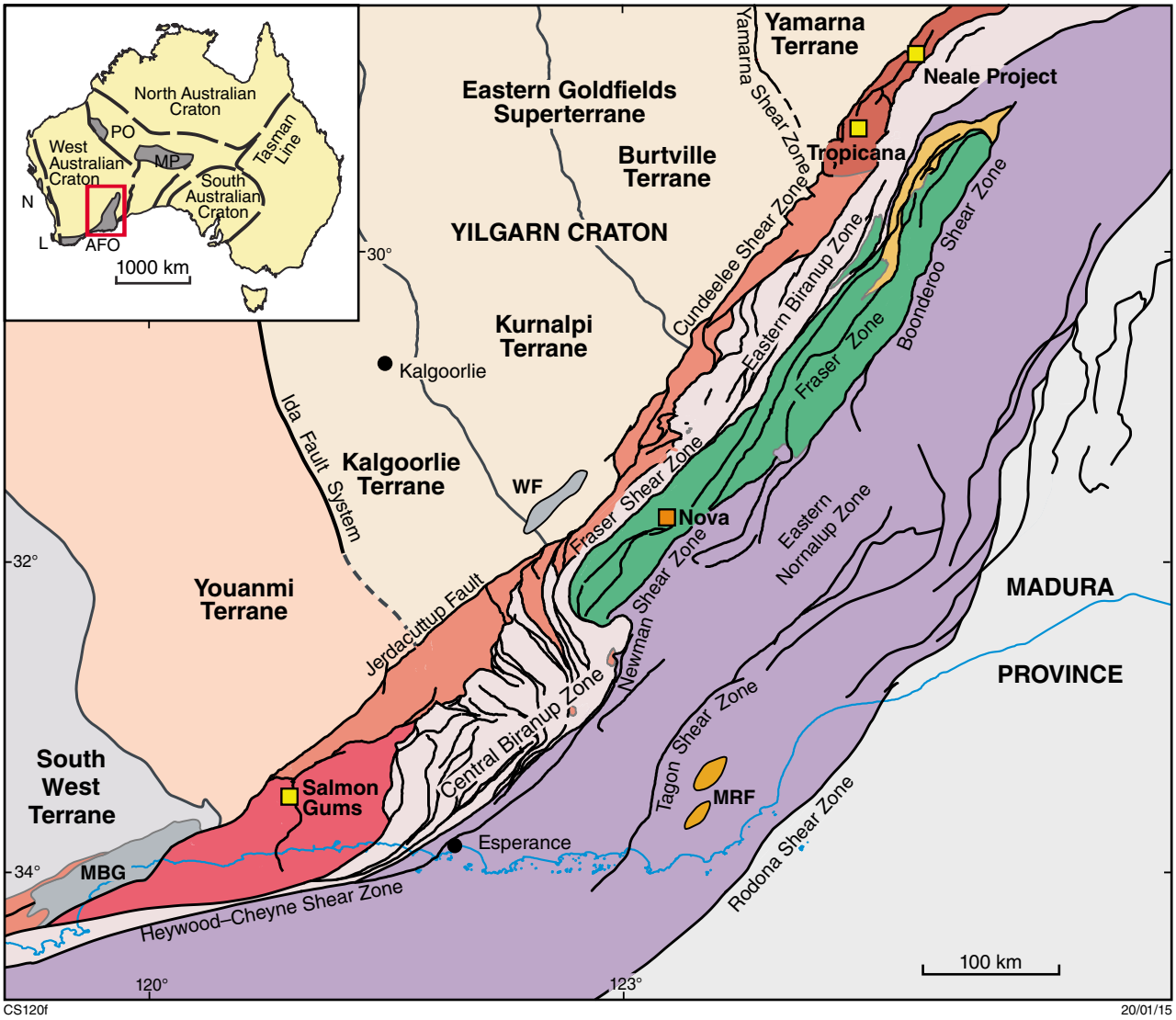

ALBANY–FRASER OROGEN

- Mount Ragged Formation
- Fraser Zone (1305–1290 Ma)
- Gwynne Creek Gneiss
- Nornalup Zone (1800–1650 Ma); Recherche (1330–1280 Ma) and Esperance (1200–1140 Ma) Supersuites (undivided)
- Biranup Zone (1800–1650 Ma) and Archean remnants
- Barren Basin (undivided)
- Tropicana Zone (2720–1650 Ma)
- Munglinup Gneiss (2800–2660 Ma)
- Northern Foreland, undivided

- Major faults
- Terrane boundary
- Geological boundary
- Coastline
- Town

Figure 1. Simplified pre-Mesozoic interpreted bedrock geology of the east Albany–Fraser Orogen (modified from Spaggiari et al., 2011) and tectonic subdivisions of the Yilgarn Craton (modified from Geological Survey of Western Australia, 2011; Cassidy et al., 2006; Pawley et al., 2012). Abbreviations used: MBG – Mount Barren Group; WF – Woodline Formation; MRF – Mount Ragged Formation; AFO – Albany–Fraser Orogen; MP – Musgrave Province; PO – Paterson Orogen; L – Leeuwin Province; N – Northhampton Province

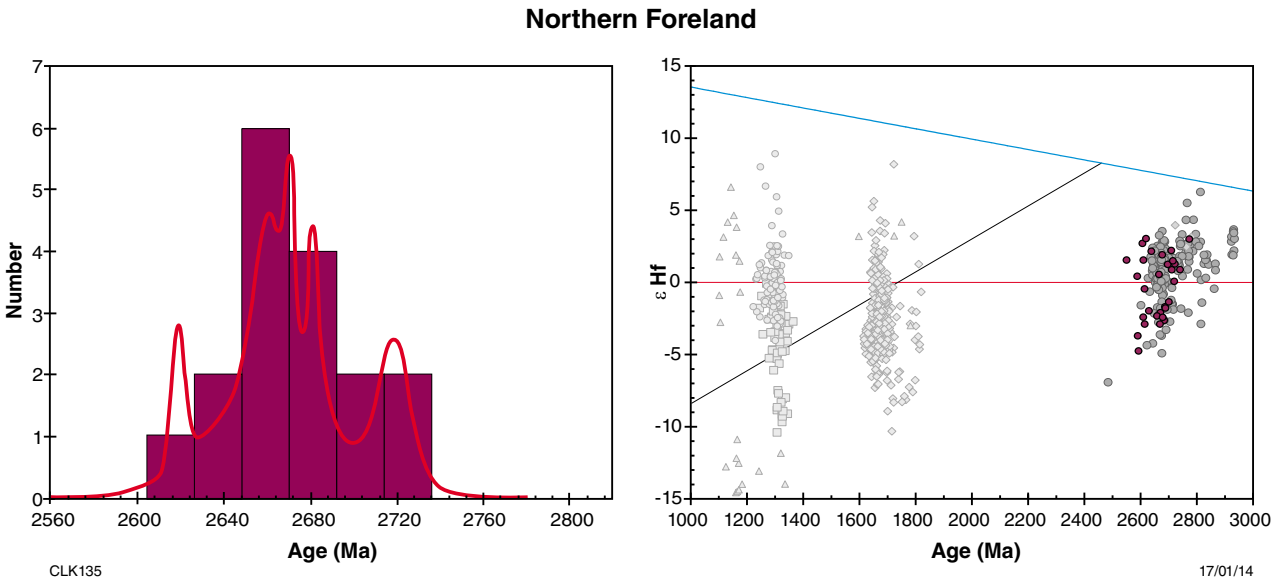

Figure 2. **Left: combined histogram/probability plot of $^{207}Pb^*/^{206}Pb^*$ crystallization ages of magmatic rocks in the Northern Foreland. Right: εHf evolution plot for the same data (coloured), other data from the Albany–Fraser Orogen in light grey, data from the Yilgarn Craton in dark grey. A reference evolution line corresponding to a $^{176}Lu/^{177}Hf$ ratio of 0.015 is shown in black.**

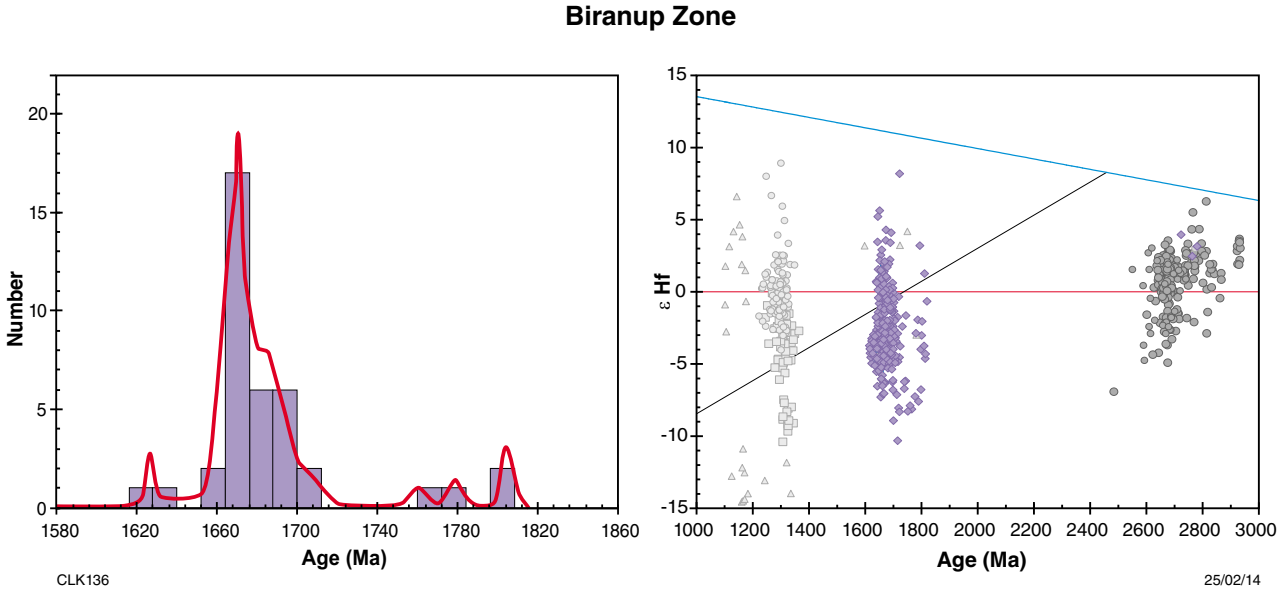

Figure 3. **Left: combined histogram/probability plot of $^{207}Pb^*/^{206}Pb^*$ crystallization ages of magmatic rocks in the Biranup Zone. Right: εHf evolution plot for the same data (coloured), other data from the Albany–Fraser Orogen in light grey, data from the Yilgarn Craton in dark grey. A reference evolution line corresponding to a $^{176}Lu/^{177}Hf$ ratio of 0.015 is shown in black.**

dated at 1299 ± 3 Ma (GSWA 194717, Kirkland et al., 2013b), 1299 ± 10 Ma, and 1291 ± 8 Ma (De Waele and Pisarevsky, 2008; Fig. 4). High-grade metamorphism occurred soon after sediment deposition and magmatic intrusion in the Fraser Zone. For example, zircon rims in a psammitic gneiss yield a date of 1292 ± 5 Ma (GSWA 194714, Kirkland et al., 2011d), and metamorphic zircons in a mafic granulite indicate high-grade metamorphism at 1292 ± 6 Ma (GSWA 194718, Kirkland et al., 2011e). Metamorphism has also been constrained at 1304 ± 7 Ma by zircon rim growth within a quartz metasandstone, which indicates a maximum depositional age of 1466 ± 17 Ma (Wingate and Bodorkos, 2007). All isotopic results from the Fraser Zone indicate a very short time interval for sediment deposition, igneous crystallization, and near-coeval granulite-facies metamorphism. The close correspondence between the age of mafic to felsic magmatism and the age of granulite-facies metamorphism implies that magmatism was the thermal impetus for metamorphism. Such similar timing of magmatism and granulite-facies metamorphism implies these rocks were emplaced in the lower-middle to lower crust, consistent with peak metamorphic conditions at c. 1290 Ma of 850°C, at pressures of 7–9 kbars. Peak metamorphism was followed by a period of isobaric cooling at pressures of about 9 kbars (Clark et al., 2014).

Barren Basin

The Barren Basin comprises Paleoproterozoic metasedimentary rocks which overlie the Yilgarn Craton and the Biranup and Nornaup Zones (Spaggiari et al., 2011, 2014a). Detrital zircon grains in sedimentary rocks of the Barren Basin indicate age peaks, in order of significance, at 2634, 1670, 2028, 1792, 1874, and 2248 Ma, defined by 156, 132, 58, 56, 44, 38 analyses, respectively (Fig. 5). Such detrital zircon ages indicate that the major sources of Barren Basin sediments were indigenous West Australian Craton rocks — mainly Proterozoic granites dominant in the Biranup Zone that have magmatic crystallization ages in the range of c. 1800 to 1670 Ma (see also Spaggiari et al., 2014a). A significant Archean c. 2630 Ma detrital zircon age peak in the Barren Basin is strongly similar in age to widespread granitic magmatism at 2640–2620 Ma in the Yilgarn Craton, which was the last major magmatic event to have affected the craton, and was responsible for craton-wide gold mineralization (Kent et al., 1996). Subordinate detrital peaks (e.g. 2030 Ma) are less well constrained but could reflect sediment derivation from the Gascoyne Province (Johnson et al., 2011). The Barren Basin developed during a protracted period of >200 Ma (1815–1600 Ma), with deposition taking place during three phases (before c. 1800 Ma, before c.1700 Ma, and between 1710 and 1600 Ma; Spaggiari et al., 2014a).

Arid Basin

Within the Fraser and Nornalup Zones, metasedimentary rocks that have maximum depositional ages younger than the Biranup Orogeny, but have been intruded by Stage I magmas, are part of the Arid Basin (Spaggiari et al., 2011, 2014a). Detrital zircons from sediments in the Arid Basin indicate age peaks, in order of significance, at 1382, 1672, 1456, 1495, 1557, 1524, and 1789 Ma, defined by 85, 75, 52, 38, 29, 28 and 16 analyses, respectively (Fig. 6).

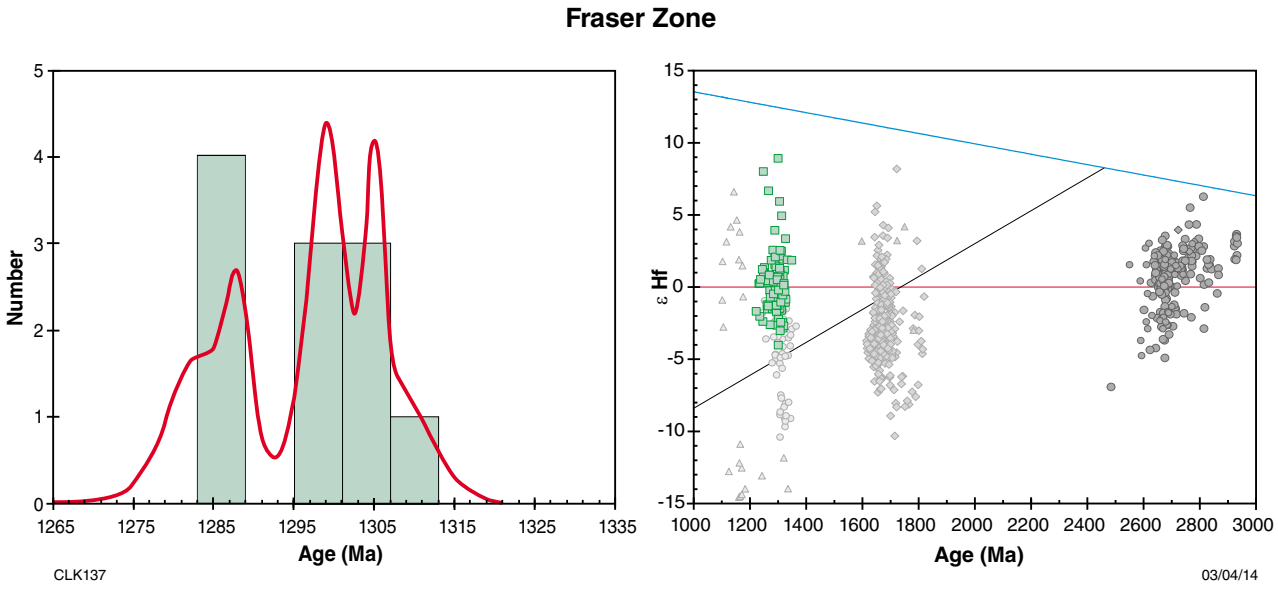

Figure 4. **Left: combined histogram/probability plot of $^{207}Pb^*/^{206}Pb^*$ crystallization ages of magmatic rocks in the Fraser Zone. Right: εHf evolution plot for the same data (coloured), other data from the Albany–Fraser Orogen in light grey, data from the Yilgarn Craton in dark grey. A reference evolution line corresponding to a $^{176}Lu/^{177}Hf$ ratio of 0.015 is shown in black.**

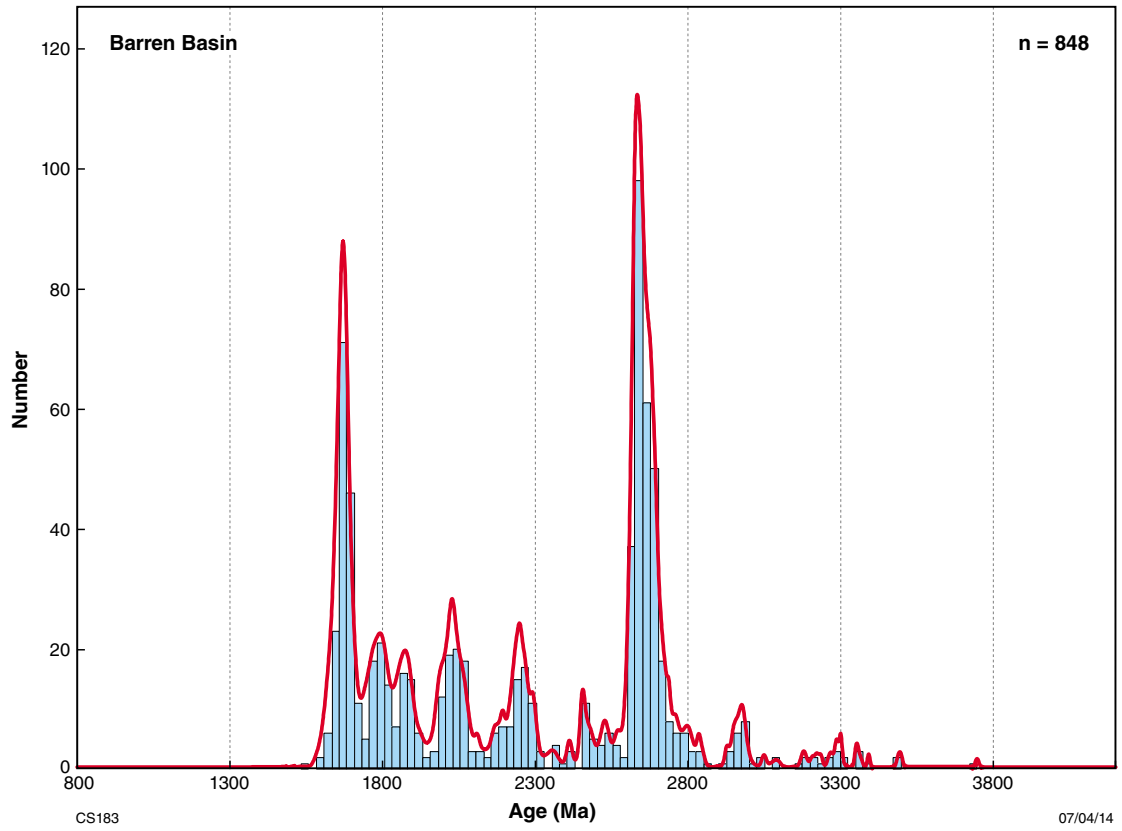

Figure 5. Combined histogram/probability plot of $^{207}Pb^*/^{206}Pb^*$ crystallization ages of detrital zircons in the Barren Basin (from Spaggiari et al., 2014a)

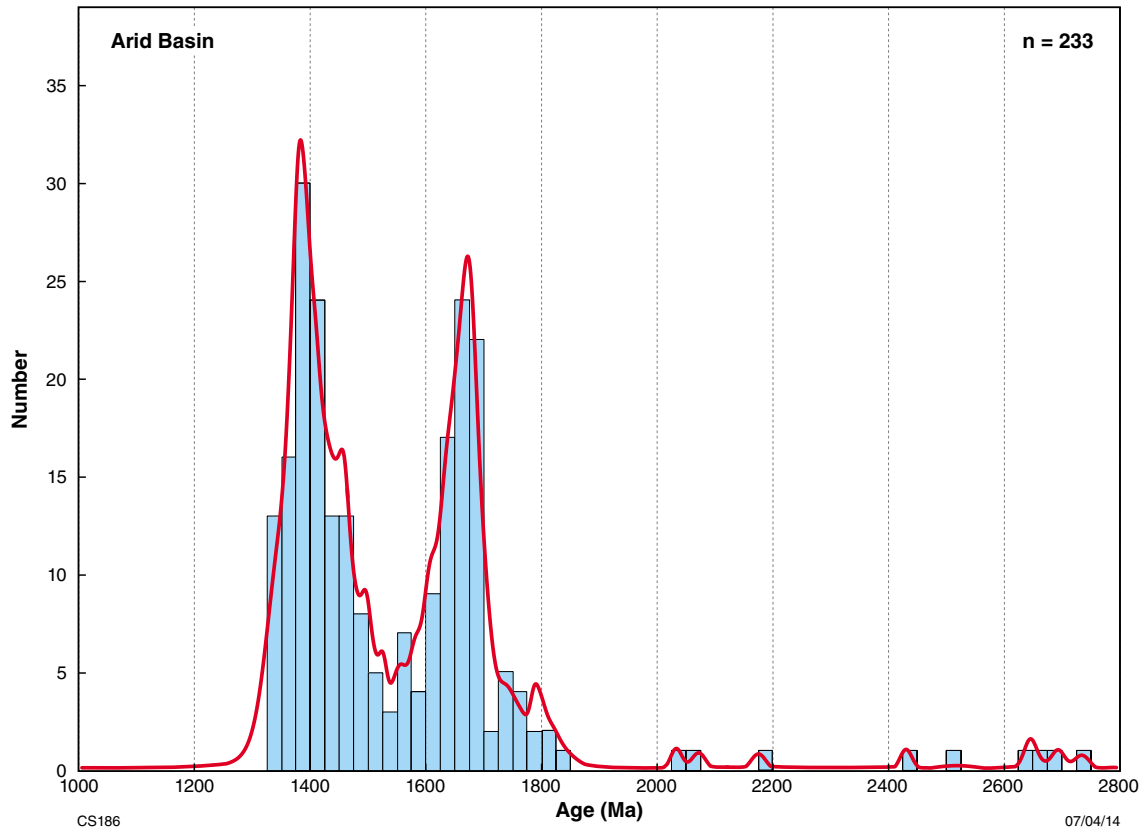

Figure 6. Combined histogram/probability plot of $^{207}Pb^*/^{206}Pb^*$ crystallization ages of detrital zircons in the Arid Basin (from Spaggiari et al., 2014a)

The 1800–1600 Ma detrital zircon ages are similar to detrital components in the Barren Basin, and suggest either a Biranup and/or Nornalup Zone hinterland for the Arid Basin, or selective reworking of less radiation damaged Proterozoic Barren Basin material (Spaggiari et al., 2014a). However, the detrital population within the Arid Basin also has some unique components not present in the Barren Basin. The dominant detrital component of 1500–1350 Ma is not recognized within the Albany–Fraser Orogen nor the Yilgarn Craton, but was likely derived from the Loongana Arc of the Madura Province to the east of the Albany–Fraser Orogen — a c. 1410 Ma piece of oceanic magmatic arc with a distinct radiogenic Hf-isotopic signature (Spaggiari et al., 2014a).

Recherche and Esperance Supersuites

The southeastern part of the Biranup Zone and the Nornalup Zone contain granitic intrusions of the 1330–1280 Ma Recherche Supersuite and the 1200–1140 Ma Esperance Supersuite (Nelson et al., 1995a; Clark et al., 1999; Smithies et al., 2014).

The Recherche Supersuite is the magmatic expression of Stage I of the Albany–Fraser Orogeny (Fig. 7), during which these rocks were metamorphosed to amphibolite or granulite facies conditions. The Recherche Supersuite contains a variety of granitic rocks including metasyenogranite, metamonzogranite, and metagranodiorite (Smithies et al., 2014). Most of these appear to be mingled with a mafic component, generally present as enclaves of various sizes. The oldest Recherche Supersuite granite presently analysed is a biotite–hornblende monzogranite with calc-silicate boudins from Poison Creek, dated at 1330 ± 14 Ma (GSWA 83662, Nelson, 1995b). Another Recherche Supersuite lithology is peraluminous, garnet-bearing, granodiorite gneiss, from Israelite Bay, dated at 1314 ± 21 Ma (GSWA 83663, Nelson, 1995c). The youngest Recherche Supersuite granite so far dated is a metamonzogranite within the Newman Shear Zone with a zircon crystallization age of 1297 ± 8 Ma (GSWA 194711, Kirkland et al., 2012c)

The Esperance Supersuite is the magmatic response to Stage II of the Albany–Fraser Orogeny (Fig. 8), which caused prolific growth of metamorphic zircon rims within rocks of the Biranup Zone. One of the youngest granites of the Esperance Supersuite is Balladonia Rock, which has a U–Pb zircon crystallization age of c. 1135 Ma (GSWA 83667, Nelson et al., 1995d), whereas the oldest is a biotite monzogranite at Mount Ridley which yielded a U–Pb zircon crystallization age of 1198 ± 11 Ma (GSWA 184374, Kirkland et al., 2012d). The Esperance Supersuite is peraluminous to metaluminous and essentially falls within the field of within plate granite in Ta vs Yb and Nb vs Y tectonic discrimination diagrams.

Hf-isotopic characteristics of the major units of the Albany–Fraser Orogen

The Lu–Hf system can be used as a geochemical tracer, providing information on both the timing of material input into the crust, as well as the process by which this material was added. Coupled with U–Pb geochronology, Hf-isotopic measurements in zircons provide unique, time-integrated information about the relative roles of juvenile mantle input versus reworking of older continental crust. The Hf-isotopic signatures of many units of the Albany–Fraser Orogen have been discussed at length elsewhere (Kirkland et al., 2011a, 2011b; Spaggiari et al., 2014a) and only a brief summary of the salient features is presented here.

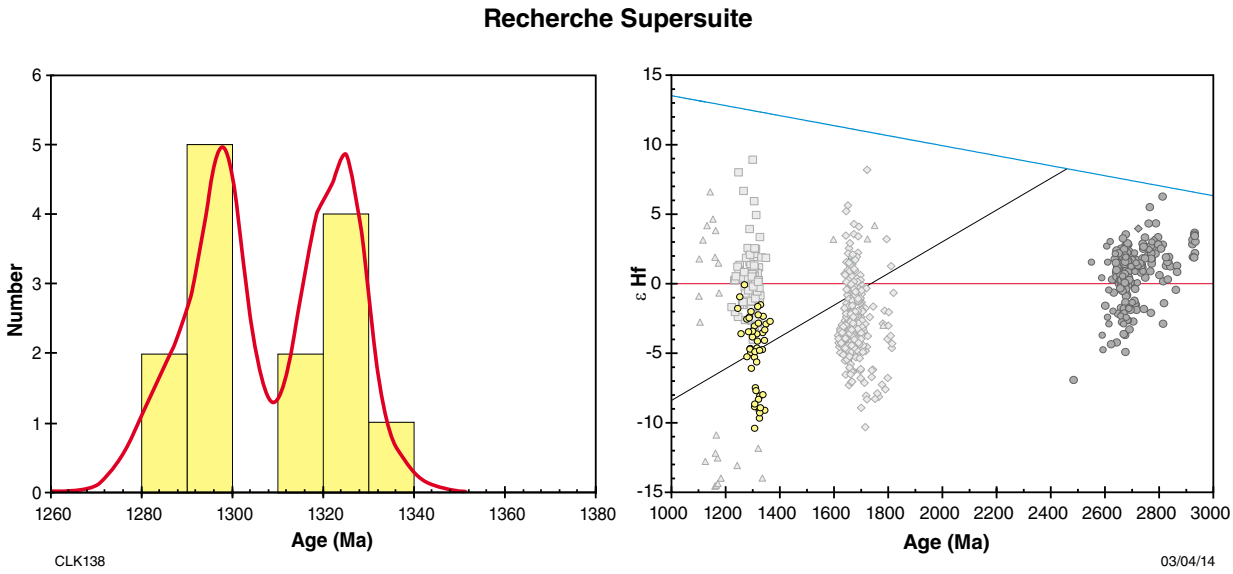

Figure 7. **Left: combined histogram/probability plot of $^{207}Pb^*/^{206}Pb^*$ crystallization ages of magmatic rocks in the Recherche Supersuite. Right: εHf evolution plot for the same data (coloured), other data from the Albany–Fraser Orogen in light grey, data from the Yilgarn Craton in dark grey. A reference evolution line corresponding to a $^{176}Lu/^{177}Hf$ ratio of 0.015 is shown in black.**

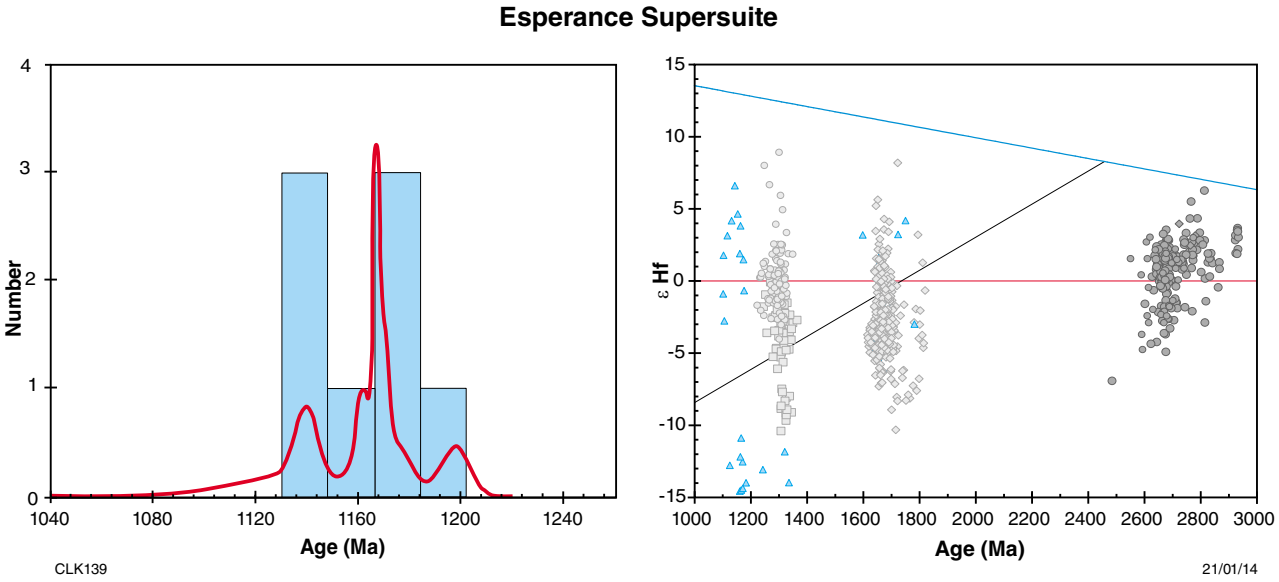

Figure 8. **Left: combined histogram/probability plot of $^{207}Pb^*/^{206}Pb^*$ crystallization ages of magmatic rocks in the Esperance Supersuite. Right: εHf evolution plot for the same data (coloured), other data from the Albany–Fraser Orogen in light grey, data from the Yilgarn Craton in dark grey. A reference evolution line corresponding to a $^{176}Lu/^{177}Hf$ ratio of 0.015 is shown in black.**

Hf signatures of the Biranup Zone

Biranup Zone magmas show a general trend towards more radiogenic values through time (Fig. 3), although there is significant complexity in this relationship (Kirkland et al., 2011a). There is a step towards more radiogenic values of up to εHf = +6 in magmatic zircons younger than 1700 Ma. The median εHf in zircons younger than 1700 Ma is -2.8 ± 3.0 (1 standard deviation [SD]), whereas in zircons older than 1700 Ma, the median εHf is -3.9 ± 3.0 (1 SD). The most evolved components of the Biranup Zone come from c. 1700 Ma zircons that lie on an andesitic crustal evolution line from the most radiogenic components of the Eastern Goldfields Superterrane of the Yilgarn Craton. The general Hf-isotope signature of the Southern Cross Domain of the Youanmi Terrane is too evolved to have been a source in the Biranup Zone. However, many of the radiogenic components in the Eastern Goldfields Superterrane are viable sources to explain the most evolved Biranup Zone magmas, assuming equilibrium melting of that source and evolution through a normal crustal reservoir. However, if the source was a more mafic residual hornblende- and garnet-bearing component, as indicated for at least some of the magmas by the strong decoupling between Nd and Hf systematics, then a steeper evolution line could explain even more of the isotopic array of the Biranup Zone magmas, with less necessity for significant mantle input. Evolution from an Archean residuum with a $^{176}Lu/^{177}Hf$ ratio of 0.036 is sufficient to evolve to the most radiogenic Biranup Zone Hf isotopic values. The isotopic features of the Biranup Zone indicate that it is not exotic to the margin of the Yilgarn Craton. Rather, it represents either a Paleoproterozoic back-arc or rift on the Yilgarn Craton, which distended and isolated Archean fragments within it (Kirkland et al., 2011a).

Hf signatures of the Arid and Barren Basins

The Hf-isotopic signatures of detritus within the Barren and Arid basins are discussed at length on a sample-by-sample basis in Spaggiari et al. (2014a). Detrital zircons in the Barren Basin have a median εHf of +1 and range from +6 to -18. Two-stage model ages reveal similarities with magmatic rocks of the Biranup Zone and Yilgarn Craton. Detrital zircons in the Arid Basin indicate a median εHf of 0 and range from +12 to -17. Two-stage model ages have similarities with model ages in the Biranup Zone, Yilgarn Craton, and include a 2.0 Ga model-age component (Fig. 9).

Hf signatures of the Fraser Zone and Recherche Supersuite

We consider the mafic to granitic magmatic rocks of the Fraser Zone (Fig. 4) and the Recherche Supersuite (Fig. 7) together, because they are all expressions of Stage I events in the Albany–Fraser Orogen. Five Recherche Supersuite samples yielded igneous zircons that preserve magmatic $^{176}Hf/^{177}Hf$ ratios. The Hf-isotopic compositions fall into two groups (Fig. 7). A radiogenic group comprises most samples and indicates εHf values of 0 to -6 (median εHf = -3.49 ± 1.81 (1SD)). The Hf-isotopic range of this material can be explained by reworking, through a typical crustal reservoir, of Biranup Zone material with moderately radiogenic isotopic compositions (e.g. -3 to + 3). One sample defines a distinctly more evolved signature with εHf values of -8 to -11 (median εHf = -8.93 ± 0.76 [1 SD]). This sample (GSWA 194786, preliminary data) is a metamonzogranite, from east of Boingaring Rocks, with

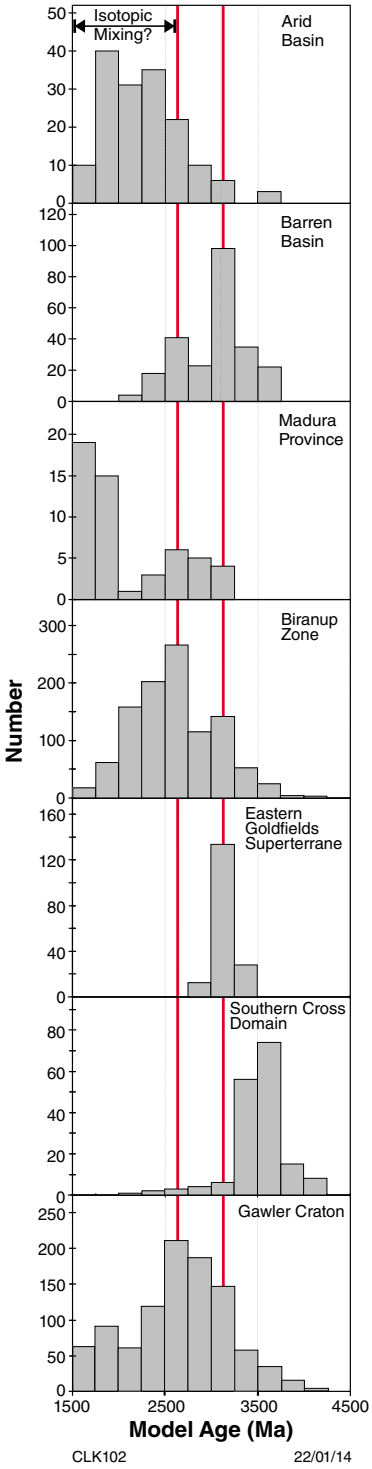

Figure 9. Stacked histograms of model ages from the Barren and Arid Basins in comparison to the Yilgarn Craton, Madura Province, and Gawler Craton. All data (excluding the Gawler Craton) is from <www.dmp.wa.gov.au/geochron/>

a zircon U–Pb crystallization age of 1320 ± 8 Ma. Its isotopic signature suggests greater incorporation of older crustal elements, potentially older Biranup Zone crust.

Ten samples of magmatic rocks in the Fraser Zone yielded igneous zircons that indicate εHf values of +9 to -4 (median εHf = -0.08 ± 2.15 [1SD]) (Fig. 4). The Hf-isotopic range of this material overlaps the more radiogenic members of the Recherche Supersuite granites, but unsurprisingly extends to more depleted values, consistent with the large volume of mafic rocks in the Fraser Zone. The Fraser Zone's isotopic pattern has been interpreted to reflect mantle input into a Biranup Zone source (Kirkland et al., 2011a). Juvenile Biranup Zone magmatic rocks have εHf values (recalculated at 1200 Ma) of c. -8, hence evolution through a normal crustal reservoir (e.g. $^{176}Lu/^{177}Hf = 0.015$) could be consistent with the most unradiogenic components of the Fraser Zone directly reworking a Biranup Zone source, which is consistent with the limited inherited zircons in the Fraser Zone magmatic rocks having ages of 1770–1604 Ma.

Geochemical considerations led Smithies et al. (2013) to suggest that the Fraser Zone magmatic rocks were generated by a mantle melt underplated and intraplated at the base of the crust, where it assimilated a <10% component of crust or melt derived from that crust. Chemically, the most likely basement component was regarded as a combination of Archean granite and Munglinup Gneiss, with high La/ Yb ratios resulting from extraction from garnet-bearing sources. This conclusion is essentially similar to that from Hf-isotopic and inherited zircon considerations which suggest a Biranup Zone source influenced by mantle melt, because the Biranup magmatic rocks contain a component of reworked Archean crust. In either case, these results indicate that the Yilgarn Craton or its reworked equivalents were present as basement when magmatic rocks of the Fraser Zone were emplaced. This has important implications for the interpretation of seismic line 12GA-AF3, which images Biranup Zone and the Udarra Seismic Province below the Fraser Zone (Plate 4), and indicates that this relationship is not solely due to subsequent thrusting or tectonic displacement (Spaggiari et al., 2014b).

Hf signatures of the Esperance Supersuite

Hf-isotope results are available for two samples of Esperance Supersuite granites (Fig. 8), although one of these (GSWA 194773, Kirkland et al., 2011f) is from the Forrest Zone of the Coompana Province, east of the Madura Province (Spaggiari et al., 2012, 2014c). Sample GSWA 194773, from ditch cuttings of a felsic rock at the bottom of the Alliance Petroleum Eucla No. 1 well, yielded a U–Pb zircon age of 1140 ± 8 Ma, interpreted as the magmatic crystallization age of the felsic protolith. This sample also indicated a median εHf value of +1.9 ± 2.8 (1 SD). In contrast, sample GSWA 182474 (Kirkland et al., 2012f), a granite vein from the Big Red prospect drillcore BRDDH001 (Plate 2), reflects pegmatite intrusion at 1167 ± 2 Ma, and has a considerably more

evolved Hf-isotopic signature (median = -15 ± 2.5 [1 SD]). This sample also contains inherited material with ages and isotopic signatures similar to Biranup Zone material. Nd-isotope analyses from other samples of the Esperance Supersuite indicate compositions ($\varepsilon_{Nd\ (1200Ma)}$ = -7 to -5) more radiogenic than can be explained by reworking of Biranup Zone or Archean crust alone and suggests further addition of juvenile mantle material into the orogen. In contrast, GSWA 182474 likely reflects in situ melting of Barren Basin paragneiss.

The Tropicana Zone: a new component of the Kepa Kurl Booya Province

The preceding information has provided the necessary background on the various lithotectonic zones of the Albany–Fraser Orogen and adjacent Yilgarn Craton, to allow discussion of the newly defined Tropicana Zone (Occhipinti et al., 2014), and to evaluate its relationship to the other elements of the orogen. Within the Tropicana Zone, an exploration prospect (Neale Project) has reported up to 23.9 grams per ton Au from rotary core drilling (Watkins, 2012). However, it is not clear if this gold represents the same mineralization as the c. 2500 Ma event at Tropicana (Blenkinsop and Doyle, 2014; Doyle et al., 2014). The tectonic setting for the mineralization event that affected Archean host rocks within the Tropicana Zone is unknown, and the gold could be late Archean, reworked Archean, or Proterozoic.

A suite of drillcore samples from the Hercules Gneiss (Neale Project) within the Tropicana Zone has been investigated to shed light on the mineralization, composition, and evolution of this zone. In the Yilgarn Craton, a class of rare low-Si granites has been referred to as 'mafic granites', and includes a LILE-enriched group of sanukitoids emplaced around 2655 Ma (Champion and Sheraton, 1997). A comparison of the dioritic rocks of the Hercules Gneiss with sanukitoids from the Yilgarn Craton, as well as from other Archean cratons, shows that the Hercules Gneiss has chemical compositions comparable to sanukitoid magmas. Together with the distinctive compositions of sanukitoids, the rarity of these rocks within any Archean craton suggests that the granitic protoliths of the Neale Project area represent a single suite of rocks intruded during a single event.

All samples of the Hercules Gneiss contain a component of near-spherical and/or multifaceted zircons consistent with formation during high-pressure metamorphism. There is considerable debate about the interpretation of U–Pb zircon dates from granulite-facies meta-igneous rocks, reflecting the wide variety of growth and/or alteration processes which may have affected zircons in such rocks. Nonetheless, initiation of granulite-facies metamorphism appears to have been essentially coeval with magmatic crystallization in these sanukitoids. Estimates of the original magmatic crystallization ages of these rocks are hindered by the intense neocrystallization and reworking of zircon during granulite-facies metamorphism. However, all gneisses may have had a magmatic crystallization age of c. 2700 Ma, shortly preceding granulite-facies zircon growth. The best estimate of the age of magmatic crystallization could be reflected in the youngest oscillatory zoned zircon cores, which have textural characteristics of zircons grown within a viscous silicate melt, and which have not been affected by radiogenic-Pb loss. Following this criteria, the date of 2692 ± 16 Ma for zircon cores in sample GSWA 192523 (preliminary data) is the best estimate for the timing of sanukitoid magmatism (Fig. 10).

The age of magmatic protolith components in the Hercules Gneiss is similar to those of many intrusive events within the Yilgarn Craton, although the Burtville Terrane and Southern Cross Domain are the most similar. However, the estimate of c. 2692 Ma for sanukitoid magmatism is distinct from the ages of compositionally similar magmatic rocks elsewhere in the Yilgarn Craton, i.e. 2.76 Ga in the western Yilgarn, and 2.65 Ga in the eastern Yilgarn. Furthermore, prolonged granulite-facies zircon growth at 2718–2554 Ma in the Hercules Gneiss (Fig. 10) is dissimilar to the timing of high-grade events in the rest of the Yilgarn Craton, although its initiation may match some granulite-facies events in the Eastern Goldfields Superterrane (Goscombe et al., 2009). This could indicate that the Tropicana Zone reflects a deeper crustal level, or an unknown component of the Yilgarn Craton, or both. This could be explained by the presence of the Plumridge Detachment, along which the Tropicana Zone has been thrust to the northwest (Plate 4; Occhipinti et al., 2014). The gneissic fabric in the Hercules Gneiss is cut by microgranite veins dated at 1783 ± 3 Ma (GSWA 192550, Kirkland et al., 2014). This indicates that thrusting of the Tropicana Zone onto the Yilgarn Craton was before 1783 Ma, given that similar magmatic events are known from the (para)autochthonous Biranup Zone. The 1783 Ma date is similar to that of the nearby McKay Creek Metasyenogranite dated at 1761 ± 10 Ma (GSWA 182424, Kirkland et al., 2012e), and also to magmatic and volcanic rocks of the Voodoo Child Formation (Plate 1; Occhipinti et al., 2014).

Re–Os analyses of pyrite suggest that gold mineralization occurred at c. 2.1 Ga. Gold and pyrite growth occurred during late alteration processes and brittle fracturing of the sanukitoid host rock. A mineralization event at c. 2.1 Ga does not obviously correlate with major Proterozoic tectonothermal events known elsewhere in the Albany–Fraser Orogen, but may reflect low-grade upgrading of an Archean source. Gold was mobilized prior to the major Proterozoic magmatic and metamorphic events, including the Biranup Orogeny and Stages I and II of the Albany–Fraser Orogeny. Given that sanukitoid magmas are well known for gold fertility, we suggest that they may have been the primary source of gold in the Neale Project area, which was subsequently remobilized and concentrated at c. 2.1 Ga into brittle structures associated with pyrite, quartz, biotite, muscovite, actinolite, clinozoisite–epidote, and chlorite.

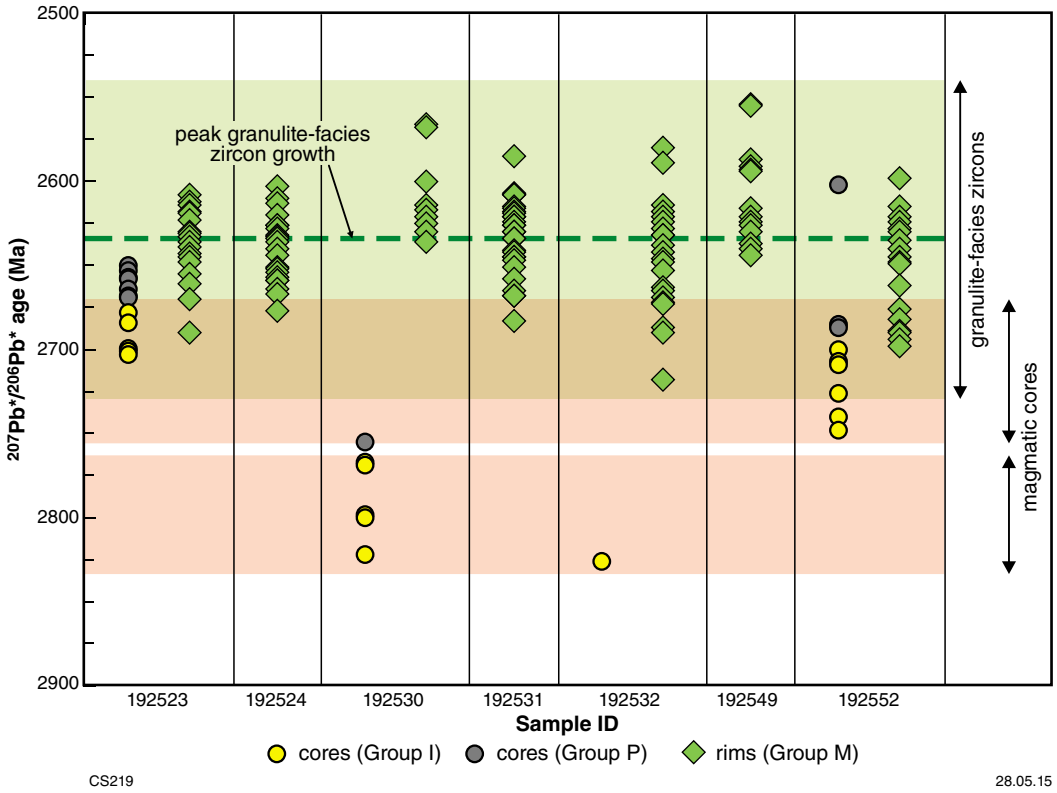

Figure 10. Sample versus age plot illustrating the prolonged granulite-facies zircon growth event within the Hercules Gneiss and the best age estimate for the protolith (sanukitoid magma) estimated to be 2692 ± 16 Ma, based on GSWA 192523 (preliminary data)

Conclusions

U–Pb zircon geochronology, integrated with Lu–Hf isotope measurements on the same dated zircons, has led to new understanding of the evolution of the major components of the Albany–Fraser Orogen:

Northern Foreland

- Crystallization ages of magmatic protoliths are 2722–2619 Ma
- Hf-isotopic signatures are similar to those of Yilgarn Craton rocks
- represents a reworked component of the Yilgarn Craton margin.

Biranup Zone

- Crystallization ages of magmatic protoliths are 1806–1627 Ma
- Hf-isotopic signatures are consistent with juvenile input into an Archean Yilgarn craton source
- numerous distinct magmatic events, including the Biranup Orogeny and prolific Stage II mineral growth
- represents a (para)autochthonous unit.

Fraser Zone

- Crystallization ages of magmatic protoliths are 1310–1283 Ma
- Hf-isotopic signatures are consistent with juvenile input into a Biranup Zone source or a reworked Archean source. Inherited zircons in magmatic rocks are consistent with the former interpretation
- high-grade metamorphism was driven by magmatism
- represents an uplifted (para)autochthonous lower-crustal hot zone.

Barren Basin

- Deposition occurred before c. 1800 Ma, before c. 1700 Ma, and between 1710 and 1600 Ma
- age and Hf-isotopic signatures indicate sediments were derived from the Yilgarn Craton and Biranup Zone.

Arid Basin

- Deposition occurred after the Biranup Orogeny and (just) prior to Stage I events
- detrital zircons were derived from the Biranup Zone, Yilgarn Craton, Loongana Arc, and possibly unknown sources.

Recherche Supersuite

- Crystallization ages of magmatic protoliths are 1330–1283 Ma
- represents the magmatic expression of Stage I of the Albany–Fraser Orogeny
- Hf-isotope signatures are consistent with reworking of a Biranup Zone source.

Esperance Supersuite

- Crystallization ages of magmatic protoliths are 1198–1135 Ma
- represents in situ melting of a range of sources from within the orogen and new radiogenic (mantle) addition into Biranup Zone crust, during Stage II of the Albany–Fraser Orogeny.

Tropicana Zone

- Crystallization age of magmatic (sanukitoid) protoliths estimated to be 2692 ± 16 Ma, but interpretation is hampered by intense granulite-facies overprinting
- the age of 2692 Ma is different to compositionally similar magmatism found elsewhere within the Yilgarn Craton
- prolonged granulite-facies metamorphic zircon growth at 2718–2554 Ma is not similar to the timing of high-grade events in the rest of the Yilgarn Craton
- may represent a deeper crustal level or a different part of the Yilgarn Craton, or both, consistent with the suggestion that it is a piece of the Yilgarn Craton not seen elsewhere, thrust onto the craton margin
- the Tropicana Zone was attached to the craton before c. 1780 Ma, based on 1780 Ma granite veins in the Tropicana Zone and the age of similar magmatism in the (para)autochthonous Biranup Zone
- Re–Os dating of pyrite suggests an age of c. 2.1 Ga for associated gold mineralization; this age is distinct from those of major Proterozoic tectonothermal events elsewhere in the Albany–Fraser Orogen
- sanukitoid magmas may have been the source of gold in the Tropicana Zone.

References

Barley, ME, Eisenlohr, BN, Groves, DI, Perring, CS and Vearncombe, JR 1989, Late Archean convergent margin tectonics and gold mineralization: A new look at the Norseman-Wiluna belt, Western Australia: Geology, v. 17, p. 826–829.

Blenkinsop, TG, and Doyle, MG 2014, Structural controls on gold mineralization on the margin of the Yilgarn craton, Albany–Fraser orogen: The Tropicana Deposit, Western Australia: Journal of Structural Geology, doi: 10.1016/j.jsg.2014.01.013.

Cassidy, KF, Champion, DC, Krapež, B, Barley, ME, Brown, SJA, Blewett, RS, Groenewald, PB and Tyler, IM 2006, A revised geological framework for the Yilgarn Craton, Western Australia: Geological Survey of Western Australia, Record 2006/8, 8p.

Champion, DC and Sheraton, JW 1997, Geochemistry and Nd isotope systematics of Archaean granites of the Eastern Goldfields, Yilgarn Craton, Australia: Implications for crustal growth processes: Precambrian Research, v. 83, p. 109–132.

Clark, C, Kirkland, CL, Spaggiari, CV, Oorschot, C, Wingate, MTD and Taylor, RJ 2014, Proterozoic granulite formation driven by mafic magmatism: An example from the Fraser Range Metamorphics, Western Australia: Precambrian Research, v. 240, p. 1–21.

Clark, DJ, Kinny, PD, Post, NJ and Hensen, BJ 1999, Relationships between magmatism, metamorphism and deformation in the Fraser Complex, Western Australia: constraints from new SHRIMP U–Pb zircon geochronology: Australian Journal of Earth Sciences, v. 46, p. 923–932.

Clark, DJ, Hensen, BJ and Kinny, PD 2000, Geochronological constraints for a two-stage history of the Albany–Fraser Orogen, Western Australia: Precambrian Research, v. 102, p. 155–183.

De Waele, B and Pisarevsky, SA 2008, Geochronology, paleomagnetism and magnetic fabric of metamorphic rocks in the northeast Fraser Belt, Western Australia: Australian Journal of Earth Sciences, v. 55, p. 605–621.

Doyle, M, Blenkinsop, T, Crawford, A, Fletcher, I, Foster, J, Fox-Wallace, LJ, Large, R, Mathur R, McNaughton, N, Meffre, S, Muhling, J, Occhipinti, S, Rasmussen, B and Savage, J 2014, Tropicana deposit, Western Australia: an integrated approach to understanding granulite-hosted gold and the Tropicana Gneiss, *in* Albany–Fraser Orogen seismic and magnetotelluric (MT) workshop 2014: extended abstracts *compiled by* CV Spaggiari and IM Tyler: Geological Survey of Western Australia, Record 2014/6, p. 69–76.

Fitzsimons, ICW 2003, Proterozoic basement provinces of southern and southwestern Australia and their correlation with Antarctica: Geological Society of London Special Publication, v. 206, p. 93–130.

Goscombe, B, Blewett, RS, Czarnota, K, Groenewald, PB and Maas, R 2009, Metamorphic evolution and integrated terrane analysis of the eastern Yilgarn Craton: rationale, methods, outcomes and interpretation: Geoscience Australia, Record 2009/23. 270p.

Johnson, SP, Sheppard, S, Rasmussen, B, Wingate, MTD, Kirkland, CL, Muhling, JR, Fletcher, IR and Belousova, E 2011, Two collisions, two sutures: Punctuated pre-1950 Ma assembly of the West Australian Craton during the Ophthalmian and Glenburgh Orogenies: Precambrian Research, v. 189, p. 239–262.

Kent, AJR, Cassidy, KF and Fanning, MC 1996, Archean gold mineralization synchronous with the final stages of cratonization, Yilgarn Craton, Western Australia: Geology, v. 24, p. 879–882.

Kirkland, CL, Wingate, MTD, Spaggiari, CV and Pawley, M 2010, 194736: metasyenogranite, Bartlett Bluff; Geochronology Record 849: Geological Survey of Western Australia, 4p.

Kirkland, CL, Spaggiari, CV, Pawley, MJ, Wingate, MTD, Smithies, RH, Howard, HM, Tyler, IM, Belousova, EA and Poujol, M 2011a, On the edge: U–Pb, Lu–Hf, and Sm–Nd data suggests reworking of the Yilgarn Craton margin during formation of the Albany–Fraser Orogen: Precambrian Research, v. 187, p. 223–247, doi:10.1016/j.precamres.2011.03.002.

Kirkland, CL, Spaggiari, CV, Wingate, MTD, Smithies, RH, Belousova, EA, Murphy, R and Pawley, MJ 2011b, Inferences on crust–mantle interaction from Lu–Hf isotopes: a case study from the Albany–Fraser Orogen: Geological Survey of Western Australia, Record 2011/12, 25p.

Kirkland, CL, Wingate, MTD and Spaggiari, CV 2011c, 194701: metagranitic gneiss, Crystal Lake; Geochronology Record 983: Geological Survey of Western Australia, 5p.

Kirkland, CL, Wingate, MTD and Spaggiari, CV 2011d, 194714: psammitic gneiss, Gnama Hill; Geochronology Record 999: Geological Survey of Western Australia, 6p.

Kirkland, CL, Wingate, MTD and Spaggiari, CV 2011e, 194718: mafic granulite, American Granulite Quarry; Geochronology Record 993: Geological Survey of Western Australia, 4p.

Kirkland, CL, Wingate, MTD, Spaggiari, CV and Tyler, IM 2011f, 194773: granitic rock, Eucla No. 1 drillhole; Geochronology Record 1001: Geological Survey of Western Australia, 4p.

Kirkland, CL, Smithies, RH, Woodhouse, E, Howard, HM, Wingate, MTD, Belousova, EA, Cliff, JB, Murphy, RC and Spaggiari, CV 2012a, A multi-isotopic approach to the crustal evolution of the west Musgrave Province, central Australia: Geological Survey of Western Australia, Report 115, 47p.

Kirkland, CL, Wingate, MTD and Spaggiari, CV 2012b, 182485: migmatitic gneiss, Burkin prospect; Geochronology Record 1054: Geological Survey of Western Australia, 4p.

Kirkland, CL, Wingate, MTD and Spaggiari, CV 2012c, 194711, metamonzogranite, Kent Dam; Geochronology Record 1044: Geological Survey of Western Australia, 4p.

Kirkland, CL, Wingate, MTD, Spaggiari, CV and Pawley, MJ 2012d, 184374: monzogranite, Mount Ridley; Geochronology Record 1045: Geological Survey of Western Australia, 4p.

Kirkland, CL, Wingate, MTD, Spaggiari, CV and Pawley, MJ 2012e, 182424: metasyenogranite, McKay Creek; Geochronology Record 1017: Geological Survey of Western Australia, 4p.

Kirkland, CL, Wingate, MTD and Spaggiari, CV 2012f, 182474: granite vein, Big Red prospect; Geochronology Record 1051: Geological Survey of Western Australia, 4p.

Kirkland, CL, Wingate, MTD and Spaggiari, CV 2013a, 192558: granitic gneiss, Haig Cave; Geochronology Record 1089: Geological Survey of Western Australia, 4p.

Kirkland, CL, Wingate, MTD and Spaggiari, CV 2013b, 194717: metagabbro, Eyre Highway; Geochronology Record 1090: Geological Survey of Western Australia, 5p.

Kirkland, CL, Wingate, MTD and Spaggiari, CV 2014, 192550: monzogranite vein, Hercules prospect; Geochronology Record 1184: Geological Survey of Western Australia, 4p.

Lawley, CJM, Selby, D, Condon, D and Imber, J 2014, Palaeoproterozoic orogenic gold style mineralization at the Southwestern Archaean Tanzanian cratonic margin, Lupa Goldfield, SW Tanzania: Implications from U–Pb titanite geochronology: Gondwana Research, v. 26, p. 1141–1158

Nelson, DR, Myers, JS and Nutman, AP 1995a, Chronology and evolution of the Middle Proterozoic Albany–Fraser Orogen, Western Australia: Australian Journal of Earth Sciences, v. 42, p. 481–495.

Nelson, DR 1995b, 83662: biotite–hornblende monzogranite gneiss, Poison Creek; Geochronology Record 86: Geological Survey of Western Australia, 4p.

Nelson, DR 1995c, 83663: granodiorite gneiss, Israelite Bay; Geochronology Record 74: Geological Survey of Western Australia, 4p.

Nelson, DR 1995d, 83667: porphyritic biotite granite, Balladonia Rock; Geochronology Record 74: Geological Survey of Western Australia, 4p.

Occhipinti, SA, Doyle, M, Spaggiari CV, Korsch, R, Cant, G, Martin, K, Kirkland, CL, Savage, J, Less, T, Bergin, L and Fox, L 2014, Interpretation of the deep seismic reflection line 12GA-T1: northeastern Albany–Fraser Orogen, *in* Albany–Fraser Orogen seismic and magnetotelluric (MT) workshop 2014: extended abstracts, *compiled by* CV Spaggiari and IM Tyler: Geological Survey of Western Australia, Record 2014/6, p. 52–68.

Smithies, RH, Spaggiari, CV, Kirkland, CL, Howard, HM and Maier, WD 2011, Petrogenesis of gabbros of the Mesoproterozoic Fraser Zone: constraints on the tectonic evolution of the Albany–Fraser Orogen: Geological Survey of Western Australia, Record 2013/5, 29p.

Smithies, RH, Spaggiari, CV, Kirkland, CL and Maier, WD 2014, Geochemistry and petrogenesis of the Albany–Fraser igneous rocks, *in* Albany–Fraser Orogen seismic and magnetotelluric (MT) workshop 2014: extended abstracts *compiled by* CV Spaggiari and IM Tyler: Geological Survey of Western Australia, Record 2014/6, p. 77–88.

Spaggiari, CV, Bodorkos, S, Barquero-Molina, M, Tyler, IM and Wingate, MTD 2009, Interpreted bedrock geology of the south Yilgarn and central Albany–Fraser Orogen, Western Australia: Geological Survey of Western Australia, Record 2009/10, 84p.

Spaggiari, CV, Kirkland, CL, Pawley, MJ, Smithies, RH, Wingate, MTD, Doyle, MG, Blenkinsop, TG, Clark, C, Oorschot, CW, Fox, LJ and Savage, J 2011, The Geology of the east Albany–Fraser Orogen — a field guide: Geological Survey of Western Australia, Record 2011/23, 97p.

Spaggiari, CV, Kirkland, CL, Smithies, RH and Wingate, MTD 2012, What lies beneath — interpreting the Eucla basement, *in* GSWA 2012 extended abstracts: promoting the prospectivity of Western Australia: Geological Survey of Western Australia, Record 2012/2, p. 25–27.

Spaggiari CV, Kirkland CL, Smithies RH and Wingate MTD 2014a, Tectonic links between sedimentary cycles, basin formation and magmatism in the Albany–Fraser Orogen, Western Australia Geological Survey of Western Australia, Report 133, 63p.

Spaggiari, CV, Occhipinti, SA, Korsch, RJ, Doublier, MP, Clark, DJ, Dentith, MC, Gessner, K, Doyle, MG, Tyler, IM, Kennett, BLN, Costelloe, RD, Fomin, T and Holzschuh, J 2014b, Interpretation of seismic lines 12GA-AF1, 12GA-AF2 and 12GA-AF3: implications for crustal architecture, *in* Albany–Fraser Orogen seismic and magnetotelluric (MT) workshop 2014: extended abstracts *compiled by* CV Spaggiari and IM Tyler: Geological Survey of Western Australia, Record 2014/6, p. 28–51.

Spaggiari, CV, Kirkland, CL, Smithies, RH, Occhipinti, SA and Wingate, MTD 2014c, Geological framework of the Albany–Fraser Orogen, *in* Albany–Fraser Orogen seismic and magnetotelluric (MT) workshop 2014: extended abstracts, *compiled by* CV Spaggiari and IM Tyler: Geological Survey of Western Australia, Record 2014/6, p. 12–27.

Wingate, MTD and Bodorkos, S 2007, 177909: monzogranite gneiss, Yardilla Bore; Geochronology Record 659: Geological Survey of Western Australia, 4p.

Watkins, R 2012, ASX announcement 24/4/12 (ASX code BDR), Beadell Resources Limited, Tropicana East – Hercules Drill Results, 4p.

Integrating outcrop, aeromagnetic and gravity data: models of the east Albany–Fraser Orogen

by

LI Brisbout, CV Spaggiari, and ARA Aitken

Introduction

Presented here is a map-view structural interpretation and two magnetic and gravity forward models that traverse the east Albany–Fraser Orogen approximately 100 km to the southwest of seismic line 12GA-AF3 (Fig. 1). The regional scale map-view structures are interpreted primarily from aeromagnetic data and include kilometre scale folds, shear zones, faults and plutons. The two forward models are approximately along strike of line 12GA-AF3 and provide crustal scale, interpreted cross-sections that satisfy the aeromagnetic and Bouguer gravity data. Forward models are constrained by petrophysical data (collected and compiled during this study) and, where outcrop information is available, by geological information (largely from other workers). The datasets used in this study and the method and results of the map-view interpretation, petrophysical data collection and forward modelling are presented below.

Datasets

Geological information

The 1:250 000 scale interpreted bedrock geology map of Spaggiari and Pawley (2012) forms the framework of this study and is used to provide information on the surface locations of tectonic units and major structures. Other geological information used includes surface geology maps at 1:100 000 (Erayinia, Yardilla and Yardina) and 1:250 000 scale (Widgimooltha, Norseman, Balladonia and Zanthus) and the Geological Survey of Western Australia's (GSWA) database of field observations (WAROX). Surface geology maps and WAROX data have been used primarily to provide structural information that has been used to constrain the orientations of regional scale structures interpreted from aeromagnetic images.

Aeromagnetic and gravity data

Aeromagnetic data in the study area was downloaded from GSWA's MAGIX database and comprises 16 airborne surveys with flight-line spacings of 50–400 m and flight-line directions of 90–180°, the majority at 90°. Total magnetic intensity data have been gridded to a cell size of 75 m then reduced to the pole (RTP) (Baranov, 1957) (Fig. 2a). RTP aeromagnetic data has also been enhanced for map-view interpretation by application of the first vertical derivative (1VD), horizontal derivative, tilt derivative, analytic signal and upward continuation.

Gravity data in the study area was downloaded from the Geophysical Archive Data Delivery System (www.geoscience.gov.au/gadds) and comprises several regional surveys with stations spaced in 2.5 and 5 km grids, and several higher resolution surveys. Bouguer gravity data (Fig. 2b) has been terrain corrected, by application of the spherical cap, gridded to 1 km cell size and enhanced by application of 1VD and upward continuation.

Map-view structural interpretation

Method

Aeromagnetic and gravity images, constrained where possible by structural information, have been used to produce a map-view structural interpretation of the study area. Aeromagnetic data, which provides information on the magnetization contrasts in the top ~18 km of the crust, is the primary dataset used to interpret the regional-scale structures in map-view. The method followed here involves drawing aeromagnetic trend lines to trace magnetization contrasts in RTP 1VD images. Aeromagnetic trend lines — treated similarly to form lines in structural geology — form a framework from which faults, shear zones and folds can be interpreted. Faults and shear zones are typically interpreted where aeromagnetic trend lines are offset, where regions of different magnetic character are juxtaposed and where structures have undergone magnetite creation or destruction (Betts et al., 2003). Folds are typically interpreted where aeromagnetic trend lines have recognizable fold geometries. Bouguer gravity data provides information on density contrasts in the lithosphere, usually at a lower resolution than

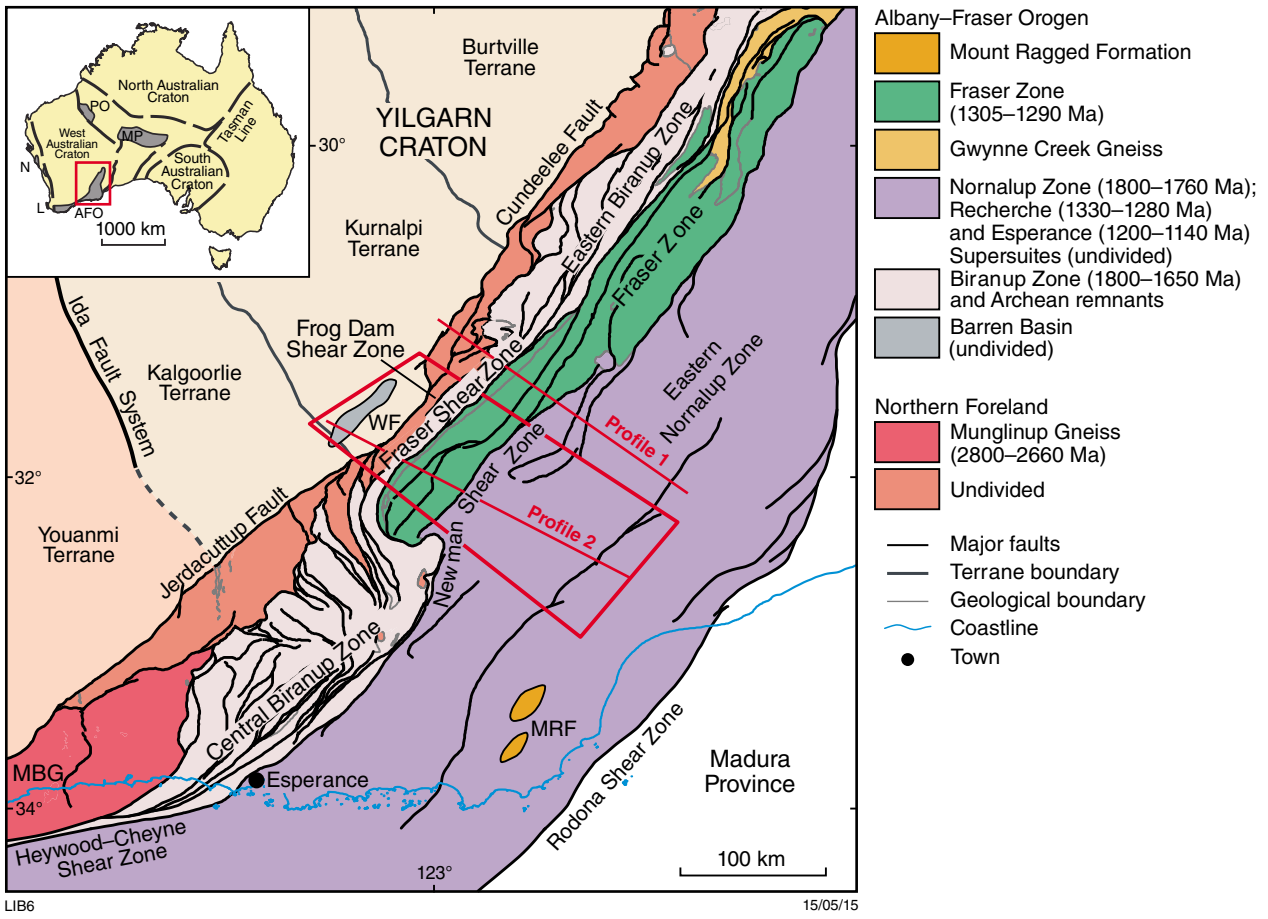

Figure 1. Simplified bedrock geology of the east Albany–Fraser Orogen (after Spaggiari et al., 2011) showing the study area, forward modelled profiles 1 and 2 and seismic line 12GA-AF3

aeromagnetic data. The density contrasts imaged in gravity data usually represent major lithological contacts or large-scale structures that juxtapose units of contrasting density. Distinguishing whether density contrasts represent lithological contacts and/or structural contacts can be achieved using aeromagnetic data and, if available, field information.

It is also possible to constrain the orientation and movement of structures mapped in aeromagnetic and gravity images, although this can be hindered by the difficulty in correlating structures observed in outcrop with structures interpreted in aeromagnetic or gravity images. The orientations of faults and shear zones can be constrained using structural information and asymmetries in the magnetic and gravity gradients. The orientation of fold axial planes can be determined from structural information, and the plunge of folds can be determined from the asymmetry in the magnetic gradient of the fold hinge. The movement direction on faults and shear zones can be determined from kinematic indicators observed in the field or, for large-scale shear zones, by using magnetic features as proxies for microstructures (e.g. Betts et al., 2007).

Map-view structure

The Northern Foreland and Biranup Zone both have low magnetizations and smooth magnetic textures that express structures poorly. On the other hand, the Fraser and Nornalup Zones have large magnetization contrasts that express structures well and based on variations in regional structures, these zones have been divided into domains and sub-domains (Fig. 3). Domains, generally, are regions with distinct structure separated by major structures, and sub-domains are regions of structural variation not necessarily bound by major structures. Some of the structural variation in the Fraser and Nornalup Zones will be described below.

The magnetic fabric of the Fraser Zone is characterized by approximately linear, high- to low-intensity magnetic horizons (~200 m in width). The magnetic horizons have not been directly correlated with features observed in outcrop but most likely represent a combination of lithological variations and subparallel structures. Magnetic horizons are parallel to the dominantly northeast-striking steeply dipping gneissic layering that is defined by sheets of metagranite, metagabbro and metasedimentary rocks (Spaggiari et al., 2011). The metagabbro, metagranite and

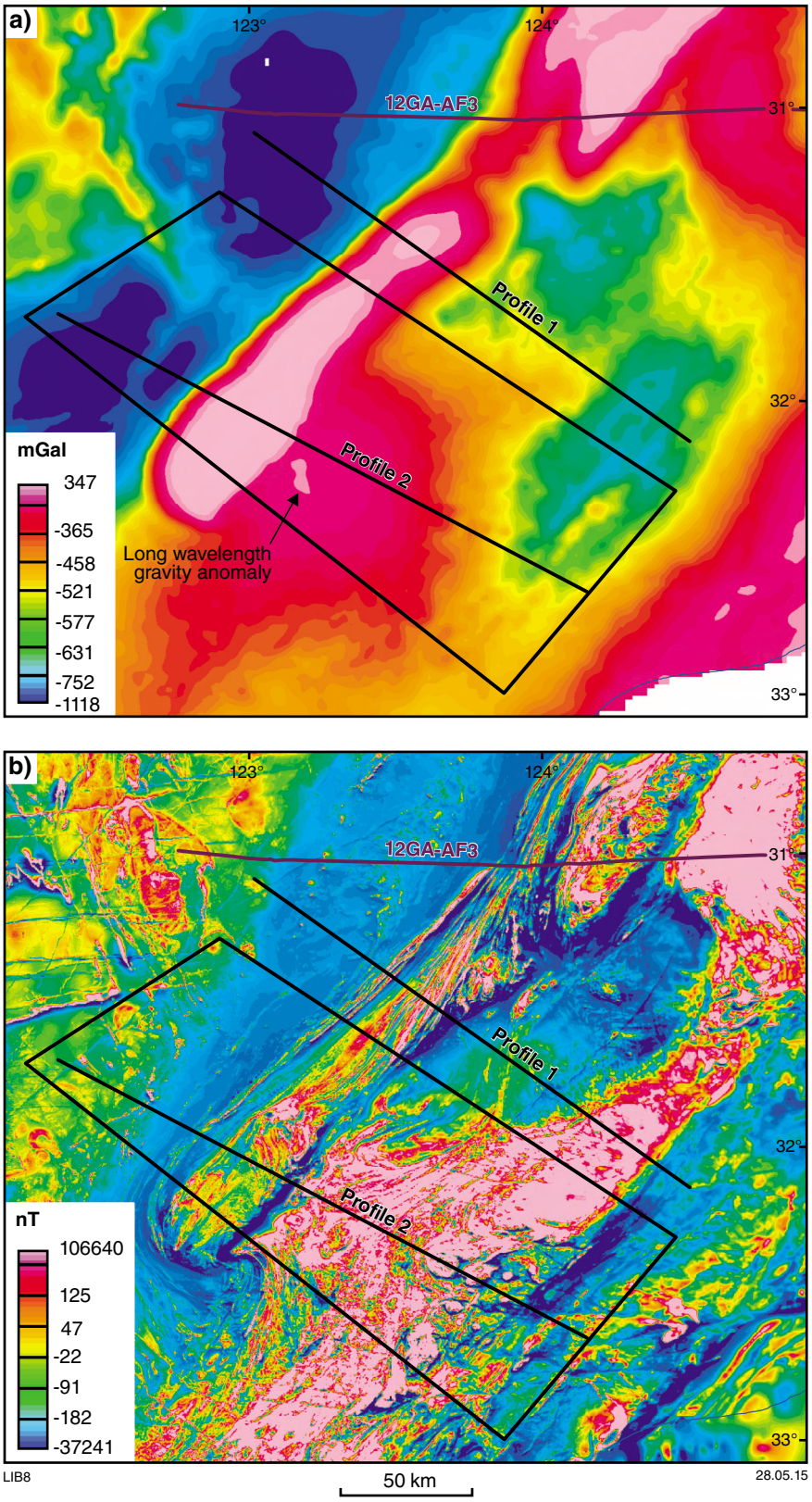

Figure 2. **a) Reduced-to-pole (RTP) total magnetic intensity image, showing the study area, modelled profiles and seismic line 12GA-AF3; b) Bouguer spherical cap corrected gravity image.**

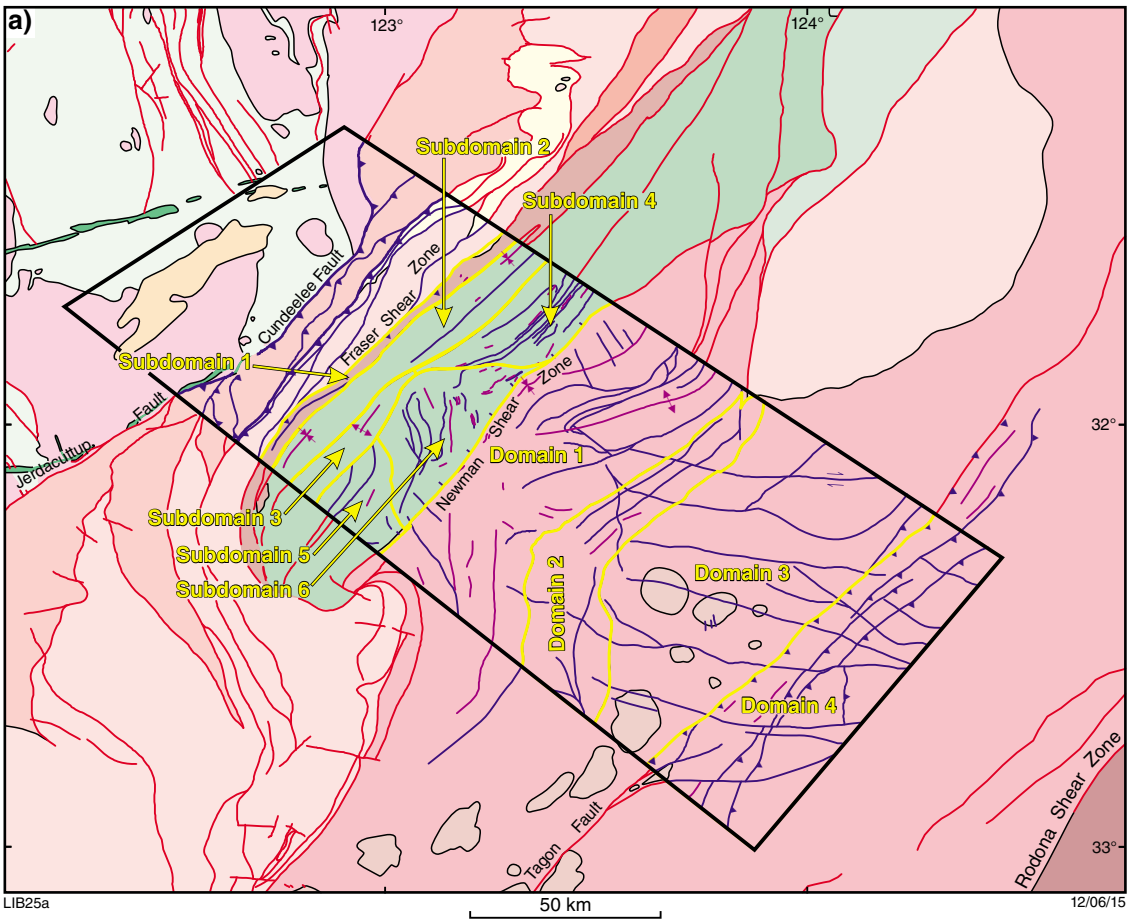

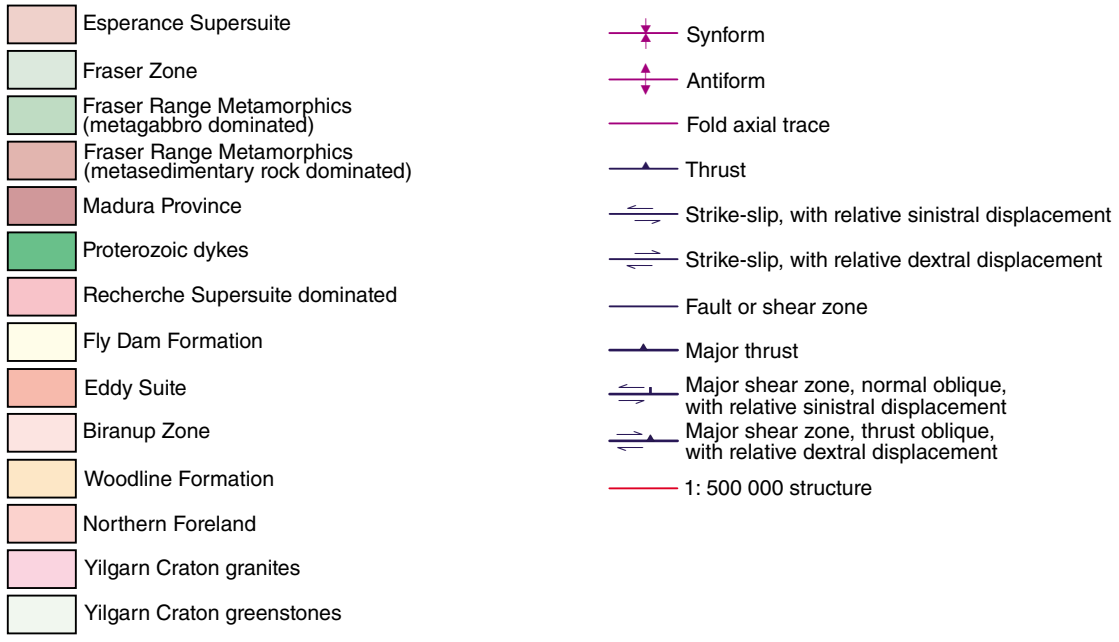

Figure 3. Structural interpretation showing, within the study area, the structures, domains and sub-domains interpreted in this study. Interpreted bedrock geology outside the study area is from Spaggiari and Pawley (2012) and GSWA 1:500 000 scale linear structure.

metasedimentary rocks of the Fraser Zone have bimodal magnetic susceptibility distributions, suggesting that the high or low intensity magnetic horizons could be any of these lithologies. In addition to the lithological layering, it is likely that some of the low intensity magnetic horizons represent demagnetized northeast-trending shear zones.

In sub-domains 2 and 3 of the Fraser Zone (Fig. 3), magnetic horizons have been folded into regional scale (~1.6 – 4.5 km wide) tight- to isoclinal folds (this study and Spaggiari and Pawley, 2012). In sub-domain 4, which is completely under cover, magnetic horizons are folded into smaller ~500 m-wide folds that are truncated by demagnetized northeast-trending shear zones (Figs 4a and b). The regional-scale northeast-trending isoclinal folds have a similar style and trend to the intrafolial isoclinal folds that are locally observed in outcrop (Fig. 4f). There are several possible relationships between the regional-scale folds and the outcrop-scale intrafolial folds. One possibility is that both folds occurred as part of a progressive deformation event that involved the formation of the gneissic layering and intrafolial folds followed by the regional-scale folds. Alternatively, it's also possible that the regional-scale folds formed during a younger deformation event, possibly during Stage II of the Albany–Fraser Orogeny. The lack of preserved U–Pb Stage II metamorphic ages in the Fraser Zone (Kirkland et al., 2011a) does not necessarily indicate a lack of Stage II deformation, it may just suggest that the Fraser Zone underwent deformation after being exhumed into the shallow crust, a setting less favourable for zircon growth (Kirkland et al., 2011).

Sub-domain 4 of the Fraser Zone also contains several eye-shaped magnetic features (Fig. 4c), including The Eye anomaly at the Nova–Bollinger Ni–Cu deposit. Further interpretation of these features is hindered by the lack of outcrop and therefore structural constraint. For example, lineations and associated kinematic indicators might have provided information on the direction of movement and the sense of shear. Despite this, a possible interpretations of these features are doubly plunging antiforms or synforms of non-cylindrical folds (Fig. 4d). Alternatively, these 'eyes' can be interpreted as large-scale proxies for sigma-mantled porphyroclasts with a slight dextral asymmetry (Fig. 4e). According to this model, magnetic horizons may represent material dominated by metagranite and/or metasedimentary rocks that wraps around more rigid metagabbro dominated 'clasts'. The interpretation of the eye-shaped magnetic features as non-cylindrical folds is perhaps more consistent with the regional-scale northeast-trending folds observed in aeromagnetic images in this study (Figs 4a and b) and in Spaggiari and Pawley (2012).

In the centre of the study area, in sub-domain 6 of the Fraser Zone, magnetic horizons appear to trend to the north-northwest, almost orthogonal to the dominant northeasterly trend. Magnetic horizons, which are subparallel to foliation measurements shown on the 1:250 000 series map sheets, are tightly folded with ~6 km wavelengths and apparent north and north-northwest trending axial traces (Fig. 4g). The regional folds interpreted in magnetic images could represent a complex, non-cylindrical geometry of an overall northeast-trending folding. The unusual trend of the fold axial traces in this sub-domain may be the result of lithological variations in the Fraser Zone, and possibly the dominance of relatively competent metagabbro.

The moderate to intense magnetic fabric of the Nornalup Zone is divided into four domains that define structural and magmatic features. In domain 1, adjacent to the Fraser Zone, the moderately continuous magnetic horizons are folded into north and northeast-trending tight folds, with wavelengths of approximately 10 km (Fig. 5a). The magnetic gradient in the hinge of the northeast-trending, southwest-closing fold shallows to the southwest, suggesting this fold is an antiform. The north-trending fold has circular magnetic anomalies along strike of the axial trace that are interpreted to be due to non-cylindrical folding (Fig. 5a).

Domain 1 contains very little outcrop and few structural measurements. Where detailed structural information is available, for example at Harms Lake, it is usually not possible to correlate structures observed in outcrop with fabrics observed in magnetic images. Harms Lake is located in a region with chaotic magnetic fabric with northwest, northeast and easterly magnetic trends, in between the regional-scale folds described above (Fig. 5b). Exposed at Harms Lake is a metagranite with a west-striking, steeply north-dipping foliation and folds with axial planes subparallel to the foliation. Approximately 2 km to the northeast of Harms Lake, metagranite of a similar composition has a northeast-striking foliation and a steep northwest dip. The complex magnetic fabric possibly reflects the complex outcrop scale structures but, due to the differences in scale between outcrop structures and magnetic features, it is not possible to directly correlate structures observed in outcrop with magnetic fabrics.

The magnetic fabric of domain 2 of the Nornalup Zone is dominated by north–northeast trending, variably continuous, highly magnetic horizons. Locally, magnetic horizons are folded into tight folds with wavelengths of ~3 km that are truncated by demagnetized, northeast-trending shear zones (Fig. 5c). The lack of outcrop and therefore structural information in this region, and the complex overlapping magnetic anomalies, make it difficult to constrain the dip direction of shear zones or the axial plane and plunge of folds. Elliptical magnetic horizons along strike of the north-trending fold axial trace are interpreted to be non-cylindrical folds, although it is also possible these anomalies represent plutons (Fig. 5c).

In domain 3 the northeast-trending fabric is crosscut by circular and subcircular highly and intensely magnetic anomalies that are interpreted as plutons, possibly belonging to the Esperance Supersuite (Fig. 5e). Several of the intensely magnetic anomalies are also coincident gravity anomalies (Fig. 5f). Some of these coincident anomalies have been drilled by Enterprise Metals NL who report intersecting magnetite-rich, intermediate intrusives (Williams and Robertson, 2011).

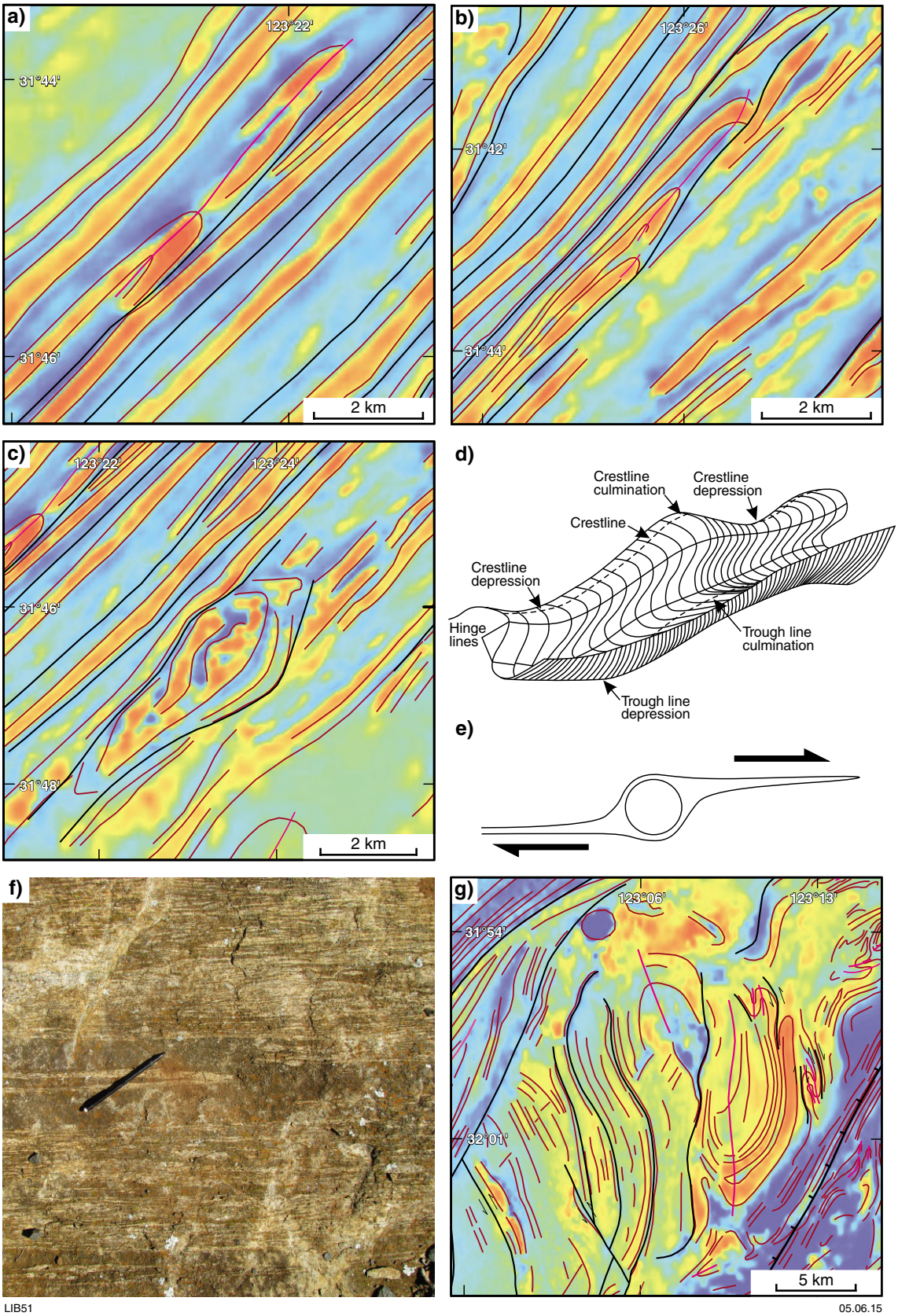

Figure 4. **Fraser Zone structures interpreted from aeromagnetic images: a) and b) isoclinal folds truncated by demagnetized northeast-trending shear zones; c) 1VD RTP total magnetic intensity images of the Fraser Zone showing an eye-shaped aeromagnetic anomaly. Possible interpretations of this anomaly include: d) doubly plunging antiforms or synforms of non-cylindrical folds (from Twiss and Moores, 1992); e) large-scale proxies for porphyroclasts (from Passchier and Trouw, 1996); f) northeast-trending intrafolial isoclinal fold; g) north and north-northwest trending isoclinal folds.**

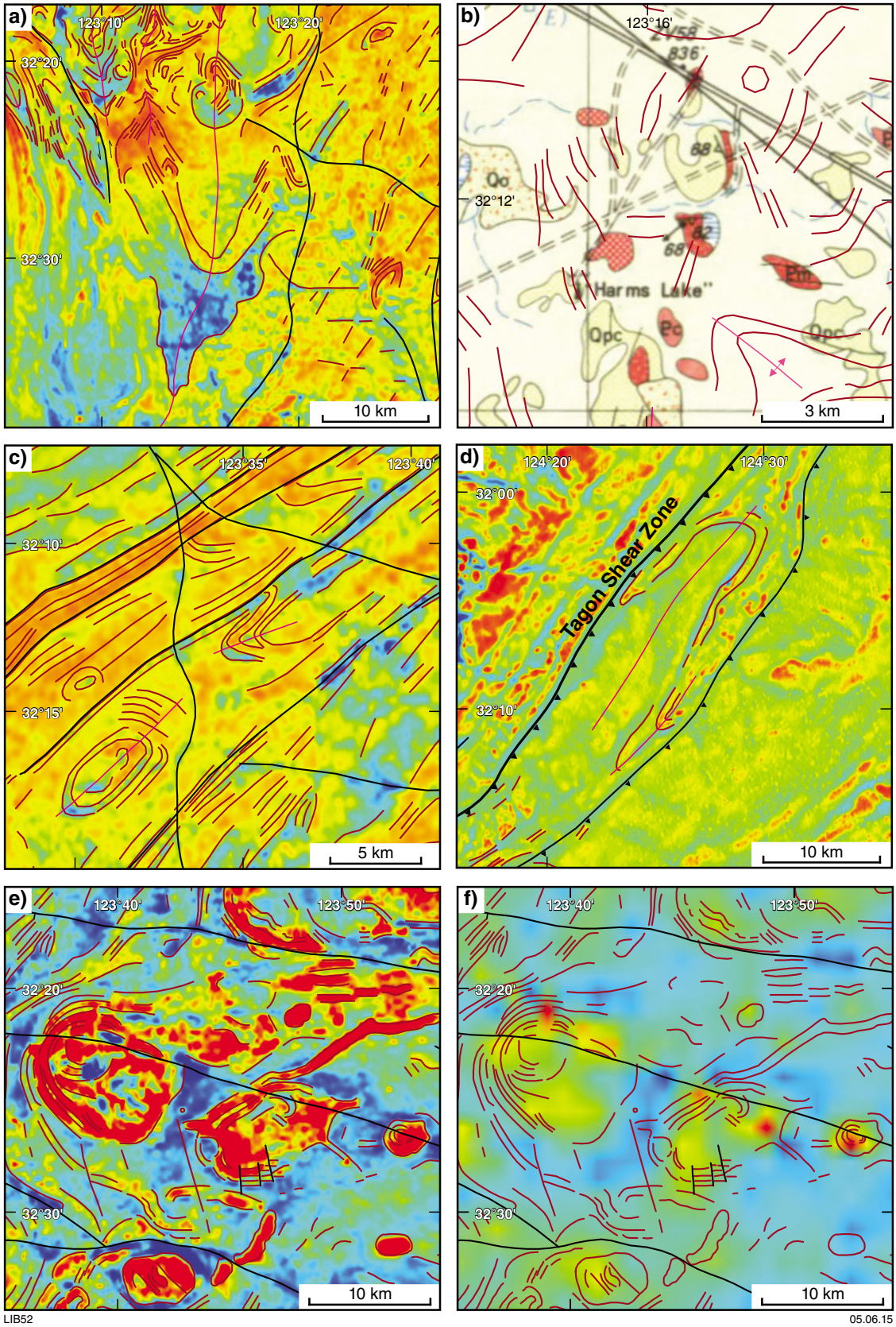

Figure 5. **Nornalup Zone structural and magmatic trends interpreted from aeromagnetic and gravity images: a) north-trending fold; b) chaotic magnetic fabric at Harms Lake; c) northeast-trending tight fold truncated by shear zone and along-strike elliptical magnetic horizons; d) isoclinal folds truncated by the Tagon Shear Zone; e) RTP magnetic image, showing the circular magnetic anomalies of interpreted intermediate intrusives; f) 1VD of Bouguer gravity image, showing the gravity anomalies of interpreted intermediate intrusives.**

Unlike other domains of the Nornalup Zone, domain 4, which is southeast of the Tagon Shear Zone, has low magnetic intensity and smooth magnetic texture with northeast-trending weakly magnetic horizons. Locally, magnetic horizons are tightly to isoclinally folded, with 2–4 km wavelengths, and are truncated by northeast-trending shear zones. One example is the isoclinal fold truncated by the Tagon Shear Zone (Fig. 5d). Domain 4 also contains interpreted intermediate intrusives, although these are smaller and less common than in domain 3. The magnetic fabric of domains 3 and 4, including the intermediate intrusions, is crosscut by a set of long (up to 70 km) demagnetized, west-northwest trending faults with apparent dextral offset (Fig. 5e).

Petrophysics

Method

Specific gravity (n = 231) and magnetic susceptibility (n = 464) data has been compiled from outcrop, hand sample and drillcore in the east Albany–Fraser Orogen. This dataset has been used primarily to constrain the physical properties assigned to magnetic and gravity forward models. Specific gravity, which is the unitless ratio of the density of the sample to the density of water, is considered to be a reasonable estimate of the density of the dominantly crystalline Albany–Fraser Orogen samples. Magnetic susceptibility measurements, which include data compiled from other GSWA workers, were made with a GMS-2 handheld magnetic susceptibility meter and calculated to be the average of five measurements made on five representative surfaces. For analysis, petrophysical data were divided into tectonic units: 1) Northern Foreland; 2) Barren Basin; 3) eastern Biranup Zone; 4) Fraser Zone; 5) eastern Nornalup Zone; and 6) Esperance Supersuite. Data for each tectonic unit have been further subdivided into five lithological groups: 1) mafic intrusive; 2) intermediate intrusive; 3) felsic intrusive; 4) metasedimentary rocks; and 5) felsic rocks of unknown protolith.

East Albany–Fraser Orogen petrophysical data

Specific gravity and magnetic susceptibility data are summarized in Table 1. Specific gravity data are also displayed in box and whisker plots, which show the minimum, maximum, lower quartile, upper quartile and median value for tectonic units (Fig. 6a) and the lithological groups within tectonic units (Fig. 6b).

The specific gravity dataset shows that density is generally determined by rock type — the mafic intrusives generally have higher specific gravities than felsic intrusives and metasedimentary rocks (Fig. 6a). The metasedimentary rocks have a broader distribution and slightly higher specific gravities than felsic intrusives (Fig. 6a). The mean and median specific gravities calculated for tectonic units are largely determined by the proportion of mafic, felsic and metasedimentary samples (Fig. 6b and Table 1). For example, the Fraser Zone, which is dominated by metagabbroic samples, has a higher specific gravity than the Nornalup Zone, which is dominated by samples of the Recherche Supersuite.

Most rock types, and therefore tectonic units, have bimodal magnetic susceptibility distributions with a non-susceptible and a susceptible population. Consequently, the mean of these bimodal populations contain large standard errors that, although not representative of either population, do provide values that can be used in forward modelling (Table 1).

Magnetic and gravity forward models

Method

Two ~200 km-long, 70 km-deep magnetic and gravity forward models were constructed traversing the east Albany–Fraser Orogen (Fig. 1). Forward modelling was performed in the Oasis Montage Add-in, GM-SYS. For the two profiles, RTP aeromagnetic and Bouguer gravity data were sampled from grids at 500 m spacing. Polygons that represent the subsurface were then constructed and attributed with physical properties. The surface locations of the modelled polygons are constrained using the available geological data and the physical properties attributed to polygons have been constrained using the east Albany–Fraser Orogen petrophysical dataset. The physical properties and geometries of the polygons were then adjusted iteratively until a suitable match was achieved between the observed RTP magnetic and Bouguer gravity data, and the magnetic and gravity response of the model.

Other constraints on the forward models include the depth to the Moho, which was sampled from the AusMOHO (the variation of Moho depth in Australia) model (Kennett et al., 2011). The Moho is approximately 37 km deep and features a trough beneath the Fraser Zone that extends to a depth of 44 km (profile 1) and 42 km (profile 2). In both profiles the top of the lower crust is assumed to be at a depth of between 20 and 17 km, parallel the Moho. Following Christensen and Mooney (1995), the lower crust has been modelled with a density of 2.8 gcm^{-3} and the upper mantle with a density of 3.2 $gcm^{-}3$. These variables were kept constant during modelling and zero magnetization in the lower-crust is assumed. The thickness of the Eucla Basin is modelled according to Lowry (1970), although it is not visible at the scale of the models shown.

Profile 1

Profile 1 is located ~50 km to the southwest of seismic line 12GA-AF3, and traverses the Northern Foreland and the Biranup, Fraser and Nornalup Zones (Fig. 1). The dominant feature in the observed gravity data is the high amplitude anomaly associated with the metagabbro dominated Fraser Zone (Fig. 2b). One of the aims of

Table 1. Summary of magnetic susceptibility and specific gravity measurements by tectonic subdivision and rock type

Tectonic unit or basin	*Lithology*	*Specific gravity*			*Magnetic susceptibility (×10^{-5})*					
		n	*Mean ± SD*	*Median*	*n*	*Mean ± SD*	*Median*	*Geometric mean (log10)*	*Min*	*Max*
Northern Foreland	mafic intrusives	9	2.901 ± 0.259	3.042	10	309.6 ± 654	0	0.638	0	1623
	felsic intrusives	13	2.653 ± 0.037	2.636	21	505.1 ± 930	0	1.258	0	3463
	all samples	35	2.770 ± 0.204	2.692	35	403.2 ± 801	0	1.118	0	3463
Barren Basin	metasedimentary rocks	16	2.771 ± 0.187	2.754	30	753.8 ± 1717	0	0.005	0	6500
Eastern Biranup Zone	mafic intrusives	26	3.023 ± 0.102	3.018	33	145.1 ± 314	0	0.702	0	1250
	intermediate intrusives	7	2.763 ± 0.122	2.762	7	35.2 ± 93	0	0.342	0	246.4
	felsic intrusives	40	2.664 ± 0.074	2.642	67	184.4 ± 395	0	0.776	0	1750
	all samples	76	2.799 ± 0.188	2.750	110	163.3 ± 357	0	0.730	0	1750
Nornalup Zone	felsic, mafic and intermediate intrusives	21	2.733 ± 0.091	2.716	89	1732.1 ± 272	678	2.405	0	9721
	all samples (incl. Esperance Supersuite)	24	2.723 ± 0.090	2.714	129	1933 ± 2635	875	2.625	0	18050
Fraser Zone	mafic intrusives (including hybrids)	60	3.010 ± 0.111	3.027	101	642.2 ± 1366	50	1.453	0	7224
	felsic intrusives	10	2.662 ± 0.081	2.629	20	328.8 ± 659	120	1.774	0	3000
	Arid Basin metasedimentary rocks	18	2.872 ± 0.173	2.853	26	486.1 ± 652	164	1.608	0	2454
	all samples	89	2.937 ± 0.173	2.995	149	565.4 ± 1185	100	1.519	0	7224
Esperance Supersuite	felsic and intermediate intrusives	3	2.660 ± 0.056	2.643	40	2823.8 ± 3541	1406	3.115	0	18050

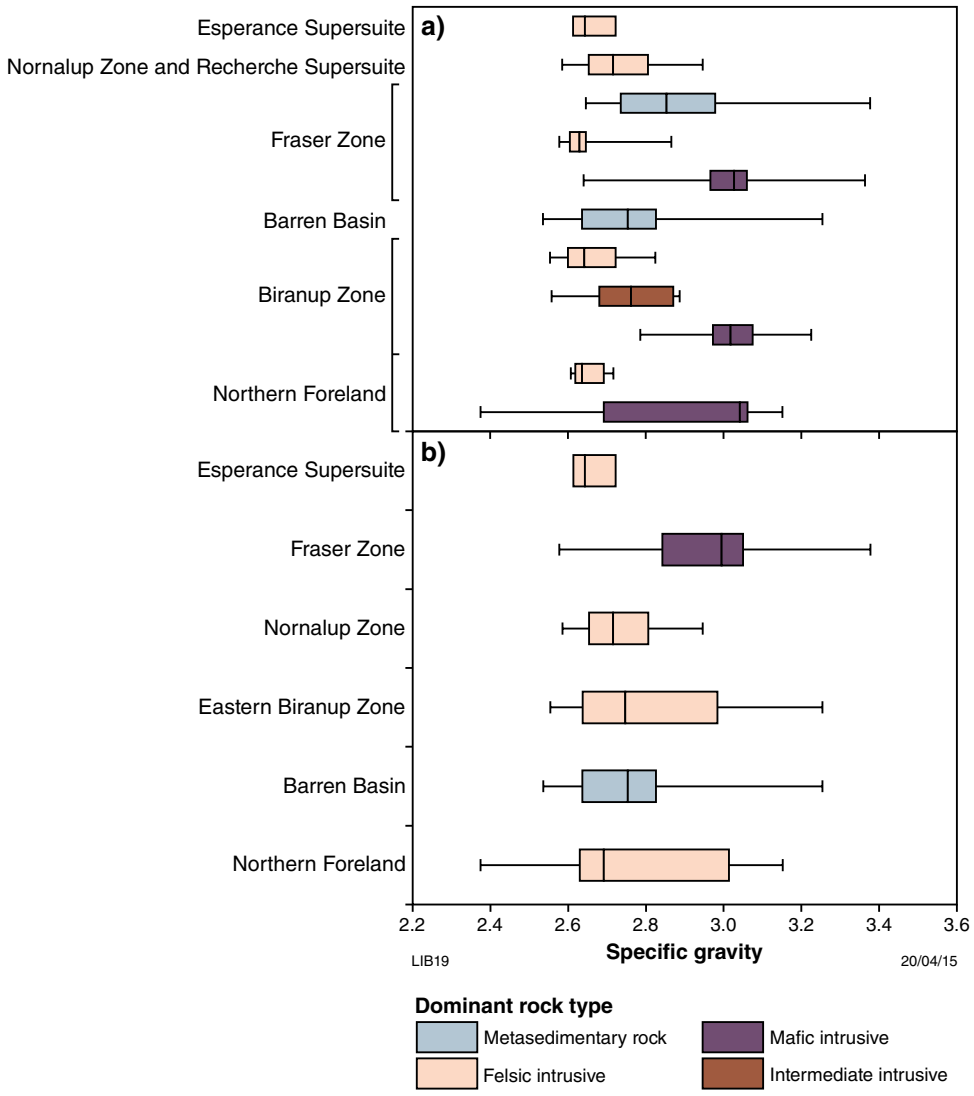

Figure 6. Box and whisker plots showing the minimum, lower quartile, upper quartile and maximum specific gravity for: a) the rock types within tectonic units; b) tectonic subdivisions of the east Albany–Fraser Orogen

modelling profile 1, and in particular the gravity data, is to determine the most likely geometry of the Fraser Zone. The observed magnetic data in the majority of profile 1 is of relatively low intensity with the exception of the high amplitude, high frequency anomalies in the Fraser Zone, and the high amplitude, moderate frequency anomaly in the Nornalup Zone, at the southeastern end of the profile (Fig. 7a).

In profile 1 the Northern Foreland is modelled as three southeast-dipping units that extend ~18km to the lower crust (Fig. 7). This geometry is based on field observations which suggest the Northern Foreland, and the adjacent southeast margin of the Yilgarn Craton, are dominated by northwest-vergent folding and thrusting. The source of the observed gravity trough in the Northern Foreland is interpreted to be the two northwestern units of the Northern Foreland (modelled with densities of 2.638 and 2.642 gcm^{-3}). The low densities of these units suggest they are dominated by granite and/or possibly metasedimentary rocks of the Paleoproterozoic Barren Basin.

To the southeast the Northern Foreland is separated from the Biranup Zone by the Frog Dam Shear Zone. There is very little magnetization or gravity contrast across the Frog Dam Shear Zone, preventing the orientation of this structure from being constrained using forward modelling. Based on the geometry of the adjacent Northern Foreland both the Frog Dam Shear Zone and the Biranup Zone are modelled as southeast dipping.

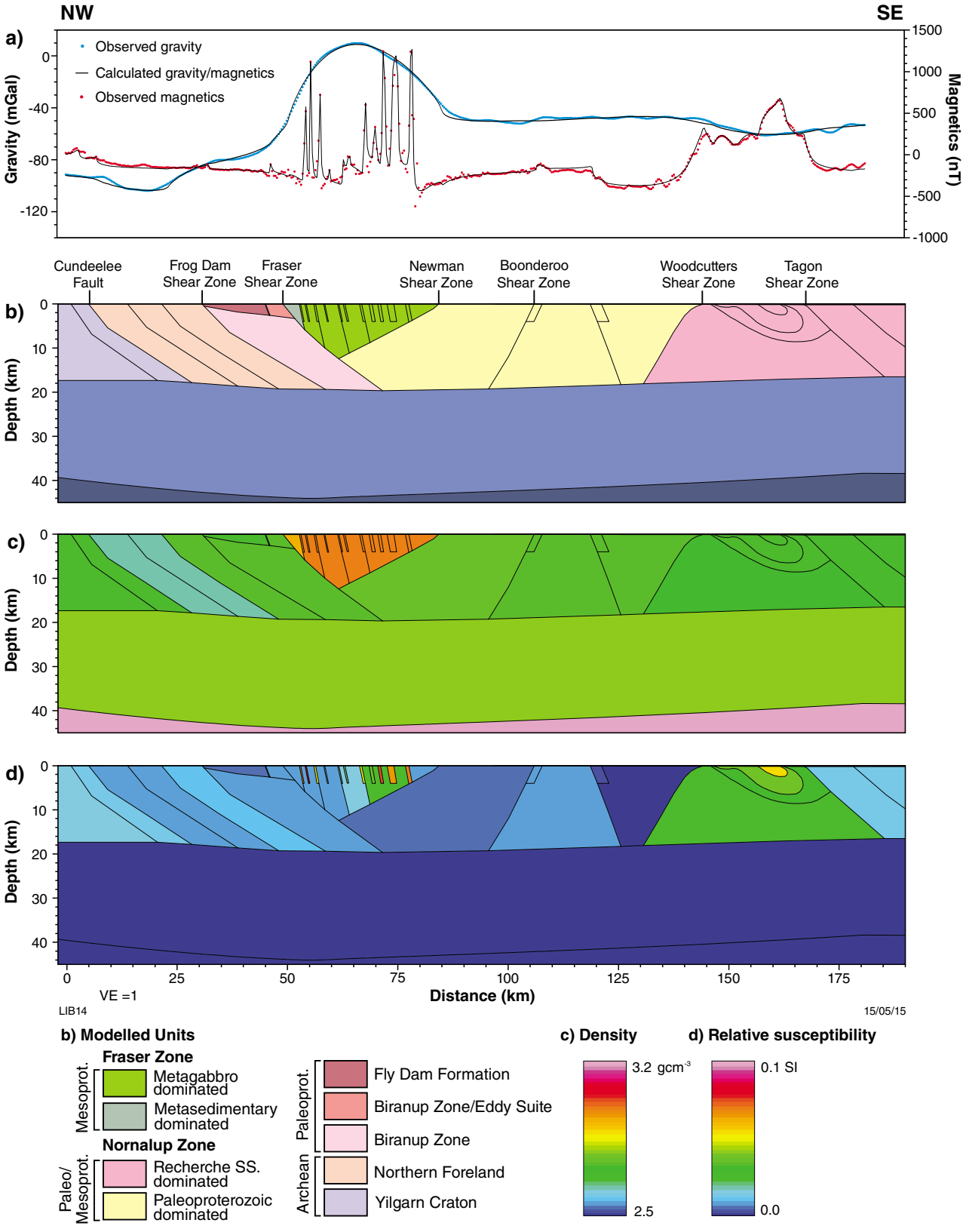

Figure 7. **Magnetic and gravity model of profile 1: a) observed and calculated magnetic and gravity data; b) modelled units; c) density model; d) relative susceptibility model**

Southeast of the Biranup Zone, the Fraser Zone is modelled in 2.5D (with an along-strike extent of 10 km to the southwest and 130 km to the northeast) and attributed a density of 3 gcm^{-3} (the median specific gravity of the Fraser Zone). Given these constraints, and honouring the surface constraints, the Fraser Zone has been modelled as near-triangular in shape and extending to a depth of 12.4 km (Fig. 7). The metasedimentary-dominated component of the Fraser Range Metamorphics (Snowys Dam Formation) lies along the northwest margin of the Fraser Zone and has been modelled with a slightly lower density of 2.95 gcm^{-3}. If the Snowys Dam Formation was modelled with an even lower density, which is possible if the proportion of metagabbro were lower, the northwestern margin of the Fraser Zone, and the Fraser Shear Zone, would steepen.

The high amplitude, high frequency magnetic anomalies of the Fraser Zone are modelled as southeast-dipping blocks that extend to a depth of 4 km, below which sensitivity is low (Fig. 7d). In magnetic images these blocks represent northeast-trending, highly magnetic horizons, some of which are isoclinally folded at a scale smaller than the resolution of the model. Blocks are modelled as southeast dipping due to the asymmetry of the magnetic anomalies in profile. The longer wavelength magnetic variations are accounted for by blocks that extend to the base of the Fraser Zone and which correspond to shear zones interpreted by Spaggiari and Pawley (2012).

Southeast of the Fraser Zone, the completely under cover crust has low magnetic intensity and smooth magnetic texture. This crust is interpreted as Biranup-like Paleoproterozoic dominated material of the Nornalup Zone, rather than Recherche Supersuite dominated granite which typically has a higher susceptibility. The interpreted Paleoproterozoic dominated crust is intersected by the Boonderoo Shear Zone (Spaggiari and Pawley, 2012) which forms a slight aeromagnetic high. However, given the lack of gravity or magnetization contrast across the Boonderoo Shear Zone, its orientation is difficult to constrain from forward modelling. At the southeastern end of the profile, the Paleoproterozoic-dominated Nornalup Zone is interpreted to be separated from the Recherche Supersuite-dominated Nornalup Zone by the Woodcutters Shear Zone (Plates 2 and 4). There is a strong magnetic and gravity contrast across the Woodcutters Shear Zone, which forward modelling suggests dips to the northwest and shallows towards the surface. The Recherche Supersuite-dominated Nornalup Zone is interpreted to lie southeast of the Woodcutters Shear Zone. The source of the high amplitude magnetic anomaly and coincident gravity low, at the southeastern end of the profile, is modelled as a magnetically zoned pluton (Fig. 7d).

Profile 2

Profile 2 is located 70 km to the southwest of profile 1 and southwest of seismic line 12GA-AF3 (Fig. 1). Dominant features in the observed gravity data include a high amplitude gravity anomaly above the Fraser Zone and a moderate amplitude, long wavelength (~150 km) anomaly to the southeast of the Fraser Zone (Fig. 2b). One of the aims of modelling profile 2, and in particular the gravity data, is to suggest a source for this long wavelength anomaly. The observed magnetic data in the Northern Foreland, Biranup Zone and the northwest Fraser Zone is of low intensity but in the southeast Fraser Zone and the Nornalup Zone contains many high frequency, high amplitude anomalies (Fig. 8a). Due to the complex, overlapping nature of the magnetic anomalies, particularly in the Nornalup Zone, only broad peaks and troughs have been modelled. Longer wavelength features in the observed magnetic data in the Nornalup Zone include a magnetic low coincident with the demagnetized Newman Shear Zone, a broad increase in magnetization to the southeast of the Newman Shear Zone, and a decrease towards the southeastern end of the profile (Fig. 8a).

The Northern Foreland, as in in profile 1, is interpreted to form three southeast-dipping units that extend to the lower crust. The gravitational field above the Northern Foreland is composed of a long wavelength Bouguer gravity low that extends along much of the Yilgarn Craton's southern margin. This long wavelength feature extends outside the limit of the model, making it difficult to constrain with these profiles. Superimposed on this long wavelength Bouguer gravity low are shorter wavelength peaks and troughs. The source of the short wavelength Bouguer gravity trough is interpreted to be the southeastern unit of the Northern Foreland. In profile 2, the density required to produce this trough is considerably lower (2.6 gcm^{-3}) than the median value for the Northern Foreland felsic intrusives (2.636 gcm^{-3}) and lower than values obtained for granites of the Agnew–Wiluna belt by Williams (2009). It is most likely that the southeastern unit of the Northern Foreland has a density higher than 2.6 gcm^{-3} and that there is a low density body at depth beneath the margin of the Yilgarn Craton. Tassell and Goncharov (2006) suggest that the source of this gravity low is a deep crustal root beneath the margin of the Yilgarn Craton and the Albany–Fraser Orogen, based on a previous deep crustal seismic and gravity study. To the southeast of the Northern Foreland, the Biranup Zone is narrower than in profile 1 and is also modelled as southeast dipping.

The Fraser Zone is modelled in 2.5D, with an along-strike length of 20 km to the southwest and 120 km to the northwest and a density of 3 gcm^{-3}. As in profile 1, the Fraser Zone is near-triangular in shape but extends to a greater depth of 15.4 km (Fig. 8). In this region the Fraser Zone is bound by the Fraser Shear Zone to the northwest and the Newman Shear Zone to the southeast. Interestingly, in forward models the boundaries of the Fraser Zone are relatively shallowly dipping (30–60°) whereas in outcrop, foliations in both the Fraser and Newman Shear Zones are steep. This suggests that an early, perhaps relatively shallow structure, has been overprinted by steeper structures. The high frequency, high amplitude magnetic anomalies in the southeastern Fraser Zone correlate with the regional-scale folded horizons of structural sub-domain 6. Based on the asymmetry of the magnetic anomalies and field-based structural observations, these folded horizons are modelled as northwest-dipping bodies (Fig. 8).

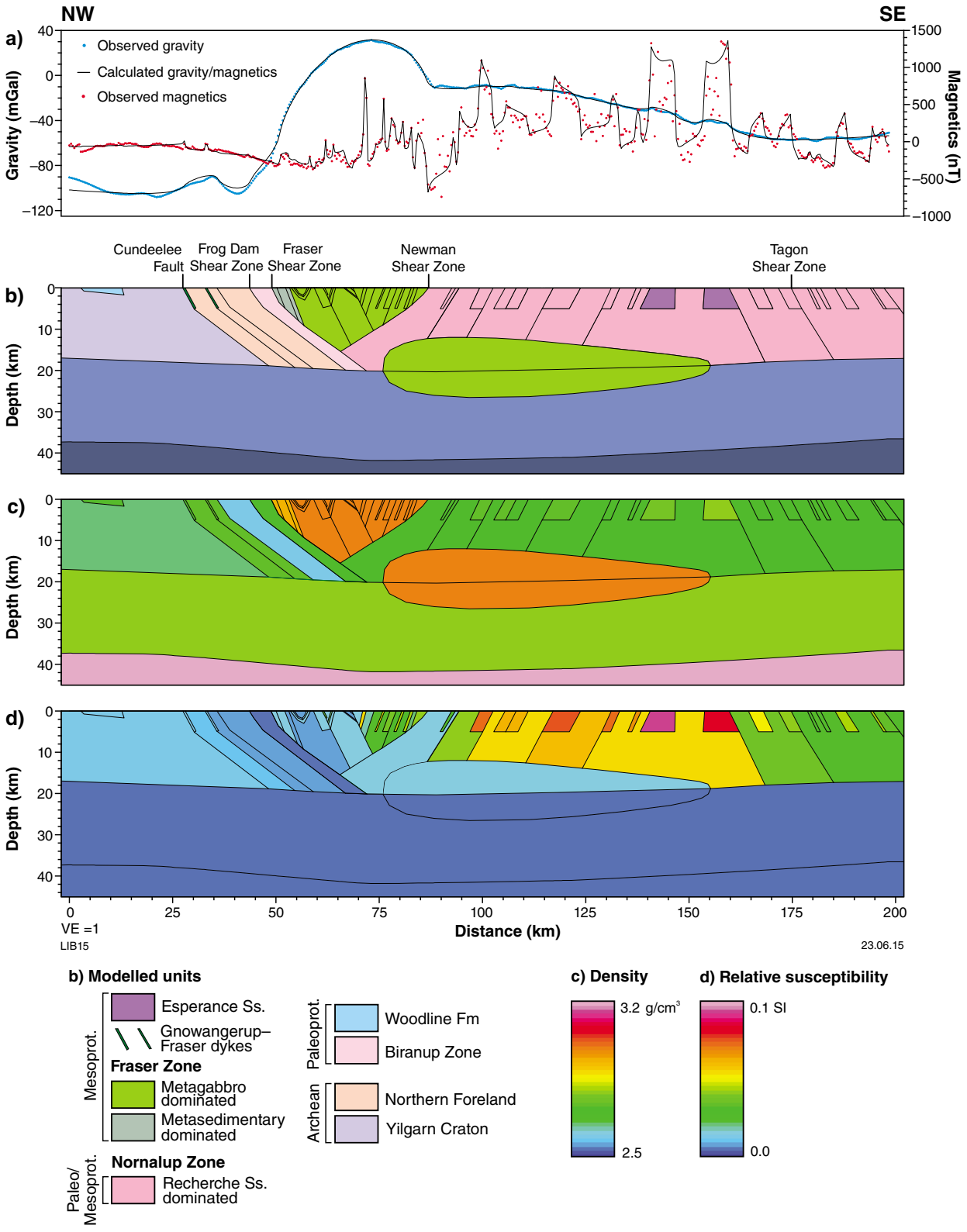

Figure 8. **Magnetic and gravity model of profile 2: a) observed and calculated magnetic and gravity data; b) modelled units; c) density model; d) relative susceptibility model**

The internal architecture of the Nornalup Zone, which lies immediately southeast of the Newman Shear Zone and extends to the end of profile 2, is difficult to constrain. This is partly because the Nornalup Zone is almost entirely under cover and partly because the magnetic data is dominated by many overlapping magnetic anomalies.

The source of the long wavelength Bouguer gravity high in profile 2 is interpreted to be a mid-crustal body with a density of 3 gcm^{-3} and a maximum thickness of ~14.5 km (Fig. 8). This body is modelled in 2.5D with an along-strike extent of 20 km to the southwest and 10 km to the northeast. The only known large mafic intrusive event in the orogen, is the intrusion of the Fraser Zone gabbros during Stage I of the Albany–Fraser Orogeny. One possible interpretation is that the source of this anomaly is a sill-like body of residual mafic material related to the Fraser Zone metagabbros. Superimposed on this long wavelength Bouguer gravity high are higher frequency gravity highs, most of which are at a scale smaller than can be represented on the model. Some of the high frequency, high density anomalies (modelled with densities of 2.78 and 2.80 gcm^{-3}) are coincident with intense magnetic anomalies, several of which have been drilled by Enterprise Resources NL, and which are reported as shallow intermediate intrusions.

The high frequency magnetic anomalies of the Nornalup Zone are modelled broadly with simple polygons to a depth of 5 km, below which sensitivity is limited. Given the complex, overlapping nature of the magnetic anomalies in the Nornalup Zone, the orientations of these features are difficult to constrain.

Sensitivity testing

The Fraser Zone in profile 1 and the mid-crustal mafic body in profile 2 have both been sensitivity tested. Sensitivity testing refers to varying the density and geometry of bodies, within constraint of the specific gravity data and the surface geology, to test the range of possible geometries and physical properties of a body. In profile 1, the Fraser Zone has been attributed densities of 2.95, 3.00 and 3.10 gcm^{-3}, and extends to maximum depths of ~19.4, 12.4 and 7.6 km, respectively (Fig. 9). Densities lower than 2.95 gcm^{-3} are not possible if the surface location of the Fraser Zone is honoured and densities higher than 3.10 gcm^{-3} are not likely given the specific gravity dataset. The models with a lower density of 2.95 gcm^{-3} represent a Fraser Zone with a higher proportion of metasedimentary rock and/or metagranite and models with a higher density of 3.10 gcm^{-3} represent a Fraser Zone with a higher proportion of metagabbro and possibly ultramafic rocks. Ultramafic intrusives, although not commonly observed outcropping in the southwest Fraser Zone, have been reported in drillcore from Nova–Bollinger (Smithes et al., 2013) and in the Fraser Zone to the northeast of the study area (Orion Gold NL, 2013).

The mafic body, interpreted to be the source of the long wavelength Bouguer gravity high in profile 2 has also been sensitivity tested. Although no petrophysical constraints are available, the specific gravity has been varied within the range of values geologically reasonable for mafic and ultramafic rocks. This Bouguer gravity high appears to be symmetric and therefore the shape of the body is assumed to be subhorizontal. The interpreted mafic body has been modelled in the mid-crust with densities of 2.95, 3.00, 3.10 and 3.2 gcm^{-3}, with the thickness of the body varying from 17.7, 14.5, 11.1 to 8.8 km, respectively (Fig. 10a). The mafic body has also been modelled in the lower crust, and with densities of 3.10 and 3.20 gcm^{-3}, where the thickness of the body varies from 17.8 to 16.3 km, respectively (Fig. 10b). Although possible, a lower crustal body with such a large thickness is considered less likely than a thinner mid-crustal body.

Conclusions

The structural interpretation, based primarily on aeromagnetic image interpretation, suggests that the Mesoproterozoic Fraser Zone contains structural domains that can be characterized by: 1) regional-scale northeast-trending tight- to isoclinal folds (~1.6 – 4.5 km in width); 2) isoclinal folds (~500 m in width) truncated by northeast-trending shear zones and eye-shaped magnetic features, interpreted as either doubly plunging antiforms or synforms of non-cylindrical folds or as magnetic porphyroclasts; and 3) regional-scale north to north-northwest trending, tight- to isoclinal folds (~6 km in width). The Paleo to Mesoproterozoic Nornalup Zone is divided into four structural domains that are characterized by: 1) north- and northeast-trending folds (~10 km in width); 2) north- and northeast-trending magnetic horizons, locally with northeast-trending tight folds (~3 km); 3) highly magnetic subcircular anomalies interpreted as plutons of the Esperance Supersuite; and 4) weakly magnetic northeast-trending horizons that locally are folded into isoclinal northeast-trending folds.

The Fraser Zone is associated with a distinct high Bouguer gravity high. Geologically and petrophysically constrained forward modelling of two profiles suggest that the Fraser Zone, if modelled with the median specific gravity of the Fraser Zone petrophysical samples (3 gcm^{-3}), is near-triangular and extends to depths of 12.4 and 15.4 km. In the crust to the southeast of the Fraser Zone, Bouguer gravity data show a long wavelength (~150 km) gravity high. This long wavelength gravity anomaly can be accounted for by a subhorizontal, mid-crustal body of mafic–ultramafic material. If attributed a specific gravity of 3 gcm^{-3} this mid-crustal body will have a maximum thickness of ~14.5 km. Given the intrusion of the Fraser Zone is the only voluminous mafic intrusive event recorded in the Albany–Fraser Orogen, the mid-crustal mafic body may have intruded with the Fraser Zone metagabbros during Stage I of the Albany–Fraser Orogeny.

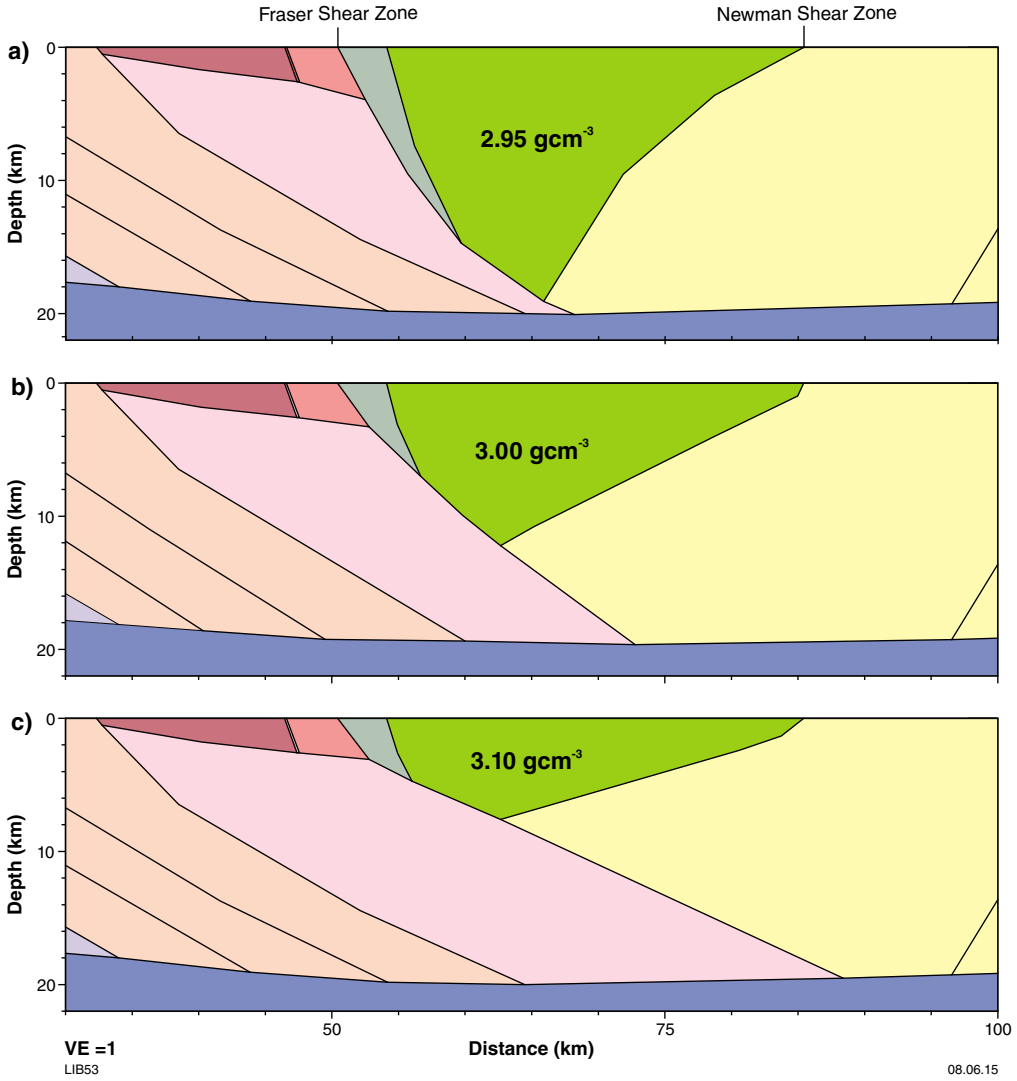

Figure 9. Profile 1 sensitivity test, Fraser Zone with densities of: a) 2.95 gcm^{-3}; b) 3.00 gcm^{-3}; c) 3.10 gcm^{-3}.

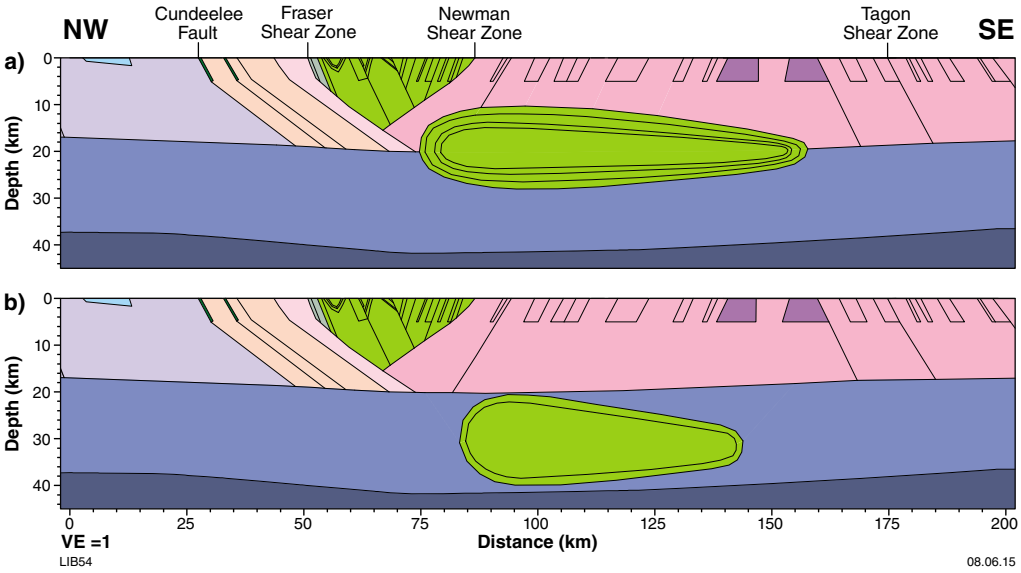

Figure 10. Profile 2 sensitivity test: a) mid-crustal body with densities, from outside to inside, of 2.95, 3.00, 3.10 and 3.20 gcm^{-3}; b) lower-crustal body with densities from outside to inside of 3.00 and 3.10 gcm^{-3}

References

Aitken, ARA and Betts, PG 2009, Multi-scale integrated structural and aeromagnetic analysis to guide tectonic model: An example from the eastern Musgrave Province, Central Australia: Tectonophysics, v. 476, p. 418–435.

Baranov, V 1957, A new method for interpretation of aeromagnetic maps: pseudo-gravimetric anomalies: Geophysics v. 22, p. 359–383.

Betts, P, Williams, H, Stewart, J and Ailleres, L 2007, Kinematic analysis of aeromagnetic data: looking at geophysical data in a structural context: Gondwana Research, v. 11, p. 582–583.

Betts, PG, Valenta, RK and Finlay, J 2003, Evolution of the Mount Woods Inlier, northern Gawler Craton, Southern Australia: an integrated structural and aeromagnetic analysis: Tectonophysics, v. 366, p. 83–111.

Christensen, NI and Mooney, WD 1995, Seismic velocity, structure and composition of the continental crust: a global view: Journal of Geophysical Research, v. 10, p. 9761–9788.

Clark, C, Kirkland, CL, Spaggiari, CV, Oorschot, C, Wingate, MTD and Taylor, RJ 2014, Proterozoic granulite formation driven by mafic magmatism: An example from the Fraser Range Metamorphics, Western Australia: Precambrian Research, v. 240, p. 1–21.

Kennett, B, Salmon, M, Saygin, E and AusMoho Working Group 2011, AusMoho: the variation of Moho depth in Australia: Geophysical Journal International, v. 87, p. 946–958, doi:10.1111/j.1365-246X.2011.05194.

Kirkland, CL, Spaggiari, CV, Pawley, MJ, Wingate, MTD, Smithies, RH, Howard, HM, Tyler, IM, Belousova, EA and Poujol, M 2011, On the edge: U–Pb, Lu–Hf, and Sm–Nd data suggests reworking of the Yilgarn Craton margin during formation of the Albany–Fraser Orogen: Precambrian Research, v. 187, p. 223–247, doi:10.1016/j.precamres.2011.03.002.

Orion Gold NL 2013, Phase 1 Drilling Completed at Peninsula Ni–Cu Project, WA: Report to Australian Securities Exchange, 19 December 2013, 12p.

Passchier, CW and Trouw, RAJ 1996, Microtectonics: Springer-Verlag, Berlin, 289p.

Smithies, RH, Spaggiari, CV, Kirkland, CL, Howard, HM and Maier, WD 2013, Petrogenesis of gabbros of the Mesoproterozoic Fraser Zone: constraints on the tectonic evolution of the Albany–Fraser Orogen: Geological Survey of Western Australia, Record 2013/5, 29p.

Spaggiari, CV, Kirkland, CL, Pawley, MJ, Smithies, RH, Wingate, MTD, Doyle, MG, Blenkinsop, TG, Clark, C, Oorschot, CW, Fox, LJ and Savage, J 2011, The geology of the east Albany–Fraser Orogen — a field guide: Geological Survey of Western Australia, Record 2011/23, 97p.

Spaggiari, CV and Pawley, MJ 2012, Interpreted pre-Mesozoic bedrock geology of the east Albany–Fraser Orogen and southeast Yilgarn Craton (1:500 000), *in* The geology of the east Albany–Fraser Orogen — a field guide *compiled by* CV Spaggiari, CL Kirkland, MJ Pawley: Geological Survey of Western Australia, Record 2011/23, Plates 1 and 1A.

Spaggiari, CV and Brisbout, LI 2014, Interpreted pre-Mesozoic bedrock geology of the east Albany–Fraser Orogen and southeast Yilgarn Craton including seismic line 12GA-AF3 (1:500 000), *in* East Albany–Fraser Orogen seismic and magnetotelluric (MT) workshop 2014: extended abstracts *compiled by* CV Spaggiari and IM Tyler: Geological Survey of Western Australia, Record 2014/6 Plate 2.

Spaggiari, CV, Kirkland, CL, Smithies, RH and Wingate, MTD 2014, Tectonic links between Proterozoic sedimentary cycles, basin formation and magmatism in the Albany–Fraser Orogen, Western Australia: Geological Survey of Western Australia Report, Report 133, 63p.

Tassell, H and Goncharov, A 2006, Geophysical evidence for a deep crustal root beneath the Yilgarn Craton and Albany–Fraser Orogen, *in* Proceedings; Extended abstracts: Geological Society of Australia: Australian Earth Sciences Convention, Newcastle, NSW, 2006, p. 6.

Twiss, RJ and Moores, EM 1992, Structural Geology: Freeman and Company, New York, 532p.

Williams, NC 2009, Mass and magnetic properties for 3D geological and geophysical modelling of the southern Agnew–Wiluna Greenstone Belt and Leinster nickel deposits, Western Australia: Australian Journal of Earth Sciences, v. 56, p. 1111–1142.

Williams, VA and Robertson, W 2011, Final report, Eucla Project E69/2603 for the period 14 May, 2010 to 13 May, 2011; Enterprise Metals Limited: Geological Survey of Western Australia, Statutory mineral exploration report, A90741 (unpublished).

Interpretation of gravity and magnetic data across the Albany–Fraser Orogen

by

RE Murdie, K Gessner, SA Occhipinti, CV Spaggiari, and J Brett

Introduction

Gravity and magnetic data can be used to deduce the distribution of physical properties and infer rock types and structures in areas where the basement geology is obscured by younger basins or regolith cover. Across the Albany–Fraser Orogen the bedrock geology is largely covered by Mesozoic–Cenozoic sedimentary rocks of the Eucla Basin, and by regolith. The Albany–Fraser seismic reflection survey data provide an opportunity to better constrain gravity and magnetic forward models, and the regional interpretation of the potential field data. Here we report the results of gravity and magnetic forward models along the seismic reflection lines 12GA-AF1, 12GA-AF2, 12GA-AF3 and 12GA-T1 (Occhipinti et al., 2014; Spaggiari et al., 2014b). The interpretations highlight variations of geological structure along the boundary between the Yilgarn Craton and the Albany–Fraser Orogen that provide important constraints for tectonic models.

Potential field data

Gravity data

Gravity data from the Australian National Gravity Database (Wynne and Bacchin, 2009) exists at 2.5 – 5 km spacing across most of the region, with pockets of higher data density where specific surveys were commissioned. However, around Esperance gravity measurements are locally spaced at 11 km (Fig. 1). To improve the previously very coarse spaced resolution of measurements in the Esperance area, gravity data were acquired at 2.5 km spacing where a helicopter survey was possible, and 1 km spacing along roads in areas where landing was not feasible. In addition to the 2013 Geological Survey of Western Australia's (GSWA) Esperance gravity survey, data was acquired at 400 m spacing along each seismic line. For the Albany–Fraser seismic survey all newly acquired gravity data were integrated with the existing data, gridded at 0.005 degrees of an arc — approximately 400 m (Fig. 2; GSWA, 2013a), and added to the Australian National Gravity Database. All data is available through the Geophysical Archive Data Delivery System (GADDS; <www.geoscience.gov.au/gadds>).

Magnetic data

The area is covered by Federal and State Government Surveys and Multiclient data of either 400 or 200 m line spacing. Where available, higher density open-file company surveys were used and merged into the Western Australian state grid merge of total magnetic intensity (TMI) data (Fig. 3). The data were gridded with a cell size of 0.0008333 degrees of an arc (~80 m) (GSWA, 2013b). A reduced-to-pole (RTP) transform was applied to the TMI data, and a map encompassing the Albany–Fraser seismic survey area was extracted (Fig. 4).

Geophysical interpretation results

The main features referred to in the following section are shown in the Bouguer anomaly map (Fig. 2) and RTP map (Fig. 4) of the study area, with reference to the interpreted bedrock geology map (Plates 1, 2 and 3). Numbers in brackets refer to tentatively defined areas, domains and structures shown in Figures 2 and 4. Upward continuation of the gravity data to 5, 10 and 20 km, enhance the longer wavelength features (Fig. 5a–c).

Long wavelength gravity features in the Albany–Fraser Orogen

A defining feature of the Albany–Fraser Orogen is a long wavelength gravity pattern that becomes obvious when imaged by upward continuations of the gravity data (Fig. 5a–c). One key element of this long wavelength pattern is the Rason regional gravity low (Fraser and Pettifer, 1980; Shevchenko, 2004), a Bouguer low that is about 100 km-wide across strike, and extends for several hundreds of kilometres along the margin of the Yilgarn Craton, from the area north of line 12GA-AF2, to the area just north of 124°E 29°S (Figs 2 and 5a–c). The Bouguer low along the Yilgarn Craton margin is in stark contrast to the adjacent Bouguer high to the east, which correlates with the Fraser Zone (Spaggiari et al., 2011). Aside from this large amplitude gravity gradient near the Yilgarn

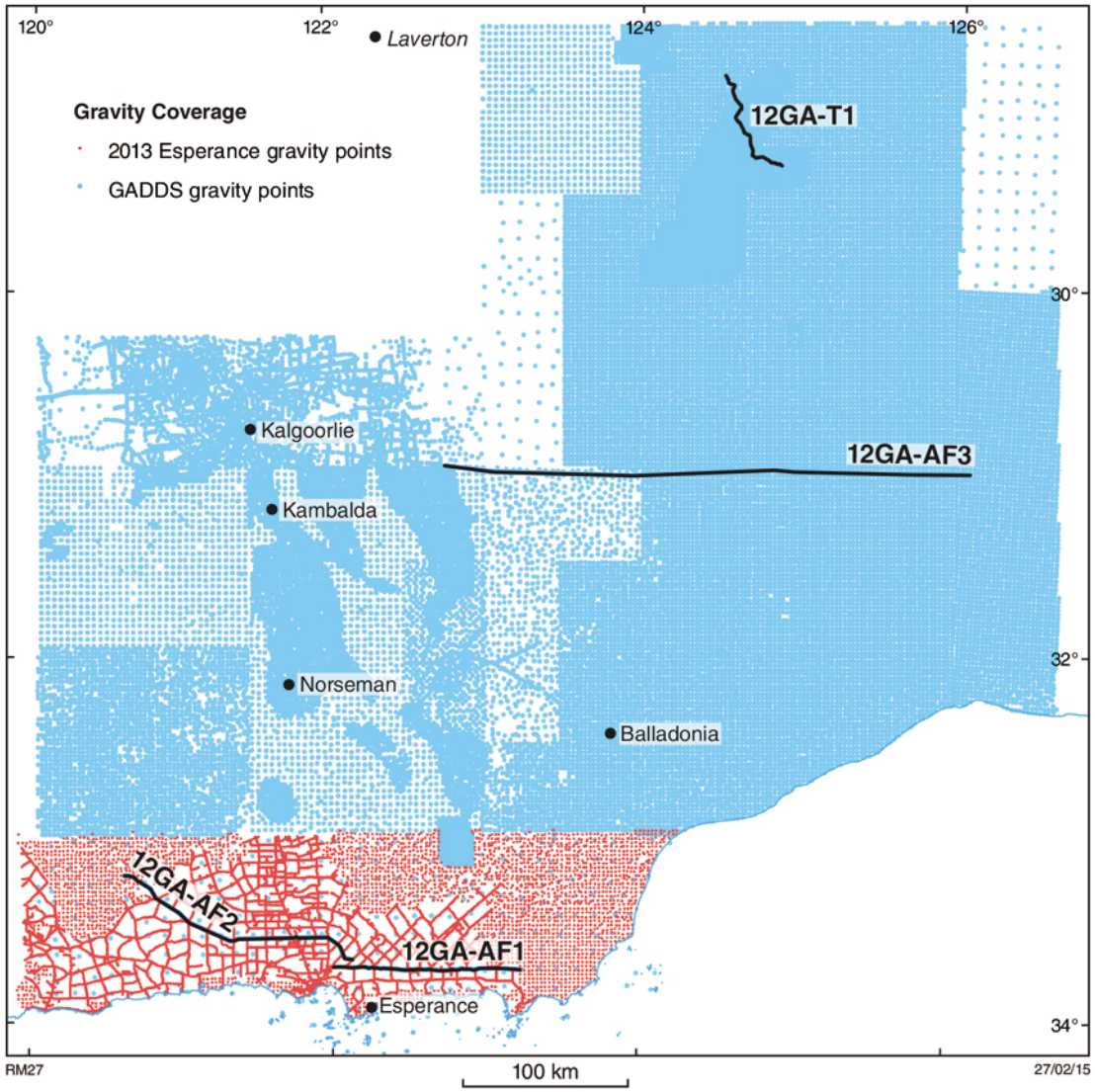

Figure 1. Distribution of the gravity data points from the pre-2013 and syn-2013 surveys

Craton margin, the Albany–Fraser crust shows a generally elevated gravity response compared to the Yilgarn Craton (Figs 2 and 5a–c).

Yilgarn Craton

In the southwestern part of the study area, the Youanmi Terrane of the Yilgarn Craton is dominated by low density and moderately high susceptibility granites (area 1a, Figs 2 and 4), whereas granites further to the east in the Eastern Goldfields Superterrane have much lower susceptibility (area 1b, Fig. 4). The greenstones in both terranes clearly trend to the north-northwest, as seen in the Bouguer and magnetic highs (areas 1a and 1b, Fig. 4). The Binneringie and Jimberlana dykes (areas B and J, Figs 2 and 4) of the c. 2410 Ma Widgiemooltha Dyke Suite (Spaggiari et al., 2011, and references therein) can be identified by their very straight, narrow and consistent trend across the Yilgarn Craton (area 1c, Figs 2 and 4). There are many east to northeast-trending smaller mafic dykes of various suites in the region (Plates, 1, 2 and 3; Spaggiari et al., 2011), which are too thin to be resolved in the gravity data, but are clearly visible in the magnetics. Previously, a transition zone between the Yilgarn Craton and the Albany–Fraser Orogen had been described from where the strong magnetic lineaments of the Yilgarn Craton greenstone belts became attenuated to where the strong northeast magnetic and gravity trends of the Albany–Fraser Orogen commenced (Shevchenko, 2004). This coincides with a wide northeast-trending gravity low, the Rason regional gravity low province (Fraser and Pettifer, 1980). Currently, the boundary of the Yilgarn Craton is marked by the Jerdacuttup Fault and the Cundeelee Shear Zone (Spaggiari et al., 2014b), shown by a marked change in character in the magnetic image, but is not well defined in the gravity image.

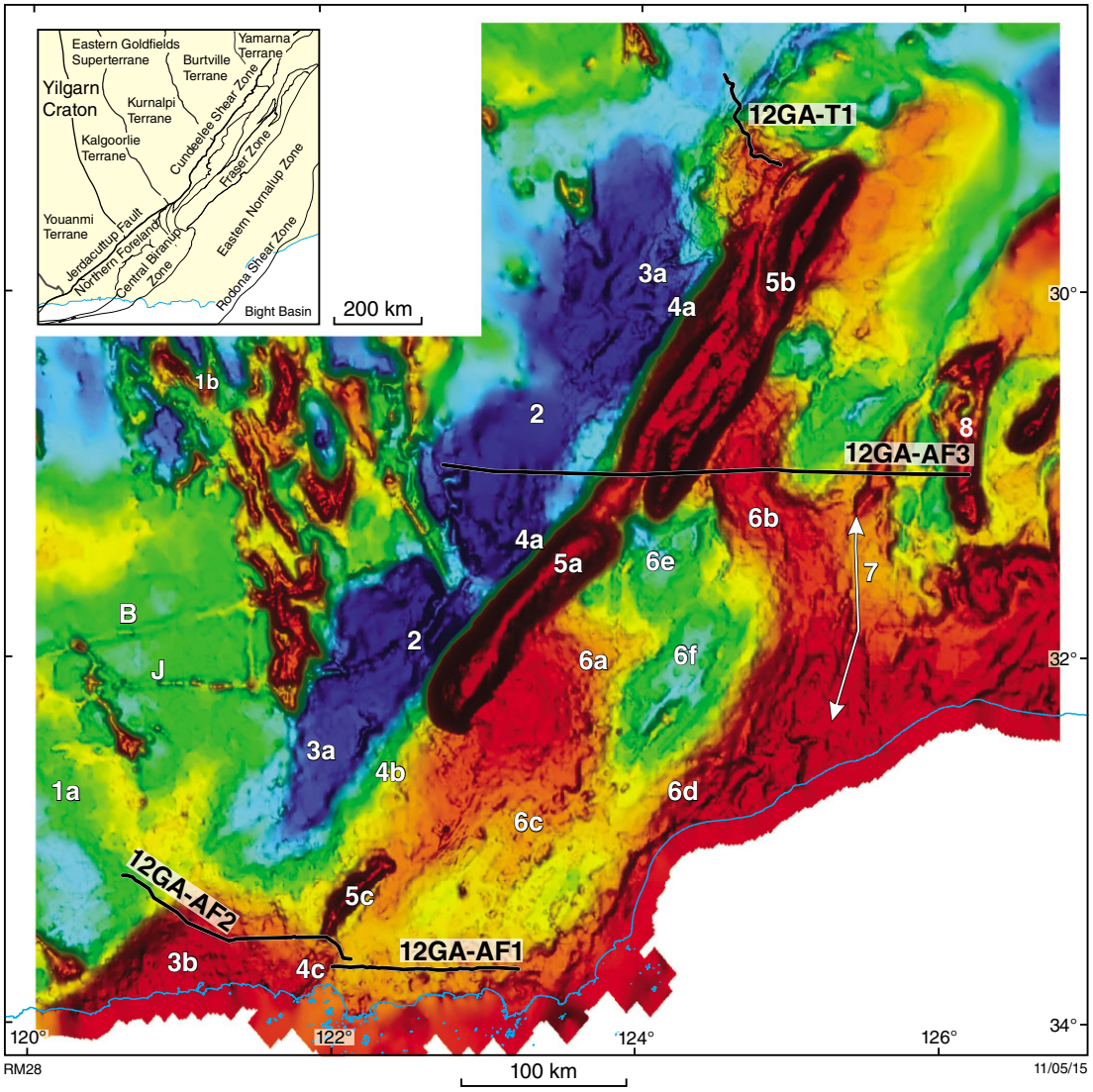

Figure 2. **Bouguer anomaly image of the central and east Albany–Fraser Orogen and adjoining Yilgarn Craton (GSWA, 2013a). Numbers indicate areas referred to in the text.**

Northern Foreland

The Northern Foreland, defined in the sense of Spaggiari et al. (2011) as Yilgarn Craton crust that was reworked during the Albany–Fraser Orogeny, has a relatively weak magnetic signature (area 3a, Fig. 4). Small volumes of magnetic rocks such as granites, parts of greenstone sequences and mafic intrusions, are local exceptions. The Northern Foreland lies within the regional Bouguer gravity low that encompasses the edge of the Yilgarn Craton. To the southwest, the Northern Foreland is dominated by the Munglinup Gneiss (Plate 3), which overall displays a moderate magnetic signature with frequent spots of high intensity and is coincident with a deep-seated gravity high (area 3b, Fig. 2) that may or may not be caused by the same body.

Biranup Zone

The Biranup Zone extends from the Northern Foreland east towards the Fraser Zone and is located on the steep eastern gradient of the regional Bouguer low as it abuts the Fraser Zone (area 4a, Fig. 4). In the southern part of the study area (Plate 3), the Biranup Zone overlies a shallow gravity gradient between the regional Bouguer low to the area of generally higher Bouger anomaly which characterizes the Albany–Fraser crust (area 4b, Fig. 2). Here the Biranup Zone has a moderate magnetic signature with linear magnetic anomalies that bend around the southern tip of the Fraser Zone (Plate 3). The southeastern Biranup Zone (area 4c, Figs 2 and 4) shows a more intense magnetic signature than the rest of the Biranup Zone.

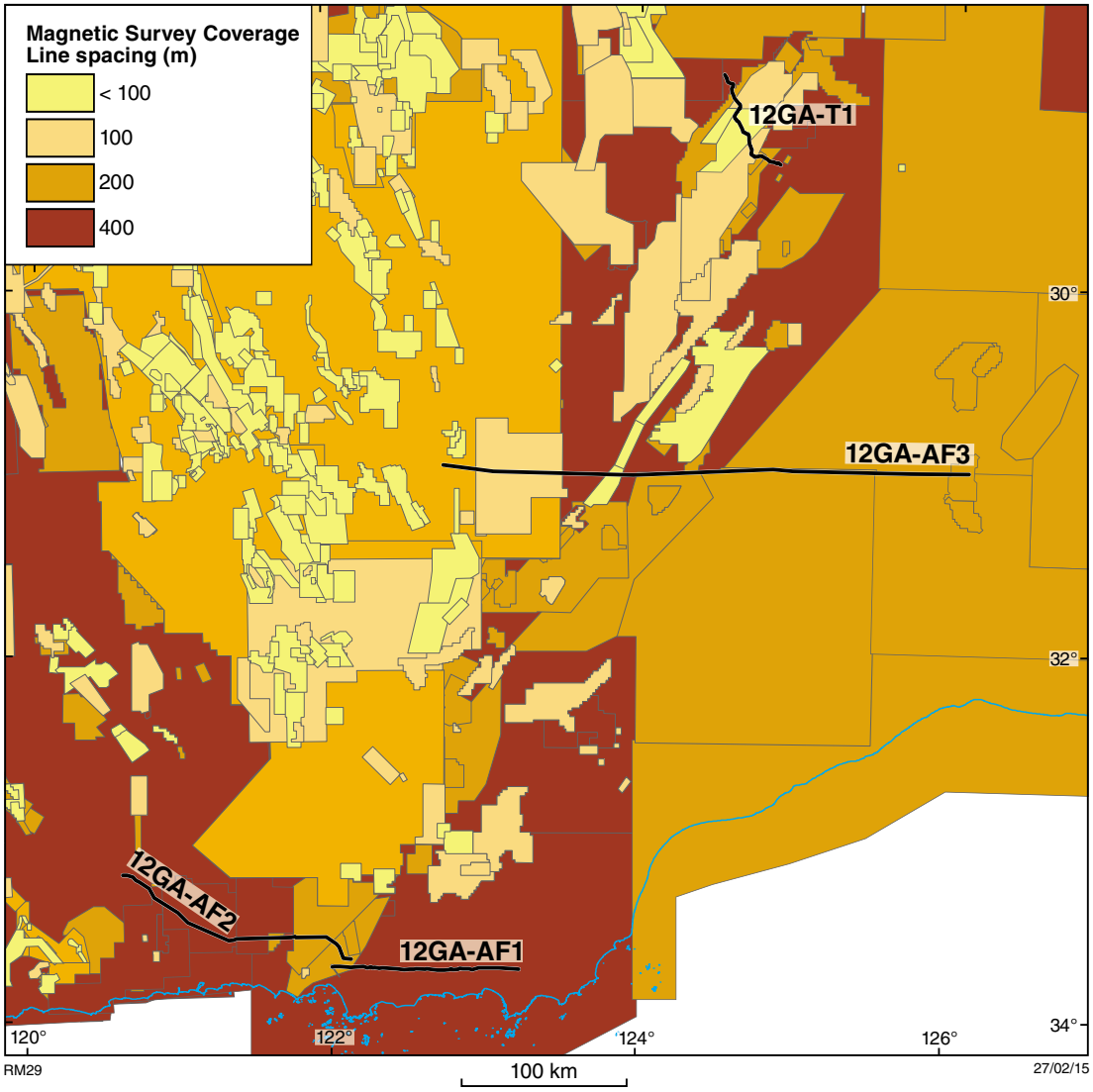

Figure 3. Density of magnetic flight lines over the study area. All data is available through the GSWA data portal.

Fraser Zone

The Fraser Zone has a very distinct Bouguer high with steep gradients (areas 5a and 5b, Fig. 2) and pronounced, thin linear, magnetic anomalies that likely reflect both the layering of dense metagabbroic rocks with metagranitic and metasedimentary rocks, and the strong metamorphic fabric (Spaggiari et al., 2011, 2014b). The different units can be seen as distinct Bouguer highs with different magnetic textures. The magnetic signature of the two central strands is different, with the southerly one extending up the west side of the northern section having a more parallel linear appearance (area 5a, Fig. 4), compared to the linked rounded packages of the central eastern half (area 5b, Fig. 4). In the upwardly continued images, the Bouguer features become merged into a single anomaly. To the south, and just north of the curved eastern end of line 12GA-AF2, an area of strong Bouguer high with steep sides and parallel strong magnetic stripes appears to have signatures similar to the Fraser Zone (area 5c, Figs 2 and 4). It includes c. 1300 Ma granitic rocks of the Recherche Supersuite, as well as c. 1200 Ma granite of the Esperance Supersuite, that are intrusive into the Biranup Zone (Plate 3). Given the geophysical signature, it is also likely to contain a significant component of mafic material. Its depth extent is shallower than the Fraser Zone, as its signal disappears by the upward continuation to 20 km (Fig. 5c).

Nornalup Zone and Recherche and Esperance Supersuites

There are two Bouguer highs with shallower dipping sides and similar textures that correspond with high magnetic intensities. The first is just east of the southeastern end of the Fraser Zone (area 6a, Fig. 4; Brisbout et al., 2014), and the second forms an ‘S’shape that links to the Fraser Zone (area 6b, Fig. 4). The gradients of the gravity

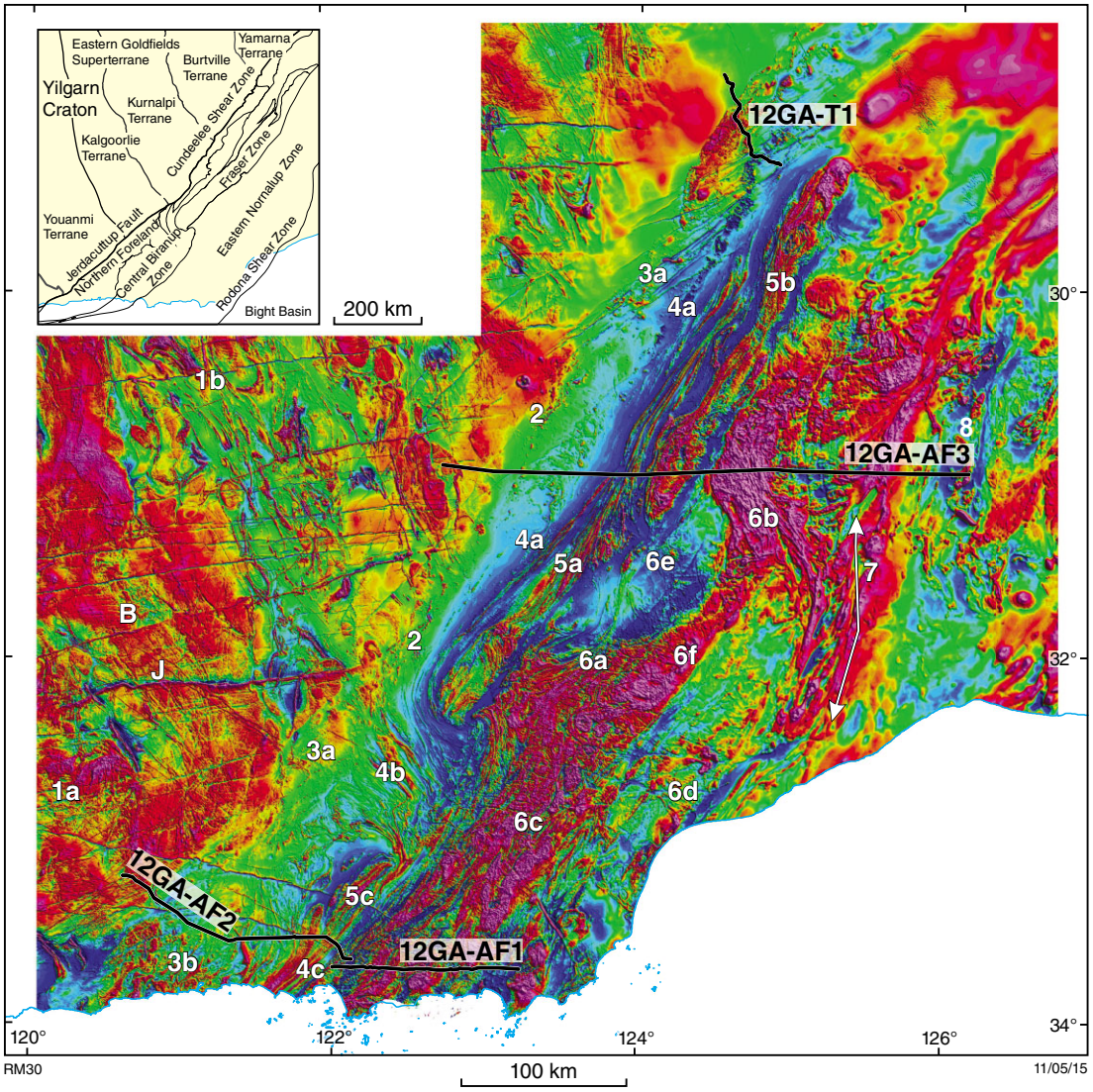

Figure 4. **Reduced-to-pole (RTP) total magnetic intensity (TMI) image of the magnetic surveys over image the central and east Albany–Fraser Orogen and adjoining Yilgarn Craton. Numbers indicate areas referred to in the text**

image would imply deeper causative bodies, but the high magnetic intensities with short wavelengths imply shallow sources. However, both the magnetic and gravity upwardly continued images retain the strength in both signals, suggesting a link between the deep and shallow bodies. Where the Recherche Supersuite is dominant in the Nornalup Zone (Plates 2 and 3), there are several distinct magnetic zones. The bulk of it is highly magnetic and includes mapped intrusions of higher density and very highly magnetic Esperance Supersuite granite (area 6c, Fig. 4; Spaggiari et al., 2014). This contrasts with a relatively moderate magnetic signature to the east, and towards the coast (area 6d, Fig. 4). Alternatively, the whole of the Recherche Supersuite may have a relatively low magnetic signature, and the high signals are due to intrusions of Esperance Supersuite granite. In which case, the Esperance Supersuite granites are substantial. There are two areas of Bouguer low within the Nornalup Zone. One (area 6e, Fig. 4) coincides with a magnetic low and the other (area 6f, Fig. 4) sits on the magnetic high associated with the Recherche and Esperance Supersuites.

Rodona Shear Zone

The Rodona Shear Zone is the boundary between the Albany–Fraser Orogen and the Madura Province (Spaggiari et al., 2011). A distinct north–south linear feature (area 7, Fig. 4) is seen on the western side of this shear zone which is several kilometres wide (Spaggiari et al., 2014b). Strong magnetic features can be seen either side of the shear zone which is interpreted to be dominated by Recherche Supersuite (Spaggiari et al., 2014b).

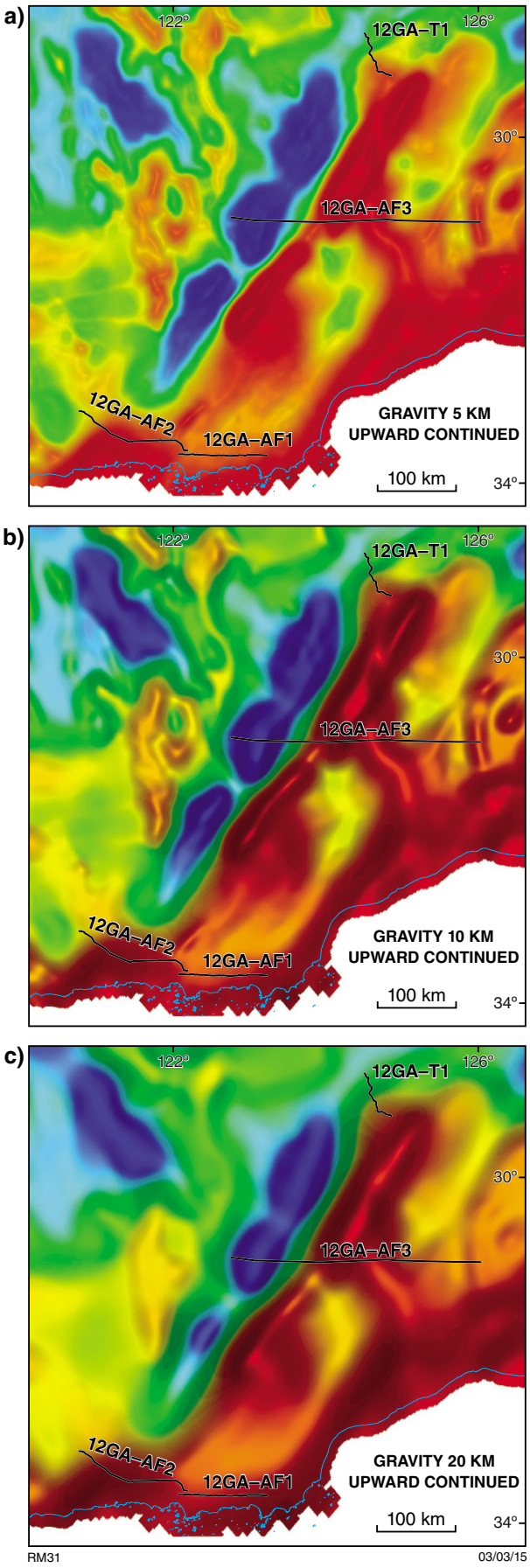

Figure 5. Upward continuation of the Bouguer anomaly data to 5, 10 and 20 km

Haig Cave Supersuite

A strong, steepsided Bouguer high at the eastern end of line 12GA-AF3 has been associated with gabbroic rocks from drillcores from the Loongana, Haig, and Serpent prospects (area 8, Fig. 2; Spaggiari et al., 2014a). It has a corresponding magnetic low signal with local highs, some of which show strong remnant magnetism.

Multiscale edge detection

Multiscale edge detection (Archibald et al., 1999) involves computation of the maximum horizontal gradients of potential field data for many levels of upward continuation. These gradients are initially computed at point locations and form strings of points, referred to as 'worms', for each upward continuation level. Worms of different upward continuation levels are interpreted as discontinuities in physical rock properties, which relate to stratigraphic, intrusive or faulted contact surfaces in the Earth's crust. Archibald et al. (1999) and Holden et al. (2000) proposed that worms derived from higher upward continuation levels can be interpreted as originating from physical property contrasts of greater depth. However, this feature must be treated with caution due to the inherently ambiguous depth information of potential field data. At lower continuation levels, the attitude of the surfaces is more likely to reflect the dip direction of the property contrasts, but not the angle.

Both the gravity and the total magnetic intensity (TMI) data were used to generate worms using the Intrepid multiscale edge detection tool; upward continuation levels were varied by a factor of 1.4 using the Canny method (Canny, 1986).

Gravity worms

The gravity worms outline the major areas of high and low gravity, but also indicate deep features in other areas which as yet have no geological explanation (Fig. 6). The gravity worms detect the junction of the Youanmi terrane and Eastern Goldfields Superterrane (area 1a, Fig. 6) and interior features of the greenstone belts in the Yilgarn Craton (area 1b, Fig. 6). The Binneringie and Jimberlana dykes also have strong worms associated with them (area 2, Fig. 6). The western contact of Fraser Zone against the Biranup Zone produced a very pronounced worm (area 3a, Fig. 6), whereas the worm on its eastern contact with the Nornalup Zone (area 3b, Fig. 6) represents a shallower gradient. On both the western and eastern limits of the Fraser Zone the worms suggest that its contact surfaces are outward dipping, which is inconsistent with the interpreted structure of the Fraser Zone (Spaggiari et al., 2014b). Towards the southwest, the gradient steepens and flips to an inward-dipping contact (area 3c, Fig. 6). A deeper, less-pronounced worm is oriented parallel to the Fraser Zone worm about 80 km to the west, and dips shallowly to the northwest (area 4, Fig. 6). This worm appears to relate to the long wavelength component of gravity increase from the pronounced regional low as seen in the upward continued images (Fig. 5) west of the Fraser Zone towards the eastern Yilgarn Craton.

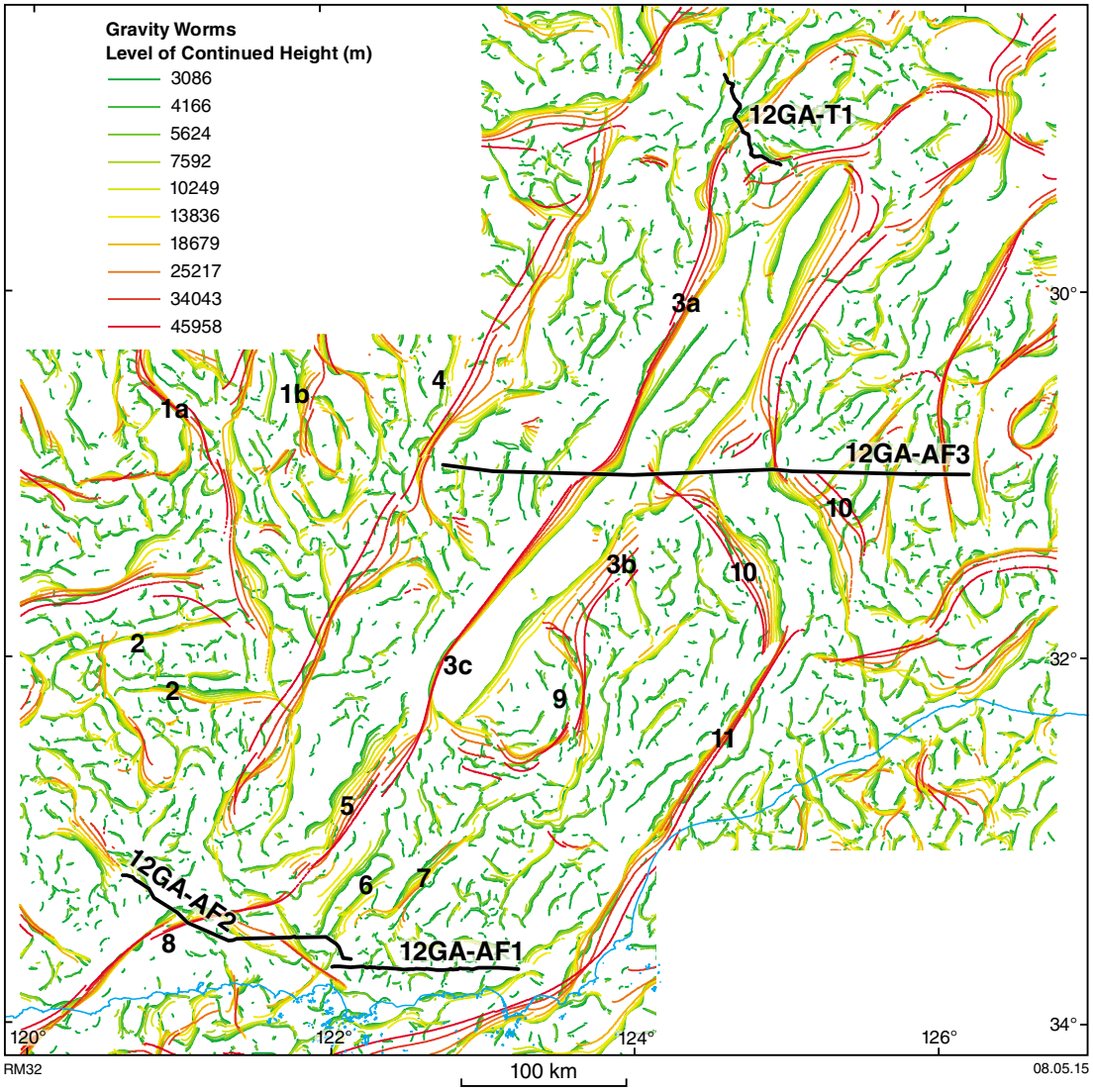

Figure 6. Multiscale edges (worms) of the Bouguer anomaly image

The edge of the Yilgarn Craton is not picked out by a worm at the surface, although the worm in area 4 may be a deeper reflection of the craton margin. The boundary of the Northern Foreland and the Biranup Zone in the south (area 5, Fig. 6) coincides with a moderately steep southeast-dipping worm and area 6 in Figure 6 has coherent local worms around the gravity high of area 5c in Figure 2. The boundary of the Biranup and Nornalup Zones has a shallow east-dipping worm (area 7, Fig. 6). A large Bouguer high in the southern part of the Munglinup Gneiss continues to great depth with a south–eastward dip (area 8, Fig. 6). The Bouguer high at the southeast limit of the Fraser Zone (area 9, Fig. 6) has almost vertical worms which are not quite as deep. The worms of the S-shaped gravity high in the Nornalup Zone dip outwards on either side of the feature (area 10, Fig. 6), indicating a dome-shape upper boundary of the structure. The structure joins with one of the most pronounced worms in the area (area 11, Fig. 6). Oriented parallel to the strike of the Albany–Fraser Orogen, this worm is continuous and deep, but does not relate to any known crustal feature — unfortunately 12GA-AF1 stops just short of this worm. The main questions that arises from the multiscale edge detection is how any of the large features, such as the steep worm associated with the Fraser Zone, or the shallow one dipping under parts of the Yilgarn Craton edge, may relate to a crustal or lithospheric boundary of the Yilgarn Craton with the Albany–Fraser Orogen.

Magnetic worms

The magnetic worms do not generally delineate the same features as the gravity worms (Fig. 7), except in the case of the Yilgarn greenstones (area 1a, Fig. 7) and mafic dykes (area 2, Fig. 7). The edge of the Yilgarn Craton is defined by steeply dipping worms at depth (area 3, Fig. 7) which disappear under the Gunbarrel Basin to the north. The Munglinup Gneiss is associated with a weak, shallowly dipping, but deep worm (area 4, Fig. 7).

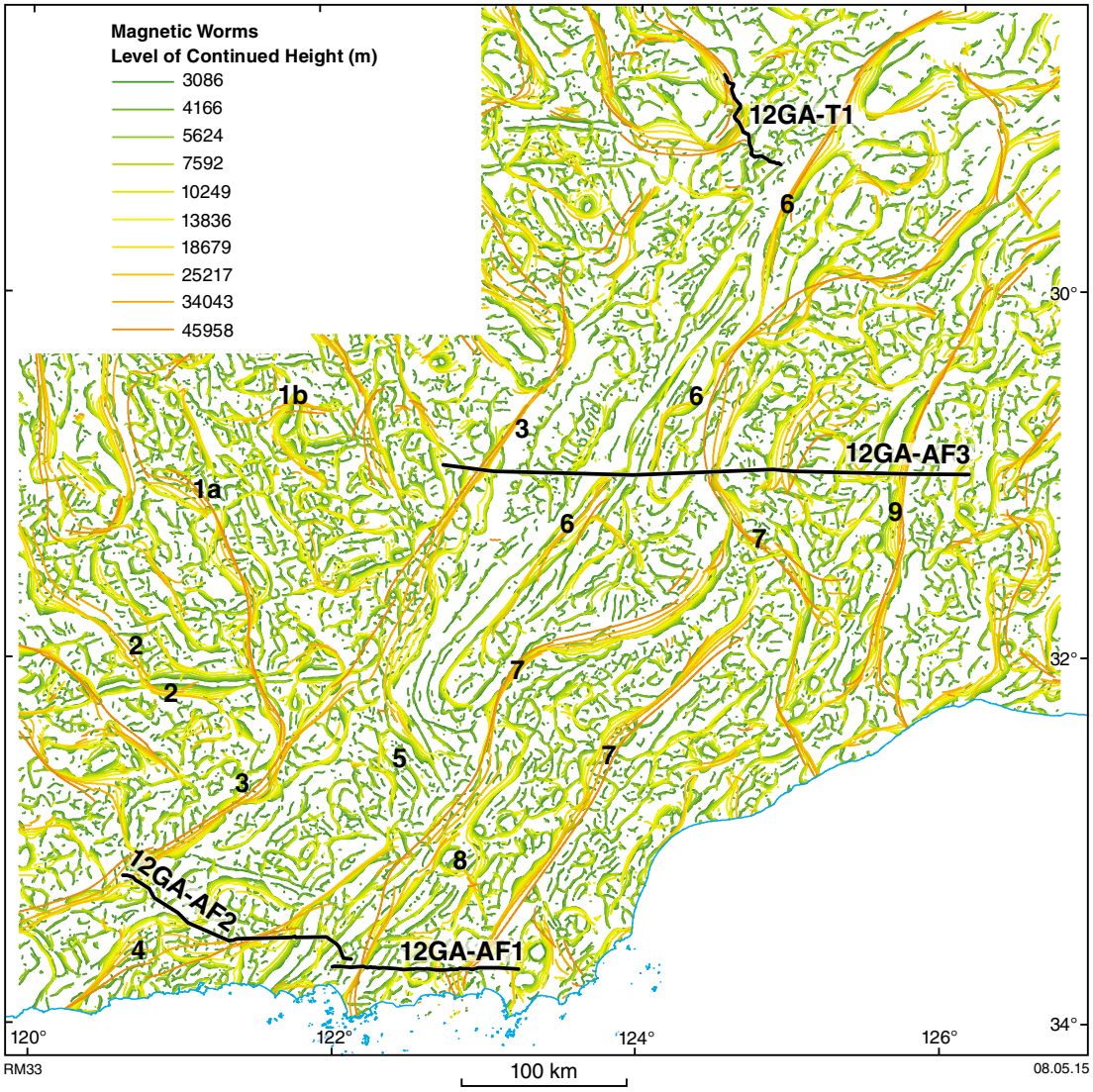

Figure 7. Multiscale edges (worms) of the TMI image

The structures in the Biranup lithologies at the southern end of the Fraser Zone are outlined by worms (area 5, Fig. 7). These worms appear to dip both to the east and west. The edges and internal parts of the Fraser Zone have steeply dipping worms adjacent to them (area 6, Fig. 7). The edges of the strongly magnetized area of the Nornalup Zone have strong steep worms which pick out different features compared to the gravity worms over the same area (area 7, Fig 7). The areas of Esperance Supersuite show as shallow coherent rings within the Nornalup Zone (area 8, Fig.7). The Rodona Shear Zone again has a strong steep worm dipping to the east (area 9, Fig. 7).

Gravity and magnetic forward modelling

Forward calculations of gravity and magnetic anomalies were produced for models derived from the seismic interpretations of Spaggiari et al. (2014b) and compared to the gridded gravity and magnetic data extracted along the seismic lines. Where possible, the architecture of the seismic interpretation was used to obtain a plausible density distribution that fitted with the surface geological mapping and the seismic interpretation. This was possible for the gravity models. However, there is far more detail in the magnetic maps than can be resolved in the seismic data, due to the detection of layering and internal folding within the seismically distinct packages. Hence, it was considered reasonable to split the surface polygons into smaller packages while maintaining the dip of the layers from the known geology, in order to represent the sheeting, interlayering and intrusions mapped at the surface.

Where possible, edge detection data was also used to infer dip directions, but where conflicts arose between the two interpretations, more weight was given to the seismic constraints. Density data was taken from a variety of sources. Actual density and susceptibility measurements of Albany–Fraser Orogen have been conducted by GSWA (Shevchenko, 2000; Brisbout et al., 2014) and from the

Yilgarn by Williams (2009). Values for the Yarraquin Seismic Province are estimates from forward modelling from Gessner et al. (2014). The calculated anomalies were compared to the observed data to infer density and susceptibility values for the rock bodies interpreted in the seismic data and at the surface by geological mapping. The primary objective of this process was to determine where the seismically inferred models correlate with the observed gravity field and where inconsistencies exist. Postulating why these inconsistencies exist can provide a new perspective on the crustal architecture. Models extending from 0 to 50 km depth were created using the GM–SYS tool within Geosoft Oasis Montaj.

Forward modelling of potential field data is inherently non-unique and therefore consistency between seismic interpretations and the observed potential field data represents only the validity of a single interpretation. Further investigation of the model space (including the addition of geological constraints) should be undertaken in order to improve the confidence of these interpretations.

Forward models along individual seismic lines

12GA-AF1

Gravity model

Seismic line 12GA-AF1 (Fig. 8) shows a relatively low amplitude, high frequency gravity response, indicating that there are no major density variations along it. The following numbers indicate areas of interest on the models (Fig. 8). The eastward-dipping Biranup Zone is modelled with a moderately high granitic density of 2730 kg/m^3 (area 1, Fig. 8b). Shevchenko (2000) measured 2740 kg/m^3 from a granitic gneiss from the Garnet Ice Quarry southwest of the Fraser Zone, and Brisbout et al. (2014) split the Biranup Zone into mafic, intermediate, and felsic intrusives, with an average density of 2750 kg/m^3. These are modelled as conforming to the fault-bound seismic package dipping to the east. The Nornalup Zone (area 2a, Fig. 8b) is of similar density to the Biranup Zone, with slightly lower density units at the surface (area 2b, Fig. 8b) and one mid-crustal layer (area 2c, Fig. 8b) implying it is more felsic than the adjacent units. The deepest layers are from the Yarraquin Seismic Province, which has a similar mid-crustal density (area 3a, Fig. 8b). This is underlain by the Gunnadorrah Seismic Province which is the lower crustal component of the Albany–Fraser Orogen. This is modelled with a higher density of 2850 kg/m^3 (area 3b, Fig. 8b; Gessner et al., 2014).

The Recherche Supersuite mostly has a density of about 2700–2720 kg/m^3, (area 4a, Fig. 8b) and has been modelled as east-dipping units with inclusions of more mafic material (higher density), most of which are imaged in the seismic survey (area 4b, Fig. 8b). Three small bodies in the western end of the Recherche Supersuite (area 4c, Fig. 8b) are interpreted as Esperance Supersuite in the seismic line (Plate 4). However, these require a relatively high density of 3000 kg/m^3 to better fit the Bouguer anomaly, with the exception of the westernmost body, which only requires a density of 2730 kg/m^3, implying that these are mafic rather than granitic inclusions. The few available samples of Esperance Supersuite are granitic rocks and have a mean density of 2650 kg/m^3. A non-reflective patch in this area coincides with a Bouguer low (area 4d, Fig. 8b), can be accounted for by modelling a granitic body with a density of 2690 kg/m^3.

A large zone of slightly lower density has been interpreted as intrusions cutting the eastward-dipping layers of Recherche Supersuite dominated crust in the centre of the section (area 4e, Fig. 8b; see Spaggiari et al. [2014b] for explanation). This interpretation is consistent with a modelled density of 2705 kg/m^3 against 2715 kg/m^3 background. Whereas this region is not a major Bouguer low in the gravity map, it could be the edge of a larger low seen to the north in the map (Fig. 2). It contains inclusions of highly reflective areas that could be mafic inclusions (area 4f, Fig. 8b; Spaggiari et al., 2014b). These inclusions are consistent with modelled densities that are slightly higher (2750–2950 kg/m^3).

At the far eastern end of the profile, three more granitic bodies were interpreted in the seismic line. Each of these bodies required a different density to fit the gravity (area 4g, Fig.8b); one of higher density, one lower and one similar to the background as shown by the relative colours on the density scale.

Magnetic model

The magnetic profile along line 12GA-AF1 can be divided in four domains (Fig. 8c). From west to east, these are: i) a large amplitude rising to a peak; ii) a magnetic low with relatively low amplitude anomalies rising towards the east; iii) an area of high susceptibility with strong high-frequency peaks; and iv) a magnetic low with short wavelength low amplitude anomalies. The background level of the magnetic data is controlled by the high susceptibilities in the west and low crustal susceptibilities in the east. However, the detailed, short wavelength features within these regions are best fit by a set of vertical or dipping intrusive bodies of a size smaller than can be resolved by the seismic line interpretation. Modelling of these smaller bodies was attempted with the same dip direction as the Recherche Supersuite and Esperance Supersuite dominated crustal domains interpreted from the seismic reflection survey (Fig. 8c).

In the western part of line 12GA-AF1, the RTP image (Fig. 4) shows thin strips of magnetic response that correspond to a zone of northeasterly trending shears between the Red Island and Heywood–Cheyne Shear Zones (area 5, Fig. 8c). The eastern side of the Heywood–Cheyne Shear Zone correlates to a peak in magnetic response (area 6, Fig. 8c). The inclusions of granite within the Recherche Supersuite appear to have varying susceptibility (area 4f, Fig. 8c). For example, intrusions of Esperance Supersuite are detected because of their generally high magnetic susceptibility. The major granitic intrusion of area 4e in Figure 8b, in the centre of 12GA-AF1, has a low magnetization for the most part but

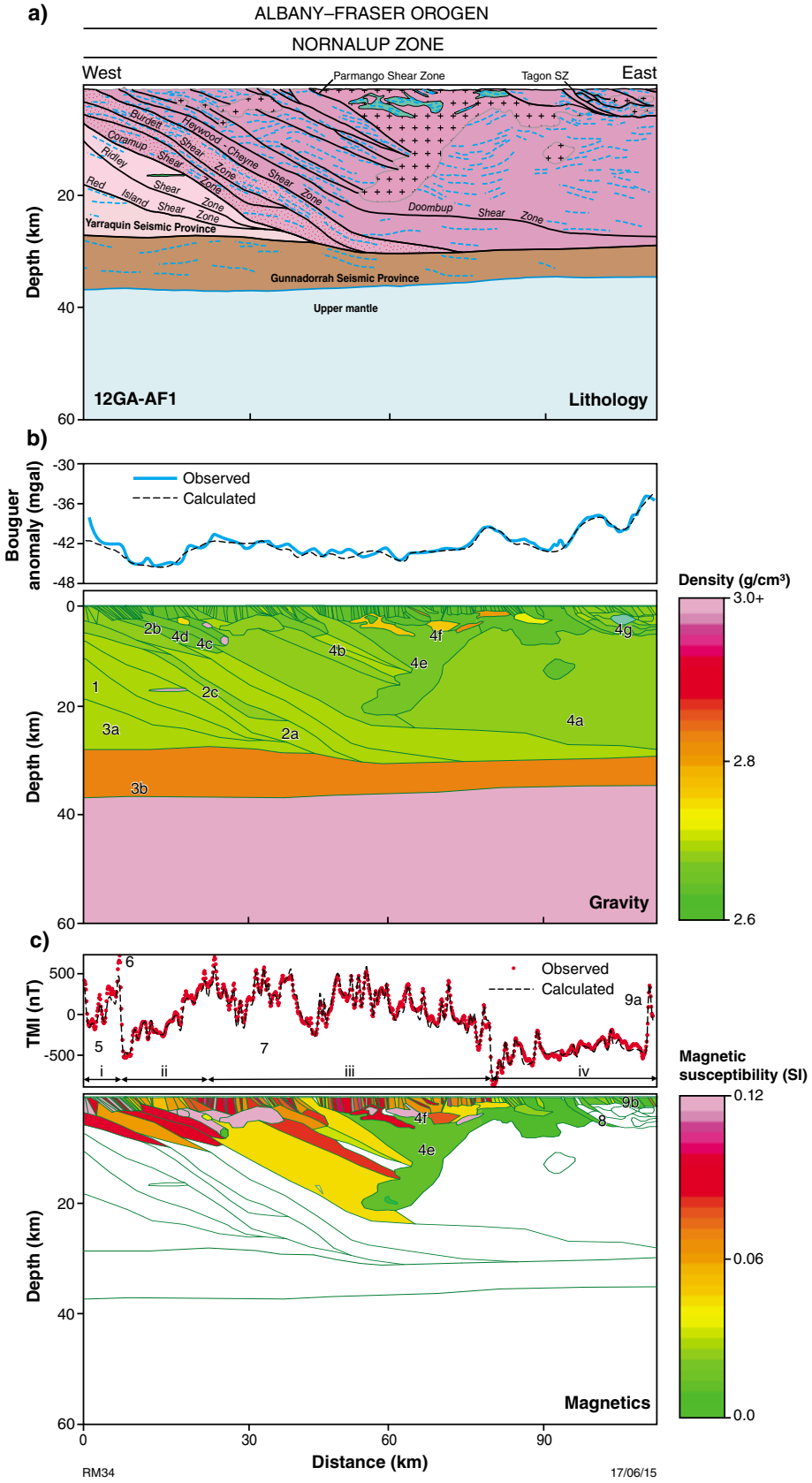

Figure 8. **12GA-AF1 forward model summary figure showing: a) lithology as defined by the seismic interpretation. The key to the units is given in Figure 12; b) observed Bouguer anomaly profile and calculated model response with model of density per lithology; c) observed magnetic susceptibility anomaly profile and calculated model response with model of susceptibility per lithology. Numbers indicate areas referred to in the text.**

appears to be overlain by very high susceptibility material with similar characteristics to Esperance Supersuite. Between domains iii and iv (Fig. 8c) there is a marked change in the magnetic field, with the background level dropping off. This feature can be correlated with the Tagon Shear Zone (Plates 3 and 4). The underlying granite has low susceptibility, accounting for the low background values from here on eastwards (area 8, Fig. 8c). Apart from a single unit at the far east (area 9a, Fig. 8c), all units in this area have low susceptibility, similar to the Recherche Supersuite granitic intrusives (area 9b, Fig. 8c).

12GA-AF2

Gravity model

The overall signature of line 12GA-AF2 is a large broad wavelength high with gentle shoulders, indicating that there is a high-density body at depth. The west of the profile is consistent with the seismic interpretation of a two-layer, Yilgarn Craton architecture with Youanmi Terrane granite–greenstone rocks on top and the Yarraquin Seismic Province below (Spaggiari et al., 2014b). The Youanmi Terrane and Northern Foreland (area 1a, Fig. 9b) has been modelled with a density of 2670–2700 kg/m^3, and the Yarraquin Seismic Province (area 1b, Fig. 9b) with 2730 kg/m^3, consistent with values used in the modelling of the Youanmi seismic lines (Gessner et al., 2014). The lower layer of the Yarraquin Seimic Province (area 1c, Fig. 9b) is thought to only exist at depth in the western portion of 12GA-AF2 and has been modelled with a slightly higher density of 2790 kg/m^3. A comparable high-density lower crustal layer (area 2, Fig. 9b) is present in the eastern part of the line and extends further eastwards into 12GA-AF1. It is proposed that it belongs to the Gunnadorrah Seismic Province (Spaggiari et al., 2014b). The Munglinup Gneiss (area 3, Fig. 9b) has been modelled with similar densities to the Yilgarn Craton units. The Biranup Zone in this line was modelled with densities of similar value to that used for the Biranup Zone in 12GA-AF1, but with the upper layers having a slightly lower density of 2670–2700 kg/m^3 (area 4a, Fig. 9b), and the lower layers having a density of 2730kg/m^3 (area 4b, Fig. 9b). The major feature of line 12GA-AF2 is the broad high which has been attributed to an area of low reflectivity and high density overlying the mantle (area 5, Fig. 9b). The Bouguer anomaly is fitted with a body slightly larger than interpreted from the seismic data. This lower crustal feature is not dissimilar to the inferred crustal root imaged further west along the margin of the Yilgarn Craton and Albany–Fraser Orogen (Tassell and Goncharov, 2006). The short wavelength strong feature at the eastern end can be modelled by a shallow unit of high density (area 6, Fig. 9b).

Magnetic model

The magnetic model for 12GA-AF2 was generated using only faults and form lines. As the form lines break the fault-bounded blocks into horizontal or shallowly dipping units, the model does not provide as good a short wavelength fit as the magnetic model of 12GA-AF1. However, the long-to-middle wavelength features fit the gross structure reasonably well. Most of the upper crust has a low susceptibility. The Youanmi Terrane (area 7a, Fig. 9c) has a moderately higher susceptibility than the Northern Foreland (area 7b, Fig. 9c). There is a magnetic spike (marked as area 8, Fig. 9c) that we interpreted as a thin slice of ultramafic greenstone near the surface, but since it is not visible in the seismic line it is not modelled it here. The Munglinup Gneiss in the model is an area of fairly uniform low-to-moderate susceptibility (area 9a, Fig. 9c) with a mafic dyke (area 9b, Fig. 9c) indicated by a small double peak. The Biranup Zone appears to have a high susceptibility (area 10a, Fig. 9c) with another mafic dyke producing a negative peak (area 10b, Fig. 9c). The central part of the Biranup Zone in 12GA-AF2 (area 11, Fig. 9c) has a moderate magnetic signature, whereas the southeastern part of the Biranup Zone drops off in susceptibility (area 12, Fig. 9c). The highly detailed folded and linear features seen in the central Biranup Zone in map view (cf. between areas 4b and 5c in Fig. 4) do not correlate well with the polygons from the seismic interpretation. The seismic imaging is not detailed enough to pick out the individual layers as seen in the RTP image, but these smaller layers are required to match the magnetic forward model.

12GA-AF3

Gravity model

The Yilgarn Craton is modelled as a two-layered architecture with low-density granites (2620 kg/m^3) of the Kurnalpi Terrane (area 1a, in Fig. 10) above the Udarra Seismic Province (Korsch et al., 2014) with average crustal densities that increase with depth to a density of 2750 kg/m^3 (area 1b, Fig. 10b), slightly less than the lower crust of 12GA-AF1 and 12GA-AF2. The low-reflective lower crustal zone (area 2, Fig. 10b) within the Udarra Seismic Province appears to have a relatively high density and has been modelled with a density of 2850 kg/m^3. The Gunnadorrah Seismic Province that constitutes the lower crust of Albany–Fraser Orogen (area 3, Fig. 10b) was modelled with a high density to account for the higher Bouguer gravity levels in the eastern half of the profile (cf. Fig 2). The Northern Foreland (area 4, Fig. 10b) has an average granitic density, whereas the Biranup Zone has a mixture of elevated (area 5a, Fig. 10b) and very high (e.g. parts of the Eddy Suite; area 5b, Fig. 10b) densities.

The Fraser Zone constitutes the biggest gravity feature of this line (area 6 in Fig. 10b) and forms two peaks with the highest density of 3230 kg/m^3 modelled at shallow depth. Brisbout et al. (2014) propose a mafic component of Fraser Zone rocks with an average density of 3027 kg/m^3 and Shevchenko (2000) measured mafic granulite samples of 2970 km/m^3, that is consistent with the surrounding polygons. East of the Fraser Zone an area of low reflectivity is interpreted as a granite with entrained mafic and ultramafic lithologies. This granite is modelled with a higher than average granite density of 2730 kg/m^3 (area 7a, Fig. 10b) with higher density inclusions at 3000 kg/m^3 (area 7b, Fig. 10b).

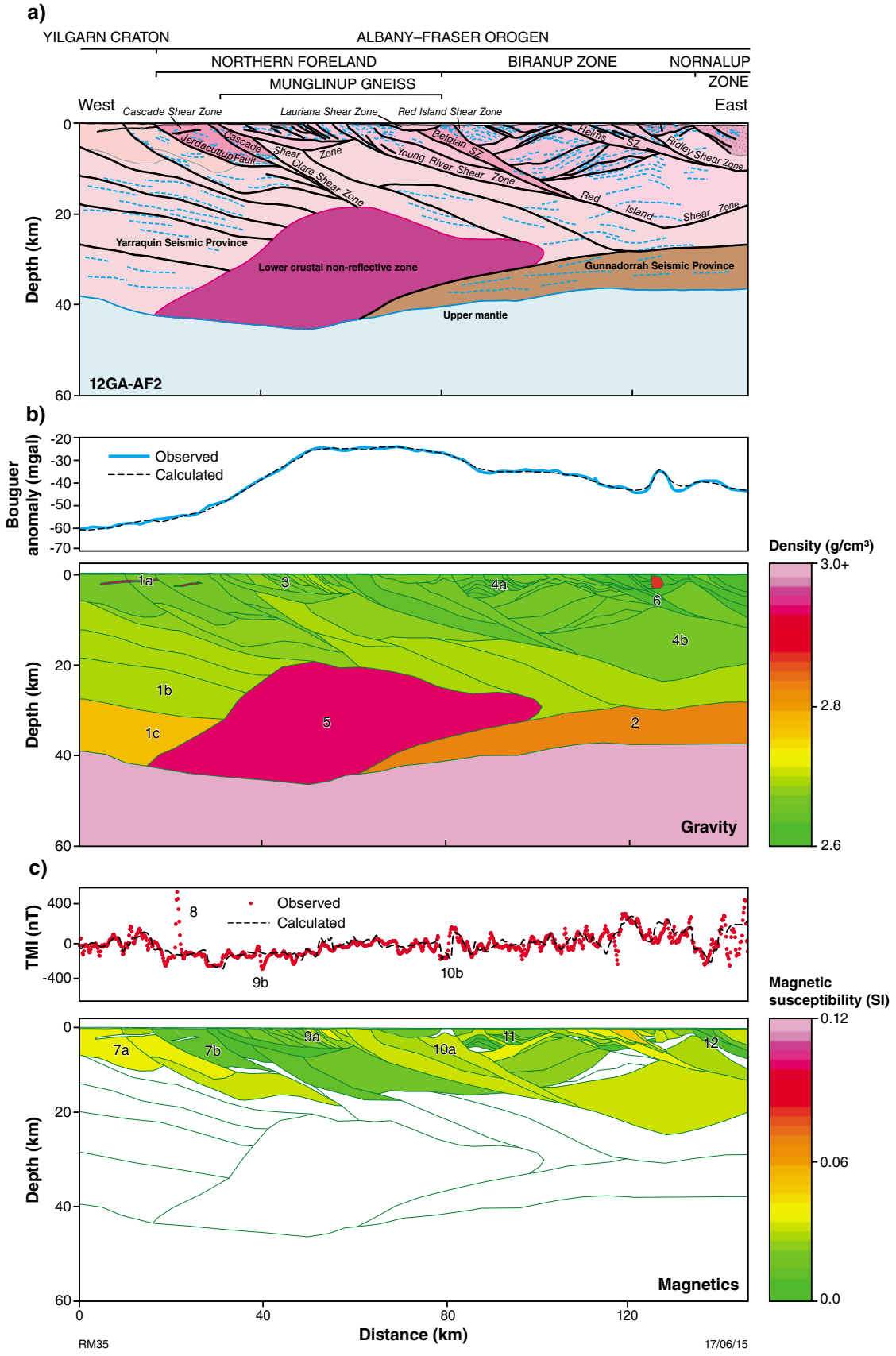

Figure 9. **12GA-AF2 forward model summary figure showing: a) lithology as defined by the seismic interpretation. The key to the units is given in Figure 12; b) observed Bouguer anomaly profile and calculated model response with model of density per lithology; c) observed magnetic susceptibility anomaly profile and calculated model response with model of susceptibility per lithology. Numbers indicate areas referred to in the text.**

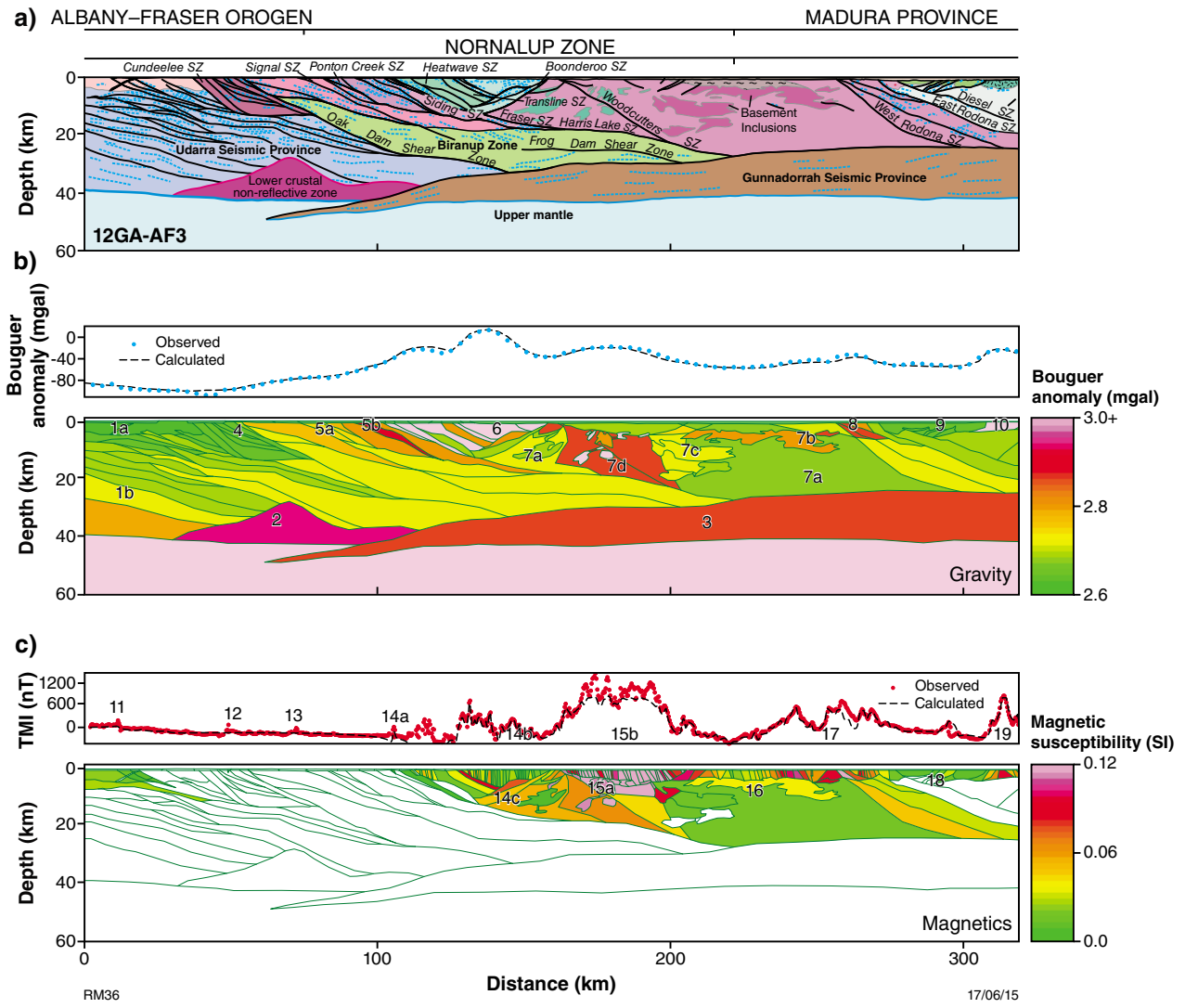

Figure 10. 12GA-AF3 forward model summary figure showing: a) lithology as defined by the seismic interpretation. The key to the units is given in Figure 12; b) observed Bouguer anomaly profile and calculated model response with model of density per lithology; c) observed magnetic susceptibility anomaly profile and calculated model response with model of susceptibility per lithology. Numbers indicate areas referred to in the text.

The central inclusions (area 7c, Fig. 10b) only require a density of 2700 kg/m^3, indicating that perhaps these are more sedimentary or granitic in origin. The third large Bouguer high in this area is unaccounted for in the seismic interpretation of the line and surface geology, but requires a large area of higher density at shallow- to mid-crustal levels (area 7d, Fig. 10b). The origin of this body is unexplained but would probably require a higher percentage of mafic material to be present. Further to the east, a small Bouguer high with a low dimple in it corresponds to the Rodona Shear Zone (area 8, Fig. 10b). The Bouguer low at the eastern end of 12GA-AF3 (area 9, Fig. 10b) is modelled by an upper crustal layer of low-density rocks of the Madura Province. The most easterly Bouguer peak (area 10, Fig. 10b) is modelled as a high-density polygon of 3000 kg/m^3 consistent with gabbroic rocks of the Haig Cave Supersuite recovered from drillcore (Plate 2). The shape of the high-density body is not well defined by the seismic data as it is located near the edge of the seismic line.

Magnetic models

The magnetic data is best fitted by modelling the upper and middle crust as sheeted intrusions. The Kurnalpi Terrane of the Yilgarn Craton in the west of 12GA-AF3 has a low magnetization, with the exception of a spike (area 11, Fig. 10c) associated with a narrow, west-dipping greenstone fragment. In 12GA-AF3 the Northern Foreland is magnetically quiet apart from a spike at area 12 (Fig. 10c) that is part of a series of high magnetic spots strung out in a northerly trend within the Northern Foreland (Fig. 4). The Biranup Zone shows a folded magnetic texture with bands of moderately magnetized

material in map view (Fig. 4), which show as small peaks within a quiet background in section view (area 13, Fig.10c). The first major magnetic peak to the east relates to a paragneiss unit (the Snowys Dam Formation) in the western part of the Fraser Zone (area 14a, Fig. 10c). Whereas this paragneiss unit is detectable in the magnetic field, it is too narrow to be imaged in the seismic reflection profile. The rest of the Fraser Zone (area 14b, Fig. 10c) is characterized by short-wavelength large-amplitude anomalies, which requires that the units as interpreted from the seismic image, are split into smaller units, and/or that the structure is more complex than can be imaged seismically. The Fraser Zone appears to be underlain by units with high magnetic susceptibility (area 14c, Fig 10c) to account for the background long wavelength base to the signal, but the surface units mainly have low-to-moderate susceptibility.

The strong short wavelength magnetic features coincident with the eastern gravity high in 12GA-AF3 (near area 7d, Fig. 10b) require a deep-seated anomaly (area 15a, Fig. 10c). This can be modelled as various granitic bodies at depth with strong susceptibility. The individual peaks cannot be resolved without invoking some extreme susceptibilities in shallow bodies (area 15, Fig. 10c). Granites further to the east define a moderate susceptibility zone (area 16, Fig. 10c) that includes basement rafts with moderate susceptibility. Further east again an area of strong susceptibility coincides with a region near the Rodona Shear Zone (area 17, Fig. 10c) where the seismic reflectors strengthen (Plate 2). Towards the eastern end of 12GA-AF3 the magnetic signal reduces to lower levels with minor variations that can be modelled based on the seismic interpretation polygons (area 18, Fig. 10c), before increasing drastically due to the gabbro of the Haig Cave Supersuite (area 19, Fig. 10c).

12GA-T1

Gravity model

The dominant gravity feature along line 12GA-T1 is a rise in Bouguer gravity from west to east (Fig. 11). The Bouguer gravity of the Tropicana Zone (area 1, Fig. 11b), the reworked Yamarna Terrane (area 2, Fig. 11b) and the Biranup Zone (area 3, Fig. 11b) is consistent with average crustal densities. The underlying Babool Seismic Province, the middle to lower crust of the Yamarna Terrane, (Korsch et al., 2014) is slightly denser (area 4a, Fig. 11b), with denser basal layers (area 4b, Fig. 11b) similar to the Yarraquin Seismic Province as seen in 12GA-AF2 and 12GA-AF3, and in the Youanmi Survey lines (Gessner et al., 2014). The major feature interpreted from the seismic data, is the presence of the Gunnadorrah Seismic Province (Korsch et al., 2014), which dips to the west and offsets the Moho. The Gunnadorrah Seismic Province has been assigned similar densities to those given to the Gunnadorrah Seismic Province in 12GA-AF3. However, unlike in 12GA-AF3, where the body had a uniform density across the whole depth range, the Gunnadorrah Seismic Province had to be split along form lines of the seismic interpretation to avoid too high a gravity signal at the eastern end of 12GA-T1 (area 5, Fig. 11b). The Gunnadorrah Seismic Province is now modelled as a layered body of upward decreasing density so that at mid-crustal levels it has similar densities to the Babool Seismic Province at the same depth.

At the surface, several short wavelength features can be explained by low-density bodies, such as the Bobbie Point Metasyenogranite (area 6, Fig. 11b) and another, even lower density body just to the east (area 7, Fig. 11b). The Salt Creek Gabbro (area 8, Fig. 11b) is interpreted as a series of gabbroic to ultramafic intrusives coincident with remnant magnetism (Occhipinti et al., 2014), but is not visible in the gravity profile. On the Bouguer map, it sits on a step in the gravity. High reflectivity areas in the seismic data have been interpreted as belonging to the Tropicana Zone high-density unit (Occhipinti et al., 2014; Plate 4). In the centre of the section, these units have a high density (area 9a, Fig. 11b), whereas at the eastern end of 12GA-T1, a large body of this high-density unit only requires an average granitic density to fit the gravity profile (area 9b, Fig. 11b).

Magnetic model

The western end of the magnetic model has a very smooth signal due to the non-magnetic, largely glacigene sedimentary cover of the Gunbarrel Basin on top of the Yamarna Terrane (area 10, Fig. 11c). Individual bands of highly susceptible material in the Tropicana Zone cause the short wavelength peaks (area 11, Fig. 11c). The pronounced magnetic low (area 12, Fig. 11c) relates to the Salt Creek Gabbro, which is interpreted to be remanently magnetized (Occhipinti et al., 2014). The Salt Creek Gabbro can be defined as the magnetic low anomalies that are strung-out on the RTP image trending northeast across the southern end of 12GA-T1 (Fig. 4). However, the magnetic modelling suggests that the Salt Creek Gabbro is confined to only one body, rather than two as interpreted from the seismic images.

Conclusions

High-resolution gravity and magnetic grids have been studied on a regional scale for insights into the geology of the Albany–Fraser Orogen which, in many areas, is covered by recent sediments and Cretaceous to Cenozoic basins. The main features in both potential fields are associated with the high-grade metamorphic Fraser Zone rocks which are aligned parallel to the trend of the Albany–Fraser Orogen. Within the Northern Foreland, Biranup and Nornalup Zones there are also very strong features but there, the main fabrics are not always parallel to the orogen. From the modelling they are inferred to have a deep-seated origin which may link to more shallow bodies, but as yet these features cannot be linked to surface geology.

A major feature is the Rason regional gravity low, which encompasses many geological bodies, and is oriented parallel to the boundary between Yilgarn Craton and the Albany–Fraser Orogen. Shevchenko (2004) suggested regional thickening of the crust during the Albany–Fraser

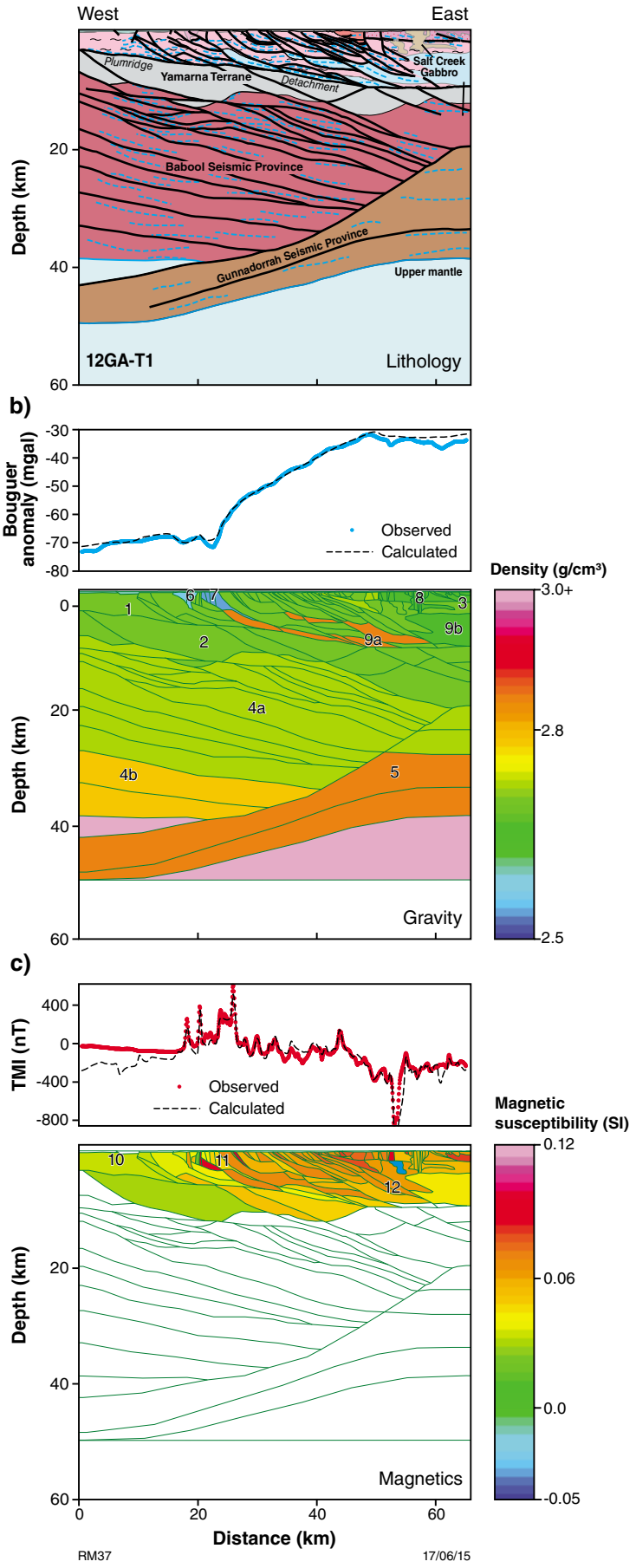

Figure 11. **12GA-T1 forward model summary figure showing: a) lithology as defined by the seismic interpretation. The key to the units is given in Figure 12; b) observed Bouguer anomaly profile and calculated model response with model of density per lithology; c) observed magnetic susceptibility anomaly profile and calculated model response with model of susceptibility per lithology. Numbers indicate areas referred to in the text.**

Orogeny as a likely explanation for this feature. However, the western part of 12GA-AF3 images typical Yilgarn east-dipping component of lower crust fabrics, with no major apparent change in the thickness of the lithospheric layers. If, therefore the reason for the Rason regional gravity low is a variation of crustal rather than mantle density, the feature is more likely due to a change in composition, e.g. where a stack of mid-crustal material has replaced denser, lower crust.

Potential field forward modelling in 2D of the profiles along the seismic lines tested the feasibility of the bodies generated by the seismic interpretation. Using densities that were in line with hand specimens or other models, gravity models were generated from the geometries defined by the seismic interpretation which fitted the observed gravity with only slight adjustments to the seismic interpretation. The models show that the areas of non-reflective lower crust are bodies of anomalously high density. Other areas of high density were required in 12GA-AF3 to explain the most easterly major peak in the gravity profile. Local anomalies helped clarify the nature of the inclusions within the less reflective areas as having a greater or lesser mafic or ultramafic content.

The magnetic data is of much higher resolution and the detail in the observed data is much greater than could be imaged on the seismic profiles. Hence, for lines 12GA-AF1, 12GA-AF3 and 12GA-T1, the bodies from the seismic interpretation were split into subparallel bodies to reflect the folding, layering and sheeting of the rock units. Line 12GA-AF2 was more magnetically quiet and so the bodies were not split. However, this led to a model with greater errors than in the other lines. All magnetism is assumed to be induced. Better models would be achieved if the remanent magnetism was taken into account.

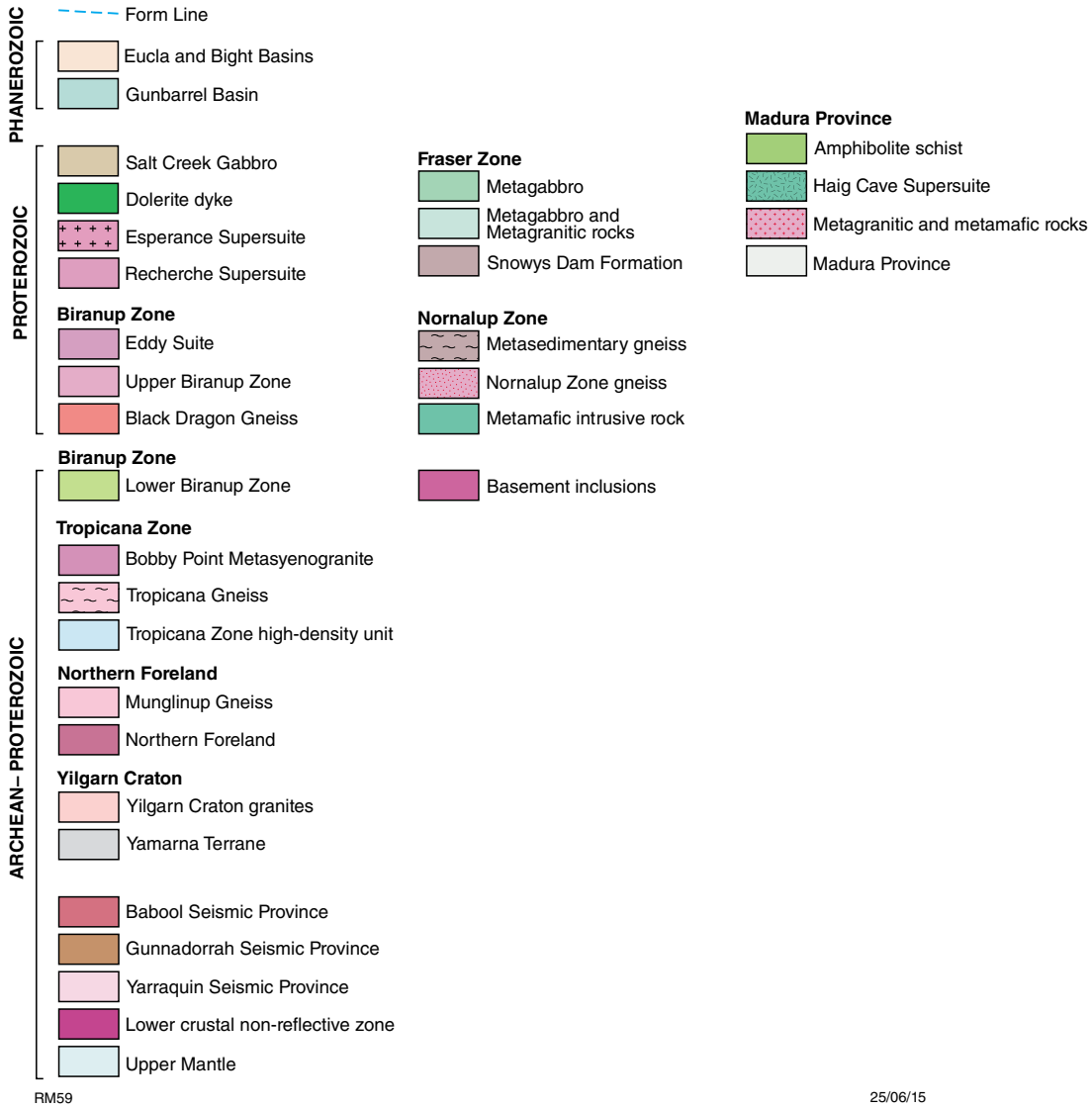

Figure 12. Legend for the units shown in the lithological sections in Figures 8, 9, 10 and 11

Individually the forward models give an insight into the density and susceptibility distribution of the orogen. However, the relationship between these anomalous areas of high density and magnetic intensity, and the regional significance of the orogen-parallel Bouguer low would benefit from a 3D modelling approach.

References

Archibald, NJ, Gow, L and Boschetti, F 1999, Multiscale edge analysis of potential field data: Exploration Geophysics, v. 30, p. 38–44.

Brisbout, LI, Spaggiari, CV and Aitken, ARA 2014, Integrating outcrop, aeromagnetic and gravity data: models of the east Albany–Fraser Orogen, *in* Albany–Fraser Orogen seismic and magnetotelluric (MT) workshop 2014: extended abstracts *compiled by* CV Spaggiari and IM Tyler: Geological Survey of Western Australia, Record 2014/6, p. 102–117.

Canny, J 1986, A computational approach to edge detection: IEEE Transactions on Pattern Analysis and Machine Intelligence, v. 8, p. 679–698.

Fraser, AR and Pettifer, GR 1980, Reconnaissance gravity surveys in WA and SA, 1969–1972: Australian Bureau of Mineral Resources, Geology and Geophysics Bulletin 196, 60p.

Geological Survey of Western Australia 2013a, Gravity anomaly grid (400m) of Western Australia (2013 – version 2), 11 November 2013 update: Geological Survey of Western Australia, digital data layer.

Geological Survey of Western Australia 2013b, Magnetic anomaly grid (80 m) of Western Australia (2013 – version 2): Geological Survey of Western Australia, digital data layer.

Gessner, K, Goodwin, JA, Gallardo, LA, Milligan, PR, Brett, J and Murdie, RE 2014, Interpretation of magnetic and gravity data across the Southern Carnarvon Basin, and the Narryer and Youanmi terranes in Western Australia: multiscale edge detection (worms), forward modelling, and cross-gradient joint inversion, *in* Youanmi and Southern Carnarvon seismic and magnetotelluric (MT) workshop 2013: extended abstracts *compiled by* TJ Ivanic, S Wyche and I Zibra: Geological Survey of Western Australia, Record 2013/6, p. 61–74.

Holden, DJ, Archibald, NJ, Boschetti, F and Jessell, MW 2000, Inferring geological structures using wavelet-based multiscale edge analysis and forward models: Exploration Geophysics, v. 31, p. 617–621.

Korsch, RJ, Spaggiari, CV, Occhipinti, SA, Doublier, MP, Clark, DJ, Dentith, MC, Doyle, MG, Kennet, BLN, Gessner, K, Neumann, NL, Belousova, EA, Tyler, IM, Costelloe, RD, Fomin, T and Holzschuh, J 2014, Geodynamic implications of the 2012 Albany–Fraser deep seismic reflection survey: a transect from the Yilgarn Craton across the Albany–Fraser Orogen to the Madura Province, *in* Albany–Fraser Orogen seismic and magnetotelluric (MT) workshop 2014: extended abstracts *compiled by* CV Spaggiari and IM Tyler: Geological Survey of Western Australia, Record 2014/6, p. 142–173.

Occhipinti, SA, Doyle, MG, Spaggiari, CV, Korsch, RJ, Cant, G, Martin, K, Kirkland, CL, Savage, J, Less, T, Bergin, L and Fox, L 2014, Interpretation of the deep seismic reflection line 12GA-T1: northeastern Albany–Fraser Orogen, *in* Albany–Fraser Orogen seismic and magnetotelluric (MT) workshop 2014: extended abstracts *compiled by* CV Spaggiari and IM Tyler: Geological Survey of Western Australia, Record 2014/6, p. 52–68.

Shevchenko, SI 2000, Gravity data — Fraser Range region, Western Australia: Geological Survey of Western Australia, Record 2000/15, 25p.

Shevchenko, SI 2004, Application of potential field data in the Officer Basin area, *in* The 2001 northeastern Yilgarn deep seismic reflection survey *compiled by* BR Goleby, RS Blewett, PB Groenewald, KF Cassidy, DC Champion, LEA Jones, RJ Korsch, S Shevchenko and SN Apak: Geoscience Australia, Record 2003/28, p. 49–58.

Spaggiari, CV, Kirkland, CL, Pawley, MJ, Smithies, RH, Wingate, MTD, Doyle, MG, Blenkinsop, TG, Clark, C, Oorschot, CW, Fox, LJ and Savage, J 2011, The geology of the east Albany–Fraser Orogen — a field guide: Geological Survey of Western Australia, Record 2011/23, 97p.

Spaggiari, CV, Kirkland, CL, Smithies, RH and Wingate, MTD 2014a, Tectonic links between Proterozoic sedimentary cycles, basin formation and magmatism in the Albany–Fraser Orogen, Western Australia: Geological Survey of Western Australia, Report 133, 63p.

Spaggiari, CV, Occhipinti, SA, Korsch, RJ, Doublier, MP, Clark, DJ, Dentith, MC, Gessner, K, Doyle, MG, Tyler, IM, Kennet, BLN, Costelloe, RD, Fomin, T and Holzschuh, J 2014b, Interpretation of Albany–Fraser seismic lines 12GA-AF1, 12GA-AF2 and 12GA-AF3: implications for crustal architecture, *in* Albany–Fraser Orogen seismic and magnetotelluric (MT) workshop 2014: extended abstracts *compiled by* CV Spaggiari and IM Tyler: Geological Survey of Western Australia, Record 2014/6, p. 28–51.

Tassell, H and Goncharov, A 2006, Geophysical evidence for a deep crustal root beneath the Yilgarn Craton and Albany–Fraser Orogen, Western Australia, in Conference abstracts: Geological Society of Australia; Australian Earth Sciences Convention 2006, Melbourne, Victoria, 2 July 2006, 6p.

Williams, NC 2009, Mass and magnetic properties for 3D geological and geophysical modelling of the southern Agnew-Wiluna greenstone belt and Leinster nickel deposits, Western Australia: Australian Journal of Earth Sciences, v. 56, no. 8, p. 1111–1142.

Wynne, P and Bacchin, M (compilers) 2009, Index of gravity surveys (2nd edition): Geoscience Australia, Record 2009/07.

The nature of the lithosphere in the vicinity of the Albany–Fraser reflection seismic lines

by

BLN Kennett[1]

Introduction

The recent and ongoing program of reflection profiling in western and central Australia has provided considerable insight into the nature of crustal architecture. Complementary information on the nature of the whole lithosphere comes from a broad range of seismological studies using both man-made and natural sources. Up to the 1980s there was an extensive program of seismic refraction studies, which provide important information on crustal structure. Since 1992, the Australian National University has carried out deployments of portable broadband seismic recorders across Australia. These instruments provide high-fidelity recording of ground motion and record both regional and distant earthquakes. In addition, the national seismic network operated by Geoscience Australia has been augmented in recent years, particularly for tsunami warning.

Figure 1 illustrates the coverage that has been achieved in the western part of Australia to the end of 2012, for both active seismic experiments and passive seismic recording. In 2011 the Yilgarn–Officer–Musgrave reflection line (YOM) linked the Yilgarn Craton and central Australia. In 2012 the set of reflection lines across the Albany–Fraser Orogen (12GA-AF1, 12GA-AF2, 12GA-AF3 and 12GA-T1; Plate 4) provided additional insight into the nature of the edge of the Yilgarn Craton further south. Previously in this area, there had been two broadband seismic stations deployed in the SKIPPY reconnaissance survey of the entire continent from 1993–96, and a couple more were later deployed in work supported by the pmd*CRC.

In November 2013, a new dense deployment of portable seismic equipment was installed across the southern part of the east Albany–Fraser Orogen. Twenty-five instruments provide relatively dense sampling around the 12GA-AF3 reflection line and a further 15 have been deployed to extend to about halfway between the northern and southern reflection lines. After a year the passive seismic stations will be redeployed to give denser coverage around lines 12GA-AF1 and 12GA-AF2, and to link across the region in between. The objective of this experiment — supported by an ARC Linkage grant between the Australian National University and the Geological Survey of Western Australia — is to apply detailed seismic tomography to the delineation of structure in the region using techniques that have proved very effective in southeastern Australia (e.g. Rawlinson et al., 2011; Tkalčić et al., 2012). It is also hoped that it may be possible to extend information on crustal structure from the reflection lines into 3D.

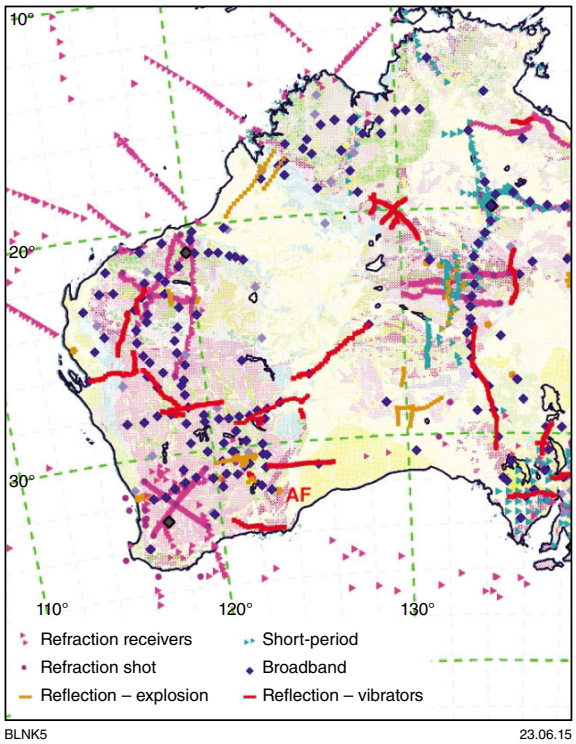

Figure 1. Distribution of active seismic experiments and passive seismic recording across western and central Australia. AF indicates the group of Albany–Fraser reflection lines. Coverage is rather sparse in the desert interior, with a few stations deployed during the SKIPPY reconnaissance survey of the continent from 1993–96 using a limited number of stations deployed for five to six months at a time.

1 Research School of Earth Sciences, The Australian National University, Canberra ACT 0200, Australia
Brian.Kennett@anu.edu.au

The seismograms from the portable and permanent seismic stations across the continent have been analysed to extract information on lithospheric structure beneath the Australian region, both in the crust and uppermost mantle. A wide variety of methods have been employed to study the lithosphere (e.g. Kennett, 2003; Kennett and Blewett, 2012).

The principal information from regional earthquakes comes from the analysis of the large amplitude surface waves late in the seismograms. These surface waves travel almost horizontally through the lithosphere and with a sufficient density of crossing paths can be used in a tomographic inversion to determine 3D structure in the lithospheric mantle. Receiver-based studies at individual stations exploit the conversions and reverberations following the onset of the P-wave energy. From distant earthquakes information can be extracted about the structure in the crust and uppermost mantle, since the paths arriving at the stations are near vertical.

Additional information has begun to be extracted from the seismic noise field, through the stacked cross-correlation of signals at pairs of stations that provide an approximation to the signal expected for a source at one station recorded at the other location. This ambient noise tomography approach was pioneered in Australia by Saygin (2007) using the continuous data recordings at the portable stations in association with permanent seismic stations to link different experiments. The main signal comes from high-frequency surface waves, which provide imaging of upper to middle crustal structure, and are particularly sensitive to the presence of sediments (Saygin and Kennett, 2010, 2012).

Recently a major synthesis of the available seismological constraints on lithospheric structure has been carried out to produce the Australian Seismological Reference Model (AuSREM). An overview of the AuSREM model is given in Kennett and Salmon (2012). A detailed description of the crustal component and its construction is presented in Salmon et al. (2013a), with a comparable treatment for the mantle component in Kennett et al. (2013). The crustal and mantle components are linked through the Moho model constructed using all available information, including reflection picks (Kennett et al., 2011; Salmon et al., 2013a,b).

We build on the results from the AuSREM model in this summary of lithospheric properties in the neighbourhood of the Albany–Fraser Orogen reflection lines. There have been only a limited number of refraction and receiver function studies in the region and so the information on crustal structure depends heavily on the ambient noise studies.

Crustal Structure

Receiver function studies

A powerful method to extract information on crustal structure is the analysis of distant earthquakes using the receiver function technique, which exploits the conversions and reverberations immediately following the onset of the P wave. The two horizontal components of motion are combined to produce records with polarization along (radial) and perpendicular (tangential) to the great circle back to the source. The rotated components are then deconvolved using the vertical component of motion that represents dominantly P waves. In this way the influence of the source is largely eliminated and attention is focused on wave propagation processes close to the receiver. When there is little energy on the tangential receiver function 3D structural variation is weak, and then an inversion may be made using a radial receiver function for an effective 1D structure in the neighbourhood of the receiver (Shibutani et al., 1996; Sambridge, 1999). Alternative approaches use stacking of receiver functions to emphasize features such as the conversion from the crust-mantle boundary, and hence, constrain the Moho depth. The moveout pattern of conversions and multiples from different source distances can be used to constrain the depth of seismic boundaries and Vp/Vs ratios (Zhu and Kanamori, 2000). It can also be advantageous to make a partial allowance for the influence of the free surface on the seismograms by a rotation of components in the vertical plane or a transformation (Reading et al., 2003a).

The first systematic treatment of receiver function results across Australia were made by Clitheroe et al. (2000a,b) with an emphasis on the thickness of the crust and also the base of sediments; just a couple of these stations lie in the zone near the Albany–Fraser profiles (Fig. 1). Since 2000, a particular focus of portable broadband deployments has been on Western Australia. A number of deployments now provide good coverage of the Archean cratons and the Proterozoic Capricorn Orogen, with some stations near the southeastern limit of the Yilgarn Craton.

AuSREM crustal model

The results from receiver functions provide S wavespeed profiles in the immediate neighbourhood of the seismic stations, together with an estimate of the ratio between P and S wavespeeds. Refraction experiments provide P wavespeed along the line of stations with full crustal penetration only near the midpoints.

From the P/S wavespeed ratio derived from more than 150 receiver functions across the continent we are able to produce a smooth interpolation of the ratio between P and S wavespeeds and use this to convert the S wavespeed distribution of Saygin and Kennett (2012) derived from ambient noise tomography to an equivalent P wavespeed model. We then combine estimates of the P wavespeed from refraction and receiver function studies with the tomographic results to produce a P wavespeed model for the continent and offshore where there are refraction experiments.

The resulting model is illustrated in Figure 2 with depth slices at 10 km intervals starting at 5 km depth. The constraints from the ambient noise tomography are rather weak below 25 km, and so there are portions of the model without direct control. We have blanked out those regions that lie further than 200 km from a refraction or receiver

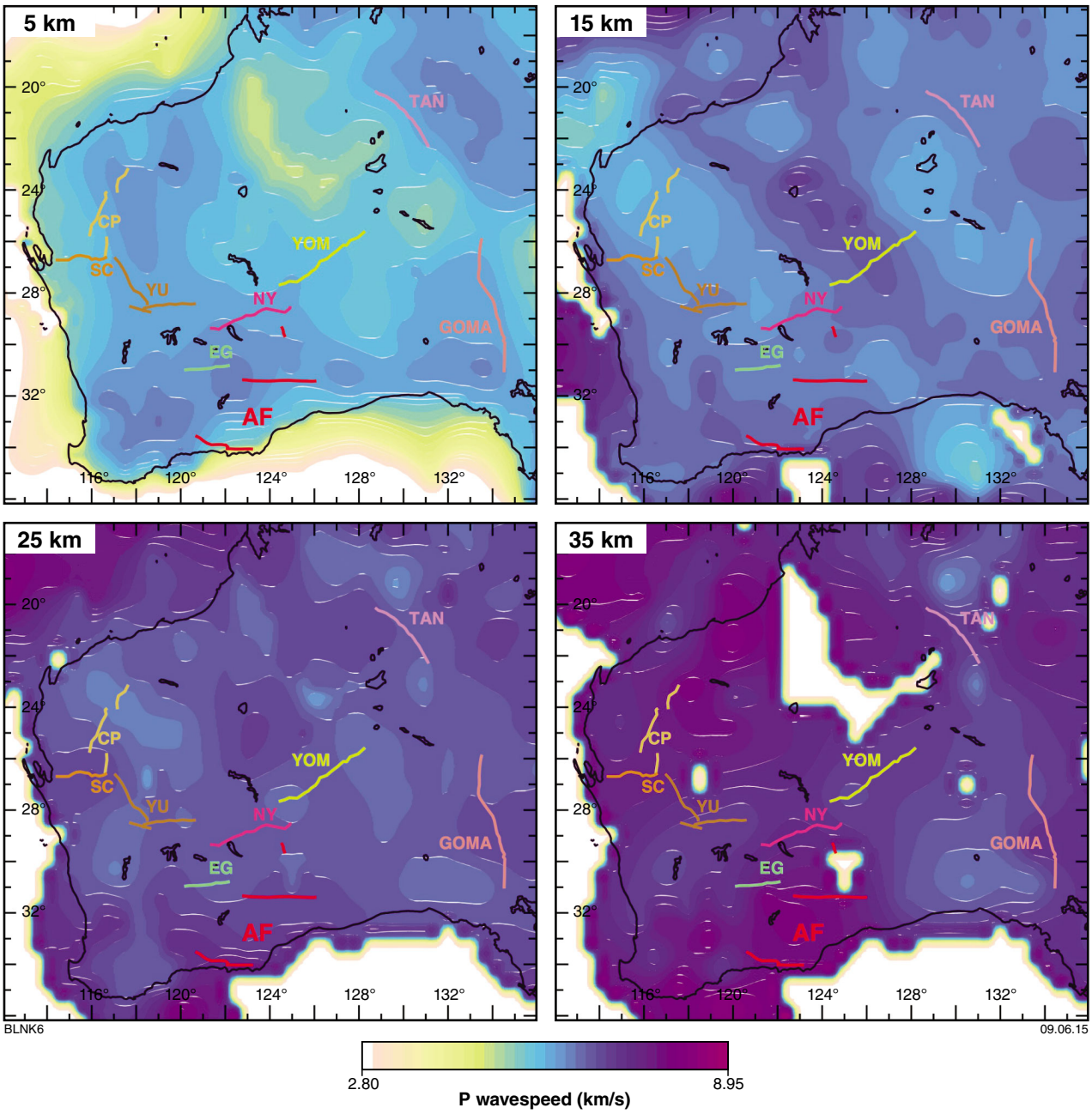

Figure 2. Depth slices through the AuSREM crustal model for P wavespeed for the region around the Albany–Fraser Orogen reflection lines. The same wavespeed scale is used for all depths, since mantle speeds are encountered at 15 km offshore. Regions without direct control on wavespeed are blanked out at depth. In each panel distinctively coloured lines indicate the locations of the recent seismic lines.

function control point in Figure 2, notably in the Canning Basin at 35 km depth and just north of the 12GA-AF3 reflection line. At 5 km depth we see the influence of the deep sediments in the Canning Basin, contrasting with the Proterozoic metasediments in the Capricorn Orogen. The transition to the Pinjarra Orogen is evident in slower P wavespeeds along the western coast of Western Australia at 5 km depth, but at greater depth there is very little contrast with the Yilgarn Craton.

Shallow control is weak for the southern reflection lines 12GA-AF1 and 12GA-AF2, but better for the more northerly line 12GA-AF3 which lies on a mild gradient of decreasing P wavespeed towards the east at both 5 and 15 km depth. The sense of the wavespeed gradient reverses at 25 km depth, but with little change along the line.

The thinner crust in the Pilbara is reflected in the presence of mantle wavespeeds at 35 km depth, and rather high P wavespeeds are encountered in the southern Yilgarn, adjacent to the Albany–Fraser Orogen. The 12GA-AF2 and 12GA-AF3 reflection lines indicate that these high seismic wavespeeds lie within the reflective crust, and hence the Moho must lie at around 40 km depth rather

than at 27 km where a distinctive discontinuity is seen in some receiver function work. The reflection results help to explain a bimodal distribution of crustal thickness in this area from earlier studies.

Crustal thickness

Kennett et al. (2011) assembled the full suite of available information on the depth to Moho across the continent drawing on results from refraction experiments, receiver functions and Moho picks from the full suite of crustal reflection profiles across the continent. For refraction or receiver function studies the crust-mantle boundary is taken at the base of the transition to mantle seismic velocities (P wavespeeds above 7.9 km/s or shear wavespeeds above 4.4 km/s). On the reflection records, the Moho is taken at the base of the set of crustal reflectors and converted to depth using an average crustal velocity of 6 km/s.

The estimates of crustal thickness from Western Australia into the centre of the continent are summarized in Figure 3. There is a close correspondence in the estimates from the different techniques and station deployments even though the methods of analysis differ significantly, e.g. the profile of crust thickness in the northern Yilgarn Craton from receiver function studies is very similar to that seen on the adjacent reflection profiles, and as a consequence the receiver function results provide a check on the calibration of the time–depth conversion for the reflection results.

As noted above the results from the Albany–Fraser reflection lines have led to a reinterpretation of crustal thickness in the area, with preference now given to a crustal thickness near 40 km rather than 27 km. The study of Gorbatov et al. (2013) using autocorrelation of seismic records to extract estimates of reflectivity beneath seismic stations show the presence of two clear discontinuities in this region. The seismic P wavespeeds below 30 km are very high for crustal material so that interpretation of a shallow Moho becomes understandable. The reflection lines also indicate a slight down bulge of the Moho at the edge of the craton accompanying a distinct change in the style of reflectivity. These features have been incorporated in an updated version of the Australian Moho map in Salmon et al. (2013b).

The background contour plot of the Moho in Figure 3 is taken from the continent-wide synthesis of results, using all receiver functions and the refraction data from the compilation of Collins et al. (2003), with additional control from reflection experiments (Kennett et al., 2011; Salmon et al., 2013b). New results from the Eucla to Gawler profile which extends 12GA-AF3 to the east suggest that the 40 km contour for crustal thickness should move close to the coastline, and the zone of thicker crust in central Australia may extend further south.

Surface wave tomography

The earthquake belts to the north of Australia along the Indonesian arc into New Guinea and to the east in the Tonga–Fiji zone provide frequent seismic events of suitable magnitude to be recorded well in Australia. There are less common events to the south along the mid-oceanic ridge between Australia and Antarctica, but these are important in providing additional directional control. A number of different techniques have been used to analyse the large amplitude surface waves that arrive late in the seismogram, and from the combinations of results from many paths 3D models of the seismic shear wavespeed distribution have been extracted (e.g. van der Hilst et al., 1998; Debayle and Kennett, 2000, 2003; Kennett et al., 2004a,b; Fishwick et al., 2005, 2008; Yoshizawa and Kennett, 2004; Fichtner et al., 2009, 2010). Most of the methods rely on some approximations to wave propagation in three dimensions, but the work of Fitchner et al. (2009, 2010) uses full seismogram calculations in a 3D model. As a consequence the frequency range used is restricted to prevent excessive computational requirements. Fortunately the results with this sophisticated analysis indicate that the longer wavelength features obtained with the approximate methods are confirmed.

We can now have considerable confidence in the main structures in the lithosphere at a horizontal scale of about 200 km and a vertical resolution around 30 km. Figure 4 illustrates the shear wave structure in Western Australia using the AuSREM mantle model developed by collaboration between the authors of a number of different studies (Yoshizawa and Kennett, 2004; Fishwick and Rawlinson, 2012; Fichtner et al., 2010). This new model benefits from the incorporation of more paths than in any individual study and includes the use of techniques that provide improved resolution at depth. The variations in seismic S-wave velocity are displayed in terms of the absolute shear wavespeed at each depth, with the neutral colour chosen to represent typical continental values.

In Figure 3, Regions with faster S wavespeed than the continental reference are indicated by bluish tones, and zones with slower S wavespeed are shown in tones of brown. Reductions in seismic wavespeed are expected from the influence of temperature or the presence of volatiles. Cooler temperatures will produce faster shear wavespeeds, but the very fast wavespeeds seen in Figure 4 are difficult to produce by temperature alone and suggest the presence of chemical heterogeneity.

The mantle lithosphere below 100 km is marked by distinct fast seismic wavespeeds, but at about 75 km there is an indication of somewhat reduced wavespeeds (Figure 4) in the east of Western Australia, that may be linked in part to the presence of thickened crust. The YOM reflection profile crosses into this lower wavespeed zone, yet at greater depth shear wavespeeds are very fast. The area of lower S wavespeed is not associated with enhanced seismic attenuation as might be expected if the cause was a concentration of radioactivity in the uppermost mantle, and its origin remains somewhat enigmatic.

At 75 km depth the Paterson Orogen is marked by high seismic wavespeeds, and there is also a distinct rather fast patch in the northern Yilgarn. There is no distinctive mantle feature associated with the Capricorn Orogen, though we note that at 225 km the Capicorn and Pilbara

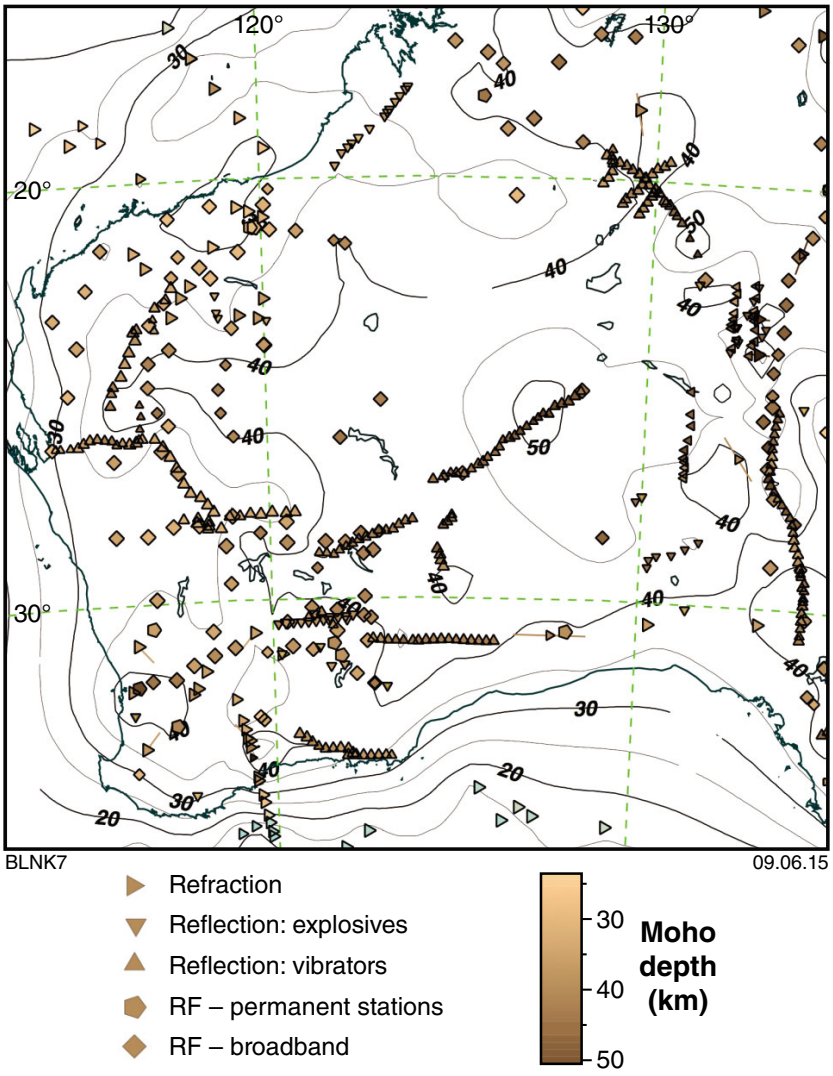

Figure 3. Estimates of crustal thickness derived from refraction experiments (triangles) and receiver function studies (diamonds – broadband stations, squares – short-period stations, less reliable results indicated by smaller symbols). Moho estimates from reflection work are indicated by the dense lines of triangles. The contours of Moho depth are derived from a continent-wide synthesis (Kennett et al., 2011; Salmon et al., 2013a,b), with notable influence from the results from the Albany–Fraser reflection lines.

show somewhat lower shear wavespeeds than in the Yilgarn Craton. The zone of fast shear wavespeeds beneath the Yilgarn Craton extends towards central Australia and remains quite fast even at 225 km depth. This zone of elevated wavespeeds is among the thickest seismic lithosphere on the Australian continent.

The area beneath the Albany–Fraser reflection lines lies just to the east of the fast seismic wavespeeds associated with the Yilgarn Craton at 75 km depth. The northern line lies along the edge of the main region of higher seismic wavespeeds at 150 and 225 km depth. Both sets of lines lie in a gradient zone of decreasing wavespeed to the east at both 150 and 225 km. Constraints on mantle structure weaken to the south because there are fewer earthquakes in this zone. As a result the apparent reduction in seismic wavespeeds may arise in part from a loss in resolution in the surface wave tomography.

Discussion and conclusions

The AuSREM model for lithospheric structure in the Australian region provides valuable controls on 3D variability that can be helpful in the interpretation of other classes of information such as reflection seismic profiles. The crustal component of AuSREM builds on information from man-made and natural sources, using refraction experiments, near receiver studies using distant earthquakes and continent-wide tomography exploiting ambient seismic noise. In the uppermost mantle surface-wave tomography is the main source of information on 3D S wavespeed variation, with the most reliable results available below 75 km depth. At shallower depth there is a strong influence from the crustal structure along the various paths and crustal structure can be mapped into the uppermost mantle, especially where the crust is thick.

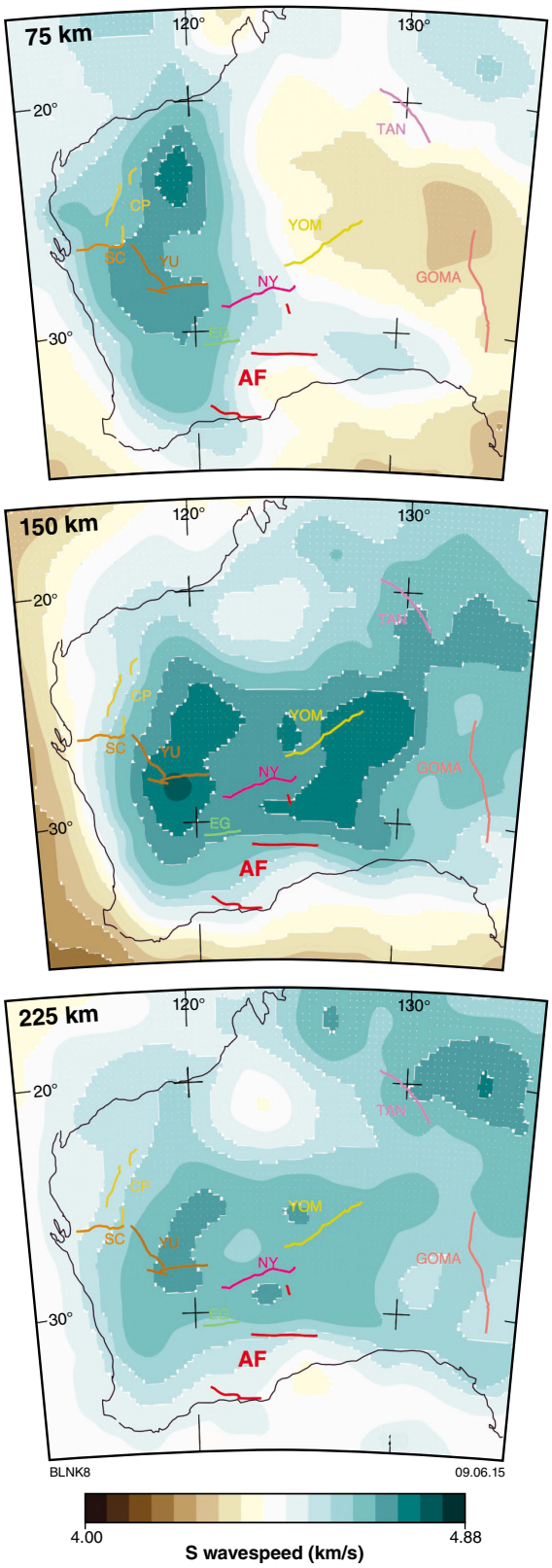

Figure 4. **Seismic shear-wavespeed structure in western to central Australia from the AuSREM mantle model, largely controlled by surface wave tomography. Continental scale estimates of seismic wavespeed variation at 75, 150, and 225 km depth, inferred from the analysis of surface waves. In each panel distinctively coloured lines indicate the locations of the recent seismic lines.**

The distinct changes in styles of crustal reflectivity as one progresses from the Yilgarn Craton into the Albany–Fraser Orogen are not matched by comparable changes in P velocity, except for a modest gradient in the near surface. The reflection line itself has changed our perceptions of the way in which the crustal components interact, with indications of a slight downward bulge of the Moho at the edge of the craton.

The Albany–Fraser reflection profiles lie at the southern edge of the main zone of fast shear wavespeeds in the mantle. Both the northern and southern lines lie at the eastern edge of the zone of fastest wavespeeds at 75 km and in a gradient of decreasing wavespeed to the east at 150 and 225 km. The structures in the mantle below 100 km depth do not show a direct correspondence with the surface geology, with high velocities that would conventionally be associated with cratons, extending below both Archean and Proterozoic domains.

Acknowledgements

The deployments of portable broadband stations across Australia have depended on the efforts of many people often working in trying circumstances. Particular thanks are due to John Grant, Steve Sirotjuk, and Qi Li for their major role in maintaining equipment and logistics, and to Armando Arciadiaco for field support and a critical role in data handling and organization. Receiver function results draw on the work of Drs Geoff Clitheroe, Anya Reading, Steve Revets, Erdinc Saygin, Michelle Salmon, and Elizabeth Vanacore. Particular thanks go to Anya Reading for her systematic studies of seismic structure in Western Australia, which have been significant in the construction of the crustal wavespeed distribution.

References

Aitken, ARA 2010, Moho geometry gravity inversion experiment (MoGGIE): a refined model of the Australian Moho and its tectonic and isostatic implications: Earth and Planetary Science Letters, v. 297, p. 71–83.

Clitheroe, G, Gudmundsson, O and Kennett, BL 2000a, The crustal thickness of Australia: Journal of Geophysical Research, v. 105, p. 13697–13713.

Clitheroe, G, Gudmundsson, O and Kennett, BLN 2000b, Sedimentary and upper-crustal structure of Australia from receiver functions: Australian Journal of Earth Sciences, v. 47, p. 209–216.

Collins, CDN, Drummond, BJ and Nicoll, MG 2003, Crustal thickness patterns in the Australian continent, *in* The Evolution and Dynamics of the Australian Plate *edited by* D Müller and R Hillis: Geological Society of Australia Special Publication 22, p. 121–128

Debayle, E and Kennett, BLN 2000, The Australian continental upper mantle — structure and deformation inferred from surface waves: Journal of Geophysical Research, v. 105, p. 25443–25540.

Debayle, E and Kennett BLN 2003, Surface wave studies of the Australian region, in The Evolution and Dynamics of the Australian Plate, *in* The Evolution and Dynamics of the Australian Plate *edited by* D Müller and R Hillis: Geological Society of Australia Special Publication 22, p. 25–40

Fichtner, A, Kennett, BLN, Igel, H and Bunge, H-P 2009, Full seismic waveform tomography for upper-mantle structure in the Australasian region using adjoint methods: Geophysical Journal International, v. 179, p. 1703–1725.

Fichtner, A, Kennett BLN, Ige,l H and Bunge, H-P 2010, Full seismic waveform tomography for radially anisotropic structure: New insights into the past and present states of the Australasian upper mantle: Earth and Planetary Science Letters, v. 290, p. 270–280.

Fishwick, S, Kennett, BLN and Reading, AM 2005, Contrasts in lithospheric structure within the Australian Craton: Earth and Planetary Science Letters, v. 231, p. 163–176.

Fishwick, S, Heintz, M, Kennett, BLN, Reading, AM and Yoshizawa, K 2008, Steps in lithospheric thickness within eastern Australia, evidence from surface wave tomography: Tectonics, v. 27, no. 4, TC0049, doi:10.129/2007TC002116.

Fishwick, S and Rawlinson, N 2012, 3D structure of the Australian lithosphere from evolving seismic datasets: Australian Journal of Earth Sciences, v. 59, p. 809–826.

Gorbatov, A, Kennett, BLN and Saygin, E 2013, Crustal properties from seismic station autocorrelograms: Geophysical Journal International, v. 192, p. 861–870.

Kennett, BLN 2003, Seismic Structure in the mantle beneath Australia, *in* The Evolution and Dynamics of the Australian Plate *edited by* D Müller and R Hillis: Geological Society of Australia Special Publication 22, p. 7–23,

Kennett, BLN and Blewett, R 2012, Lithospheric framework of Australia: Episodes, v. 35, p. 9–22.

Kennett, BLN and Salmon, M 2012, AuSREM: Australian seismological reference model: Australian Journal of Earth Sciences, v. 59, p. 1091–1103.

Kennett, BLN, Fishwick, S, Reading, AM and Rawlinson, N 2004a, Contrasts in mantle structure beneath Australia – relation to Tasman Lines?: Australian Journal of Earth Sciences, v. 51, p. 563–569.

Kennett, BLN, Fishwick, S and Heintz, M 2004b, Lithospheric structure in the Australian region — a synthesis of surface wave and body wave studies, Exploration Geophysics, v. 35, p. 258–266.

Kennett, BLN, Salmon, M, Saygin, E and AusMoho working group 2011, AusMoho: the variation in Moho depth across Australia: Geophysical Journal International, v. 187, p. 946–958

Kennett, BLN, Fichtner, A, Fishwick, S and Yoshizawa, K 2013, Australian Seismological Reference Model (AuSREM): mantle component: Geophysical Journal International, v. 192, p. 871–887.

Rawlinson, N, Kennett, BLN, Vanacore, E, Glen, RA and Fishwick, S 2011, The structure of the upper mantle beneath the Delamerian and Lachlan orogens from simultaneous inversion of multiple teleseismic datasets: Gondwana Research, v. 19, p. 788–799.

Reading, A, Kennett, B and Sambridge, M 2003a, Improved inversion for seismic structure using transformed S-wavevector receiver functions: removing the effect of the free surface: Geophysical Research Letters, v. 30, no. 19, doi: 10.1029/2003GL018090.

Reading, AM, Kennett, BLN and Dentith, MC 2003b, The seismic structure of the Yilgarn Craton: Western Australia, Australian Journal of Earth Sciences, v. 50, p. 427–438.

Reading, AM and Kennett, BLN 2003, Lithospheric structure of the Pilbara Craton, Capricorn Orogen and northern Yilgarn Craton, Western Australia, from teleseismic receiver functions: Australian Journal of Earth Sciences, v. 50, p. 439–445.

Reading, AM, Kennett, BLN and Goleby, B 2007, New constraints on the seismic structure of West Australia: Evidence for terrane stabilization prior to the assembly of an ancient continent? Geology, v. 35, p. 379–379.

Reading, A, Tkalčić, H, Kennett, BLN, Johnson, SP and Sheppard, S 2012, Seismic structure of the crust and uppermost mantle of the Capricorn and Paterson Orogens and adjacent cratons, Western Australia, from passive seismic transects: Precambrian Research, v. 196, p. 295–308.

Salmon, M, Kennett, BLN and Saygin, E 2013a, Australian Seismological Reference Model (AuSREM): crustal component: Geophysical Journal International, v. 192, p. 190–206.

Salmon, M, Kennett, BLN, Stern, T and Aitken, ARA 2013b, The Moho in Australia and New Zealand: Tectonophysics, v. 609, p. 288–298.

Sambridge, MS 1999, Geophysical inversion with a neighbourhood algorithm – I. Searching a parameter space: Geophysical Journal International, v. 138, p. 479–494.

Saygin, E 2007, Seismic receiver and noise correlation based studies in Australia: Australian National University, PhD Thesis (unpublished).

Saygin, E and Kennett, BLN 2010, Ambient noise tomography for the Australian Continent: Tectonophysics, v. 481, p. 116–125, doi:10.106/j.tecto.2008.11.013.

Saygin, E and Kennett, BLN 2012, Crustal structure of Australia from ambient seismic noise tomography: Journal of Geophysical Research, 117, B01304; doi:10.1029/2011JB008403.

Shibutani, T, Sambridge, M and Kennett, BLN 1996, Genetic algorithm inversion for receiver functions with application to crust and uppermost mantle structure beneath Eastern Australia: Geophysical Research Letters, v. 23, p. 1829–1832.

Tkalčić, H, Rawlinson, N, Arroucau, P, Kumar, A and Kennett, BLN 2012, Multistep modelling of receiver-based seismic and ambient noise data from WOMBAT array: crustal structure beneath southeast Australia, Geophysical Journal International, v. 189, p. 1681–1700.

Yoshizawa, K and Kennett, BLN 2004, Multi-mode surface wave tomography for the Australian region using a 3-stage approach incorporating finite frequency effects: Journal of Geophysical Research, v. 109, B02310; doi: 10.129/2002JB002254.

Zhu, L and Kanamori, H 2000, Moho depth variation in southern California from teleseismic receiver functions: Journal of Geophysical Research, v. 105, p. 2969–2980.

Geodynamic implications of the 2012 Albany–Fraser deep seismic reflection survey: a transect from the Yilgarn Craton across the Albany–Fraser Orogen to the Madura Province

by

RJ Korsch[1], CV Spaggiari, SA Occhipinti[2], MP Doublier[1], DJ Clark[1], MC Dentith[3], MG Doyle[2], BLN Kennett[4], K Gessner, NL Neumann[1], EA Belousova[5], IM Tyler, RD Costelloe[1], T Fomin[1], and J Holzschuh[1]

Introduction

From April to June 2012, 672 line km of vibroseis-source, deep seismic reflection and gravity data were acquired along four traverses (12GA-AF1, 158.4 km; 12GA-AF2, 114.04 km; 12GA-AF3, 319.12 km; and 12GA-T1, 80.32 km), collectively referred to as the Albany–Fraser seismic survey. Magnetotelluric (MT) data were collected along seismic lines 12GA-AF3 and 12GA-T1. The lines started in the southern and eastern part of the Archean Yilgarn Craton (in the Youanmi, Kurnalpi and Yamarna Terranes), and crossed the major elements of the east Albany–Fraser Orogen, before ending to the east of the Rodona Shear Zone in the Madura Province (Figs 1, 2 and 3; Plates 1, 2 and 3; figure 1, Spaggiari et al., 2014b). This seismic survey is the first to provide deep crustal images of the onshore component of the Albany–Fraser Orogen. The project is, in part, a collaborative project between Geoscience Australia (GA) and the Geological Survey of Western Australia (GSWA), and is part of the ongoing cooperation under the National Geoscience Agreement (NGA). It was primarily funded through the Western Australian Government's Royalties for Regions Exploration Incentive Scheme (EIS), with acquisition and processing of the data being managed by GA as part of its program of precompetitive data acquisition and analysis to support mineral resources exploration. Acquisition of line 12GA-T1 was funded by the Tropicana Joint Venture (being AngloGold Ashanti Australia Ltd and the Independence Group NL). Interpretation of the data was undertaken jointly by GSWA, GA and the Tropicana Joint Venture.

A key aim of the Albany–Fraser seismic survey was to image the crustal architecture in the region. Specific aims to understand the regional geodynamics were to:

- image the crustal architecture of the southeastern Yilgarn Craton margin and its relationship to the Albany–Fraser Orogen
- establish the subsurface extent of the Yilgarn Craton beneath the Albany–Fraser Orogen, and look for mantle-tapping structures that may have provided fluid pathways for mineralization. The seismic lines were designed to cross several major structures, such as the Cundeelee Shear Zone, the Fraser Shear Zone, the Boonderoo Shear Zone, and the Red Island Shear Zone
- examine the deep crustal structure of the Albany–Fraser Orogen and investigate the processes that drove Paleoproterozoic rifting and magmatism along the craton margin, and Mesoproterozoic tectonic assembly
- test models of Mesoproterozoic fold and thrust belt architecture in the Albany–Fraser Orogen
- examine structural relationships between tectonic units mapped at the surfac
- image the crustal architecture of the Yilgarn Craton margin and its relationship to the Albany–Fraser Orogen in the vicinity of the Tropicana gold deposit
- understand the structural geometry around the Tropicana gold deposit to help define areas elsewhere along the belt which may be prospective for mineralization.

1 Minerals and Natural Hazards Division, Geoscience Australia, GPO Box 378, Canberra ACT 2601

2 AngloGold Ashanti Ltd, Level 13, St Martins Tower, PO Box Z5046, Perth WA 6831

3 Centre for Exploration Targeting, School of Earth and Environment, The University of Western Australia, 35 Stirling Highway, Crawley WA 6009

4 Research School of Earth Sciences, The Australian National University, Canberra ACT 0200

5 GEMOC ARC National Key Centre, Department of Earth and Planetary Sciences, Macquarie University, Sydney NSW 2109

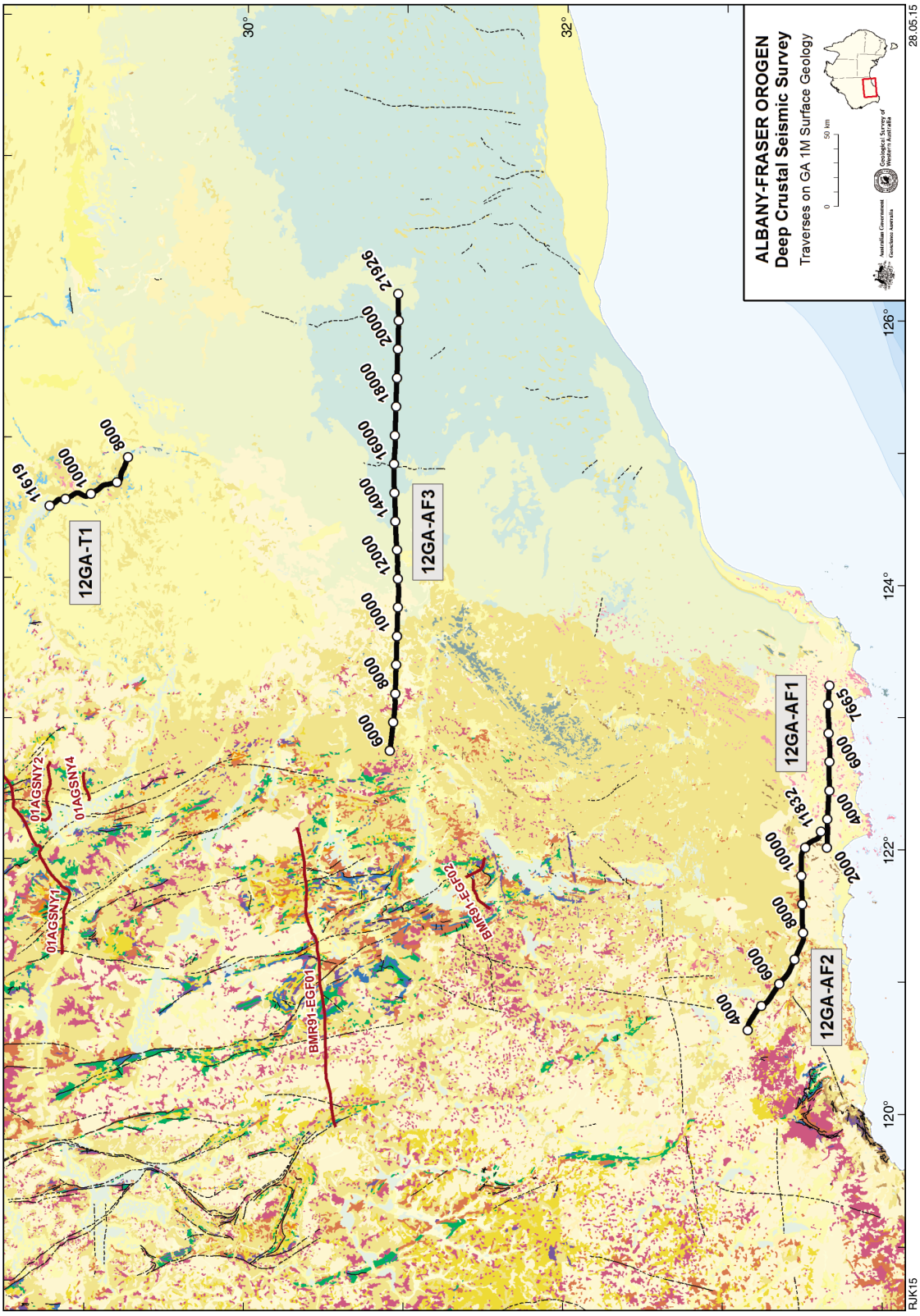

Figure 1. Map showing the surface geology of the region covered by the Albany–Fraser seismic survey, from the Yilgarn Craton in the west, across the Albany–Fraser Orogen, to the Madura Province in the east. The surface geology is from the 1:1 000 000 scale geology map of Australia (Raymond, 2009, which also contains the legend). The seismic lines have CDP stations labelled.

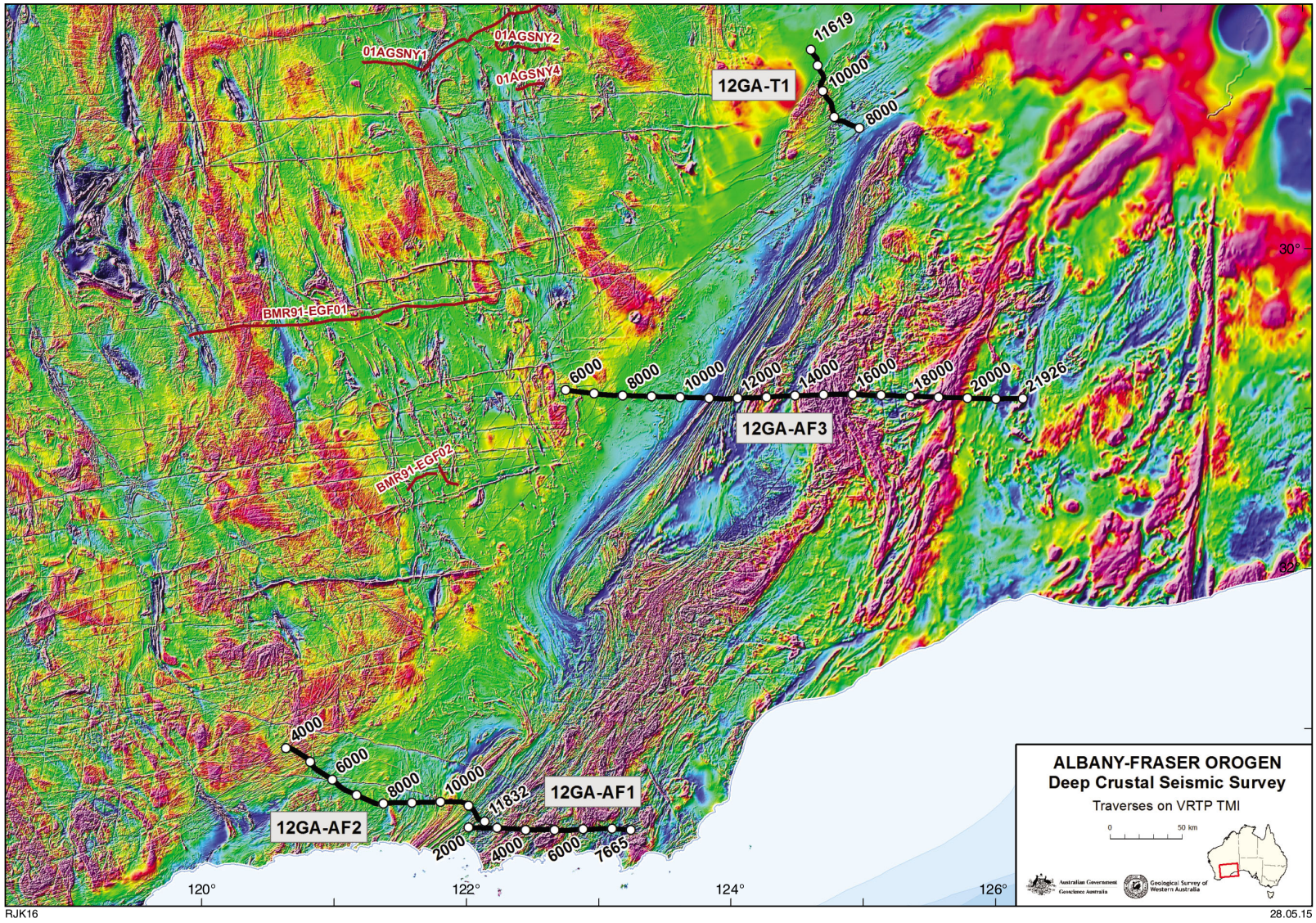

Figure 2. **Map showing a regional aeromagnetic image for the region covered by the Albany–Fraser seismic survey, from the Yilgarn Craton in the west, across the Albany–Fraser Orogen, to the Madura Province in the east (extracted from Milligan et al., 2010). Warm colours are high magnetic intensities; cool colours are low magnetic intensities. The seismic lines have CDP stations labelled.**

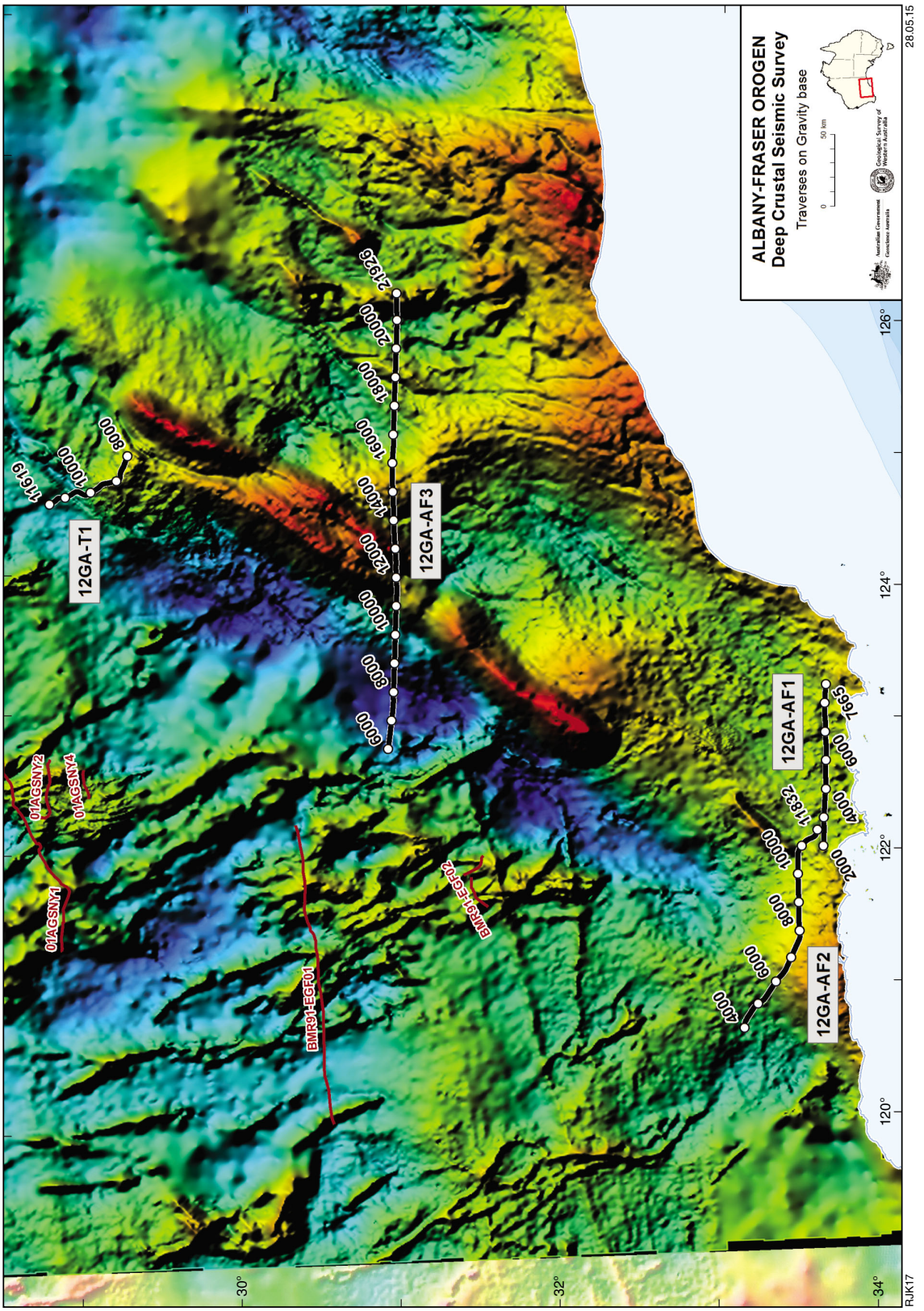

Figure 3. Map showing a regional gravity image for the region covered by the Albany–Fraser seismic survey, from the Yilgarn Craton Terrane in the west, across the Albany–Fraser Orogen, to the Madura Province in the east (extracted from Bacchin et al., 2008, with the addition of the new data from the Esperance gravity survey from GSWA). Warm colours are gravity highs, cool colours are gravity lows. The seismic lines have CDP stations labelled.

Companion papers in this volume present summaries of the geological evolution of the region and preliminary interpretations of the Albany–Fraser seismic lines (Spaggiari et al., 2014a,b; Doyle et al., 2014; Occhipinti et al., 2014), discussions of the potential field geophysics (Murdie et al., 2014; Brisbout et al, 2014), MT (Spratt et al., 2014) and implications for mineral systems (Tyler et al., 2014). The northwest-southeast to east-west orientations of the seismic lines are essentially perpendicular or slightly oblique to the major domains and structures in the region (Figs 1, 2 and 3), and provide crustal-scale geometries which can be compared with existing geological interpretations. Overall, the crust in the vicinity of the seismic sections has quite variable reflectivity, with some parts of the sections containing strong reflections, and other areas having very low reflectivity (Figs 4, 5, 6, 7 and 8; Plate 4).

Here, we discuss some of the geodynamic implications which arise from interpretation of the new deep seismic reflection and MT data obtained during the Albany–Fraser seismic survey. Of particular interest is the relationship, at a crustal scale, between the Yilgarn Craton and the Albany–Fraser Orogen. For example, is there evidence for a suture between the Yilgarn Craton and the Albany–Fraser Orogen, or outboard of the Albany–Fraser Orogen, and how far to the east does the Yilgarn Craton extend beneath the zones of the Albany–Fraser Orogen? The current surveys build on the existing network of deep-crustal seismic surveys, acquired since 1991, and will improve the understanding of the crustal structure and geodynamics of Western Australia.

Details of the acquisition and processing techniques followed for the deep seismic survey are provided in Costelloe et al. (2014). We undertake conversion from two-way travel time (TWT) to depth using an effective P-wave velocity for the crust of 6000 ms^{-1}, so that 1 s TWT is approximately equal to 3 km depth, with the exception of sedimentary rocks in the Eucla and Bight Basins and for the Cenozoic regolith, where we assume much slower P-wave velocities of 2500–3800 ms^{-1}. Because of the 2D nature of the seismic lines, the orientations of structures, mentioned below, are apparent dips, and apparent dip directions.

Structure of the Moho

In the region of the Albany–Fraser seismic survey, the crust below the Albany–Fraser Orogen is generally thicker than that below the Yilgarn Craton (Figs 4, 5, 6 and 8; Plate 4). The Mohorovičić discontinuity (Moho) has an undulating topography, varying in depth from about 11.5 s TWT (~35 km), beneath the eastern Nornalup Zone on line 12GA-AF1, to about 16.3 s TWT (~49 km) at about common depth point (CDP) 9000 on line 12GA-AF3, beneath the Biranup Zone, and also at about CDP 10 900 on line 12GA-T1, beneath the Tropicana Zone (Figs 4, 6 and 8; Plate 4). The Moho is quite variable in seismic character. In places, for example, at about CDP 11 000 on line 12GA-AF2, it is imaged as a very sharp discontinuity, at the base of strongly to moderately reflective packages, above non-reflective material which is interpreted as the upper mantle. In other places, however, the Moho is very poorly imaged, and the transition from crust to mantle appears gradational, for example, on line 12GA-AF2 at about CDP 6200 (Fig. 5; Plate 4).

In the region of the Albany–Fraser seismic survey, the Moho beneath the terranes of the Yilgarn Craton is mostly defined by a contrast between moderately reflective lower crust and mainly non-reflective upper mantle (Figs 4, 5, 6 and 8; Plate 4). Several deep seismic reflection profiles collected previously across the Yilgarn Craton show that, with the exception of the Narryer Terrane in the northwest, the Moho gradually deepens towards the east. From a depth of about 11 s TWT (~33 km) beneath the Youanmi Terrane (Korsch et al., 2013a), it deepens to about 12 s TWT (~36 km) under the Kalgoorlie Terrane (Drummond et al., 1993, 2000). It then deepens further, from about 13.5 s TWT (~40 km) under the Kurnalpi Terrane to about 15.5 s TWT (~46 km) under the western part of the Yamarna Terrane (Goleby et al., 2004). On seismic line 12GA-AF2, the Moho beneath the Youanmi Terrane has been interpreted to deepen to the east, from about 12.8 s TWT (~38 km) to about 14.1 s TWT (~42 km) at about CDP 4850 (Fig. 5; Plate 4). Thus, it is slightly deeper than observed on seismic lines to the north, for example, on line BMR91-EGF01, where it occurs at about 11 – 12.5 s TWT (~33-37 km) (Drummond et al., 1993, 2000) and on lines 10GA-YU1 and 10GA-YU2, where it is remarkably flat, and at a depth of about 11 s TWT (~33 km) (Korsch et al., 2013a).

On seismic line 12GA-AF3, the Moho below the Kurnalpi Terrane has been interpreted to occur at about 13.0 – 13.7 s TWT (~39–41 km) (Fig. 6; Plate 4), which is at approximately the same depth as the Moho beneath this terrane on line 01AGS-NY1 (Goleby et al., 2004). On seismic line 12GA-T1, the Moho has been interpreted to occur beneath the Yamarna Terrane at about 13.0 s TWT (~39 km) (Fig. 8; Plate 4), which is significantly shallower than where it has been interpreted on seismic line 01AGS-NY1 (~15.5 s TWT, Goleby et al., 2004) and on line 11GA-YO1 (~15 s TWT, Korsch et al., 2013b).

Beneath the Albany–Fraser Orogen, the Moho is generally much less distinctive than beneath the Yilgarn Craton, and is usually interpreted as the base of a weakly to moderately reflective domain. Apart from three specific regions discussed below, the Moho is relatively flat, and is interpreted to occur at about 12.2 s TWT (~37 km) in the eastern part of line 12GA-AF2, shallowing slightly to about 11.5 s TWT (~34 km) at the eastern end of line 12GA-AF1) (Figs 4 and 5; Plate 4). On the eastern half of line 12GA-AF3, the Moho is interpreted to be slightly deeper, at about 13.7 – 14.4 s TWT (~41–43 km), whereas at the eastern end of line 12GA-T1 it occurs at a depth of about 13 s TWT (~39 km) (Fig. 8).

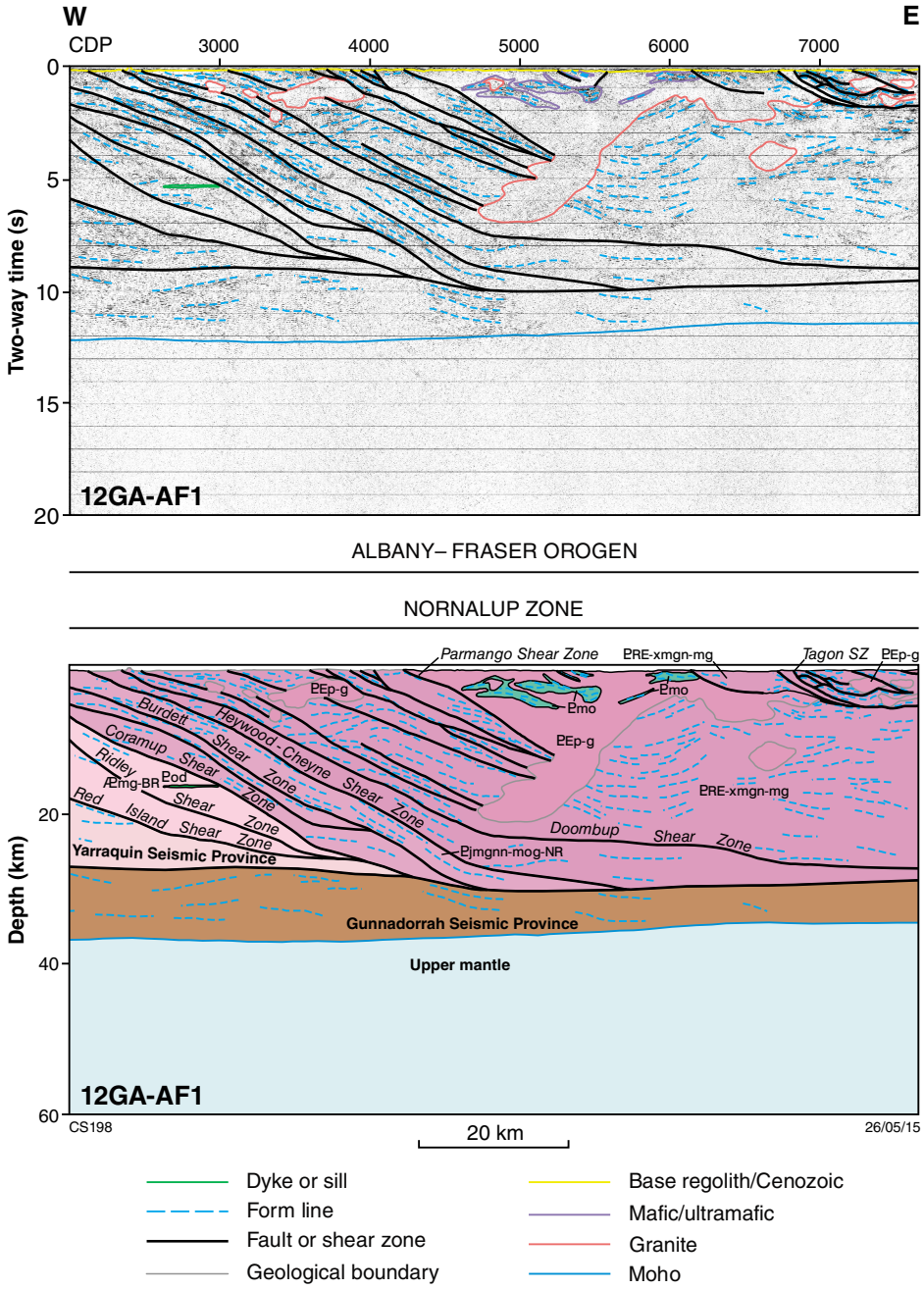

Figure 4. Migrated section for seismic line 12GA-AF1, showing the seismic image with interpreted linework (upper) and solid geology interpreted section (lower). Display is to 20 s TWT (~60 km) depth, and shows vertical scale equal to the horizontal scale, assuming a crustal velocity of 6000 ms^{-1} for the entire section. See Figure 7 for the units legend.

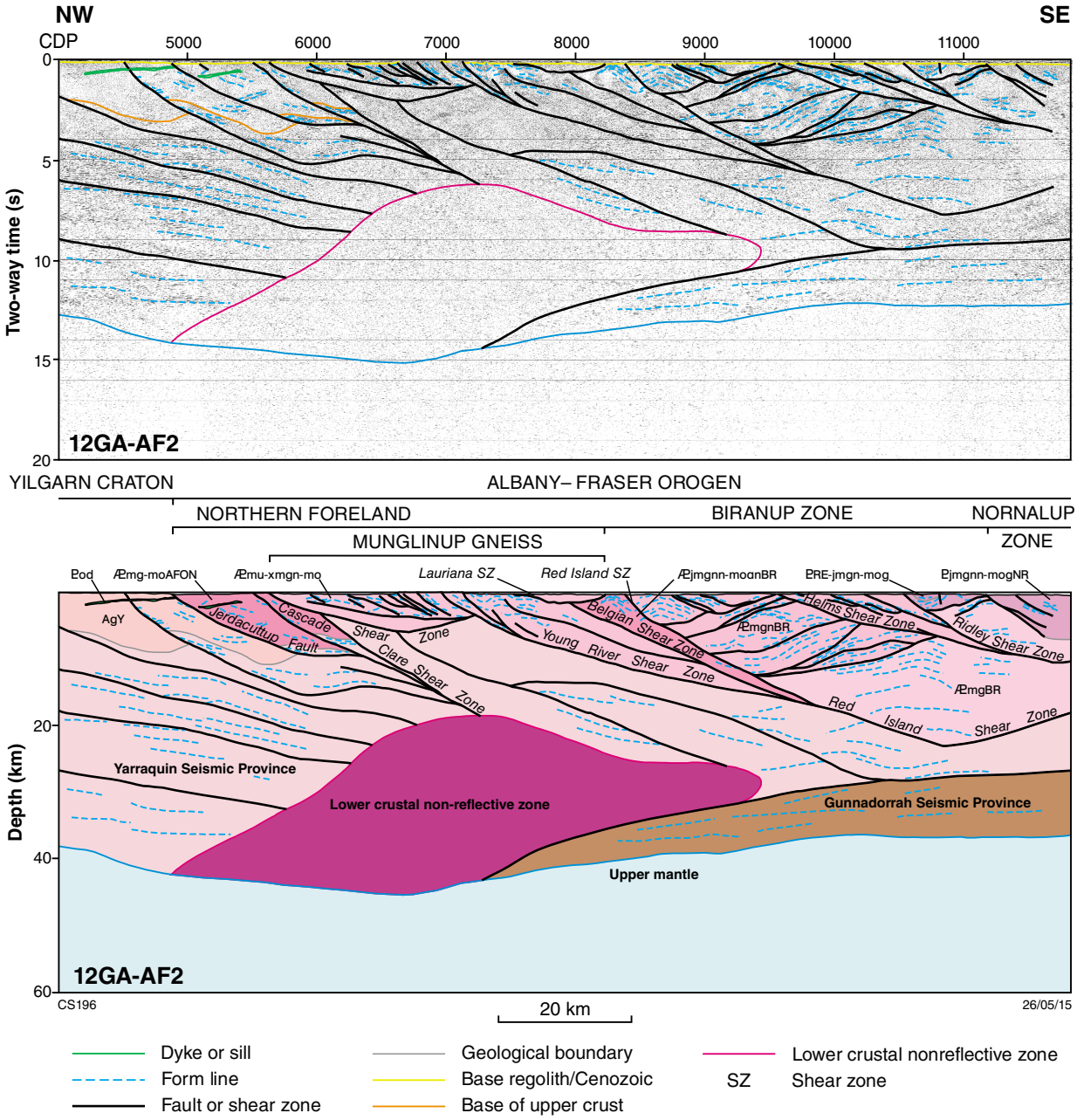

Figure 5. Migrated section for seismic line 12GA-AF2, showing the seismic image with interpreted linework (upper) and solid geology interpreted section (lower). Display is to 20 s TWT (~60 km) depth, and shows vertical scale equal to the horizontal scale, assuming a crustal velocity of 6000 ms^{-1} for the entire section. See Figure 7 for the units legend.

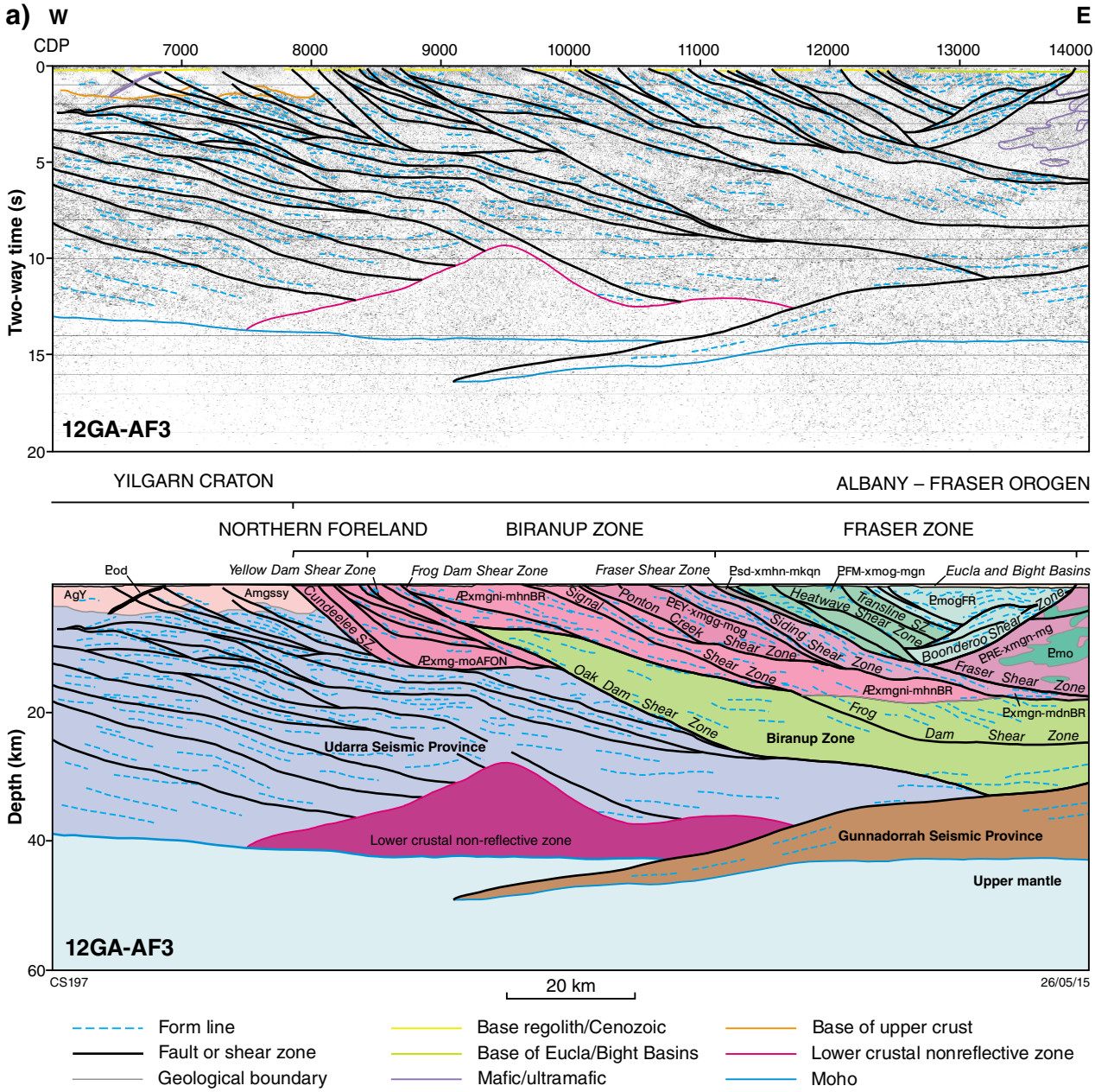

Figure 6. Migrated sections for seismic line 12GA-AF3, showing the seismic image with interpreted linework (upper) and solid geology interpreted section (lower). Display is to 20 s TWT (~60 km) depth, and shows vertical scale equal to the horizontal scale, assuming a crustal velocity of 6000 ms^{-1} for the entire section. The western part of the section is shown in a), and the eastern part in b). See Figure 7 for the units legend.

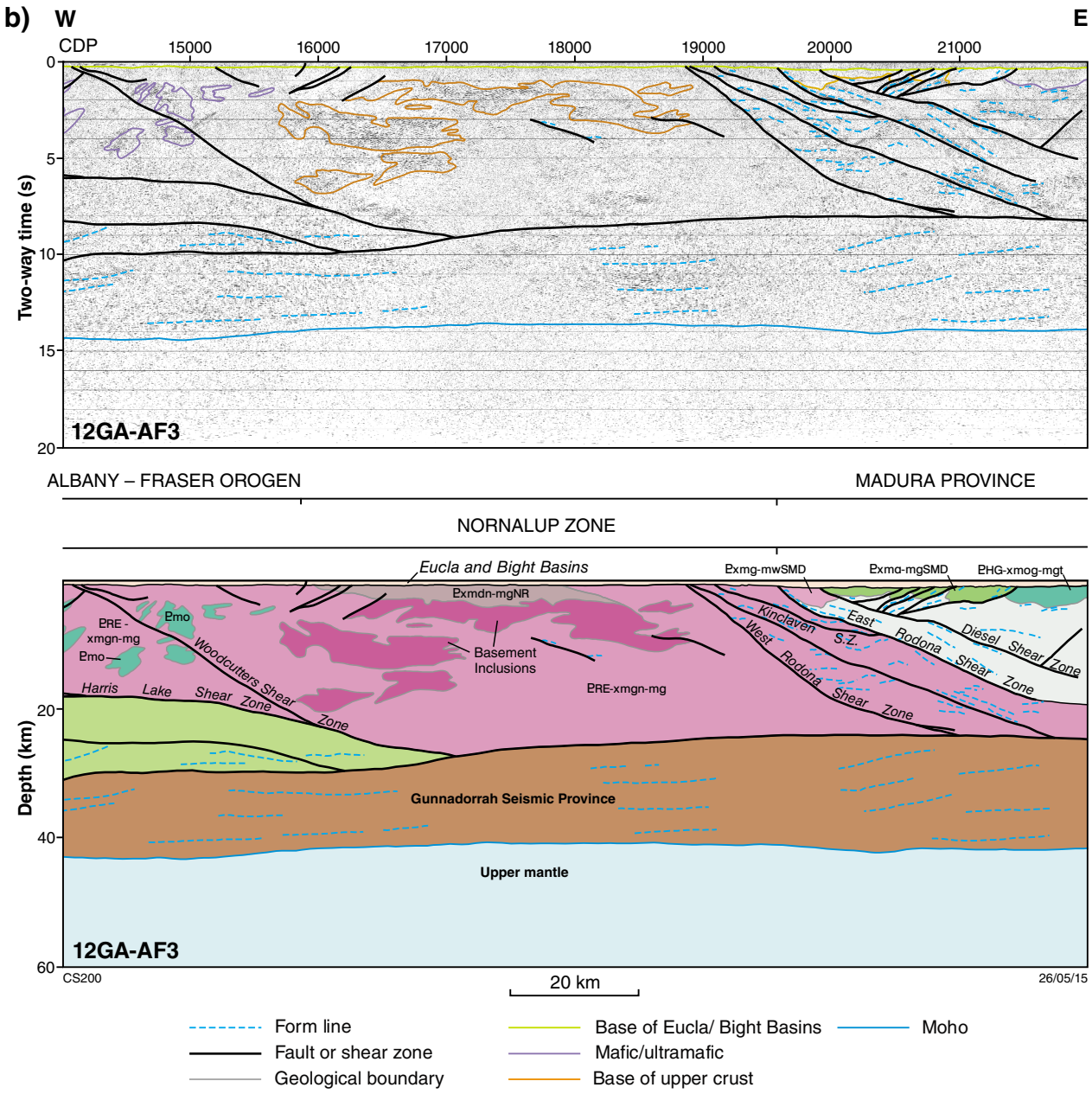

Figure 6. continued

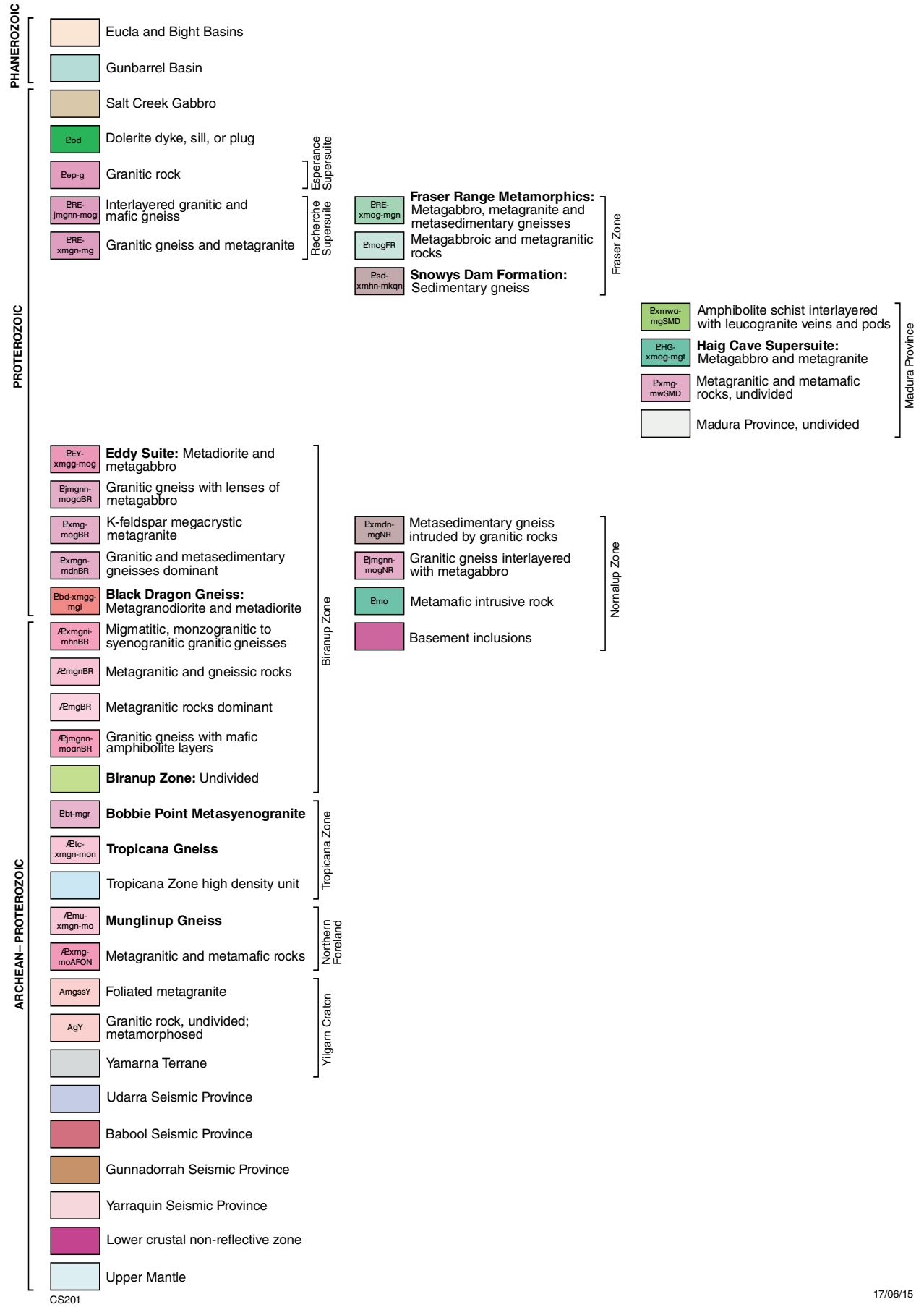

Figure 7. Reference for the units shown in the migrated sections in Figures 4, 5 and 6

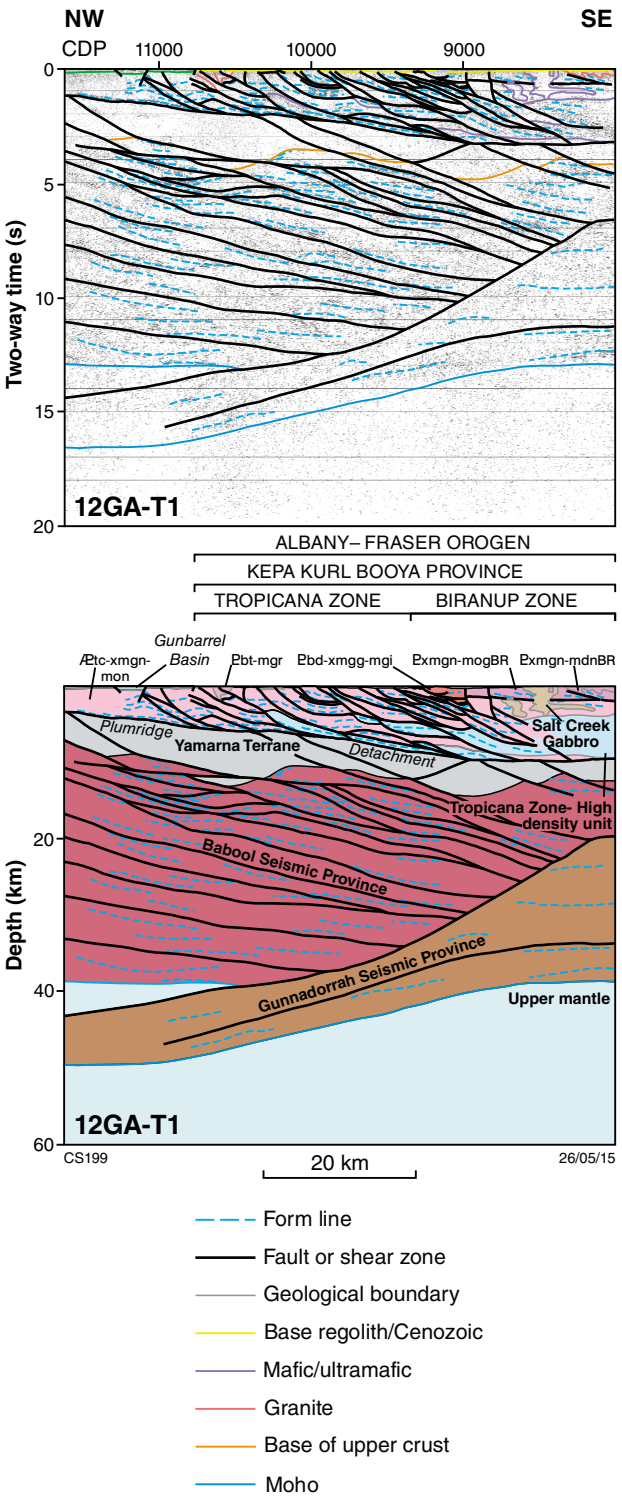

Figure 8. Migrated section for seismic line 12GA-T1, showing both uninterpreted and interpreted versions. Display is to 20 s TWT (~60 km) depth, and shows vertical scale equal to the horizontal scale, assuming a crustal velocity of 6000 ms^{-1} for the entire section.

In line 12GA-T1, we have interpreted the Moho as being displaced along a low-angle fault, with a northwest-dip component, at about CDP 10 550, and a vertical displacement of about 3.5 s TWT (~10 km) implying a thrust sense of movement with a top-to-the-southeast sense of displacement (Fig. 8; Plate 4). At the southeastern end of the line, lower crustal subhorizontal reflections define the Moho at about 13 s TWT (~39 km). This reflective package can be tracked towards the northwest, becoming gently northwest-dipping and penetrating deeper to at least 16.3 s TWT (~49 km) in the lower crust. At the northwestern edge of seismic line 12GA-T1, we have interpreted the Moho to occur beneath subhorizontal reflections, at about 13 s TWT (~39 km). We have mapped this fault upwards to a depth of about 6.6 s TWT (~19 km) in the middle crust, at the southeastern edge of the line (Fig. 8). An alternative interpretation by Kennett (2014) is that the Moho deepens progressively towards the northwestern margin of the line, and is not faulted.

In our interpretation of line 12GA-AF3, we map the Moho as being displaced by a low-angle, west-dipping fault, at about CDP 10 650, with a vertical displacement of about 2.3 s TWT (~7 km) showing a top-to-the-east thrust movement, similar to that observed on seismic line 12GA-T1 (Fig. 6; Plate 4). We have mapped this fault as flattening in the middle crust, as it does not appear to cut through the crust to the surface. An alternative interpretation by Kennett (2014) is that the Moho is not faulted, but that the crust thickens considerably from about 13 s TWT (~39 km) at the western end of the line to about 16.3 s TWT (~49 km) centred below CDP 10 650, and then shallows eastwards to a depth of about 14 s TWT (~42 km).

In seismic line 12GA-AF2, we have shown the Moho to be continuous, but interpreted the crust to be thicker in the central part of the line (about 15.2 s TWT, ~46 km) than on the western side (about 12.8 s TWT, ~38 km) and on the eastern side (about 12.2 s TWT, ~37 km) (Fig. 5; Plate 4; see also Kennett, 2014). Nevertheless, the position of the Moho is poorly constrained where the crust is thickest, and it is possible that the Moho could be faulted, similar to our interpretations for lines 12GA-AF3 and 12GA-T1 (Figs 6 and 8). There does not appear to be any Moho offset in line 12GA-AF1 (Fig. 4).

Crustal architecture

In the region of the Albany–Fraser seismic survey, the upper crust can be subdivided into several discrete provinces and overlying basins (Fig. 9), based principally on surface geological mapping, the interpretation of potential field data, and drillhole data. These are the Youanmi, Kurnalpi and Yamarna Terranes of the Yilgarn Craton, several tectonic units in the Albany–Fraser Orogen (Northern Foreland including the Munglinup Gneiss; Tropicana, Biranup, Fraser and Nornalup Zones of the Kepa Kurl Booya Province), the Madura Province, as well as the Carboniferous–Permian Gunbarrel Basin, the Mesozoic Bight Basin and the Cenozoic Eucla Basin (Plates 1, 2 and 3). By comparison, much of the middle to

lower crust appears to have a different seismic character, which is distinctive from that imaged in the upper crust immediately above it. Following Korsch et al. (2010), we use the term 'seismic province' to refer to a discrete volume of middle to lower crust, which cannot be traced to the surface, and whose crustal reflectivity is different to that of laterally or vertically adjoining provinces. Thus, we interpret the Babool Seismic Province (as defined by Korsch et al., 2013b) to occur in the middle to lower crust beneath the Yamarna Terrane, and the Yarraquin Seismic Province (as defined by Korsch et al., 2013a) to occur in the middle to lower crust below the Youanmi Terrane (Figs 4, 5 and 8; Plate 4). Here, we term the middle to lower crust beneath the Kurnalpi Terrane, the Udarra Seismic Province (new name, after Udarra Soak) (Fig. 6; Plate 4), as we are not yet able to demonstrate that it is the equivalent of either the Yarraquin Seismic Province to the southwest or the Babool Seismic Province to the northeast.

Beneath part of the Albany–Fraser Orogen, we infer the presence of a new seismic province, the Gunnadorrah Seismic Province (new name, after Gunnadorrah Homestead), which occurs mainly beneath the eastern Nornalup Zone, and has been mapped on all four seismic lines (Figs 4, 5, 6 and 8; Plate 4).

Yilgarn Craton

The Yilgarn Craton in Western Australia is a large (~1000 by ~1000 km) Archean granite–greenstone terrain which forms a major part of the West Australian Craton, and represents well over one billion years of craton formation. The craton has been subdivided into several terranes (Fig. 9; Cassidy et al., 2006; Pawley et al., 2012), and consists of metamorphosed mafic and felsic volcanic and intrusive rocks, and metasedimentary units, intruded by granite and gneissic granite, which formed mainly between 3050 and 2620 Ma (Cassidy et al., 2006). However, in the Narryer Terrane in the northwest of the craton, there are rocks with ages of c. 3730 Ma (Kinny et al., 1988). These are the oldest known rocks in Australia. The Albany–Fraser seismic survey provides images of parts of three terranes along the southeastern margin of the craton (Fig. 9).

Youanmi Terrane

The Youanmi Terrane contains greenstone belts, consisting of mafic and felsic volcanic successions and associated sedimentary rocks, mainly in the age range 2760–2620 Ma, but with some as old as c. 3000 Ma (Pidgeon and Wilde, 1990; Van Kranendonk et al., 2013). Granite and gneissic granite intrusions volumetrically form much of the terrane. Although there are some granites with ages up to c. 3010 Ma, the large majority are younger than c. 2720 Ma (Cassidy et al., 2006; Ivanic et al., 2012).

Seismic line 12GA-AF2 crosses part of the southernmost, poorly exposed part of the Southern Cross Domain of the Youanmi Terrane, between CDP 4002 and 4865 (Fig. 5; Plate 4). Here the crust consists of two layers: 1) a weakly to moderately reflective upper crust of variable thickness, ranging from about 2.0 s TWT (~6 km) at about CDP 4100 to about 3.7 s TWT (~11 km) at about CDP 8500; 2) a strongly reflective middle to lower crust, with the reflections dipping gently to the southeast (Fig. 5; Plate 4).

Because of the very distinct change in the seismic character at the boundary between the upper and middle crust, we follow Korsch et al. (2013a) and confine the Youanmi Terrane (sensu stricto) to only the upper crust. We define its base as the contact with the Yarraquin Seismic Province (Korsch et al., 2013a), as defined by relatively non-reflective upper crust and the package of strong reflections in the middle to lower crust.

In the vicinity of line 12GA-AF2, the Youanmi Terrane is only weakly reflective, so is likely to consist predominantly of granite, which, seismically, is typically weakly to non-reflective. Weak parallel reflections probably relate to gneissic fabric in deformed granites. We have interpreted a set of very strong reflections in the upper crust at 0.3 to 0.7 s TWT (~1–2 km depth) to be a mafic sill, similar to those imaged on previous seismic lines farther to the north in the Youanmi Terrane (Ivanic et al., 2013). In the vicinity of the seismic line, the Youanmi Terrane has been intruded by mafic dykes. These are typically mapped as subvertical, and hence have not been imaged in the seismic section.

Kurnalpi Terrane

The Kurnalpi Terrane contains greenstone belts, consisting of mafic and felsic volcanic successions and associated sedimentary rocks, which range in age from c. 2715 to 2704 Ma (e.g. Kositcin et al., 2008), and granites having very similar, and younger, crystallization ages (see summary in Korsch et al., 2011). The volcanic rocks have a calc-alkaline geochemistry consistent with an island-arc signature (e.g. Barley et al., 2008). There is also limited evidence for older, c. 2800 Ma granite, greenstone and sedimentary successions in the terrane (e.g. Kositcin et al., 2008). Nevertheless, based on Sm–Nd data from younger granites, the Kurnalpi Terrane is isotopically the most juvenile terrane in the Yilgarn Craton (Champion and Cassidy, 2008).

Seismic line 12GA-AF3 crosses part of the southernmost Kurnalpi Terrane, between CDP 6002 and 7850 at the surface (Fig. 6a; Plate 4). Here the crust consists of two layers: 1) a thin, upper crust, which, in general, is only weakly to moderately reflective, and variable in thickness, ranging from about 0.5 s TWT (~1.5 km) at about CDP 7070 to about 1.5 s TWT (~4.5 km) at about CDP 7900; 2) a thick, strongly reflective middle to lower crust, with the reflections dipping gently to the east (Fig. 6a; Plate 4).

Because of the very distinct change in the seismic character at the boundary between the upper and middle crust, and because we are unable to track the strong reflections in the middle to lower crust to the surface, at this stage we confine the Kurnalpi Terrane (sensu stricto) to only the upper crust. We define its base as the contact

with the Udarra Seismic Province, as defined by thin, relatively non-reflective upper crust and a package of strong reflections in the middle to lower crust. Previous work on seismic lines BMR91-EGF01 (Drummond et al., 1993, 2000) and 01AGS-NY1 (Goleby et al., 2004) noted the presence of the reflective middle to lower crust, but, at that time, did not define it as a discrete seismic province.

In the vicinity of line 12GA-AF3, the lack of strong reflections in the Kurnalpi Terrane suggests that, in this area, the terrane consists predominantly of granite. Weak parallel reflections are probably due to gneissic fabric in deformed granites. We have interpreted a set of very strong reflections dipping to the west in the upper crust at 0.3 – 0.7 s TWT (~1–2 km depth) to be a mafic sill (Fig. 6a; Plate 4). Farther to the north, seismic line 01AGS-NY1 crossed almost the entire Kurnalpi Terrane. There, it has a similar, weakly reflective uppermost crust, but is considerably thicker, up to 3 s TWT (~9 km) thick (Goleby et al., 2004, 2006).

Yamarna Terrane

The easternmost terrane in the Yilgarn Craton, the Yamarna Terrane, (Fig. 9), is mostly concealed beneath cover. Nevertheless, it contains greenstone belts which are all younger than 2720 Ma. This is in contrast to the other terranes in the Yilgarn Craton (with the exception of the Kalgoorlie and Kurnalpi Terranes) which also contain older greenstone belts (Cassidy et al., 2006; Pawley et al., 2012). Seismic line 12GA-T1 is interpreted to cross part of the southernmost Yamarna Terrane, now concealed beneath the Tropicana Zone (Fig. 8; Plate 4).

We follow Korsch et al. (2013b) in confining the Yamarna Terrane (sensu stricto) to only the upper crust, which consists of granite–greenstone units. Its base is defined as the contact with the Babool Seismic Province (Korsch et al., 2013b), defined by the relatively non-reflective upper crust above the package of strong reflections in the middle crust which have an apparent dip to the southeast (Fig. 8; Plate 4). In seismic line 12GA-T1, this boundary is shown to be displaced by a series of extensional faults which dip to the southeast (Fig. 8).

The top of the Yamarna Terrane in seismic line 12GA-T1 is at a depth of about 1.2 s TWT (~3.5 km) at CDP 11 500 and deepens to about 3.3 s TWT (~10 km) at about CDP 8450. This terrane is up to just over 2 s TWT (~6 km) thick (Fig. 8; Plate 4). The seismic character of the Yamarna Terrane in line 12GA-T1 is very similar to that observed on seismic line 11GA-YO1 to the north (Korsch et al., 2013b), but it is not as reflective as observed on seismic lines 01AGS-NY1 and 01AGS-NY3 (Goleby et al., 2003, 2004).

Albany–Fraser Orogen

All of the lines in the Albany–Fraser seismic survey cross most of the tectonic units mapped in the east and central Albany–Fraser Orogen. In combination, these seismic lines provide a cross-section from the southern Yilgarn Craton across the orogen to the Madura Province to the east. Seismic lines 12GA-AF1, 12GA-AF2 and 12GA-AF3 are described in detail by Spaggiari et al. (2014b), and seismic line 12GA-T1 is described in detail by Occhipinti et al. (2014). A summary of the interpretations of these lines is provided below.

Northern Foreland including Munglinup Gneiss

The Northern Foreland consists of rocks from the southeastern part of the Yilgarn Craton which have been reworked during the Albany–Fraser Orogeny (Myers, 1990; Spaggiari et al., 2009, 2011). It is predominantly granitic in character, and includes the Munglinup Gneiss in the southern part of our study area (Plate 3). U–Pb SHRIMP crystallization ages for the granitic rocks range from c. 2722 to 2619 Ma, typical of ages from the Yilgarn Craton (Spaggiari et al., 2011; Kirkland et al., 2014). One granodioritic gneiss has a crystallization age of c. 1300 Ma (Nelson, 1995), corresponding to Stage I of the Albany–Fraser Orogeny. High-temperature metamorphism has been dated from 1210 to 1180 Ma, corresponding to Stage II of the Albany–Fraser Orogeny (Spaggiari et al., 2011; Kirkland et al., 2011a).

The Northern Foreland is imaged on seismic lines 12GA-AF2 and 12GA-AF3 (Figs 5 and 6a; Plate 4), whereas the Munglinup Gneiss is imaged only on line 12GA-AF2 (Fig. 5; Plate 4). On seismic line 12GA-AF2, the Northern Foreland occurs between two southeast-dipping faults, the Jerdacuttup Fault at CDP 4865 and the Cascade Shear Zone at CDP 5640. Farther east, the Northern Foreland is represented by the Munglinup Gneiss, which extends from the Cascade Shear Zone to the Red Island Shear Zone at about CDP 8380 (Fig. 5; Plates 3 and 4). In seismic line 12GA-AF2, Northern Foreland crust lacking Munglinup Gneiss has a similar seismic character to the Youanmi Terrane immediately to the west, being a weakly reflective zone interpreted to occur above the more highly reflective Yarraquin Seismic Province. On line 12GA-AF3, the Northern Foreland again occurs between two east-dipping shear zones, the Cundeelee Shear Zone at CDP 7850 and the Frog Dam Shear Zone at CDP 8680 (Fig. 6a; Plate 4). In this seismic section, the western half of the Northern Foreland has a similar seismic character to the Kurnalpi Terrane immediately to the west, being a weakly reflective zone. However, east of the Yellow Dam Shear Zone at CDP 8370 the Northern Foreland is highly reflective, with a series of strong reflections dipping to the east and subparallel to the bounding Yellow Dam and Frog Dam Shear Zones (Fig. 6a; Plate 4).

In the vicinity of seismic line 12GA-AF2, there is a major increase in metamorphic grade across the Cascade Shear Zone. Rocks of the Northern Foreland to the west are greenschist facies, whereas rocks of the Munglinup Gneiss to the east are recrystallized to upper amphibolite facies. This suggests relative uplift of the eastern block across this shear zone.

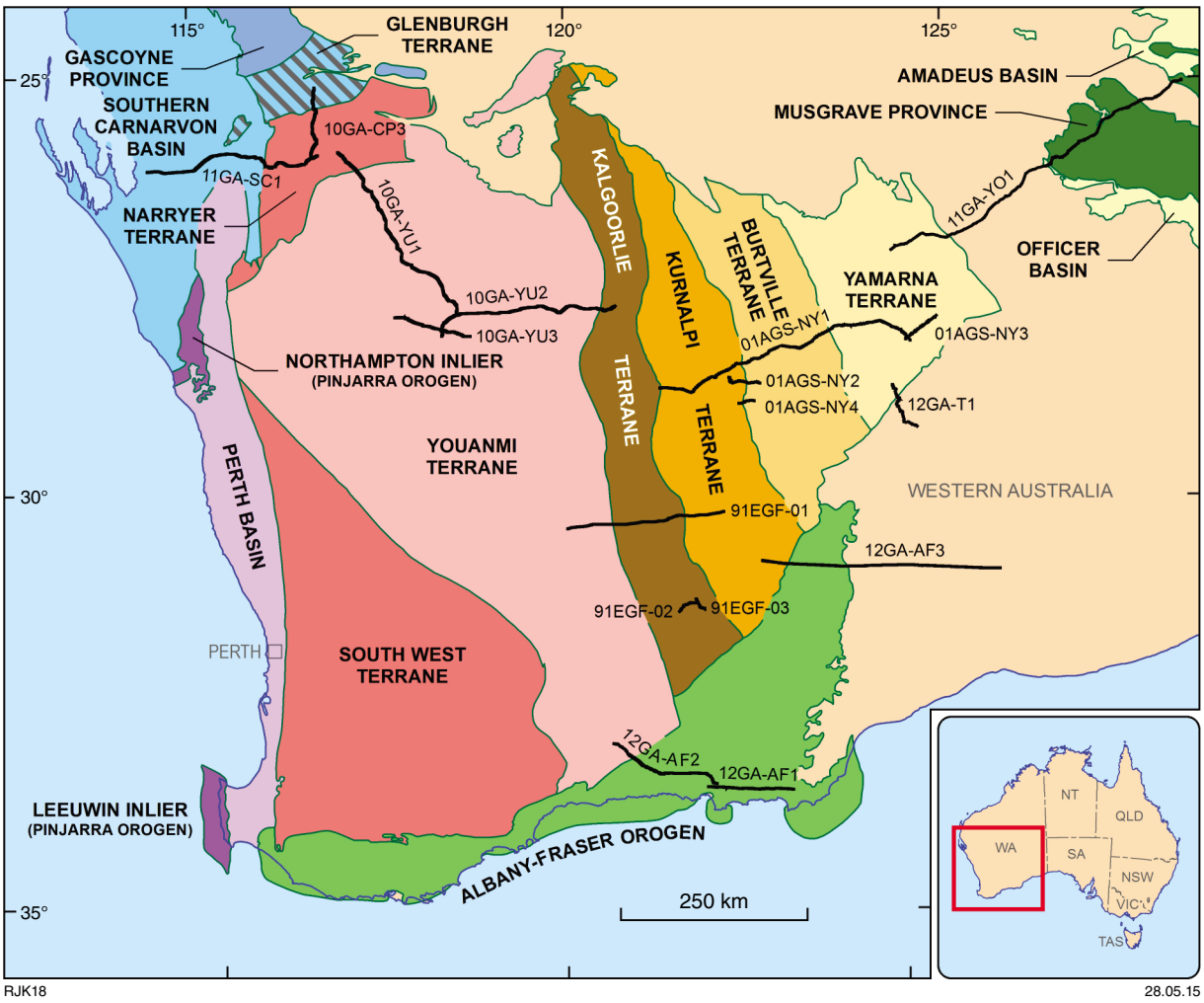

Figure 9. Map of the key tectonic units in the vicinity of the Albany–Fraser seismic survey in Western Australia, showing the locations of the major deep crustal seismic reflection lines

The western part of the Munglinup Gneiss, between CDP 5800 and the Young River Shear Zone at CDP 6960 on seismic line 12GA-AF2, is interpreted to be very thin skinned, with a maximum thickness of about 2 s TWT (~6 km). It can be subdivided into an upper, strongly reflective part and a lower, weakly reflective part, separated by a gently southeast-dipping fault, which occurs at a maximum depth of about 1.5 s TWT (~4.5 km) (Fig. 5; Plate 4). Farther to the east, from the Young River Shear Zone to the Red Island Shear Zone, are a series of thrusts in the Munglinup Gneiss which we interpret to cut more deeply into the crust, eventually linking onto the Red Island Shear Zone at a depth of about 5.7 s TWT (~17 km) at about CDP 9850 (Plate 4). East of CDP 6040, the Cascade and Young River Shear Zones separate the Munglinup Gneiss from the Yarraquin Seismic Province below.

Tropicana Zone

The Tropicana Zone consists of high-grade metamorphic rocks that include the Tropicana Gneiss (Occhipinti et al., 2014). The paucity of outcrop in the Tropicana Zone limits our understanding of the relationship between different units in the region, and the description below taken from Doyle et al. (2014) is based on analysis of rock from drillcore and reverse circulation drill chips. Precursor granitic rocks of orthogneisses belonging to the Tropicana Gneiss have been dated between 2700 and 2640 Ma. The Tropicana Gneiss also contains garnet gneiss, amphibolite, mafic granulite, quartzofeldspathic gneiss, metaferruginous chert, and metapegmatite, metamorphosed to amphibolite to granulite facies (Doyle et al., 2013). It is likely that these rocks form part of a metamorphosed granite–greenstone terrane. Without detailed geochemistry and analysis of the volumetric abundance of different rock types that could be attributed to granites or components of a greenstone belt; however, it is difficult to be certain of this.

Both large- and small-scale, apparently shallow to moderately southeast or east-dipping structures within the Tropicana Gneiss have been interpreted in the region from limited field observations and analysis of magnetic

data (Spaggiari et al., 2011; Occhipinti et al., 2014). Change in magnetic character within the Tropicana Zone is often attributable to the juxtaposition of different units, sometimes due to faulting. Such structures have been observed in seismic line 12GA-T1, thus supporting the interpretation of structures from magnetic data.

Previously, part of the Tropicana region has been included in the Northern Foreland of the Albany–Fraser Orogen, based on the presence of Archean Yilgarn Craton-like rocks (e.g. Spaggiari et al., 2011). Based on new work (Blenkinsop and Doyle, 2014; Doyle et al., 2014; Occhipinti et al., 2014), and the interpretation that the Tropicana region appears to have been thrust an unknown distance over the Yamarna Terrane via the Plumridge Detachment, it is no longer included in the Northern Foreland (Plate 1). It does share the Paleoproterozoic history of the Albany–Fraser Orogen, however, as it is clearly intruded by igneous rocks of Biranup Zone age and affinity, and is thus named the Tropicana Zone of the Kepa Kurl Booya Province (Spaggiari et al., 2014a; Kirkland et al., 2014, Occhipinti et al., 2014).

Seismic line 12GA-T1 provides an excellent image of the upper crust in the vicinity of the Tropicana gold deposit (Fig. 8; Plate 4; Doyle et al., 2007). A series of linked, listric faults dip to the southeast and sole onto a gently-dipping detachment (named the Plumridge Detachment by Occhipinti et al., 2014), which extends across the entire seismic section, from a depth of about 1.2 s TWT (~3.5 km) at CDP 11 500 to a depth of about 3.3 s TWT (~10 km) at about CDP 8450. The presence of hangingwall anticlines suggests that the listric faults dominantly have a thrust sense of displacement.

On seismic line 12GA-T1, the northwestern part of the Tropicana Zone extends beneath the Gunbarrel Basin to a depth of up to 200 ms TWT (about 350 m). At the southeastern end of the line, between CDP 8002 and the Blue Robin Shear Zone at CDP 9340, a thin sliver of rock has been interpreted to have been thrust over the top of the Tropicana Zone on a very low angle to subhorizontal fault (Fig. 8; Plate 4; Occhipinti et al., 2014). The sliver has a maximum thickness of about 700 ms TWT (~2 km) and contains rocks of the Biranup Zone (Spaggiari et al., 2011). Thus, the Tropicana Zone extends beyond the limits of the seismic line, both to the northwest under cover of the Gunbarrel Basin, and to the southeast for an unknown distance beneath the Biranup Zone.

At this stage, the southern limit of the Tropicana Zone is yet to be defined. At the latitude of line 12GA-AF3, Biranup Zone rocks with a similar geological history to the Tropicana Gneiss within the Tropicana Zone have, as yet, not been found. One possibility is that a rock package interpreted to occur beneath the upper crust of the Biranup Zone on line 12GA-AF3 could be equivalent to the Tropicana Gneiss of the Tropicana Zone. This package extends from a depth of 2.1 s TWT (~6 km) at CDP 9200 well into the middle crust to a depth of about 9.8 s TWT (~32 km) at CDP 16 150 (Fig. 8; Plate 4). The top of this package is defined as the Frog Dam Shear Zone, which extends to the surface where it is juxtaposes the Biranup Zone over the Northern Foreland. Alternatively, this package could represent the lowermost part of the Biranup Zone, or even the upper part of the mid- to lower crustal Udarra Seismic Province.

Biranup Zone

The Biranup Zone consists of Paleoproterozoic mid-crustal rocks with crystallization ages in the range c. 1810 to 1625 Ma, within which occurs fragments of granite with Archean crystallization ages consistent with being remnants of the Yilgarn Craton (Spaggiari et al., 2011; Kirkland et al., 2011a, 2014). The southeastern part of the zone has been intruded by 1330–1280 Ma granites of the Recherche Supersuite during Stage I of the Albany–Fraser Orogeny. Parts of the Biranup Zone have been imaged on all four seismic lines in the Albany–Fraser seismic survey.

On seismic line 12GA-AF2, the Biranup Zone extends from the Red Island Shear Zone at CDP 8380 to the Coramup Shear Zone at CDP 11 150 (Fig. 5; Plate 4). Here, the upper crust is mostly highly reflective, with packages of reflections dipping both to the east and to the west. The zone is dominated by east-dipping shear zones, although, in places, there are west-dipping shear zones which we interpret to sole onto, or are truncated by, major east-dipping shear zones which cut deep into the crust. The Biranup Zone extends to the east, in the subsurface, onto seismic line 12GA-AF1, bounded by the Red Island and Coramup Shear Zones (Fig. 4; Plate 4). Below the Biranup Zone, the Yarraquin Seismic Province forms the middle to lower crust (see below).

On seismic line 12GA-AF3, the Biranup Zone extends from the Frog Dam Shear Zone at CDP 8680 to the Fraser Shear Zone at CDP 11 100 (Fig. 6a; Plate 4). The zone is highly reflective, with east-dipping reflective packages interpreted to be bound by subparallel faults, with the major ones cutting deep into the middle crust. Rollover anticlines in the hangingwalls of some faults indicate a predominant thrust sense of displacement. The zone can be tracked deep into the crust to the top of the lower crust, below which the Gunnadorrah Seismic Province is interpreted (see below).

At the southeastern end of line 12GA-T1, between CDP 8002 and the Blue Robin Shear Zone at CDP 9340, a thin sliver of rock, with a maximum thickness of about 700 ms (~2 km), has been interpreted as part of the Biranup Zone (Fig. 8; Plate 4; Occhipinti et al., 2014). It has been thrust over the top of the Tropicana Zone on the very low angle to subhorizontal Blue Robin Shear Zone (Occhipinti et al., 2014).

Fraser Zone

The Fraser Zone predominantly consists of sheets of c. 1300 Ma amphibolite to granulite-facies metagabbroic rocks, interlayered with sheets of similar aged granitic material and sedimentary rocks which were also metamorphosed at c. 1300 Ma (Spaggiari et al., 2011; Kirkland et al., 2011a; Clark et al., 2014). The Fraser Zone was only imaged in seismic line 12GA-AF3,

where it is bound to the west by the east-dipping Fraser Shear Zone at CDP 11 100, and to the east by the west-dipping Boonderoo Shear Zone at CDP 13 880. The latter is interpreted to sole onto, or be cut by, the Fraser Shear Zone at CDP 12 740 at a depth of about 4.2 s TWT (~13 km). Thus, the Fraser Zone is interpreted to have a V-shaped geometry between the two main shear zones (Fig. 6a; Plate 4; Spaggiari et al., 2014b). This is consistent with the extruded, pop-up architecture proposed by Spaggiari et al. (2013).

The western two-thirds of the Fraser Zone is dominated by moderately to strongly reflective packages separated by a series of east-dipping shear zones. There is a large antiform between CDP 13 000 and CDP 13 400, and the eastern edge of the zone is defined by at least two west-dipping fault-bound rock packages, which terminate against the Fraser Shear Zone at depth (Fig. 6a; Plate 4).

Eastern Nornalup Zone

The eastern Nornalup Zone is the easternmost zone recognized in the east Albany–Fraser Orogen, and is dominated by the 1330–1280 Ma Recherche Supersuite and the 1200–1140 Ma Esperance Supersuite, formed during Stages I and II of the Albany–Fraser Orogeny, respectively. Rare granitic gneisses within the eastern Nornalup Zone have crystallization ages of c. 1809 and 1763 Ma (Spaggiari et al., 2011), similar to ages found in the Biranup Zone to the west (Kirkland et al., 2011a). The zone has been imaged on lines 12GA-AF1, 12GA-AF2 and 12GA-AF3, occurring to the east of the Coramup Shear Zone at CDP 11 150 on seismic line 12GA-AF2, across the entire line, at the surface, on line 12GA-AF1, and between the Boonderoo Shear Zone at CDP 13 880 and the East Rodona Shear Zone at CDP 19 540 on seismic line 12GA-AF3 (Figs 4, 5 and 6b; Plate 4).

Repeated intrusion of magma, along with contemporaneous deformation, has led to variable reflectivity in the seismic sections across the eastern Nornalup Zone (Fig. 6b; Plate 4; see also Spaggiari et al., 2014b). Consequently, the seismic sections across the eastern Nornalup Zone have been difficult to interpret. The western one-third of the eastern Nornalup Zone, between the Coramup Shear Zone on line 12GA-AF2 and the Parmango Shear Zone at CDP 4250 on line 12GA-AF1, is dominated by east-dipping, highly reflective packages separated by a series of east-dipping shear zones (Figs 4 and 5). Several rollover anticlines in the hangingwalls indicate a dominant thrust sense of displacement. The seismic packages are interpreted to have been intruded locally by irregularly shaped bodies of granite assigned to the Esperance Supersuite (Figs 4, 5 and 6b; Plate 4).

Farther east on line 12GA-AF1, between the Parmango Shear Zone and the Tagon Shear Zone at CDP 6700, the eastern Nornalup Zone is dominated by weak reflections, interpreted to be granitic material (Fig. 4; Plate 4). Segments of highly reflective material, likely representing rafts, surrounded by the weakly reflective granitic material, are interpreted to be mafic in composition (Spaggiari et al., 2014b). East of the Tagon Shear Zone, the upper crust is dominated by a series of east-dipping listric faults, with rollover anticlines in the hangingwall indicating a dominant thrust sense of displacement. Alternatively, when combined with the next shear zone to the east, these curved features could be interpreted as an S–C fabric, indicative of extensional movement along the Tagon Shear Zone. These listric faults link onto a sole thrust, which has a maximum depth of about 1.8 s TWT (~5 km). Several of these listric faults appear to have been folded during later deformation (Fig. 4; Plate 4).

On seismic line 12GA-AF3, the eastern Nornalup Zone occurs between the Boonderoo Shear Zone and the East Rodona Shear Zone (Fig. 6b; Plate 4). Here, the seismic character of the zone is very similar to the central part of the zone on line 12GA-AF1. It is mostly weakly reflective, consistent with granitic material, and contains rafts of irregularly shaped, highly reflective material. These are interpreted to be mafic in composition in the west, and metasedimentary or basement inclusions in the east (Spaggiari et al., 2014b).

Madura Province

Because of its width of about 14 km in the vicinity of line 12GA-AF3, we have divided the Rodona Shear Zone into the West Rodona Shear Zone and East Rodona Shear Zone (Fig. 6b; Plate 4). The East Rodona Shear Zone is inferred to bound the eastern edge of the Albany–Fraser Orogen (Spaggiari et al., 2011, 2012, 2014b,c). East of the East Rodona Shear Zone at CDP 18 820, seismic line 12GA-AF3 crosses about 50 km of the western part of the Madura Province. Basement rocks of the Madura Province are completely covered by younger rocks of the Cretaceous–Eocene Bight and Eucla Basins, and, to the north, also by the Neoproterozoic Officer Basin, which underlies the younger cover. Hence, the geology of the Madura Province is poorly understood, only being sampled in a few drillholes (Spaggiari et al., 2012).

Drilling at the Burkin prospect, approximately 65 km north of seismic line 12GA-AF3, intersected gneissic and metasedimentary rocks, as well as amphibolite (Spaggiari et al., 2012). U–Pb SHRIMP zircon geochronology on a sample of interpreted migmatitic gneiss highlighted the complexity: three zircon cores (either inherited or detrital) were dated at c. 2408 to 2293 Ma, four grains provided a possible maximum depositional age of c. 1538 Ma (if the gneiss is interpreted to have a sedimentary protolith), and possible high temperature migmatization (which post-dated deformation) is interpreted to have occurred at c. 1478 Ma (Kirkland et al., 2012). Alternatively, the c. 1478 Ma date may also be of detrital origin. Importantly, all ages in this rock are distinct from crystallization ages of igneous rocks in the Albany–Fraser Orogen (Spaggiari et al., 2012).

The Loongana, Haig and Serpent drillholes, in the vicinity of seismic line 12GA-AF3, intersected weakly layered cumulate metagabbro and ultramafic rocks intruded by trondhjemitic plagiogranite (Spaggiari et al., 2014c). U–Pb SHRIMP geochronology on five samples of metamorphosed gabbro, tonalite and granite from the Loongana LNGD001 and LNGD002 drillholes provided crystallization ages within error of c. 1410 Ma, which is

younger than the ages from the sample of gneiss from the Burkin prospect (summarized in Spaggiari et al., 2011, 2012). Whole-rock geochemistry indicates that these gabbroic rocks are primitive, subduction-related intrusions, consistent with formation in an ocean-arc environment (Spaggiari et al., 2014c). This is supported by the Hf isotopes of zircons, which also indicate a juvenile source (Spaggiari et al., 2014c). Again, the c. 1410 Ma age is not recognized as crystallization ages of igneous rocks west of the Rodona Shear Zone in the Albany–Fraser Orogen.

Much farther south, metasedimentary rocks, collectively termed the Salisbury Gneiss, are exposed on offshore islands. A migmatitic leucosome from Salisbury Island provided U–Pb zircon SHRIMP ages of c. 1214 and 1182 Ma, interpreted as crystallization or metamorphic ages, which is within the age range of Stage II of the Albany–Fraser Orogeny (Clark et al., 2000).

In seismic line 12GA-AF3, between the West Rodona and Diesel Shear Zones at CDP 19 860, are packages of moderate to strong reflections of variable dip which are bound by east-dipping faults showing a thrust sense of displacement (Fig. 6b; Plate 4). Farther east, towards the eastern end of the line, are a series of west-dipping faults which sole onto, or are cut by, the Diesel Shear Zone. This package of rocks has variable reflectivity, with the uppermost non-reflective part being penetrated for 200 m by the GSWA MAD002 drillhole.

Lower crustal seismic provinces

Across the four seismic lines, we have mapped several areas in the middle to lower crust which have a different seismic reflectivity to the upper crust above them. When we are unable to track these rock packages to the surface, we refer to them as seismic provinces, and have almost no constraints on their geological composition or age.

Yarraquin Seismic Province

The Yarraquin Seismic Province was defined by Korsch et al. (2013a) as the highly reflective middle and lower crust, in the Youanmi seismic survey, which occurs below the entire Youanmi Terrane (sensu stricto), from the Yalgar Fault in the northwest to the Ida Fault in the east. Here, we use the term to refer to the moderately to strongly reflective middle and lower crust below the Youanmi Terrane on line 12GA-AF2 (Fig. 5; Plate 4). Our interpretations imply that this seismic province extends, in the subsurface, below the Northern Foreland, Munglinup Gneiss and Biranup Zone, to the top of the Gunnadorrah Seismic Province at about CDP 4600 on line 12GA-AF1 (Fig. 4; Plate 4), a distance of over 210 km.

Neodymium model ages for granites show that the eastern Youanmi Terrane has an average crustal age of 3500–3000 Ma (Champion and Cassidy, 2008; Wyche et al., 2012). If the granites were derived from the middle or lower crust, this would imply that the age of the Yarraquin Seismic Province is not significantly older than the oldest rocks currently found at the surface in the Youanmi Terrane. Hf data on zircon crystals, however, suggest that granites of the eastern Youanmi Terrane have sampled 4300–3100 Ma model-aged material at depth, presumably from the Yarraquin Seismic Province (Wyche et al., 2012).

Udarra Seismic Province

On seismic line 12GA-AF3, the middle to lower crust is highly reflective, and substantially different in seismic character to the Kurnalpi Terrane at the surface (Fig. 6a; Plate 4). As we have not been able to track these rocks to the surface, we have no direct constraints on their lithology or age. We are not able to demonstrate that this rock package forms part of the Kurnalpi Terrane, albeit with a different structural fabric. Hence, at this stage, we treat this seismic province as a discrete package of rocks which forms the current basement to the granite–greenstone rocks of the Kurnalpi Terrane, and is here termed the Udarra Seismic Province (see above). It extends from the western edge of the seismic section to the boundary with the Gunnadorrah Seismic Province at a depth of about 11 s TWT (~33 km) at about CDP 13 000, a distance of about 140 km (Fig. 6a; Plate 4).

The Kurnalpi Terrane was crossed by seismic line 01AGS-NY1 (Goleby et al., 2004, 2006), and showed a similar crustal reflectivity to that imaged in line 12GA-AF3, with a weakly reflective upper crust and a strongly reflective middle to lower crust. Goleby et al. (2004, 2006), however, did not identify the middle to lower crust as a separate seismic province.

The Kurnalpi Terrane predominantly contains volcanic and intrusive rocks with calc-alkaline geochemistries which range in age from c. 2720 to 2700 Ma. They are interpreted to represent an oceanic island arc (Barley et al., 2008; Kositcin et al., 2008; Korsch et al., 2011). A greenstone succession that is older than 2800 Ma is also present in the eastern part of the terrane. Neodymium model ages for granites show that the Kurnalpi Terrane has an average crustal age of 2950–2800 Ma (Champion and Cassidy, 2008; Wyche et al., 2012), and is the most juvenile terrane in the Yilgarn Craton. Model ages of Hf data from zircons suggest that granites of the Kurnalpi Terrane have sampled 3400–3000 Ma material at depth (Wyche et al., 2012), presumably from the Udarra Seismic Province. If the granites were derived from the middle or lower crust, this would imply that the Udarra Seismic Province contains a component that is older than the oldest rocks currently found at the surface in the Kurnalpi Terrane.

Babool Seismic Province

The Babool Seismic Province was defined by Korsch et al. (2013b) as the highly reflective middle and lower crust, which occurs below the Yamarna Terrane (sensu stricto), as observed in the Yilgarn–Officer–Musgrave seismic reflection line (11GA-YO1). Here, we use the term to

refer to the moderately to strongly reflective middle and lower crust below the Yamarna Terrane on line 12GA-T1 (Fig. 8; Plate 4). Our interpretation implies that, in the middle crust, this seismic province extends across the entire seismic line, but that in the lower crust it extends to the boundary with the Gunnadorrah Seismic Province (see below).

Geochronological and isotopic data from the Yamarna Terrane are relatively sparse, and SHRIMP U–Pb zircon ages from greenstones and associated granites range between c. 2711 and 2645 Ma, with rare inherited zircons as old as 2940 Ma (see Pawley et al., 2012). The Nd model ages for granites from the Yamarna Terrane suggest an average crustal age of 3000–2900 Ma (Champion and Cassidy, 2008). Zircon Hf-isotope data collected on two samples from the Yamarna Terrane reveals a substantial juvenile input (εHf values are positive), and a mantle extraction age of c. 3200 to 3000 Ma (Wyche et al., 2012). Thus, the Babool Seismic Province, may form older basement below the Yamarna Terrane.

If the model ages described above are representative of each seismic province, then it is apparent that the Udarra Seismic Province has significantly younger Nd and Hf model ages than those inferred from the Yarraquin Seismic Province, and younger Nd model ages than those inferred from the Babool Seismic Province. Thus, we are unable to determine whether the Udarra Seismic Province is the same crust as the Yarraquin Seismic Province to the west, and the Babool Seismic Province to the northeast. Hence, at this stage, they are regarded as separate seismic provinces.

The Yarraquin, Udarra and Babool Seismic Provinces all have similar seismic reflectivity beneath terranes of the Yilgarn Craton, predominantly defined by strong, subhorizontal to gently east dipping reflections. A similar origin for each province could be inferred, possibly relating to large-scale crustal extension. Analogue centrifuge modelling by Harris et al. (2002) and Bédard et al. (2013) have produced scenarios which resemble the current seismic architecture of these seismic provinces. However, to produce the current thickness of the seismic province only by extension, the crust would have to have been originally of Himalayan thickness (i.e. about 70 km). A possible solution is that large-scale extension of a crust of normal thickness was followed by later contraction, which thickened the crust to approximately its current thickness.

Gunnadorrah Seismic Province

In the eastern half of seismic line 12GA-AF3, the lower crust predominantly consists of subhorizontal reflections with moderate to strong reflectivity (Fig. 6; Plate 4). This reflectivity is significantly different to that observed in the Fraser Zone, eastern Nornalup Zone and Madura Province in the upper to middle crust above it. Hence, we refer to it as a separate seismic province, the Gunnadorrah Seismic Province. At the eastern end of seismic line 12GA-AF3, the seismic province is up to 5.5 s TWT (~16 km) thick, and gradually thins to the west. We have mapped it as far west as the inferred fault in the Moho at about CDP 9200 (Fig. 6; Plate 4). Major structures in the upper and middle crust, such as the Frog Dam and Fraser Shear Zones, appear to sole onto the top of the seismic province, rather than penetrate through the seismic province to the Moho. A possible interpretation is that the Gunnadorrah Seismic Province represents lower crust that has been reworked, overprinting any previous structures.

A similar change in seismic character in the lower crust is observed at the southeast end of seismic line 12GA-T1. Here, very strong, southeast-dipping reflections in the Babool Seismic Province are separated from moderately reflective subhorizontal reflections across a fault interpreted to cut and displace the Moho (Fig. 8; Plate 4). Because of the similar seismic character in the lower crust between the eastern end of line 12GA-AF3 and the southeastern end of line 12GA-T1, we consider these areas to be part of the Gunnadorrah Seismic Province.

In the eastern half of seismic line 12GA-AF2, and on all of seismic line 12GA-AF1, the lowermost crust immediately above the Moho is weakly to moderately reflective, with the reflections being essentially subhorizontal (Figs 4 and 5). This segment is up to 3.3 s TWT (~10 km) thick, and we have interpreted it to be the Gunnadorrah Seismic Province, as it has a similar seismic character to where that seismic province has been interpreted in seismic lines 12GA-AF3 and 12GA-T1 (Figs 6 and 8).

Lower crustal non-reflective zones

Near the western end of seismic line 12GA-AF2, beneath the Munglinup Gneiss, is a large, anomalous region of low reflectivity occurring within the Yarraquin Seismic Province in the lower crust. It extends for about 75 km laterally, is up to 8.5 s TWT (~25 km) thick and occurs immediately above the thickest portion of crust in this section (Fig. 5; Plate 4). Possible explanations for this zone of reduced impedance contrast could be that it is a large alteration zone associated with crustal thickening, a possible large source region for magmatism, or a large zone of extensive deformation which has obliterated the earlier seismic fabric.

A zone of reduced impedance contrast, of similar size to that interpreted on line 12GA-AF2, has been interpreted in the lower crust near the western end of seismic line 12GA-AF3. Here, it again occurs where the crust is thickest, but immediately above where we have interpreted the Moho to have been cut and displaced (Fig. 6a; Plate 4).

Similar zones of reduced impedance contrast have been observed in mineralized regions such as within the middle crust of the Kalgoorlie region, where an anomalous region of low reflectivity has been interpreted to represent either extensive deformation or large-scale alteration within the area (Drummond et al., 2000). Another zone of reduced impedance contrast occurs in the lower crust beneath the Olympic Dam deposit in South Australia, which Drummond et al. (2006) interpreted to be the source-region for the magma of the Hiltaba Suite granite hosting the deposit.

Younger successions

Paterson Formation

The late Carboniferous to early Permian Paterson Formation occurs on seismic line 12GA-T1, between the Gunbarrel Fault at CDP 10 760 and the northwestern end of the line at CDP 11 671, overlying rocks of the Tropicana Zone (Fig. 8; Plate 4). The formation is generally poorly imaged, possibly because it is mainly glaciogene in origin (e.g. Jackson and Van de Graaff, 1981). Based on drillhole information, it is at least 300 m thick just west of the Gunbarrel Fault (R Hocking, in Spaggiari et al., 2011, p. 60). On the seismic line, the Paterson Formation is thickest in the vicinity of CDP 11 200, where it is about 200 ms TWT thick (about 350 m, based on a P-wave velocity of 3500 ms^{-1}).

Eucla and Bight Basins

The Eucla Basin was defined originally by Lowry (1970) to include both Cretaceous and Cenozoic successions found onshore north of the Great Australian Bight. Hill (1991), however, included the Cretaceous successions in the mainly offshore Bight Basin, thus limiting the Eucla Basin to the Cenozoic succession, including its offshore components. At the surface, seismic line 12GA-AF3 crosses the western portion of the Eucla Basin, and part of the Bight Basin in the subsurface. The western limit of the Eucla Basin occurs at about CDP 12 670, and the basin extends to the east, to well beyond the eastern end of the seismic line (Fig. 6; Plate 4). The Eucla Basin component is only weakly reflective and is poorly imaged, for example, around CDP 14 500 (Plate 4). The maximum thickness of the Eucla and Bight Basins in the vicinity of the seismic line is constrained by the GSWA MAD002 stratigraphic drillhole, where the base of the Bight Basin is at approximately 375 m true depth (Spaggiari et al., 2014b), and by the Haig prospect drillholes where it is at approximately 400 m (Tillick, 2011).

Regolith

In the region of the Albany–Fraser seismic survey, basement is usually masked by a thin regolith. On the seismic sections, a strong reflection or set of reflections often occurs near the surface; this represents the change from very slow velocities in the thin regolith to fast velocities in the underlying bedrock.

New geochronology from the Coompana Province

Here, we refer to the basement in the region between the Mundrabilla Shear Zone (eastern edge of the Madura Province) and the western edge of the Gawler Craton in South Australia as the Coompana Province (after Flint and Daly, 1993; Myers et al., 1996). It is not exposed, being completely covered by sedimentary rocks of the Eucla and Bight Basins, and/or the Officer Basin. Hence, its geology is poorly known, being based on a few drillhole intersections. Note, however, that Shaw et al. (1996) subdivided the Coompana Province into three separate units based on interpretation of geophysical datasets — the Forrest, Waigen and Coompana Provinces. Here, we do not use those subdivisions, but consider the westernmost unit as the Forrest Zone of the Coompana Province. In an attempt to further understand the Coompana Province, and its relationship to the Madura Province and Albany–Fraser Orogen, geochronological and related studies have been conducted as part of this project on currently available drillcore samples.

The only published geochronology on basement rocks in southeast Western Australia, east of the Mundrabilla Shear Zone, comes from the Eucla 1 petroleum exploration well (Stach, 1964), which intersected granitic basement at a depth of 214 m. U–Pb SHRIMP zircon geochronology undertaken by GSWA on cuttings from the 215–225 m intervals provided a crystallization age of 1140 ± 8 Ma (GSWA 194773, Kirkland et al., 2011b), which is within the age range of the Esperance Supersuite of Stage II of the Albany–Fraser Orogeny (Spaggiari et al., 2012). A single zircon age of c. 1600 Ma could represent an inherited basement component to the Coompana Province.

In South Australia, the Coompana Province predominantly consists of mafic volcanic rocks with interlayered sedimentary rocks, along with mafic and granitic intrusive rocks (Flint and Daly, 1993). In the petroleum exploration well Mallabie 1, gneissic granite was intersected below mafic volcanic and sedimentary rocks (Scott and Speer, 1969). The gneissic granite has an interpreted U–Pb LA-ICPMS zircon crystallization age of c. 1505 Ma (Wade et al., 2007), an age not found in the Albany–Fraser Orogen. K–Ar dating of biotite and hornblende from the gneissic granite provided an age of c. 1180 Ma (Webb et al., 1982), indicating likely thermal resetting coincident with Stage II of the Albany–Fraser Orogeny.

Two petroleum exploration wells were drilled recently by Rodinia Oil (Australia) Pty Ltd in the western Officer Basin in South Australia, and penetrated basement of the Coompana Province at a depth of 2639 m in Mulyawara 1 (Baily et al., 2012a), and a depth of 2390 m in Kutjara 1 (Fig. 10; Baily et al., 2012b). Petrographic analysis of basement rocks in both wells has identified quartz monzonite (Baily et al., 2012a). The dating by SHRIMP U–Pb zircon geochronology of cuttings of a basement sample from each of these wells was undertaken at GA (Neumann and Korsch, 2014).

GA sample number 2152083 (GSSA R1964856) is a sample of drill cuttings collected over the depth interval 2682–2691 m from the Mulyawara 1 well, approximately 42 m below the base of the Officer Basin. It contains three inherited grains (c. 1615 to 1532 Ma), with 22 analyses giving an interpreted magmatic crystallization age of this granitoid of 1168 ± 6 Ma (Fig. 11; Neumann and Korsch, 2014).

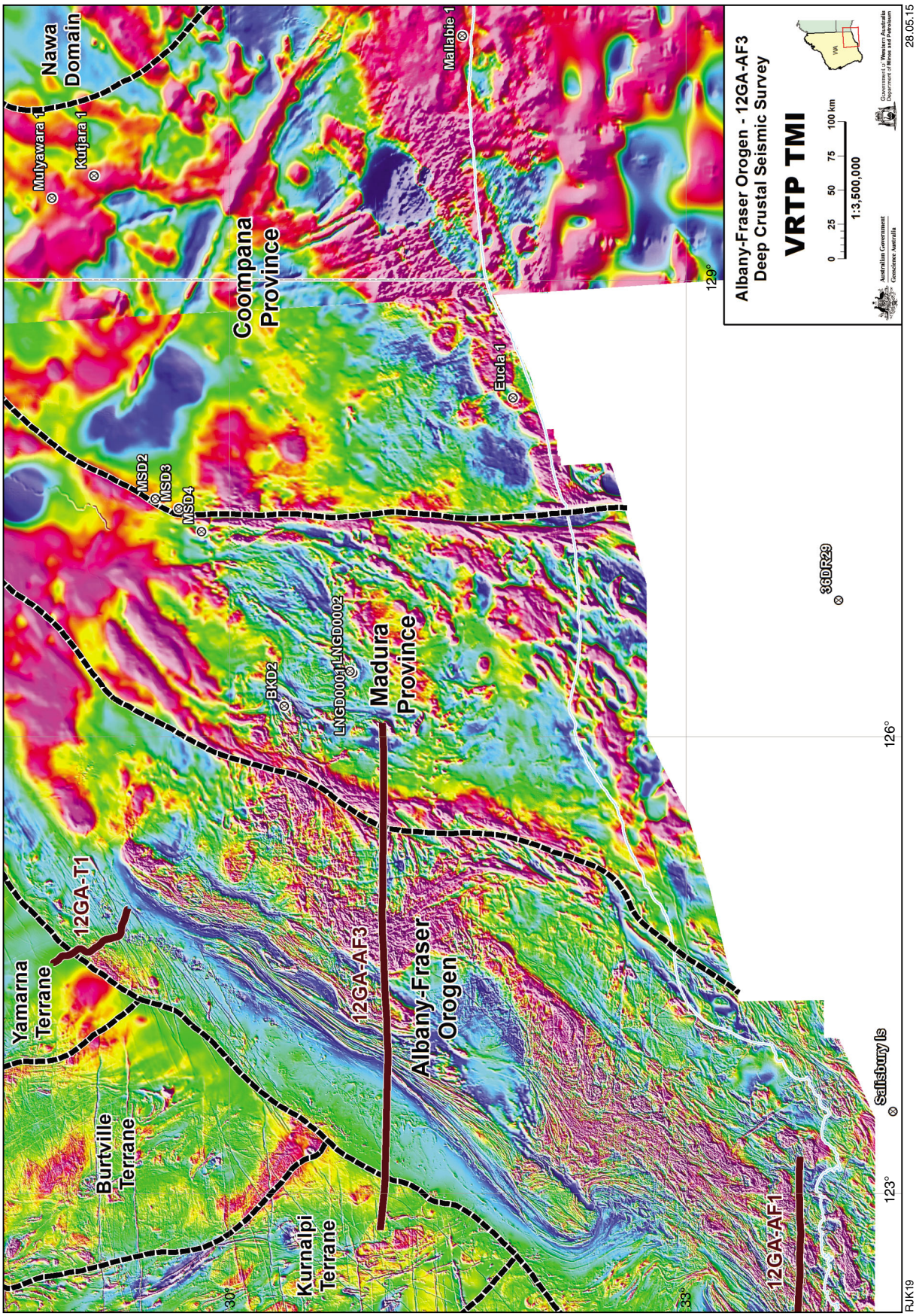

Figure 10. Map showing regional aeromagnetic data and locations of sample localities and key drillholes discussed in the text from the Madura and Coompana Provinces

GA sample number 2152082 (GSSA R1964851) is a sample of drill cuttings collected over the depth interval 2445–2454 m from the Kutjara 1 well, approximately 55 m below the interpreted base of the Officer Basin. It contains one inherited grain (c. 1657 Ma), with 30 analyses giving an interpreted magmatic crystallization age of this granitoid of 1591 ± 11 Ma (Fig. 11; Neumann and Korsch, 2014). A further 24 analyses from zircon rims with low Th/U values yielded an age of 1167 ± 7 Ma, which is interpreted to represent a metamorphic event affecting the granitoid (Fig. 11; Neumann and Korsch, 2014).

In addition, previously unpublished geochronology results on samples from mineral exploration drillholes by WMC Resources Ltd (Richardson, 2005) from the Mundra South prospect, in the vicinity of the Mundrabilla Shear Zone (Fig. 10), are summarized here. These include U–Pb zircon geochronology by LA-ICPMS and Hf-isotopic data by LA-MC-ICPMS collected by GEMOC (Table 1; Griffin et al., unpublished report).

Sample RA55309 is of gneiss from drillhole MSD4, in the Madura Province, just to the west of the Mundrabilla Shear Zone. It contains two inherited grains at c. 1560 Ma and has an interpreted magmatic crystallization age of 1500 ± 11 Ma (Fig. 12). This age has not been encountered so far as an igneous crystallization age in the Albany–Fraser Orogen, and, although unknown from the Madura Province (see above), is essentially identical in age to the granitic gneiss from the Coompana Province in South Australia (Wade et al., 2007). The maximum Hf model age is c. 2.1 Ga (Fig. 13) but, given the evidence for possible mixing with juvenile input (e.g. range of five εHf units), the actual maximum model age could be greater.

Sample RA55307 is of granite from drillhole MSD3, in the Forrest Zone of the Coompana Province, just to the east of the Mundrabilla Shear Zone. It has an inferred magmatic crystallization age of 1280 ± 11 Ma, and a possible metamorphic resetting age of c. 1215 Ma (Fig. 12). These ages are consistent with Stages I and II of the Albany–Fraser Orogeny, respectively. Two inherited grains are c. 1460 and 1430 Ma, similar in age to detrital zircons from metasedimentary rocks in the Fraser

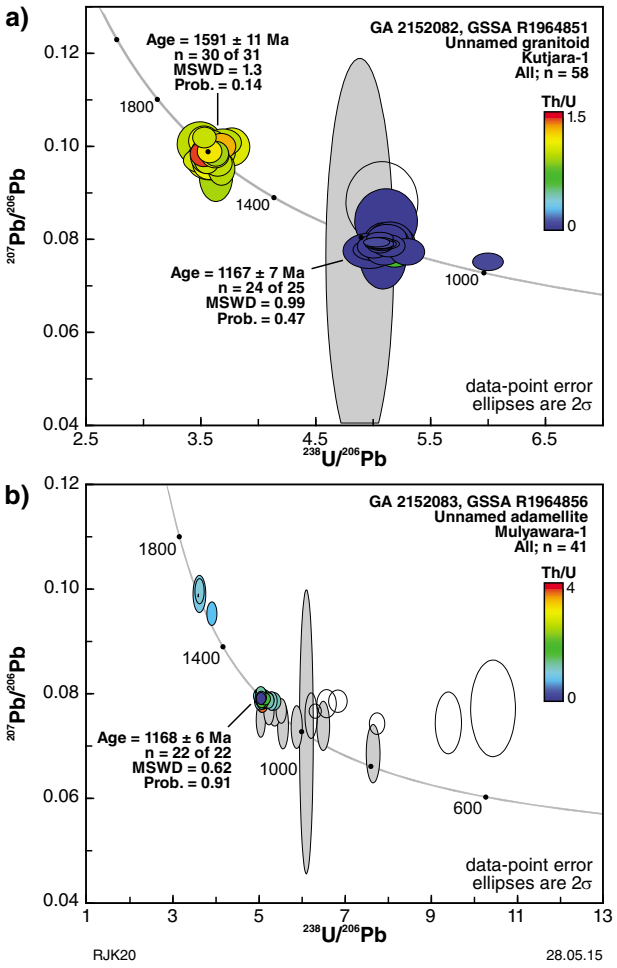

Figure 11. Tera-Wasserburg concordia diagram showing results of zircon analyses from: a) unnamed granitoid, Kutjara 1 (sample GA 2152082, GSSA R1964851); b) the unnamed adamellite Mulyawara 1 (sample GA 2152083, GSSA R1964856), coloured according to Th/U values (after Neumann and Korsch, 2014). Open ellipses represent analyses greater than 10% discordant, and grey-coloured ellipses represent analyses with a common ^{206}Pb content higher than an arbitrary value of 0.5%.

Table 1. Summary of new geochronology results for samples from drillholes in the region

Drillhole	*Sample*	*Lithology*	*Inheritance (Ma)*	*Magmatism (Ma)*	*Resetting/ metamorphism (Ma)*	*Hf model age (Ga)*
MSD3	RA55307	granite	c. 1460, 1430	1280 ± 11 (N = 14)	1216 ± 12 (N = 11)	c. 1.7
MSD3	RA55308	alkaline intrusive	2980, 2550–2380 (N = 4)	c. 1287 (N = 3)		
MSD4	RA55309	gneiss	c. 1560 (N = 2)	1500 ± 11 (N = 18)		c. 2.1
MSD2	RA55310	basalt	c. 3300 (N = 3), 1800, c. 1470 (N = 2), c. 1380 (N = 2), 1205	?610 (N = 1)		
Mulyawara 1	GA2152083	granitoid	1615–1532 (N = 3)	1168 ± 6		
Kutjara 1	GA2152082	granitoid	1657 (N = 1)	1591 ± 11	1167 ± 7	

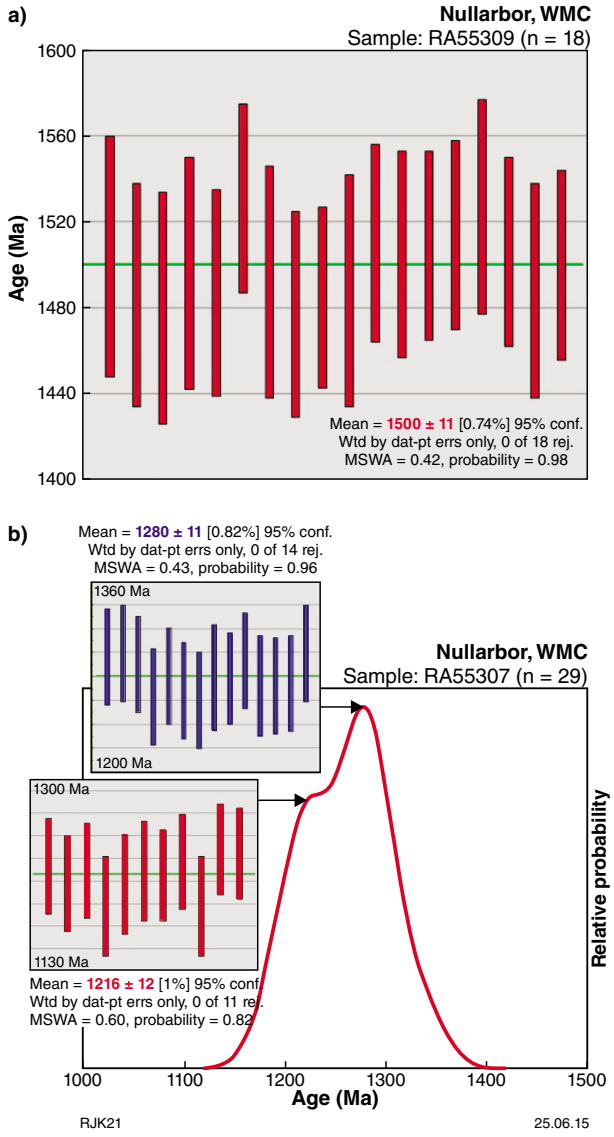

Figure 12. a) Weighted mean age diagram showing $^{207}Pb/^{206}Pb$ ages of zircons from Madura Province gneiss, WMC sample RA55309 (hole MSD4); b) relative probability and weighted mean age diagrams showing $^{207}Pb/^{206}Pb$ ages of zircons from the Forrest Zone, Coompana Province granite, WMC sample RA55307 (hole MSD3)

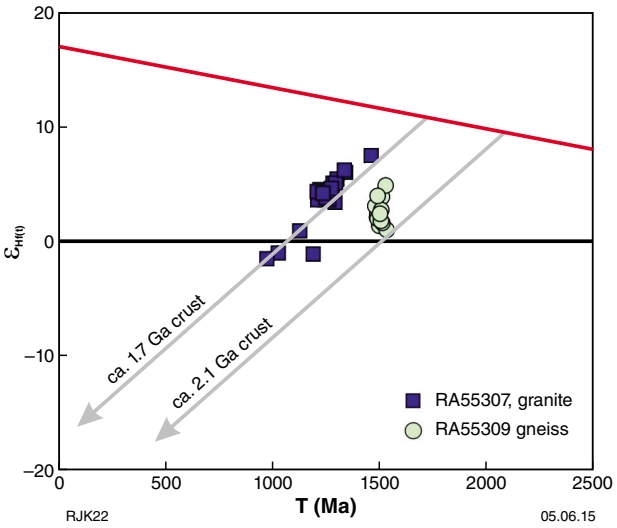

Figure 13. εHf versus time diagram for zircons from the gneiss (Madura Province) and granite (Coompana Province) WMC samples shown in Figure 12. Evolution lines for c. 1.7 Ga crust and c. 2.1 Ga crust illustrate different protoliths for the granite and the gneiss.

Zone, which are interpreted as derived from the Madura Province (Spaggiari et al., 2011, 2014c). The average Hf model age for this sample is c. 1.7 Ga (Fig. 13), which could indicate a different protolith to that of the gneiss in sample RA55309 (Fig. 13). Thus, it is possible that the Mundrabilla Shear Zone represents a major crustal structure separating different pieces of crust, which was reactivated as a late stage intraplate shear zone (Crawford et al., 2012). Sample RA55308 is a possible alkaline intrusive from the same drillhole. Zircons were scarce, and were mainly inherited grains at c. 2980 to 2380 Ma, and three grains at c. 1287 Ma, similar to the crystallization age of the granite sample RA55307.

Sample RA55310 is of basalt from drillhole MSD2, in the Forrest Zone of the Coompana Province, just to the east of the Mundrabilla Shear Zone. Zircons were rare and predominantly inherited, with ages at c. 3300 Ma (N = 3), c. 1800 Ma, c. 1470 Ma (N = 2) and c. 1380 Ma (N = 2). The two youngest single grains have ages of c. 1205 and 610 Ma, the significance of which is unclear.

Crustal-scale shear zones

The entire region of the Albany–Fraser seismic survey is dominated by east-dipping shear zones. With the exception of the Boonderoo Shear Zone on line 12GA-AF3, which bounds the eastern side of the Fraser Zone, all the shear zones which bound the provinces or zones are interpreted as west-directed thrusts, although some of these are likely to have an oblique sense of movement.

The most fundamental, crustal-scale shear zone mapped on seismic lines 12GA-AF2 and 12GA-AF1 (Figs 4 and 5; Plate 4) is the Red Island Shear Zone, the boundary between the Northern Foreland (Munglinup Gneiss) and the Biranup Zone. We have interpreted this shear zone to cut deep into the crust. The Cascade Shear Zone links onto the Young River Shear Zone, which eventually links onto the Red Island Shear Zone at a depth of about 5.7 s TWT (~17 km) at CDP 9800 (Fig. 5; Plate 4). The Coramup Shear Zone, the boundary between the Biranup and Nornalup Zones, cuts the Red Island Shear Zone at a depth of about 9 s TWT (~27 km) at about CDP 3800 in 12GA-AF1 (Fig. 4; Plate 4). In combination, these shear zones, as well as several internal shear zones, can be interpreted as part of a major, really extensive, hard-linked imbricate thrust system (Figs 4 and 5; Plate 4) with a likely transpressional component, for example, a dextral shear component on the Coramup Shear Zone.

Farther to the north, in the vicinity of seismic line 12GA-AF3, the major crustal-scale shear zones are the Cundeelee, Frog Dam and Fraser Shear Zones, but these do not appear to form part of a hard-linked thrust system (Fig. 6; Plate 4). Near the eastern end of the seismic line, the West Rodona and East Rodona Shear Zones combine with the Diesel Shear Zone farther to the east to form a broad, east-dipping shear system, which is about 20 km wide at the surface.

The crustal architecture in the vicinity of the Tropicana gold deposit is significantly different to that observed on the seismic lines to the south, with the shallow, low-angle Plumridge Detachment acting as the floor to the Tropicana Zone on seismic line 12GA-T1 (Fig. 8; Plate 4).

Cenozoic faulting

The Albany–Fraser deep crustal seismic lines cross several faults associated with Neogene and younger surface expressions. These scarps are the product of reactivation of pre-existing structures favourably oriented for failure in the prevailing horizontal east–west trending compressive stress field (e.g. Hillis et al., 2008), and provide important tie points constraining the interpretation of the seismic data, and of existing geophysical datasets.

Seismic line 12GA-AF2

The Lort River Scarp (Thom, 1972) is developed in highly deformed rocks of the Munglinup Gneiss. It is 40 km long and up to 3 m high (east side up), and is crossed by seismic line 12GA-AF2 between CDP 7100 and 7115 (Figs 5 and 14; Plate 4). The scarp is associated with an aeromagnetic lineament which is mapped as a fault along strike to the southwest. Trenches excavated across the scarp indicate that it is underlain by a 30–40° (at the surface) east-dipping thrust fault (Estrada, 2009). Single event displacement values obtained in the trenches suggest that the fault has ruptured three times in the last c. 100 ka, twice along the full length of the scarp. Standard relations between scarp length and earthquake rupture dimensions (Leonard, 2010) indicate that such an event would rupture to 10–13 km depth (23–30 km down the fault plane), assuming the dip range cited above is preserved to depth. A surface rupture is hence likely to originate on the Young River Shear Zone at depth.

The northeast-trending Esperance Scarp is ~50 km long. Surface expression, as observed in 10 m DLI DEM (Western Australia Department of Land Information digital elevation model) data, is subtle over much of its length. Towards its northern end, the scarp vertically displaces sandplain deposits by up to 2 m, with a southeast side up sense of movement. A dune field overlying a paleochannel is similarly vertically displaced. This suggests that the scarp is underlain by an east-dipping thrust fault. Surface expression relating to the fault is lost 2.5 km northeast of the seismic line. The projection of the trace, however, intersects line 12GA-AF2 at about CDP 11 540 to 11 550 (Figs 5 and 14; Plate 4). Although the fault does not appear to have been directly imaged in the seismic data, the surface scarp is parallel with the Heywood–Cheyne Shear Zone, suggesting that the fault scarp is possibly the result of a reactivation of a Proterozoic fault within the Heywood–Cheyne Shear Zone.

Seismic line 12GA-AF3

The top of the uppermost lithological unit of the Eucla Basin, the Nullarbor Limestone, was subaerially exposed approximately 15 Ma ago (de Broeckert and Sandiford, 2005; Sandiford, 2007; Hou et al., 2008), forming a vast limestone terrace (the Nullarbor Plain). Very low relief, an almost total absence of fluvial processes (van de Graaff et al., 1977; de Broeckert and Sandiford, 2005), and low bedrock erosion rates (Stone et al., 1994), has resulted in excellent preservation of the c. 15 Ma gently dipping depositional surface (e.g. Hillis et al., 2008). During the course of regional geological mapping, a number of small-displacement (up to several tens of metres), generally north-striking faults were discovered dissecting the plain (Lowry, 1970). The availability of regionally extensive digital elevation data has allowed for the mapping of many more fault displacements of the Nullarbor Plain surface (Fig. 14; Hillis et al., 2008; Clark et al., 2012), and also of the latest Pliocene Roe Plain surface (James et al., 2006). In many cases these features correspond to basement structures (faults and shear zones) imaged in aeromagnetic data. Some appear to cut major aeromagnetic trends; however, indicating that Neogene and younger faults exploit a combination of lithological and structural features most suitable for reactivation in the current east–west horizontal compressive stress field (see Hillis and Reynolds, 2003).

Scarps with distinct surface displacements, which cross seismic line 12GA-AF3, include the Cundeelee Scarp (coincident but distinct from the Boonderoo Shear Zone), the Naretha Scarp (not related to a mapped fault) and scarps associated with the Rodona Shear Zone (Endeavour and Rawlinna scarps).

The Cundeelee Scarp is about 24 km long and up to 8 m high (west side up) where line 12GA-AF3 crosses it between CDP 13 875 and 13 885 (Figs 6a and 10; Plate 4). The scarp is northerly trending, and so the underlying west-dipping fault is likely to be distinct from the northeast-striking Boonderoo Shear Zone. A weakly developed surface expression trending northeast from the southern end of the Cundeelee Scarp is coincident with the mapped position of the Boonderoo Shear Zone, suggesting a structural linkage between the two features.

The 54 km long, west side up, Naretha Scarp is about 12.5 m high where line 12GA-AF3 crosses it between CDP 15 870 and 15 880 (Figs 6b and 10; Plate 4). The underlying west-dipping fault apparently crosscuts the local northwest-trending magnetic grain. At its southern end, the fault terminates proximal to the along-strike continuation of the Tagon Shear Zone, but is poorly imaged in the seismic reflection data.

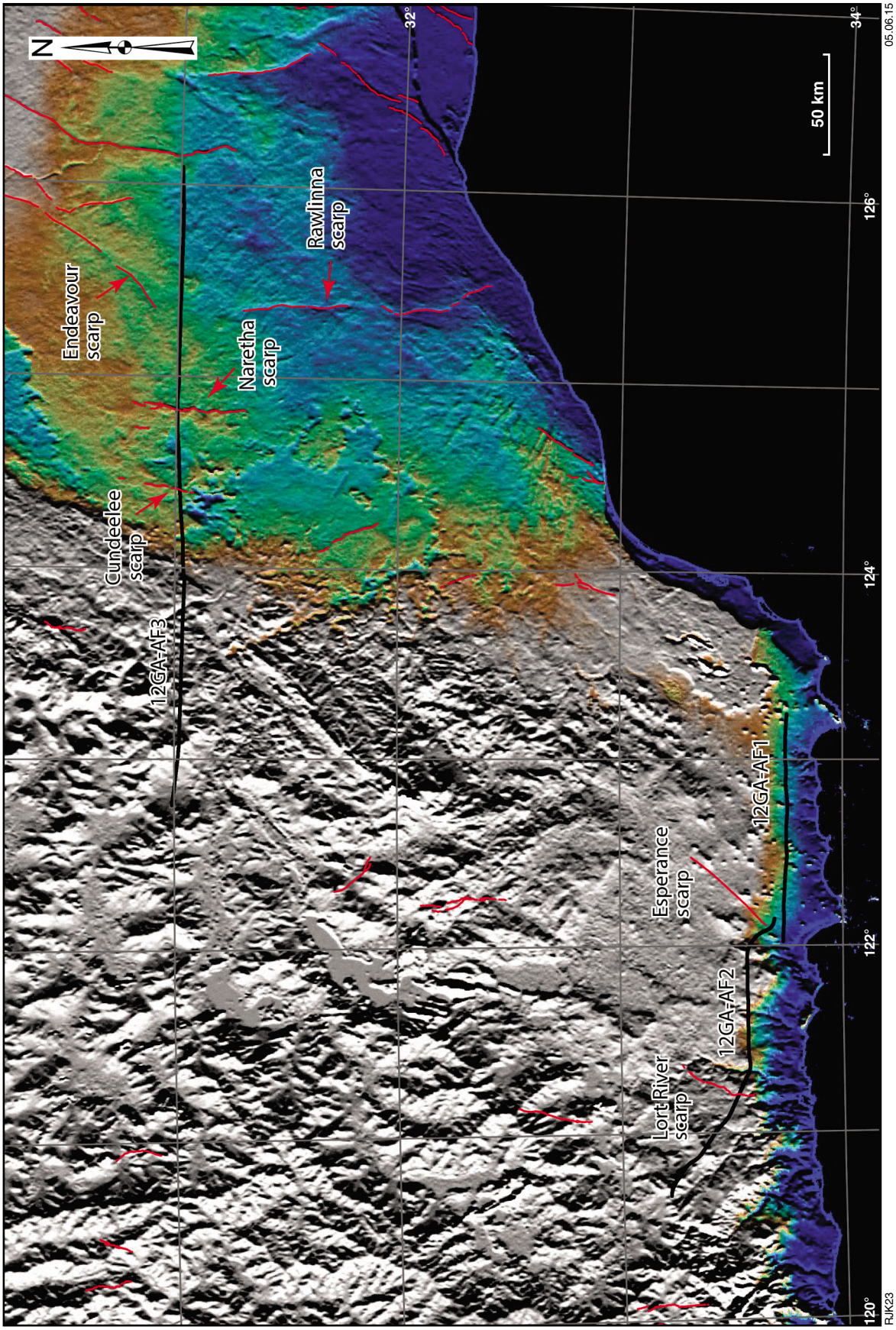

Figure 14. Cenozoic faults on a background image derived from the 3 s shuttle radar topography mission (SRTM) DEM, with hill shading illumination from the west. Colour-drape has been modified to highlight scarps relating to faults displacing rocks of the Eucla Basin. Red lines highlight the scarps.

Seismic line 12GA-AF3 crosses the Rodona Shear Zone, as imaged in aeromagnetic data, between CDP 18 765 and 18 885 (Fig. 6b; Plate 4). West-facing scarps overlie elements of the Rodona Shear Zone to the north (the Endeavour Scarp) and to the south (Rawlinna Scarp) of the line. These attain maximum vertical displacements of about 5–10 m, and overlie east-dipping faults. While relief is evident where the seismic line crosses the Rodona Shear Zone, it is relatively degraded, presumably as the result of paleofluvial action.

Geodynamic implications

The new deep-seismic imaging, extending from the eastern Yilgarn Craton, across the Albany–Fraser Orogen, into the Madura Province, provides, for the first time, a holistic view of the crustal architecture across this poorly exposed part of Western Australia. Based on the nature of the seismic reflectivity, the Youanmi, Kurnalpi and Yamarna Terranes in the Yilgarn Craton are here confined to the upper crust. The crust which underlies them is seismically distinct, and cannot be tracked anywhere to the surface. The middle to lower crust below the Youanmi Terrane is interpreted as the Yarraquin Seismic Province, and that below the Yamarna Terrane as the Babool Seismic Province. A new seismic province, the Udarra Seismic Province, is proposed for the middle to lower crust below the Kurnalpi Terrane. The eastern part of the east Albany–Fraser Orogen is underlain by the Gunnadorrah Seismic Province, which is confined to the lower crust and has a distinctly different seismic reflective character to the eastern Nornalup Zone in the upper to middle crust. It should be noted, however, that the eastern Nornalup Zone on line 12GA-AF1 is heavily affected by Mesoproterozoic magmatism, which appears to have produced a zone of non-reflectivity, and may have masked earlier features. Nevertheless, the seismic images, combined with geological and geophysical data, can be used to help constrain geodynamic models for the region.

Amalgamation of the Yilgarn Craton

The overall architecture of the Yilgarn Craton is dominated by a central nucleus, consisting of the Youanmi Terrane and the underlying Yarraquin Seismic Province (Korsch et al., 2013a,c). Based on Nd-isotopic data, it has been proposed that the Youanmi Terrane has behaved as a coherent crustal block since at least 3000–2900 Ma (Champion and Cassidy, 2010; Ivanic et al., 2012; Van Kranendonk et al., 2013). Following this, the Youanmi Terrane acted as a nucleus, or protocraton, onto which the Narryer Terrane was accreted in the northwest and the Eastern Goldfields Superterrane developed to the east (e.g. Cassidy et al., 2006; Wyche et al., 2012). Terranes on either side of the Youanmi Terrane are interpreted to be bound by crustal-scale faults which dip away from the nucleus, towards the west and northwest on the northwestern side, and towards the east on the eastern side (Korsch et al., 2013c).

Assuming a convergent plate tectonic model, based on analogies with modern day plate tectonic processes, several groups of workers (e.g. Barley et al., 1989; Myers, 1995; Krapez and Barley, 2008; Korsch et al., 2011) have proposed geodynamic models for the Eastern Goldfields Superterrane of the Yilgarn Craton which involve the accretion of allochthonous continental slivers as discrete terranes. Cassidy et al. (2006) considered that formation of the Eastern Goldfields Superterrane by amalgamation of a series of terranes to form the composite Yilgarn Craton was completed by about 2655 Ma. Alternatively, it has been proposed that, rather than a series of allochthonous continental slivers, the Eastern Goldfields Superterrane represents the extended margin of the Youanmi Terrane (Czarnota et al., 2010; Pawley et al., 2012). In this scenario, the older Burtville Terrane would be analogous to a horst of the basement, whereas the greenstone rocks of the younger terranes were deposited in a series of basins following extension after 2720 Ma. In either case, cratonization was essentially complete by c. 2630 Ma (see Champion et al., 2002; Korsch et al., 2013a).

Geodynamic implications of the Tropicana Zone

The Tropicana Zone has been thrust to the northwest onto the Yamarna Terrane of the Yilgarn Craton, along the gently dipping Plumridge Detachment. Internally, the Tropicana Zone is dominated by low-angle thrust faults which sole onto the detachment, as a linked system. Retrograde metamorphism and mineralization in the Tropicana Zone is dated between c. 2520 and 2505 Ma (Doyle et al., 2013, 2014), suggesting that a significant tectonic event occurred at this time; this event has not been recognized in either the Yilgarn Craton or in other zones in the Albany–Fraser Orogen. Extensional faults cutting the base of the Yamarna Terrane show that this terrane has been extended, prior to being overthrust by the Tropicana Zone. This extension, followed by movement on the thrusts and detachment on the Tropicana Zone, may be related to this end-Archean event.

Paleoproterozoic extensional structures

The lack of clearly identified piercing points makes determination of the sense of displacement across faults mapped in the seismic sections very difficult. Nevertheless, the base of the upper crust below the terranes of the Yilgarn Craton can be used as a marker horizon. In seismic line 12GA-AF3, this horizon has been interpreted as being displaced by a series of east-dipping faults, which, in general, show an extensional (down-to-the-east) sense of displacement (Fig. 6a; Plate 4). A similar, extensional sense of displacement is shown for the base of the Yamarna Terrane across east-dipping faults below the Tropicana Zone in seismic line 12GA-T1 (Fig. 8; Plate 4). However, on seismic line 12GA-AF2 the base of the Youanmi Terrane is interpreted to have a thrust sense of displacement on east-dipping faults. This can

be reconciled with the other two seismic sections if the amount of inversion by later thrusting is greater than the amount of initial extension. It is plausible that some of the structures imaged in the seismic sections and interpreted as thrusts, could have been early extensional faults which were later inverted during contractional events.

Crust recognizable as the Yilgarn Craton, and/or its underlying seismic provinces, extends well to the east beneath the Albany–Fraser Orogen. The packages thin eastwards, eventually terminating at about CDP 4300 on line 12GA-AF1 and at about CDP 13 200 on line 12GA-AF3 (Figs 4 and 6a; Plate 4). Thus, it appears that the southeastern part of the Yilgarn Craton has undergone a period of extension and crustal attenuation, possibly during the development of an early Paleoproterozoic passive margin, or when breakup occurred, with removal of the southeastern margin of the Yilgarn Craton. Alternatively, rifting of the southeastern portion of the Yilgarn Craton may have occurred (or have been repeated) during formation of the Paleoproterozoic Barren Basin and synchronous Biranup and Nornalup Zones. This process may have occurred purely as a rift, or in a distal back-arc setting (Spaggiari et al., 2014c).

Barren Basin

The name Barren Basin collectively refers to successions of Paleoproterozoic metasedimentary rocks which were deposited on top of the Yilgarn Craton, and also found outboard in the east Albany–Fraser Orogen (Spaggiari et al., 2011, 2014c). The shallow marine to tidal Stirling Range Formation (Cruse and Harris, 1994) has a maximum depositional age of c. 2016 Ma, based on U–Pb dating of detrital zircon, and a minimum age of c. 1800 Ma, based on U–Pb dating of authigenic xenotime (Rasmussen et al., 2002, 2004). The shallow marine or fluvial Woodline Formation has a maximum depositional age of c. 1737 Ma — based on three U–Pb ages from a single zircon grain (Hall et al., 2008). The deltaic, shallow marine to fluvial Mount Barren Group has a maximum depositional age of c. 1792 Ma, based on U–Pb dating of detrital zircon, and a minimum age of c. 1693 Ma, based on U–Pb dating of authigenic xenotime (Dawson et al., 2002; Vallini et al., 2002, 2005).

The question arises as to whether the sedimentary rocks of the Barren Basin, or at least the older successions, were deposited on a passive margin, as suggested by Hall et al. (2008) in a rift setting, or in a distal back-arc setting during the early stages of formation of the Albany–Fraser Orogen at a convergent margin (Kirkland et al., 2011a), or possibly both. The recent dating of granites as old as 1806 Ma in the Biranup and Nornalup Zones suggests that active margin processes had commenced by about this time. If the Barren Basin was the product of rifting, this may have led to the development of a marginal basin and adjacent passive margin by c. 1600 Ma (Spaggiari et al., 2014c).

Assembly of the southeastern part of Western Australia

The tectonic evolution of the Albany–Fraser Orogen took place between c. 1810 and 1140 Ma (Spaggiari et al., 2011, 2014c). There has been some debate as to the nature and timing of the relationship between the Archean Yilgarn Craton and, to its south and southeast, the Paleoproterozic–Mesoproterozoic Albany–Fraser Orogen. Previous plate tectonic models proposed that part of the Albany–Fraser Orogen was separated by oceanic crust from the Yilgarn Craton, and that a southeast-dipping subduction system closed the ocean between them, with collision and amalgamation occurring at about 1345–1300 Ma (e.g. Myers et al., 1996; Clark et al., 2000; Bodorkos and Clark, 2004b; Spaggiari et al., 2009). More recently, however, Kirkland et al. (2011a,b) and Spaggiari et al. (2011, 2014c) have proposed that, in the Albany–Fraser Orogen, widespread magmatism, sedimentation, high-temperature metamorphism and deformation prior to and during the Biranup Orogeny occurred between c. 1810 and 1665 Ma, as crust of the southeast Yilgarn Craton was extended and thinned, possibly due to rollback of a northwest-dipping subduction zone located outboard, well to the southeast.

Rocks with juvenile, oceanic affinities (Spaggiari et al., 2014c; Kirkland et al., 2014) dated at c. 1410 Ma (summarized in Spaggiari et al., 2011, 2012) occur in the Madura Province and provide support for the existence of an oceanic realm outboard of the Nornalup Zone, at some stage at least, between the end of the Biranup Orogeny at c. 1650 Ma and the start of Stage I of the Albany–Fraser Orogeny at c. 1345 Ma.

Kirkland et al. (2011a,c) and Spaggiari et al. (2011) inferred that prior to Stage I of the Albany–Fraser Orogeny (c. 1345 to 1260 Ma), a northwest-dipping subduction zone may still have been located to the east, outboard of the Biranup and Nornalup Zones, having stepped back farther east (Fig. 15). Gabbros in the Fraser Zone, dated at c. 1300 Ma, have been interpreted by Smithies et al. (2013) and Clark et al. (2014) possibly to have formed in a distal back-arc environment, again suggesting that the subduction zone was located well to the east. We speculate that the arc could have been near the current location of the Mundrabilla Shear Zone, as evidenced by the 1280 Ma age of granite in drillhole MSD3 (see above). If our speculation is correct, the subduction zone must have had a similar polarity to the earlier (c. 1710 to 1650 Ma) subduction event, and the resulting oceanic closure led to the amalgamation of the southeast margin of the West Australian Craton and the combined South Australian Craton – Mawson Craton (see also Bodorkos and Clark, 2004b; Giles et al, 2004). Here, the South Australian Craton is considered to consist of the Gawler Craton, and probably the poorly understood Coompana Province. The Madura Province was possibly an outboard terrane with oceanic affinities which possibly was swept up and accreted to the West Australian Craton during

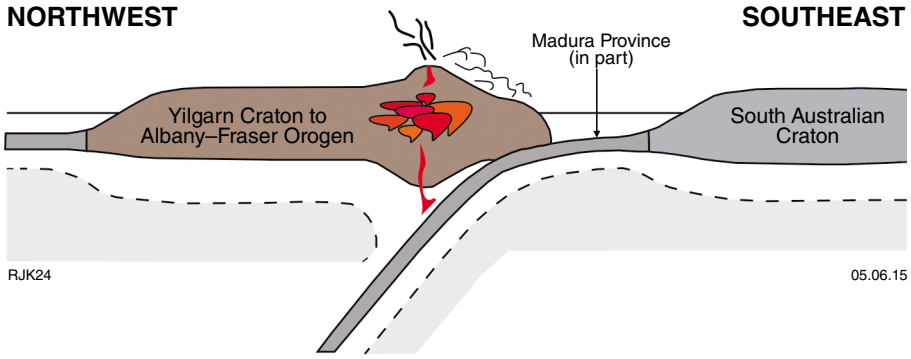

Figure 15. Schematic cross-section, showing a possible scenario for the formation of the 1330–1280 Ma Recherche Supersuite, with a northwest-dipping subduction zone beneath the Yilgarn Craton and Albany–Fraser Orogen, immediately prior to collision with the South Australian Craton

continent–continent convergence, which resulted in Stage I of the Albany–Fraser Orogeny (cf. Spaggiari et al., 2014c). As virtually the entire basement between the eastern part of the Albany–Fraser Orogen and the western part of the Gawler Craton, a distance of over 850 km, is under cover, geological information is patchy. Until much more information becomes available, it will not be possible to provide a comprehensive tectonic model based on the limited data currently available.

Stage II of the Albany–Fraser Orogeny, at c. 1215 to 1140 Ma (Clark et al., 2000; Bodorkos and Clark, 2004a), is generally considered to result from intracratonic reworking at the former plate margin (e.g. Myers et al., 1996; Clark et al., 2000; Giles et al., 2004; Spaggiari et al., 2009), which resulted in high-temperature metamorphism, deformation and emplacement of the 1200–1140 Ma Esperance Supersuite. Given that seismic sections represent present day images of the crust, and that the youngest structures overprint older structures and are usually the best imaged seismically, we speculate that the dominant age of thrusting interpreted in the Albany–Fraser seismic sections occurred during Stage II of the Albany–Fraser Orogeny.

Transect from Yilgarn Craton to Madura Province

It is now possible to combine the interpreted seismic sections from the current Albany–Fraser survey with seismic sections from earlier deep crustal seismic surveys (Fig. 9) to produce an approximate northwest–southeast oriented ~1200 km long transect across southwest Western Australia from the Pinjarra Orogen to the Madura Province (Fig. 16). Key seismic surveys used here are:

- the Southern Carnarvon and Youanmi surveys (lines 11GA-SC1, 10GA-YU1, 10GA-YU2 and 11GA-SC1; Korsch et al., 2013c)
- the Eastern Goldfields survey, acquired in 1991 (line BMR91-EGF01, commonly known as EGF1; Drummond et al., 1993, 2000; Swager et al., 1997)
- the Northeast Yilgarn survey, acquired in 2001 (lines 01AGS-NY1 and 01AGS-NY3; Goleby et al., 2004, 2006)
- the current Albany–Fraser survey.

The surveys across the Yilgarn Craton showed that the terranes which make up the Eastern Goldfields Superterrane are separated from each other, and from the Youanmi Terrane by major, crustal-scale, east-northeast dipping faults or shear zones, which penetrate to the Moho (Korsch, 2013a,c). By contrast, the Albany–Fraser Orogen is dominated mainly by southeast-dipping shear zones which are confined to the upper and middle crust (Fig. 16). These are dominantly west- to northwest-directed thrusts, probably the end result of at least the major shortening events during Stage I and Stage II of the Albany–Fraser Orogeny. The thrusts likely represent the reactivation of older, possibly extensional structures as well as the development of new structures during each event.

Summary

In our interpretation of the four Albany–Fraser deep seismic reflection lines, we have investigated the crustal architecture of an area in Western Australia which is poorly exposed, extending from the southeastern part of the Yilgarn Craton, across the Albany–Fraser Orogen, to the Madura Province. Our preliminary interpretation defines two new seismic provinces, which are probably older basement beneath both the Kurnalpi Terrane of the Yilgarn Craton and the Albany–Fraser Orogen. Neither is exposed. The Albany–Fraser Orogen is dominated by east- to southeast-dipping shear zones, often forming linked thrust systems. It is likely that some of these shear zones are inverted, earlier extensional faults. The Tropicana Zone sits above the newly defined, very shallowly dipping, Plumridge Detachment. The Albany–Fraser seismic sections, combined with previous deep seismic traverses, provide a crustal-scale transect from the Pinjarra Orogen in the west to the Madura Province in the southeast.

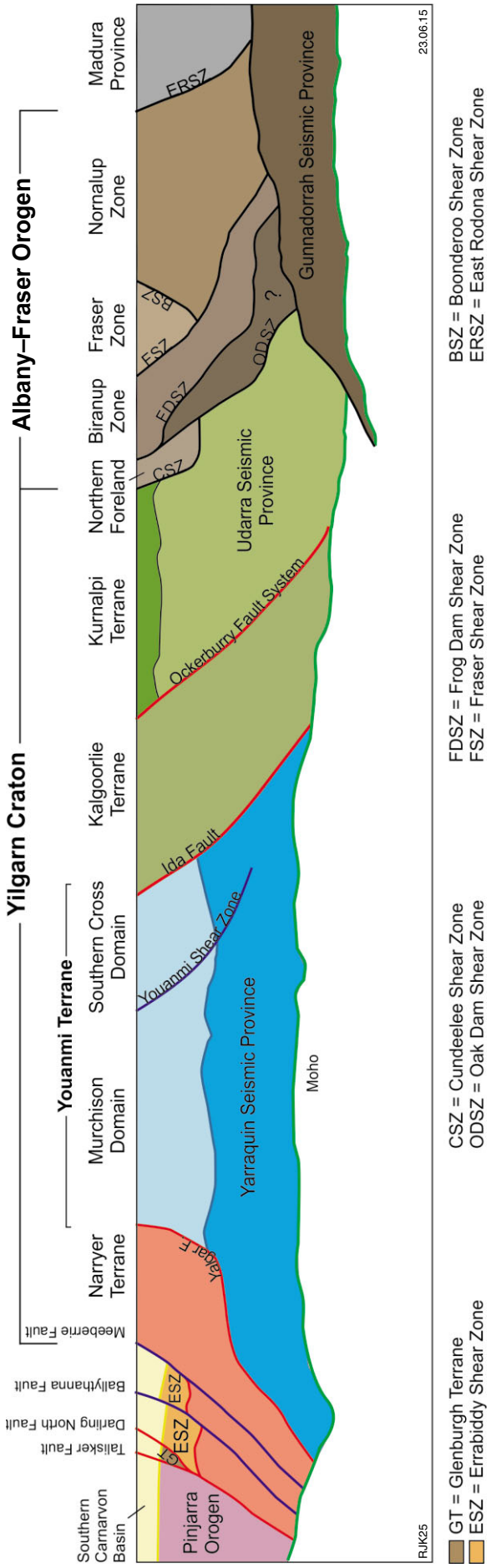

Figure 16. Cartoon of the present day architecture of the crust in Western Australia, based on deep seismic reflection profiling. The cross-section extends from the Pinjarra Orogen near the coast in the west, across the Yilgarn Craton, from the Narryer Terrane to the Kurnalpi Terrane, and then across the Albany–Fraser Orogen to the Madura Province in the east, showing the key tectonic elements and significant faults.

Acknowledgements

This paper forms part of a collaborative project between Geoscience Australia, the Geological Survey of Western Australia and the Tropicana Joint Venture. We thank Lindsay Highet, Weiping Zhang and Natalie Kositcin for producing some of the figures. We also thank David Champion and Geoff Fraser for their reviews of the manuscript, Andrew Cross and Chris Kirkland for their comments on the geochronology and isotope data, and Rodinia Oil (Australia) Pty Ltd for permission to analyse samples from the basement in the Kutjara 1 and Mulyawara 1 petroleum exploration wells.

References

Bacchin, M, Milligan, PR, Wynne, P and Tracey, R 2008, Gravity anomaly map of the Australian region (3rd edition), 1:5 000 000 scale: Geoscience Australia, Canberra.

Baily, T, Clark, R, Rowland, B and Nicolson, J 2012a, Mulyawara-1 well completion report: Rodinia Oil (Australia) Pty Ltd [Department for Manufacturing, Innovation, Trade, Resources and Energy South Australia, Well Completion Report 2011/000091], 58p.

Baily, T, Clark, R, Rowland, B and Nicolson, J 2012b, Kutjara-1 well completion report: Rodinia Oil (Australia) Pty Ltd [Department for Manufacturing, Innovation, Trade, Resources and Energy South Australia, Well Completion Report 2011/000279], 50p.

Barley, ME, Eisenlohr, BN, Groves, DI, Perring, CS and Verancombe, JR 1989, Late Archean convergent margin tectonics and gold mineralization: a new look at the Norseman-Wiluna Belt, Western Australia: Geology, v. 17, p. 826–829.

Barley, ME, Brown, SJ, Krapež, B and Kositcin, N 2008, Physical volcanology and geochemistry of a late Archaean volcanic arc: Kurnalpi and Gindalbie terranes, eastern Goldfields Superterrane, Western Australia: Precambrian Research, v. 161, p. 53–76.

Bédard, JH, Harris, LB and Thurston, PC 2013, The hunting of the snArc: Precambrian Research, v. 229, p. 20–48.

Blenkinsop, TG and Doyle, MG 2014, Structural controls on gold mineralization on the margin of the Yilgarn craton, Albany–Fraser orogen: The Tropicana deposit, Western Australia: Journal of Structural Geology, v. 67 p. 189–204.

Bodorkos, S and Clark, DJ 2004a, Evolution of a crustal-scale transpressive shear zone in the Albany Fraser Orogen, SW Australia: 1. P–T conditions of Mesoproterozoic metamorphism in the Coramup Gneiss: Journal of Metamorphic Geology, v. 22, p. 691–711.

Bodorkos, S and Clark, DJ 2004b, Evolution of a crustal-scale transpressive shear zone in the Albany Fraser Orogen, SW Australia: 2. Tectonic history of the Coramup Gneiss and a kinematic framework for Mesoproterozoic collision of the West Australian and Mawson cratons: Journal of Metamorphic Geology, v. 22, p. 713–731.

Brisbout, LI, Spaggiari, CV and Aitken, ARA 2014, Integrating outcrop, aeromagnetic and gravity data: models of the east Albany–Fraser Orogen, *in* Albany–Fraser Orogen seismic and magnetotelluric (MT) workshop 2014: extended abstracts *compiled by* CV Spaggiari and IM Tyler: Geological Survey of Western Australia, Record 2014/6 p. 102–117.

Champion, DC, Cassidy, KF and Budd, A 2002, Overview of the Yilgarn Craton magmatism: Implications for crustal development, *in* The characterization and metallogenic significance of Archaean granitoids of the Yilgarn Craton *edited by* KF Cassidy, DC Champion, NJ McNaughton, IR Fletcher, AJ Whitaker, IV Bastrakova and AR Budd: Australian Mineral Industry Research Association (AMIRA) Project P482/MERIWA Project M281, Final Report, p. 8.1–8.21.

Cassidy, KF, Champion, DC, Krapez, B, Barley, ME, Brown, SJA, Blewett, RS, Groenewald, PB and Tyler, IM 2006, A revised geological framework for the Yilgarn Craton, Western Australia: Geological Survey of Western Australia, Record 2006/8, 8p.

Champion, DC and Cassidy, KF 2008, Geodynamics: using geochemistry and isotopic signatures of granites to aid mineral systems studies: an example from the Yilgarn Craton: Geoscience Australia, Record 2008/09, p. 7–16.

Champion, DC and Cassidy, KF 2010, Granitic magmatism in the Yilgarn Craton: implications for crustal growth and metallogeny: Geological Survey of Western Australia, Record 2010/20, p. 12–18.

Clark, C, Kirkland, CL, Spaggiari, CV, Oorschot, C, Wingate, MTD and Taylor, R 2014, Proterozoic granulite formation driven by magmatism: an example from the Fraser Range Metamorphics, Western Australia: Precambrian Research, v. 240, p. 1–21.

Clark, DJ, Hensen, BJ and Kinny, PD 2000, Geochronological constraints for a two-stage history of the Albany–Fraser Orogen, Western Australia: Precambrian Research, v. 102, p. 155–183.

Clark, D, McPherson, A and Van Dissen, R 2012, Long-term behaviour of Australian Stable Continental Region (SCR) faults: Tectonophysics, v. 566-567, p. 1–30.

Costelloe, RD, Holzschuh, J and Fomin, T 2014, Acquisition and processing of the 2012 Albany–Fraser deep reflection seismic survey, *in* Albany–Fraser Orogen seismic and magnetotelluric (MT) workshop 2014: extended abstracts *compiled by* CV Spaggiari and IM Tyler: Geological Survey of Western Australia, Record 2014/6 p. 1–6.

Crawford, B, Betts, P and Ailleres, L 2012, A geophysical investigation of deformation and reactivation of a major intraplate shear zone: Geological Society of Australia, Abstracts 102, p. 26–27.

Cruse, T and Harris, LB 1994, Ediacaran fossils from the Stirling Range Formation, Western Australia: Precambrian Research, v. 67, p. 1–10.

Czarnota, K, Champion, DC, Goscombe, B, Blewett, RS, Cassidy, KF, Henson, PA and Groenewald, PB 2010, Geodynamics of the eastern Yilgarn Craton: Precambrian Research, v. 183, p. 175–202.

Dawson, GC, Krapež, B, Fletcher, IR, McNaughton, NJ and Rasmussen, B 2002, Did late Palaeoproterozoic assembly of proto-Australia involve collision between the Pilbara, Yilgarn and Gawler Cratons? Geochronological evidence from the Mount Barren Group in the Albany–Fraser Orogen of Western Australia: Precambrian Research, v. 118, p. 195–220.

de Broeckert, P and Sandiford, M 2005, Buried inset-valleys in the eastern Yilgarn Craton, Western Australia: geomorphology, age, and allogenic control: Journal of Geology, v. 113, p. 471–493.

Doyle, MG, Kendall, BM and Gibbs, D 2007, Discovery and characteristics of the Tropicana gold district, *in* Proceedings of Geoconferences (WA) Inc. Kalgoorlie '07 Conference, *edited by* FP Bierlein and CM- Knox-Robinson: Geoscience Australia, Record 2007/14, p.186–190.

Doyle, MG, Savage, J, Blenkinsop, TG, Crawford, A and McNaughton, N 2013, Tropicana – Unravelling the complexity of a +6 million ounce gold deposit hosted in granulite facies metamorphic rocks, *in* World Gold Conference, Brisbane, Queensland 26–29 September 2013: Australasian Institute of Mining and Metallurgy Publication Series 9/2013, p. 87–93.

Doyle, MG, Blenkinsop, TG, Crawford, AJ, Fletcher, IR, Foster, J, Fox-Wallace, L, Large, RR, Mathur, R, McNaughton, NJ, Meffre, S, Muhling, JR, Occhipinti, SA, Rasmussen, B and Savage, J 2014, Tropicana deposit, Western Australia: an integrated approach to understanding granulite-hosted gold and the Tropicana Gneiss, *in* Albany–Fraser Orogen seismic and magnetotelluric (MT) workshop 2014: extended abstracts *compiled by* CV Spaggiari and IM Tyler: Geological Survey of Western Australia, Record 2014/6 p. 69–76.

Drummond, BJ, Goleby, BR, Swager, CP and Williams, PR 1993, Constraints on Archaean crustal composition and structure provided by deep seismic sounding in the Yilgarn Block: Ore Geology Reviews, v. 8, p. 117–124.

Drummond, BJ, Goleby, BR and Swager, CP 2000, Crustal signature of Late Archaean tectonic episodes in the Yilgarn craton, Western Australia: evidence from deep seismic sounding: Tectonophysics, v. 329, p. 193–221.

Drummond, B, Lyons, P, Goleby, B and Jones, L 2006, Constraining models of the tectonic setting of the giant Olympic Dam iron oxide–copper–gold deposit, South Australia, using deep seismic reflection data: Tectonophysics, v. 420, p. 91–103.

Estrada, B 2009, Neotectonic and palaeoseismological studies in the southwest of Western Australia: The University of Western Australia, School of Earth and Environment, Perth, PhD thesis, (unpublished).

Flint, RB and Daly, SJ 1993, Coompana Block, *in* The geology of South Australia Volume 1 The Precambrian *edited by* JF Drexel, WV Preiss and AJ Parker: Geological Survey of South Australia, Bulletin 54, p. 168–170.

Giles, D, Betts, PG and Lister, GS 2004, 1.8–1.5-Ga links between the North and South Australian Cratons and the early-middle Proterozoic configuration of Australia: Tectonophysics, v. 380, p. 27–41.

Goleby, BR, Blewett, RS, Groenewald, PB, Cassidy, KF, Champion, DC, Jones, LEA, Korsch, RJ, Shevchenko, S and Apak, SN 2003, The 2001 Northeastern Yilgarn deep seismic reflection survey: Geoscience Australia, Record 2003/28, 143p.

Goleby, BR, Blewett, RS, Korsch, RJ, Champion, DC, Cassidy, KF, Jones, LEA, Groenewald, PB and Henson, PA 2004, Deep seismic reflection profiling in the Archaean northeastern Yilgarn Craton, Western Australia: implications for crustal architecture and mineral potential: Tectonophysics, v. 388, p. 119–133.

Goleby, BR, Blewett, RS, Fomin, T, Fishwick, S, Reading, AM, Henson, PA, Kennett, BLN, Champion, DC, Jones, LEA, Drummond, BJ and Nicoll, M, 2006, An integrated multi-scale 3D seismic model of the Archaean Yilgarn Craton, Australia: Tectonophysics, v. 420, p. 75–90.

Hall, CE, Jones, SA and Bodorkos, S 2008, Sedimentology, structure and SHRIMP zircon provenance of the Woodline Formation, Western Australia: implications for the tectonic setting of the West Australian Craton during the Paleoproterozoic: Precambrian Research, v. 162, p. 577–598, doi:10.1016/j.precamres.2007.11.001.

Harris, LB, Koyi, H and Fossen, H 2002, Mechanisms for folding of high-grade rocks in extensional tectonic settings: Earth-Science Reviews, v. 59, p. 163–210.

Hill, AJ 1991, Revisions to the Cretaceous stratigraphic nomenclature of the Bight and Duntroon basins, South Australia: Geological Survey of South Australia, Quarterly Geological Notes, no. 120, p. 2-20.

Hillis, RR and Reynolds, SD 2003, In situ stress field of Australia, *in* Evolution and dynamics of the Australian Plate *edited by* RR Hillis and RD Muller: Geological Society of Australia, Special Publication, no. 22, p. 49-58.

Hillis, RR, Sandiford, M, Reynolds, SD and Quigley, MC 2008, Present-day stresses, seismicity and Neogene-to-Recent tectonics of Australia's 'passive' margins: intraplate deformation controlled by plate boundary forces, *in* The Nature and Origin of Compression in Passive Margins *edited by* H Johnson, AG Dore, RW Gatliff, R Holdsworth, ER Lundin and JD Ritchie: Geological Society of London, Special Publications 306, p. 71–90.

Hou, B, Frakes, LA, Sandiford, M, Worrall, L, Keeling, J and Alley, N F 2008, Cenozoic Eucla Basin and associated palaeovalleys, southern Australia — Climatic and tectonic influences on landscape evolution, sedimentation and heavy mineral accumulation: Sedimentary Geology, v. 203, p. 112–130.

Ivanic, TJ, Van Kranendonk, MJ, Kirkland, CL, Wyche, S, Wingate, MTD and Belousova, EA 2012, Zircon Lu–Hf isotopes and granite geochemistry of the Murchison Domain of the Yilgarn Craton: Evidence for reworking of Eoarchean crust during Meso-Neoarchean plume-driven magmatism: Lithos, v. 148, p. 112–127.

Ivanic, TJ, Wingate, MTD, Korsch, RJ, Blewett, RS, Jones, LEA, Wyche, S, Zibra, I, Doublier, MP, Romano, SS, Pawley, MJ, Van Kranendonk, MJ, Gessner, K, Hall, CE, Chen, SF Patison, N and Costelloe, RD 2013, Preliminary interpretation of the Youanmi deep seismic reflection lines for Proterozoic intrusive rocks, *in* Youanmi and Southern Carnarvon seismic and magnetotelluric (MT) workshop *compiled by* S Wyche, TJ Ivanic and I Zibra: Geological Survey of Western Australia, Record 2013/6, p. 77–81.

Jackson, MJ and van de Graaff, WJE 1981, Geology of the Officer Basin, Western Australia: Bureau of Mineral Resources, Bulletin 206, 102p.

James, NP, Bone, Y, Carter, RM and Murray-Wallace, CV 2006, Origin of the Late Neogene Roe Plains and their calcarenite veneer: implications for sedimentology and tectonics in the Great Australian Bight: Australian Journal of Earth Sciences, v. 53, p. 407–419.

Kennett, BLN 2014, The nature of the lithosphere in the vicinity of the Albany–Fraser seismic lines, *in* Albany–Fraser Orogen seismic and magnetotelluric (MT) workshop 2014: extended abstracts *compiled by* CV Spaggiari and IM Tyler: Geological Survey of Western Australia, Record 2014/6 p. 134–140.

Kinny, PD, Williams, IS, Froude, DO, Ireland, TR and Compston W 1988, Early Archaean zircon ages from orthogneisses and anorthosites at Mount Narryer, Western Australia: Precambrian Research, v. 38, p. 325–341.

Kirkland, CL, Spaggiari, CV, Pawley, MJ, Wingate, MTD, Smithies, RH, Howard, HM, Tyler, IM, Belousova, EA and Poujol, M 2011a, On the edge: U–Pb, Lu–Hf, and Sm–Nd data suggests reworking of the Yilgarn Craton margin during formation of the Albany–Fraser Orogen: Precambrian Research, v. 187, p. 223–247.

Kirkland, CL, Wingate, MTD, Spaggiari, CV and Tyler, IM 2011b, 194773: granitic rock, Eucla No. 1 drillhole; Geochronology Record 1001: Geological Survey of Western Australia, 4p.

Kirkland, CL, Spaggiari, CV, Wingate, MTD, Smithies, RH, Belousova, EA, Murphy, R and Pawley, MJ 2011c, Inferences on crust–mantle interaction from Lu–Hf isotopes: a case study from the Albany–Fraser Orogen: Geological Survey of Western Australia, Record 2011/12, 25p.

Kirkland, CL, Wingate, MTD and Spaggiari, CV 2012, 182485: migmatitic gneiss, Burkin prospect; Geochronology Record 1054, Geological Survey of Western Australia, 4 p.

Kirkland, CL, Spaggiari, CV, Smithies, RH and Wingate, MTD 2014, Cryptic progeny of craton margins: Geochronology and Isotope Geology of the Albany–Fraser Orogen with implications for evolution of the Tropicana Zone, *in* Albany–Fraser Orogen seismic and magnetotelluric (MT) workshop 2014: extended abstracts *compiled by* CV Spaggiari and IM Tyler: Geological Survey of Western Australia, Record 2014/6 p. 89–101.

Korsch, RJ, Preiss, WV, Blewett, RS, Cowley, WM, Neumann, NL, Fabris, AJ, Fraser, GL, Dutch, R, Fomin, T, Holzschuh, J, Fricke, CE, Reid, AJ, Carr, LK and Bendall, BR 2010, Deep seismic reflection transect from the western Eyre Peninsula in South Australia to the Darling Basin in New South Wales: Geodynamic implications, *in* South Australian Seismic and MT Workshop, extended abstracts *edited by* RJ Korsch and N Kositcin: Geoscience Australia, Record 2010/10, p. 105–116.

Korsch, RJ, Kositcin, N and Champion, DC 2011, Australian island arcs through time: geodynamic implications for the Archean and Proterozoic: Gondwana Research, v. 19, p. 716–734. doi: 10.1016/j.gr.2010.11.018.

Korsch, RJ, Blewett, RS, Wyche, S, Zibra, I, Ivanic, TJ, Doublier, MP, Romano, SS, Pawley, MP, Johnson, SP, Van Kranendonk, MJ, Jones, LEA, Kositcin, N, Gessner, K, Hall, CE, Chen, SF, Patison, N, Kennett, BLN, Jones, T, Goodwin, JA, Milligan, PM and Costelloe, RD 2013a, Geodynamic implications of the Youanmi and Southern Carnarvon deep seismic reflection surveys: a ~1300 km traverse from the Pinjarra Orogen to the eastern Yilgarn Craton, *in* Youanmi and Southern Carnarvon seismic and magnetotelluric (MT) workshop *compiled by* S Wyche, TJ Ivanic I and Zibra: Geological Survey of Western Australia, Record 2013/6, p. 141–158.

Korsch, RJ, Blewett, RS, Pawley, MJ, Carr, LK, Hocking, RM, Neumann, NL, Smithies, RH, Quentin de Gromard, R, Howard, HM, Kennett, BLN, Aitken, ARA, Holzschuh, J, Duan, J, Goodwin, JA, Jones, T, Gessner, K and Gorczyk, W 2013b, Geological setting and interpretation of the southwest half of deep seismic reflection line 11GA-YO1: Yamarna Terrane of the Yilgarn Craton and the western Officer Basin, *in* Yilgarn Craton-Officer Basin-Musgrave Province seismic and MT workshop *edited by* NL Neumann: Geoscience Australia, Record 2013/28, p. 24–50.

Korsch, RJ, Blewett, RS, Smithies, RH, Quentin de Gromard, R, Howard, HM, Pawley, MJ, Carr, LK, Hocking, RM, Neumann, NL, Kennett, BLN, Aitken, ARA, Holzschuh, J, Duan, J, Goodwin, JA, Jones, T, Gessner, K and Gorczyk, W 2013c, Geodynamic implications of the Yilgarn Craton–Officer Basin–Musgrave Province (YOM) deep seismic reflection survey: part of a ~1800 km transect across Western Australia from the Pinjarra Orogen to the Musgrave Province, *in* Yilgarn Craton–Officer Basin–Musgrave Province Seismic and MT Workshop *edited by* NL Neumann: Geoscience Australia, Record 2013/28, 168–196.

Kositcin, N, Brown, SJA, Barley, ME, Krapež, B, Cassidy, KF and Champion, DC 2008, SHRIMP U-Pb zircon age constraints on the Late Archaean tectonostratigraphic architecture of the Eastern Goldfields Superterrane, Yilgarn Craton, Western Australia: Precambrian Research, v. 161, p. 5–33.

Krapez, B and Barley, ME 2008, Late Archaean synorogenic basins of the Eastern Goldfields Superterrane, Yilgarn Craton, Western Australia Part III. Signatures of tectonic escape in an arc-continent collision zone: Precambrian Research, v. 161, p. 183–199.

Leonard, M 2010, Earthquake fault scaling: self-consistent relating of rupture length, width, average displacement, and moment release: Bulletin of the Seismological Society of America, v. 100, p. 1971–1988.

Lowry, DC, 1970, Geology of the Western Australian part of the Eucla Basin: Geological Survey of Western Australia, Bulletin 122, 201p.

Milligan, PR, Franklin, R, Minty, BRS, Richardson, LM and Percival, PJ 2010, Magnetic anomaly map of Australia (5th Edition), 1:5 000 000 scale: Geoscience Australia, Canberra.

Murdie, RE, Gessner, K, Occhipinti, SA, Spaggiari, CV and Brett, J 2014, Independent constraints of the Albany–Fraser seismic interpretations using models of gravity and magnetic data, *in* Albany–Fraser Orogen seismic and magnetotelluric (MT) workshop 2014: extended abstracts *compiled by* CV Spaggiari and IM Tyler: Geological Survey of Western Australia, Record 2014/6 p. 117–133.

Myers, JS 1990, Albany–Fraser Orogen: Geological Survey of Western Australia, Memoir 3, p. 255–263.

Myers, JS 1995, The generation and assembly of an Archaean supercontinent: evidence from the Yilgarn Craton, Western Australia, *in* Early Precambrian Processes, *edited by* MP Coward and AC Ries: Geological Society of London, Special Publication 95, p. 143–154.

Myers, JS, Shaw, RD and Tyler, IM 1996, Tectonic evolution of Proterozoic Australia: Tectonics, v. 15, p. 1431–1446.

Nelson, DR 1995, 83690: biotite granodiorite gneiss, Bald Rock; Geochronology Record 78: Geological Survey of Western Australia, 4p.

Neumann, NL and Korsch, RJ 2014, SHRIMP U–Pb zircon ages from Kutjara 1 and Mulyawara 1, northwestern South Australia; Geoscience Australia, Record 2014/05, 18p.

Occhipinti, SA, Doyle, M, Spaggiari CV, Korsch, R, Cant, G, Martin, K, Kirkland, CL, Savage, J, Less, T, Bergin, L and Fox, L 2014, Interpretation of the deep seismic reflection line 12GA-T1: northeastern Albany–Fraser Orogen, *in* Albany–Fraser Orogen seismic and magnetotelluric (MT) workshop 2014: extended abstracts *compiled by* CV Spaggiari and IM Tyler: Geological Survey of Western Australia, Record 2014/6 p. 51–67.

Pawley, MJ, Wingate, MTD, Kirkland, CL, Wyche, S, Hall, CE, Romano, SS and Doublier, MP 2012, Adding pieces to the puzzle: episodic crustal growth and a new terrane in the northeast Yilgarn Craton, Western Australia: Australian Journal of Earth Sciences, v. 59, p. 603–623.

Pidgeon, RT and Wilde, SA 1990, The distribution of 3.0 Ga and 2.7 Ga volcanic episodes in the Yilgarn Craton of Western Australia: Precambrian Research, v. 91, p. 309–325.

Rasmussen, B, Bengtson, S, Fletcher, IR and McNaughton, N 2002, Discoidal impressions and trace-like fossils more than 1200 million years old: Science, v. 296, p. 1112–1115.

Rasmussen, B, Fletcher, IR, Bengtson, S and McNaughton, N 2004, SHRIMP U–Pb dating of diagenetic xenotime in the Stirling Range Formation, Western Australia: 1.8 billion year minimum age for the Stirling biota: Precambrian Research, v. 133, p. 329–337.

Raymond, OL (coordinator) 2009, Surface geology of Australia 1:1 million scale digital geology data: Geoscience Australia, digital geology map. <https://www.ga.gov.au/products/servlet/controller?event=GEOCAT_DETAILS&catno=69455>.

Richardson, SP 2005, Joint relinquishment report C76/2003 for the period 16 April 2003 to 27 May 2005 and combined annual report for the period 16 April 2004 to 15 April 2005 — Mundra South project: WMC Resources Ltd, Belmont, (unpublished), 13p.

Sandiford, M 2007, The tilting continent: a new constraint on the dynamic topographic field from Australia: Earth and Planetary Science Letters, v. 261, p. 152–163.

Scott, AF and Speer, GW 1969, Mallabie No. 1 well completion report: Outback Oil Company NL; Primary Industries and Resources South Australia, Open File Envelope No. 1172, 92p.

Shaw, RD, Wellman, P, Gunn, P, Whitaker, AJ, Tarlowski, C and Morse, M 1996, Guide to using the Australian crustal elements map: Australian Geological Survey Organisation, Record 1996/30, 44p.

Smithies, RH, Spaggiari, CV, Kirkland, CL, Howard, HM and Maier, WD 2013, Petrogenesis of gabbros of the Mesoproterozoic Fraser Zone: constraints on the tectonic evolution of the Albany–Fraser orogen: Geological Survey of Western Australia, Record 2013/5, 29p.

Smithies, RH, Spaggiari, CV, Kirkland, CL and Maier, WD 2014, Geochemistry and petrogenesis of the Albany–Fraser igneous rocks, *in* Albany–Fraser Orogen seismic and magnetotelluric (MT) workshop 2014: extended abstracts *compiled by* CV Spaggiari and IM Tyler: Geological Survey of Western Australia, Record 2014/6 p. 77–88.

Spaggiari, CV, Bodorkos, S, Barquero-Molina, M, Tyler, IM and Wingate, MTD 2009, Interpreted bedrock geology of the south Yilgarn and central Albany–Fraser Orogen, Western Australia: Geological Survey of Western Australia, Record 2009/10, 84p.

Spaggiari, CV, Kirkland, CL, Pawley, MJ, Smithies, RH, Wingate, MTD, Doyle, MG, Blenkinsop, TG, Clark, C, Oorschot, CW, Fox, LJ and Savage, J 2011, The geology of the east Albany–Fraser Orogen — a field guide: Geological Survey of Western Australia, Record 2011/23, 97p.

Spaggiari, CV, Kirkland, CL, Smithies, RH and Wingate, MTD 2012, What lies beneath — interpreting the Eucla basement, *in* GSWA 2012 extended abstracts: promoting the prospectivity of Western Australia: Geological Survey of Western Australia, Record 2012/2, p. 24–26.

Spaggiari, CV, Smithies, RH, Kirkland, CL, Howard, HM, Maier, WD and Clark, C 2013, melting, mixing, and emplacement: evolution of the Fraser Zone, Albany–Fraser Orogen, *in* GSWA 2013 extended abstracts: promoting the prospectivity of Western Australia: Geological Survey of Western Australia, Record 2013/2, p. 1–5.

Spaggiari, CV, Kirkland, CL, Smithies, RH, Occhipinti, SA and Wingate, MTD 2014a, Geological framework of the Albany–Fraser Orogen, *in* Albany–Fraser Orogen seismic and magnetotelluric (MT) workshop 2014: extended abstracts *compiled by* CV Spaggiari and IM Tyler: Geological Survey of Western Australia, Record 2014/6 p. 12–27.

Spaggiari, CV, Occhipinti, SA, Korsch, RJ, Doublier, MP, Clark, DJ, Dentith, MC, Gessner, K, Doyle, MG, Tyler, IM, Kennett, BLN, Costelloe, RD, Fomin, T and Holzschuh, J 2014b, Interpretation of seismic lines 12GA-AF1, 12GA-AF2 and 12GA-AF3: implications for crustal architecture, *in* Albany–Fraser Orogen seismic and magnetotelluric (MT) workshop 2014: extended abstracts *compiled by* CV Spaggiari and IM Tyler: Geological Survey of Western Australia, Record 2014/6 p. 28–51.

Spaggiari, CV, Kirkland, CL, Smithies, RH and Wingate, MTD 2014c, Tectonic links between sedimentary cycles, basin formation and magmatism in the Albany–Fraser Orogen, Western Australia: Geological Survey of Western Australia, Report 133, 63 p.

Stach, LW 1964, Completion report, Alliance Eucla well No. 1 (PCL-2-N 12 000 38): Alliance Petroleum Australia NL, Melbourne; Geological Survey of Western Australia, Statutory Petroleum Exploration Report, S141 A2, 30p.

Stone, J, Allan, G and Fifield, LK 1994, Limestone erosion measurements with cosmogenic Cl-36 in Calcite: preliminary results from Australia: Nuclear Instruments and Methods in Physics Research, Section B-Beam Interactions with Materials and Atoms, v. 92, p. 311–316.

Swager, CP, Goleby, BR, Drummond, BJ, Rattenbury, MS and Williams, PR 1997, Crustal structure of granite–greenstone terranes in the Eastern Goldfields, Yilgarn Craton, as revealed by seismic reflection profiling: Precambrian Research, v 83, p. 43–56.

Thom, R 1972, A Recent Fault Scarp in the Lort River Area, Ravensthorpe 1:250,000 sheet: Geological Survey of Western Australia, Annual Report 1971, p. 58-59.

Tillick, D 2011, Final Report of Co-funded Government – Industry Drilling Program at the Haig Prospect, Eucla Project, August 2011, Teck Australia Pty Ltd, 24 p.

Tyler, IM, Spaggiari, CV, Occhipinti, SA, Kirkland, CL and Smithies, RH 2014, The Albany–Fraser deep reflection seismic and MT survey: Implications for mineral systems, *in* Albany–Fraser Orogen seismic and magnetotelluric (MT) workshop 2014: extended abstracts *compiled by* CV Spaggiari and IM Tyler: Geological Survey of Western Australia, Record 2014/6 p. 174–182.

Vallini, DA, Rasmussen, B, Krapež, B, Fletcher, IR and McNaughton, NJ 2002, Obtaining diagenetic ages from metamorphosed sedimentary rocks: U–Pb dating of unusually coarse xenotime cement in phosphatic sandstone: Geology, v. 30, p. 1083–1086.

Vallini, DA, Rasmussen, B, Krapež, B, Fletcher, IR and McNaughton, N 2005, Microtextures, geochemistry and geochronology of authigenic xenotime constraining the cementation history of a Paleoproterozoic metasedimentary sequence: Sedimentology, v. 52, p. 101–122.

van de Graaff, WJE, Crowe, RWA, Bunting, JA and Jackson, J 1977, Relict early Cainozoic drainage in Western Australia: Zeitschrift Fur Geomorphologie, v. 21, p. 379–400.

Van Kranendonk, MJ, Ivanic, TJ, Wingate, MTD, Kirkland, CL and Wyche, S 2013, Long-lived, autochthonous development of the Archean Murchison Domain, and implications for Yilgarn Craton tectonics: Precambrian Research, v. 229, p. 49–92. http://dx.doi.org/10.1016/j.precamres.2012.08.009

Wade, BP, Payne, JL, Hand, M and Barovich, KM 2007, Petrogenesis of ca 1.50 Ga granitic gneiss of the Coompana Block: filling the 'magmatic gap' of Mesoproterozoic Australia: Australian Journal of Earth Sciences, v. 54, p. 1089-1102.

Webb, AW, Thomson, BP, Blissett, AH, Day, SJ, Flint, RB and Parker, AJ 1982, Geochronology of the Gawler Craton, South Australia: South Australia Department of Mines and Energy, Report Book 82/00086, 136p.

Wyche, S, Kirkland, CL, Riganti, A, Pawley, MJ, Belousova, EA and Wingate, MTD 2012, Isotopic constraints on stratigraphy in the central and eastern Yilgarn Craton, Western Australia: Australian Journal of Earth Sciences, v. 59, p. 657–670.

The Albany–Fraser deep reflection seismic and MT survey: implications for mineral systems

by

IM Tyler, CV Spaggiari, SA Occhipinti, CL Kirkland, and RH Smithies

Introduction

The acquisition of the Albany–Fraser deep seismic reflection and magnetotelluric (MT) survey in 2012 was carried out as a collaborative project between the Geological Survey of Western Australia (GSWA), Geoscience Australia (GA), the National Research Facility for Earth Sounding (ANSIR), AngloGold Ashanti Limited (AGA) and Independence Group, and the Centre for Exploration Targeting (CET) at The University of Western Australia. Funding for reflection seismic lines 12GA-AF1, 12GA-AF2 and 12GA-AF3, and for the regional MT survey carried out by CET, was provided by the Western Australian Government's Exploration Incentive Scheme (EIS), administered by GSWA and funded from the Royalties for Regions program, together with in-kind support from GA. Funding for seismic line 12GA-T1 across the Tropicana gold deposit was provided by AngloGold Ashanti and Independence Group through ANSIR. Gravity stations at 400 m spacing were acquired on all four lines.

The aim of the seismic lines was to:

- image the crustal architecture of the Archean Yilgarn Craton margin and its relationship to the Paleo- to Mesoproterozoic Albany–Fraser Orogen
- establish the subsurface extent of the Yilgarn Craton beneath the Albany–Fraser Orogen, and look for mantle-tapping structures that may have provided fluid pathways for mineralization. The seismic lines were designed to cross several major faults, including the Cundeelee Fault, the Fraser Fault, the Newman Shear Zone, the Red Island Shear Zone and the Rodona Shear Zone
- examine the deep crustal structure of the Albany–Fraser Orogen and investigate the tectonic processes that drove the development of the Yilgarn Craton margin from the Neoarchean through Paleoproterozoic rifting and magmatism to Mesoproterozoic tectonic assembly
- test models of fold and thrust belt architecture
- examine primary and structural relationships between geological and tectonic units mapped at the surface.

The survey provided new insights into the architecture of the southeastern margin of the Yilgarn Craton, and of the adjacent Albany–Fraser Orogen. This has refined our understanding of the geodynamic setting and tectonic history of the region through the Neoarchean and Paleo- to Mesoproterozoic (Spaggiari et al., 2014a,b,c; Korsch et al., 2014). This improved understanding of the development of the Albany–Fraser Orogen can be used to evaluate the mineral systems in both the Archean and Proterozoic rocks, and the implications for regional-scale mineral exploration targeting.

Central to an understanding of the prospectivity of a region is the knowledge that most giant orebodies are generated by lithospheric-scale deep plumbing systems that concentrate fluids, energy, and metals into specific sites in the crust (Hronsky and Groves, 2008; McCuaig et al., 2010; Hronsky, 2011; Griffin et al., 2013). These often reflect sites of fossil subduction zones or lithospheric boundaries around old cratonic margins (Wyborn et al., 1994; McCuaig et al., 2010). The setting of the Albany–Fraser Orogen on the Yilgarn Craton margin is one of high prospectivity, given their combined history of granite–greenstone development, rifting and break-up, back-arc basin development, arc accretion and continental collision during the Neoarchean and Paleo- and Mesoproterozoic (Spaggiari et al., 2011, 2013, 2014c; Kirkland et al., 2011).

Mineral systems in the southeastern margin of the Yilgarn Craton, and the adjacent Albany–Fraser Orogen

The Albany–Fraser Orogen and its Northern Foreland, which developed in the adjacent Yilgarn Craton, had not been considered prospective for the development of major ore deposits. However, perceptions of the region's prospectivity were dramatically changed by the discovery in 2005 of the 7.89 million ounce Tropicana gold deposit by AngloGold Ashanti Limited and their Joint Venture

partners Independence Group (Doyle et al., 2009; 2013; 2014). This changed view has been confirmed by the discovery in 2012 of the Nova Ni–Cu–Co deposit by Sirius Resources, which has a maiden resource estimate of 242 kt Ni, 100 kt Cu, and 7.7 kt Co (Sirius Resources, 2012, 2013).

Several mineral systems are now recognized:

- Neoarchean (c. 2500 Ma) thrust-related shear zone Au hosted in amphibolite to granulite facies ortho and paragneisses (Tropicana, Tropicana east)
- Paleoproterozoic (c.1760 Ma) intrusion-related Au–Ag (Voodoo Child)
- Paleoproterozoic stratabound sedimentary clastic-hosted Pb–Zn–Ag–Cu–Au (Trilogy)
- Paleoproterozoic (1800–1600 Ma) magnetite iron ore (Southdown)
- Mesoproterozoic (c. 1300 Ma) orthomagmatic mafic intrusion-related Ni–Cu–Co (Nova).

There is potential also for Neoarchean intrusion-related Au associated with c. 2720 Ma sanukitoids (Kirkland et al., 2014; Smithies et al., 2014), and for reworked or metamorphosed orogenic lode-gold mineralization. In addition, remobilization to deposit Proterozoic shear zone-hosted gold is also possible, as well as the formation of intrusion-related deposits associated with Palaeoproterozoic magmatism. Other potential Proterozoic mineral systems include basin-related stratabound volcanic and sedimentary, and sediment-hosted Au and base metal deposits (VMS, SEDEX). Orthomagmatic mafic intrusion-related deposits could also occur associated with the widespread Paleo- and Mesoproterozoic magmatic events. The Mesoproterozoic A-type granitic intrusions of the Esperance Supersuite have potential to host Sn and W, Mo mineralization or to host iron oxide–copper–gold style (IOCG) mineralization.

Tectonic subdivisions and geodynamic setting

The Albany–Fraser Orogen is developed along the southern and southeastern margin of the Yilgarn Craton (Fig. 1), with the eastern extent currently interpreted as the Rodona Shear Zone separating the orogen from the Madura Province (Spaggiari et al., 2012, 2014b,c). Reworking of the Yilgarn Craton margin took place during the Paleo- to Mesoproterozoic from at least 1810 Ma through to 1125 Ma (Kirkland et al., 2011, 2014; Spaggiari et al., 2011).

The orogen is divided into two main tectonic units: the Northern Foreland and the Kepa Kurl Booya Province (Plates 1, 2 and 3). The Northern Foreland originated as part of the Archean Yilgarn Craton, with a strong isotopic similarity observed between the two (Kirkland et al., 2011). The Kepa Kurl Booya Province (Spaggiari et al., 2009, 2011), is defined as the crystalline basement of the Albany–Fraser Orogen. It includes four fault-bound geographical and structural zones (Tropicana, Biranup, Fraser, and Nornalup) that contain rocks with variable protolith ages and geological histories (Spaggiari et al., 2009, 2011, 2014a; Occhipinti et al., 2014). Archean events include c. 2720 Ma magmatism, followed by medium to high-grade metamorphism until c. 2600 Ma, followed by thrust emplacement and accompanying hydrothermal mineralization at 2520 Ma (Occhipinti et al., 2014; Kirkland et al., 2014). Paleoproterozoic events include a further hydrothermal event at c. 2110 Ma, felsic magmatism at 1810–1800 Ma and 1780–1760 Ma, and the 1710–1650 Ma Biranup Orogeny (Kirkland et al., 2014). The Mesoproterozoic Albany–Fraser Orogeny took place as the 1345–1260 Ma Stage I, and the 1215–1140 Ma Stage II events.

Three sedimentary basins are present: the 1815–1600 Ma Barren Basin, the 1455–1305 Ma Arid Basin and the 1280–1215 Ma Ragged Basin (Spaggiari et al., 2014c). Within the Biranup Zone and throughout the Nornalup Zone granitic intrusions belong to either the 1330–1280 Ma Recherche Supersuite or to the 1200–1125 Ma Esperance Supersuite, coinciding with Stages I and II of the Albany–Fraser Orogeny respectively.

Recent work indicates that the Albany–Fraser Orogen has developed entirely within the extended margin of the Yilgarn Craton, with Paleoproterozoic magmatism in the Biranup Zone strongly linked physically and isotopically to the Yilgarn Craton, demonstrated by the preservation of Yilgarn-like Archean metagranite in the Biranup Zone and Biranup Zone intrusions extending into the Northern Foreland and Tropicana Zone (Spaggiari et al., 2011; Kirkland et al., 2011). Isotopic evidence indicates that Archean material is preserved in the lower crust as far east as the Rodona Shear Zone (Kirkland et al., 2014). This suggests an extended continental margin or distal back-arc basin setting during the Paleoproterozoic (Barren Basin) evolving to a marginal basin flanked by a passive margin (Arid Basin) (Spaggiari et al., 2014c). During the Mesoproterozoic initiation of a subduction zone to the east led first to the accretion of a c. 1410 Ma oceanic arc (Loongana Arc, Madura Province) at c. 1330 Ma and the closure of the Arid Basin via east-dipping subduction. Continued outboard, west-dipping subduction then put the orogen into a back-arc setting before final collision with the Mawson Craton (Smithies et al., 2013; Clark et al., 2014; Spaggiari et al., 2014c). Stage II represents orogenesis during intracratonic reactivation and is largely responsible for the preserved crustal architecture.

Northern Foreland

The Northern Foreland is the portion of the Archean Yilgarn Craton that was intruded by Paleoproterozoic magmatic rocks, and reworked during the Paleoproterozoic Biranup Orogeny and the Mesoproterozoic Albany–Fraser Orogeny (Myers, 1990; Nelson et al., 1995; Spaggiari et al., 2009, 2011; Spaggiari and Pawley, 2012). It consists of greenschist and amphibolite to granulite facies, Archean gneisses and granites, remnant greenstones, and younger dolerite dykes (Myers, 1995; Spaggiari et al., 2009). The Munglinup Gneiss, with protolith ages of 2717–2640 Ma, is a major component of the Northern Foreland and is preserved in thrust sheets in the central part of the orogen (Plate 3; Nelson et al., 1995; Spaggiari et al., 2009, 2011).

Figure 1. Major resource projects and operating mines, southeast Yilgarn Craton and Albany–Fraser Orogen

Gold occurrences

The Northern Foreland contains known gold mineralization and a number of prospects have been explored (Plates 2 and 3). Sipa Resources and Newmont Exploration reported that their Woodline Project consists of chlorite schists, mafic schists and quartz mica schists, which they suggest represent reworked Yilgarn Craton (Newmont Exploration, 2009).

The AngloGold Ashanti – Independence Group Tropicana Joint Venture Beachcomber project lies within the Northern Foreland between the Yellow Dam Shear Zone and the Frog Dam Shear Zone (Plate 2), which marks the boundary with the Biranup Zone to the east (AngloGold Ashanti Australia, 2013). Gold mineralization of 4 m at 43.5 grams per tonne has been reported from drilling at the project (MiningNews, 2006).

Considering the range in metamorphic grade of Archean rocks within the Northern Foreland, and their variable state of reworking (Newmont Exploration, 2009), Archean orogenic lode-Au mineralization, reworked Archean Au, or even shear-zone hosted Proterozoic Au mineralization may have developed and have been preserved.

Kepa Kurl Booya Province: Tropicana Zone

The newly named Tropicana Zone is defined as part of the Kepa Kurl Booya Province (Occhipinti et al., 2014). Although the Tropicana Zone contains Archean rocks that have an affinity to the Yilgarn Craton and include felsic and mafic gneisses, metagranite and metamorphosed banded iron-formation, their geological evolution is distinct and cannot be correlated with adjacent terranes, such as the Yamarna Terrane (Occhipinti et al., 2014; Kirkland et al., 2014). Furthermore, the Tropicana Zone has been emplaced into its current position over the Yamarna Terrane of the Yilgarn Craton an unknown distance via the c. 2500 Ma Plumridge Detachment (Occhipinti et al., 2014). It is for this reason that it is not included in the Northern Foreland of the Albany–Fraser Orogen, i.e. because it has formed in a different tectonic setting. The Tropicana Zone shares a similar geological history to the Northern Foreland and Biranup Zone from at least 1800 Ma, with deposition of Barren Basin sedimentary rocks (Lindsay Hill Formation), and intrusion of Paleoproterozoic granitic rocks such as the c. 1800 Ma Black Dragon Gneiss, the c. 1763 Ma McKay Creek Metasyenogranite (associated with the Voodoo Child Formation), the c. 1710 Ma Bobbie Point Metasyenogranite, and most likely 1690–1670 Ma metagranitic and metagabbroic rocks similar to those dated in the adjacent Pleiades Lakes area of the Biranup Zone (Plate 1; Spaggiari et al., 2011; Occhipinti et al., 2014).

Tropicana, Havana and Tropicana East Au

AngloGold Ashanti Limited's large (7.89 million ounce) Tropicana gold deposit, which includes the Boston Shaker, Tropicana, and Havana North and South deposits, is located 330 km east-northeast of Kalgoorlie in the Great Victoria Desert (Doyle et al., 2009). Sixty kilometres to the northeast are Beadell Resources' Atlantis and Hercules Au prospects discovered in 2012 (Tropicana East; Beadell Resources, 2014).

The Tropicana gold deposit, and the Tropicana East prospect are all hosted within Neoarchean rocks of the Tropicana Zone (Spaggiari et al., 2014; Occhipinti et al., 2014; Doyle et al., 2014; Kirkland et al., 2014). They are dominated by granitic orthogneisses, with the oldest unit dated at c. 2720 Ma, followed by further granite intrusion, and amphibolite to granulite facies metamorphism at c. 2640 Ma (Kirkland et al., 2013). At Hat Trick Hill near Tropicana metamorphosed banded iron formation is present (Fox et al., 2012) together with felsic to mafic paragneiss and associated felsic to ultramafic intrusions interpreted as a sequence of volcano-sedimentary rocks deposited in a deep, quiet water submarine setting (Doyle et al., 2009).

The rocks hosting the Tropicana–Havana deposit are bounded by large-scale shear zones and faults interpreted to be within an imbricate fold and thrust belt (D_2 of Blenkinsop and Doyle, 2014), consistent with the interpretation of seismic line 12GA-T1 (Occhipinti et al., 2014; Plate 1). Thrusting has transported the upper amphibolite to granulite facies rocks to the northwest over what is interpreted in line 12GA-T1 as typical low reflectivity Yilgarn Craton granite–greenstone upper crust of the Yamarna Terrane (Blenkinsop and Doyle, 2014; Occhipinti et al., 2014; Korsch et al., 2014).

Gold deposition is structurally controlled within a network of moderately east to southeasterly dipping biotite–pyrite shear zones formed during northeast-southwest shortening (Blenkinsop and Doyle, 2014). Rather than representing a separate event from the D_2 northwest directed thrusting, the compression direction is consistent with that expected within a D_2 lateral thrust ramp occurring orthogonal to the transport direction. The D_2 and D_3 events of Blenkinsop and Doyle (2014) can occur contemporaneously within the observed map pattern of linked imbricate thrusts and lateral ramps (see Plate 1). Mineralization, and therefore thrust emplacement, is interpreted to post-date peak high-grade metamorphism and has been dated as occurring at 2524–2515 Ma, 140 million years younger than typical Yilgarn Craton orogenic lode gold deposits (Doyle et al., 2009; Blenkinsop and Doyle, 2013; 2014). Blenkinsop and Doyle (2014) have interpreted the deposit as forming by hydrothermal fluid flow within the developing margin of the proto-Albany–Fraser Orogen.

Re–Os dating of gold-bearing pyrite in brittle fractures associated with mineralization in similar Archean gneisses (Hercules Gneiss, Plate 1) at Tropicana East has given an age of c. 2110 Ma (Kirkland et al., 2014). This suggests that mineralization in the Tropicana Zone was not confined to one discrete event but may have occurred episodically from the latest Neoarchean into the early Paleoproterozoic, prior to large-scale magmatic and tectonic events that affected the orogen during the later Paleoproterozoic and the Mesoproterozoic.

Voodoo Child Au–Ag

The Voodoo Child Au–Ag deposit is located 50 km to the northeast of Tropicana and is hosted in Paleoproterozoic greenschist facies mafic and felsic intrusive and dacitic volcanic rocks within barren granites (Less, 2013). Mineralization is intrusion-related and occurs within biotite- and sericite-altered microgranodiorite, with electrum grains associated with chalcopyrite, pyrite and sphalerite. In addition Au–Ag mineralization accompanies disseminated pyrite and biotite-sericite ± silica alteration of a reactive quartz diorite.

Less (2013) noted that mineralization is later than at Tropicana with the intrusions and adjacent volcano-sedimentary rocks dated at c. 1760 Ma. This is provides additional evidence of multiple Au mineralizing (or upgrading) events within the Albany–Fraser Orogen.

Archean sanukitoids as a source of Au in the Tropicana Zone

Archean metadiorites, metamonzodiorites, and metagranites analysed at Tropicana East (Hercules Gneiss, Plate 1) indicate a suite of rocks dated at around c. 2720 Ma that is high-Mg and LILE-enriched and can

be classified as sanukitoid (Smithies et al., 2014; Kirkland et al., 2014). These intrusive rocks are indicative of direct derivation from a mantle source region enriched by subducted slab-derived melts. Sanukitoids have been linked to gold fertility and may provide a repeatedly remobilized source for gold in the Tropicana Zone.

Barren Basin

The Barren Basin comprises Paleoproterozoic metasedimentary rocks belonging to the Stirling Range Formation, Mount Barren Group, Lindsay Hill Formation, Woodline Formation (Woodline Sub-basin), the Fly Dam Formation, and unnamed occurrences of psammitic to semipelitic schist and gneiss (Spaggiari et al., 2014c). These units overlie the Yilgarn Craton, Northern Foreland, and the Biranup and Nornalup Zones (Muhling and Brakel, 1985; Thom et al., 1977, 1984; Hall et al., 2008; Spaggiari et al., 2009, 2011).

The basin formed in an extended continental margin or distal back-arc basin setting (Spaggiari et al., 2014c), with deposition dominated by siliclastic rocks, although volcanic rocks such as those at the Voodoo Child prospect (Less, 2013) may be related to the early stages of basin development. Components of the Barren Basin may be prospective for sediment-hosted base metal deposits, unconformity- and sandstone-hosted U, and volcanic-hosted massive sulfide style deposits.

Trilogy Pb–Zn–Ag–Cu–Au

The Trilogy Pb–Zn–Ag–Cu–Au deposit (Fig. 1) has been described by Sampson and Bourne (2001) based on the original exploration by Homestake Gold of Australia Limited and by Tectonic Resources NL. The deposit was discovered by Homestake in 1997 and is located 25 km south of Ravensthorpe within the c. 1696 Ma amphibolite facies metasedimentary rocks of the Mount Barren Group, deposited in the Barren Basin (Vallini et al., 2002; 2005). The Mount Barren Group here was deposited unconformably on the Archean Cocaranup and Carlingup greenstones belts, which contain Au, Cu and Ni mineralization, but was affected by a northwest-directed fold and thrust system (Witt, 1998).

The deposit probably represents a clastic-hosted stratabound sedimentary deposit made up of polymetallic massive sulfide mineralization hosted within graphitic phyllites. Pb–Zn–Ag sulfide mineralization is cut by Cu–Au stringer mineralization, contained within a silicified envelope suggestive of Mount Isa-style mineralization. The deposit has resources of 163 000 oz Au, 9.3 million oz Ag and 65 t Cu (Silver Lake Resources, 2014).

Kepa Kurl Booya Province: Biranup Zone

The Biranup Zone of the Kepa Kurl Booya Province is a belt of predominantly mid-crustal rocks that lies along the entire southern and southeastern margin of the Yilgarn Craton (Myers, 1990; Spaggiari et al., 2009, 2011). In the eastern part of the orogen, the Biranup Zone is in fault contact to the southeast with the Mesoproterozoic Fraser and Nornalup Zones (Plates 2 and 3). In an area denoted the 'S-bend', it is primarily tectonically interlayered with reworked rocks of the Yilgarn Craton within the Northern Foreland, but also contains fragments of Yilgarn Craton granite within it (Spaggiari et al., 2009; 2011). The Biranup Zone is dominated by intensely deformed orthogneiss, metagabbro, and paragneiss, with ages ranging 1800–1625 Ma (Kirkland et al., 2011).

Southdown Fe

Grange Resources Limited's Southdown magnetite deposit is located 90 km northeast of Albany. No age information is available, but it is interpreted here as iron-rich metasedimentary rocks deposited originally as part of an unassigned sedimentary succession, possibly within the Barren Basin, and then deformed and metamorphosed at high grade during the Biranup and Albany–Fraser orogenies.

The deposit is 12 km long consisting of an overturned, tight to isoclinal, gently easterly plunging syncline (Grange Resources, 2005; 2014). The core of the fold is occupied by high-grade quartz–magnetite–clinopyroxene gneiss, quartz–sulfide–garnet gneiss, feldspar–pyroxene–magnetite gneiss and garnet–biotite gneiss.

Grange Resources (2014) have reported mineral resources of 1256.9 Mt @ 33.7% DTR and ore reserves totalling 387.7 Mt @ 35.6% DTR.

Gold occurrences

International Goldfields'/Segue Resources Corvette prospect at their Plumbridge Project occurs within the Biranup Zone (Plate 2).

Kepa Kurl Booya Province: Fraser Zone

The Fraser Zone is bounded by the Fraser Shear Zone along its northwestern edge and southern tip, and by the Newman and Boonderoo Shear Zones along its southeastern edge (Plate 1, 2 and 3). It is dominated by high-grade metagabbroic rocks that have a strong, distinct, geophysical signature in both aeromagnetic and gravity data (Spaggiari et al., 2011). Most of the northeastern part of the Fraser Zone is obscured by younger rocks of the Eucla Basin, but geophysical data show that it is a northeasterly trending, fault-bounded unit that is approximately 425 km long and up to 50 km wide.

The Fraser Zone contains the 1305–1290 Ma Fraser Range Metamorphics (Spaggiari et al., 2009; 2011), which are dominated by sheets of metagabbroic rocks, interlayered with sheets of granitic material, and layers or slivers of pelitic, semipelitic, and calcic metasedimentary rocks of the Arid Basin. Metamorphism took place in the granulite facies up to 850° C and 7–9 kbars soon after magmatism

(Clark et al., 2014). The tectonic setting is interpreted as a lower crustal hot zone, possibly formed in a rift-like setting within a distal back-arc basin related to a subduction zone at a Mesoproterozoic continental margin to the east (Smithies et al., 2013; Clark et al., 2014).

Fraser Range Ni–Cu–Co

Sirius Resources announced the discovery of the Nova Ni–Cu–Co deposit within the Fraser Zone in July 2012 (Sirius Resources, 2012, 2013; Plate 2). It is interpreted as a primary magmatic nickel sulfide deposit made up of pyrrhotite, pentlandite, and chalcopyrite within gabbroic granulites that define a structure known as The Eye (Sirius Resources, 2012; 2013). The deposit has a maiden resource estimate of 242 kt Ni, 100 kt Cu and 7.7 kt Co (Sirius Resources, 2013). Sirius Resources have announced a further discovery at Bollinger, located to the east of Nova (Plate 2).

The main gabbros of the Fraser Zone have relatively high Ni/Cu ratios and depleted PGE contents (Ni/Cu = 2–3; Smithies et al., 2013; Smithies et al., 2014), and this also appears to be a feature of the Nova discovery (Sirius Resources, 2012). The suggestion that these gabbros might be cogenetic makes the entire Fraser Zone prospective for similar Ni–Cu mineralization. Sirius Resources has drawn comparison with the geological setting of the Proterozoic Circum-Superior Belt in Canada, which similarly fringes an Archean craton and hosts world-class nickel deposits at Thompson, Raglan, and Voiseys Bay.

Other mineral systems

There is potential for further Proterozoic shear zone and intrusion-related Au throughout the orogen associated with events that have been defined as occuring prior to the Biranup Orogeny (the Salmon Gums and Ngadju Events, Spaggiari et al., 2014a), the Biranup Orogeny itself, and with Stage I and Stage II of the Albany–Fraser Orogeny. The Arid and Ragged basins could have developed in a back-arc tectonic setting that was conducive to the formation of basin-related stratabound volcanic and sedimentary-hosted Au and base metal deposits (VMS, SEDEX).

Gabbros of the Salt Creek Complex purported to have intruded into the Tropicana Zone and Northern Foreland late in Stage II of the Albany–Fraser Orogeny have been explored for orthomagmatic Ni–Cu mineralization by Mithril Resources (2003, 2005). These rocks form a semi-contiguous north-northeast trending belt east of the Fraser Zone and have potential for orthomagmatic mafic intrusion-related mineralization.

The Esperance Supersuite is made up of A-type granitic rocks that have the potential for greisen- or breccia-related Sn and W, for porphyry Mo and for IOCG deposits. Orthomagmatic mafic intrusion-related deposits may also occur associated with the Biranup Orogeny magmatic rocks, with the Recherche Supersuite, and with the Esperance Supersuite. The considerably older, mingled gabbroic rocks of the c. 1660 Ma Eddy Suite are difficult to distinguish geochemically from the Fraser gabbros, and may have a similar upper mantle source component (Smithies et al., 2014). The Eddy Suite occurs as an east-dipping, fault-bound package beneath the Fraser Shear Zone (Plate 4, Spaggiari et al., 2014b). At c. 1210 Ma mafic intrusions related to the Marnda Moorn large igneous province were intruded into the Yilgarn Craton margin (Wingate and Pidgeon, 2005; Wang et al., 2014). This event occurred shortly after the start of high-grade metamorphism during Stage II of the Albany–Fraser Orogeny (now thought to be c. 1225 Ma, Spaggiari et al., 2014c). In the Yilgarn Craton margin the Marnda Moorn large igneous province consists of dolerite or gabbro dykes of the Gnowangerup – Fraser Dyke Suite. The dykes do not appear to cut across the Albany–Fraser Orogen but may be represented by irregular, mingled and mixed mafic rocks within migmatitic Munglinup Gneiss and Biranup Zone gneisses, and in the older part of the Esperance Supersuite.

Setting of mineral systems in the Albany–Fraser Orogen

The Albany–Fraser deep seismic reflection and MT survey was designed to cross the southeastern boundary of the Yilgarn Craton, into the adjacent Albany–Fraser Orogen. This region is an underexplored greenfields terrain whose mineral prospectivity was largely ignored up until 2005, when the discovery of the Tropicana Au deposit dramatically changed perceptions. The following discovery of the Nova Ni–Cu–Co deposit in 2012 further increased the prospectivity of the belt for a range of commodities, not just Au. Both deposits differ significantly in age and style from the world class Au and Ni deposits in the adjacent Archean Yilgarn Craton to the northwest.

The deep seismic reflection and MT lines, together with new surface geological mapping, medium-resolution airborne magnetic and ground gravity surveys, whole-rock geochemistry, geochronology and isotopic studies have provided insights into the architecture and the geological evolution of the region and its related mineral systems. The orogen does have characteristics that have been recognized as prospective by modern targeting philosophies. It is an old cratonic margin, reactivated by plate margin processes related to collision, and by repeated rifting in continental margin and back-arc settings. There are large-scale structures evident in the seismic and MT profiles (Plate 4) that provide links through the crust, tapping into an underlying, apparently fertile lithospheric mantle.

The Plumridge Detachment imaged in 12GA-T1 (Plate 4), is dated at c. 2520 Ma as a latest Neoarchean, northwest directed thrust system carrying the allocthonous Archean Tropicana Zone onto the granite–greenstone basement of the Eastern Goldfields Superterrane. The rocks within the Tropicana Zone include a c. 2720 Ma suite of sanukitoids, derived from metasomatized mantle above a subducting slab, and therefore possibly formed at a c. 2720 Ma continental margin. These have a similar crystallization age to the supposed plume-related komatiite related

Ni–sulfide mineral system at the base of the greenstones in the Kalgoorlie and Kurnalpi Terranes of the Eastern Goldfields Superterrane consistent with a different tectonic setting. Prolonged granulite facies metamorphism until c. 2600 Ma in the Tropicana Zone spanned the ensuing evolution of the Eastern Goldfields, and the associated orogenic lode-gold mineral system that deposited the Golden Mile. This suggests that the Tropicana Zone was buried to a deeper crustal level for an extended period before being thrust onto the southern Eastern Goldfields Superterrane from the southeast at c. 2520 Ma, accompanied by the development of a major hydrothermal gold-bearing mineral system sourced from the buried craton margin. This buried source region, possibly within the Gunnadorah Seismic Province (Korsch et al., 2014) had the potential to be tapped repeatedly during the subsequent Proterozoic evolution of the Albany–Fraser Orogen via structures such as those evident in 12GA-AF3 (Plate 4), forming shear and intrusion-related deposits.

The Paleoproterozoic Trilogy polymetallic stratabound sedimentary deposit is within the c. 1700 Ma Barren Basin and is adjacent to the Jerdacutup Fault, which on line 12GA-AF2 and 12GA-AF1 (Plate 4) can be linked through the crust to the mantle via a series of east-dipping shear zones that separate the Archean Yarraquin Seismic Province, forming the lower crust of the Yilgarn Craton, from the Munglinup Gneiss and the Biranup and Nornalup Zones.

The Fraser Range Ni–Cu–Co deposits are present in the Fraser Zone, which is bound by the Fraser and Boonderoo Shear Zones. On 12GA-AF3 (Plate 4) the Fraser Zone is interpreted as a wedge-shaped unit in the upper crust above a system of easterly dipping shear zones, and was apparently thrust into place from deeper in the crust, after intrusion at c. 1300 Ma (Spaggiari et al., 2014b). The underlying shear zones link to the top of the Gunnadorah Seismic Province (Plate 4), and again suggest a link to the buried Archean plate margin and to the associated fertile metal source in the underlying lithospheric mantle.

Later, c. 1200 Ma mafic magmatism may relate to the early evolution of post-melting residual hot zones interpreted as the lower crustal, non-reflective zones on 12GA-AF2 and 12GA-AF3 within Yilgarn Craton lower crust of the Yarraquin and Udarra seismic provinces (Plate 4).

References

AngloGold Ashanti Australia Limited 2007, Annual Report, Tropicana Project: Geological Survey of Western Australia, Statutory mineral exploration report, A76262 (unpublished).

AngloGoldAshanti Australia Limited 2013, Tropicana JV Project, Tropicana Group 4 Project – Final Surrender Report: Geological Survey of Western Australia, Statutory mineral exploration report, Combined Report number, C58-2005 (unpublished).

Beadell Resources Limited 2014, Beadell Resources Limited, West Perth Western Australia, viewed 3 March 2014, <www.beadellresources.com.au/irm/content/tropicana-east.aspx?RID=228>.

Blenkinsop, TG and Doyle, MG 2013, Structural controls on gold mineralization on the margin of the Yilgarn craton, Albany Fraser orogeny: the Tropicana deposit, Western Australia, *in* Future understanding of tectonics, ores, resources, environment and sustainability *edited by* Z Chang, R Goldfarb, T Blenkinsop, C Palczek, D Cooke, K Camuti and J Carranza: FUTORES Conference, Economic Geology Research Unit Contribution 68, James Cook University, Townsville, Australia, 2–5 June 2013, p. 37.

Blenkinsop, TG and Doyle, MG 2014, Structural controls on gold mineralization on the margin of the Yilgarn craton, Albany–Fraser orogen: The Tropicana Deposit, Western Australia: Journal of Structural Geology, doi: 10.1016/j.jsg.2014.01.013.

Clark, C, Kirkland, CL, Spaggiari, CV, Oorschot, C, Wingate, MTD and Taylor, R 2014, Proterozoic granulite formation driven by magmatism: an example from the Fraser Range Metamorphics, Western Australia: Precambrian Research, v. 240, p. 1–21.

Doyle, MG, Gibbs, D, Savage, J and Blenkinsop, TG 2009, Geology of the Tropicana Gold Project, Western Australia, *in* Smart science for exploration and mining: Economic Geology Research Unit, James Cook University; 10th Biennial SGA Meeting of the Society for Geology Applied to Mineral Deposits, Townsville, Queensland, 17 August 2009: Proceedings volume 1, p. 50–52.

Doyle, M, Savage, J, Blenkinsop, T, Crawford, A and McNaughton, N, 2013, Tropicana – Unravelling the complexity of a +6 Million Ounce Gold Deposit Hosted in Granulite Facies Metamorphic Rocks: The Australian Institute of Mining and Metallurgy Publication Series, no. 9/2013, p. 87–93.

Doyle, MG, Blenkinsop, TG, Crawford, AJ, Fletcher, IR, Foster, J, Fox-Wallace, L, Large, RR, Mathur, R, McNaughton, NJ, Meffre, S, Muhling, JR, Occhipinti, SA, Rasmussen, B and Savage, J 2014, Tropicana deposit, Western Australia: an integrated approach to understanding granulite-hosted gold and the Tropicana Gneiss: *in* Albany–Fraser Orogen seismic and magnetotelluric (MT) workshop 2014: extended abstracts, *compiled by* CV Spaggiari and IM Tyler: Geological Survey of Western Australia, Record 2014/6, p. 69–76.

Fox, LJ, Blenkinsop, TG and Doyle, MG 2012, Geology of the Hat Trick Prospect, Tropicana Region, Northern Foreland of the Albany Fraser orogeny, WA: Geological Society of Australia, Abstracts 102, p. 39–40.

Grange Resources Limited 2005, Grange Resources Limited, Burnie Tasmania, viewed 3 March 2014, <www.grangeresources.com.au/clients/grange/downloads/item60/17~Southdown%20Preliminary%20Final%20Report%20(358.62%20Kb)%20%20-%2014%20Sep%2005.pdf>.

Grange Resources Limited 2014, Grange Resources Limited, Burnie Tasmania, viewed 3 March 2014, <www.grangeresources.com.au/clients/grange/downloads/item178/grange_resources_updated_resource_and_reserve_statement_-_southdown_project__-_28_february_2014.pdf>.

Griffin, WL, Begg, GC and O'Reilly, SY 2013, Continental-root control on the genesis of magmatic ore deposits: Nature Geoscience, v. 6, p. 905–910.

Hall, CE, Jones, SA and Bodorkos, S 2008, Sedimentology, structure and SHRIMP zircon provenance of the Woodline Formation, Western Australia: Implications for the tectonic setting of the West Australian Craton during the Paleoproterozoic: Precambrian Research, v. 162, p. 577–598.

Hronsky, JMA 2011, Self-organized critical systems and ore formation: The key to spatial targeting? Society of Economic Geology Newsletter, v. 84, p. 14–16.

Hronsky, JMA and Groves, DI 2008, Science of targeting: Definition, strategies, targeting and performance measurement: Australian Journal of Earth Science v. 55, p. 3–12.

Kirkland, CL, Spaggiari, CV, Pawley, MJ, Wingate, MTD, Smithies, RH, Howard, HM, Tyler, IM, Belousova, EA and Poujol, M 2011, On the edge: U–Pb, Lu–Hf, and Sm–Nd data suggests reworking of the Yilgarn Craton margin during formation of the Albany–Fraser Orogen: Precambrian Research, v. 187, p. 223–224.

Kirkland, CL, Spaggiari, CV, Smithies, RH and Wingate, MTD 2014, Cryptic progeny of craton margins: Geochronology and Isotope Geology of the Albany–Fraser Orogen with implications for evolution of the Tropicana Zone, *in* Albany–Fraser Orogen seismic and magnetotelluric (MT) workshop 2014: extended abstracts *compiled by* CV Spaggiari and IM Tyler: Geological Survey of Western Australia, Record 2014/6, p. 89–101.

Korsch, RJ, Spaggiari, CV, Occhipinti, SA, Doublier, MP, Clark, DJ, Dentith, MC, Doyle, MG, Kennett, BLN, Gessner, K, Neumann, NL, Belousova, EA, Tyler, IM, Costelloe, RD, Fomin, T and Holzschuh, J 2014, Geodynamic implications of the 2012 Albany–Fraser deep seismic reflection survey: a transect from the Yilgarn Craton across the Albany–Fraser Orogen to the Madura Province, *in* Albany–Fraser Orogen seismic and magnetotelluric (MT) workshop 2014: extended abstracts *compiled by* CV Spaggiari and IM Tyler: Geological Survey of Western Australia, Record 2014/6, p. 142–173.

Less, T 2013 Newly recognized Paleoproterzoic gold–silver mineralization in the Albany-Fraser orogeny, *in* Future understanding of tectonics, ores, resources, environment and sustainability *edited by* Z Chang, R Goldfarb, T Blenkinsop, C Palczek, D Cooke, K Camuti and J Carranza: FUTORES Conference, Economic Geology Research Unit Contribution 68, James Cook University, Townsville, Australia 2–5 June 2013, p. 31.

McCuaig, TC, Beresford, S and Hronsky, JMA 2010, Translating the mineral systems approach into an effective exploration targeting system: Ore Geology Reviews, v. 38, p. 128–138.

Mining News 2006, Tropicana expands with hits at Beachcomer: MiningNews, Friday 10 November 2006.

Mithril Resources Limited 2003, Annual Report, 2003, Plumridge Project EL39/871,872,873,874,931,934 and E69/1573 2002/2003: Geological Survey of Western Australia, Statutory mineral exploration report, Combined Annual Technical Report A66752 (unpublished).

Mithril Resources Limited 2005, Final Report, 2005, Plumridge Project ET 39/871: Geological Survey of Western Australia, Statutory mineral exploration report A070970 (unpublished).

Muhling, PC and Brakel, AT 1985, Geology of the Bangemall Group: the evolution of a Proterozoic intra-cratonic sedimentary basin: Geological Survey of Western Australia, Bulletin 128, 266p.

Myers, JS 1990, Albany–Fraser Orogen, in Geology and mineral resources of Western Australia: Geological Survey of Western Australia, Memoir 3, p. 255–263.

Myers, JS 1995, Geology of the Esperance 1:1 000 000 sheet (2nd edition): Geological Survey of Western Australia, 1:1 000 000 Geological Series Explanatory Notes, 10p.

Nelson, DR, Myers, JS and Nutman, AP 1995, Chronology and evolution of the Middle Proterozoic Albany–Fraser Orogen, Western Australia: Australian Journal of Earth Sciences, v. 42, p. 481–495.

Newmont Exploration Proprietary Limited 2009, Partial relinquishment report for E28/1483 for the period 2 March 2005 to 1 March 2008, Woodline Project — Sipa JV, Western Australia: Geological Survey of Western Australia, Statutory mineral exploration report, CR34075.

Occhipinti, SA, Doyle, M, Spaggiari CV, Korsch, R, Cant, G, Martin, K, Kirkland, CL, Savage, J, Less, T, Bergin, L and Foz, L 2014, Interpretation of the deep seismic reflection line 12GA-T1: northeastern Albany–Fraser Orogen, *in* Albany–Fraser Orogen seismic and magnetotelluric (MT) workshop 2014: extended abstracts, *compiled by* CV Spaggiari and IM Tyler: Geological Survey of Western Australia, Record 2014/6, p. 52–68.

Sampson, L and Bourne, B 2001, The geophysical characteristics of the Trilogy massive sulphide deposit, Ravensthorpe, Western Australia: Exploration Geophysics, v. 32, p. 181–184.

Silver Lake Resources 2014, Silver Lake Resources, South Perth Western Australia, viewed 4 March 2014, <www.silverlakeresources.com.au/projects/great-southern-project>.

Sirius Resources NL 2012, Sirius Resources NL, Balcatta Western Australia, viewed 3 March 2014, <www.siriusresources.com.au/documents/SiriusASXannouncement-120726-Significantnickel-copperdiscovery.pdf>.

Sirius Resources NL 2013, Sirius Resources NL, Balcatta Western Australia, viewed 3 March 2014, <www.siriusresources.com.au/documents/130320MaidenNovaResourceEstimate.pdf>.

Smithies, RH, Spaggiari, CV, Kirkland, Howard, HM and Maier, WD 2013, Petrogenesis of gabbros of the Mesoproterozoic Fraser Zone: constraints on the tectonic evolution of the Albany–Fraser Orogen: Geological Survey of Western Australia, Record 2013/5, 29p.

Smithies, RH, Spaggiari, CV, Kirkland, CL and Maier, WD 2014, Geochemistry and petrogenesis of igneous rocks in the Albany–Fraser Orogen, *in* Albany–Fraser Orogen seismic and magnetotelluric (MT) workshop 2014: extended abstracts *compiled by* CV Spaggiari and IM Tyler: Geological Survey of Western Australia, Record 2014/6, p. 77–88.

Spaggiari, CV, Bodorkos, S, Barquero-Molina, M, Tyler, IM and Wingate, MTD 2009, Interpreted bedrock geology of the south Yilgarn and central Albany–Fraser Orogen, Western Australia: Geological Survey of Western Australia, Record 2009/10, 84p.

Spaggiari, CV, Kirkland, CL, Pawley, MJ, Smithies, RH, Wingate, MTD, Doyle, MG, Blenkinsop, TG, Clark, C, Oorschot, CW, Fox, LJ and Savage, J 2011, The geology of the east Albany–Fraser Orogen — a field guide: Geological Survey of Western Australia, Record 2011/23, 97p.

Spaggiari, CV, Kirkland, CL, Smithies, RH, Wingate, MTD, 2012, What lies beneath — interpreting the Eucla basement, *in* GSWA 2012 extended abstracts: promoting the prospectivity of Western Australia: Geological Survey of Western Australia, Record 2012/2, p. 25–27.

Spaggiari, CV and Pawley, MJ 2012, Interpreted pre-Mesozoic bedrock geology of the east Albany–Fraser Orogen and southeast Yilgarn Craton (1:500 000), *in* The geology of the east Albany–Fraser Orogen — a field guide *compiled by* CV Spaggiari, CL Kirkland, MJ Pawley, RH Smithies, MTD Wingate, MG Doyle, TG Blenkinsop, C Clark, CW Oorschot, LJ Fox and J Savage: Geological Survey of Western Australia, Record 2011/23, Plates 1 and 1A.

Spaggiari, CV, Smithies, RH, Kirkland, CL, Howard, HM, Maier, WD and Clark, C 2013, melting, mixing, and emplacement: evolution of the Fraser Zone, Albany–Fraser Orogen, *in* GSWA 2013 extended abstracts: promoting the prospectivity of Western Australia: Geological Survey of Western Australia, Record 2013/2, p. 1–5.

Spaggiari, CV, Kirkland, CL, Smithies, RH, Occhipinti, SA and Wingate, MTD 2014a, Geological framework of the Albany–Fraser Orogen, *in* Albany–Fraser Orogen seismic and magnetotelluric (MT) workshop 2014: extended abstracts *compiled by* CV Spaggiari and IM Tyler: Geological Survey of Western Australia, Record 2014/6, p. 12–27.

Spaggiari, CV, Occhipinti, SA, Korsch, RJ, Doublier, MP, Clark, DJ, Dentith, MC, Gessner, K, Doyle, MG, Tyler, IM, Kennett, BLN, Costelloe, RD, Fomin, T and Holzschuh, J 2014b, Interpretation of Albany–Fraser seismic lines 12GA-AF1, 12GA-AF2 and 12GA-AF3: implications for crustal architecture, *in* Albany–Fraser Orogen seismic and magnetotelluric (MT) workshop 2014: extended abstracts, *compiled by* CV Spaggiari and IM Tyler: Geological Survey of Western Australia, Record 2014/6, p. 28–51.

Spaggiari CV, Kirkland CL, Smithies RH, and Wingate MTD, 2014c, Tectonic links between sedimentary cycles, basin formation and magmatism in the Albany–Fraser Orogen, Western Australia Geological Survey of Western Australia, Report 133, 63p.

Thom, R, Lipple, SL and Sanders, CC 1977, Ravensthorpe, Western Australia: Geological Survey of Western Australia, 1:250 000 Geological Series, Explanatory Notes.

Thom, R, Chin, RJ and Hickman, AH 1984, Newdegate, Western Australia: Geological Survey of Western Australia, 1:250 000 Geological Series, Explanatory Notes.

Vallini, DA, Rasmussen, B, Krapež, B, Fletcher, IR and McNaughton, NJ 2002, Obtaining diagenetic ages from metamorphosed sedimentary rocks: U–Pb dating of unusually coarse xenotime cement in phosphatic sandstone: Geology, v. 30, p. 1083–1086.

Vallini, DA, Rasmussen, B, Krapež, B, Fletcher, IR and McNaughton, N 2005, Microtextures, geochemistry and geochronology of authigenic xenotime constraining the cementation history of a Paleoproterozoic metasedimentary sequence: Sedimentology, v. 52, p. 101–122.

Wang, X-C, Li, Z-X, Li, J, Pisarevsky, SA and Wingate, MTD 2014, Genesis of the 1.21 Ga Marnda Moorn large igneous province by plume–lithosphere interaction: Precambrian Research, v. 241, p. 85–103.

Wingate, MTD and Pidgeon, RT 2005, The Marnda Moorn LIP, a late Mesoproterozoic large igneous province in the Yilgarn craton, Western Australia: LIP of the Month, July 2005, <www.largeigneousprovinces.org>.

Witt, WK 1998, Geology and mineral resources of the Ravensthorpe and Cocanarup 1:100 000 sheets: Geological Survey of Western Australia, Report 54, 152p.

Wyborn, LAI, Heinrich, CA and Jaques, AL 1994, Australian Proterozoic Mineral Systems: Essential Ingredients and Mappable Criteria: Australasian Institute of Mining and Metalurgy Publication Series 5/94, p. 109–115.

RECORD 2014/6

ALBANY–FRASER OROGEN SEISMIC AND MAGNETOTELLURIC (MT) WORKSHOP 2014: EXTENDED ABSTRACTS

Spaggiari and Tyler

This Record is published in digital format (PDF) and is available as a free download from the DMP website at <www.dmp.wa.gov.au/GSWApublications>.

Further details of geological products produced by the Geological Survey of Western Australia can be obtained by contacting:

Information Centre
Department of Mines and Petroleum
100 Plain Street
EAST PERTH WESTERN AUSTRALIA 6004
Phone: (08) 9222 3459 Fax: (08) 9222 3444
www.dmp.wa.gov.au/GSWApublications

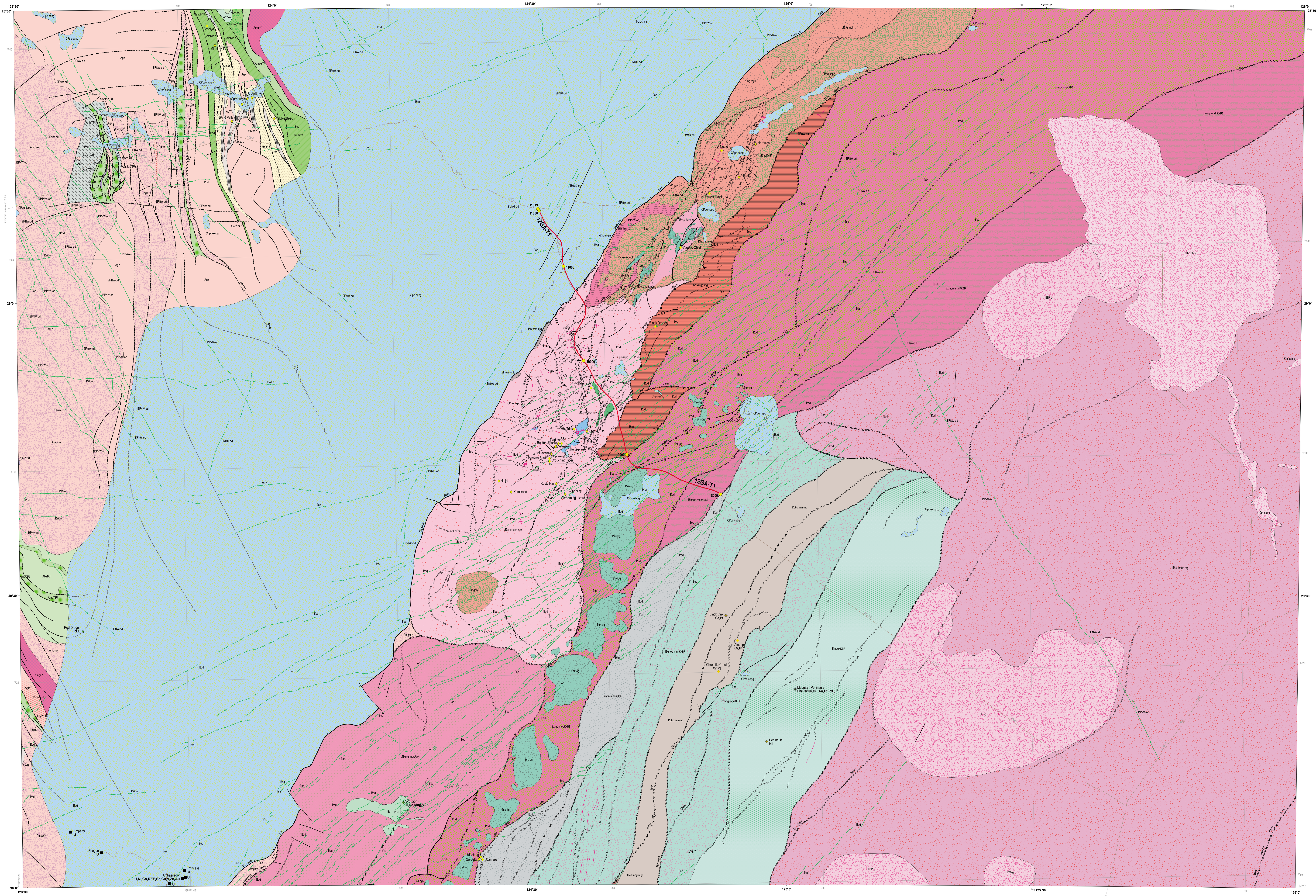

PALEOZOIC — CARBONIFEROUS–PERMIAN

CPpa-sepg — **PATERSON FORMATION:** conglomerate (including diamictite), sandstone, and siltstone; largely glacigene

CAMBRIAN — 508 ±5 Ma

Cth-xbb-s — **TABLE HILL VOLCANICS:** basalt (in part vesicular and/or amygdaloidal) in multiple flows; minor interbedded sandstone and siltstone

PROTEROZOIC–PHANEROZOIC

ƁPNW-od — **Cosmo Newbery Dyke Suite:** northwest-trending mafic dykes; interpreted from aeromagnetic data; concealed where dashed

Ɓo — Undivided mafic intrusive rock
Ɓod — Dolerite dyke, sill, or plug; fine- to medium-grained dolerite and gabbro; concealed where dashed

Ɓsk-og — **SALT CREEK GABBRO:** gabbro or gabbronorite; locally intrusive into metasedimentary rocks

PROTEROZOIC — MESOPROTEROZOIC

Albany–Fraser Orogeny Stage II (1225–1140 Ma)

Esperance Supersuite — 1220–1140 Ma — ƁEP-g — Granitic rock; undeformed to moderately deformed

Gnowangerup–Fraser Dyke Suite — c. 1210 Ma — ƁMMG-od — Dolerite and gabbro dykes; trending east-northeast to northeast; mostly interpreted from aeromagnetic data

Albany–Fraser Orogeny Stage I (1330–1260 Ma)

Recherche Supersuite — 1330–1280 Ma — ƁRE-xmgn-mg — Granitic gneiss and metagranite; heterogeneous; locally with pods or lenses of metagabbro; may include intrusions of Esperance Supersuite and remnants of Paleoproterozoic basement

1310–1283 Ma — ƁFM-xmog-mgn, ƁmogKKBF, Ɓxmog-mgnKKBF

ƁFM-xmog-mgn — **FRASER RANGE METAMORPHICS:** sheeted and mostly strongly deformed metagabbro, metagranite, and minor metasedimentary rocks; includes hybrid rocks and mafic and felsic granulite
ƁmogKKBF — Metagabbroic rock; may include felsic granulite, metagranitic and metasedimentary rocks
Ɓxmog-mgnKKBF — Metagabbroic and metamafic rocks; may include metagranite and metasedimentary rocks, mafic and felsic granulite

1483–1297 Ma — Ɓgk-xmtn-mo — **GWYNNE CREEK GNEISS:** psammitic gneiss with minor semipelitic layers; includes minor metagranitic rocks, metamafic, and meta-ultramafic rocks

1600–1305 Ma — Ɓxmtn-monAFOA — Psammitic and semipelitic gneiss, locally garnet-rich; interlayered with mafic amphibolite to granulite and granitic gneiss

PALEOPROTEROZOIC

Biranup Orogeny (1710–1620 Ma)

1694–1625 Ma — Ɓxmg-mogKKBB — K-feldspar megacrystic metagranite and metasyenogranite, mingled with metagabbroic rock; hybrid rocks; may include remnants of Archean rocks and younger gabbroic rocks
1700–1625 Ma — Ɓxmgn-mdnKKBB — Granitic and sedimentary gneisses dominant; may include remnants of Archean rocks

c. 1708 Ma — Ɓbt-mgr — **BOBBIE POINT METASYENOGRANITE:** metasyenogranite; weakly foliated to mylonitic; includes minor mingled mafic rocks and minor banded iron-formation rafts; may include remnants of McKay Creek Metasyenogranite, and Tropicana or Hercules Gneiss

1752–1600 Ma — Ɓlh-xmf-mtq — **LINDSAY HILL FORMATION:** quartzite and metasandstone, interbedded with metasiltstone; locally interbedded with metaconglomerate and pebbly metasandstone

Ngadju Event (1780–1760 Ma)

c. 1760 Ma — Ɓkc-xmgr-mgi — **McKAY CREEK METASYENOGRANITE:** metasyenogranite, mingled with metagabbro; may include intrusions of Bobbie Point Metasyenogranite, and remnants of Voodoo Child Formation and Hercules or Tropicana Gneiss

1780–1700 Ma — Ɓvc-xmog-mfd — **VOODOO CHILD FORMATION:** interlayered mafic to ultramafic intrusive rocks, metabasaltic to metadacitic volcanic rocks, and metasedimentary rocks; may include Paleoproterozoic metagranite

Salmon Gums Event (1815–1800 Ma)

1815–1790 Ma — Ɓbd-xmgg-mgi — **BLACK DRAGON GNEISS:** metagranodiorite and metadiorite; may include remnants of Archean rocks and Tropicana Gneiss

ARCHEAN–PROTEROZOIC — NEOARCHEAN–PALEOPROTEROZOIC

2800–1600 Ma — ÆmgKKBT — Metagranite; intrudes Tropicana or Hercules Gneiss

Ætc-xmgn-mon — **TROPICANA GNEISS:** interlayered granitic gneiss including tonalitic and dioritic compositions, mafic gneiss, garnet gneiss, and minor metachert and metamorphosed iron formation; may include intrusions of Paleoproterozoic metagranite
Ætc-xmin-mog — Metamorphosed banded iron-formation, metagabbro and metaleucogabbro; may include Archean or Paleoproterozoic metagranite
Ætc-xmog-mue — Metagabbro and metamorphosed ultramafic rocks; intruded by metagranite
Æhg-mgin — **HERCULES GNEISS:** metadiorite and quartz metamonzodiorite gneiss; locally intruded by Paleoproterozoic granite and mafic rocks

Widgiemooltha Dyke Suite — c. 2410 — ƁWI-o — Dolerite and gabbro; includes cumulate and granophyric differentiates; concealed where dashed

2800–1140 Ma — Æxmg-moAFON — Metagranitic and metamafic rocks; Archean granite and greenstone and Proterozoic granitic and mafic rocks deformed and metamorphosed during the Albany–Fraser Orogeny

ARCHEAN

3010–2600 Ma — AmgnY, AmgssY, AgY, AgmY

AmgnY — Granitic gneiss, locally migmatitic; includes local mafic bands and enclaves
AmgssY — Foliated metagranite, locally gneissic; may include amphibolite lenses; includes deeply weathered rock
AgY — Granitic rock, undivided; metamorphosed
AgmY — Monzogranite; common biotite and rare local hornblende; minor granodiorite and syenogranite; fine to coarse grained; equigranular to porphyritic; massive to weakly foliated; metamorphosed

Atb-xs-o — **TOBIN FORMATION:** wacke, lithic sandstone, siltstone, abundant chert and banded iron-formation, and minor felsic volcaniclastic rocks; metamorphosed

Atp-xf-s — **TOPPIN HILL FORMATION:** felsic volcanic and volcaniclastic rocks, with minor siliciclastic sedimentary rocks; metamorphosed

AmnqfYYA — Quartzofeldspathic gneiss, locally strongly foliated; protolith unknown

AmwYYA — Metamorphosed igneous mafic rock; undivided

AmbYYA — Metamafic volcanic rock dominant

AoYYA — Mafic intrusive rock dominant; metamorphosed
AbYYA — Mafic volcanic rock dominant; metamorphosed
Axb-ogYYA — Mafic volcanic rock with minor gabbro; metamorphosed

AmnfqYBU — Quartzofeldspathic gneiss, protolith unknown

AmdYBU — Metasedimentary rock, undivided; includes metamorphosed sandstone, siltstone, shale, and chert

AmcYBU — Metachert

AmfaYBU — Meta-andesite

AmoYBU — Metamorphosed mafic intrusive rock dominant

AmbYBU — Metamorphosed mafic volcanic rock dominant

AmuYBU — Metamorphosed ultramafic rock, undivided; includes talc–chlorite(–carbonate) and tremolite–chlorite schists

AsYBU — Siliciclastic rocks, undivided; metamorphosed

AoYBU — Mafic intrusive rock dominant; metamorphosed

AbYBU — Mafic volcanic rock, undivided; metamorphosed

ALBANY–FRASER OROGEN: Fraser Zone; ARID BASIN; Biranup Zone; Tropicana Zone; BARREN BASIN

Geological boundary
Fault, major
- normal, tick on downthrown side
- thrust, triangle on upthrown side

Fault
- movement not specified
- normal, tick on downthrown side
- thrust, triangle on upthrown side
- reverse, triangle on upthrown side
- strike-slip, showing relative dextral displacement
- strike-slip, showing relative sinistral displacement
- concealed
- thrust, concealed, triangle on upthrown side

Shear zone, major
- movement not specified
- thrust, triangle on upthrown side
- strike-slip, showing relative dextral displacement
- strike-slip, showing relative sinistral displacement
- thrust oblique, triangle on upthrown side, showing relative dextral displacement
- concealed
- thrust, concealed, triangle on upthrown side
- strike-slip, concealed, showing relative dextral displacement

Shear zone
- movement not specified
- thrust, triangle on upthrown side
- reverse, triangle on upthrown side
- strike-slip, showing relative dextral displacement
- strike-slip, showing relative sinistral displacement
- thrust oblique, triangle on upthrown side, showing relative dextral displacement
- concealed
- thrust, concealed, triangle on upthrown side
- strike-slip, concealed, showing relative dextral displacement

Fault or shear zone
- movement not specified
- concealed

Fold axial trace
- axial trace
- anticline
- antiform
- synform
- antiform, concealed

Seismic line, with common depth point (CDP) symbol — 10000

Major track
Track

MINERAL SITES

MINERALIZATION STYLE
- Kimberlite, lamproite, and carbonatite
- Orthomagmatic mafic and ultramafic
- Vein and hydrothermal
- Stratabound sedimentary and/or sedimentary banded iron-formation

COMMODITY GROUP
- Precious metal
- Steel alloy metal
- Speciality metal
- Energy

All precious metal sites are gold unless otherwise indicated

SITE NAME

Mine, deposit, prospect, or occurrence............Scorpion

Mineralization sites on this map have been extracted from GSWA's MINEDEX database. For clarity, names have been shown only for selected sites. Full details of site numbers, site locations, site status, mineralization, and commodities can be obtained from the MINEDEX database, accessed at <www.dmp.wa.gov.au/minedex>.

COMMODITY

Chromium	Cr
Cobalt	Co
Copper	Cu
Gold	Au
Heavy Minerals	HM
Iron	Fe
Magnetite	Mag
Nickel	Ni
Palladium	Pd
Platinum	Pt
Rare Earth Elements	REE
Scandium	Sc
Titanium	Ti
Uranium	U
Vanadium	V
Zinc	Zn

DATA SOURCES

Theme	Data Currency	Organization†
Geology *	2015	Geological Survey of Western Australia, Department of Mines and Petroleum
Mineral sites *	2014	Geological Survey of Western Australia, Department of Mines and Petroleum
Structural data	2015	Geological Survey of Western Australia, Department of Mines and Petroleum
Topography	2014	Landgate

* DMP data can be viewed interactively via GeoVIEW.WA <www.dmp.wa.gov.au/geoview>, and related datasets can be downloaded from the GSWA Data and Software Centre <www.dmp.wa.gov.au/datacentre>

† WA State Government unless otherwise indicated

Compiled by CV Spaggiari 2009–15 (Albany–Fraser); east Yilgarn compiled by MJ Pawley 2010–11.
Geology by CV Spaggiari 2008–15, SA Occhipinti 2008–15, CL Kirkland 2008–11,
and MJ Pawley 2008 (Albany–Fraser); CM Doyle, SA Jones, and SS Romano 2008 (east Yilgarn)
Cartography by I Lesiak
Edited by K Greenberg, B Striewski, F Eddison and MA Ferland
Published by Geological Survey of Western Australia
Department of Mines and Petroleum
100 Plain Street
East Perth, Western Australia 6004
Phone: +61 8 9222 3459 Fax: +61 8 9222 3444
Website: www.dmp.wa.gov.au/gswa Email: geological.survey@dmp.wa.gov.au

The recommended reference for this plate is:
Spaggiari, CV and Occhipinti, SA 2015, Interpreted pre-Mesozoic bedrock geology of the Albany–Fraser Orogen and southeast Yilgarn Craton including seismic line 12GA-T1 (1:250 000), *in* Albany–Fraser Orogen seismic and magnetotelluric (MT) workshop 2014: extended abstracts *compiled by* CV Spaggiari and IM Tyler: Geological Survey of Western Australia, Record 2014/6, Plate 1.

SHEET INDEX

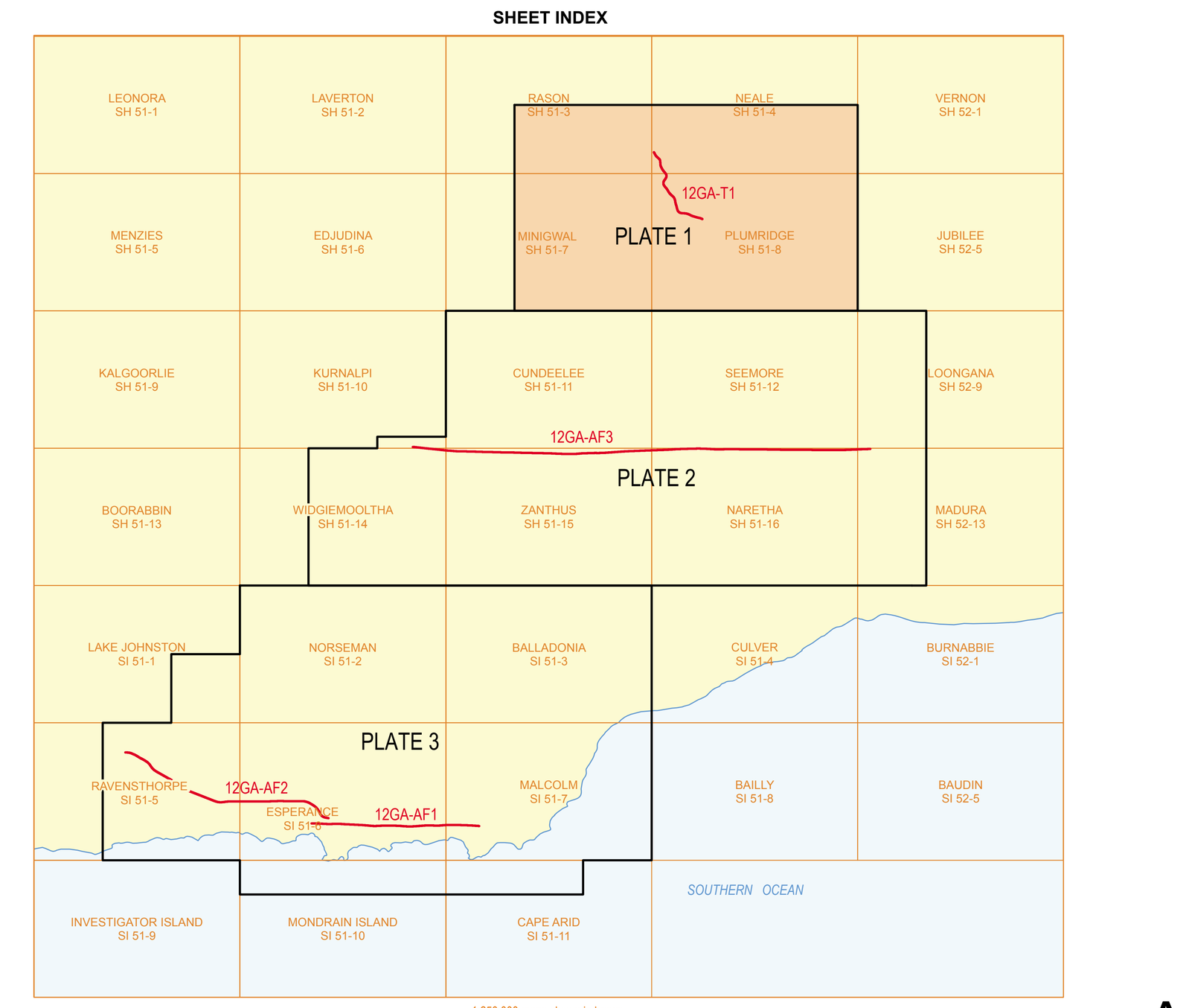

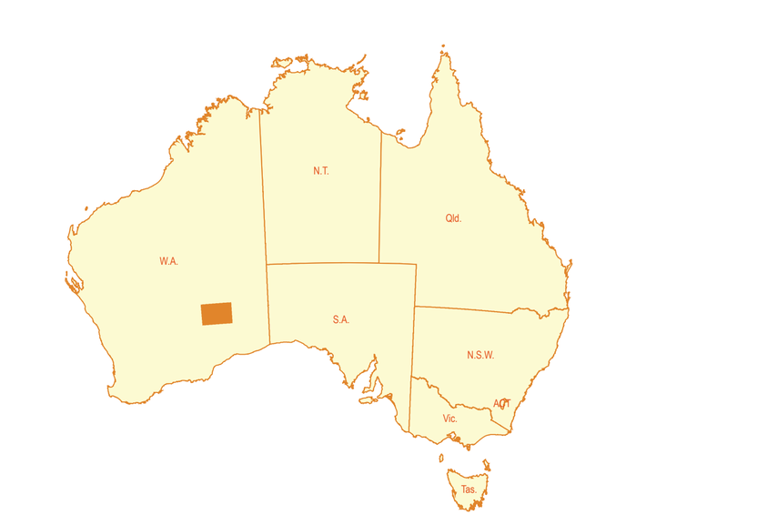

Government of Western Australia
Department of Mines and Petroleum

Geological Survey of Western Australia

HON. BILL MARMION MLA
MINISTER FOR MINES AND PETROLEUM

RICK ROGERSON
EXECUTIVE DIRECTOR

SCALE 1:250 000

2 500 0 5 10 15 20 25
Metres Kilometres

UNIVERSAL TRANSVERSE MERCATOR PROJECTION
HORIZONTAL DATUM: GEOCENTRIC DATUM OF AUSTRALIA 1994
VERTICAL DATUM: AUSTRALIAN HEIGHT DATUM

Grid lines indicate 20 000 metre interval of the Map Grid Australia Zone 51

The Map Grip Australia (MGA) is based on the Geocentric Datum of Australia 1994 (GDA94)
GDA94 positions are compatible within one metre of the datum WGS84 positions

GEOLOGICAL SURVEY OF WESTERN AUSTRALIA

RECORD 2014/6 PLATE 1

INTERPRETED PRE-MESOZOIC BEDROCK GEOLOGY OF THE ALBANY–FRASER OROGEN AND SOUTHEAST YILGARN CRATON

INCLUDING SEISMIC LINE 12GA-T1

December 2015

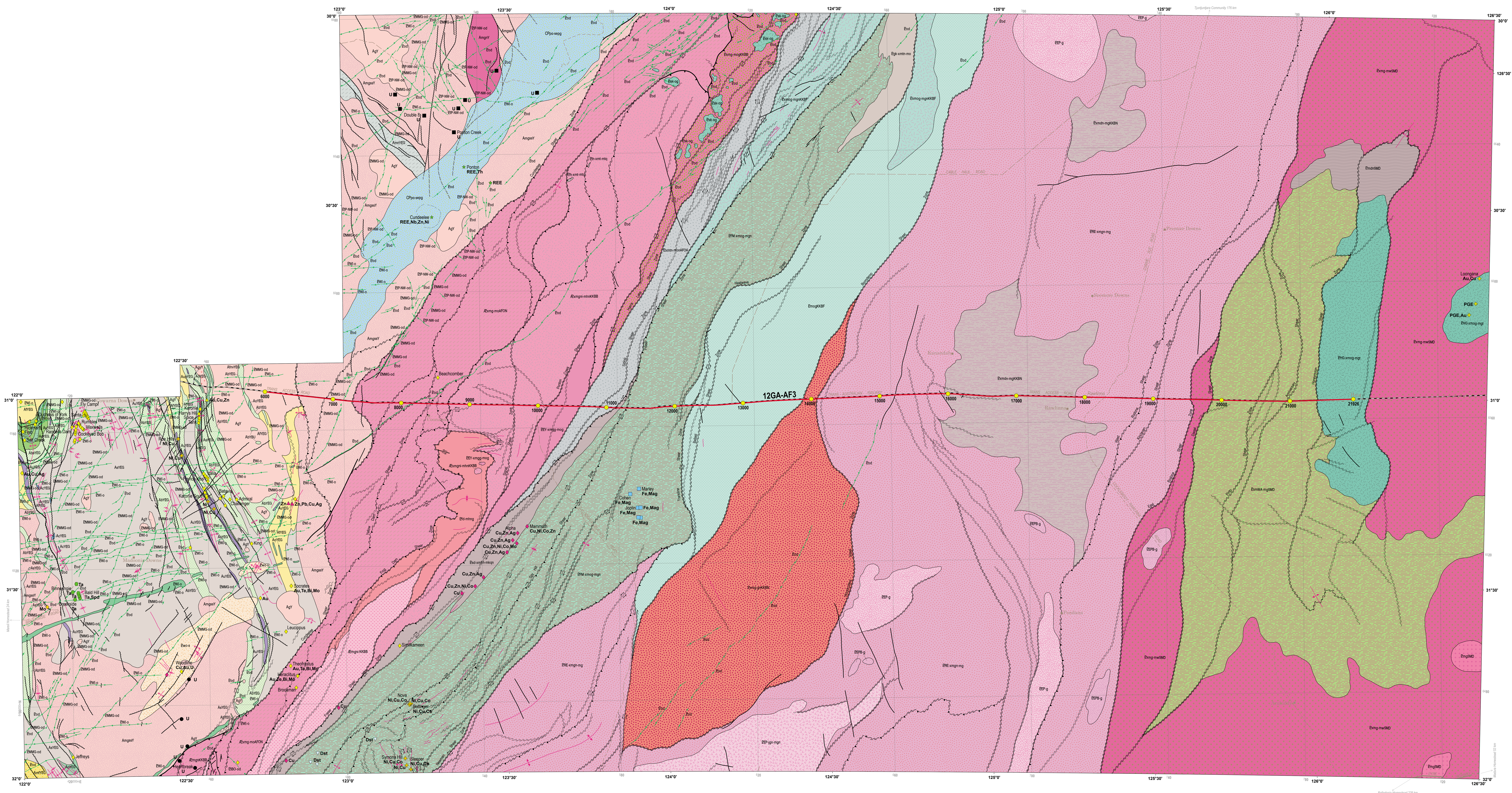

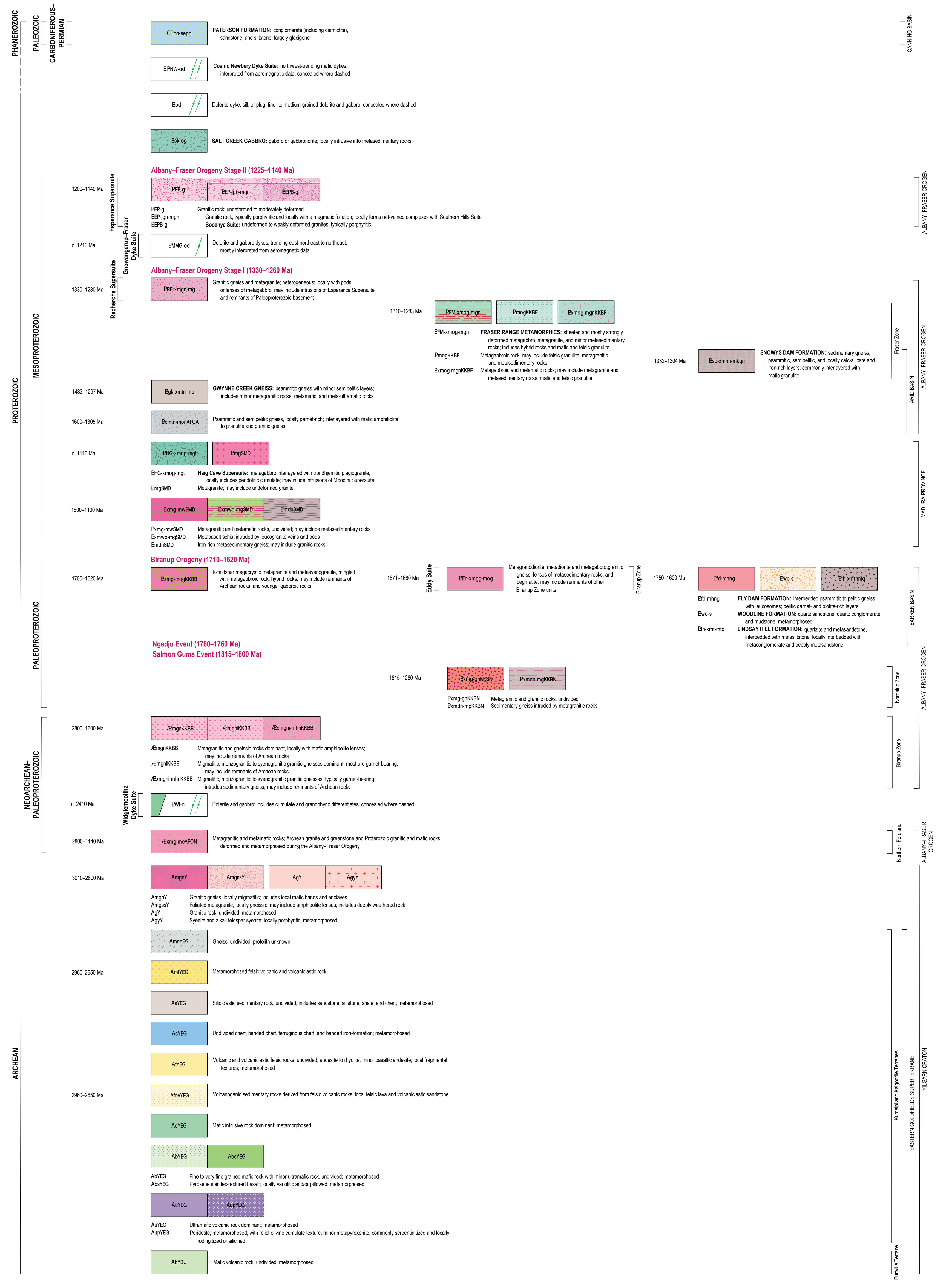

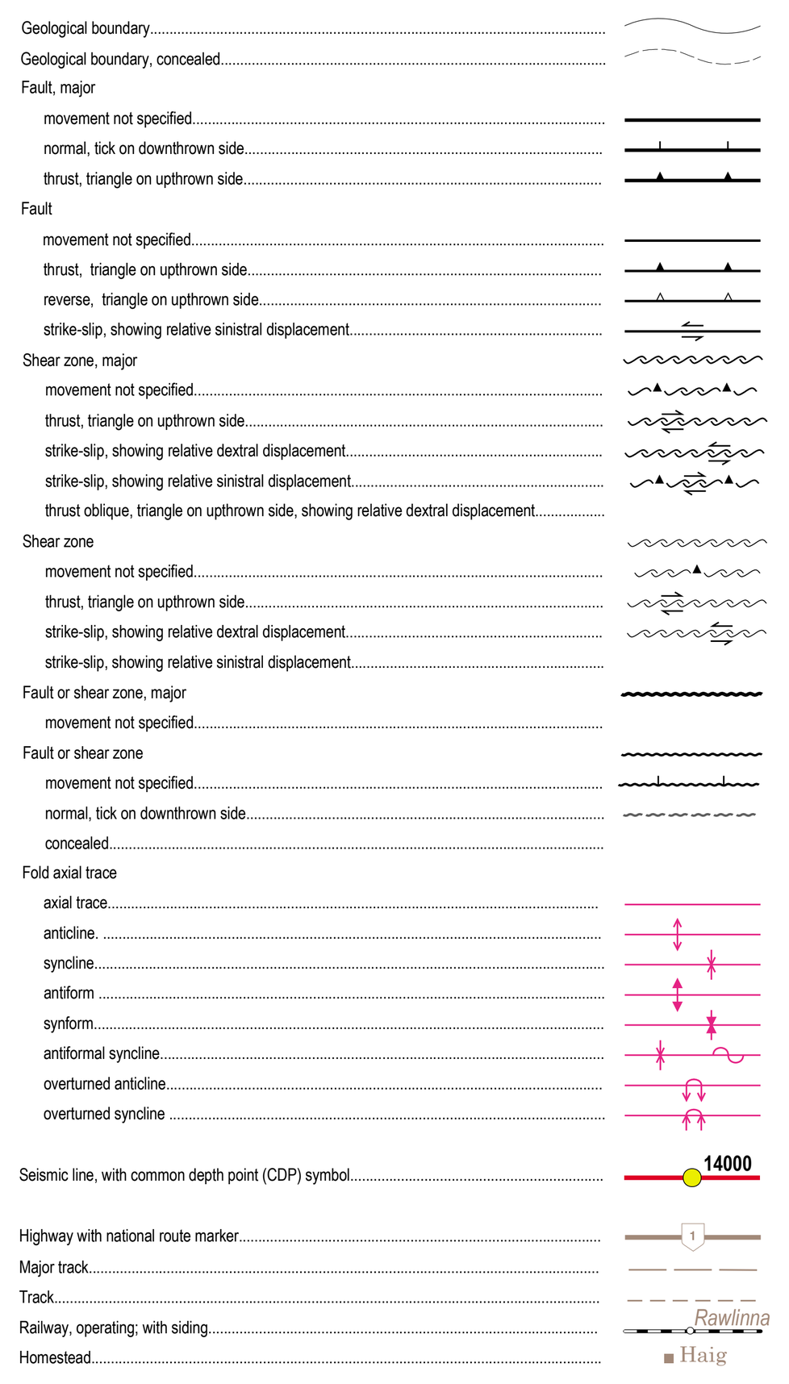

MINERAL SITES

MINERALIZATION STYLE

- Kimberlite, lamproite, and carbonatite
- Porphyry, pegmatite, greisen, and skarn
- Orthomagmatic mafic and ultramafic
- Vein and hydrothermal
- Stratabound volcanic and sedimentary
- Stratabound sedimentary and/or sedimentary banded iron-formation
- Basin hosted
- Unknown/unassigned

COMMODITY GROUP

- Precious metal
- Steel alloy metal
- Speciality metal
- Base metal
- Iron
- Energy
- Construction material

All precious metal sites are gold unless otherwise indicated

COMMODITY

Bismuth	Bi
Cobalt	Co
Copper	Cu
Dimension stone	Dst
Gold	Au
Iron	Fe
Lead	Pb
Magnetite	Mag
Molybdenum	Mo
Nickel	Ni
Niobium	Nb
Platinum Group Elements	PGE
Rare Earth Elements	REE
Silver	Ag
Spodumene	Spd
Tantalum	Ta
Tellurium	Te
Thorium	Th
Uranium	U
Zinc	Zn

SITE NAME

Mine, deposit, prospect, or occurrence.......... Socrates

Mineralization sites on this map have been extracted from GSWA's MINEDEX database. For clarity, names have been shown only for selected sites. Full details of site numbers, site locations, site status, mineralization, and commodities can be obtained from the MINEDEX database, accessed at <www.dmp.wa.gov.au/minedex>.

Compiled by CV Spaggiari 2009–15 and LI Brisbout 2013 (Albany–Fraser); east Yilgarn compiled by MJ Pawley 2010–11; southeast Yilgarn extracted from Geological Survey of Western Australia 2005 and 2008, 1:500 000 scale IBG.

Geology by CV Spaggiari 2008–15, CL Kirkland 2008–11, LI Brisbout 2013 and MJ Pawley 2008 (Albany–Fraser); SA Jones 2002–03, AA Ross 2005, CE Hall 2005, B Goscombe 2005, TJ Griffin 1980–84 and AH Hickman 1979–81 (southeast Yilgarn).

Cartography by I Lesiak

Edited by K Greenberg, B Striewski, F Eddison and MA Ferland

Published by Geological Survey of Western Australia

Department of Mines and Petroleum
100 Plain Street
East Perth, Western Australia 6004
Phone: +61 8 9222 3459 Fax: +61 8 9222 3444
Website: www.dmp.wa.gov.au/gswa Email: geological.survey@dmp.wa.gov.au

The recommended reference for this plate is:
Spaggiari, CV and Brisbout, LI 2015, Interpreted pre-Mesozoic bedrock geology of the Albany–Fraser Orogen and southeast Yilgarn Craton including seismic line 12GA-AF3 (1:500 000), *in* East Albany–Fraser Orogen seismic and magnetotelluric (MT) workshop 2014: extended abstracts *compiled by* CV Spaggiari and IM Tyler: Geological Survey of Western Australia, Record 2014/6, Plate 2.

DATA SOURCES

Theme	Data Currency	Organization†
Geology *	2015	Geological Survey of Western Australia, Department of Mines and Petroleum
Mineral sites *	2014	Geological Survey of Western Australia, Department of Mines and Petroleum
Structural data	2015	Geological Survey of Western Australia, Department of Mines and Petroleum
Topography	2014	Landgate

* DMP data can be viewed interactively via GeoVIEW.WA <www.dmp.wa.gov.au/geoview>, and related datasets can be downloaded from the GSWA Data and Software Centre <www.dmp.wa.gov.au/datacentre>

† WA State Government unless otherwise indicated

SHEET INDEX

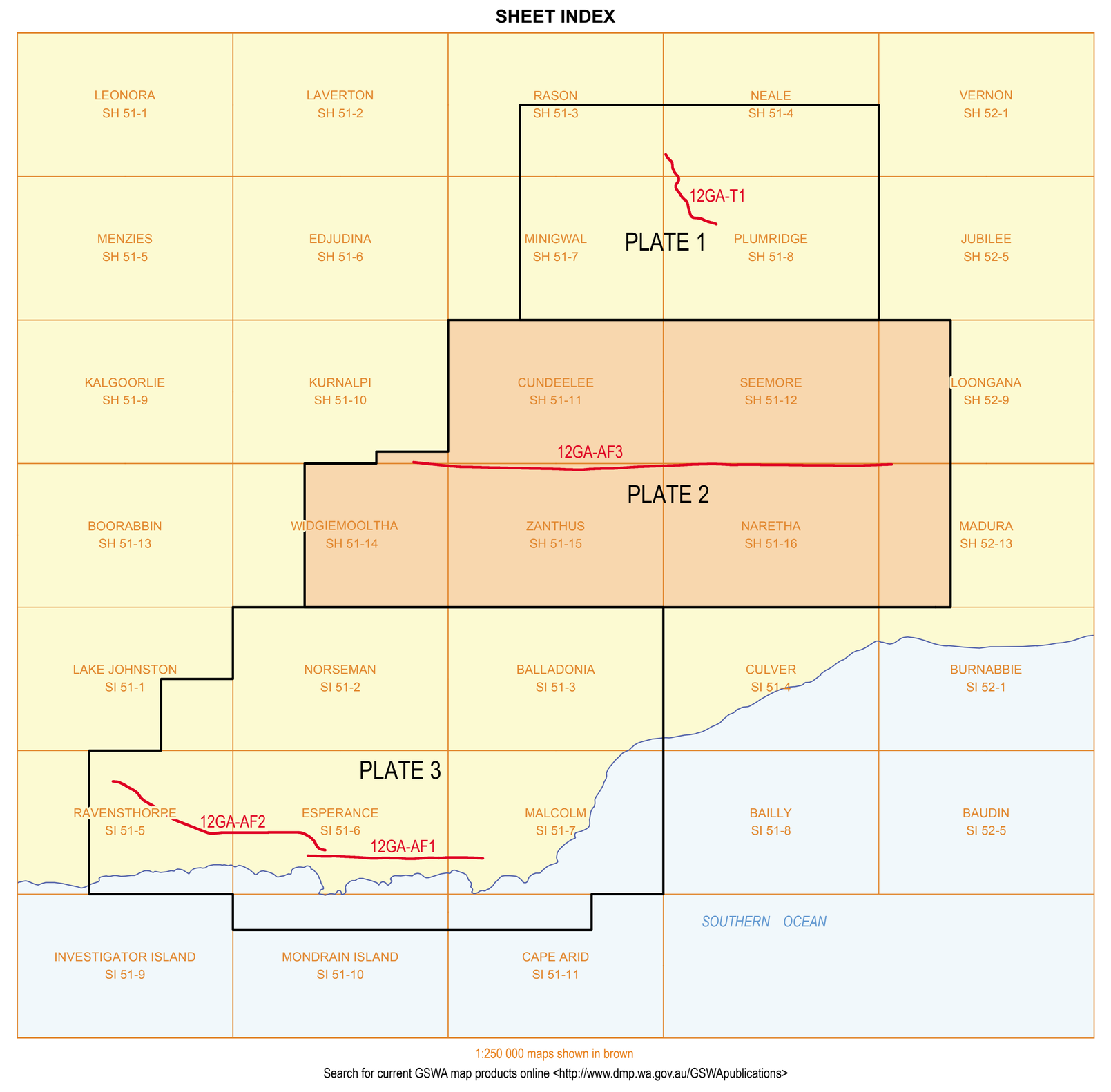

Government of **Western Australia**
Department of **Mines and Petroleum**

HON. BILL MARMION MLA
MINISTER FOR MINES AND PETROLEUM

Geological Survey of Western Australia

RICK ROGERSON
EXECUTIVE DIRECTOR

SCALE 1:500 000

5 000 Metres 0 10 20 30 40 50 Kilometres

UNIVERSAL TRANSVERSE MERCATOR PROJECTION
HORIZONTAL DATUM: GEOCENTRIC DATUM OF AUSTRALIA 1994
VERTICAL DATUM: AUSTRALIAN HEIGHT DATUM

Grid lines indicate 20 000 metre interval of the Map Grid Australia Zone 51

GDA

The Map Grip Australia (MGA) is based on the Geocentric Datum of Australia 1994 (GDA94)
GDA94 positions are compatible within one metre of the datum WGS84 positions

GEOLOGICAL SURVEY OF WESTERN AUSTRALIA

RECORD 2014/6 PLATE 2

INTERPRETED PRE-MESOZOIC BEDROCK GEOLOGY OF THE ALBANY–FRASER OROGEN AND SOUTHEAST YILGARN CRATON

INCLUDING SEISMIC LINE 12GA-AF3

December 2015

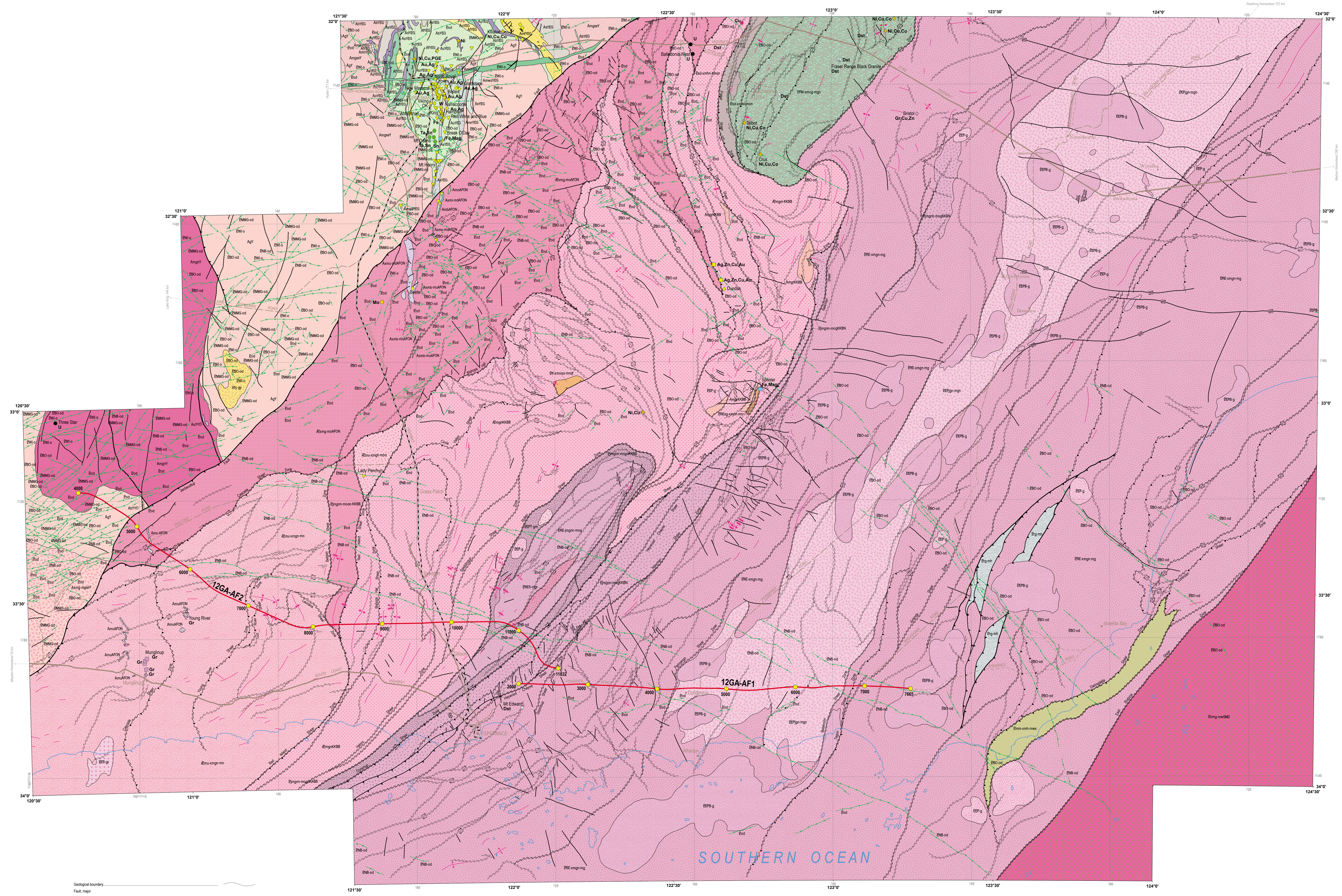

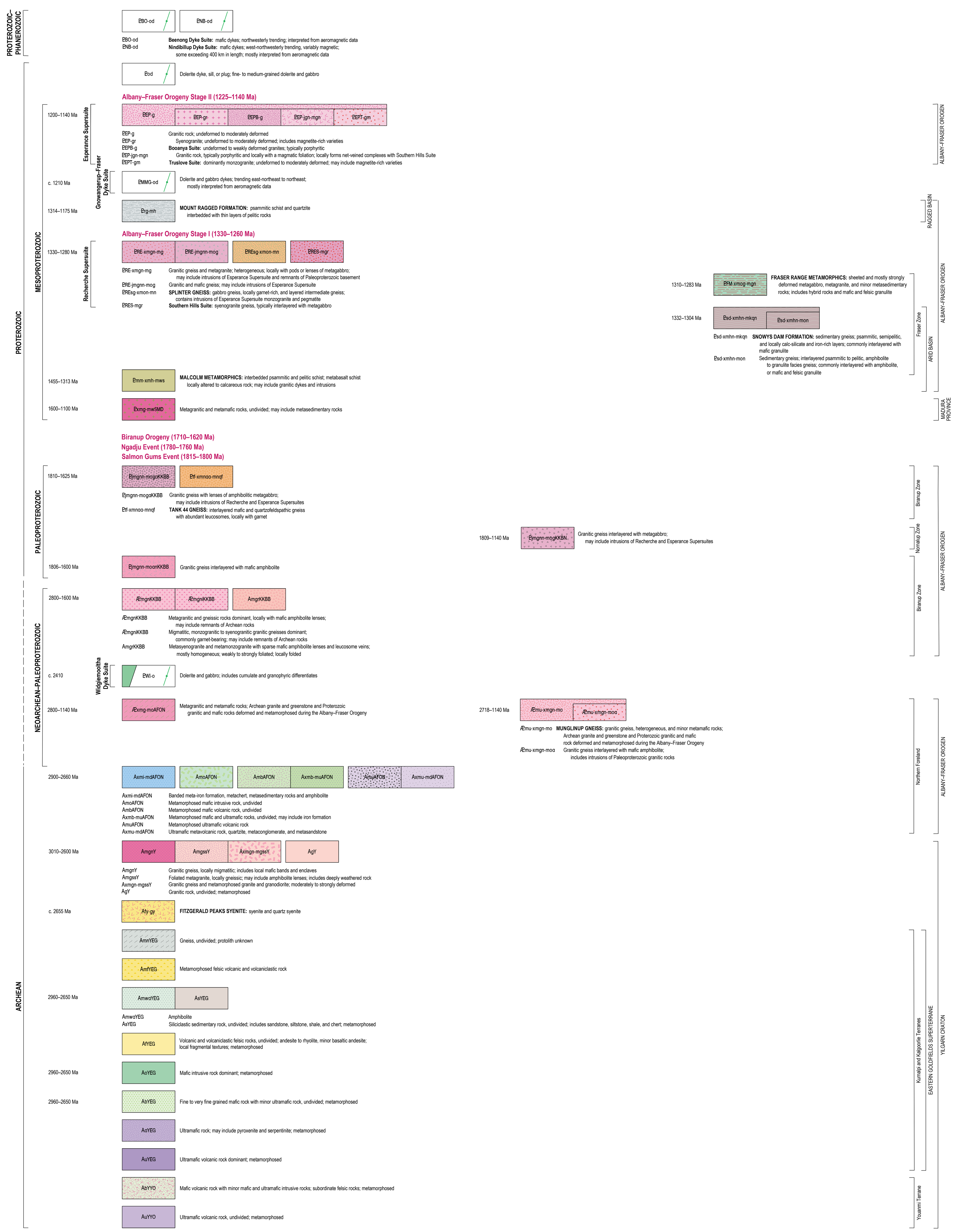

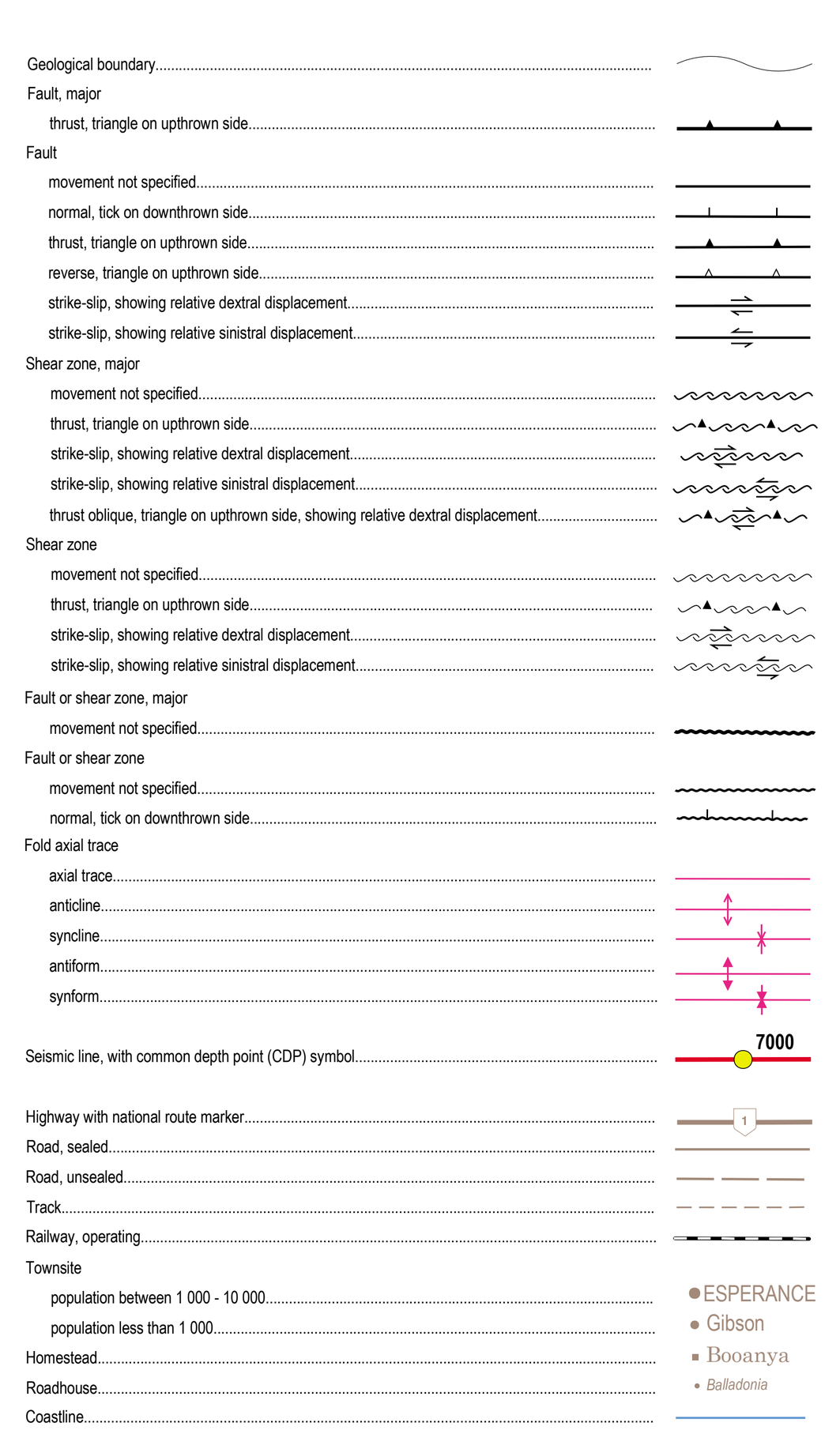

MINERAL SITES

MINERALIZATION STYLE

- Porphyry, pegmatite, greisen, and skarn
- Orthomagmatic mafic and ultramafic
- Vein and hydrothermal
- Stratabound sedimentary and/or sedimentary banded iron-formation
- Basin hosted
- Unknown/unassigned

COMMODITY GROUP

- Precious metal
- Steel alloy metal
- Speciality metal
- Iron
- Energy
- Industrial mineral
- Construction material

All precious metal sites are gold unless otherwise indicated

COMMODITY

Cobalt	Co
Copper	Cu
Dimension stone	Dst
Gold	Au
Graphite	Gr
Iron	Fe
Magnetite	Mag
Molybdenum	Mo
Nickel	Ni
Platinum Group Elements	PGE
Silver	Ag
Tantalum	Ta
Tungsten	W
Tin	Sn
Uranium	U
Zinc	Zn

SITE NAME

Mine, deposit, prospect, or occurrence .... Bullen

Mineralization sites on this map have been extracted from GSWA's MINEDEX database. For clarity, names have been shown only for selected sites. Full details of site numbers, site locations, site status, mineralization, and commodities can be obtained from the MINEDEX database, accessed at <www.dmp.wa.gov.au/minedex>.

Compiled by CV Spaggiari 2006–15 and LI Brisbout 2013 (Albany–Fraser); southeast Yilgarn extracted from Geological Survey of Western Australia 2005 and 2008, 1:500 000 scale IBG.

Geology by CV Spaggiari 2006–15, LI Brisbout 2013, CL Kirkland 2008–11, and MJ Pawley 2008 (Albany–Fraser); CF Gower, JA Bunting, R Thom and SL Lipple, 1971, P McGoldrick 1988–90 (southeast Yilgarn).

Cartography by I Lesiak

Edited by K Greenberg, B Striewski, F Eddison and MA Ferland

Published by Geological Survey of Western Australia

Department of Mines and Petroleum
100 Plain Street
East Perth, Western Australia 6004
Phone: +61 8 9222 3459 Fax: +61 8 9222 3444
Website: www.dmp.wa.gov.au/gswa Email: geological.survey@dmp.wa.gov.au

The recommended reference for this plate is:
Spaggiari, CV and Brisbout, LI 2015, Interpreted pre-Mesozoic bedrock geology of the Albany–Fraser Orogen and southeast Yilgarn Craton including seismic lines 12GA-AF1 and 12GA-AF2 (1:500 000), *in* Albany–Fraser Orogen seismic and magnetotelluric (MT) workshop 2014: extended abstracts *compiled by* CV Spaggiari and IM Tyler: Geological Survey of Western Australia, Record 2014/6, Plate 3.

DATA SOURCES

Theme	Data Currency	Organization†
Geology *	2015	Geological Survey of Western Australia, Department of Mines and Petroleum
Mineral sites *	2014	Geological Survey of Western Australia, Department of Mines and Petroleum
Structural data	2015	Geological Survey of Western Australia, Department of Mines and Petroleum
Topography	2014	Landgate

* DMP data can be viewed interactively via GeoVIEW.WA <www.dmp.wa.gov.au/geoview>, and related datasets can be downloaded from the GSWA Data and Software Centre <www.dmp.wa.gov.au/datacentre>
† WA State Government unless otherwise indicated

SHEET INDEX

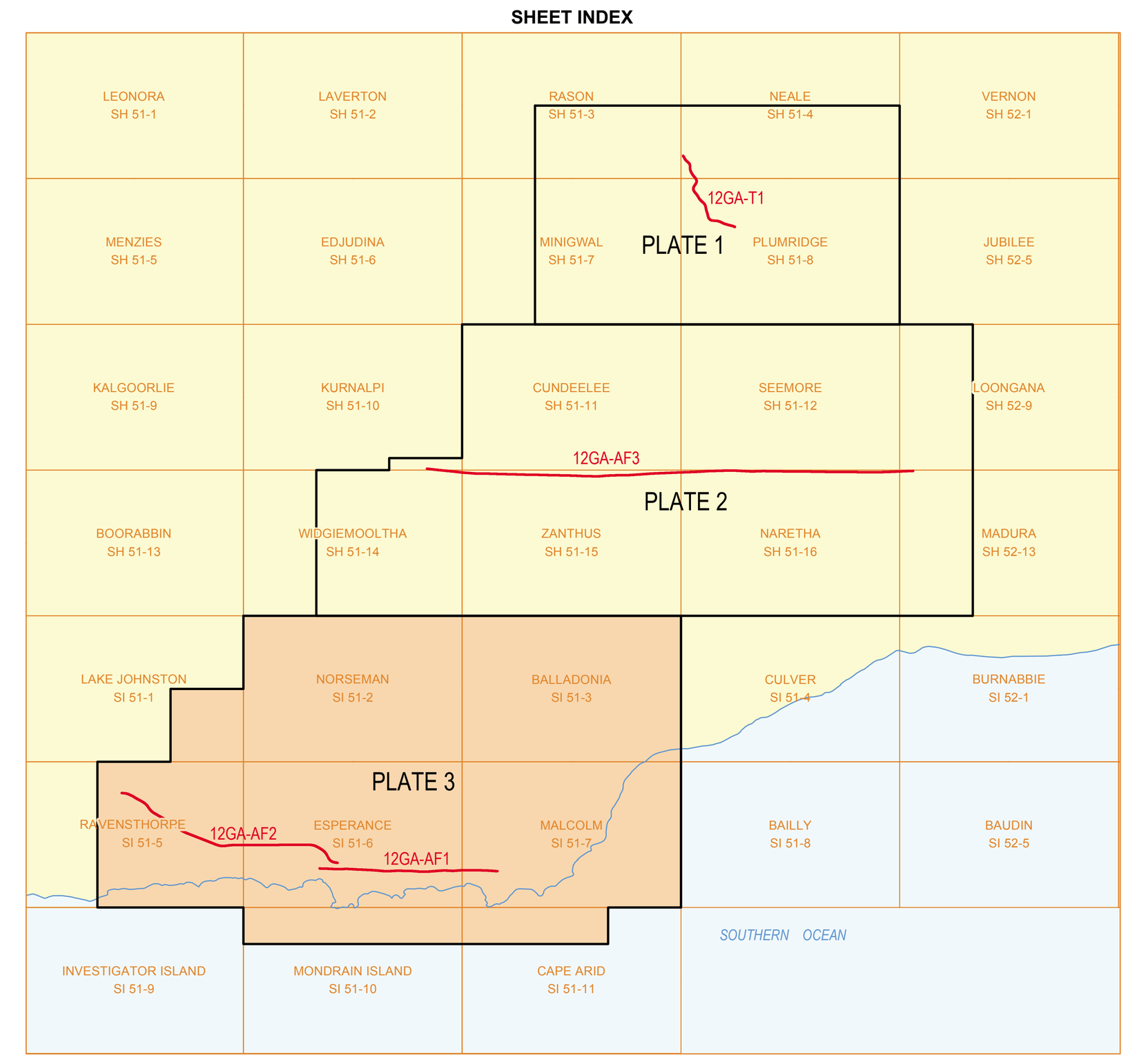

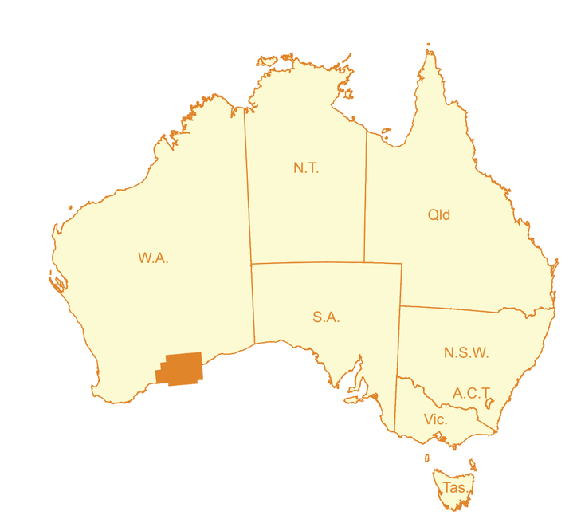

Government of Western Australia
Department of Mines and Petroleum

Geological Survey of Western Australia

SCALE 1:500 000

UNIVERSAL TRANSVERSE MERCATOR PROJECTION
HORIZONTAL DATUM: GEOCENTRIC DATUM OF AUSTRALIA 1994
VERTICAL DATUM: AUSTRALIAN HEIGHT DATUM

Grid lines indicate 20 000 metre interval of the Map Grid Australia Zone 51

The Map Grip Australia (MGA) is based on the Geocentric Datum of Australia 1994 (GDA94)
GDA94 positions are compatible within one metre of the datum WGS84 positions

GEOLOGICAL SURVEY OF WESTERN AUSTRALIA
RECORD 2014/6 PLATE 3

INTERPRETED PRE-MESOZOIC BEDROCK GEOLOGY OF THE ALBANY–FRASER OROGEN AND SOUTHEAST YILGARN CRATON

INCLUDING SEISMIC LINES 12GA-AF1 AND 12GA-AF2

December 2015

INTERPRETED MIGRATED SEISMIC SECTIONS

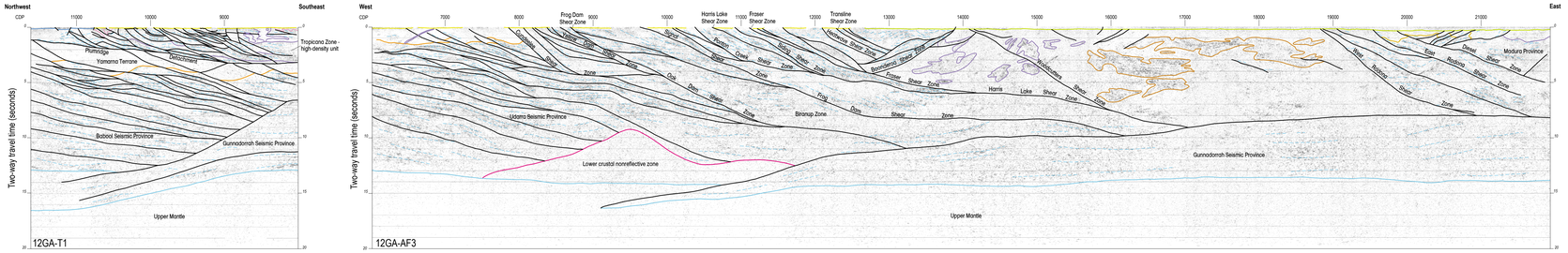

INTERPRETED GEOLOGICAL SECTIONS

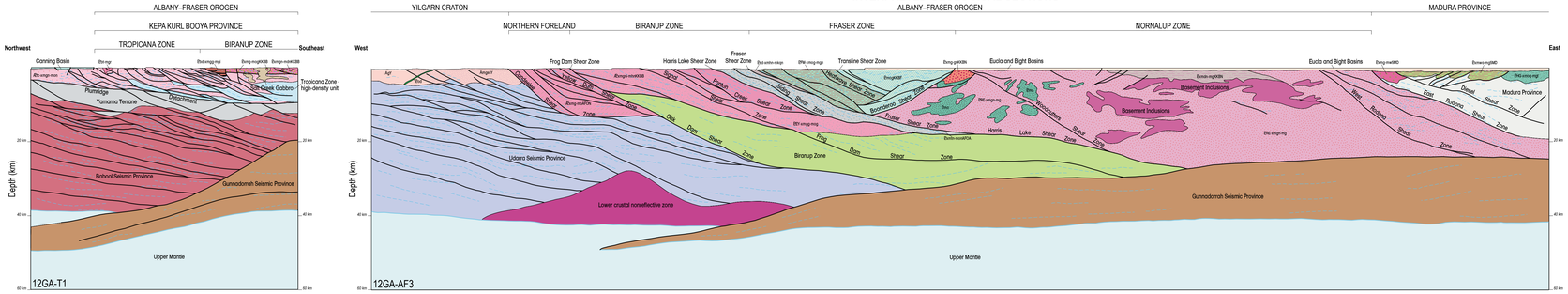

INTERPRETED MIGRATED SEISMIC SECTIONS

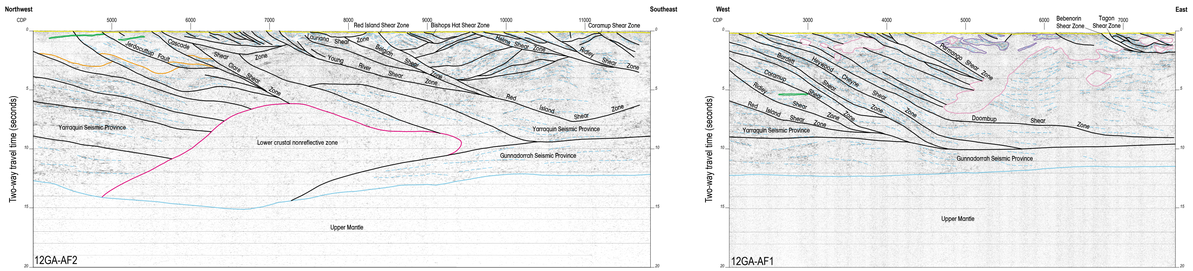

INTERPRETED GEOLOGICAL SECTIONS

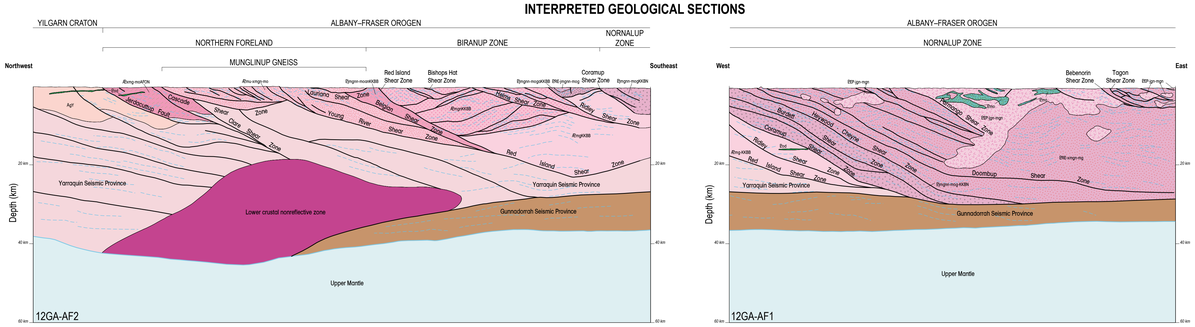

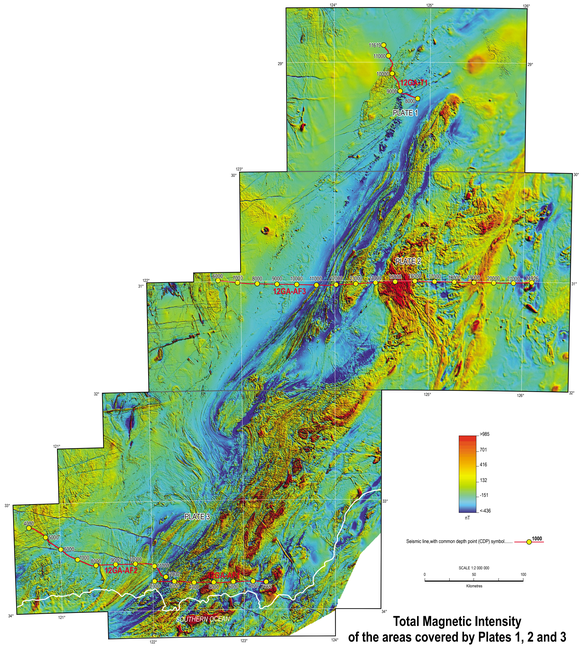

Total Magnetic Intensity of the areas covered by Plates 1, 2 and 3

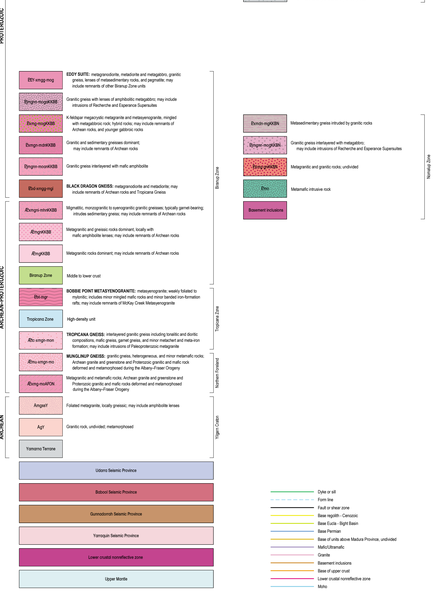

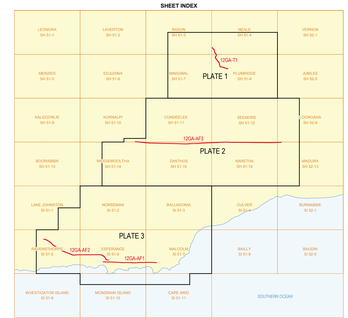

Compiled by CV Spaggiari and SA Occhipinti
Interpretation by CV Spaggiari, SA Occhipinti, RJ Korsch, MP Doublier, DJ Clark, MC Dentith, K Gessner, MG Doyle, IM Tyler, BLN Kennett, T Lees, J Savage, K Martin, RD Crabtree, T Fenton and J Holzschuh
Cartography by I Lewis
Edited by K Greenberg, B Grewcock, F Kildison and MA Farland
Published by Geological Survey of Western Australia
This map is published in digital format (PDF) and is available online at <www.dmp.wa.gov.au/GSWApublications>
Copies are available from:
Information Centre
Department of Mines and Petroleum
100 Plain Street
East Perth, Western Australia 6004
Phone: +61 8 9222 3459 Fax: +61 8 9222 3444
Website: www.dmp.wa.gov.au/geosa Email: geological.survey@dmp.wa.gov.au
The recommended reference for this plate is:
Spaggiari, CV and Occhipinti, SA 2015, Geological interpretation of the Albany–Fraser Orogen and southeast Yilgarn Craton seismic lines 12GA-AF1, 12GA-AF2, 12GA-AF3, and 12GA-T1: Albany–Fraser Orogen seismic and magnetotelluric (MT) workshop 2014, extended abstracts, compiled by CV Spaggiari and IM Tyler: Geological Survey of Western Australia, Record 2014/6, Plate 4.

ANSIR NATIONAL RESEARCH FACILITY FOR EARTH SOUNDING
ANGLOGOLD ASHANTI
INDEPENDENCE GROUP NL
ROYALTIES FOR REGIONS
Australian Government Geoscience Australia
Government of Western Australia Department of Mines and Petroleum
HON. BILL MARMION MLA MINISTER FOR MINES AND PETROLEUM
Geological Survey of Western Australia
REX ROGERSON EXECUTIVE DIRECTOR
SCALE 1:600 000
0 5 10 20 30 40 50
Miles Kilometres
UNIVERSAL TRANSVERSE MERCATOR PROJECTION
HORIZONTAL DATUM: GEOCENTRIC DATUM OF AUSTRALIA 1994
VERTICAL DATUM: AUSTRALIAN HEIGHT DATUM
GDA
The Map Grid Australia (MGA) is based on the Geocentric Datum of Australia 1994 (GDA94). GDA94 positions are compatible within one metre of the datum WGS84 positions.

GEOLOGICAL SURVEY OF WESTERN AUSTRALIA
RECORD 2014/6 PLATE 4

GEOLOGICAL INTERPRETATION OF THE ALBANY–FRASER OROGEN AND SOUTHEAST YILGARN CRATON SEISMIC LINES 12GA-AF1, 12GA-AF2, 12GA-AF3, AND 12GA-T1

December 2015